Proceedings of the European Telemetry Conference

Garmisch - Partenkirchen, Germany

May 22 to 25, 2000

etc2000

European Telemetry Conference

with Exhibition

Edited by: German Society of Telemetering

Arbeitskreis Telemetrie e.V.

German Society of Telemetering
Arbeitskreis Telemetrie e.V.

Vorstand / President: Hans - Joachim Klewe
Im Ziegenförth 54
D-38108 Braunschweig

Printed in Germany by: Döring - Druck, Braunschweig

CONTENTS / INHALTSVERZEICHNIS

Europäische Telemetriekonferenz mit Ausstellung

European Telemetry Conference with Exhibition

22. - 25. 05. 2000 / Garmisch-Partenkirchen, Kongresshaus Germany

Veranstaltet von: **Arbeitskreis Telemetrie e.V.**
organized by: ***Geman Society for Telemetering***

in Zusammenarbeit mit:
in cooperation with:

- **International Foundation for Telemetering (IFT)**
- **International Society on Biotelemetry (ISOB)**
- **Société des Électriciens, des Électroniciens et des Radioélectriciens (SEE), Section 17**
- **Deutsche Gesellschaft für Luft- u. Raumfahrt e.V. (DGLR) Fachausschuß 6.1 "Telemetrie"**
- **Technische Universität München Lehrstuhl für Flugantriebe**
- **International Society of Air Safety Investigators [ISASI] Flight Recording Working Group**

etc2000:	*Hans-Joachim Klewe*
ETSC / ICTS:	*Gerhard V. Mayer*
AIMS2000:	*Hans-Peter Kau*
ISASI *:*	*Paul Mayes / Mike Pool*
Ausstellung: *Exhibition:*	*Werner R. Lange* *Daniela Fessl*
Organisationsbüro: *Registration and* *Conference Secretariat:*	*Brigitte Rüba* *Inge Schade* *Isolde Böhringer*
Exkursionen: *Tours:*	*Herta Klewe*
Europäischer Abend: *European Dinner:*	

Arbeitskreis Telemetrie e.V.

Ganghoferstraße 29
D-82216 Gernlinden

Vorstand:

Hans-Joachim Klewe	**Präsident**
Dr. Gerhard V. Mayer	**Vizepräsident**
Herbert Wutz	**Vizepräsident**
Werner R. Lange	**Schatzmeister**
Daniela Fessl	**Schriftführerin**

Fachbeirat / *Advisory Council:*

Jürgen Bendix / Arbeitskreis Telemetrie e.V.

Dr. Michael Bornhausen / Arbeitskreis Telemetrie e.V.

Peter Claaßen / PC-ELECTRONIC GmbH

Josef Heim / Arbeitskreis Telemetrie e.V.

Dr. Hans-Wolfgang Helb / Universität Kaiserslautern

Dr. Hans-Peter Kimmich / T & T - Zürich

Hans-Joachim Klewe / Arbeitskreis Telemetrie e.V.
/ International Society on Biotelemetry

Werner R. Lange / Lange Electronic GmbH

Prof. Dr. Gerhard V. Mayer / Aero Sensing Radarsysteme GmbH

Hans Heiko Renner / Wehrtechnische Dienststelle 61

Peter Taubenreuther / STT Systemtechnik Taubenreuther

Bernd Uwe Wiese / Wehrtechnische Dienststelle 61

Herbert Wutz / TEL DATA SYSTEM GmbH

Einführung

Die EUROPÄISCHE TELEMETRIEKONFERENZ **etc 2000** findet vom 22.-25.Mai 2000 als Kongress und Ausstellung für Telemetrie, Versuchsinstrumentierung und Fernwirken in Garmisch-Partenkirchen statt. Die Veranstaltung wird vom Arbeitskreis Telemetrie e.V./ DGLR-Fachausschuß 6.1"Telemetrie" durchgeführt und informiert über Innovationen und den Stand der Technik dieser Fachgebiete.
Wie bei den vorhergehenden Europäischen Telemetriekonferenzen wird auch bei der **etc 2000** der internationale Charakter der Veranstaltung durch eine große Zahl von Vortragenden und Teilnehmern aus Europäischen und Überseeischen Ländern belegt. Die Vorträge werden, der Internationalität der Veranstaltung entsprechend, in englischer Sprache gehalten. Die große Zahl der Konferenzbeiträge macht es erforderlich, Parallelsitzungen in den zur Verfügung stehenden Konferenzräumen durchzuführen.
Besonders hervorgehoben ist bei der **etc 2000** die effiziente Modulationstechnologie FQPSK, zu der in Form eines Forums vorgetragen wird. Ebenfalls im Rahmen der **etc 2000** findet eine Tagung des Europäischen Telemetrie Standardisierungs Komitees [ETSC] mit Teilnehmern aus Deutschland, England, Frankreich sowie Delegierten des TSCC/USA statt. Weiter wird eine Tagung der International Group of Telemetry Practioners (ICTS**)** durchgeführt, deren Thema die Sicherstellung von Frequenzen für Telemetrie-Anwendungen ist.
Zusammen mit der **etc 2000** findet das Symposium "Aircraft Integrated Monitoring Systems" **AIMS 2000** statt. Diese Symposium wird ergänzt durch den 4.Biennial Workshop der International Society of Air Safety Investigators (ISASI) Flight Recording Work Group.
Kongressteilnehmern stehen die Vortragsreihen beider Veranstaltungen offen.

Erstmals wird dem vorliegenden Tagungsband eine CD beigefügt, die alle Vortragsreihen sowie einen Teil des Aussteller-Katalogs enthält. Da alle Beiträge mittels elektronischer Textverarbeitung erstellt wurden, haben sehr viele Autoren von der Möglichkeit Gebrauch gemacht, Grafiken und Bilder farbig darzustellen. Da der Tagungsband aus Kostengründen nicht farbig gedruckt werden konnte, stellt die CD eine hervorragende Ergänzung dar,da nunmehr die Farbdarstellungen auf dem Bildschirm erkennbar gemacht werden können.
Der Arbeitskreis Telemetrie e.V. [German Society of Telemetering] als Veranstalter der **etc 2000** wird sich im Gespräch mit den Teilnehmern der Konferenz und im Dialog mit anderen nationalen und internationalen Organisationen wie der International Foundation for Telemetering [IFT] in den USA, der Société des Electriciens, des Electroniciens et des Radioelectriciens [SEE] Section 17, der International Society on Biotelemetry [ISOB] sowie der Low Power Radio Association [LPRA] weiterhin bemühen,Trends und Entwicklungen im Bereich der Telemetrie und Fernwirktechnik zu erkennen und bei künftigen Veranstaltungen zu berücksichtigen.
Die mit der Konferenz verbundene Ausstellung gibt einen umfangreichen Überblick über den Stand der Technik und die Vielzahl des Angebots von Hard-und Software bei Geräten, Anlagen und Systemen im Bereich der Telemetrie, der Versuchsinstrumentierung und des Fernwirkens. 70 Hersteller und Organisationen stellen auf 60 Ständen aus.
Im Namen der Arbeitskreises Telemetrie e.V. danke ich Allen, die bei der Organisation der **etc 2000** mitgewirkt haben, sowie allen Vortragenden und Ausstellern, die zum Erfolg der Veranstaltung beigetragen haben.

Hans-Joachim Klewe
Conference-Chairman

Introduction

The EUROPEAN TELEMETRY CONFERENCE ***etc 2000*** *will be held in form of a Congress*
with Exhibition for Telemetry,Test Instrumentation and Telecontrol in Garmisch-Partenkirchen Germany, from May 22 to 25, 2000. The event will be organized by the German Society of Telemetering [Arbeitskreis Telemetrie e.V./ DGLR-section 6.1"Telemetrie"] and will inform the experts on innovations and the latest state of the art in this field.

The international character of the ***etc 2000*** *again is stated by a large number of lecturers and participants from european and overseas countries. The papers will be presented in english language, according to the internationality of the event.Due to the number of conference contributions it is necessary to held parallel meetings.*
In particular extended on ***etc 2000*** *is the field "Efficient Modulation Technologies" which will be presented in form of a "Forum FQPSK".*
Also along ***etc 2000*** *the Annual Plenary Meeting of the European Telemetering Standardization Committee [ETSC] with delegates of Germany, France, Great Britain and TSCC/USA will take place. In addition questions of the future availability of frequencies for telemetering purposes are discussed in a meeting of the International Group of Telemetry Practioners [ICTS]*
Together with ***etc2000*** *the Symposium "Aircraft Integrated Monitoring Systems"* ***AIMS2000*** *will take place.Jointly with this symposium the International Society of Air Safety Investigators*
(ISASI) Flight Recording Working Group is holding ist 4th.Biennial Workshop.
Participants of ***etc 2000*** *and* ***AIMS 2000*** *are free to attend the presentations of both events as well as to visit the common exhibition.*
First time a CD, which contains all presentations of ***etc 2000*** *and* ***AIMS 2000*** *as well as a part of the exhibitors catalogue, will be added to this Proceedings Volume.Due to the fact, that all contributions have been established by means of computerized text- and graphic processing, many authors made use of coloured pictures and diagrams in their papers. Because of cost reasons the Proceedings Volume could not be printed in colour, the CD is a great supplement serving to show the coloured graphis on the screen of a computer monitor.*
The German Society of Telemetering as organizer of the ***etc 2000*** *will further endeavour itself in discussions with the participants of the conference, as well as in dialogue with other national and international organisations, e.g. the "International Foundation for Telemetering [IFT]" in the USA, the "Société des Electriciens,des Electroniciens et des Radioelectriciens [SEE],section 17" in France, the "International Society on Biotelemetry [ISOB]" and the "Low Power Radio Association [LPRA]" in England, in order to recognize trends and developments in the field of Telemetry, Test Instrumentation and Telecontrol and to take this into account in future events.*
The joint exhibition gives an extensive overview of the latest developments in technology and on the great variety of hardware and software for instrumentation, installation and systems concerning Telemetry, Test Instrumentation and Telecontrol. 70 manufacturers and organisations are exhibiting on 60 booths.
On behalf of the Arbeitskreis Telemetrie e.V. may I thank all of those who participated in the organisation of the ***etc 2000****, as well as all lecturers and exhibitors contributing to the success of the event.*

Hans-Joachim Klewe
Conference Chairman

Opening Presentations

TELEMETRY SPECTRUM ENCROACHMENT— LESSONS LEARNED

Mikel R. Ryan
Head, Mid-Atlantic Area Frequency Coordination Office
Naval Air Warfare Center Aircraft Division
Patuxent River, Maryland, United States of America

Abstract

Over the past five years the United States (US) Congress has passed legislation mandating the reallocation of 255 MHz of radio frequency bands from Federal to non-Federal or "MIXED USE." Several of the frequency bands supporting telemetering functions were affected, and more legislation of this nature is forecasted, both in the US and in numerous countries around the world. This threat **can** be met and countered by the international telemetering community if the "Lessons Learned" in the last five years are adapted.

Introduction

Aeronautical flight testing is an expensive, technically sophisticated and, at times, dangerous production. A number of complex and organizationally independent functions must be successfully coordinated to complete a mission. Examples of some of these are: range safety, chase aircraft, weather, radars, recorders, and, of course, aeronautical telemetry support. Because a mission relies on so many disparate factors, the availability of sufficient dedicated frequencies and frequency bands is essential.

The US aeronautical flight test community is heavily dependent on access to four portions of the electromagnetic spectrum. Specifically, the 1435-1525 MHz and 2310-2390 MHz bands (also referred to as "L-Band" and "Upper S-Band" respectively) are used by the US Department of Defense (DOD), the National Aeronautics and Space Administration and the civil aerospace industry for the development and checkout of manned aircraft. The 2200-2290 MHz band ("Lower S-Band") is restricted to telemetering of unmanned flight vehicles such as drones and missiles. Although the 1710-1850 MHz band was reallocated to other functions many years ago several ranges still retain frequency assignments in this band for air/ground video telemetry operations. Loss of access to these bands, or portions of these bands, would have a significant cost to the USA telemetering community.

Body

A Bit of History . . .

The history of this issue really began back in the 1920's, when the US Federal Government first began allocating the nation's electromagnetic spectrum. From then until the early 1980's the Government gave away free airway licenses after dubious hearings in which applicants competed to prove who was worthiest. After that slow and complicated system broke down in 1984, the Federal Communications Commission (FCC) tried another scheme: the licenses were still free, but distributed by random selection, or lotteries. This new system was a fiasco. Smelling no-risk money, hoards of speculators (and not a few charlatans) banded together as quickie companies to join these lotteries—**400,000** "firms" for cellular telephone licenses alone. After paying nothing at all, lottery winners were free to turn around and sell their valuable rights. For example, the RCDG partnership, which won a cellular license for Cape Cod, Massachusetts, in December 1989, never spent a dime to put its system on the air. Instead, investors sold their windfall 10 months later to Southernwestern Bell Corp. for $41.5 million. The FCC figures that 85% of the cellular licenses awarded to firms other than local telephone companies changed hands from 1984 to 1992. Transition fees to cellular license brokers **alone** topped $1 billion. Just the cellular licenses the Government gave away in the 1980's were worth an estimated (by the US Department of Commerce) $46 billion.

Ever since the late 1950's, economists such Nobel Prize winner Ronald Coase argued that it was absurd for the FCC to give out those licenses for free. It's not simply that the Treasury was passing up billions of dollars that could be used to reduce the US Federal Deficit. Auctions were also the most economically efficient to allocate any scarce resource. The reasoning was that those who value something the most normally would use it the best. Finally, in August 1993, a wiser Congress passed the Communications Licensing and Spectrum Allocation Improvement Act, allowing the sale of spectrum rights.

The Grab (Part 1)

Eighteen months later, then-USA Secretary of Commerce Ronald H. Brown issued the National Telecommunications and Information Administration's (NTIA) "Spectrum Reallocation Final Report." Mandated by Title IV of the Omnibus Budget Reconciliation Act of 1993 (OBRA-93), this report identified 235 MHz of radio frequency bands (including our 1710-1755 MHz band) for reallocation from Federal to non-Federal or "MIXED USE*."

*Four of the reallocated bands were designated "MIXED USE." This means that limited amounts of some classes of Federal transmitters will be conditionally permitted to operate in these bands. In addition to this

clemency, the transfer of certain bands at specified locations will be delayed (in many cases indefinitely) to protect certain high-value users.

Why?

There were three primary objectives to this legislation. The first was to increase the efficiency of spectrum use and the effectiveness of the spectrum management process. The second, to promote and encourage the use of new spectrum-based technologies in telecommunications applications. The third, to add several billion dollars to Government coffers through competitive bidding (auctions) for the reassignment and licensing of the reallocated bands to the private sector by the FCC.

Why Us?

These noble goals were of little comfort to those spectrum orphans who were expected to:

- Locate unoccupied Government spectrum and get replacement assignments for their expelled equipment. And with fewer frequency bands and more systems to accommodate, spectrum congestion and conflict would increase.
- In some cases, totally re-engineer the expelled equipment to fit the characteristics and standards of the new band; a wretched and expensive burden indeed. Since Title VI did not provide a mechanism to compensate Federal agencies for the costs of this reallocation, the **user** was responsible for funding, converting, retuning and replacing his displaced frequencies and equipment.

The NTIA was tasked to research and identify the spectrum for reallocation. To make the transfer as painless and efficient as possible, the NTIA sought out the Government spectrum that:

- Was not required for the Government's present or future needs.
- If transferred, would not result in costs or loss of services that were excessive in relation to the benefits.
- Had the greatest potential for productive uses and public benefits (and auction profits) when sold to the private sector.

OBRA-93 was more of a nuisance than a handicap to the telemetering community. Although the few remaining telemetry assignments in the 1710-1755 MHz band were deleted, the rest of the 1755-1850 MHz band remained in our hands.

In summary, after two years of thorough search and sometimes painful negotiation the NTIA succeeded in minimizing the reallocation impact to most Federal users. Of the

thousands of types of emitters used by Government agencies, just a few dozen were affected to any extent. Most of these lost a fraction of their allocated operating band, meaning their operators would merely have to shift their assignments a few MHz up or down. Only a few major systems, none of them telemetering, were seriously impacted.

The Grab (Part 2)

However, despite the word "FINAL" in the title of the reallocation report, the raids on Federally-allocated spectrum continued. When the initial spectrum auctions produced several billion quick and painless dollars for the US Treasury, members of Congress took notice and generated further spectrum reallocation proposals, many of them rash and irresponsible. On 7 June 1995, Senate Bill S.888 was brought before a vote. This bill proposed reallocation of another 275 MHz of Government spectrum, including the entire 225-400 MHz band. In 1993 the US DOD declared that the 225-400 MHz band was the single most critical spectrum resource of the military tactical forces, both nationally and within the North Atlantic Treaty Organization. Despite this proclamation Bill S.888 **passed** by a voice vote. Once the Bill passed the US House of Representatives and was signed into law by the President the DOD would have nine months to vacate the band.

The US DOD was stunned. Not only had the Senate totally overlooked the significance of the band to the national defense but the DOD had no notice this Bill was even being contemplated until the day of the vote. The resulting outcry quickly persuaded the Senate to strike the “reallocation of the 225-400 MHz band” provision from the Bill, but the DOD knew this was just a brief respite. Realizing the gravity of the threat to its electromagnetic spectrum assets the DOD mobilized to:

- Ensure there are no more breakdowns in liaison between the DOD and Congress concerning proposed spectrum reallocation legislation.
- Educate all echelons of the DOD on the criticality of access to the electromagnetic spectrum and the threat spectrum encroachment posed to its mission.
- Document and justify its use and possession of its remaining frequency bands against further encroachment.
- Somehow predict the access it will have to crucial spectrum assets in the near and far terms; an access largely dependent on national-level legislating and budgeting whims.

There were other circumstances that slowed the impetuous of the reallocation frenzy. Pressured by a voracious Congress the FCC increased the pace of the spectrum auctions. As a result too much spectrum was dumped on the market too soon, resulting in a glut. One auction was predicted to pull in about $1.8 billion; instead it only raised $13.6

million, or less than 1% of the expected amount. At the same time many of the earlier auction winners were declaring bankruptcy; they belatedly discovered that neither the market or the required technology was prepared to accommodate their pricey electromagnetic investments.

Despite these alarms, on 8 August 1997, President Clinton signed into law the Balanced Budget Act of 1997 (BBA-97). Title III of the BBA required the Federal Government to surrender 20 more MHz of spectrum below 3 GHz for future auctions no later than 8 February 1998. It is important to note that the BBA-97 required identification of reallocatable frequencies in a report to the Congress within six months. In contrast, the report to Congress on OBRA-93 was submitted after 18 months of analysis and negotiation.

This loss included the 2385-2390 MHz band. This band is used at US DOD test ranges and by the private sector aerospace industry for flight test telemetry for manned aircraft such as the F/A-18E/F, V-22, F-22, Joint Strike Fighter and the Boeing 777. Since the 2310-2360 MHz band was reallocated in 1992 to the Digital Audio Broadcasting industry, its usability will soon be lost to the flight test community. Loss of the 2385-2390 MHz band will mean increased program schedule slippage and range operations costs because only 25 MHz of spectrum (2360-2385 MHz) will be available for aeronautical telemetry in the Upper S-Band.

A Hard-Earned Success

Recently however, the US DOD and telemetering community won a victory, and a consequential one at that. On 5 October 2000, President Clinton signed into law the "National Defense Authorization Act for Fiscal Year 2000." The first provision of Section 1062 ("Assessment of Electromagnetic Spectrum Reallocation") requires the NTIA ***to return*** a total of eight MHz of spectrum recently reallocated by BBA-97. We **will not** have to provide alternative spectrum to replace the returned eight MHz. Still, the loss of the 235 MHz to the OBRA-93 and the remaining 12 MHz to the BBA-97, which includes 2385-2390 MHz, remains unchanged.

But more significant, Section 1062 also authorizes the future surrender of frequencies **only** if the Secretary of Defense, the Chairman of the Joint Chiefs of Staff, and the Secretary of Commerce jointly certify to Congress that this surrender will not degrade essential military capability. If necessary, alternative frequencies with the necessary comparable technical characteristics would have to be identified and made available to the DOD to restore the essential military capability lost.

Finally, the Act directs an interagency review, assessment and report to Congress and the President on the progress made in implementation of national spectrum planning, the reallocation of Federal Government spectrum to non-Federal use, and the implications of such reallocations to the affected federal agencies. The report (due 1 October 2000) is to include the effects of the reallocation on critical military and intelligence capabilities, civil space programs, and other Federal Government systems used to protect public safety.

Lessons Learned

Not surprisingly, other country's governments have been following the reallocation efforts and results (particularly the auction revenues) of the US Government with keen interest. Dozens of them (if they haven't already) intend to start their own spectrum reallocation/auctioning programs, while hopefully avoiding the mistakes of their American cousins. The frequency management and telemetering communities in the US are grizzled, hardened veterans of the spectrum encroachment wars. From them we can glean several valuable strategies to survive, influence and perhaps even win the upcoming spectrum conflicts:

- **Organize/Mobilize/Educate Your Community.**

Reallocation legislation adversely affects numerous spectrum users, commercial and Federal, individuals and agencies. They are all potential allies in your efforts to survive. Bringing them into the fold focuses their efforts and prevents wasteful duplication of effort. Most important this allows your community to speak as **one voice**. This consistency will impress and be appreciated by the harried policy-makers. If your leadership cannot look past ancient quarrels/slights, egos and petty rivalries to forge an effective coalition with other organizations than they need to be replaced with personalities who can. The stakes are that significant.

The frequency management and telemetering communities quickly realized that few people comprehended the importance of our continued access to the electromagnetic spectrum. We began a concerted effort to alert, brief and periodically update the players (especially the important ones) on our concerns, positions and solutions. Also, this education served as a "rumor control" to head off much of the counterproductive speculation and misconception that followed the different surges of reallocation legislative proposals.

One promising assemblage is the International Consortium on Telemetry Frequencies (ITCS). Comprised of an international, diverse group of telemetry practitioners, it was

recently established as an advocate for the protection and future availability of spectrum for telemetering.

- **Document/Justify Your Usage NOW.**

You will be expected to present your plea for continued usage of a candidate frequency band in writing, the more detailed and voluminous the better. Concentrate on operational and monetary impacts to your valuable service; all other factors are given little consideration. Since you will usually have little or no time to respond to a data call, begin compiling the pertinent statistics, usage surveys and position statements **now**. Continuously update them. If you **do not** respond, or respond in what is perceived to be a half-hearted manner, the policy-makers will assume that the candidate band is not important to you and proceed accordingly.

- **Make Your Spectrum Assets As Unappetizing As Possible.**

The reallocators are looking for readily available, commercially attractive spectrum, not a war. Your motto: "We may not win this fight but I promise you won't win it either. I will come after you like a rabid dog." If they become convinced that even a cursive examination of your turf will automatically earn them a bloody nose they will learn to avoid you and your property. Their reallocation efforts **will** go on, but will then be directed toward bands that have less alert and zealous defenders.

- **Make Relocation THEIR burden, Not Yours.**

Despite your gallant efforts you are about to lose a band or sub-band. Press for concessions, exemptions and delays. For example: "I will accept the nationwide reallocation gracefully IF I can retain band usage within a 50 kilometer of each of my six test sites" or "Because of a lack of funds I need an extra five years past the reallocation timetable to move to a new band."

This is not the time to be shy or defeatist. You **DEMAND** that the reallocators accommodate your legitimate needs: "**YOU** have booted me out of my telemetry bands, now **YOU** tell me ***where*** and ***how*** to move."

- **Don't Become Discouraged.**

Those of us in the US frequency management and telemetering communities never had to deal with an issue like this before. As a result we were tentative and clumsy in our initial efforts to confront it. Further confounding us was the non-stop bombardment of reallocation proposals we were expected to respond to immediately (remember: silence = concurrence). We were exhausted with the extra workload and demoralized by our

impotence. At best it seemed we were fighting a haphazard rear-guard action.

But we learned and matured. We became more streamlined and politically sophisticated. Leaders emerged, we assumed a "war footing" and went on the offensive. And today we are seeing the results. Remember this is a long-term issue that will not go away or be resolved. *The Genie Is Out Of The Bottle*: everyone now knows the value of a finite resource like the radio frequency spectrum will only increase, making it perpetually desired and contested.

Conclusion

Both the US House and Senate Commerce Committees predicted in the BBA-97 revenues of $26.3 billion over the first five years from spectrum sales. In light of recent shortfalls in predicted auction profits this figure is certainly over-optimistic. Still, while not the bottomless piggy bank some partisans anticipated, the spectrum sales **have** proven profitable, and Governments world-wide have noted this new possible source of revenue. As a result, the pressure on the international telemetering community to surrender more spectrum to commercial use for eventual auctioning will continue for the foreseeable future.

For more information consult the "DOD Spectrum Encroachment WWW Page." This is an unclassified, continuously updated compendium of US spectrum reallocation-related documents, reports, bulletins, summaries and sources. It can be used as a tool for informing and educating other spectrum users and defending against loss of their spectrum assets. The Web Address is:

http://spectrum.nawcad.navy.mil

References

Brown, Ronald, "PRELIMINARY SPECTRUM REALLOCATION REPORT: Response to Title VI – Omnibus Reconciliation Act of 1993," NTIA Special Publication 94-27, National Telecommunications and Information Administration, U.S. Department of Commerce, Washington, DC, February, 1994.

Brown, Ronald, "SPECTRUM REALLOCATION FINAL REPORT: Response to Title VI – Omnibus Reconciliation Act of 1993," NTIA Special Publication 95-32, National

Telecommunications and Information Administration, U.S. Department of Commerce, Washington, DC, February, 1995.

U.S. General Accounting Office, "DEFENSE COMMUNICATIONS: Federal Spectrum Sale Could Impair Military Operations," GAO/NSIAD-97-131, Washington DC, June, 1997.

Daley, William, "SPECTRUM REALLOCATION REPORT: Response to Title III of The Balanced Budget Act of 1997," NTIA Special Publication 98-36, National Telecommunications and Information Administration, U.S. Department of Commerce, Washington, DC, February, 1998.

Biography

Mr. Mikel R. Ryan is the Head of the Mid-Atlantic Area Frequency Coordination Office at the Naval Air Warfare Center Aircraft Division, Patuxent River, Maryland, USA. He served in the US Army 82nd Airborne Division and the 11th & 19th Special Forces Groups (Airborne), and retired a Master Sergeant in 1994. In September 1997, Mr. Ryan was given a Congressional Tribute by the HONORABLE Steny H. Hoyer (D-Maryland) for his tenure as the Chairman of the Frequency Management Group of the Range Commanders Council. Mr. Ryan has been heavily involved with defending Federal spectrum (especially telemetry) from reallocation since 1994.

Introduction to Patents and Intellectual Property

Michael W. Landry
Registered Patent Attorney
San Diego California, USA
mike@iprguy.com

Abstract

Increasing efforts towards standardization and growing patent portfolios will present new challenges to the telemetry industry in both technology development and contracting. This paper presents an introduction to the principals of intellectual property with the main emphasis on patents. The discussion will include treatment of the United States patent system, highlighting some important differences to the European patent system.

Keywords: Patents, Intellectual property rights, IP, IPR, Standards, Contracts

Introduction

In the United States, approximately 154,000 utility patents and nearly 15,000 design patent issued in 1999. The rate of technology development is accelerating, and along with it the number of patent applications filed. The recent recognition of the patentability of software has contributed to the increase.

Patents serve several purposes to a business. Licensing out a patent provides a potential source for royalty income to increase earnings. A patent covering a product feature can be used as a marketing tool, exploiting the perception that a patented feature must have some advantage. A patent also can be used to reduce or eliminate competition, or at least create barriers to entry into an industry. A patent holder who is not an active producer in an industry would generally only use a patent portfolio offensively to seek royalties. An industry participant would apply all the offensive uses, but also may use its patents defensively or as a counter attack, leading to a cross license agreement with a competitor.

Today, there is a growing crossover between commercial and defense technology. There is a greater interest in commercializing defense technology, and a greater interest in utilizing commercial equipment for defense needs. Incorporating more current technology into defense systems also increases the chance of encountering an unexpired patent.

Intellectual Property

Intellectual property is intangible, non-physical property which has value because of the rights represented. The intellectual property owner, as with physical property owners, has the right to exclude others from using and interfering with the property. There are limitations on the rights to use intellectual property; laws place limits on the permissible uses and the rights are always subject to the rights of others. All these characteristics are analogous to physical property rights.

Sometimes referred to as intellectual property rights (IPR), the most prominent forms are patents, trademarks, copyrights, and trade secrets. A brief understanding of the other forms of IP will aide in understanding the distinction to patents, which are the main focus of this paper.

A trademark is a distinctive word, name, symbol, sound, or color (or combination of these) used to identify goods made or sold and to distinguish them from goods made or sold by others. Trademarks are used to allow a buyer to recognize a particular brand of product when choosing among similar products sold by competitors. Trademark law protects a mark from infringement by a similar mark used on a competing product or service. The trademark ownership arises by actual use of the mark. State and federal registration of a trademark is available to create certain legal presumptions that benefit the owner.

A copyright is the exclusive right of the author to reproduce an original work fixed in a tangible medium, such as paper, phonorecord, computer disk, or later developed medium. Copyrights do not protect any idea, concept, process, procedure, principle, or discovery. Copyright law protects against copying the embodiment, but the idea embodied is not protected. (17 USC §102, 106) Copyright protection is useful for documents, drawings, brochures, cartoon characters, and computer programs. Copyright would protect software from copying, but a patent would be required to protect the functional aspects of the software. Copyright exists at the time the work is created. Federal registration of copyrights is available, which provides additional enforcement rights to the owner.

A trade secret is information that has economic value from not being generally known and is subject to reasonable efforts to maintain its secrecy. Trade secret law provides a remedy for the misappropriation of protected information against those that have improperly acquired and used the trade secret. No right is created that prevents others from using the information if they have properly obtained it, such as by reverse engineering, independent development, or accessing publicly available documents. Trade secrets are valuable to protect property that may not fall within the subject matter requirements of a patent, such as customer lists, a formula, or manufacturing process. While a patent has a finite term, a trade secret potentially last forever as long as it is not generally known. The essential characteristic being secrecy, there are no registration requirements and none is available.

All forms of intellectual property can be sold and licensed by contract, in manners similar to tangible property transfers. Unlike physical property, many people can possess the same IP at the same time.

Patent Law

A patent grants to the patent owner, for the term of the patent, the right to exclude others from making, using, selling, or importing the claimed invention in the United States. The definition is presented in these specific terms to emphasize the rights provided by a patent, and to distinguish the rights not provided. A patent is only issued after a formal examination by the patent office.

A patent is not a "right to use"; the only right granted is the right to sue another who infringes the patent. A patent owner may be prevented from using his own invention because of the rights of another patent owner. The right to sue is only for infringement of the claimed invention. Many ideas and embodiments may be disclosed in the patent, but the exclusive right is defined by the claims, that

difficult to understand language at the end of the document beginning with "I claim..." or "The invention claimed is...". The right lasts only for the term of the patent, starting with the issue date and ending 20 years from the application date (or 17 years from the issue date if the application date was before June 8, 1995, whichever is longer.) When the patent expires the invention is in the public domain. The exclusive right is only for activity in the jurisdiction where the patent is issued; there are no rights in other countries unless a patent is issued in that jurisdiction.

The word "patent" means "open". An issued patent is completely open to the public; the patent document itself can be copied freely. In fact, the entire case file created during the prosecution of the patent is available to the public once the patent issues. This file includes the original application and all correspondence between the patent office and the applicant. The patent office maintains secrecy over the patent application and office proceedings until issuance, although the application may be published 18 months after filing. (35 USC §122) The applicant is generally free to disclose the invention while the patent is pending, unless the disclosure is deemed to be detrimental to national security (35 USC §181, 186).

In exchange for the grant of the exclusive right, the inventor must provide a written description of the invention. This allows others to learn from the invention and improve on it. By granting the exclusive right to the invention and the same time allowing the public to learn about it, new innovation is encouraged as the public attempts to solve the problem addressed by the invention in other ways to avoid infringing the patent.

The description must meet specific requirements (35 USC §112). The patent must describe the invention in full, clear, concise, and exact terms sufficient to enable a person of ordinary skill in the field of the invention to make and use the invention. The patent must also set forth the "best mode" contemplated by the inventor to carry out the invention. It is grounds for invalidating a patent to fail to provide an enabling disclosure or to omit the embodiment preferred by the inventor. If there are secrets known to the inventor to achieve a working invention they must be disclosed. The policy is that an inventor should not be granted the valuable rights of the patent without fulfilling the obligation to teach the public how to practice the invention.

Strictly speaking, a patent does not protect the idea, but the embodiment of the idea; therefore, an operative description of a functional invention is required. Non-operative inventions, such as perpetual motion machines or other attempts to defy the laws of physics, or inventions lacking a proper description will be rejected during the patent examination process.

Requirements for a Patent

There are three type of patents: Design, Plant, and Utility. A design patent is available for an original and ornamental design for an article of manufacture. It does not cover the functional aspects of a design, only its appearance. A plant patent is available for a distinct variety of plant that is propagated by means other than with seeds. When the term "patent" is used by itself, the reference is to a utility patent. Utility patents comprise 95% of the issued patents and are generally of primary interest.

Utility patents are granted for the invention or discovery of any new and useful (1) process, (2) machine, (3) article of manufacture, or (4) composition of matter, or any new and useful improvement to an item

in these categories. (35 USC §101) These four categories are called statutory subject matter. Unless an invention is statutory subject matter it cannot be patented, no matter how new, useful, or lucrative. Most things that can be conceived and built can fit into one of these categories. A patent cannot be obtained for an abstract idea, mathematical formula, or something that is performed solely in the mind.

In addition to the affirmative requirements of new, useful, and non-obvious, there are also factors that may cause loss of the right to a patent. (35 USC §102) The factors are: a) The invention was known or used by others before it was invented by the applicant. The inventors' notebook can be used to establish the date of invention, and whether it pre-dates the invention by others. b) The invention was described in a printed publication more than one year prior to the date of filing a patent application. c) The invention was sold or offered for sale more than one year prior to the date of filing a patent application. d) The inventor abandoned the invention. e) The applicant did not invent the invention.

Claims

The claims define the rights in the patent. There are two basic types of claims, a method claim and an apparatus claim. The method is a sequence of steps by which something is transformed or processed. An apparatus is a structure that performs some function. Each claim recites a number of elements and defines the connection or interrelation between them. An element is a basic component that has some identifiable property. The elements are also called limitations, because the inclusion of each element limits the scope of the claim, narrowing the range of possible products it covers.

The first claim in a patent is an independent claim; it is self-contained and lists the complement of elements that comprise the invention. Another claim may be dependent on an earlier recited claim (in the same patent), inheriting the elements of that claim and adding or refining some element.

One difficulty in reading patent claims is the formal style used in claim drafting. The requirement is to particularly point out and distinctly claim the subject matter which the applicant regards as his invention, and in doing so the claim drafter must follow the present rules of the patent office as well as follow tradition. The resulting claim is many times unclear to technologists, lawyers, and the courts.

Another obstacle to reading patent claims is the use of the word "means". The use of "means" in claim language is encouraged by the patent statute allowing for an element to be expressed as a means for performing a specified function without the recital of structure. The claim is construed to cover the corresponding structure described in the specification and its equivalents. (35 USC §112) "Means for..." is short hand reference for all the possible structures disclosed in the description. This language is used to attempt to broaden the scope of the claim.

Infringement

A patent is infringed by making, using, selling, offering to sell, or importing the patented invention without authority. (35 USC §271) Authority is present in the owner and anyone who has a license granted by the owner of the patent. The "patented invention" means the invention defined by the claims of the patent. A patent may have many claims, infringement occurs if at least one of the claims is infringed. The "accused product" is the potentially infringing product in question.

A patent claim is infringed when the accused product has present every element recited in the claim of the patented invention. If the accused product does not have every element in the claim, then it does not infringe. If the accused product has every element in the claim, and adds some others, it still infringes. (Although, if the additional elements are new, useful, and non-obvious, then the accused product might have been a good candidate for another patent, improving upon the infringed patent.)

Figure 1 models the infringement of a patent using familiar circuit functions. The first step is to identify each element of the patent claim and compare it to the accused product, element by element, to see if they match. If each comparator output is TRUE, the condition for the AND gate is satisfied and infringement of the claim is TRUE. If at least one claim is infringed, the condition for the OR gate is satisfied and infringement of the patent is TRUE. Note the addition of the fuse, representing validity of a claim. If a claim is invalid, a determination potentially made during litigation, the fuse is open preventing a condition of infringement. A dependent claim, which depends on another claim, has an input from the result of the corresponding base claim. It can be seen from this logic that there can be no infringement of a dependent claim unless there is infringement of the independent claim on which it depends.

The comparing operation is shown with an "approximately equal" symbol. This is because the literal meaning may be expanded somewhat by a judicially established rule known as the doctrine of equivalents. This doctrine has undergone varying interpretations in recent years, with the present trend being to limit its application. The doctrine of equivalents states that an accused product may infringe a claim, although not literally according to the words used in the claim, if the element at issue in the accused product performs substantially the same function in the substantially same way to obtain the same result. Graver Tank & Mfg. Co. v. Linde Air Prods. Co., 339 U.S. 605 (1950).

Designing Around

Intentional "designing around" the claims of a patent is not by itself a wrong. Designing around a patent is, in fact, one of the ways in which the patent system works to the advantage of the public in promoting progress in the useful arts, its constitutional purpose.

The designing around effort would start by analyzing the claim that is intended to be avoided. As illustrated by the discussion of Figure 1, if the competing product has eliminated one of the elements of the claim, there is no infringement. If a claim element can be substituted with another element that is substantially different in its function, way, or result then infringement is probably avoided. One cannot know for certain that changes are sufficient to avoid infringement until a judge or a jury has made that determination. The Read Corp. v. Portec, Inc., 970 F.2d 816 (Fed.Cir. 1992). Designing around is a serious endeavor and should only be done with the advice of legal counsel.

European Patents Compared To U.S. Patents

The European Patent Convention (EPC) establishes a common system of law and procedure for granting patents, called European patents. There are currently 19 contracting States of Europe that have adopted the EPC. The European Patent Office is in Munich with branch offices and additional suboffices in other locations.

Many of the concepts of the EPC are similar to provisions of U.S. patent law. There are a number substantive and procedural differences. Recent changes to U.S. law, partially motivated by an effort to harmonize the laws of the two jurisdictions, have reduced the differences.

Subject Matter. Subject matter for patentable inventions specifies the range of inventions which are permitted to be patented. 35 USC §101 defines the categories of patentable subject matter, as discussed above.

Article 53 EPC specifically excludes aesthetic creations, methods of doing business, programs for computers, and medical procedures, all of which are possible candidates for patents in the U.S. Aesthetic creations could be covered by a U.S. design patent.

Right to Invention. According to U.S. patent law, the first inventor is entitled to a patent (with the qualification that the first inventor did not abandon, suppress, or conceal the invention and was the first to conceive the invention and was reasonably diligent in the "reduction to practice" of the invention). This rule leads to Interferences, were two applicants have claimed the same invention and the patent office must determine the priority of the invention based on evidence produced by each applicant as to the dates of conception and reduction to practice. Outside the U.S., the general rule of law is that the first inventor to file a patent application on an invention is entitled to the patent. Administratively, this is much simpler but the fairness can be debated. The "first to file" rule tends to lead to a rush to patent filings.

Novelty. A requirement for patentability in all jurisdictions is that the invention is new, meaning that it is not part of the state of the art known by the public. Novelty can be destroyed by actions of the inventor, as well as others, making the invention available to the public, thus placing it in the state of the art. U.S. patent law, 35 USC §102(b) allows a one year grace period for filing a patent application after the occurrence of a publication describing the invention, an offer to sell or sale of the invention, or public use of the invention. This period of time allows normal commercial activities associated with invention to happen without a loss of right to a patent.

This U.S. grace period is contrasted with Article 54 EPC providing an invention is not considered to be new if it was made available to the public by means of a written or oral description, by use, or in any other way, before the date of filing of the European patent application. The novelty requirement of Article 54 EPC, with certain exceptions provided in Article 55 EPC, has the effect of requiring a patent application to be filed prior to any public use or disclosure.

Patent Term. In an effort to harmonize U.S. patent law with other industrialized countries, the term of a patent is now measured from the patent application date instead of the issue date. This averts attempts by patent applicants to delay issuance of a patent while amending claims to increase the chance there is infringement once the patent issues. The patent term begins on the issue date and ends 20 years from the filing date. In late 1999, a further change to U.S. law was enacted which takes back some of the change. (American Inventors Protection Act of 1999) The term of a patent may be extended if the issuance was delayed due to patent office failing to meet a certain schedule for examination and processing of the application.

Article 63 EPC provides for the European patent term of 20 years from the application filing.

Publication of Pending Applications. Until the 1999 changes, no U.S. patents were published until issued. (Foreign counterparts to U.S. application were published if filed by countries providing for such publication.) This meant that pending applications were unknown until the patent issued, which could be many years. Under currently enacted law, a patent application will be published 18 months after filing date, unless the applicant certifies that the application will not be filed in another country providing for 18 month publication. (35 USC §122(b)) The effect of this change appears to be minimal because the category of applications effected are already published in the other countries 18 months from the U.S. filing date, the operative change being that now the application will also be published by the U.S.

Article 93 EPC provides for publication 18 months from the filing date or priority date.

Provisional Rights. Historically, in the U.S. there had been no rights created by a patent application. Only an issued patent created rights and there was no ability to obtain royalties for infringement during the pendency of the application. With the recent changes to U.S. law, 35 USC §154(d) now provides provisional rights for patent applications if the infringer has actual notice of the published application and the claims of the issued patent are substantially identical to the published application. This provisional right only applies to applications that are published under 35 USC §122(b) as discussed above.

Article 67 EPC recognizes provisional rights in published patent applications, providing for the recovery of royalties for infringement of a granted patent during the period between publication and grant of the patent.

Post Issuance Opposition. In the U.S., a petition for reexamination may be filed after issuance of the patent, by the patent owner or a third party, raising a substantial new question of patentability on the basis of prior art patent or printed publications. Typically the information would be prior art not known at the time of the original examination. The petition may be filed at any time during the period of enforceability, which is up to 6 years after expiration. If the petition is accepted, the patent office reexamines the patent application along with the new information. A new patent may issue with the same or narrower claims, or may be rejected completely. Opposition upon publication is not available in the U.S. (35 USC §122(c))

Article 99 EPC provides for a notice of opposition to the EPO within 9 months of the European patent grant. Opposition may be filed on the grounds that the invention is not patentable because it is obvious, is not new, lacks industrial application, or that the patent does not sufficiently disclose the invention in order for it to be carried out by a person skilled in the art.

Standards Covered By Patents

Commercial communications systems are almost always covered by some industry standard in order to support multiple suppliers of compatible products. Although not a recipe for a product, the standard discloses all the technical information necessary for a product to comply with the standard. The standards are readily available to the public for purchase at a nominal price.

While the non-public nature of a trade secret is incompatible with the public nature of a standard, patents covering standards are common. Participants from the effected industry, including producers and users, meet in standardization committees to develop an acceptable standard. A company representative may contribute proposals embodying their patented or planned-to-be-patented techniques. In the commercial context, standards are developed through consensus among members of industry supported organizations and the membership votes to approve the standards. The voting is influenced by technical as well as political and commercial considerations.

The commercial communications industry develops standards under procedures developed by organizations such as IEEE (Institute of Electrical and Electronic Engineers) or ANSI (American National Standards Institute). ANSI is an organization that coordinates the development of United States voluntary standards. Numerous government agencies are ANSI members, including the Department of Defense, National Aeronautics and Space Administration (NASA), and the Federal Communications Commission (FCC). ANSI is the U.S. member of non-treaty international standards organizations such as the International Organization for Standardization (ISO) and coordinates the activities associated with U.S. participation. Although not compulsory, the procedures established by ANSI for the development of standards are instructive.

A proposed American National Standard may be drafted in terms that include the use of a patented item if it is justified based on technical reasons. The ANSI Patent Policy requires a patent holder to provide a statement of assurance that a) a license will be made available without compensation or b) a license will be made available to applicants who desire to utilize the license for purpose of implementing the standard under reasonable terms and conditions that are demonstrably free of any unfair discrimination. Since a supplier would be infringing a patent by supplying a product conforming to the standard, a license would be necessary. If the owner of the patent could deny a license, an unfair and uncompetitive condition would result.

An adopted standard does not specifically reference any patents, but will provide a notice that compliance with the standard may require use of an invention covered by patent rights. A standard should not include proper names, trademarks, commercial terms, or provisions for business relationships. The standard developing body is not responsible for identifying all patents which may cover the standard nor for establishing the validity and scope of any patent. These tasks are addressed by the industry.

When specific technology is adopted by a standard, it can be done so in more than one way. Language incorporating the technology can be drafted in specific and precise terms as to the algorithm or processes. It can also be drafted in terms of the requirements sought to be achieved, leaving the supplier to utilize the appropriate technology. To insure that products from each supplier will be compatible, many functions of a system must be specified in detail, thereby restricting alternatives. When specifying implementation structure in a restrictive way, the choice of structure must be selected carefully. Using specific language that locks in technology available in the present may preclude the use of other technology available in the future.

Conclusion

A brief discussion of the complex field of patents has been provided along with a comparison of United States and European patents. Standards activities and industry participants can be effected by patents covering proposed or adopted technology. The objective has been to arm the reader with some familiarity of the general principles. Caution must be used when applying this knowledge because the law changes and the specific facts pertaining to an issue will influence the outcome.

Disclaimer

This publication is intended to provide accurate and authoritative information in regard to the subject matter covered. It is not intended to render legal advice, or apply to any particular situation. If legal advice or other expert assistance is required, the services of a competent professional person should be sought.

References

Title 35 United States Code §§ 1-376

European Patent Convention Article 1-178

M. W. Landry, “A Primer on Patents”, Proceedings of the International Telemetering Conference, Vol XXXV, pp. 299-309, October 1999.

INFRINGEMENT LOGIC DIAGRAM

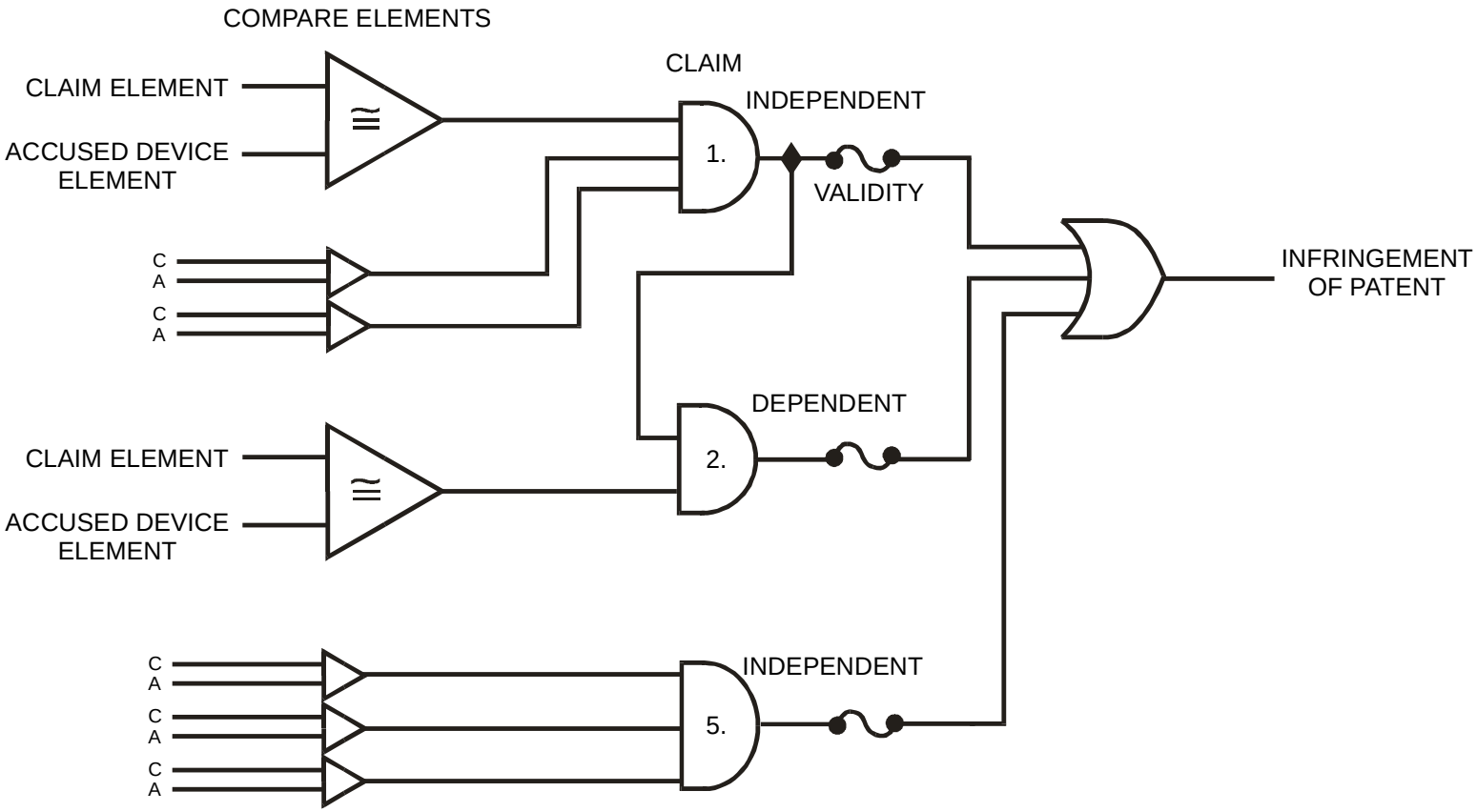

DATA RECORDING AND STORAGE

Telemetry Recording Systems for the Year 2000 and Beyond

David N. Kortick
Product Manager
Astro-Med, Inc.
Test & Measurement Systems
West Warwick, RI USA

Abstract
Telemetry recording systems have evolved from simple pen-writing instruments to thermal array printing systems over several decades. Today's Telemetry Recording Workstations not only provide a permanent hard copy of telemetry data, but also offer high resolution videographic displays with real-time point-of-writing representation, customizable user interfaces and the ability to efficiently store data digitally. Built-in Ethernet network connectivity provides an efficient mechanism for command and control as well as the transfer of digital data to the recording system. The many advances in recording, data display, and networking technologies make the Telemetry Recording Workstation a fundamental instrument for any telemetry application or installation.

Introduction

The strip chart telemetry recorder has been an important part of telemetry systems for many decades. Its unique ability to graphically represent real-time data has continued to be useful for a variety of applications. These recorders are used in many applications including flight testing, rocket and missile launch monitoring, and satellite testing. The telemetry recorder, like most technologies, has constantly evolved to fulfill the needs of its users.

A Brief History of Telemetry Recorders

Telemetry recorders were originally galvanometer-based pen-writing instruments. The typical recorder drew eight waveforms on eight separate pre-printed grids of 40 mm width. The point-of-writing mechanism changed over many years, from free-flowing capillary ink styli to pressurized ink, to heated elements on thermally sensitive paper. Some of these pen recorders continue to serve the telemetry community usefully due to the fact that the real-time point-of-writing is constantly visible. The drawbacks to these methods include the mechanical limitations of the galvanometer for high frequencies, the high maintenance costs of these systems, and the untidiness of ink-based recorders. This type of recorder also has very limited communications capability, if any at all.

The next generation of telemetry recorders utilized a light-beam to mark a photo-sensitive paper. There were a number of advantages to this method including the ability to record high frequency signals and overlapping waveforms. One of the drawbacks to this recording method was a small latency period while the hardcopy was developing. Another disadvantage was that the photo-sensitive media was very expensive and did not archive well. The light-beam recorder did not offer host control interfaces. However, these recorders continue to be used today in a few high frequency applications.

The next evolution in telemetry recorders was the electrostatic array recorder introduced in the late 1970's. This was the first introduction of digital recording in a previously analog field and offered advancements such as overlapping channels, alphanumeric annotation, graphics, and host control capabilities. Another key advantage was that the time-skew associated with pre-printed grids was eliminated with this technology. One of the shortcomings of the electrostatic array recorder was the digitization effect due to a recording technique that only offered 100 dots per inch (dpi) of resolution. Even when 200 dpi versions became available, the print quality of pen and light-beam recorders were preferred because of the seemingly smooth traces.

The thermal array recorder followed shortly after the electrostatic array recorder. This printing method, still the most widely used today, has a number of benefits including high resolution (300 dpi) printing, high frequency response, flexible chart formats, and alphanumeric annotation. Full host control was a major advancement for thermal array recorders, finally closing the loop between telemetry system and recording system. Thermal array recorders were also designed as platform instruments, which meant that options could be added as new technologies became available. Over the many years since the introduction of the first thermal array recorder, features such as video display, large memory capacities and digital signal processing were added to these instruments. High-speed digital data inputs became widely used with the thermal array recorders, eliminating the high costs and constant need for calibration of digital-to-analog converters (DAC) at telemetry installations. The thermal array recorder became much more than a basic recorder and evolved into a recording system.

The Latest Advances in Telemetry Recording Systems

The latest generation of telemetry recording systems greatly expand upon the thermal array platform. These instruments not only perform the traditional strip chart functions, but offer the engineer a complete data collection and review workstation. These systems offer complete customization of the data viewing and printing and also allow the user to define the control interface. The network connectivity of the telemetry recorder make it an integrated component of the telemetry installation.

The most recent designs of telemetry recorder-workstations offer inputs for analog or digital data. This ensures compatibility with the latest telemetry installations, as well as legacy systems. These advanced designs also employ a modular architecture, proven to be a success with the previous generation of recorders, which allows the system to be expanded in the future.

Large Displays with Touch Panel Interfaces

One of the major advancements in the latest generation telemetry recorder is a large real-time display which shows the signals in a waterfall format. While waveform displays have been available on telemetry recorders for a number of years, they were limited by size and resolution and only allowed the user to make approximate measurements. The latest displays are 18-inch backlit color LCD's with 1280x1024 resolution. This type of display offers the significant advantage of allowing the user to see a large amount of data on the screen. The use of color allows for instant waveform identification and adds the ability for the signal to change color based on a preset alarm limit. The increased resolution also allows for graphical templates indicating grid values and annotation, similar to the paper-based templates that flight test engineers have used with pen-based recorders for many years (figure 1). In addition, split-screen displays and multiple real-time XY plots can be viewed on the screen, without compromising the viewing of real-time data.

These displays also offer the important benefit of a real-time pen emulation. In many applications such as flutter and flight safety testing, the ability to see the pens move is paramount. For the first time, these high-resolution displays allow a realistic simulation of an analog pen movement (figure 1). In addition, a pen-sound simulation can be found in some of the latest recorder designs. The visual and audible feedback from the pen movement create a realistic equivalent to a pen-based analog strip chart recorder.

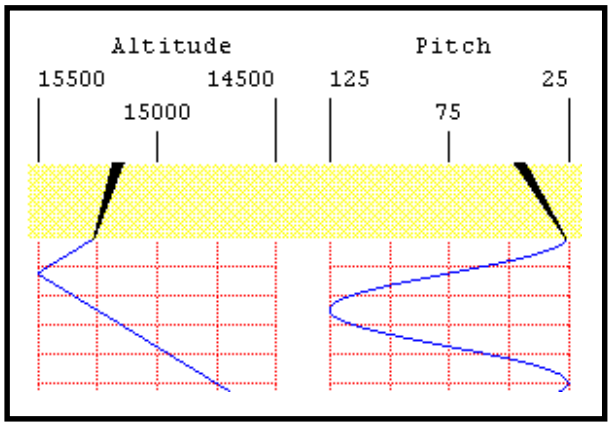

Figure 1: Real-time pen tip display with annotation and chart template

Touch-panel interfaces are also used on the more advanced telemetry recorders. This type of interface replaces the hardware knobs and buttons that have historically been the controls for telemetry recorders. A well designed touch-panel interface, with a quick response and intuitive layout, offers benefits for both new and seasoned users. Some of the recorder designs allows users to create macros, which can perform a number of repetitive functions quickly. The latest recorder designs allow users to create the entire front panel. This is known as a customized control panel (figure 2), and gives the user complete flexibility over which controls are on the front panel. For example, a user with a simple application may need a few chart speed buttons and a recording start/stop button. A more advanced exercise may need to instantly access controls for signal adjustments, triggering, data capture and historical data review. These control panels can also be password protected for security purposes, which will prevent unauthorized modifications to an existing custom setup.

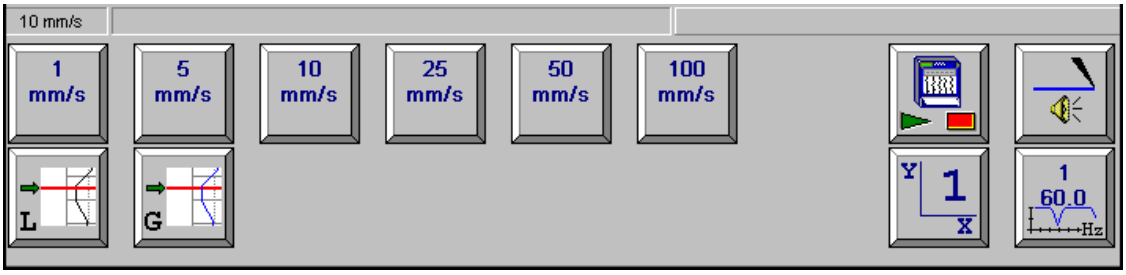

Figure 2. A custom control panel allows users to define their front-panel interface.

During a flight test, an engineer watching a strip-chart will often write on the chart when a planned maneuver is performed, or if something unexpected happens. With a touch-panel interface, the engineer can simply touch the display at a specific point and add annotation to the data. This can be in the form of pre-defined phrases or free-form text. A mark is placed at that point in time and the annotation is saved and printed with the waveform data. Touch-panel interfaces also allow for on-screen cursor measurements that can be activated by touching a specific data point. A large touch-panel is well suited for measurements such as timing, amplitude and frequency.

A touch-panel interface also has the advantage of an environment that has the "touch and feel" of paper. A flight engineer could use a split-screen mode, for example, that allows for viewing of historical data without interrupting real-time recording. The portion of the screen with the historical data can be reviewed by touching and dragging, analogous to flipping through sheets of paper. The designs of these touch-panel interfaces are such that the engineer who may be familiar with using pen-based recorders will quickly become proficient with the new technologies.

Large Capacity Storage Media

The latest telemetry recorders have been designed with the ability to store large amounts of data to hard drives or other magnetic media. Engineers are increasingly using strip-chart hardcopy output only when necessary and prefer to store data in a digital format more suited for analysis. The latest telemetry recorder designs utilize storage media that enables the user to save data independent of paper recording, while at the same time giving them the opportunity to play back data to paper later.

Telemetry recorders typically employ multi-gigabyte hard drives for data storage. SCSI is most often used due the robustness of these types of drives. Some designs utilize a Redundant Array of Independent Disks (RAID) architecture to provide more storage capacity. While the capacity of hard drives gets larger as costs come down, many engineers are also looking for ways to reduce this large volume of data while preserving its fidelity. One solution can be taken from the advances in paper recording.

Paper is a good medium for data storage for lower frequency signals because of the high volume of data that can be included in a chart output. Traditionally, if the engineer needed more data resolution in the time axis, the paper speed would be increased. Due to the mechanical limitations of pen recorders, there was signal attenuation at frequencies greater than 60 Hz. Thermal array recorders solved this problem by using min/max algorithms which offer the ability to print higher frequency signals regardless of the chart speed.

The most recent data storage technique utilizes a similar min/max algorithm to store line segments a hard drive. This data is stored exactly as it would appear on a chart and at a rate to match the equivalent chart speed. The resultant record acts as a Virtual Chart™ and allows a user to run a test with or without real-time paper output and still create hard copy after the test. The chart output is identical to a chart created in real-time, showing any changes to signal conditioner settings, annotation, or chart speed.

A key benefit of this technique is an efficient use of storage space. For example, a standard pack of z-fold chart paper is approximately 120,000 mm or 1,440,000 line segments at a print resolution of 12 dots per millimeter. A single chart segment (equivalent to 1 print line) requires 192 Bytes. This means that the Virtual Chart equivalent of a pack of paper requires 276 MB of disk space, which includes IRIG timing and grid synchronization. As another example, running a Virtual Chart for 5 hours at 100 mm/s requires approximately 4 billion bytes. This data, since it is digital, can be used for post-mission review and analysis as well.

Network Connectivity

An increasingly important characteristic of telemetry recorders is their ability to communicate with other telemetry systems and sub-systems. The latest telemetry recorders utilize Ethernet (100BaseT or 10BaseT) for this communication. This interface offers a number of advantages such as high bandwidth, standard protocols, and inexpensive implementation. In addition to communication from a host system to a telemetry recorder, Ethernet also allows communication between telemetry recorders. The Ethernet interface can be used for a number of different functions. Figure 3 illustrates a block diagram of a host interface for telemetry recorders.

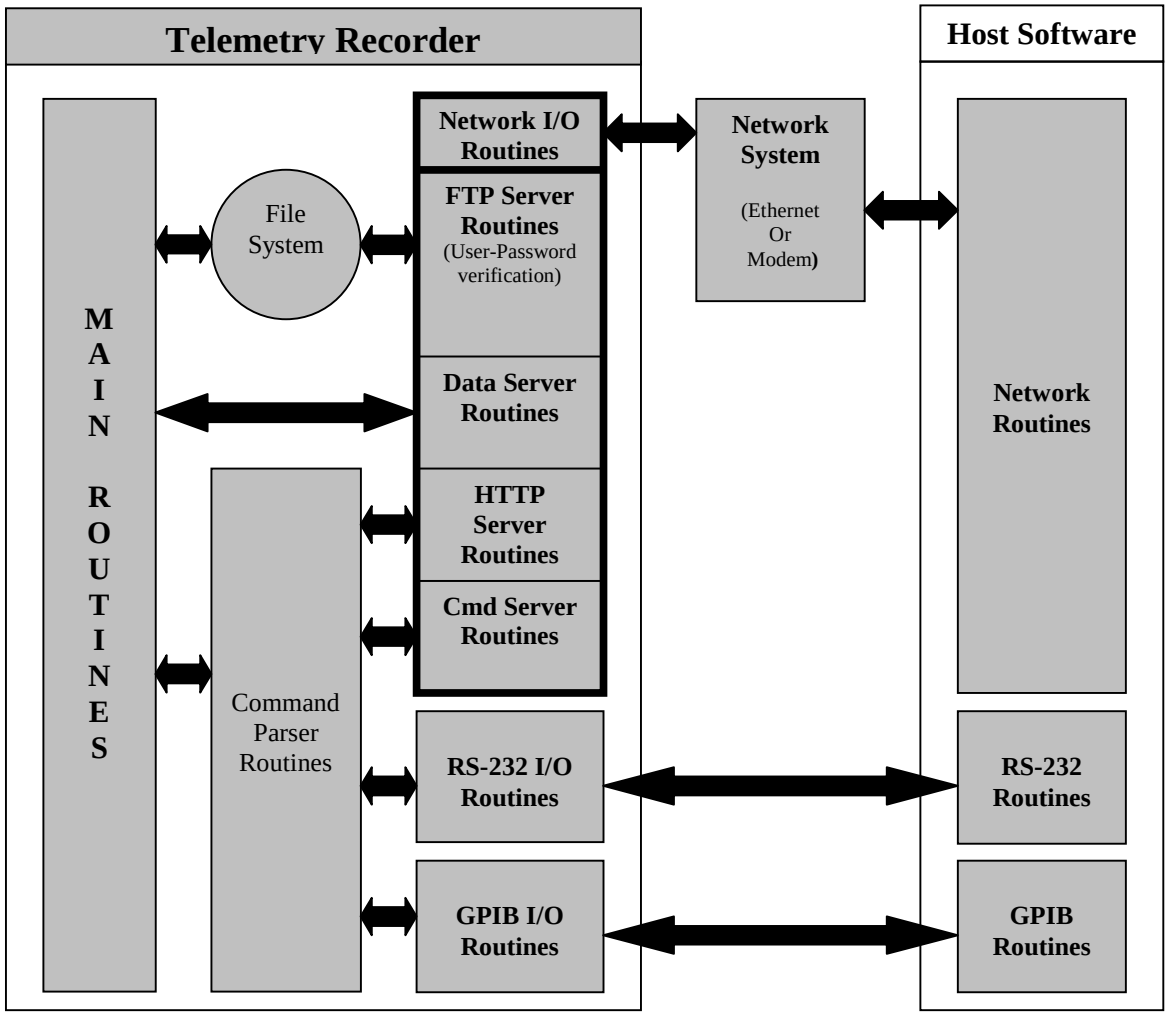

Figure 3. Block diagram of Ethernet and other host interfaces

One of the uses of Ethernet is for transferring recorder configurations to and from a host workstation. Using the TCP/IP and FTP protocols, setup files can be quickly transferred to the telemetry recorder prior to a mission. This eliminates the costly set-up time associated with previous generations of recorders. Using this method, a library of configurations can be stored and used when necessary.

Another important use of Ethernet is for command and control of the telemetry recorder. Telemetry recorders have traditionally utilized RS232 or IEEE-488 for host control. While the latest designs also offer these interfaces, as seen in figure 3, Ethernet is a more efficient and cost-effective interface to implement. Host control commands available for telemetry recorders include recording start/stop, change chart speeds, edit annotation buffers and analog settings modifications as well as queries for alarm limit status and system status.

Ethernet can also be used to send digitized data to the telemetry workstation. The traditional approach to sending digitized waveforms is to have the recorder look like a DAC where the host streams data points for each channel in real-time or close to real-time. Data rates and resultant loads on both host and recorder can be high. This method becomes risky when non-deterministic networks are used because of the problem of time synchronization.

An alternative method is to send line segments based on the minimum and maximum waveform values for a delta T. The value of delta T depends on chart speed. Raw signal sample rates are set by the host to maintain required bandwidth. The impact of transmission delays is minimal because the line segments are built in the host using a fixed time period that the telemetry recorder also uses to control the rate of printing and display. The data set containing the line segments can include time marks, an IRIG time stamp and grid information that provide the host with expanded control over the chart.

The segment approach eliminates the need for special hardware by using the telemetry recorder operating system to handle the incoming data. Optimum performance at higher speeds is obtained by having the host transmit segment data in blocks that are separated by at least 50 milliseconds. This limit implies that at chart speeds above a few millimeters per second, the host should send multiple segments in each block.

The network connectivity of the latest generation of telemetry recorders offers greatly capabilities for configuration, host control and data transfer. The interface also lends itself well to other possibilities. One of the concepts currently being explored is a host control mechanism that can be accessed via a standard web browser. When using Ethernet for host control, a thin server and web menu structure can be implemented. Any host computer that can establish a network or modem connection and is running a standard web browser can access the thin server. The host control server software could detect the host browser level and adjust the menus accordingly.

Conclusion

The telemetry recorder-workstation continues to be an important tool for the telemetry community. The significant advances made by the latest generation of these instruments make them even more useful since the users have unprecedented control over how their data is viewed, printed and analyzed. As a direct result of the needs of telemetry engineers, today's telemetry recorder-workstation employs some of the newest technologies available and utilizes an architecture that ensures the fulfillment of future requirements.

Keywords

recorder, videographic display, data recording, strip-chart

The Merging of Instrumentation Recording and Consumer Storage Technologies

Jim Matthews
Metrum-Datatape Inc.

Abstract

For the last decade or more, traditional instrumentation recorder technologies and traditional consumer storage technologies have been on a merging path. This paper outlines this trend and investigates the impact it is having on the instrumentation recording industry as a whole. It will look at both the upside and downside of using computer peripherals intended for the consumer market in the test and instrumentation environments.

The test and instrumentation industry has gradually been shifting from recording products that adhere to strict standards such as IRIG to a proliferation of consumer storage products such as DLT and AIT. Developing technologies such as optical and solid state storage devices are beginning to appear on telemetry and instrumentation recorder manufacturers' product lists.

Interfaces that make traditional instrumentation recorders behave like computer peripherals have become common place at test ranges. The Range Commanders Council (RCC) is adopting IRIG standards for data formats that are easily LAN & WAN transferable and allow easy software reconstruction of multiplexed data.

Introduction

When PCs first hit the consumer market in the early 70's the test and instrumentation community considered them nothing more than toys. Who was to know that the PC consumer market would turn out to be a major driving source for test and instrumentation storage in the 90's. There are more than 1 million DLT drives and over 6 million 4mm drives in use today. Instrumentation recorder manufacturers, to either make their heritage products function like a computer peripheral or to make a computer peripheral function like an instrumentation recorder, have spent thousands of man-hours.

Some of the success stories include Metrum-Datatape's MARS-II, MARS-IIe and MARS-II-L with its COTS DLT storage device. Since its introduction in 1994 more than 300 units have been delivered. When compared to the consumer market, this does not sound much like a success story but for a flight test instrumentation recorder this is phenomenal. The majority of MARS-II sales have been in the United States. An example of a European success is Racal-Heim's DATaREC D series. The DATaREC D series, also a flight test instrumentation recorder, was designed around DAT and DLT technology. A not so successful story was Veridian's RDRU which was also designed around DLT technology. It could not penetrate the instrumentation recorder market dominated by Metrum-Datatape, Racal Heim and Ampex and was abandoned by Veridian.

The introduction of newer, faster and smarter consumer storage devices has escalated in the last five years, as has the proliferation of formats. This is of great concern to the test and instrumentation community. The Range Commanders Counsel (RCC), which sets the IRIG standards for all range users, is, for the first time, having to consider standards for storage devices designed by and for the consumer markets. They are having to consider standards for command and control as opposed to standards for the tape footprint.

At this point it might be wise to discuss the difference between an instrumentation recorder and a consumer storage device. Instrumentation recorders have the ability to capture real time test data at a constant rate over a period of time without interruption. The source of data is invariant in terms of rate. Looking at the problem mathematically, the data behaves as a uniform distribution function. This is much different with a consumer storage device where data arrives in a non-uniform manner. This data can be best described as *"clumps and bunches".*

Data that is acquired in real time can be reproduced in the same "unyielding" fashion at a constant invariant rate. The fundamental aspect of real time data is that it exists once and only once in time and space. Examples of this are: Missile and rocket launches, radar and sensor arrays, and satellite up and down links. If the data acquisition/retrieval equipment is not able to keep up with the data rates in these examples, the data is simply lost forever — something that is obviously unacceptable.

When a computer processing data encounters a "busy" indication, in the consumer storage environment, the user simply waits until processing time is available or comes back later to try again. Virtually, all consumer storage devices behave in this manner. In order to use such a device, in an instrumentation and test environment, an interface that will capture the data, buffer it and translate it into a format that can be stored on a computer peripheral must be designed. The size of the buffer depends on the native speed of the device.

The remainder of this discussion will, after a brief history, center around the technology found in the instrumentation and test community today and give an example of how instrumentation manufacturers are adapting to new technologies.

A Brief Data Storage History

In the 80's, when the first consumer driven products were introduced to the test and instrumentation market they were received with a lot of skepticism. The telemetry giants, EMR and Loral Instrumentation, were caught completely off guard by the widespread acceptance of these PC based telemetry front-end ground stations. This allowed upstart companies like Terametrix and Veda Systems to get wholesale acceptance in the test and instrumentation industry. At this point in time there was little or no impact on instrumentation recorder manufacturers. Technology didn't catch up with longitudinal recorders until a decade later.

Consumer storage devices were too slow and not rugged enough to displace instrumentation tape recorders. Metrum-Datatape's family of MARS longitudinal flight recorders was the standard for flight test until the MARS-II with its DLT drive

was introduced in 1994. From the introduction of the MARS 1000 in 1966 to the introduction of the MARS II in 1994, Metrum-Datatape fielded more than 4000 of longitudinal MARS flight test recorders.

In 1992 Metrum-Datatape introduced a buffered version of their VLDS. The addition of a 16 Megabyte buffer provided the end user with the means to record and reproduce a broader range of data rates. This major enhancement to the VLDS, now called Buffered VLDS (BVLDS), offered two operating modes. In the streaming mode, data was transferred to the recorder at a constant rate in order to provide backward compatibility with VLDS drives. Sustained data rates could be recorded ranging from 800 kilobits per second to 32 megabits per second. The other mode of operation was called burst mode. In the burst mode data was transferred at various rates ranging from 0 to 160 megabits per second up to the capacity of the buffer. This variable rate capability was a significant departure from earlier generations of the VLDS and allowed the BVLDS to find a market in ground station recording.

Another break through for instrumentation recording came in 1992 with Calculex's introduction of the ARMOR (Asynchronous Real-time Multiplexer and Output Reconstructor) multiplexer/demultiplexer. The integration of the ARMOR and VBLDS greatly expanded the range of data recording applications. Applications such as the missile launch programs at White Sands Missile Range and NASA's space shuttle mission monitoring at Johnson Space Center quickly became heavy users of the Buffered VLDS ARMOR.

The Model 64 was released in 1996. In addition to all the capabilities offered with the Buffered VLDS, the Model 64 contained a standard 64 Megabyte buffer, provided a sustained data rate of 64 megabits per second and stored 27.5 gigabytes of data on a cassette. This unit also allowed burst data rates up to 160 megabits per second. Like the Buffered VLDS the Model 64 could reproduce tapes recorded on all previous generations of VLDS.

The year 1996 also marked a significant milestone for the VLDS product family. The VLDSB, Model 64 and HE Class tape formats became IRIG standards. Also in 1996, a SCSI II fast and wide interface was introduced with an 8 megabyte per second sustained transfer rate and 20 megabyte per second burst transfers. The significance of these developments was users could now take a storage device designed solely for the instrumentation and test markets and use it like a computer peripheral.

The Harsh Environment (HE) class of recorders was added to the Metrum-Datatape product family when engineering released it to production in 1997. HE class recorders are the newest members of the VLDS product family that has more than 2500 units installed world wide.

Each generation of MARS and VLDS recorders have extended the performance and functions of the family. For each new model an approach of evolution rather than revolution has been taken. In this way the proven characteristics of the in-service products have been retained and new generations have benefited from field user feedback. The three prime areas of enhancement over the product life have taken place in the servo system, the data channel and the variable rate buffer.

The Buffered VLDS, Model 64 and HE class recorders, now IRIG 106 and ANSI formats, addressed applications far beyond the capabilities of any of their longitudinal ancestors. Using the ARMOR, COTS components, a UNIX workstation and specially developed fault tolerance control software, the Buffered VLDS and Model 64 have become an integral part of range activities such as missile and commercial launch programs in the United States including THADD, Space Shuttle, Delta and Atlas Centaur.

The next generation of solid state and RAID recording systems will continue the tradition of giving users the ability to bridge legacy products with state of the art technologies.

One would think that with success stories like MARS, MARS-II and VLDS Metrum-Datatape would have such a large share of the instrumentation and test storage market, they could never be displaced. However, companies like Calculex, Orbital Sciences and L3 have introduced solid-state devices that are receiving serious consideration. Orbital Sciences' solid-state recorder, HSSR, is now the recorder of choice on the F-22 and Calculex's solid-state recorder, MONSSTR, is getting a serious look in the industry. In its effort to maintain its market share Metrum-Datatape has introduced three new state of the art products designed solely for instrumentation and test, while incorporating the latest in consumer technology. These three products, a Disk Recorder and two Solid State recorders will be discussed later in this paper.

Today's Instrumentation and Test Marketplace

Data storage is probably the fastest developing technology on the planet. Most users in the consumer storage market are not concerned with the type of storage their computer uses, as long as they can get their programs and information when they want them as fast as possible. In the world of instrumentation and test the opposite is true. Real time instrumentation and test data exists in time for a brief moment unless it is captured and stored. The technology consumer PC users most want to ignore and instrumentation and test users lose the most sleep over is constantly pushing the bounds of the possible. Ironically, it is the consumer PC users who are pushing the technology. Table 1 shows a sampling of storage devices that are in use today in the instrumentation and test environment. Though far from complete, this list should demonstrate the problems associated with data distribution between ranges.

As consumer storage devices continue rocketing to faster speed, higher capacity, better reliability, instrumentation test pundits are predicting the demise of slow and unreliable electromechanical “dinosaurs-to-be” instrumentation tape recorders. Design engineers are constantly stretching the envelope in diverse regions of science and technology. Today's consumer storage devices depend on mind-bending combinations of aerodynamics, signal-processing algorithms, and quantum mechanics.

Media	Size	Type	Native Capacity	Native Data Rate
56x CD-ROM	n/a	Optical Disk	.65 Gbytes	8.4 Mbyte/sec
8x CD-R	n/a	Optical Disk	.65 Gbytes	1.2 Mbyte/sec
ADR	8mm	Tape	25 Gbytes	2 Mbyte/sec
AIT	8mm	Tape	50 Gbytes	6 Mbyte/sec
DD-2 L	19mm	Tape	330 Gbytes	15 Mbyte/sec
DDS-4	4mm	Tape	20 Gbytes	3 Mbyte/sec
DLT III	1/2"	Tape	10 Gbytes	1.25 Mbyte/sec
DLT IV	1/2"	Tape	40 Gbytes	6 Mbyte/sec
DTF	1/2"	Tape	42 Gbytes	12 Mbyte/sec
Fixed Disk	n/a	Hard Drive	22 Gbytes	12 Mbyte/sec
LTO	1/2"	Tape	100 Gbytes	20 Mbyte/sec
Magneto Optical	n/a	Optical Disk	5.2 Gbytes	1.2 Mbyte/sec
Mammoth	8mm	Tape	20 Gbytes	3 Mbyte/sec
VLDS S-VHS	1/2"	Tape	27.5 Gbytes	8 Mbyte/sec
VXA	8mm	Tape	33 Gbytes	3 Mbyte/sec

Table 1 - A sampling of storage devices used for real time instrumentation and test storage.

Flash memory manufacturers are saying that silicon chips can store data indefinitely, without electrical power. This technology remains too pricey to dethrone tape in the instrumentation and test world, but it continues to boost storage density and threatens to lower prices. As flash memory keeps conquering more non-computer fields, such as digital cameras and answering machines, this challenger may someday take the place of tape.

All these advances in storage are radically changing the world of instrumentation and test data storage. Larger and faster hard drives that are plug and play compatible with existing digital tape recorders already support RAID storage systems. The remainder of this paper will be spent discussing new solid state and RAID technology as it applies to instrumentation and test.

Flash memory

Flash memory has become big in products that need a small amount of nonvolatile storage for programs or data. According to In-Stat, a Scottsdale, Arizona market research firm, in 1995 only about 25 percent of flash-memory products went into computers, making computers the number-two users, behind communications products. Even in computers, however, most flash-memory applications were replacements for EPROMs and EEPROMs (code storage) rather than data storage.

The big push for data-storage flash memories did not come from computers. Consumer items, such as digital cameras and voice recorders, played that role. Today's demand for flash memory has outstripped supply, and manufacturers have found a market no matter what their technology. This demand has kept the supply down and prices up and this is not likely to change for another three to five years.

With all the advances and alternatives, why hasn't flash memory recorders toppled tape recorders yet? It is the price that is holding back the inevitable. Flash memory is still 5 to 10 times as expensive as tape storage. Flash memory's backers point out this differential is much less than it was a few years ago. Still, even the most optimistic say it will take perhaps another five years before solid state flash recorders replace tape recorders.

Instrumentation and test storage manufacturers have to choose which type of flash memory is best for their applications. In applications where capacity is more important, slower access may be worth the sacrifice. However, in a real time data acquisition environment, the speed of access may outweigh all other considerations. Consumer applications are typically forgiving on the speed issue, while real time instrumentation and test applications usually demand speed above all else.

Solid State Recorders

Solid State Instrumentation Recorders are starting to generate a lot of interest in the high performance flight test community. The demand for smaller footprints and higher reliability is the driving force. The compact ruggedness and the lack of moving parts are making solid-state instrumentation recorders very attractive for carrier suitability testing. On the plus side the density of flash memory components is rising along with access speed. On the down side, though, the commercial demand for flash memory is keeping manufacturers at full capacity while driving down the supply and driving up cost. For the next several years the demand for popular commercial devices such as digital cameras will force flash memory prices to stay at the current level or rise slightly. The flight test community will continue to use tape as long as the comparative cost of solid state instrumentation recorders is two to three times higher.

The flight test community is in the process of evaluating the various solid-state instrumentation recorders that are on the market today. The majority of the high-performance SSDRs that are being evaluated require expensive and bulky data transfer devices. Most of these devices were designed with the airborne reconnaissance market as the primary target. The flight test market was only a secondary target. The sustained rates and capacities of these devices tend to be very high (see table 2) but the higher data rates and capacities come at a substantial cost. When you include the expense of replacing the ground support equipment currently in use the price tag quickly becomes prohibitive.

Product	Manufacturer	Maximum Capacity	Maximum Sustained Data Rate
Solid State HE	Metrum-Datatape	76 Gbytes	30 Mbytes
Solid State MARS	Metrum-Datatape	38 Gbytes	13 Mbytes
MONSSTR	Calculex	207 Gbytes	128 Mbytes
S/TAR	L3	100 Gbytes	50 Mbytes
HSSR	Orbital Sciences	200 Gbytes	45 Mbytes

Table 2 - Solid State Data Recorder Manufacturers
(Note: The Solid State HE & MARS are not fully released and specifications may change)

Metrum-Datatape has assumed a strategy that has the flight test community as the primary target and airborne reconnaissance as secondary. They intend to build on the hugely successful MARS family of recorders and their Harsh Environment (HE) class recorders. The solid state MARS-IIe is plug-and-play compatible with the DLT MARS-IIe. Current MARS-II and IIe users will only have to replace their current Storage Modules (SM) when they have an application where a SSDR is required. Playback or data transfer occurs in the MARS-II-L.

As with the solid state MARS-IIe, Metrum-Datatape's solid-state HE class recorder enhances the product line instead of replacing it. With VLDS as an IRIG standard and over 2500 VLDS type digital recorders in use Metrum-Datatape did not want to abandon their users. The solid state HE will utilize the same chassis and interfaces as the 32HE and 64HE including the popular ARMOR compatible Single Board Multiplexer. Removable storage modules that will reproduce or transfer data to the Model 80 or 80i are replacing the tape transport. Expensive pallets and wiring harnesses will not have to be replaced when switching between VHS and Solid State. Additional memory modules can accommodate capacity and sustained rates without a change in footprint.

RAID Systems

RAID, Redundant Array of Inexpensive Disks, is a collection of methods; implemented in hardware, software, or both which uses one or more disk drives in a RAID system to increase data performance, data reliability, or both while minimizing cost.

In order to accomplish the conflicting goals of increasing data performance verses increasing data reliability, while reducing cost, several popular RAID levels have evolved from the consumer storage market. The current RAID levels are 0, 1, 0+1, and 5.

RAID level 0, also known as data striping, attempts to increase data performance by breaking up a larger block of data into several smaller blocks which are simultaneously written to or read from several disk drives at once.

RAID level 1, also know as data mirroring or data shadowing, increases data reliability by writing or reading the same block of data to two or more different disk drives or partitions on disk drives simultaneously.

RAID Level 0+1, also known as Mirrored Stripes or Striped Mirrors, are configured to both increase performance and reliability at the same time. This is done by both striping data over multiple disk drives as well as mirroring the same data to another set of disk drives at the same time.

RAID level 5, also known simply as RAID5, increases reliability while reducing cost but at the expense of reduced performance. This is accomplished by creating a parity disk. A parity disk is the mathematical XOR function of a set of two or more data disks, the result of which is stored in the parity disk. The simplest RAID5 implementation requires three drives or drive partitions. Two of the three disks are data disks and the third is the parity disk. Mathematically, Disk1 XOR Disk2 = Disk3.

There are many variants of RAIDs. For example, the Sun MicroSystems Netra product is an eleven-+1 RAID system. It uses eleven data disks and one parity disk with a pure software RAID implementation. This is about a $1B per year product for Sun MicroSystems.

Since the goals of an instrumentation and test storage system are very different from a consumer COTS RAID system, a look at the underlying technical issues is required in order to avoid serious future reliability and performance problems.

Hard Disk Drives

Tape drives are a very high technology with peculiarities unique to them. Hard disk drives have their own peculiarities which effect their reliability and performance and the reliability and performance of the RAID systems in which they are used.

For disk drives to maintain head-to-media tracking reliably they periodically go through a head-to-media re-calibration. This re-calibration attempts to adjust for the constantly changing temperature inside the disk drive. Temperature changes cause the drive platters to change shape and size thus affecting head-to-media tracking. Factors, which affect drive temperature, are: ambient room temperature, power-on hours, I/O operations per seconds, amount of random 1s or 0s, mechanical bearing wear and size and rpm rating of the drive itself. Modern disk drives, especially Fibre Channel Arbitrated Loop (FC-AL), frequently have a temperature sensor on-board the drive, which can be read from either the host RAID system or the Enclosure Services (ES) module.

If a disk drive fails to successfully write data or read data there is a mechanism to retry the data. This usually requires at least one or more extra revolutions, which can take from 16µ seconds at 3600 rpm to about 5µ seconds at 10000 rpm. Also, a maximum seek is usually added to each retry attempt, taking up to 50µ seconds. After 'N' attempts to unsuccessfully write a disk sector, the SCSI or Fibre Channel disk drive will attempt to re-map the bad sector. This can take up to150µ seconds.

Today's applications are requiring faster, higher performance drives. It would seem that if you wanted a faster drive, you spin the disk faster. That is precisely what some manufacturers have done by introducing a motor that spins 1000 rpm. Prior to that, the fastest motor was 7,200 rpm. This accelerated speed increases the data transfer rate by 30%. The time for the head to align with the desired data track (latency time) decreases by almost 40 %.

As drive companies squeeze data tighter and tighter onto the disk, heads are forced to read smaller, weaker signals. To remedy this, scientists are working on technology that enables thin film inductive heads to fly closer to the disk to strengthen the output signal. The closer the head flies to the disk the smaller the magnetic area it can read or write and the greater amount of data can be stored.

The goal is to get the head as close as possible to the spinning disk and still avoid a collision, known as a head crash. Head crashes can damage the data stored in the disk's magnetic coating. To avert this, the head is mounted to an aerodynamically designed slider that in turn is mounted on a light suspension allowing the head to fly

1µ inch above the spinning disk. In real terms, that's the equivalent of flying a 747 jet .025 inches above the ground.

Drive manufacturers are very reluctant to reveal their write/read retry algorithms. This is a piece of information that is critical to using hard drives successfully in real time instrumentation and test RAID applications. The write retry numbers can be derived by experimentation, but is a very long and difficult task.

The formatting of a hard disk drive, the setting of the dozens of parameters available in the mode select format pages is an independent task all its own. The goal of course is to level the differences between drive manufacturers as much as possible. Selecting the default formatting supplied by the various host bus adapter manufacturers is often undesirable.

Many commercial RAID solutions provide some means of hot sparring of hard drives. Hot sparring is the technique of replacing a failed disk with a good or new disk together with the dynamic rebuilding of the new disk with the data it should contain. This is undesirable in a real time instrumentation and test RAID systems because this may cause the available data rate to drop to near zero for a considerable length of time.

Most SCSI and Fibre Channel drives allow for a read-after-write or verify function. This requires an additional revolution per sector of data written. While increasing the reliability of the data written to disk, it also significantly reduces data performance.

To compensate for all of the undesirable traits of hard disk drives in real time instrumentation and test RAID systems, a comprehensive buffering/caching scheme must be developed to substitute for the time it takes to do thermal re-calibrations, write retries, sector re-mappings, seek and revolution times, etc.

There are numerous hardware RAID System suppliers in the consumer storage market. Popular hardware RAID suppliers are Mylex, DPT, CMD, DEC/Compaq, Adaptec, Symbios/LSI, EMC and IBM. These companies account for perhaps 90% of all RAID sales worldwide. These hardware RAID suppliers, all in the consumer storage market, range from very inexpensive PC/PCI base RAID host bus adapters selling for less than $1K to external RAID systems selling for more than $1M. None of these systems are tuned for Real time instrumentation and test data acquisition, nor will they be easily convinced to do so. It is up to the manufacturers of instrumentation and test storage systems to design I/O and buffer electronics that will adapt these devices to their applications.

Disk Recorder

Metrum-Datatape's Model 80 Disk Recorder is the market's latest instrumentation recorder incorporating a COTS RAID designed for the consumer storage market. When you examine all of the current offerings on the market today, this product comes the closest to maintaining its identity as a pure instrumentation storage device. It is "Plug & Play" compatible with Metrum-Datatape's very successful Model 64 S-VHS digital data recorder and ARMOR multiplexer/demultiplexer.

The Model 80 disc recording system acquires data through a COTS 8 bit parallel PCI interface, the PCI-V64, which is compatible with the ARMOR multiplexer/demultiplexer. To the ARMOR, the Disk Recorder appears to be a Model 64 tape drive to which ARMOR data may be recorded and from which recorded data can be played back. Additionally, to the ARMOR, the Disk Recorder also appears to be the host computer from which the ARMOR receives its setup and operational commands.

Basically, the Disk Recorder is a Pentium III®-class, Windows NT® workstation, complete with system disk, RAM, and floppy diskette, containing a RAID 0 subsystem consisting of up to four hard drives and a RAID controller assembly.

A touch screen flat panel display that is supported by a VGA flatscreen video adapter, touchscreen controller, and flat panel inverter enhances the basic workstation.

Data and control interface with the ARMOR are provided by the workstation's on-board RS-232 serial interface, a PCI-V64 parallel data interface circuit card assembly which emulates the Model 64 tape drive, and a parallel control interface circuit card assembly.

The workstation's on-board IDE and SCSI buses support the installation of various archival recording devices.

Conclusion

The community probably saw the last ever tape transport designed solely for real time instrumentation and test data storage with the release of Metrum-Datatape's 32HE and 64HE. Consumer storage technology has advanced to the point where it is no longer economically feasible for traditional instrumentation and test manufacturers to design transports. The focus of new design efforts will be in the selection of commercial COTS devices and designing suitable housing, electronics and software to make the device look and perform like a real time instrumentation and test storage device. Manufacturers that can do this while leaving a bridge to their heritage products that are still in use will thrive in the new millennium.

An Open-Architecture Approach to Scaleable Data Capture

Terry Mason
Avalon Electronics Ltd

Abstract

The ultra high capacity disk-based data recorders now entering service offer not just a convenient and inexpensive alternative to conventional tape systems for applications like Telemetry and Flight Test but also a unique opportunity to rethink the classical models for data capture, analysis and storage. Based on ‘open architecture’ interface standards – typically SCSI – this new generation of products represents an entirely new approach to the way data is handled. But the techniques they employ are equally applicable to any SCSI storage device. This Paper discusses a range of practical scenarios illustrating how it is now possible to `mix-and-match' recording technologies at will – disk-array, AIT, DLT, DTF, ExaByte, JAZ, ZIP, DVD, etc. – to produce an almost infinite combination of readily scaleable plug-and-play data capture, analysis and archiving solutions. The cost and reliability benefits arising from the use of standard mass-produced storage sub-systems are also considered.

Introduction

An Open Forum at the 1998 European Telemetry Conference addressed once again the perennial question "Is Tape Dead?" Various alternative storage technologies were discussed – solid-state (dynamic and static), disks, etc. – but as ever, no clear challenger emerged. Much has changed in the intervening two years however. In particular, a new class of disk-based recorders has appeared whose high performance, low cost and flexibility now make this technology an attractive proposition for many data capture applications. One example of this new approach is Avalon Electronics' new AE7000 disk array recorder.

At the same conference, Avalon Electronics showed how it had been possible to adapt a commercial off-the-shelf SCSI computer peripheral such as a Digital Linear Tape (DLT) drive into a flexible, general purpose data recorder for digital and analog applications[1]. Figures 1 and 2 summarise how this was done. The enabling innovation was essentially to move the problem of computer interfacing from the *reproduce* side of the classical data recording model to the *record* side of a standard SCSI data storage device (in this case a high capacity DLT drive). Once the data had been converted into SCSI format, it became very simple to manipulate and process by computer.

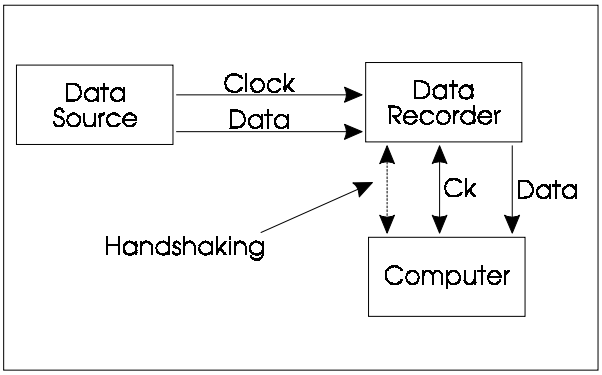

Figure 1. Classical Data Recording modes

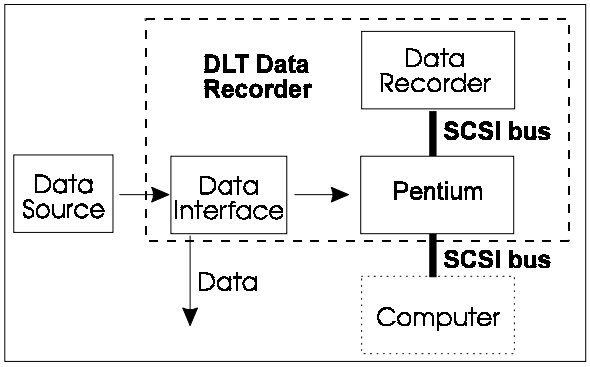

Figure 2. DLT Recorder Architecture

This concept has now evolved from its simple `stand-alone' roots into an entirely new *scaleable* approach to the way data is captured, analysed, transported and archived. Furthermore, using essentially the same schematic diagram – but with alternative, faster storage devices such as disk arrays – it has even been possible to push sustained data transfer rates beyond anything currently possible with magnetic tape. But when these extremely fast data capture devices are fitted with generic analog and/or SCSI interfaces data can readily be migrated to less sophisticated storage media for subsequent transportation, analysis or archiving. This ‘horses-for-courses’, scaleable architecture mean that it is no longer necessary to equip an entire data handling network with expensive storage equipment. The disk array implementation is used as the foundation for this paper in order to demonstrate the full possibilities of this approach.

High Rate Data Capture Using Disk Technology (AE7000)

The storage ‘engine’ of the 1 Gbit/s Avalon AE7000 disk recorder (Figure 3) is an array of eight 18 GigaByte (GB) hard disks, giving a total storage capacity of approximately 144 GB (1.15 Terabits), or almost 50% more than the largest ID-1 tape cartridge. The unit’s architecture (Figure 5), which is the subject of a number of international patent applications, is similar to that of the DLT recorder (Figure 2) in that data (either analog or digital) is first converted to 16-bit SCSI format in a Data Interface controlled by an embedded Pentium computer. In this case however, the formatted data is fanned out over the array of disks which appears to the Pentium as a single SCSI "`Direct Access" device. It is important to emphasise here that AE7000 is not a RAID (Redundant Arrays of Independent Disks). The inherent integrity and reliability of today’s disk technology means that there is no need to operate them in *redundant-array* mode, leaving virtually the entire capacity of the media available for data storage. It so happens that data is recorded on several disks in parallel, but there the similarity ends. Input/Output interfaces are modular, the range at present including serial and parallel digital interfaces with aggregate sustained throughputs to 1 Gbit/s, single channel wideband analog inputs to 50 MHz and flexible mixed analog and digital interfaces for telemetry and similar multi-channel applications. To overcome the twin needs to store sensitive data securely when not in use and to be able to install extra capacity when required, the disk array is housed in a single hot-swappable crate (Figure 5). This can be locked away in an approved safe. The various methods of reading data are discussed later.

Figure 3: AE7000 1 Gbit/s Disk Recorder.

Figure 4: Hot-swappable Crate Containing up to 1.15 Tbits of Data on Eight Disks

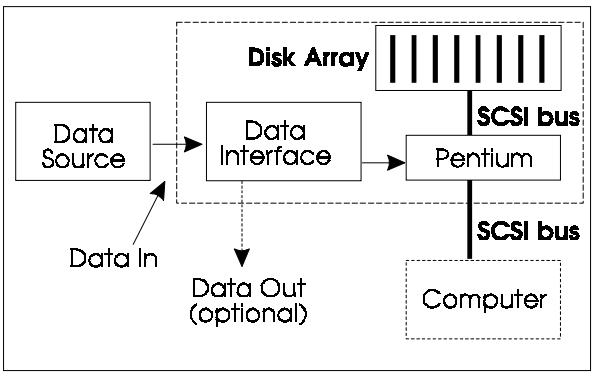

Figure 5: Disk Array Architecture

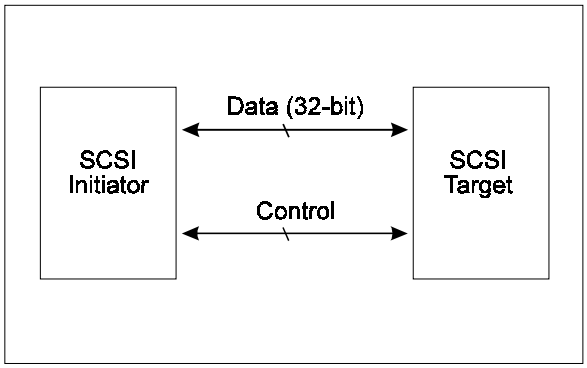

Figure 6: SCSI Data/Control Interface (fast/wide implementation)

Data Management

One of the most difficult aspects of adapting computer storage devices for data capture applications is data management. Invariably, 'really world' data is some form of time history where the instantaneous changes of one or more physical parameters (pressure, temperature, force, amplitude, etc.) are 'plotted' against a timebase. Multi-track linear magnetic tape recorders are particularly suited to this application, since the timebase is effectively the tape movement itself. Helical and transverse scan recorders operate in a similar manner (albeit with some temporary manipulation of the data to accommodate head switching). Computer peripherals behave somewhat differently – typically writing in a disjointed manner which bears little or no relationship to 'real time'. Yet many potential users, while attracted by the advantages of peripheral-based solutions, are nevertheless principally concerned in what is happening to their signals between specific points in time. This problem is compounded when edited portions of the data are transcribed from one medium to another – say from the disk array to a JAZ disk. It is invariably the *original time history* which is of interest, not the time when the data was transcribed.

In the Avalon approach (Figure 5), these difficulties are overcome in an ingenious yet simple way. The basic unit of storage on a disk is the *sector* (512 Bytes). In order to minimise the amount of overhead written to disk, input data is cached until there is enough to write a *cluster* (defined as 1,000 *sectors,* or 512 kB). As the eight disks effectively write or read in parallel, the basic unit *of system* storage is therefore 8,000 sectors (4.096 MB). Each time a cluster is written to disk a directory entry is made as an ASCII space delineated file with entries for cluster number, time (in seconds since 1980) and any related user event marks. Each time the recording process is terminated – always at the end of a complete cluster – the complete directory is written to a flash memory which is integral to (and therefore travels with) the removable disk crate. The time source can be the unit's internal generator or one of a number of external timecode options (IRIG, GPS, etc.). To avoid the complexities of multiplexing any low rate *housekeeping data* (range timecode, voice annotation, etc.) into the primary high rate data stream, these ‘tracks’ are stored in flash memory too, suitably linked to the timeframes to which they pertain.

One of the advantages of using the SCSI interface (Figure 6), rather than say Ethernet, is that it has no protocol layer, meaning that data can be simply manipulated as a variable number of blocks. All SCSI interface vendors provide drivers that bring the SCSI device to a common software interface such as ASPI (Adaptec SCSI Protocol Interface). Handshaking commands and responses (ATN, BSY, ACK, etc.) are transmitted between the Initiator and Target on separate dedicated lines. Another major advantage is the limited number of commands needed to move data around the system. For example, consider the need to transfer to RAM a passage of data of known duration which was recorded commencing at a certain moment in time. It is simply necessary to convert this *start time* into seconds (from 1980), relate this to its associated *cluster number* in the flash memory and then multiply this value by 8,000. This is the *start sector* which is then placed in the SCSI *command block* along with the appropriate transfer length (expressed in *blocks*). Once transferred, this data can be given a filename and resaved, if required.

The foregoing scenario described the use of AE7000 as a SCSI *Target* in which it appears to the host as a single 144 GB hard drive. But it is probably in its role as an *Initiator* that it makes its greatest contribution to the concept *of scalability.* As an Initiator, it is able to download portions of data to any other suitable SCSI archival or transfer medium including, AIT, DLT, DTF, ExaByte, JAZ, DVD or other large capacity disk. Typically, in this mode the beginning and end data points are selected manually using a pair of cursors at the unit's graphical interface (Figure 8). Pressing the TRANSFER button causes the system’s control computer to make the proper calculations and then transfer the dataset to the selected data in its original form. For example, an important passage of analog data could be transcribed from one AE7000 in computer compatible form onto, say, a JAZ disk for transportation to another location where it could be imported to a second AE7000 and displayed in its original analog form again. The normal error checks associated with data interchange between SCSI devices apply, meaning that no errors are introduced during the transcription process.

System Interfacing

Before going on to consider the range of practical implementations, it may be helpful to describe several important system interfacing possibilities. AE7000 is designed initially to operate as a stand-alone recorder/reproducer with a minimum of user controls and a clear Graphical User Interface (Figure 6). The primary pushbutton controls are: STOP, RECORD, PLAY and GOTO. In addition to the usual displays for gain, offset, etc. AE7000 also includes a range of RECORD TRIGGER options. These can be used to define when recording should take place. A typical screen used during PLAY is shown in Figure 7. Here, the cursors are used to define the start and finish points for a passage of data to be write-inhibited, replayed or marked for later analysis or transcription.

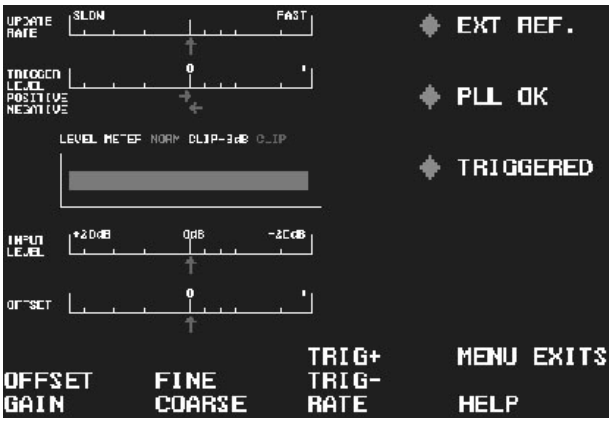

Figure 6: AE7000 Monitor Screen

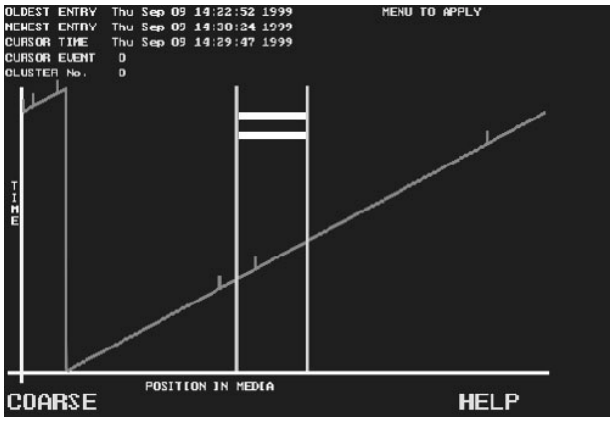

Figure 7: AE7000 Replay Control Screen

But in the context of a scaleable data capture strategy, a number of more adventurous possibilities exist (Figure 9). Bearing in mind that disk-based systems are essentially *temporary* storage devices, it is important that there should be a convenient means of copying data for transportation, off-line analysis and/or archiving. As many applications are still (and are likely to remain, at least in the foreseeable future) analog in nature (telemetry, SIGINT, etc.), the simplest possibility is to transcribe selected passages in analog form to a suitable analog tape recorder. An alternative is to transcribe data directly to a standard SCSI device. Virtually any SCSI system can be used, provided that it has the required capacity and transfer rates for the data sets involved. Since AE7000 can operate as either an Initiator or a Target, analog (or digital) data stored on a SCSI device can at any time be up-loaded again and restored to its native format.

It is an often-heard truism that 95% of all stored instrumentation data is ‘garbage’. Yet any missile test range or flight test center is likely to have a massive warehouse of large, expensive, open-reel and/or cartridge tapes, only a tiny fraction of whose contents are classified as ‘valuable’ data. It will be immediately obvious, therefore, that the flexibility of the disk-capture approach offers important advantages in this respect. Data acquired at rates beyond the reach of even the fastest tape recorders can readily be transcribed to any suitable low cost medium provided only that the passages of

interest can be identified by time of acquisition and/or simple event marker. It has been found that the optional built-in AIT drive often has sufficient capacity to house the entire output of a day's trials although it is equally possible to employ higher capacity media such as DTF for larger datasets.

An interesting extension to this is the concept of *remote data capture*. In this case, data is captured on disk at the acquisition site while selected passages are transmitted to a remote location over a high speed link for further analysis on a similar disk recorder. This concept is particularly relevant in applications where several remote acquisition sites are controlled by a single central monitoring facility.

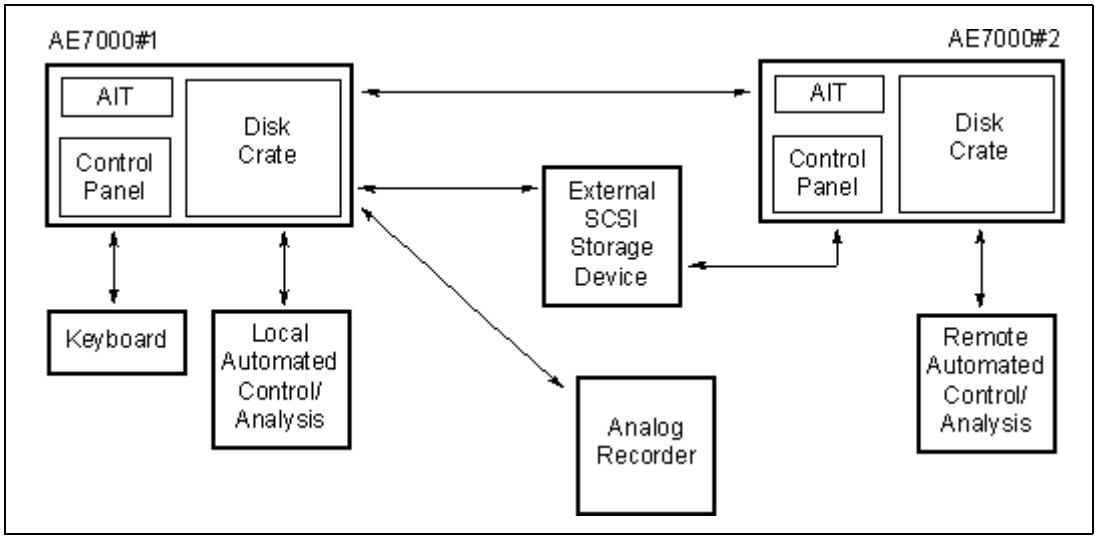

Figure 8: AE7000 Typical Data Flows

Disk-Based Data Capture in Telemetry

From the standpoint of the capture and analysis of telemetry data, some important advantages of a scaleable disk-based solution are:

1) ***'Instant-on'* buffered data capture**. There is no need to run the recorder up to speed in anticipation of the arrival of data. Take the case of an airborne test firing of a missile. It is normal for the aircraft to make one or more circuits of the range while the missile's instrumentation packages are calibrated, checked and their outputs recorded for future reference. Then, typically, there will be a pause before permission is given to launch the missile. There is the permanent dilemma as to whether to leave the tape(s) running (with the possibility of running out before the actual firing), or alternatively to stop the tape and hope to be up to speed again in time for the test. These problems do not exist with a disk recorder which can record instantly up to its maximum data rate (1 Gbit/s aggregate or 50 MHz aggregate in the case of AE7000). Capacity is also unlikely to be an issue since the unit's 1.15 Terabit storage is probably more than adequate to hold a full day's data at the most busy range facility.

2) ***'Loop store'* mode.** The previous comments assume a typical scenario where the data capture process conforms to a pre-planned schedule–and in any event in which personnel at the recording facility have some control over events.

There are many situations however when the exact timing of an event of interest are outside the control of the recorder operator. Where high rate tape recorders are used to capture such unpredictable events, it is normal to use two or more units working in series–with someone in attendance to change the tapes as necessary. A disk-based recorder can overcome this problem by working in *loop store* mode, whereby as the medium becomes full the earliest data is overwritten ensuring that it always holds a 'loop' of 'pre-event' data. In this situation it is normal to further program the system to stop recording at a predetermined interval after the event of interest has been identified, freezing a finite time history leading up to and following the event for analysis.

3) ***Instant Access* to recorded data**. There is no 'rewind time' with disk recorders. Once a test run has been recorded it is available *immediately* for verification and/or analysis. The operator simply has to select the timeframe of interest using the cursors and then press the GOTO button. *Looping* mode is also available on replay, allowing an event to be played again and again without stress to the instrument or recording medium.

4) ***Data Distribution***. Once initial validation of the data has been confirmed it is available for immediate transcription in analog or digital form (as appropriate) to another storage device, (Figure 9). This is another area where the flexibility and scalability of the concept is important. Provided only that a human or automatic 'operator' at the acquisition site is able to identify the data of interest, it may immediately be reduced in volume to something as manageable (and inexpensive) as a medium format cartridge or JAZ disk. Nothing is lost however, since any data migrated to a SCSI or analog device in this way can always be restored to its original form, simply by reversing the process and returning it to the disk recorder. Secondary copies can be distributed to the Test Range's Client, if required. Alternatively, the data can be transmitted over a high speed data link to a remote location for further analysis.

5) ***Cost***. Compared to 'traditional' data recorders, the relatively low cost of the disk system itself, the analog and SCSI devices it is designed to interface with and the media they use offer immediate advantages. Less obvious perhaps, are the cost savings surrounding the introduction of the package into an existing data collection facility. For example, the multi-channel data input/output interfaces can be made to emulate exactly the user's existing interface (IRIG, DCRsi or ID-1, for example). Where a possible change of recording technology is linked to a move from an analog to a digital environment, the traditional horrors of 'going digital' are eliminated. AE7000 for example, fits equally well into either regime, and will perform the analog-to-digital conversion (i.e. to SCSI) 'for free'.

6) ***Reliability and Logistics***. The principal moving parts in a disk array system are the disk drives themselves, and these are effectively field-replaceable 'throw-away' items. Other SCSI devices in the network can be considered equally expendable, or at least inexpensive enough to carry an adequate number of spare units. Furthermore, experience has shown that the inherent reliability of mass-produced computer peripherals can be retained when they are adapted for field data capture applications provided care is taken in the re-engineering process. For example, Avalon Electronics offers a 5-year warranty on the disk

drives used in its AE7000 product. These considerations mean that expensive maintenance contracts and high-value spares holdings could soon be a thing of the past as the instrumentation world embraces these new technologies.

Conclusions

Over the years there have been many ‘false dawns’ in the quest for COTS (commercial off-the-shelf) solutions to complex data capture, manipulation and archiving problems. In many cases, tape and disk-based products have failed to deliver on their initial promise. Now, however, it can be seen that a whole family of SCSI-based devices hold the key to a new, genuinely flexible approach. Compared to traditional recording tools they are inexpensive to own, simple to integrate into existing set-ups and require little or no special software code. But above all, they offer a degree of scalability to the problem unimaginable just a few years ago. As has been shown, the concept is as applicable to a simple AIT, ZIP or JAZ drive as it is to a massive 1.15 TB disk array– indeed an identical proprietary software package could probably control either. It is predicted with some certainty therefore that multi-technology solutions, based on common generic interfaces like SCSI, represent the ‘next generation’ for many data storage applications.

---

[1] T.Mason, “A New Generation of Data Recorders based on DLT Technology”, Proceedings of European Telemetry Conference, 1998.

Solid State Recorders Gain Ground

Chris Duckling
Consultant European Markets

L-3 Communications, Communication Systems-East

Abstract

For many years the data collected by instrumentation acquisition systems has used magnetic tape as its storage medium. Tape offers advantages of creating an instant archive source but in the harsher environments commonly found in instrumentation acquisition tape represents a 'compromise technology'.

Solid state memory has always had significant advantages over all other storage media in the areas of size, weight, power, reliability and bit error rate - but price has been a penalty. The explosion in the use of NAND FLASH semiconductor chips over the past few years, resulting in falling prices, and ever-increasing chip density has brought Digital Solid State Recorders (DSSR's) within the grasp of most instrumentation applications.

This paper explains the technology, advantages for instrumentation designers and users, standardisation efforts under IRIG and NATO committees and looks at available products. It will be of interest to all designers and specifiers of instrumentation systems that require real-time high performance storage.

Introduction

At ETC 1998 held in Garmisch-Partenkirchen, an expert panel was convened to discuss 'Is Tape Dead?' At that time only a few manufacturers could offer solid state product and it was concluded that the price tag and lack of available standardisation was a major inhibitor to the adoption of this technology in instrumentation applications.

Technology moves fast - especially when fuelled by commercial rather than aerospace needs! In the two years that have followed many firms have introduced solid state products which are targeted at the instrumentation market. This paper will describe the benefits of the technology and our company's approach to producing a product for this market.

Review of technologies

There have been many reviews of storage technologies for instrumentation and other data storage applications [ref. 1, 2 & 3]. The paper at reference 1 provides a comprehensive comparison of technologies and this summary is taken from there. It is assumed that the requirement is for a reliable data storage device to work in an industrial or airborne environment and requires a method, or methods, of downloading/removing the data from the acquisition system for subsequent replay and analysis on a ground analysis station.

Magnetic Tape:

Advantages:	Disadvantages:
• The devil we know! • Low cost per bit • multiple sources of supply (but declining) • Instant archive copy made.	• Moving parts require routine maintenance and lower reliability • Media is temperature and humidity sensitive • High data rates equate to physically large machines • Need heaters for low temperatures • power hungry • Need care in mounting due to mechanical issues of shock and vibration

Magnetic Disks:

Advantages:	Disadvantages:
• Uses cheap and readily available 'laptop' disc drives • Can produce high data rates and capacities by combining into RAIDs or JBODs. • Small, light	• Another mechanical device! • Mounting needs attention • Reliability in harsh environments is difficult to predict • Obsolescence issues abound due to commercial technology employed • Not suitable for archiving • Need to address data download

Solid State:

Advantages:	Disadvantages:
• High reliability • High data rates • Excellent BER performance • Wide temperature performance • Excellent vibration performance • Excellent humidity tolerance • High vibration & shock tolerance • Instant replay • Can be 'hard-mounted' • Small, light, low power	• Not suitable for archiving • Need to address data download

Figure 1 below shows the relative performance of the three technologies reviewed against typical specification requirements found in instrumentation applications.

Figure 1 Comparison of Data Storage Technologies

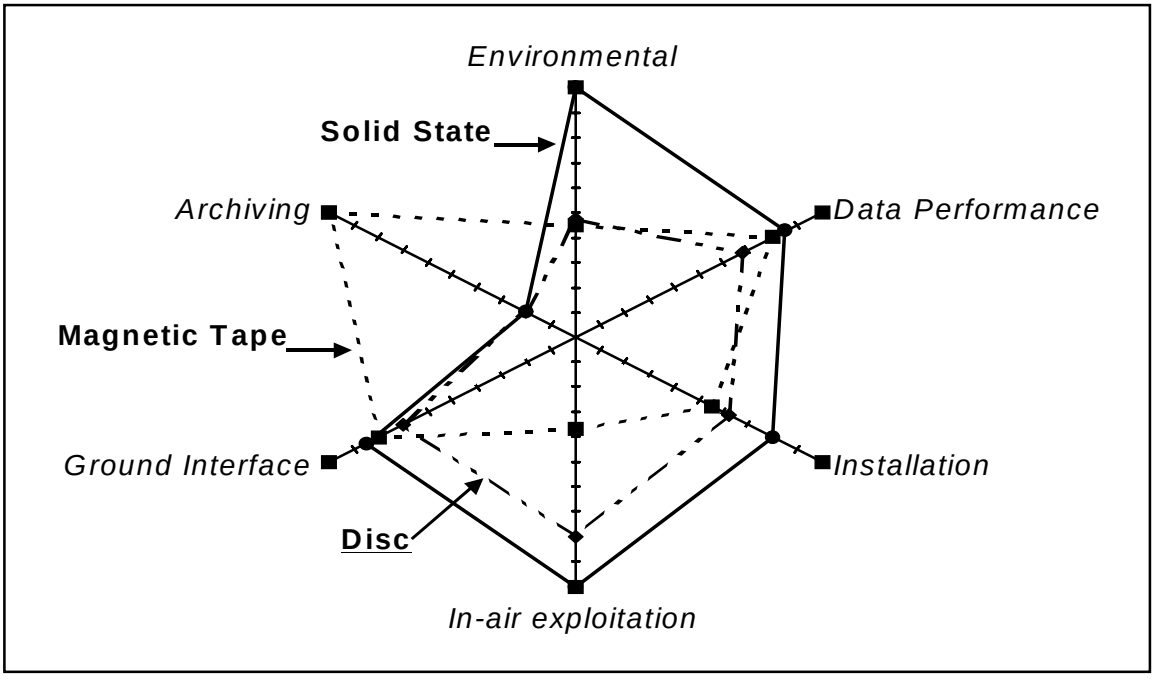

As can be seen, if the designer or user has a requirement to collect data in a harsh environment, requires high reliability with ease of installation, and can address the archiving arrangement - solid state will always provide the most viable solution.

Archiving

Most systems require an archived copy of the collected data - but applications are changing. In the past it was common to archive raw, unprocessed data, as this was the only permissible source input for many ground stations. With the advent of solid state decommutation systems [ref. 4], it is now more likely that the ground analysis station will consist of a PC or work station and the archive will be held in an industry standard e.g. Exabyte, AIT, ZIP, LTO format. In this case it becomes less important to have the archive in the raw data format or on the original media and more important to have an industry recognised COTS standard. This is the approach taken by the solid state community; to establish a removable module with a standard interface that can readily, and inexpensively be transposed into an industry standard archive by the ground system. This provides the best of both worlds - a tailored acquisition system using the appropriate technology and an inexpensive ground replay approach which archives on (probably) existing media types.

Solid State Technology

There is a common belief that solid state memories are simply a case of taking computer SIMM or PCMCIA cards and connecting them into mass memories. This is non-optimal and to be avoided at all costs. As in all systems designed for long life and high integrity, system architecture is critical. Figure 2 shows the architecture of the L-3 Communications S/TAR™ recorder at top level. It can be seen that attention to input and output data flows is critical to optimise performance. This is particularly important where read/write or read-while-write capabilities are called for. It should be noted that such facilities are easily implemented in solid state recorders.

The Digital Solid State Recorder (DSSR)

It is possible to produce a DSSR of almost any capacity and data rate, but most offerings are in the 0.5GByte to 100 GByte range with data rates continuously variable from zero to 400+ Mbps. To gain additional capacity or data rate it is a question of parallelism of memory chips to achieve the result. This is not without its challenges and careful thought must be given to read/write cycles if fault detection and correction is to be optimised.

The following sections look at how a solid state recorder addresses the users needs for various performance parameters.

Figure 2 DSSR Architecture

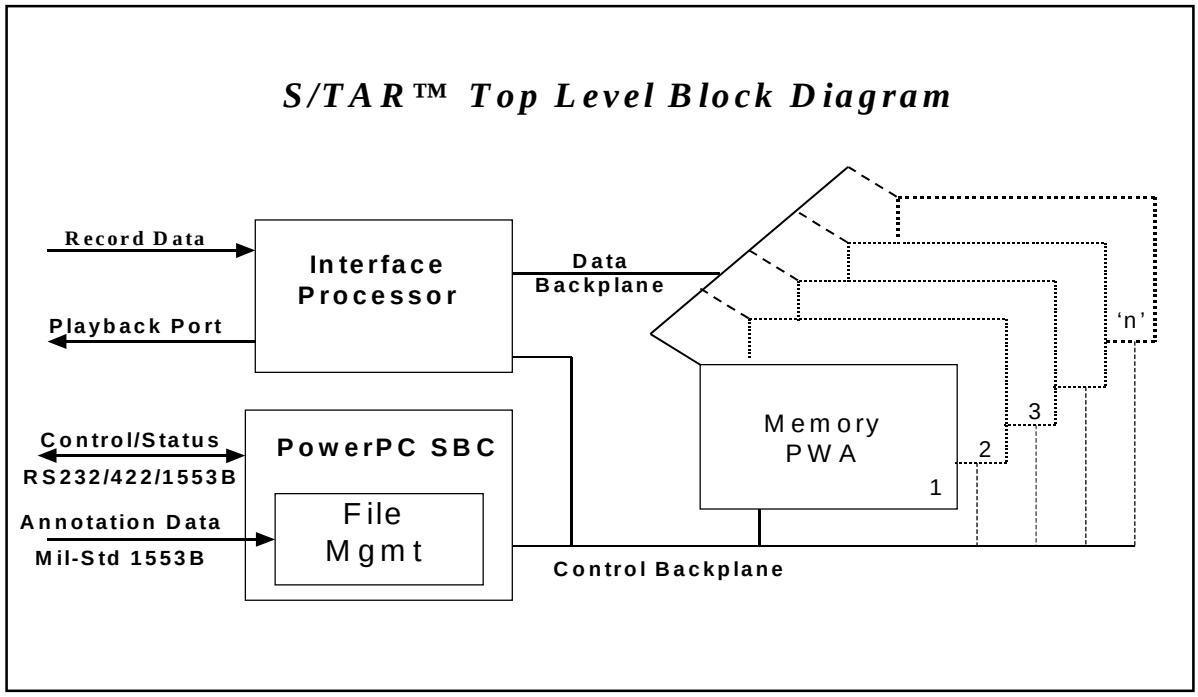

Data Integrity

Loss of data is catastrophic to a user - the costs of re-acquisition far outweighing the cost of the recorder in most cases. In magnetic media systems, be they tape or disc, it has been possible to define errors as transient or permanent. Transient errors being those caused by physical perturbations within the magnetic circuit. Generally this class of error stems from the difficult environment (vibration, temperature, humidity, shock etc.) in which the moving parts have to operate. Head to tape or head flying height are necessarily microscopic to achieve the high performance demanded by modern instrumentation systems. On rare occasions system noise disturbing the low signal level circuits within the read amplifiers causes transient errors. All electro-mechanical data storage systems suffer these problems and designers at best 'cope' with them rather than truly design them out [ref. 5].

Permanent errors are caused either by a magnetic media defect or an electronic circuit failure, generally the former.

Solid State Recorders suffer none of the electro-mechanical problems of tape or disc storage systems. Indeed their data integrity is dictated predominantly by the electronic circuit components themselves. In simple terms this would suggest that data integrity could equal MTBF - an interesting thought knowing that the component reliability is orders better that any electro-mechanical part.

However, good system design looks further into the failure mechanisms and into the memory cells themselves. High density memory is ‘mostly good’ i.e. it comes with failed cells - it is the designers job to track those and any future failing cells to ensure maximum utilisation of all memory. This is a real-time activity and the L-3 Communications S/TAR™ DSSR, for example, has a range of fault detection and mapping algorithms that run in both background and foreground modes.

Figure 3 L-3 Communications S/TAR™ RM3016 DSSR

What is particularly important is to recognise that cell failures occur randomly and as such L-3 Communications, based on their experience of space solid state recorders, have designed in Reed-Solomon error detection and correction circuits to protect the data integrity at all times. This is far more powerful than the simple read-after-write.

As a result DSSR’s are able to guarantee BER at least 10,000 times greater than their tape predecessors. This is clearly significant and it needs to be remembered that these figures are achieved without maintenance of any sort on the DSSR.

Table1 shows typical data performance that can be achieved by off-the-shelf DSSRs.

Table1 Data Performance currently available from DSSRs

Data Rate	0 - 800 Mbps	User clock defined
Memory size	1 - 100 GBytes	
BER	10E-12	

Environmental performance

This is where the lack of magnetic media and the lack of moving parts really comes into its own. Essentially using industrial grade components it is possible to extend the temperature range from -54^{0}C to +71^{0}C and to survive at altitudes up to 50,000 ft without forced-air cooling. Furthermore, the robustness of a properly designed solid state solution will permit a hard-mounted (i.e. no anti-vibration mounts) installation to withstand 12G RMS random vibration and 20G shock *operationally*.

Indeed with L-3 Communications' experience with space-borne DSSR's we are confident that DSSR's will outperform all other storage types in the harsh environments experienced in typical instrumentation applications.

Table 2 shows the environmental performance to be expected from a DSSR

Table 2 Environmental Performance of Airborne DSSRs

Parameter	**Operational Spec**	**Comment**
Temperature	-54C to +71C	No heaters, no forced air
Humidity	95%	
Altitude	50,000 feet	Without forced air cooling
Random vibration	12G RMS	Hard mounted
Shock	20G	Operational

Source L-3 Communications S/TAR™ data sheet

Size, Weight and Power

Relative to a tape based system the savings on size, weight and power are impressive. If for example a radar output recording was required, with a high data rate and high capacity demand, savings on installed size, weight and power could be as much as 80% on all three parameters by utilising a DSSR. Clearly this allows installations where there would otherwise be no possibility of data recording. A 'tight-fit' installation of a DSSR is shown in figure 4 below.

Table 3 shows typical size, power and weight for a 16Gbytes recorder with integrated acquisition interfaces.

Table 3 Size, Weight and Power for Airborne DSSRs

Parameter	Operational Spec	Comment
Size	10 - 25 litres	Depending on memory size
Power	30 - 80 watts	Depending on memory size
Installed weight	5 - 15 Kgs	Depending on memory size

Source L-3 Communications S/TAR™ data sheet

Figure 4 A typical 'tight-fit' installation of a 100Gbyte DSSR into a Saab Draken aircraft

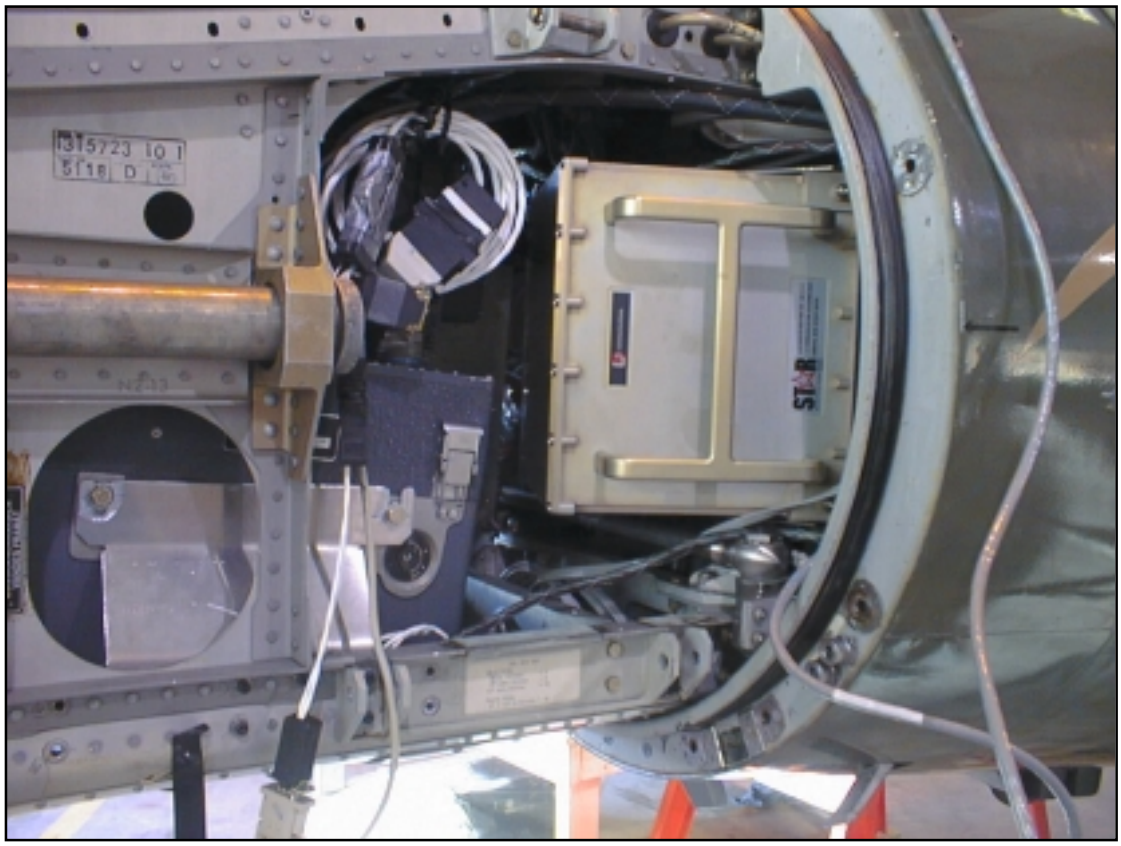

System Integration

A solid state recorder allows additional benefits to the designer/user. One of these is the ability to read almost any previously written data while still recording. Additionally 'almost instant' search to any segment of recorded data is available by addressing the file structure register. Finally, and of great benefit to ground analysis, a DSSR has the ability to record and replay data at any rate from zero to its specified maximum and to have asynchronous record/replay rates. Thus segments of a mission with an average collection data rate of 10 Mbps could be sent down a 5Kbps telemetry link without data compression and that same data could be replayed once on the ground at 1

Gbps! The S/TAR™ DSSR has been designed to offer all of the above facilities, but it should be noted that other manufacturer's products may offer all, none or different sub-sets of them.

The market has become accustomed to fewer and fewer boxes for a typical application. Currently it is possible to get tape systems with some of the signal processing built in - this is also possible with solid state.

Figure 5 shows how two L-3 Communications divisions, Communication Systems-East - creators of the S/TAR™ DSSR and Aydin Systems - creators of the Mini-ARMOR have integrated their two equipments into one box. Such an approach offers standard ARMOR interfaces and performance with all of the advantages of a solid state recorder. The removable part is easily transported to the ground analysis equipment where it requires only power to permit access to the stored data.

Figure 5 L-3 Communications Single box Instrumentation DSSR

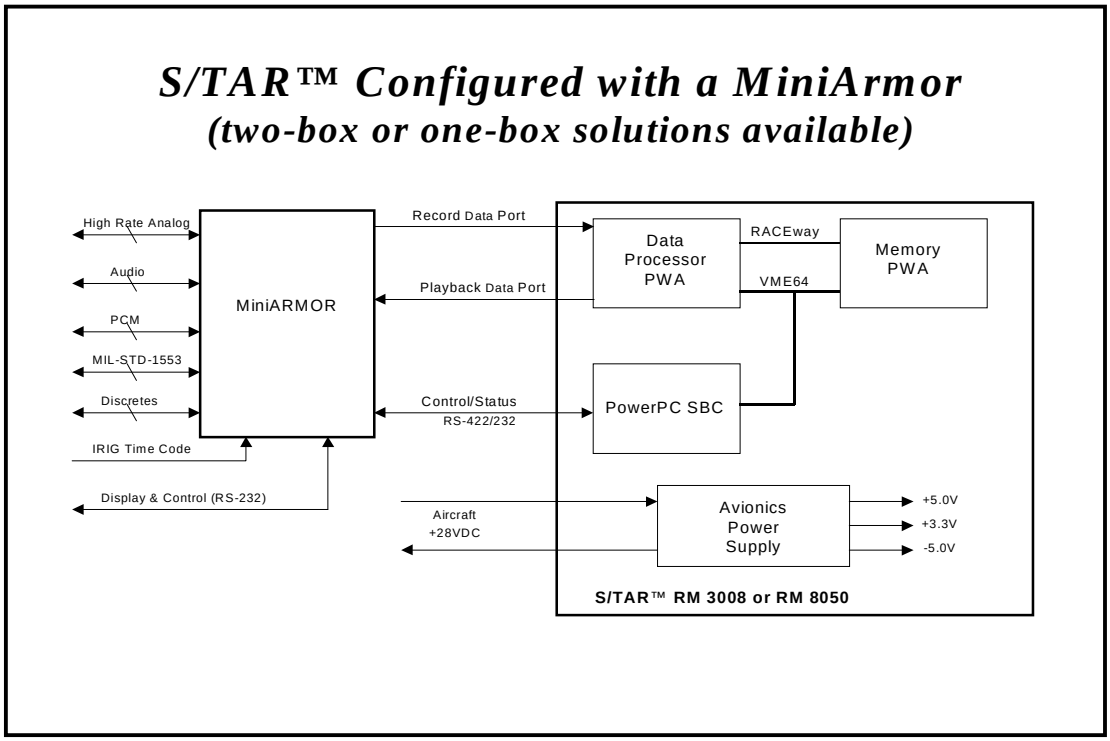

With an on-board processor and with careful application, it has been easily possible to emulate tape recorder interfaces. For example demonstrations have been performed where a an Ampex DCRsi tape recorder has been replaced by a S/TAR™ solid state recorder without any changes to the host system hardware or software. For new installations it is possible to avoid the restrictions of legacy emulation and benefit from the simplicity of the DSSR's smaller command set, the more powerful status reporting regimes, and enables direct and immediate access to the file structure of the stored data.

Simpler controllers and ground replay systems reduce overall costs and increase user flexibility.

Life Cycle Costs

In today's climate of reducing budgets and longer life-cycles the lifetime cost issue is paramount in most procurer's minds. Life cycle costing may be broken down into three major areas: routine maintenance, planned overhauls and breakdowns. Tape based systems require routine cleaning and have planned replacement of items such as rotary heads and capstans. It is too early to assess the life of commercial disc drives - none have been used in harsh environments for long enough and the market into which they are designed to be sold expects a two to three year user life before upgrade.

Solid State recorders suffer none of these problems. They require no routine or planned maintenance and with MTBFs of greater than10,000 hours in a harsh environment, it is clear that with normal usage failures will rarely be seen. Indeed a duty cycle of 10, two hour duration flights per week, 45 weeks per year - far greater than most instrumentation applications - would yield a statistical MTBF of over 10 years - with no maintenance! It is easy to see that on a true life cycle costing model a DSSR will always win.

Standardisation Status

The Range Commanders Council has long been the guiding body for tape data storage under the IRIG formats. Not all companies have adhered to these and there are many disparate, non-interchangeable tape formats in existence. NATO standardised on ID-1 and DCRsi formats in its Standard NATO Agreement (STANAG) 7024 and was keen to avoid a proliferation of standards for 'new data stores'. Accordingly, NATO convened a group of Government and Industry representatives to derive a standard which will permit data download compatibility. A representative of the Range Commanders Council sits as a full member of the group. Progress has been rapid since the first meeting in March 1999.

In essence the STANAG will define a data port through which a user can download the data stored in the device. This data port will be specified in terms of physical (connector), Electrical (power requirements, data protocol) and logical (data sets, file structures). Being a STANAG this will be available free of charge via a web download. The target is to release the standard in 2001, but the major manufacturers, being representatives on the committee, are already working towards product that will comply.
The status is changing rapidly and those persons with an interest are recommended to contact their NATO representative or the author would be pleased to assist in gaining further information.

Conclusions

Solid State technology has been with us for more than three decades but has been either volatile memory or too expensive. This has changed and for harsh environments the cost of ownership equation has swung firmly towards DSSRs. Tape will now struggle to find application in harsh environments and in higher data rate/higher capacity requirements. Tape may not yet be dead but a young pretender with amazing maturity will dominate the future.

References

1. Duckling, C. *Airborne Data Storage Options.* Paper given at SAR/SLAR Conference Scotland, September 1998 and available on request from the author: chris@manyoaks.co.uk

2. Herskovitz, D. *A Sampling of Military Data Storage/Recording Systems*. Journal of Electronic Defence, December 1999: available on-line at http://www.jedonline.com/

3. Kempster, L. *Media Mania - The Fundamentals and Futures of Removable Mass Storage Media*. Avedon Associates Inc. Potomac MD

4. Duckling, C. *Software Decom Comes of Age*. Paper given at ETC98 and published in the proceedings pp184 - 192

5. Duckling, C. *Developing a Harsh Environment Recorder*. Paper given at THIC July 1997 and available at www.thic.org

Any Chance to Have a New Tape Standard?

Dr. Balázs Bagó,
Racal-Heim Systems GmbH
Bergisch Gladbach, Germany

Abstract

In a foreseeable future all recorded data will be processed by computers but the uncountable variety of digital data acquisition, transmission and storage formats will be a nightmare for the person who is responsible for data analysis.

There is an effort by the missile ranges and weapons test centres in the United States to standardise on on-tape formats, which permit and facilitate the inter-organisational and external interchange of recorded data. The US Range Commanders Council (RCC) Telemetry Group (TG) recently issued the Digital Data Acquisition and On-Board Recording Standard (DORS) as an Inter-Range Instrumentation Group (IRIG) 107-98 document.

That means, tapes of all sizes, i.e., DLT, S-VHS, AIT, ID-1 or other media like Solid State Storage or magnetic or optical discs from all recorder manufacturers can be read and transmitted into processing computers with the data appearing in identical data blocks.

How is the Packet Telemetry concept applied in IRIG-107? How far is the standardisation process? Who uses it? Is there a chance to use it beyond the scope of the RCC?

Introduction

As a known fact, the need for acquiring, transmitting, analysing, storing and retrieving measurement data is continuously increasing. Today, almost everywhere, digital data processing methods are used, and a large number of unique data structures have been developed for specific data representation. Earlier, the recorded data were replayed and reconstructed in the analogue domain; today data can be analysed more precisely and effectively with digital computers. While the unique data formats of the recording devices were in most cases hidden from the user, the need for analysis of the digital representation opens the question of compatibility. Efforts have already been made to define standard tape formats - e.g. see the IRIG-106 standard [1] - but the fast changes in storage technology make those standards obsolete. The lack of effective standardisation among various digital data formats requires immense efforts to interpret the data formats with data analysis software.

Timetable of the IRIG-107 Standard

In February 1993 the US Range Commanders Council (RCC) Telemetry Group (TG) decided to start working on a new data format standard. The ad hoc "Digital Data Acquisition and Processing" working committee was formed and a case study was conducted to define a new data format.

Among other possible data formats, the working committee has selected the Packet Telemetry Recommendation [2,3] of the international space organisation of Consultative Committee on Space Data Systems (CCSDS) - currently hosted by NASA - as the basis for the new data format. The standard was adopted with only a few changes - mainly simplifying some control possibilities supported by CCSDS.

The first draft, called "pink sheets", was issued and published in September 1996. The committee has obtained more than 100 comments on the draft from 15 organisations from many different points of view - vendors, telemetry users, software companies, within and outside the Ranges. The working committee of RCC finally made decisions about the comments in November 1997, and the first Issue of the standard was published in June 1998 [4].

The Objectives of IRIG-107

The purpose of the IRIG 107 standard has been declared as follows [2]:

Currently there are a large number of unique data structures that have been developed by vendors and government for specific on-board data recording applications. These unique data structures require unique decoding software programs. Writing unique decoding software, checking the software for accuracy, and decoding the data tapes is extremely time consuming and costly.

A necessity was identified to develop a digital data acquisition and on-board recording standard that will support the multiplexing of multiple data streams and maintain the accuracy of data correlation with time.

The digital data acquisition standard should allow the use of a common set of playback/data reduction software, take advantage of emerging random access recording media, improve efficiency over traditional PCM for asynchronous data, and take advantage of the rapid improvement in commercial communication technology.

Concept

The basic concept of IRIG-107 has been taken over from the layering system design method of networking. Within each layer, the functions exchange data according to established standard rules or "protocols". Each layer draws upon a well-defined set of services provided by the layer below, and provides a similarly well-defined set of services to the layer above. Therefore, an entire layer within a system may be removed and replaced as dictated by user or technological requirements without destroying the integrity of the rest of the system. Layering is therefore a powerful tool to design structured systems that change due to new recording media, changed communication protocol or other technological improvements.

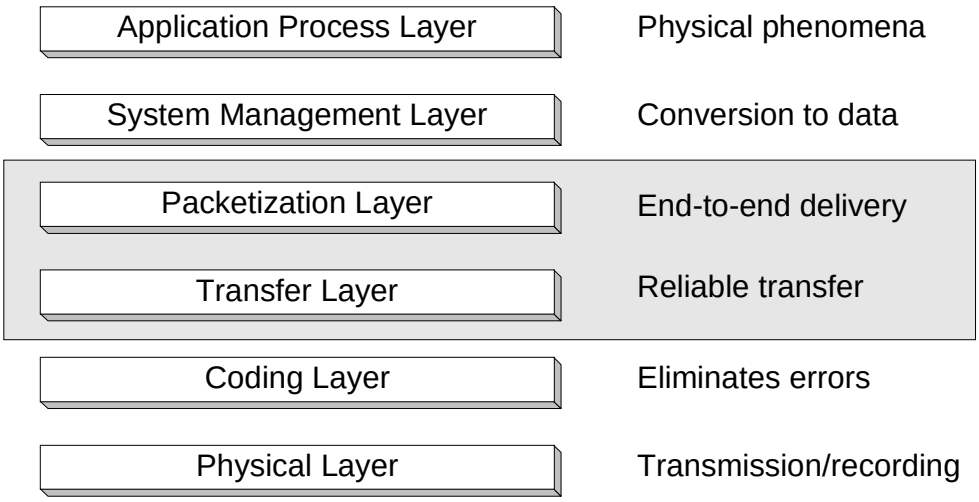

Figure 1 - Layered Model of IRIG-107

The scope of IRIG-107 is to define two of the above layers: the Packetisation Layer and the Transfer Layer.

Packet Recording

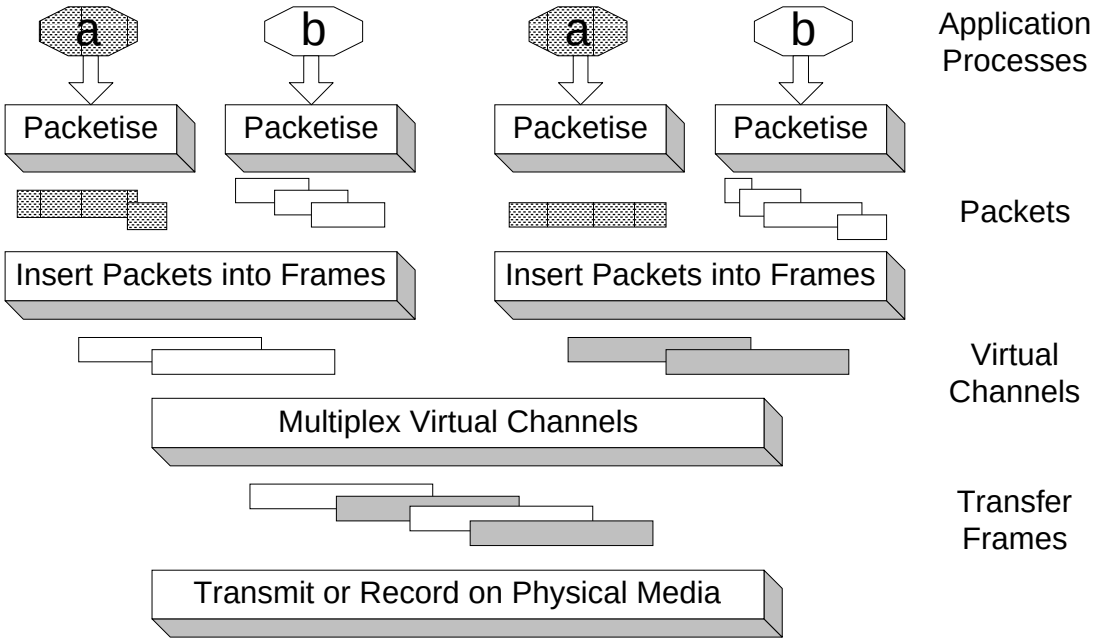

Figure 2 - Data Flow of Packetisation and Transfer Layers

Packet telemetry represents an evolutionary step from the traditional Time-Division Multiplex (TDM) method of acquiring, recording, and playing back data from instrumented vehicle sources to ground data systems sinks. The essence of the packet telemetry concept is to permit multiple application processes running in on-board sources to create units of data (packets) as best suits each data

source. The concept permits the on-board data system to record these packets in a way that enables the ground playback system to recover the individual packets with high reliability and to provide them to the data sinks in sequence.

To accomplish these functions, the standard defines the data structures: *Source Packet* (or packets) and *Transfer Frame* (or frames) and a multiplexing process called *Virtual Channels* to allow interleaving Source Packets from various application processes into different Transfer Frames.

Packet Format

The source packets are data structures generated by a packetisation device from data acquired by on-board application processes "a" and "b". The packets can be generated at fixed or variable intervals and may be fixed or variable in length. The only common requirement of the packetisation devices is to tag the data with an Application Process Identifier to route the packet to its destination sink. An optional secondary header is allowed for standardised time tagging of source packets to support time analysis between different application data.

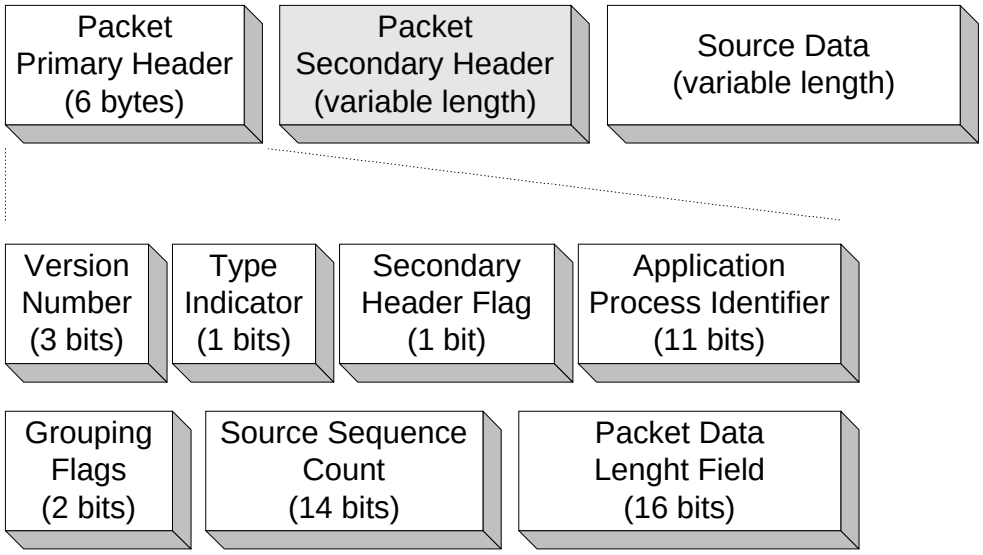

Figure 3 - Packet Format

The Source Sequence Count sub-field calls for each packet to be numbered in a sequential manner, thus providing a method of checking the order of source application data at the receiving end of the system.

Transfer Frame

The Transfer Frame is a data structure that provides an envelope for recording packetised data. The transfer frame has a fixed length for a given physical channel during a mission phase.

A 32-bit frame synchronisation market is attached to the beginning of the transfer frame primary header. This is used by the ground station to acquire synchronisation with the frame boundaries during playback. The Frame Error

Control Field at the end of the frame provides the capability for detecting errors that have been introduced into the frame during the data handling processes.

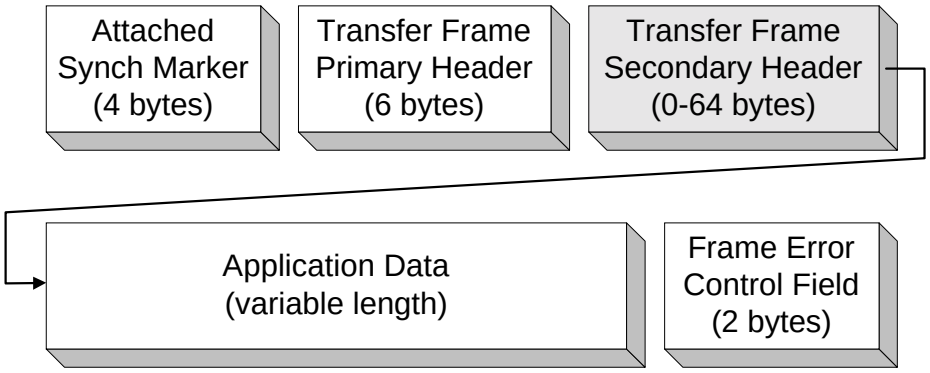

Figure 4 - Format of the Transfer Frame

The transfer frame primary header provides the necessary elements to allow the variable-length source packets from a number of application processes on a vehicle to be multiplexed into a sequence of fixed-length frames. Short packets may be contained in a single frame, while longer ones may span two or more frames. Since a packet can begin or end at any place in a frame, the entire data field of every frame can be used to carry data; there is no need to tune the sizes of packets or their order of occurrence to fit the frames.

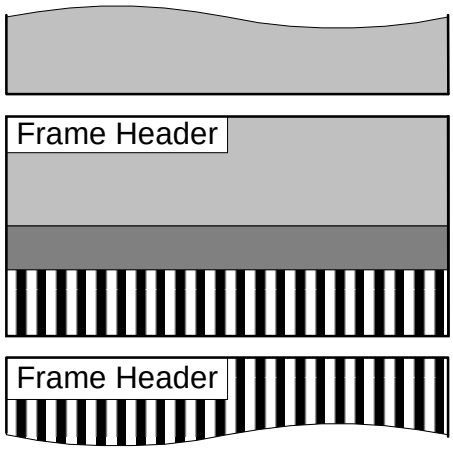

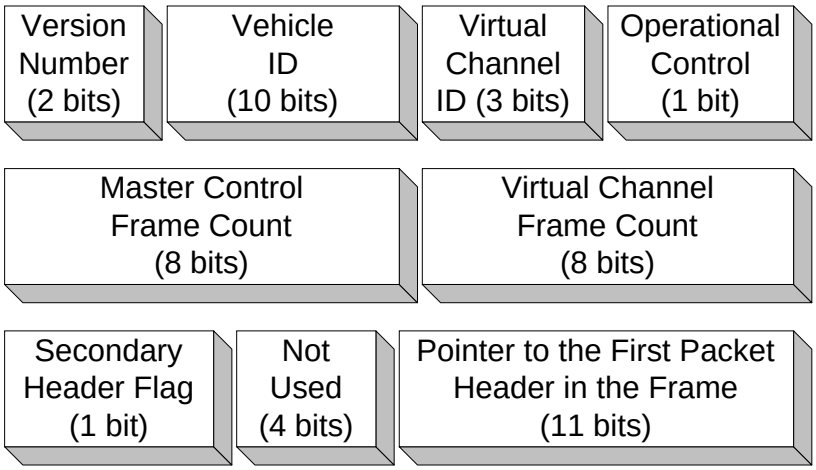

Figure 5 - Primary Frame Header

The Master and Virtual Channel Frame Count fields provide sequential count (modulo 256) of the number of frames transmitted by a single physical data

channel. The counter is long enough to provide a reasonable probability of detecting a discontinuity, in a sequence of frames, when the physical channel is briefly interrupted.

Recommended Time Stamping

The IRIG-107 standard recommends the usage of standard CCSDS format time stamping [5]. All these time formats have a common preamble (P) field to identify the format, length and resolution of the attached time information. Time stamping can be placed in the Transfer Frame Secondary Header, in the Packet Secondary Header or even all data words can be uniquely time-tagged in the packet data field. The allowed time formats can be seen on Figure 6.

General Self-Identifying Time Structure

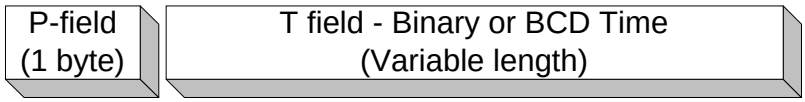

CUC - Unsegmented Time Code (binary)

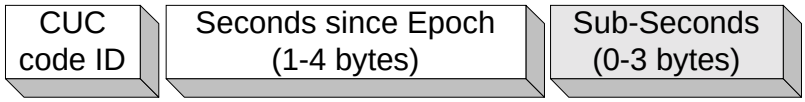

CDS - Day Segmented Time Code (binary)

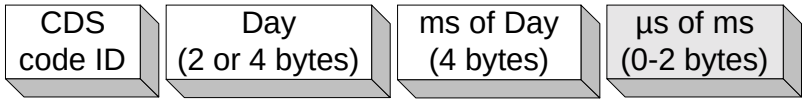

CCS - Calendar Segmented Time Code ***(BCD coded)***

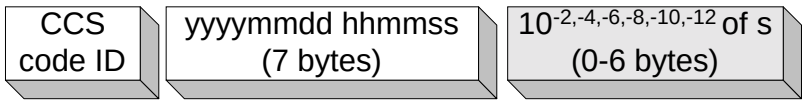

Figure 6 - Allowed Time Tags in IRIG-107

Virtual Channels

Packets are inserted into Transfer Frames comprising optional Virtual Channels. Each transfer frame is identified as belonging to one of the up to eight Virtual Channels. Virtual Channels are normally used to separate sources or destinations with different characteristics. For example, if a vehicle contains an imaging instrument which produces huge data structures, and a number of other instruments which generate smaller packets, a possible system architecture would be to assign the imaging instrument packets to one Virtual Channel and to handle the rest by multiplexing them onto a second Virtual Channel.

Transmitting with Constant Rate

Three mechanisms (idle frames, idle packets or idle data) are provided for cases where a frame must be released and insufficient packet data is available. The method allows a minimal or constant frame rate even if no data is available.

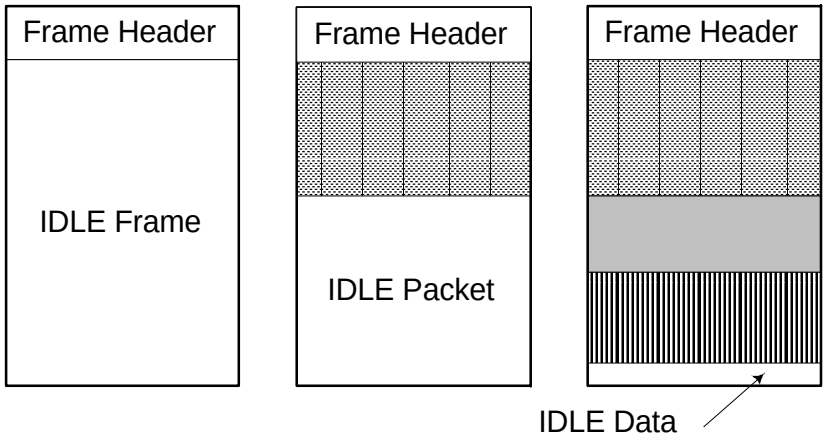

Figure 7 - Mechanism to Transfer Frames with insufficient Data

Ground Station Replay

The ground station application must reverse the packetisation process. Each data packet is selected and de-multiplexed to the sink identified by its source identifier. If the packets are tagged by time stamps, time based measurements or real time signal reconstruction can be easily achieved.

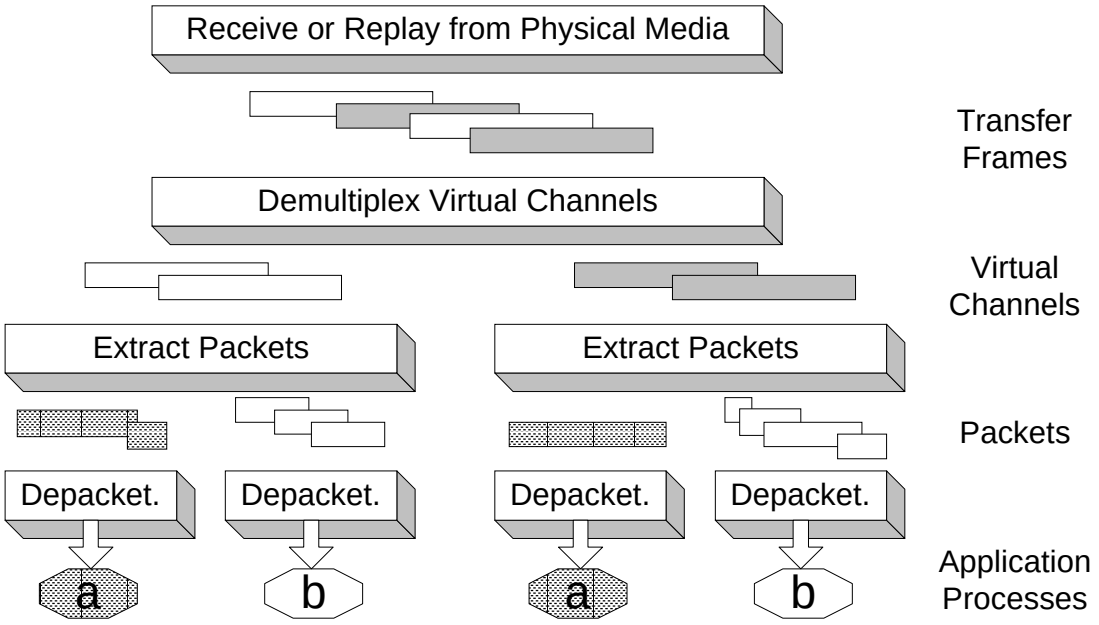

Figure 8 - Reconstructing Application Data at Ground Station

Application Data Formats Included in IRIG-107

The IRIG-107 standard recommends data formats for Pulse Code Modulation (PCM) telemetry data and MIL-STD-1553 messages.

It allows for PCM data recording in a wide range of formats - from the most strict to the most free way in the following four modes:

- Frame aligned to data packet
  - One Packet is one PCM minor frame
  - One Packet is several PCM minor frames
- Frame not aligned to data packet
  - PCM words aligned to byte boundaries
  - PCM words are placed freely into the data stream

On the other hand, the IRIG-107 standard recommends strictly only one way to store MIL-STD-1553 data in the packets, and defines a format where the messages are converted to 24-bit PCM words as it is defined in IRIG-106 standard Chapter 8. In this format the MIL-STD-1553 messages are considered as a single word, each being stored in a 24-bit PCM word as an 8-bit ID + 16-bit data. All command and status words are time stamped with 3 x 24-bit 1 µs time stamps, which are - in contradiction with the IRIG-107 standard itself - not within the recommended CCSDS time formats discussed above.

Interestingly enough, while the PCM stream format is strictly adopted in spite of the contradicting time format, the PCM frame synchronisation word and idle word usage of the IRIG-106 Chapter 8 format is not recommended. The only recommendation is that the 24-bit words and 3 x 24-bit word time stamping should not be split over packets.

The standard itself declares: "*To release the first issue of this standard, only the MIL-STD-1553 A/B application data format contained in IRIG 106 [1] was considered. Future issues of this standard will consider other more efficient techniques for packetization of MIL-STD-1553 A/B application data".*

Application Data Formats Not Included In IRIG-107

The most important criticism of the IRIG-107 standard is, that it seems to be only half complete. As an objective of the standardisation, it says: *"…the Digital Data Acquisition and On-Board Recording Standard should be compatible with the multiplexing of both synchronous and asynchronous digital inputs such as Pulse Code Modulation (PCM), MIL-STD-1553 asynchronous data bus, digital voice, time, discrete, video, and RS-232/422 communication data.",* however, the issued standard has detailed recommendation only for PCM and MIL-STD-1553 data formats, and doesn't recommend any data format for such important data sources as: analogue data, voice, pictures, video, general digital data (parallel, contact closure, frequency input), ARINC-429, ARINC-629, Honeywell ASCB, CSDB and other avionics buses, Serial data (RS232, RS422, RS485 asynchronous and synchronous), GPS, networking formats (Ethernet, Fibre Channel), etc…

Most probably there is no way to specify all possible formats, but at least a general recommendation for user specific data formats would be necessary, otherwise the application or user specific data format decoding remains an unresolved problem forever.

Pros and Cons of IRIG-107

The following table tries to summarise the facts for and against IRIG-107 to be a successful candidate for an emerging new recording standard:

Pro IRIG-107	Con IRIG-107
- Flexible way to merge together many data sources with different data rate and format - Fits modern distributed data acquisition concepts - Computer friendly format - Time stamping recommendations support easy reproduction and analysis with time correlation - Media independent format, it will not be useless with any obsolete media - Adapts an already proven CCSDS standard	- Very telemetry oriented, doesn't allow adaptation for modern media (e.g. very limited frame size) - Doesn't specify packet data formats in general - just a framework for packetisation and transmission - Some existing data format recommendations need already reconsideration - Software unfriendly way of allowing packet headers to overlap frames (e.g. cannot use structures)

IRIG-107 Usage Today

The IRIG-107 standard should be the recommended data interchange format within areas supervised by RCC. All software development should support the IRIG-107 format as at least an alternative. Some vendors are already using the IRIG-107 standard in some of their products, as follows: Calculex, SBS, Reach Technologies, Racal-Heim (the list is definitely not complete, and the author apologises to everyone not included).

Conclusions

The 5 year's effort invested in defining a new data recording standard has achieved some results, it provides good basics for common data structure. It fits well with computer data processing techniques, and its layered structure is appropriate to the current need for quick media changes.

It does not try to define an interchangeable media and hardware but rather defines the data structure only - which can reduce dramatically the continuously increasing development costs of the ground station analysis and data exchange software products.

To achieve a new standard the standardisation process must continue. It seems, that after issuing the first version the project has slowed down within RCC - either because the acceptance was too low or because the effort required to agree recommendation for other data structures was too great due to lacking interest of vendors and users.

In order to keep the process running, more organisations must support it, and in the end the users should force the vendors to support it - otherwise the vendors themselves will not put extra efforts in their developments to change their already existing proprietary data formats to IRIG-107.

References

[1] “Telemetry Standards,” Range Commanders Council Telemetry Group, IRIG Standard 106-96, May 1996.

[2] “Telemetry: Concept and Rationale,” Green Book, CCSDS 100.0-G-1, December 87.

[3] “Packet Telemetry,” Blue Book, CCSDS 102.0-B-4, November 1995.

[4] “Digital Data Acquisition and On-Board Recording Standard; Packet Telemetry” Range Commanders Council Telemetry Group, IRIG Standard 107-98, 1998.

[5] “Time Code Formats,” Blue Book, CCSDS 301.0-B-2, April 90.

DATA ACQUISITION, PROCESSING AND MONITORING

Hardware- vs. Software-Driven Real-Time Data Acquisition

Richard Powell, Sr. Principal Engineer
L-3 Communications Telemetry & Instrumentation
San Diego, CA 92128

Abstract

There are two basic approaches to developing data acquisition systems. The first is to buy or develop acquisition hardware and to then write software to input, identify, and distribute the data for processing, display, storage, and output to a network. The second is to design a system that handles some or all of these tasks in hardware instead of software. This paper describes the differences between *software-driven* and *hardware-driven* system architectures as applied to real-time data acquisition systems. In explaining the characteristics of a hardware-driven system, a high-performance real-time bus system architecture developed by L-3 will be used as an example. This architecture removes the bottlenecks and unpredictability that can plague software-driven systems when applied to complex real-time data acquisition applications. It does this by handling the input, identification, routing, and distribution of acquired data without software intervention.

Introduction

Data acquisition systems come in two generic flavors: software-driven and hardware-driven. As used in this paper, these terms refer to how data is routed through the system (i.e., with software or with hardware). In both cases, the systems are data-driven, meaning that the operations are initiated by the arrival of data as opposed to being scheduled via software. But once the data is acquired, what mechanisms transfer the data from the input modules to the application processes that require the data? How is data input, identified, merged, correlated, routed to different processes, routed to different workstations, sorted, and selected to specific destinations? Are these tasks done primarily with software or with hardware? These questions form the basis of defining software-driven and hardware-driven architectures.

In a software-driven architecture, data movement is controlled by real-time software with hardware assistance from tools like DMA controllers. Data input is handled with software drivers that typically send the data from the hardware to some software distribution process (Data Manager). From here, it is sent to different applications (client processes) using inter-process communication techniques. Hardware can be involved (i.e., DMA controllers, Ethernet ports, etc.), but all data movement and coordination is controlled by, and requires, software processes. The system is still considered data-driven because the arrival of a block of data causes an interrupt to the software, and the software responds to the arrival of the data. But the software still manages most, or all of, the data movement through the system, making the system software-driven.

In a hardware-driven system, data is input into the system, routed to hardware modules and software processes, and sent to other systems ***without*** software involvement during real-time operations. Software is required to set up the data flow process, but is not used during the actual movement of data. Data is acquired, input, identified, routed through the system, and output without software intervention, making the system hardware-driven.

In real-time data acquisition systems, all of the incoming data must be handled as it arrives; otherwise, it is lost. For some applications, a software-driven architecture is completely adequate and appropriate. In other more demanding systems, this may not be the case. Because software-driven systems have inherent bottlenecks and latencies, there are many real-time applications for which software-driven systems are not appropriate.

As the number of inputs increase, as the data rates of the inputs increase, as the number of processes on the data increase, and as the number of clients for the data increase, real-time management using only software to drive the data through the system becomes more complex, more unpredictable, and more unreliable (i.e., non-deterministic). There is a point in complexity and performance where it is necessary to drive the data through the system using more hardware assistance.

This paper examines the two extremes of these approaches. The software-driven approach is exemplified by a standard computer system employing only a single bus for input/out (I/O) module data traffic. The hardware-driven approach is exemplified by a specialized system designed specifically for real-time data acquisition. It employs not only a second bus for I/O module data traffic, but also several other mechanisms for moving and routing data through the system and to other systems and applications.

Typical Software-Driven Data Acquisition Process

A software-driven architecture is the traditional approach to acquiring real-time data. It involves installing one or more data input modules on a computer bus, servicing the input module with the main processor when data is ready, and distributing the data to the client applications requiring the data. These applications include storage, processing, display, and networking.

Figure 1 shows a typical Compact PCI hardware design used for software-driven architectures. In this case, the single board computer (SBC) board and the I/O modules plug into a Compact PCI backplane. The figure shows the main data paths through which acquired data will travel during the acquisition process. It also shows the CPU, memory, and main components, as well as their relationship to the data buses.

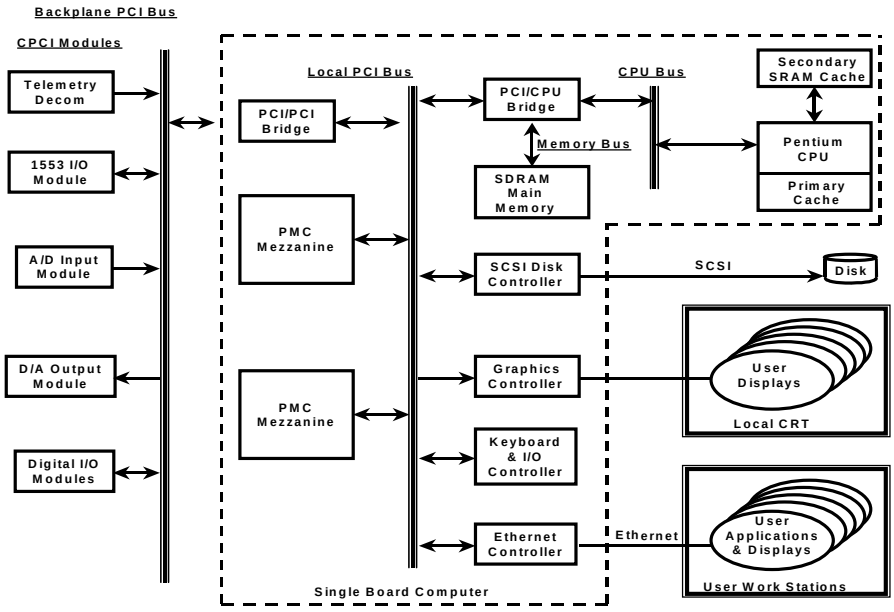

Figure 1. cPCI Hardware Architecture

Figure 2 shows a simplistic view of the software design required to support a real-time data acquisition application and drive the data through the system. Figure 3 shows a more complete, but still simplistic view of the same process. It shows the data paths though which the data must travel for various applications, and it shows the main software components and the interaction paths between them.

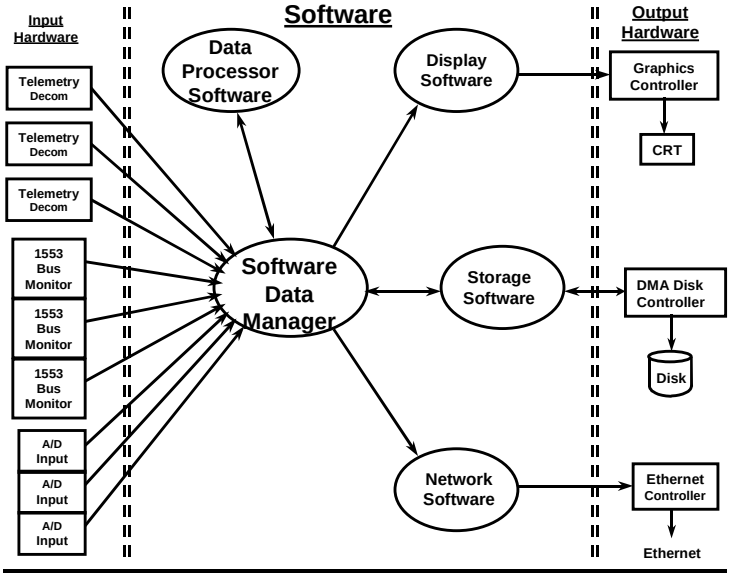

Figure 2. Simple Software Architecture Diagram

What follows is a simplified description of the software process required to support the acquisition of real-time data via a software-driven approach (see Figure 3). The system

can be a standard computer, like a Windows NT-based PC, or it can be a more sophisticated system running a real-time operating system networked to a workstation.

1. Buffer Data on Input Module → Purpose: Collect Data and Reduce Interrupt Frequency

- Collect incoming data in on-board buffer.
- Buffer size is dependent on data rates and desired interrupt frequency.
- Interrupt frequency usually needs to be less than 100 Hz or 10+ milliseconds/interrupt. (This gives latency to the incoming data, with more latency at the beginning of the buffer.)

2. Interrupt Processor and Run Driver → Purpose: Move Data from Input Module to Main Memory

- Assert interrupt when buffer is full while continuing to collect data in second buffer.
- Halt current execution of CPU.
- Save context of current execution.
- Execute Module Driver ISR (interrupt service routine).
- Clear interrupt and schedule Module Driver.
- Execute Module Driver (sometimes at the task level).
  - Get pointer to next memory buffer.
  - Start DMA process.
  - Return to previous execution.

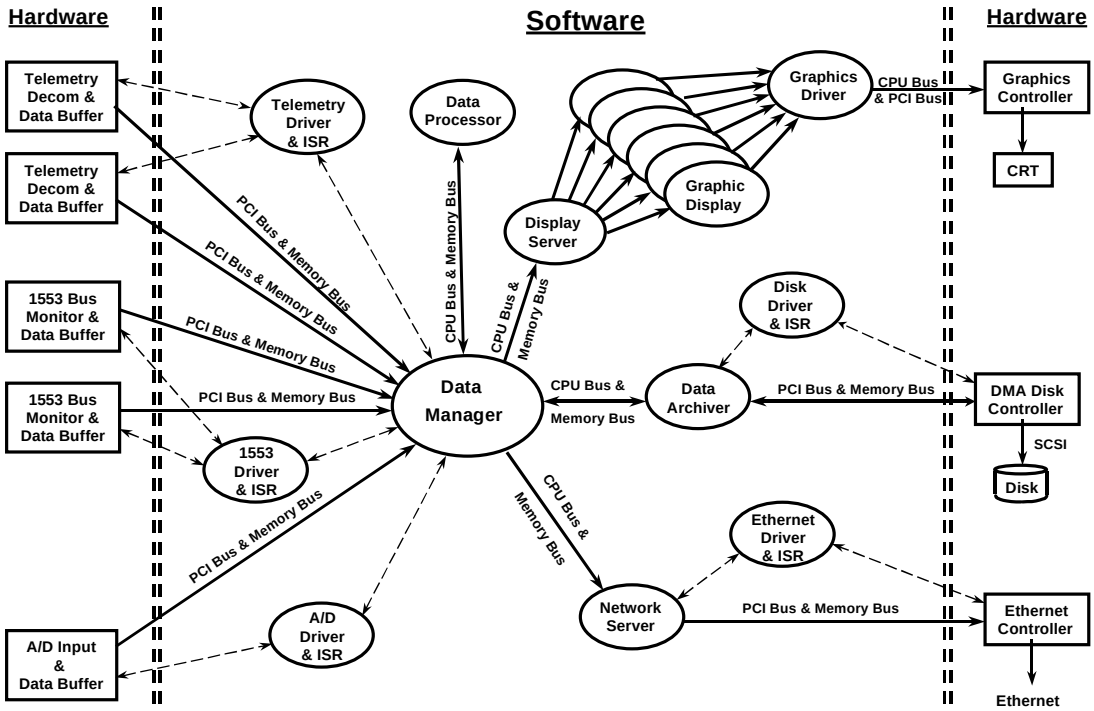

Figure 3. Detailed Software Architecture Diagram

3. Interrupt Processor and Run Driver → Purpose: Notify Data Manager of Arrival of New Data

- Assert interrupt when DMA is complete.
- Halt current execution.
- Save context of current execution.
- Execute Module Driver ISR (interrupt service routine).
- Clear interrupt and schedule Module Driver.
- Execute Module Driver (sometimes at the task level).
  - Send event to Data Manager with pointer to new data buffer.
  - Return to previous execution.

4. Run Data Manager → Purpose: Distribute Data to Client Processes

- Depending on priority of Data Manager relative to other tasks, Data Manager starts execution after previous task is suspended and scheduler starts Data Manager.
- Data Manager reads and identifies new block of data.
- Data Manager searches input lists of all client processes.
- For each client process that wants new data, Data Manager sends an event to each of those processes with a pointer to the new data block. Data Manager increments "use" count for the block for each client that gets the block.
- Data Manager checks to see if previous blocks have been freed by all client processes. If so, Data Manager frees the block for Module Driver to use again.

5. Run Client Processes → Purpose: Display, Archive, Network and Process Input Data

- Depending on priority of each client process relative to other tasks, processes execute one at a time after previous task is suspended and Scheduler starts new process. (This involves a complete context switch to the new process.)
- Client process "copies" its data from Data Manager input buffer to its own memory and decrements "use" count.
- Client process reads ID block of data and searches its list of incoming data to determine what operation to perform.
- Client processes perform their operations on data and then send data to next process or output. (These sometimes involve calls to other drivers, more interrupts, more sending of events to other processes, sending processed data back to the Data Manager, more task switching, more inter-process communication, etc.)

This is the procedure for receiving one block of data from one source. In each step of this procedure, there are caching, virtual memory, context switching, and higher priority tasks to contend with, not to mention other data sources. These tasks contribute to added latency, non-determinism, and lower performance. All processes and data movement must use the same resources (i.e., CPU, PCI Bus, main memory, CPU data bus, etc.). Even with multiple processors, there remain many bottlenecks and resource issues as described below.

Caching

All data and instructions must be in the primary cache for the CPU to access them. If needed data or instructions are not present, they are copied in from the secondary cache or main memory, thereby flushing other data or instructions out. If the data/instructions are still not in the secondary cache, then access from main memory is required, which is much slower.

Virtual Memory

Each software process needs a certain amount of memory for data and instructions. As new processes are started (displays, user applications, etc.), more memory is needed. In virtual memory systems, when more memory is needed than is physically present, the hard disk is used for additional memory. In this case, if the needed data/instructions are not in memory, there is a much greater delay in the processing of a single data block since disk access is also required to complete the operation.

Context Switching

Every time a different process (thread) runs, the system requires a call to the Scheduler, a full context switch, often primary and secondary cache updates, data copying, and sometimes swapping of memory in and out of disk.

Task Priorities

Every process (task) has a priority (at least this is true in real-time operating systems). If the Data Manager or client processes have lower priority than other tasks, they can be preempted or delayed in running. This again adds to non-determinism and lower performance.

Other Data Sources

With multiple data sources, even of the same type, the number of interrupts, calls to the Data Manager, events to the client processes, context switches, etc. multiplies proportionally. However, because of the interdependence of the application, and the contention for resources, the increased loading can be greater than a simple proportional increase and can actually increase exponentially.

Determinism and Predictability

Every time a new display is opened, more processing is required (not to mention the startup time of that process). Every time the user holds down the mouse button, the loading on the system is increased. Every time a data packet or a broadcast packet is received from the network, the loading of the system momentarily increases (including loading on the CPU, loading on the buses, additional processes waiting to run). Every time a data rate changes or a block size changes, the loading on the system changes and the performance of the system changes. The number of interrupts per second, the input data rates, the storage rates to disk, the processing rates on the data, the quantity of data to be displayed, and how quickly data can be displayed are all interdependent and very difficult to determine in a software-driven architecture. Every new input

requires more inter-process and/or inter-processor communication and sharing of the same resources.

Other Factors

Time Stamping of Data

Unless the time source is located on the hardware, it is not possible to accurately time stamp incoming data to better than a few milliseconds. Time stamping can only occur after the Module Driver is called. Normally, a driver talks to its own hardware and no other. Therefore, to get time, it must make a call to another driver (time board) and wait for the time to be returned. This process is subject to all the delays and latencies cited above. In some systems, it is possible to violate this convention, but even when the input module driver reads the time directly, it can still involve tens to hundreds of microseconds' worth of delays and errors. Also, since the data is blocked, time is assigned to the block, not to individual data words. Deriving the time for individual data words can be difficult and requires even more processing resources.

Data Merging, Correlation, and Synchronization

Data arrives in blocks and in time intervals of tens to hundreds of milliseconds. Data from different sources, even when they are of the same type, cannot be easily merged and correlated with data from different sources. Synchronizing events and data becomes difficult, processing-intensive, and usually low in fidelity.

Replaying or Output of Data in Correct Time Intervals

Because data in a software-driven architecture is blocked and driven by interrupts and software tasks that cannot run continuously, it is impossible to output data in the same time sequence and interval in which it was received. This makes it difficult to output acquired data to analog outputs (for strip charts, etc.) or for replaying the acquired data for post-analysis, which requires original timing.

Distributed Applications

Spreading the application across multiple processors or across a network to multiple workstations increases the loading on the front-end acquisition system. The bottleneck of the input section of the software-driven architecture is now further burdened by having to distribute more data to more destinations, while not being relieved of the loading required for servicing the input sources.

Parallel Processing

Parallel processing is difficult because it requires the software to distribute, coordinate, and synchronize the application, all adding to the processing load.

Modularity

Modularity is limited because of the interdependence of the system and the inherent bottlenecks involved. All input modules must interact with other resources of the system. Client processes must know the structure of the data buffers for each input, which must

remain fixed in real time and is different for every input source. Modularity has a very limited definition in a highly interdependent, software-driven architecture.

Expandability

Adding more data sources, increasing data rates, or adding applications that use the data, all impact the loading and throughput of the system. All of these require complicated and detailed analysis and usually require software changes, while still having limited expansion capability. Because of the interdependence of the system, doubling the data rate or number of input sources can more than double the loading on the system and the system's complexity.

Complexity and System Reliability

Because of the interdependence of the software-driven architecture, as more data sources and applications are added, the complexity of the system increases significantly. Determining the performance limits of the system is difficult and usually can be done only through thorough testing with all possible scenarios. Predicting performance limits ahead of time is almost impossible. The complexity and lack of predictability cause system reliability to be questionable when high performance is required. Increasing input sources or data rates compounds this problem.

Development and Maintenance Costs

Development and maintenance costs are often grossly underestimated in software-driven real-time data acquisition systems. Because of the complexity and non-predictability of a software-driven system, budgeting, scheduling, and designing such a system is extremely difficult and takes a great deal of experience. Customers and suppliers, as well as managers and engineers, all tend to underestimate the complexity and unpredictability of a software-driven architecture applied to a high-performance real-time requirement. There is a tendency to over-simplify the problem and assume that one can buy a few off-the-shelf data acquisition modules, install them in a high-end computer, write some glue software for the vendor-supplied drivers, and easily integrate them into the desired application.

There have been numerous cases where the long-term cost of a system was tens or hundreds of times more than the cost of the initial inexpensive COTS hardware. Sometimes the system never does what it was expected, and frequently it cannot be upgraded to do more. Users often spend fortunes in vain attempting to modify their investment to do what it was supposed to do at the outset. The problem is that there are applications where systems just do not have the correct architecture to ever do what is needed. The only answer is to switch to (or start with) a system that is designed and architected for real-time data acquisition; one that does not have the inherent bottlenecks, complexity, and unpredictability of a software-driven system.

Hardware-Driven Architecture

To eliminate the bottlenecks and interdependencies associated with a typical software-driven design, L-3 designed a real-time data acquisition system using a hardware-driven architecture. It was designed to have all those characteristics required to reliably

perform real-time data acquisition from multiple high-speed data inputs of various types. The characteristics of the system include the following:

- Predictable and deterministic
- High-performance
- No bottlenecks and minimal shared resources
- Non-interrupt-driven I/O
- No data blocking, except for storage
- No unnecessary data copying
- Very low latency
- Accurate time stamping of data
- Able to merge, correlate, and synchronize data
- Able to output processed data in correct time sequence (strip charts)
- Simple software interfaces
- No unnecessary inter-process and inter-processor communication
- Supports distributed applications
- Parallel processing and parallel data paths
- Modular, expandable, and reconfigurable

Figure 4 illustrates the basic system design. It shows I/O modules of various types plugged into a high-speed backplane, along with the basic support hardware for processing, archiving, and exporting the data.

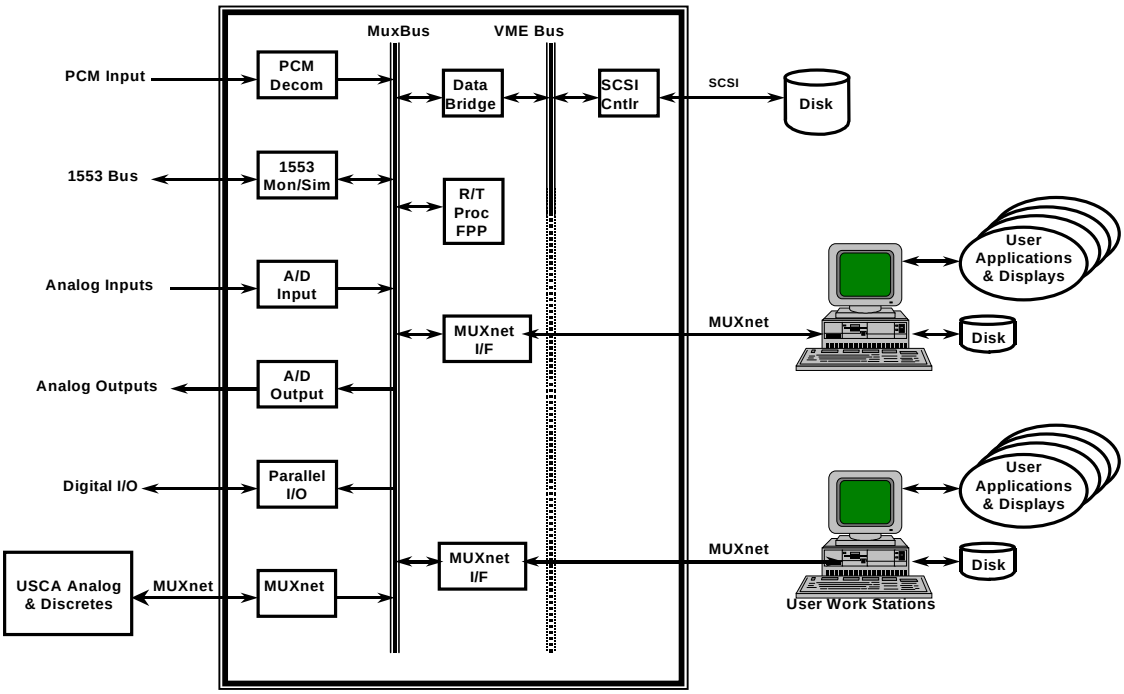

Figure 4. Real-Time Hardware-Driven Distributed Architecture

Figure 5 illustrates the data flow and software design of the hardware-driven architecture. Note the minimal software required to drive the data through the system. The only data path requiring software support is for high-speed storage to disk. But in this case the driver only sets up the DMA process on the disk controller; it never touches the data. The data is transferred to the disk without any other software involved, and all data transfers between the Data Bridge and the disk controller are handled via hardware.

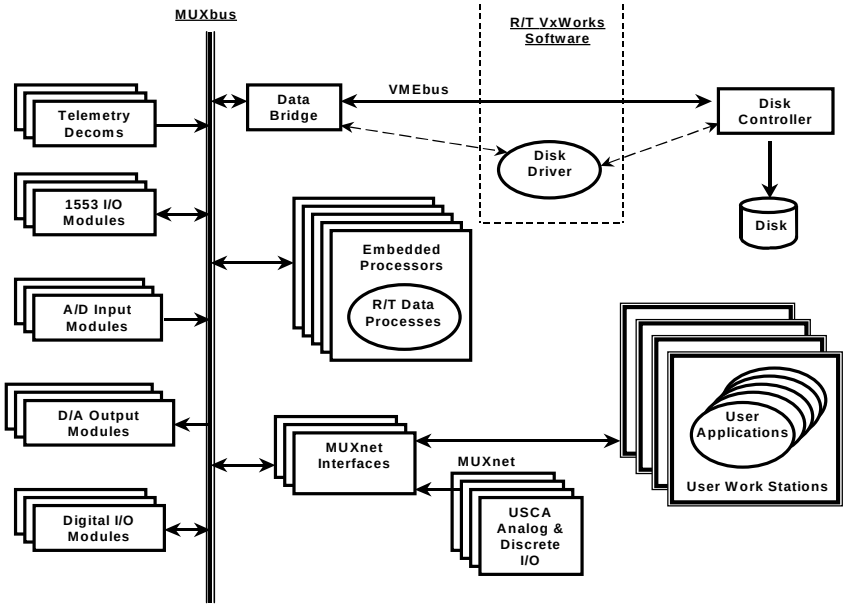

Figure 5. Hardware-Driven Architecture

The system's data acquisition process is described below:

1. Input module acquires and outputs data to the high-speed backplane (MUXbus) one sample at a time.

- Each data measurement to be received by an input module is assigned a 16-bit ID tag.
- When a data word is received, the input module immediately requests an output cycle to the MUXbus.
- With a guaranteed maximum latency of one microsecond, the data is output to the MUXbus with the 16-bit ID tag.
- Input modules do not buffer input data. Data is identified and output to the MUXbus when it is received by means of hardware only and no software interaction.

2. The MUXbus broadcasts the data to all I/O modules on the bus.

- Using a broadcast mode, the MUXbus broadcasts the data word to all modules in the system on the same bus cycle on which it was received by the input module.
- The MUXbus uses a rotating priority arbitration, which guarantees every input module between 1M and 8M output cycles per second, depending on how many other input modules are in the system. Each input module receives 1/N of the 16M cycle/sec MUXbus, where N is the number of input modules.

- Each data word occurs on the MUXbus only once. In that one cycle, the data word is received by all receiving modules taking data from the bus. These receiving modules include embedded processors (FPPs), a data bridge to the VMEbus, MUXnet (real-time network) I/O modules, analog and digital output modules, as well as many others. Multiples of each of these modules can be present without any change in MUXbus performance.

3. Each MUXbus receiving module inputs only the data it needs from the MUXbus.

- All receiving modules have hardware-decoding RAMs for selecting which data words to take off the MUXbus. These RAMs are programmed to select only those data words needed by the module.
- The modules compare the ID tag of the data word with the contents of its tag decoder RAM, and, if there is a match, the data is input into the receiving module's input FIFOs.
- The data is immediately processed by the receiving module. Output modules, like the Parallel I/O and MUXnet I/O, output the data immediately without any processing. Other modules, like the FPP and the A/D module, process the data immediately.

4. Embedded processors (FPPs) perform real-time processes on the data.

- The FPP constantly monitors its input FIFO for new data. It is not interrupt-driven and does not wait for more than one data word to arrive before it starts processing.
- For performing real-time processes, the FPP vectors immediately to the algorithm needed by the data word that was read from its input FIFO.
- As soon as the data word is processed, it is output back to the MUXbus with a new 16-bit ID tag.
- The FPP contains canned algorithms, like EU conversion, limit checking, bit manipulation, etc. It can also be programmed with user algorithms written in C.
- Multiple FPPs can be installed in a system. The existence of an FPP has no impact on the performance of other FPPs. This provides an efficient parallel processing environment with a linear increase in computing power as additional FPPs are added.
- FPPs can perform different processes on the same data words, or the same/different processes on different data words.
- All data routing to and from FPPs is handled in hardware, with no software intervention.

5. Embedded processors (FPPs) collect data for network distribution.

- FPPs are also used to collect data for distribution on Ethernet, FDDI, or ATM.
- One sample, all samples, or a statistical sample is collected for each data word needed by the network.
- The real-time (VxWorks) VME CPU periodically reads the data from the FPP.
- The VME CPU outputs the data directly to the client processes on the network.

6. The Data Bridge buffers data for storage.

- The Data Bridge has its tag decoder RAM programmed to collect those data words that are to be archived to disk.
- For efficiency and performance, the Data Bridge buffers data in a 4-MB RAM FIFO.
- When 2 MB of data have been collected, the Data Bridge interrupts the VME CPU.
- The VME CPU programs the SCSI Disk Controller to read the 2-MB block from the Data Bridge to the disk.
- The SCSI Controller then DMAs the data directly from the Data Bridge to itself across the VMEbus and out to disk.
- The sustained data rate to disk is 36 MB/sec and is independent of the number of input, output, and processing modules required by the system.

7. The MUXnet Module outputs data words directly to external workstations and PCs.

- The MUXnet Module is typically set up to collect all data on the MUXbus.
- When the data word and ID tag are received from the MUXbus, they are immediately output on the MUXnet. No processing or network protocols are involved.
- Latency from the MUXbus to the MUXnet Receiver Module of the workstation is about
  1 microsecond.
- The receiving workstation can filter the data with its own on-board tag decoder RAM for input into its local FIFOs, or it can read the most recent value of any desired data word in the Current Value Table of the MUXnet Receiver Module.
- Using the MUXnet Output Module, data can be distributed in real time to an unlimited number of workstations over distances up to several miles.
- MUXnet is a bi-directional interface, so workstations can also output data back to the MUXbus.
- The MUXnet Module handles all I/O in hardware; no software is involved. The number of MUXnet modules in a system, or the number of workstations connected to MUXnet, has no impact on the performance of other modules.
- The MUXnet eliminates all bottlenecks in distributing real-time data to real-time applications running on a distributed network.

Figure 6 illustrates a high-end data acquisition system with multiple types of inputs and with multiple client workstations and applications. Because data movement in the system is hardware-driven and independent of software, the components of the system operate independently. This makes the system extremely predictable and deterministic. The storage rate to disk is 36 MB/sec, independent of the number of input sources, types of input sources, number of output destinations, number of embedded processors, etc. The storage rate is always predictable because it is independent of software and other hardware modules.

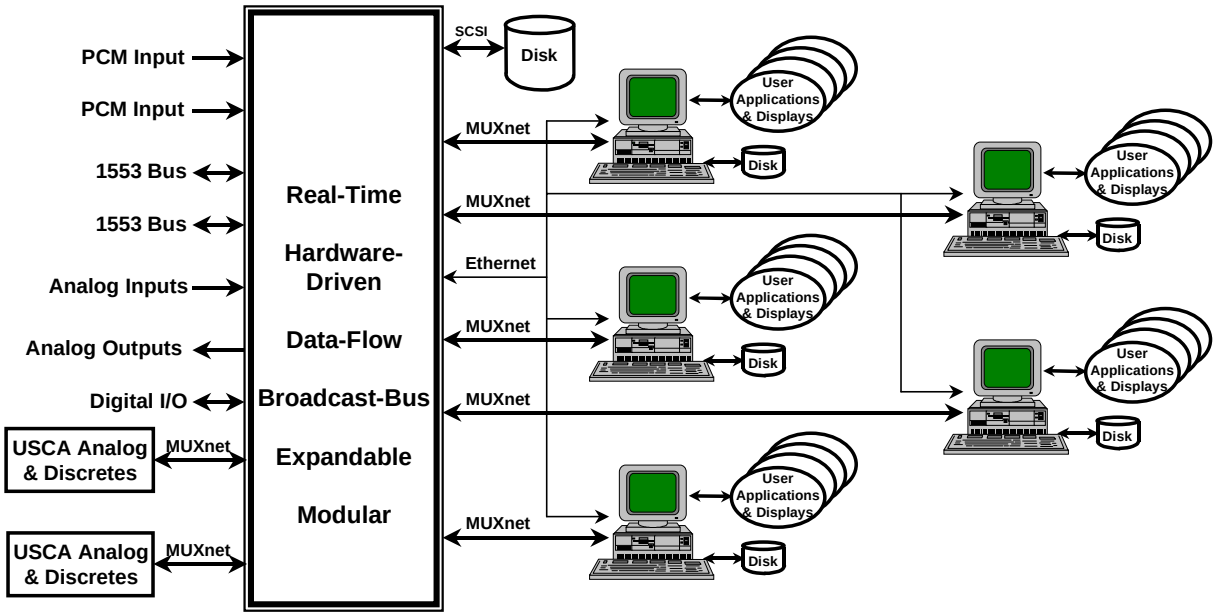

Figure 6. High-End Data Acquisition System with Multiple Data Sources and Client Workstations

Likewise, one input source has no impact on another input source, and destinations for the data have no impact on the input sources. Input sources require no software for identifying the data and placing it on the broadcast bus. Input sources also need no knowledge of the destination of the data, thereby completely decoupling them from any interaction associated with where the data is going. Modules that receive the data need not know where the data originated, or the format in which the data was buffered. Receiving modules only need to know the ID tag of the data, thereby decoupling them from the input sources.

The only shared resource is the MUXbus itself, which is extremely predictable. It provides 16M data samples per second, with all input modules guaranteed an equal share of the bandwidth. All of these factors combine to make the system predictable, deterministic, flexible, and very high in performance.

The system also provides for other features. The MUXbus automatically merges and time correlates data because each data word is immediately identified and broadcast onto the MUXbus as soon as it is received, with an overall latency on the order of one microsecond. This allows the data to be accurately time stamped in hardware as it

arrives on the MUXbus. Since the data is not blocked, the merged data from all sources can be played back from the hard disk in the same time sequence and time intervals as it occurred in real time. This enhances post-processing and playback to strip chart recorders.

Conclusion

The independence of the input, output, and processing modules, with no required inter-process communication, makes hardware-driven systems very modular and makes system software very simple. If new capabilities or higher rates are needed, the required modules can be added with known results and without added complexity. As new modules are required, the impact on the system, and the added performance are predictable. Parallel processing, parallel data paths, and distribution of data to other systems is easily accomplished with deterministic results.

These factors permit configuring a system that can be easily matched to almost any application's requirements. Because of the modularity and independence of modules, various configurations are made with no change to software. This provides for low-risk and cost-effective solutions for many real-time data acquisition applications. It also lowers the cost of future upgrades and long-term support.

In summary, for high-performance and/or complicated real-time data acquisition requirements, a system with a hardware-driven architecture eliminates the bottlenecks and unpredictable performance of conventional computer designs for real-time applications.

Auto-adaptative Software for automatic screening of massive Numerical Signals Data Bases

Robert Azencott
Miriad Technologies
Paris, France

Abstract

This communication presents Miriad DataScan, a new auto-adaptive software dedicated to automatic anomaly detection on high-rate recorded signals. Ease of use and fast learning ability focused on sophisticated curve shapes memorization and discrimination are the main features of *MdScan*™. Typical applications to Test flight Data analysis are described (collaboration with Dassault, Aerospatiale-Airbus, CNES-SEP).

Introduction

Miriad Technologies is a Paris based high tech start-up company created in 1998 by Robert Azencott and Alain Mamou-Mani. In 1999, the company raised 2.5 million $ in venture capital to commercialise new auto-adaptive software dedicated to Operational Data Analysis.

Miriad DataScan (*MdScan*™) is a generic software dedicated to automatic anomaly detection on high rate recordings of signals by systems of sensors. *MdScan*™ is the first of a suite of software products to be launched by Miriad Technologies in 2000.

In this paper, we present an overview of three recent evaluations of *MdScan*™ for test flight data analysis. These evaluations were conducted in collaboration with Dassault, Aerospatiale-Airbus, and CNES-SEP.

MdScan : a generic software for anomaly detection

1. The challenge of automatic anomaly detection :

Visual scanning of bench tests data for rocket engines, or telemetry data recorded during test flights constitutes an essential but painstaking task for trained engineers in charge with test data analysis.

Quite often, anomaly detection by a human expert is based on his trained visual memory of similar signals, so that potentially abnormal signal patterns are implicitly compared to the thousands of normal patterns he has observed in the past.

After this preliminary visual detection of potential abnormalities, the human expert will proceed with a second task, namely the certification of detected abnormal event, by patient methodical cross-correlations across the whole system of sensors, and sophisticated technological reasoning.

For *MdScan*™, one of the basic challenges was to emulate the flexibility and the auto-adaptability of the human eye for visual detection of abnormal patterns.

A startling ability of human vision is of course the very fast (and almost unconscious) memorization of geometric shapes.

This type of unsupervised on-line "learning" of the typical geometric patterns present on a recorded signal is one of the crucial technological barriers overcome by the software *MdScan*™.

2. The intrinsic limits of standard artificial neural networks :

In the past 15 years, computer scientists all over the world have intensively investigated the learning ability of artificial neural networks, in particular to automatically train "neural" pattern classifiers.

Many neural networks architectures have been tested in this context, the most popular being the multilayer perceptrons. Standard "training" of multilayer perceptions, usually implemented by the celebrated retro-propagation rule, requires first the availability of a training data base of signal partners, explicitly divided into normal patterns and abnormal patterns.

To be reliable, this type of automatic learning definitely requires to have a sufficiently high proportion of abnormal patterns in the training data base, to achieve good generalization ability for the neural classifier.

In general this situation is not realized for engine bench tests or test flight analysis, where abnormal events are fairly rare. Hence in the conception of *MdScan*™, we had to go beyond standard neural networks technology.

3. The intrinsic limits of standard data mining techniques :

Commercialized data mining approaches for detection of abnormal data often rely on standard statistical modelization of observed data. These statistical models are typically assumed to be gaussian, which leads to linear discrimination techniques.

In the world of curves indexed by time (data flows recorded at high rates), we deal with very high dimensional data, and statistical modelization of data is confronted with the so called "curse of high dimensionality".

Theoretical statisticians have clearly identified this technological challenge: the number of actual observations needed to estimate reliably a probability density for sets of K-dimensional observations grows exponentially with K. Moreover, typical curve patterns distributions are often highly non gaussian. Thus to create *MdScan*™, we had to develop an original point of view, to break trough the barrier of high dimensionality in stochastic models.

4. The MdScan philosophy :

One of our guidelines in the conception of *MdScan*™ has been the emulation of the main human vision strategies for fast shape identification. According to a widely accepted point of view, the early stages of the human vision process involve thousands of natural filters analogous to "wavelet filters", and information content criteria are quite essential to control the human memorization of elementary shape descriptors. The radically new approach of *MdScan*™ thus combines multi-scale

wavelet coding of the signals, with information content filtering, and fast adaptive compressions to automatically create highly compact sets of pattern descriptors.

Information theoretical criteria are then systematically applied to create efficient auto adaptative discrimination between abnormal events and the bulk of standard patterns. A natural by-product of the *MdScan*™ techniques is a powerful and fast identification of anomaly types. This last functionality is of particular interest to identify undesirable noise sources in acoustics data analysis.

The technological advances and concepts of *MdScan*™ are protected by a pending patent.

5. The functionalities of MdScan™ :

5.1 The software *MdScan*™ offers a bank of ready to use autoadaptative anomaly detectors, designed to cover a broad range of anomaly types, including for instance sudden spectral fluctuations, burst of spectral energies, unusual spectral rays, unexpected signal jumps, abrupt trend changes, shocks and bumps, etc…..

The autocalibration principle implemented for these *MdScan*™ detectors is essentially “one-shot learning”, where one single fast scan of a large segment of the available signal is enough to automatically learn the main signal characteristics. To complete the calibration, the user can specify a rarity threshold (or an intensity threshold) for the anomalies to be detected, as well as an anomaly duration range . Explicit examples of abnormal events are not required during autocalibration but if available, they will be taken into account. Detected anomalies can be automatically displayed on screen, edited to print reports, or exported towards other data bases.

A configuration module facilitates the selection of detectors to be applied to each sensor.

5.2 *MdScan*™ 1.0 is the first release of our *MdScan*™ software suite.
MdScan™ 1.0 runs off-line, on standard PC workstations (minimal configuration 128 Mo, 350 Mhz) under Windows NT.
MdScan™ 1.0 can typically handle and display 30 to 40 sensors.

Standardized installation procedures provide easy implementations of adequate access interfaces between *MdScan*™ 1.0 and the data base of the user (within the range of standard protocols such as ODBC, ORACLE,…).

In configuration mode *MdScan*™ 1.0 offers an interactive graphic environment where the user can very easily select the sensors to be monitored by *MdScan*™, and specify the types of *MdScan*™ detectors to be applied to each sensor. For each selected pair (sensor, detector) the user may freely specify a level of intensity (or of rarity) to filter the detected anomalies.

In “detection mode”, *MdScan*™ 1.0 can then launch off-line the massive data scanning just specified with the configuration module.

First a fast prescan of actual sensors data autocalibrates the hidden parametres of all selected detectors. Then anomalies are automatically detected, graded, and localized on all the sensors selected at configuration stage.
Visual inspection of the detected anomalies is immediately available.

Facilities are provided to quickly edit and print summary reports, or to export the actual results for later uses.

Typical off-line anomaly detection on a sensor recorded at 1000 Hz requires a computing time roughly comparable to acquisition time.

6. Evaluation of MdScan™ performances on Aerospace applications

6.1. Rocket engine test data

In collaboration with CNES and SEP we have tested early version of *MdScan*™ on launching data recorded on the ARIANE 5 engine .

The goal was to automatically detect undesirable very slow oscillations on continuous recorded signals

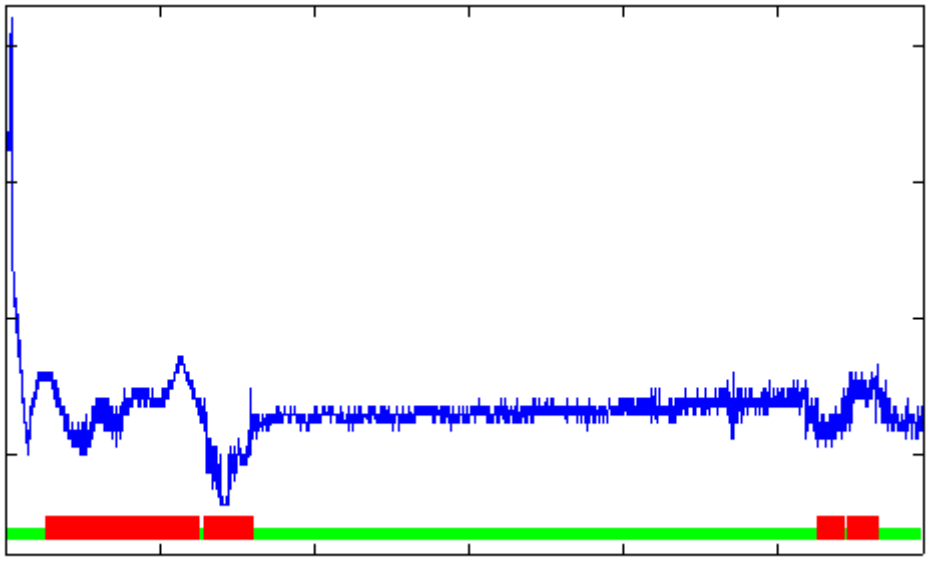

6.2. Test Flight Data (Vibrations)

With the Test Flight Data Exploitation Center and the DPR of DASSAULT AVIATION, we conducted a preliminary evaluation for *MdScan*™, on 20 vibratory signals, recorded during Rafale test flights at roughly 1000 Herz.

One shot learning and subsequent detections of unexpected special fluctuations were quite successful.

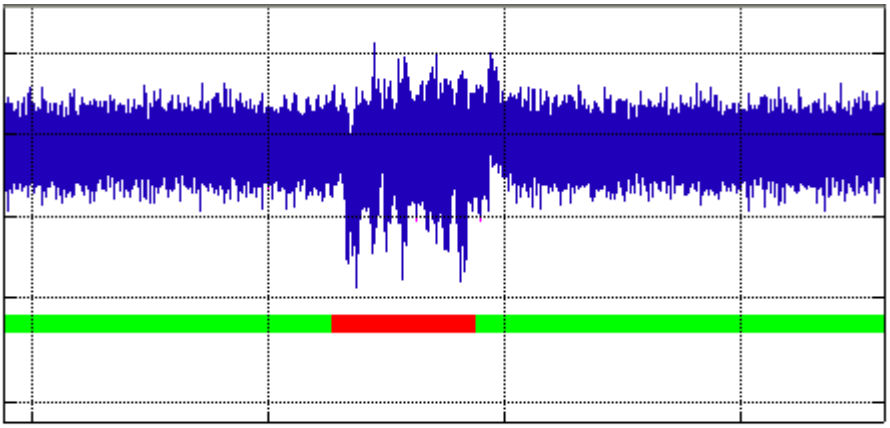

6.3 Test Flight Data (Acoustics)

Several successful validations of *MdScan*™ (Beta version) were conducted with the Test Flight Data Center of Aerospatiale-Airbus at Toulouse.

The goal was the automatic detection and identification of undesirable noise sources on Acoustics Data recorded on flight by 8 microphones, with a frequency range of 100Hz to 20.000Hz.

A library including a few examples of each undesirable noise source was available in this application.

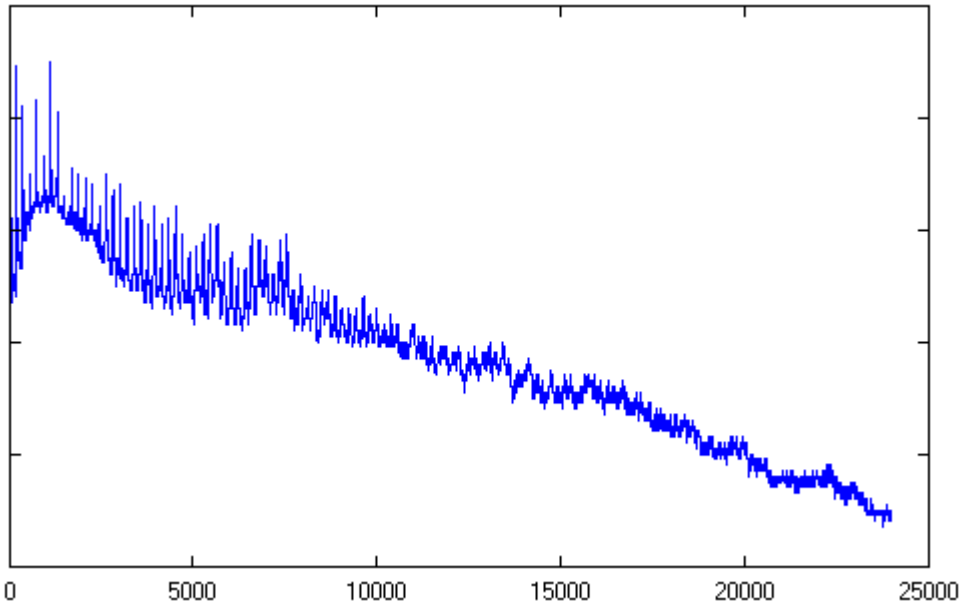

7. Potential applications of MdScan™

In the Aerospace Industry, *MdScan*™ should become a highly efficient generic software tool to reduce the workload of expert engineers in charge with test-flight Data Analysis, or bench test engine data. Vibratory signals, Continuous signals, Acoustics signals can be handled.

Systematic off line anomaly detections on commercial flight data can be a powerful add-on for anticipative maintenance programs.

In the automotive or railway industries, *MdScan*™ can be applied to anomaly detection on Bench Test Engine Data.

Early diagnosis of engine problems due to automatic anomaly detection on vibratory or acoustics data is also a potential. *MdScan*™ application.

In the manufacturing industries (Chemicals, Pharmacy, etc…), automatic anomaly detections on process data recorded during batch production, can provide early warnings for batch quality evaluations.

Realtime Visualisation of Target Telemetry

Peter G. Brown and Owen Hesford
T & E Ranges Telemetry Facility

Defence Evaluation and Research Agency,
Aberporth, Ceredigion, United Kingdom
(abetele @ dera.gov.uk)

Abstract

With the increasing complexity of target telemetry and customer requirements for multiple missile-target scenarios, the traditional telemetered data display no longer lends itself to easy assimilation by an observer. A solution is presented using techniques developed for synthetic environments that rely on a commercial off-the-shelf (COTS) package running on a PC-based system. This incorporates all current data in an easy-to-view form while retaining considerable potential for expansion.

Introduction

Due to the inherent dangers of testing missiles against manned target aircraft an unmanned drone, the *Jindivik* (Aborigine for 'The Hunted One'), was initially designed by the Australian and British Governments in 1948 and has since been under continuous development. This jet-powered aircraft is radio-controlled and flown by two pilots in control cells on the airfield. All aircraft parameters are telemetered back to the target base in real time as well as front- and rear-facing television pictures. As each Jindivik costs over £1m it is not generally practical to use the aircraft itself as the target: each aircraft carries two towed targets which can be streamed behind the main body at distances of up to 500 feet (150 metres). These tows can be either semi-active radar targets (SARTs) or infrared (IR) flare packages.

SARTs were developed to present a larger radar signature than the Jindivik, so any radar-controlled missile would choose the SART in preference to the more expensive Jindivik. Each SART can simulate a number of different types of aircraft by varying the apparent radar cross-section. Early SART trials resulted in a number of Jindivik losses and the customer wanted to know why the missile was locking on to the Jindivik and not the SART. To determine this, SART parameters were sent along the tow cable to the Jindivik telemetry sender and transmitted with the main Jindivik telemetry. By monitoring these before firing the missile, the customer could be confident that the missile was locked on to the SART and not the Jindivik.

History

Up to the last few years, the most prevalent model of Jindivik was the Mark 3, or 700 Series. This model, although it carried two tows, only had the ability to stream a single tow. Therefore, for the average trial the customer would have to monitor about six parameters from the Jindivik and a similar number from the tow. The Jindivik telemetry transmitter is a pulse amplitude modulation type (PAM), i.e. an analogue sender. The telemetry frame consisted of a 24 channel histogram in which some channels contained information relating to the tow, some to the Jindivik and some required only by the pilots

who were relying on this telemetry to fly the aircraft. Initially this histogram was displayed on an oscilloscope triggered by the synchronisation pattern of the sender resulting in the tow channels always appearing in the same place on the screen (figure 1).

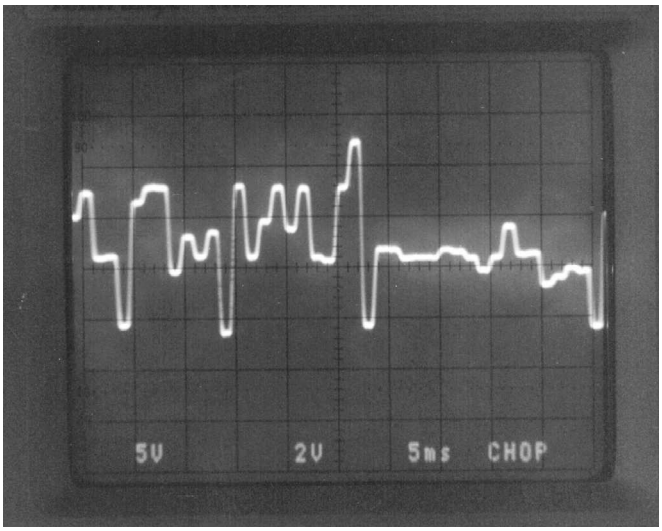

Figure 1 – Mark 4 Jindivik histogram

The customer could then mark these places, observe changes in the channel and deduce the object of the missile lock and the state of the tow. The SARTs used with Mark 3 Jindiviks could be in one of five states, so the channel displayed on the oscilloscope had five possible levels. This method, while tolerable, was not ideal and led to a substantial amount of irrelevant information cluttering the customer's view. A solution was created whereby the required channels were located in relation to the synchronisation pattern, separated out then re-multiplexed and fed to the oscilloscope (figure 2). This reduced the background clutter and left only essential information on the screen, though the representation was necessarily qualitative.

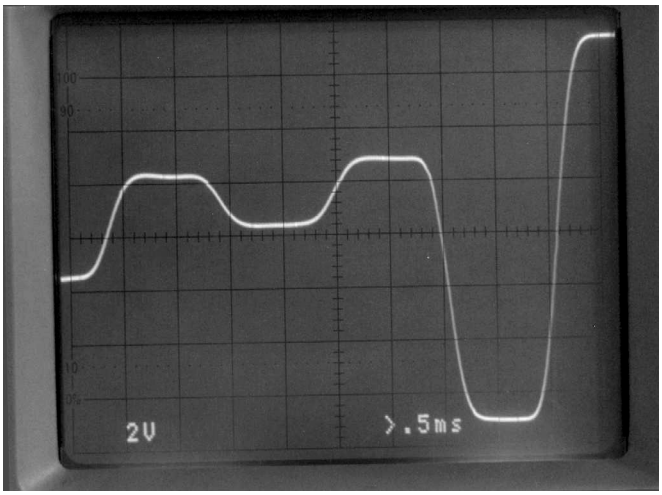

Figure 2 – Remultiplexed histogram

The Mark 4 (or 800 Series) Jindivik was introduced with the enhanced ability to stream two tows simultaneously. The telemetry frame had also altered with this model and now contained 48 channels. The next incarnation of display used a PC-based

decommutator, and displayed the channels in iconic or numeric form, which made visualisation of the target a great deal simpler (figures 3 and 4).

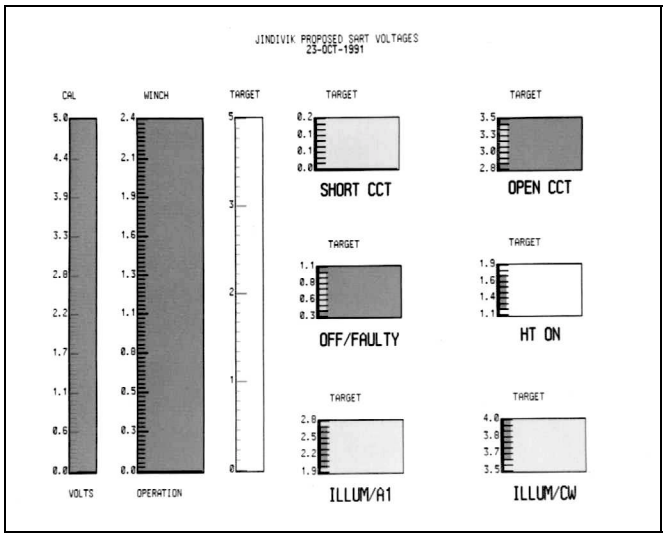

Figure 3 – Mark 3 Jindivik icon display

It then became necessary to fly two Jindiviks each streaming a tow, leading to two sets of icons to be monitored before and during a trial. This increased the complexity of the customer's task in assimilating the displays, but was still within the bounds of possibility because a separate decommutator handled each Jindivik and the information was displayed on different screens. There was no change in the design of the SARTs at this time. Production of the Mark 4 ceased in 1986 and the current production model is the 900 Series, which is a pulse code modulation (PCM) sender. This is not currently operational within DERA and as such is not part of this project.

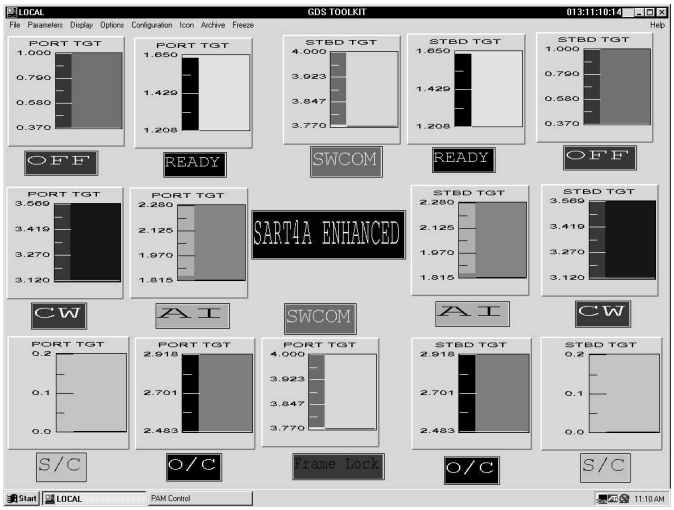

Figure 4 – Mark 4 Jindivik icon display

An enhanced SART has since been developed that doubles the number of possible states to 10. Hence ten icons per tow, two tows per Jindivik, and possibly two Jindiviks... The limit to customer assimilation of data was reached with the introduction of the SARTIP: a third, non-deployable SART mounted on a wingtip. This had five possible states and behaved just like a SART. With this addition, there is a maximum of

50 icons to be watched and checked pre-firing; any one of these icons being out of limits at any moment of the trial could cause an immediate abort for safety reasons. To assimilate such a number is beyond what can reasonably be expected of an observer under normal circumstances, and a new approach is required.

The Concept

When it was realised that the quantity of telemetered data was becoming excessive, a means was sought to present the data in a more manageable form. At this time, our primary customer suggested that if modifications to the display were to be made, they would like to see Jindivik attitude information incorporated. This is desirable because at certain attitudes of turn, the aircraft body masks the transmitting aerial from the receiving site, and it is not always obvious that this is the reason for loss of telemetry. Research into this topic found that other groups within DERA were using a third-party, commercial off the shelf (COTS) package called RealiMation to visualise data in an animated, synthetic-environment-based form. These methods are currently used by (among others) DERA Boscombe Down for black-box flight recorder visualisation and DERA Aberporth Data Analysis Facility for full-scenario post-trial information. Having examined their work and discussed the issues with the software company, it was decided to use this product for our application, thus keeping compatibility with these other groups and maintaining a knowledge base within the sector. It is worth noting that this is the first *realtime* use of visualisation for trials telemetry data within DERA.

As discussions progressed it was decided to dispense with the use of icons, and to display all information on the animated Jindivik image. Thus, tow states are indicated by a text box attached to the tow in question (in the manner of “Tooltips” in Microsoft Windows). The only telemetry parameters to be displayed away from the Jindivik are height (from an onboard radar altimeter) and airspeed. IRIG time is also displayed with these parameters, though it is fed by the Central Timing Unit and is not a true telemetry parameter. All these are displayed in text boxes at the top of the screen.

The Application

The majority of Aberporth’s target telemetry capability is based around PC-based decommutators. These distribute telemetry data locally within the telemetry bay and via an Ethernet link to a pair of client machines in the Operations building. In order to prevent unnecessary loading of the decommutators a separate machine is required to run the RealiMation application. As the two main decommutators are already broadcasting Ethernet packets to the two client machines in Operations, it seemed sensible to add another packet to the broadcast that would be picked up by the RealiMation machine. Ethernet broadcast was chosen over IP-addressing so that if another RealiMation machine is required, it can be simply plugged into the hub and it will begin receiving data immediately. It is foreseen that when this application is operational several facilities within DERA Aberporth may request sight.

The format of the Ethernet broadcast packet is shown in Tables 1-3. Analogue data are allocated words in the main packet and digital data are grouped according to their source (port tow, starboard tow, Jindivik) and stored in a sub-packet. The RealiMation software interrogates the packet and drives the display accordingly. To minimise confusion when twin tows are deployed, tow information is displayed beside the tow to which it pertains and is colour-coded red or green depending on the tow.

Size in bits	Description
16	Counter increments on each packet
16	Number of sub-packets in this packet
	--- First sub-packet ---
8	Number of bytes in this sub-packet
8	Sub-packet identification
32	Port tow flags
32	Starboard tow flags
32	Jindivik (including SARTIP) flags
32	Height
32	Pitch
32	Roll
32	Yaw
32	Airspeed
64	Time (integer in microseconds)

Table 1 – Main packet structure (including one sub-packet)

Value	Description
0	Sub-packet refers to Jindivik #1
1	Sub-packet refers to Jindivik #2

Table 2 – Sub-packet identification values

Bit number	Description
0	Illuminated AI
1	Illuminated CW
2	Illuminated ILL
3	Short circuit
4	Open circuit
5	Unserviceable
6	On
7	Switching
8	Fire flare
9	Tow OK
10	Mode 1
11	Mode 2
12	Mode 3
13	Switching command
14	Ready
15	Winch active

Table 3 – Port, starboard and Jindivik flags

One problem was discovered in identifying whether a winch is active. Winch activity is indicated by one channel describing a rapid square wave between minimum and maximum values, which obviously has to be processed to provide a steady logical 1, otherwise the winch behaviour will be absurd. The criteria for choosing a method of processing (there were obviously several operations possible to reduce a periodic waveform to a steady state) were that such an algorithm must be mathematically swift and simple to implement on the decommutator. A time average was chosen as fulfilling both these points. Winch activity is monitored in blocks of 1.2 seconds and averaged. If the winch is inactive, the winch channel will be either high or low and the average identical. If the winch is active, the winch channel will be varying equally between high and low and the average will be set at the halfway point. A logical comparison is then performed: if the average is above or below the halfway mark, the winch is deduced to be inactive.

Figure 5 – The RealiMation Application

The Future

This is a tool with vast implications for both realtime trial visualisation and synthetic trial simulation. Aberporth Telemetry, during a firing trial, has the capability to monitor two missiles and two Jindiviks. The missile decommutators could easily be modified to broadcast missile telemetry to the RealiMation computer. Neither Jindivik nor the majority of missiles sends positional information, so visualisation of a full scenario would require external input of position for both vehicles. Positional data for all relevant airborne objects is distributed throughout the range via RS-232 protocol from all Time-Space Position Indicators. There is no obstacle to accepting serial data into the RealiMation computer and using it to position Jindivik and missile relative to each other and to the range surveyed datum point.

By telemetering 1553 avionics bus data the possibility of adding the firing aircraft into the scenario becomes very real. If this occurs, DERA T & E Ranges Telemetry will be able to provide a visualisation of the entire trial *in realtime* from any perspective the customer desires. A virtual camera could be provided in the fighter cockpit, and aircraft parameters could be displayed, in a cockpit layout if necessary, thus giving the same view as the pilot to the observers on the ground. A virtual camera could be attached to the missile and follow it throughout its flight (seeker look angle could even be incorporated here).

Once a number of trials have been performed with this tool, there is no reason why its data cannot be incorporated into a simulation – after all, data for fighter, missile and target will reside in one place. If the fighter data is replaced with a pilot in a simulator, the target can be driven by any of the previous, *real*, flight patterns and the missile could be driven by a statistical estimate of its behaviour based on previous firings.

Conclusion

Although this is the first version of the application and refinements are obviously possible, there has been a significant reduction in screen clutter and an increase in presented data. It is believed that this tool has great potential and can benefit our customers both present and future.

Acknowledgements

The authors wish to acknowledge the contributions of Apollotek Ltd. (Sunbury, UK) and RealiMation Ltd. (Derby, UK) in the design and integration of the visualisation tool.

Any views expressed or implied are those of the authors and do not necessarily represent those of DERA, MOD or any other UK government department.

TEDAS II - High Speed Data Acquisition, Storage and Distribution

Bernd Gelhaar
Institute of Flight Research, DLR
Braunschweig, FRG

European Telemetry Conference
Garmisch-Partenkirchen 22.05.-25.05.2000

1 Abstract

This paper describes the development of the measurement system for the rotor test stand of the Institute of Flight Research. The different topics like sensors, instrumentation, analog-to-digital conversion using delta sigma converters and real time high speed data distribution and storage are covered. A layer based model will be described consisting of data acquisition, collection storage and distribution. According to this layer based model the new system is under development. Its parameter and specifications are discussed. The system will have 512 channels of 24 bit resolution, 100 kHz sample rate each. Thus the sum data rate will be about 100 Mbytes/s being subject to be stored and distributed in real time. Finally the current status of the system and future plans will be discussed.

Dieser Beitrag beschreibt die Entwicklung der Meß- und Datentechnik des Rotorversuchs-standes des Instituts für Flugmechanik des DLR. Es werden die verschiedenen Entwicklunstadien bis zum heutigen technischen Stand erläutert. Hierbei wird auf die verwendete Sensorik, die Analog-Digital-Wandlung mit Delta-Sigma-Wandlern sowie die Problematik der Speicherung und Verteilung der gewonnenen Daten eingegangen. Aufbauend hierauf wird das zukünftige Schichtenmodell für Erfassung und Bündelung sowie Verteilung und Speicherung der Meßdaten diskutiert. Danach wird das in Entwicklung befindliche Upgrade der Meßdatenerfassung in seinen technischen Anforderungen und Parametern erläutert. Abschließend wird der momentane Stand dargestellt und ein Ausblick auf die Zukunft gegeben

Keywords: Delta sigma converter, high speed data acquisition, high speed data recording, high speed data distribution, real time data distribution, rotor test stand, fibre channel, wind tunnel.

2 Introduction

Since 1973 DLR operates rotor test stands for wind tunnel experiments. Using this technology mach number scaled down models are tested and characterized. The results are used for research purposes as well as for industrial customers in order to perform optimization of efficiency, reduction of noise and reduction of vibration [1,2,3]. The scaling factor of the rotor model is 1:2.5 . The rotational speed is scaled up in the same ratio in order to get the same mach numbers at the blade tips compared with the original. This leads to 2 m diameter of the rotor and a speed of 1050 rpm. The test stand falls into the following components (Fig. 1, Fig. 3) :

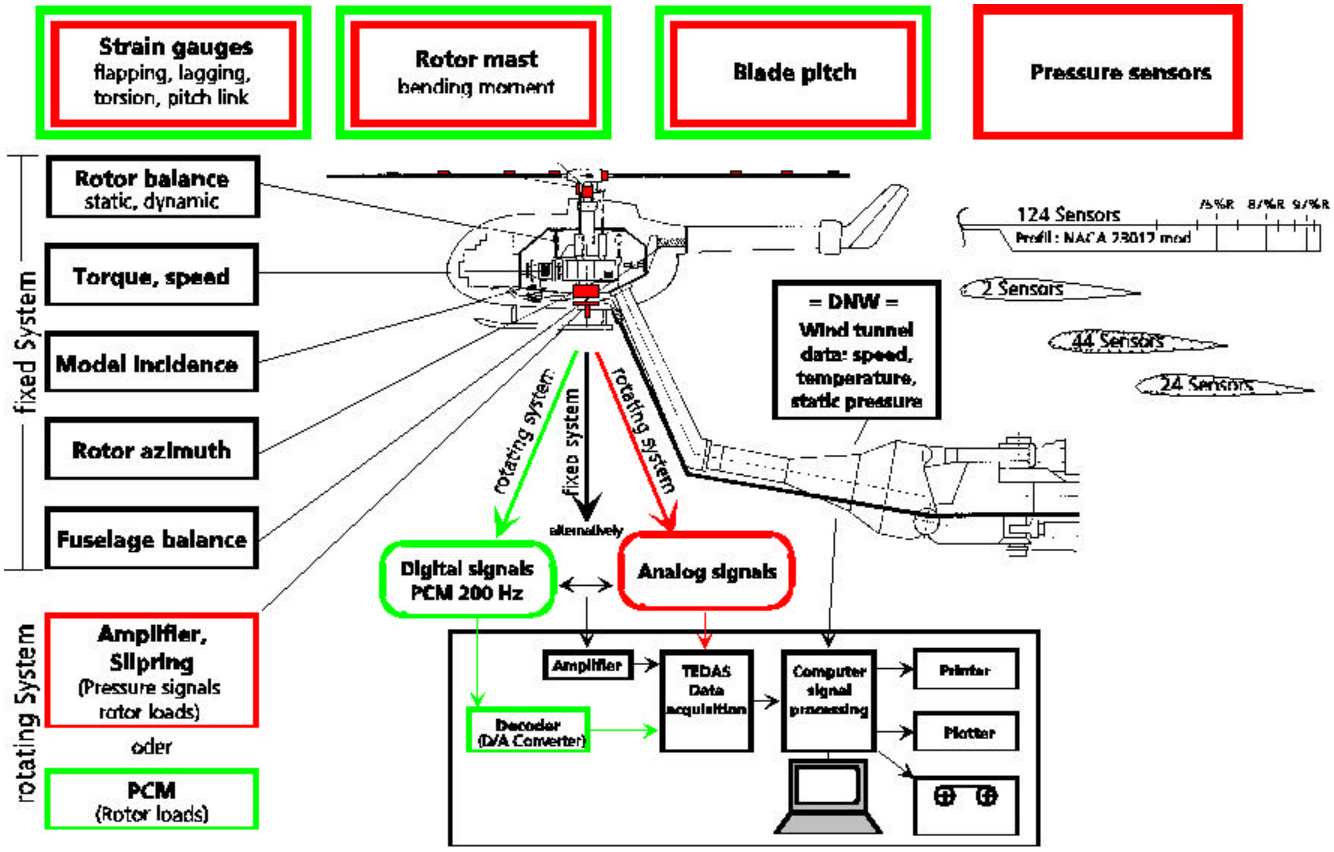

Fig.1 : Rotor Test Stand

Fig. 2 : Wind tunnel testing in DNW

- Hydraulic motor with control electronics (Fig. 4),
- rotor head with instrumentation on all movable parts,
- rotor blades with strain gauges and pressure sensors,
- model fuselage with aerodynamic surface and static pressure sensors,
- 6 component fuselage balance for measuring all moments and forces injected into it,
- 6 component rotor balance for measuring all moments and forces introduced into the rotor,
- swash plate for cyclic and collective control of the rotor blades,
- electric or electrohydraulic actuators for control of the swash plate,
- torque sensor system for measuring of power and speed,
- incremental encoder for measuring the azimuth angle of the rotor,
- slip ring for transferring sensor signal from the rotational part to the fixed part,
- amplifiers and signal conditioning units in the rotational part as well as in the fixed part,
- actuators inside the blades (flaps, smart materials).

The complete system is integrated and fully tested at the Institute of Flight Research, with the exception that no wind is applied. Then the system is carried to the Dutch German Wind Tunnel where the measurement takes place (Fig. 2).

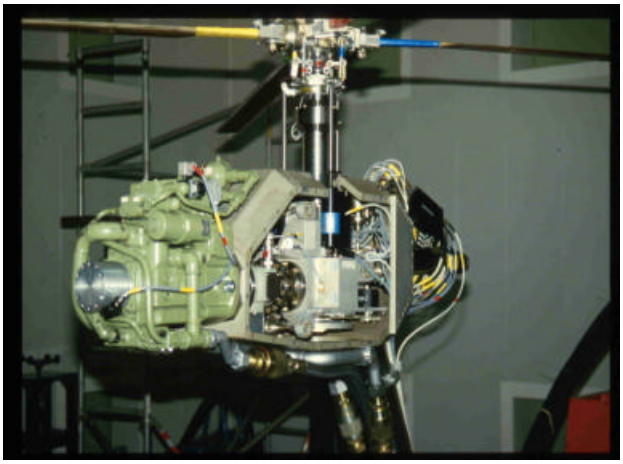

Bild 3 : Modular wind tunnel model

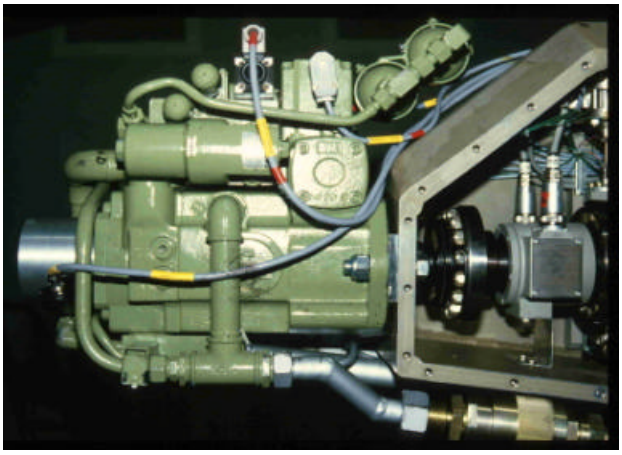

Bild 4 : Hydraulic Motor

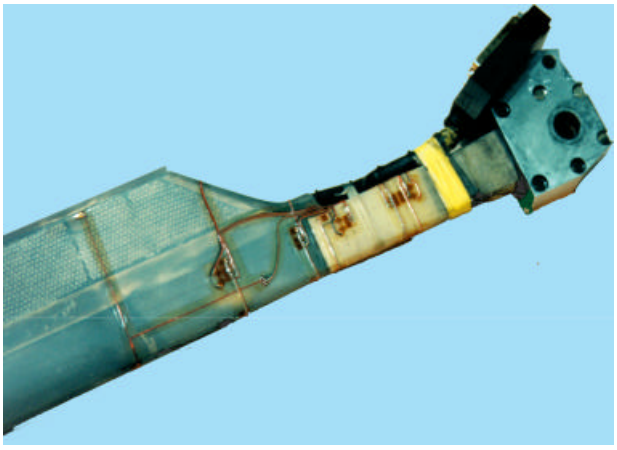

Bild 5 : Strain gages at blade root

3 Sensors

The sensors used are experiment specific and therefore change often. The following sensor groups can be identified:

3.1 Sensors in the rotating part of the system

- Strain gauges on blades (Fig. 5), control rods and mast,
- pressure sensors integrated into the blades (Fig. 6),
- angle sensors and position sensors at all movable parts (using potentiometers and magnetic sensors).

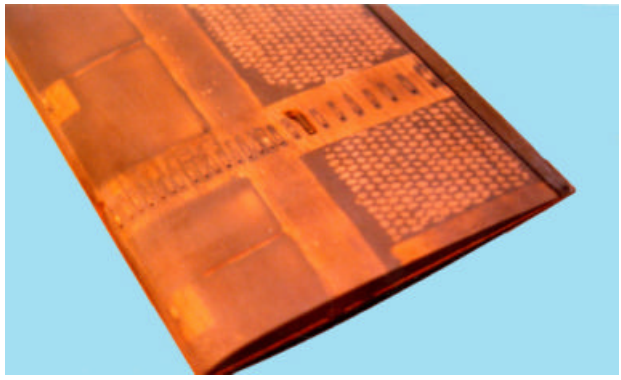

Bild 6 : Pressure sensors in rotor blade

3.2 Sensors in the fixed part of the system

- Force sensors (DMS, piezo) for the rotor balance,
- torque sensor system,
- accelerometers (Piezo),
- pressure sensor at the fuselage,
- angle encoders.

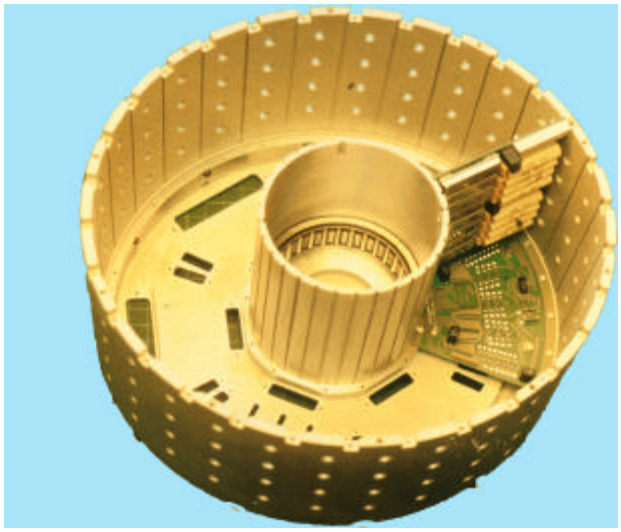

Bild 7 : Amplifier housing

The force sensors for the balance are based on strain gauges for low frequencies delivering high precision signals. For measuring high frequencies piezo based sensors are built in series. The high frequency components have reduced precision.

Most sensors in the rotating part of the system deliver only low voltages. A good signal to noise ratio before feeding the signals into the slip ring is achieved by amplifiers which are also part of the rotating system. To make the amplifiers small enough special hybrid components have been developed at DLR. These hybrids are inside a „pot“ at the lower end of the rotor mast (Picture 7). Then the signals are fed into a 250 channel slip ring. Alternatively at low signal frequencies (low sum sample rates) also a rotating pcm system can be used. This system can measure 64 channels* using a one channel slip ring. The pcm data stream is decommutated at the fixed part and then d/a converted and sampled again in the main data acquisition system together with other analog signals.

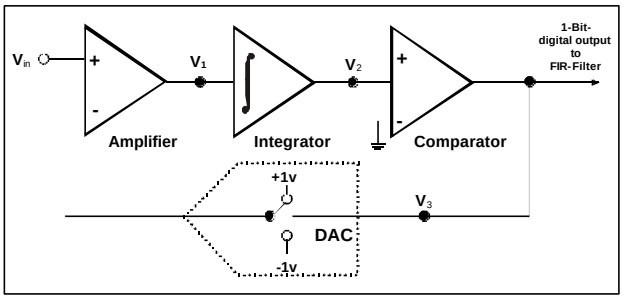

Fig. 8 : Delta Sigma Modulator

4 A/D- conversion

Sampling of all signals is done synchronously to the rotor azimuth angle. Therefore a high resolution angle encoder generates a clock signal which is used to clock the ADCs. This allows exactly 2048

samples per revolution. The sample rate is a power of 2 because this allows the usage of FFT. Otherwise the much slower DFT would have to be used. Sampling with reference to rotor angle has the consequence that the sample data are no longer data in time domain instead they are in angle domain. Thus all following computation steps like filtering must be synchronized and scaled with rotor speed as well.

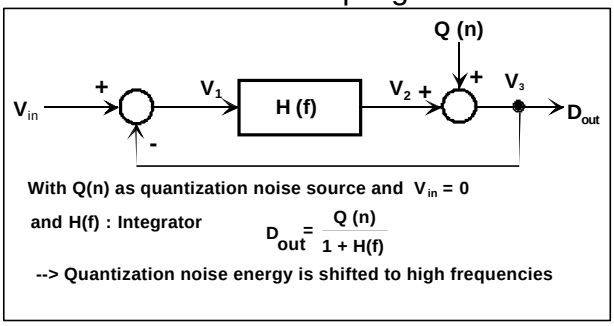

Fig. 9 : Principle of Noise Shaping

In the past A/D- conversion was done using a S&H stage followed by an successive approximation ADC. The resolution was normally 12 bit. This scheme has some disadvantages:

- Relatively expensive converters.
- High order analog antialiasing filters are needed. The analog implementation introduces a frequency dependent group delay which introduces pulse distortion.
- The filter behavior does not scale with the sample rate. As sample rate is derived from non constant rotor speed this would be necessary to remain in angle domain instead of time domain.
- The filter cost dominate the channel cost, if high requirements have to be matched.

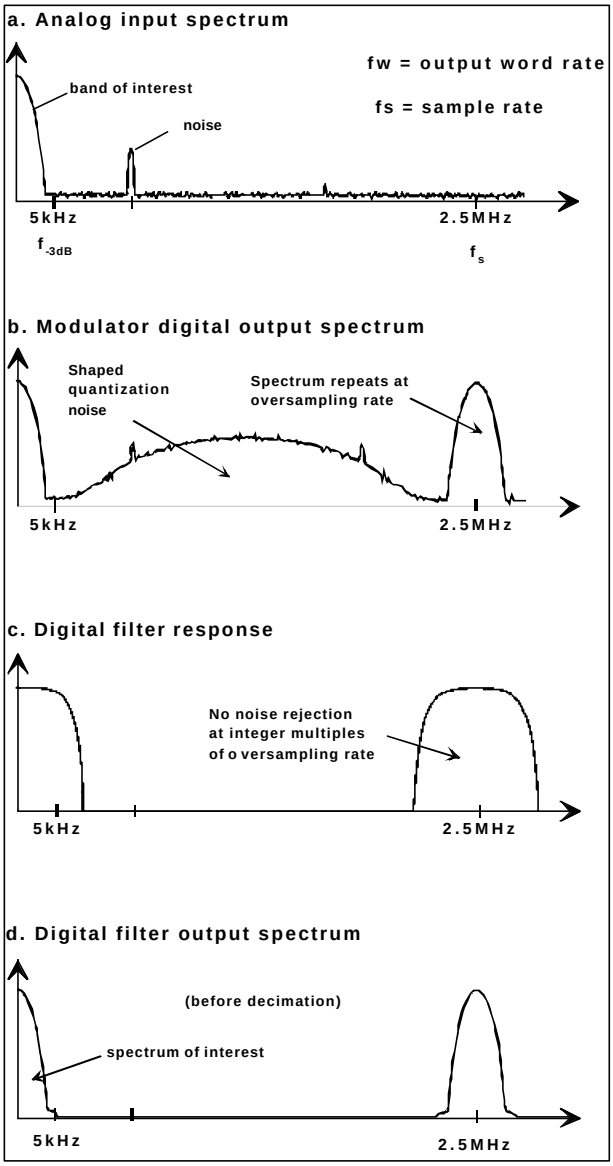

Fig. 10 : Spectral Situation at Delta Sigma Converter

4.1 Delta-Sigma-Converter

With the introduction of the delta sigma technology for consumer electronics in the 80s a revolution in conversion technologies happened. These low cost converters sample the signal with a multiple of the required output word rate (64X, 128X). Therefore a delta sigma modulator (Fig. 8) is used which produces a bit density modulated signal. This 1 bit conversion (modern chips even use 2 bit modulators) is FIR filtered. Thus no signal components above half of the output word rate are present. Now it is allowed without violating the Nyquist criterion to use every n_{th} (n=64,128) output word (in Fig. 9 the output word rate would be about 20 kHz). This gives output words with a dramatically reduced word rate compared with the sample rate of the modulator. This is called decimation. The FIR filtering process calculates sums of

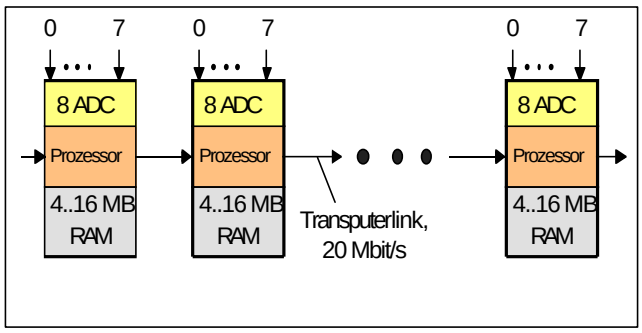

Fig. 11 : Structure of TEDAS

Fig. 12 : TEDAS

products (convolution). This increases the word width from 1bit to 16..24 bit). This scheme in combination with noise shaping for reduction of quantization noise (Fig. 9, Fig. 10) inside the modulator results in a converter with the following features:

Advantages

- Low price because it is a consumer mass product.
- Simple and low cost anti aliasing filter (1st order low path).
- Digital filter scales with sample rate.
- Excellent dynamic behaviour.
- Excellent signal to noise ratio.
- High resolution 16 bit .. 24 bit.

Disadvantages

- Due to oversampling the converter needs a high frequency clock which is derived in our case using a high resolution incremental encoder in combination with a frequency multiplying PLL (phase locked loop).
- Delta sigma converters must be operated continuously instead of start/stop operation because the FIR filter is an energy storing element (like an analog filter).
- The internal structure allows no sample rate down to zero. A 100 kHz converter for example can be used down to 2 kHz.

For our application the advantages are dominating. Thus DLR at 1990 was one of the first companies using this „consumer technology“ (audio) for industrial measurement purposes. The result was TEDAS I (Transputer Based Expandable Data Acquisition system [4].

5 TEDAS

The motivation for the development of TEDAS (Fig.12) was the demand for an increasing number of channels at 1990. Before this year the requirement was 64 channels with a sample rate of 2 kHz each, but now more than 200 channels with 35 kHz

sample rate were needed. The result is an enormous increase in sum sample rate. This could not be handled by standard computers at that time. Also the computational power for the FFT calculations needed was not available. Thus the TEDAS development was started. TEDAS is an “unlimited” number of data acquisition modules connected by serial links in a linear arrangement. Each module has its own processor and serves 8 delta sigma ADCs with 16 bit resolution. A module has 4 or 16 Mbytes local RAM. A measurement point is stored in local RAM. After data acquisition the FFT computation is done locally and the raw data and computed results are transferred to the host. Quicklook is done by doing a short measurement cycle over one rotor revolution. Advantages of this system are the unlimited number of channels and the high conversion quality introduced by delta sigma conversion. The design of 1990 still finds new customers. Systems with 400 channels have been sold to in house customers. In total 8 system have been built. But from today‘ s point of view this arrangement also has some disadvantages:

- The duration of measurement is limited by the size of local RAM.
- The speed of modern computers makes the use of transputers obsolete.
- The data transport to the host (800kByte/s) is not fast enough.
- This system is not able to do measurement over a long time period (hours ..days). Therefore it can not be used as a crash recorder.
- During measurement the computation of results or data transportation is not possible.

Although TEDAS delivers high availability and excellent signal quality the limits of this system are reached.

6 The new concept

Today’s requirement for a new multi channel data acquisition system are:

- Sample rate per channel 100 kHz,
- number of channels > 256,
- integrated crash recorder function,
- continuous measurement,
- quicklook for different users,
- high resolution, good dynamic behavior,
- conversion inside rotating part of system in order to avoid a complex slip ring system,
- modularity for longer life cycle,
- low system cost.

Based on experience gained in the past and from new requirements basic functions can be identified which need to be fulfilled by the new measurement system TEDAS II (Throughput Enhanced Data Acquisition system) being under development (Fig. 13).:

- Data acquisition,
- isochronous fusion of all data sources in order to obtain a consistent data stream,

- continuous data storage (crash recorder),
- data distribution.

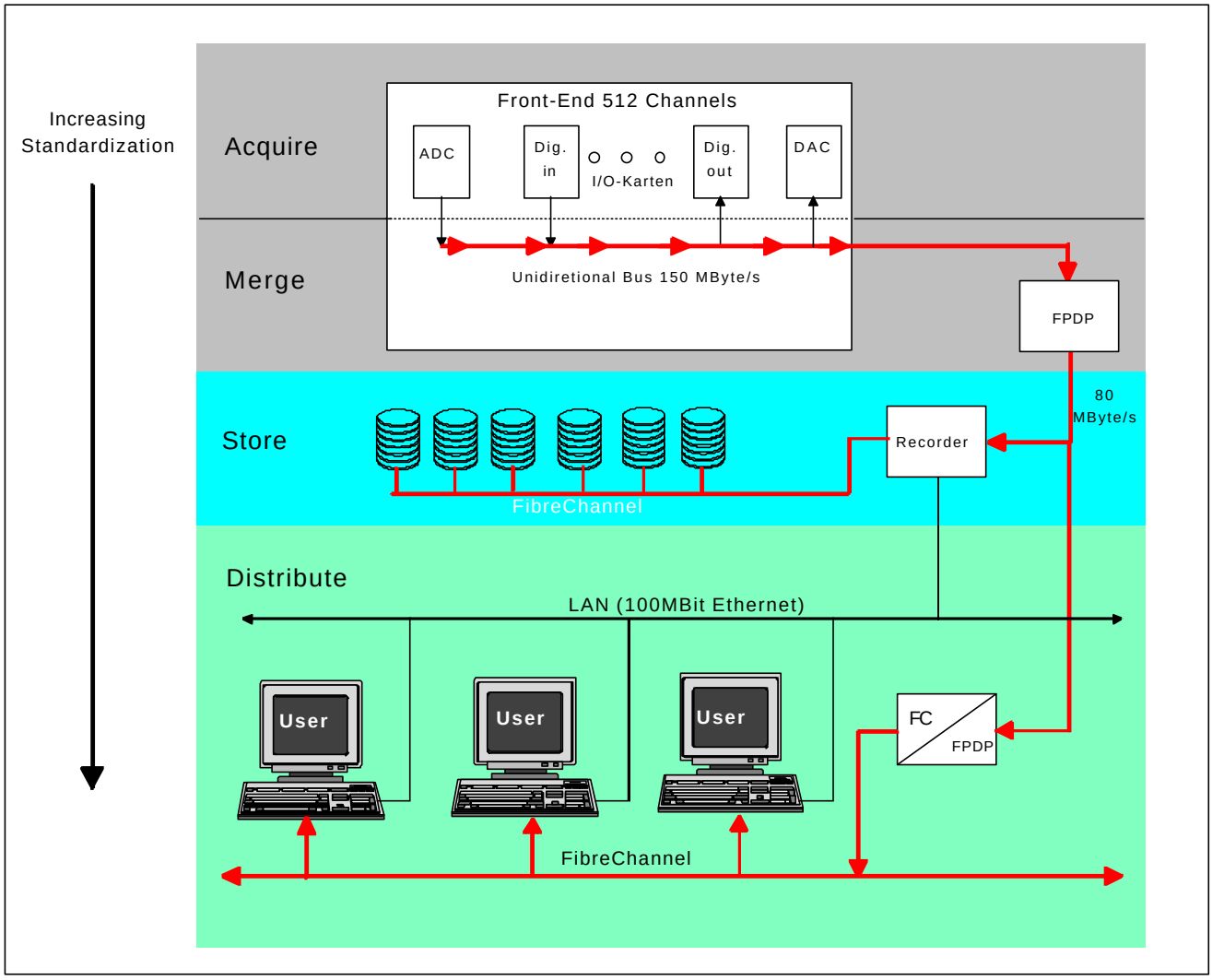

Fig. 13 : Structure of TEDAS II

These functions are the layers of the complete system. Each layer can be developed and optimized separately. Some layers can be realized with components of the shelf. Well established standards will be used, if available. Standardization increases corresponding to the signal flow from experiment specific instrumentation to data distribution which should be done using turn key solutions from the market.

Important system aspects are the high sum sample rate, the real time capability and the corresponding transport mechanism and media.

6.1 Data Distribution

Assuming a maximum channel count of 512, a maximum sample rate of 100 kHz per channel and 16 bit resolution the data throughput will be :

S=512*100000*2 Byte/s =102MByte/s.

Normally the rotor speed is 17.5 rev/sec using 4096 samples/rev. This results in a data rate of about 80 Mbytes/s. This amount of data has to transferred in real-time to different users. Therefore broadcasting transfer mode with the absence of acknowledges is required.

From the networking products available on the market the Fibre Channel (FC) has been selected. This product is available from several manufacturers and allows presently a transfer rate of 1 Gbit/s and is to be standardized for 2,4,8 Gbit/s in future. Thus this medium has enough grow potential. The media itself is copper as well as fibre optic. The FC carries all measurement data in real time. Data is distributed in blocks of one rotor revolution which provide blocks of about 6 Mbytes. The user computer, normally a SUN workstation will be equipped with FC interface boards and with a large memory and thus is able to always receive the next n blocks of the broadcasted data. As all data are available on the media, different users can receive independently different parts of the data either a little number of blocks (=rotor revolutions) for quicklook purposes or a large number for performing a measure.

6.2 Data Storage (Crash Recorder)

The crash recorder function can be seen as a very large ring buffer holding the last minutes or hours of data. If the buffer is full the oldest data will be overwritten. This function has been ordered from the market. It is a VME bus computer equipped with a FPDP interface (FPDP = Front Panel Data Port), a FC-interface and a JBOD (Just A Bunch Of Disks) storage. Data is received from the data acquisition unit via FPDP and is then transferred to the JBOD. The JBOD consists of disks equipped with a FC interface. The required data rate is achieved using striping. Striping distributes consecutive blocks of data on different disks. Thus each disk receives a moderate amount of data and can use its internal cache for intermediate storage. All disks together are able to store a continuous data stream of 80 Mbytes/s.

The FPDP parallel interface is a well proven industrial standard. It can be used with data rates up to 160 Mbytes/s. In the present application 100 Mbytes/s are used. The crash recorder can be parameterized via RS232 interface as well as via Ethernet. In the case of a crash the data can be read by the user workstations via Ethernet. As these data are already stored there are no real-time requirements.

6.3 Data Acquisition and Fusion (Front-end)

This part of the system (Fig. 14) is under development in house because market components do not fulfill the requirements and a lot of experience is available. The front-end consists of a unidirectional shift register bus which can be loaded at every sample time. During the time between two samples data is shifted out to a buffer memory. The bus may contain any kind of input or output cards. The bandwidth is 150 Mbytes/s. Input cards are ADC cards or digital in cards or in future the connection to digital data from the rotating system. Output cards normally will be DAC cards allowing to view measurement data on an oscilloscope or other devices.

The input cards in cooperation with the shift bus merge and synchronize signals from different analog or digital sources. The output cards are used for monitoring purposes. The front end is parameterized via RS232. Maximum channel count is 512. The analog signal are converted using A/D cards with following parameters:

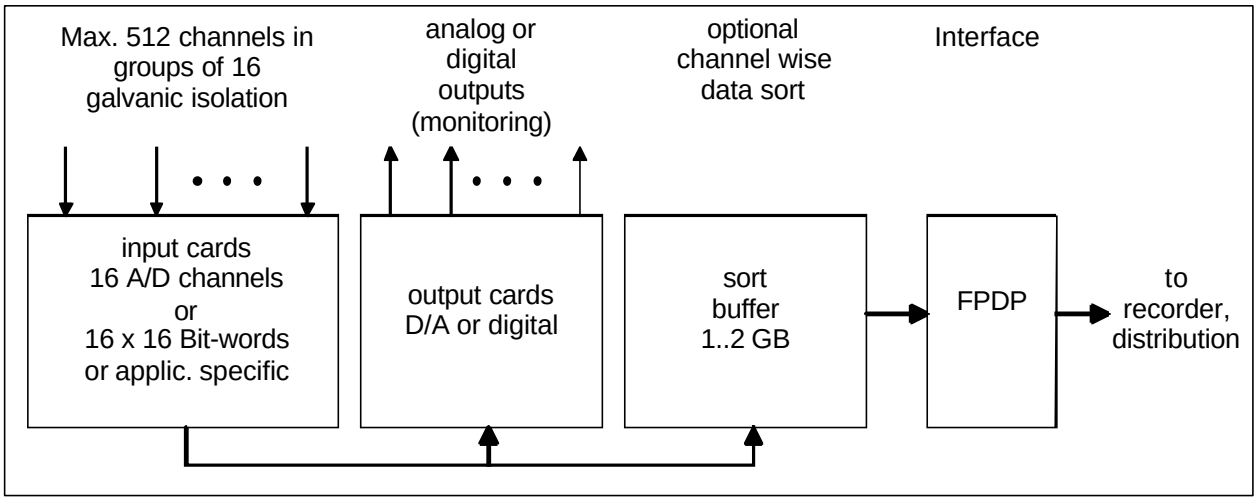

Fig. 14 : Structure of Front-End

- 16 channels,
- 2 to 100 kHz sample rate,
- delta sigma converters with 24 bit resolution,
- selectable word width 16..24 Bit including saturation logic,
- optical overflow indicator,
- 2 monitor outputs per card (16 channels),
- selectable „low group delay“ configuration, if the signals are part of a control loop,
- programmable gain from -90 dB to + 37 dB in 0,5 dB steps,
- full scale jumper programmable +-5V or +-10V
- programmable offset with 18-Bit DAC,
- each card can be isolated from the others.

The ADCs including analog signal conditioning are modules which can be expanded to be application specific modules. If the data source is already a digital signal, instead of an ADC module a digital interface is used. Especially the galvanic isolation feature is a great advantage for large scale measurement systems which are widely spread in space. This avoids the well known grounding problem which was time consuming to solve in the past.

6.3.1 Data Sorting

A big problem is the sorting of the data. Normally data appear sample wise (ch1 s1, ch2 s2.....chn, sm). The user instead wants to have the data channel wise (s1 ch1, s2, ch1..sm ch1; s1 ch2, s2, ch2 ....sm ch2) . Therefore the data have to be sorted in the way the user wants them. If required this is done in real time in a dual port buffer of several Gbyte size. This happens before the data is sent to the users. Of course the sorting introduces a delay, the first block of data can be sent after all samples of that block are in the buffer. The block size is configurable. The readout of data is channel wise if se-

lected. Of course the sorting can also happen inside the user computer, but this is very time consuming if there is a large amount of data.

6.3.2 Recorder Interface and Data Distribution

The connection between the system layers uses a well established industrial standard. The front-end has a FPDP interface connected to the same type of interface of the recorder. Another FPDP is used to make the connection to a fibre channel system for data distribution. At this time it has not yet been decided to use the pure fibre channel as it is standardized because the functionality of broadcasting has not been proved up to now. An alternative would be a special hardware which is available and uses only the physical and the signaling layers of fibre channel. If the front-end is running both the recorder and the distribution network are supported continuously with data. The destination must be able to read the data in time otherwise data are lost. For the recorder this is a strong requirement and part of its specification. For the users this has only to be assured for a given number of data blocks. This normally is defined by the size of the main memory.

7 Status of TEDAS II And Developments

The front-end is under development. The ADC modules and the carrier cards are manufactured. The large buffer is being designed. The recorder has been delivered by industry. The data distribution mechanism to the users will be defined after the fibre channel market analysis has been done. The system is planned to be ready at the end of 2000.

One requirement TEDASII can not fulfill at present: The data acquisition and conversion inside the rotating system. But many components like ADC modules are designed for being able to be integrated in the rotational part with minor changes. With the FPFD as the interface there is already a solution visible which can be realized with components of the shelf. There are components available which transform the simple FPDP protocol to the fibre channel physical layer and vice versa. Thus on both ends are FPDPs and between them is an optical fibre. This fibre can be used with an optical slip ring in order to transfer the data between the system areas.

If the data conversion inside the rotating system can be done, the large multi channel slip ring can be avoided. Another advantage is the absence of tons of cable between the slip ring and the data acquisition system which are separated by about 60 m with a very complicated cable path. Instead then we have only one thin fibre optic lane. This add on is planned after the end of the current development.

8 Conclusion

Since many years DLR operates large data acquisition systems for wind tunnel testing. The requirements are increasing continuously. In 1990 DLR introduced the use of delta sigma ADCs for industrial data acquisition purposes. This in combination with the usage of transputer was a new generation of measurement systems. Nevertheless today's requirements must ask for new architectures. The answer is TEDAS II. This system is layer oriented allowing each layer to be developed and optimized separately. The separation into the layers storage, fusion and distribution guarantees a long life cycle and growth potential. The problem of the appropriate ADC technology and of the handling of large amount of data has been discussed. Finally the status of the present development and future plans of digitalization inside the rotating system using an optical slip ring for data transportation have been discussed.

Literature

[1] Splettstoesser, B., Wall, B.G. van der, Junker, B., Schultz, K.J., Beaumier, P., Delrieux, P, Leconte, P., Crozier, P., „The ERATO Programme: Wind Tunnel Test Results and Proof of Design for an Aeroacoustically Optimized Rotor“, to be published at the 25 Eu European Rotorcraft Forum, Rome, Italy, Sept. 14-16,1999.

[2] Langer, H.-j. „Highlights of Project Work – Use of the Wind Tunnel for Helicopter Development risk Reduction“, DNW Annual Report 1993, pp. 8-9.

[3] Yu, Y.H., Gmelin, B. L., Heller, H.H., Philippe, J. J., Mercker, E., and Preisser, J.S., „HHC Aeroacoustic Rotor Test at the DNW – The Joint German/French/US Project“, 20th European Rotorcraft Forum, Amsterdam, Netherlands, Vol. 2, 1994, Paper No. 115.

[4] Gelhaar, B., Alvermann, K., and Dzaak, F. „ A Multichannel Data acquisition System based on Parallel Processor Architecture“, Proceedings of the International Telemetering Conference, San Diego, USA, Oct. 22-28, 1992.

Abbrevations

FFT	Fast Fourier Transform
DFT	Discrete Fourier Transform
FIR	Finite Impulse Response Filter
PCM	Pulse Code Modulation
PLL	Phase Locked Loop
FC	FibreChannel
FPDP	Front Panel Data Port
JBOD	Just a Bunch Of Disks
TEDAS	Transputer Based Data Acquisition System
TEDAS II	Throughput Enhanced data Acquisition System
DLR	Deutsches Zentrum für Luft- und Raumfahrt
A/D	Analog-Digital (conversion)
D/A	Digital-Analog (conversion)

HELIDAT - a Complex Measurement System is Described with a Database

Stephan Graeber, Henrik Oertel
Deutsches Zentrum für Luft- und Raumfahrt e.V. (DLR)
Institute of Flight Research
Braunschweig, Germany

Abstract

A complex measurement system, which has to be operated and maintained over a long period of time, requires a consistent documentation and change management. In this paper we describe a solution to this problem on the basis of a database. This database called “HELIDAT” describes the on-board experimental system of the ACT/FHS research helicopter in terms of hardware documentation and signal flows.

1 Introduction

Within the ACT/FHS project (**A**ctive **C**ontrol **T**echnology Demonstrator and **F**lying **H**elicopter **S**imulator) [1,2] the Institute of Flight Research currently develops the experimental on-board equipment. The objective of the ACT/FHS project is the development of a technology testbed for test and validation of key technologies for future military and civil helicopters. This helicopter will be available as a multipurpose test vehicle for the evaluation of new control technologies, cockpit designs, sensor systems and man machine interfaces. The test helicopter is based on the civil helicopter EC135 re-fitted with fly-by-light-technology, smart actuators, high-speed processors, intelligent sensors, and state-of-the-art display technology.

2 Objectives and Concepts

2.1 Historical review

From the beginning the ACT/FHS project demanded a documentation of all available signals and their parameters being used within the experimental system. A signal is a piece of information being transmitted from one hardware device to another.

This “signal list” should provide the possibility to recover old versions of the experimental system. This could be necessary if old data needs to be evaluated and there were doubts about the configuration of the experimental system at the time of this former flight experiment. Thus a version or configuration management had to be installed to ensure that no old data is overwritten, but that any old state of this so called “signal list” could be recovered.

Additionally for our embedded system a complete hardware documentation is necessary and has to be maintained. Furthermore the on-board software relies on parameters, e.g. which interface is used for each signal, unit and calibration conversions. This data has to be automatically extracted from the database.

The combination of these two requirements resulted in the idea of the database “HELIDAT”. At a first glance it seems, that these different aspects coming from the hardware and software development do not match together. But looking at it in more detail shows several interconnections between these two aspects.

2.2 Requirements Analysis

After a detailed analysis and feasibility study, which resulted in a specification document [3], we decided to engage the company *unilab Software GmbH* to help us with the design of such a database [4].

Two main objectives needed to be considered for HELIDAT:

1. Maintenance and documentation of the experimental system.
2. Provide a link between the raw signal and the physical quantity for the user, who controls the experiments with the system.

The database HELIDAT has to describe the structure of the experimental system at any given point in time as exact as necessary to fulfil the two above mentioned objectives. To reduce conflicts and inconsistencies the database needs to be installed at a central position, and it has to maintain several versions of data. A history mechanism ensures that old versions can be recovered.

2.3 User Concept

In a complex database being used by several users, it is necessary to define precisely, who is allowed to insert and change data in the different areas of the database. In some database tables, where sensitive information is stored, even the read access has to be restricted. A specific user concept defines the roles of the different users and their privileges. The concept of HELIDAT allows changes and insertions into the database from different users. Users that are responsible for e.g. special devices also maintain the respective information in the database.

2.4 History Management and Archive

The experimental system will change several times during its lifetime mainly due to changes in configuration originating from different requirements for specific experiments. This illustrates the need for a history management and a concept for backup and recovery.

To solve this problem the data stored in HELIDAT is divided into two categories. Tables are defined which contain data that will change never or seldom. New required entries in these tables will be solved by inserting the new data, but not by updating old data. Tables with a higher change frequency will be supplied with a version column. This way every entry in these tables is equipped with a version mark, in fact these version marks are itself links to a place in the database, where all versions are administered. In these tables normally no data is deleted.

The result is, that the database will grow and grow with every new version. This may be no problem in the first time, but later on it may cost performance, and there might be data in the database, which will be never used again. For this case we also foresee the possibility to export data into an archive.

Because it should not be possible to change any data in old versions of the database, the versions are kept in several states, i.e. they may be “fixed” or “under construction”, depending whether insertions to these versions are allowed or not.

2.5 Implementation

The central database system with more than 60 tables was implemented on the basis of an Oracle DBMS (database management system) by *unilab Software GmbH.*

Presently the database is ready and we are feeding in the real data. Front-ends to the database are currently under development, they will be described in the next chapter.

3 Context and Relationships

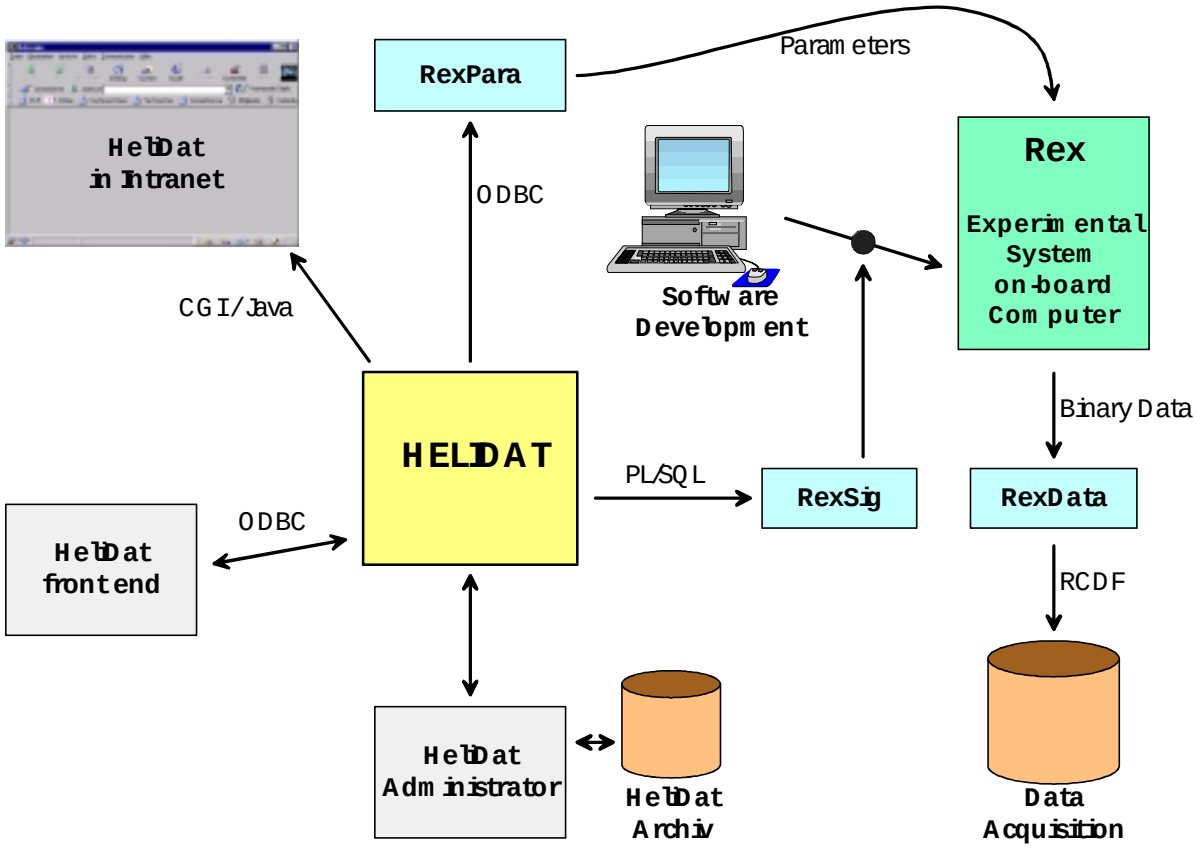

Fig 1: The Database HELIDAT within its environment

Fig 1 shows, that the database HELIDAT plays a central role in the development and operation of the experimental system (REX) for the helicopter testbed. For the real on-board computers of the experimental system a highly flexible software is being developed, which can be configured via parameters. These parameters describe amongst others for example the connections of sensors to the experimental on-board computers and the configuration of displays. The information stored in the database, which is needed for the REX software, can be split into two parts:

- Run time parameters: Values that are not hard coded in the software, but can be inserted during the start up process of the software. These parameters are collected and evaluated by a software tool (RexPara), and then written onto PCMCIA cards

(which hold this information for actually starting the on-board system). Additionally the user can set up several parameters to preconfigure the system before going into flight experiments.

- Compile constants: Values that are necessary for the start-up procedure of the software. These parameters can be read from the database during compile process (RexSig). This helps to set up consistent software versions for our system which continuously needs to handle changing requirements.

After flight campaigns the recorded flight data contains a number of the used version of the database, in order to reconstruct the hardware and signal flow of the on-board system being used to acquire this data.

3.1 Front-ends

For data retrieval, data input, and administration we presently develop several front-ends to the database. An Intranet front-end will give the users the possibility to retrieve information from the database. Information about the flow of signals, the installed devices with their connections, and the calibration data can be queried by an easy-to-use interface. The user fills out a kind of query form, which is automatically sent to the web server, evaluated, answered by the database and sent back to the users web browser. The answer may contain further links to detailed information which can be selected by the user.

For database administration and for the input of data we use other interfaces to access the database, e.g. ODBC (open database connectivity). The application runs on the users desktop computer and connects to the central database server via network. Insertions to the database are done this way due to security reasons.

Standard office software (e.g. MS Access) can be used as well as a front-end to the database. The ODBC standard allows any compatible application to access the database, if the user has the required permissions. That way a user can connect his Office application to the database. To obtain a well designed paper output this may be very useful.

3.2 Consistency

Such a complex database like ours demands several consistency conditions, which have to be checked every time, when an input or update is done into the database. These conditions are mainly checked by the central database itself, in our case either via “constraints” or “stored procedures”. The advantage of doing the consistency checks within the database is, that the checking algorithm only has to be implemented once in the central system, but the front-ends do not have to take care about the correctness of the user inputs.

All input into HELIDAT is done via stored procedures. This enables us to log all activities changing the data content. Thus it is possible to gain an overview of changes and to find out differences between versions. The latter is an essential point, because the user may ask why he gets different data from different flights. A question to the database like “what are the differences between version A and B” will give hints on the reason. For example another sensor may have been used for the acquisition of a specific signal.

4 Design and Structure

To cover the different aspects of the database, it is divided into several parts, which are strongly interconnected. Figure 2 shows the different parts and their dependencies.

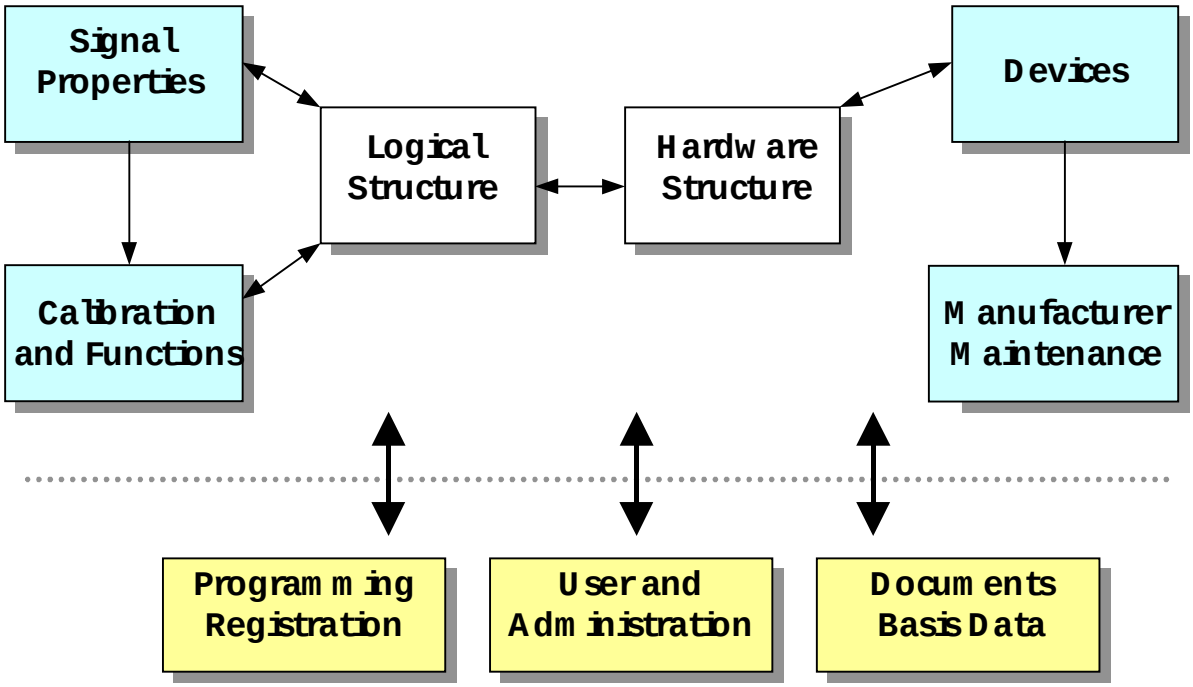

Fig. 2: Overview of HELIDAT structure

4.1 Logical Structure

The computers within the experimental system receive their information from different sensors and transfer this data to other systems. The way information takes is called a “signal way”. Such a signal way starts in the real world with a physical quantity, is converted into an electrical signal by the sensor and transferred through e.g. amplifiers, filters and A/D converters into some interface card in the computer and from there to a data storage device.

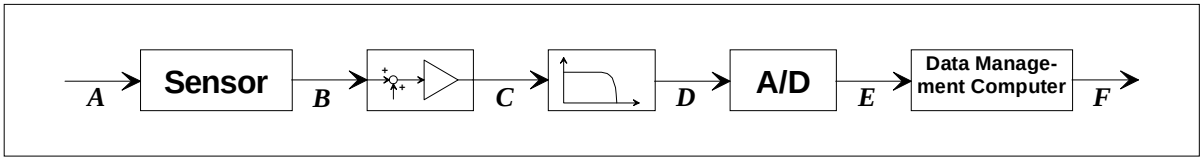

Fig 3: Example for a signal way

A piece of information may encounter several transfer media on such a signal way (e.g. serial or analogue interface). Additionally a signal may be combined with others to messages. At each point a signal needs to be described with several parameters:

1. Signal name (to identify the signal among others).
2. Signal dynamics, scan rate, sending frequency.
3. Physical unit.
4. Signal type (e.g. digital / analogue).

5. Range, minimal and maximal values, resolution.
6. Coding of a digital signal is given by parameters like position of MSB and LSB in the word, position of the sign, the number of significant bits.
7. Coordinate system being used.
8. Parameters depending on the transfer medium or channel:

Channel type	Parameters
ARINC channel	Speed, parity
Serial channel	Baud rate, data bits, stop bits, handshake
Ethernet	Protocol type, sending / receiving port address
Memory address	Memory address and block size

9. For each message we handle: sending frequency, size, number of signals, some label(s), and additionally (depending on the message type):

Message type	Parameters
ARINC message	Arinc label, resolution, remarks upon SDI, SSM
Milbus message	Remote terminal address, subaddress
Stream message	Header / Footer length, separating character, checksum

Each signal way consists of several signals being described with the above mentioned parameters. The interrelationship between two successive signals within a specific signal way is defined by transfer functions. Such a transfer function enables us to define all required connections within this signal network, dealing with calibration data (e.g. filter functions) as well as with the definition of a complex combination of different input signals to one output signal (e.g. bus structure). Note that this describes the logical, not the hardware aspect of such a network.

4.2 Hardware Structure

The hardware structure is the second big domain of the HELIDAT database. Data is stored describing devices, cables and plugs. Even the pinning of the plugs is documented.

The administration of the hardware objects (which can be seen as a superclass of the devices, cables, plugs, and other hardware parts not directly involved in the signal flow) is done via a kind of (imaginative) hardware pool, which holds all devices or other hardware objects which may be part of the experimental system for certain flights. For each entity in this pool we store

- Name.
- Serial number.
- Weight and power consumption.
- Date of purchase.
- Maintenance information (e.g. maintenance interval).
- Manufacturer data (name, address, contact etc.).
- Responsible person for the device to be contacted in case of problems.
- Links to the user documentation.

If such a device is physically installed in the experimental system, we then do the same with the database. This means that from now on an entity is created in the hardware object table, containing a link to this “real” hardware entity. We only need to define the

data depending on the integration within the system and describing the interconnections with other hardware objects:

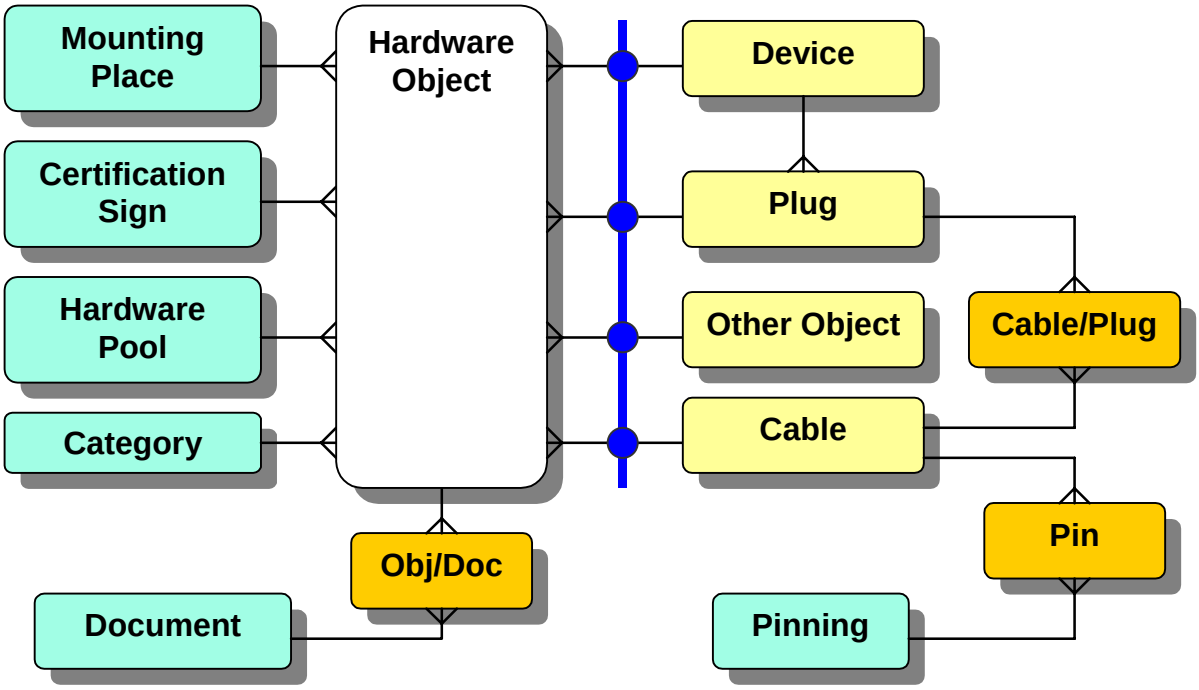

Fig 4: Overview of hardware entities and their relations

- Mounting place, centre of gravity.
- Certification data, corresponding with electrical drawings.
- Links to documents describing the object (blueprints).

4.3 Administrative data

Additionally we use some central data tables, which are connected to several areas of the database. The version management is an example for such a central service, which is used at several points in the database. A special mechanism allows to store data of several versions of all necessary entities in the database to ensure, that different configurations of the experimental system (corresponding to different versions of HELIDAT) can be maintained in parallel. Particular versions of the database can be exported to an archive.

The “stored procedures” described above also are used to automatically store administrative information like logging and error messages. This data is kept in the database and can be viewed by the administrator.

5 Conclusion

We described the basic structure and usage of a relational database, being needed to document and operate a complex on-board system for a helicopter testbed. This database is a central part for the development and maintenance of our embedded system, since it documents signal flows and hardware configurations and additionally assists the software development process by providing hardware related parameters.

Besides a description of these aspects, the paper also covers user interfaces and internal consistency checks. We expect that our approach can be used in other cases as well, where requirements for system documentation, maintenance and automatic parameter generation for a complex, always changing system demand a database solution.

6 References

[1] U. Butter, M. Dion, B. Gelhaar, H.-J. Pausder: *ACT/FHS - A New Fly By Light Research Helicopter*. Proceedings of the European Telemetry Conference, Garmisch-Partenkirchen, Germany, 1998.

[2] K. Alvermann, R. Gandert, B. Gelhaar, S. Graeber, C.-H. Oertel: *The ACT/FHS On Board Computer System*. Proceedings of the European Telemetry Conference, Garmisch-Partenkirchen, Germany, 1998.

[3] S. Graeber, C.-H. Oertel: *Spezifikation Signalliste*. DLR Document SP L 220 R 0913 D01, Ausgabe A001, 1998.

[4] J. Schniete: *Pflichtenheft 'Datenbank Flugversuchsträger'*, unilab Software GmbH, internes Dokument Projekt 986141, Braunschweig, 1998.

Multi-channel Programmable Signal Conditioning Module Using Digital Signal Processing

Michael W. Landry
Director, Technology and Intellectual Property
L3 Communications, Conic Division
San Diego California, USA

Abstract

This paper discusses the hardware and software design of an 8-channel signal conditioning module using an embedded single chip DSP. Each channel has independently programmable gain, offset, and filter cutoff frequency. Hardware and software techniques are employed to achieve an efficient design. The stacking module is a miniature assembly for use in airborne instrumentation.

Keywords: Digital filtering, Digital Signal Processing, DSP, Data acquisition, Signal Conditioning

Introduction

An ideal signal conditioner presents high impedance to the signal source, allows for scaling of the measured signal, provides bandwidth limiting, and may need to provide an excitation signal to the transducer.

The quantizing stage of a measurement system (the analog to digital converter) will be limited by finite resolution, a maximum signal range, and finite sampling rate. The wide range of possible measured signal levels requires that a general purpose measurement system have programmable gain between the source and the A/D.

Finite sampling rate requires that the bandwidth of the measured signal to be limited. Frequency components present above one-half the sample rate (Fs/2) will be converted to a frequency below Fs/2. These aliased signals are unwanted and degrade the signal-to-noise ratio of the measurement. Ideally, frequency components above Fs/2 must be attenuated to a level below the quantizing resolution in order to be eliminated. A general purpose measurement system should have a programmable bandlimiting filter that can be matched to the sample rate needed to recover the useful information in the signal.

Programmable gain and filtering can be done exclusively with hardware. Gain can be achieved using resistor programmable instrumentation amplifiers. Filtering can be achieved using state variable filters or switched-capacitor filters. These approaches lead to high component count and cost. Component tolerance and temperature stability present extra design challenges.

The approach of the signal conditioning module presented here is to use a combination of hardware and software techniques. An embedded programmed digital signal processor (DSP) performs the software functions. Using a simple anti-aliasing filter in the analog domain, signals are over-sampled at a high fixed rate followed by digital filtering, which can be programmed by a choice of filter coefficients and cascaded stages.

This module is designated as the VIB620, one of many available signal conditioning and data interface modules for the PCM600 telemetry encoder product line. The PCM600 system is miniature modular telemetry encoder suitable for applications requiring instrumentation and data acquisition. Each PCM600 is configured with a base unit containing a power supply and program control functions and one or more stacking modules. The modules are selected to meet the requirements of each application. A pre-modulation filtered output from the base unit directly drives an FM transmitter with the formatted telemetry stream. The system operates from a 28 VDC supply.

DSP Signal Conditioning Module Implementation

Signal conditioning for 8 channels is provided on one 2.5 in. by 3.5 in by 0.375 in. (63.5 mm by 89 mm by 9.5 mm) module. Each channel has independently programmed gain, offset, and cutoff frequency. High density packaging is employed using fine pitch surface mounted devices.

Input signals are received using high impedance instrumentation amplifiers. Gain is user programmable from 1 to 500 in 256 steps, providing a selectable input range of 20 mV to 10 Volts full scale. Offset is user programmable from –50% to +50% of full scale in 256 steps. Filter cutoff frequency is user programmable from 10 to 5000 Hz with 10 filter frequencies per octave.

The module produces a 12-bit output at 160 kilo-samples-per-second (ksps), configured as 20 ksps on 8 channels. The DSP receives 100 ksps for each input channel, performs a series of filter and down sample operations, then applies gain and offset correction to produce the final output sample sequence. The output samples are made available to the base unit for insertion in the telemetry stream through addressable registers.

Analog Processing

Differential input signals are converted to single-ended by instrumentation amplifiers. With the gain set to one, the maximum input signal swing is 10 Volts peak to peak. The module provides a maximum gain of 500, which corresponds to 20 mV full scale input. Offset is programmable over +/-50 % of full-scale range relative to the 0-10v A/D input range, providing an input range of +/- 5V to 0-10V.

Gain and offset are both achieved through the use of coarse adjustment in the hardware and fine adjustment calculation in the DSP. A programmable gain instrumentation

amplifier (PGIA) is controlled by the DSP through select signals driven by the FPGA. The PGIA provides gains of 1, 10, and 100.

An analog 3-pole anti-aliasing filter with a corner frequency of 6 kHz is present on each channel. Frequency components existing above 95 kHz will fold over into the 5kHz desired signal passband, and therefore must be attenuated below the quantizing threshold of the 12 bit A/D. The corner frequency and response provides 72 dB of attenuation at 95 kHz and beyond, which suppresses aliases below the A/D resolution.

Multiplexed Gain and Offset Stages

After anti-alias filtering, a common signal processing path is shared by all 8 channels. This helps to minimize variations from channel to channel and reduces component count at the expense of operating at a higher speed. This approach supports the use of a single A/D converter to sample all 8 channels in sequence.

It is necessary to scale the input signal to maximize the use of the full-scale input range of the A/D. With only a decade gain selection available with the PGIA, the full-scale signal to the A/D for some gain settings would be only 1/10th of the input range. This would result in a loss of precision in the quantizing, resulting in effectively only 8-9 bits. Therefore, a second coarse gain stage is used to scale the signal to utilize at least 75% of full scale. The gains available at the second coarse gain stage are:

1.000, 1.333, 1.778, 2.371, 3.162, 4.217, 5.623, 7.500

Computed from:

$$G_i = 10^{\frac{i-1}{8}}$$

for values of i from 1 to 8.

The method used to derive these choices for gain is to further divide the decade gain ranges of the PGIA into uniform logarithmic steps. This approach maximizes the utilization of the A/D input range for all gain selections. When 75% of the dynamic range of the A/D is used, the effective number of bits is reduced to 11.5 bits. The number of effective bits is increased as the over-sampled input is filtered and reduced in rate from 100 ksps to 20 ksps, thus restoring the 12 bit resolution.

An 8 input multiplexer is driven by three address lines supplied from the FPGA to select one of eight gain setting resistors for an inverting stage. A register table in the FPGA is set by the DSP based on the gain setting programmed for each channel. This stage changes gain with each sample at the A/D converter rate of 800 kHz requiring a topology that is optimized for fast settling time. The actual gain at each setting will change over temperature, primarily due to changes in the series resistance of the multiplexer. For this reason, a low resistance multiplexer is used and gain setting resistors are selected to be as large as possible consistent with the fast settling time

needed. The change that does occur is corrected by temperature compensation in the DSP.

The offset range of +/- 50% is achieved through the use of coarse offset performed in hardware and fine offset calculated in the DSP. Hardware offsets available are:

+50.0%, +35.7%, +21.4%, +7.14%, -7.14%, -21.4%, -35.7%, -50.0%

These available offset settings uniformly divide the range of +/- 50%. The objective, as with the gain stage, is to maximize the utilization of the A/D input range without producing an overflow. The FPGA drives an 8 input multiplexer to select a resistor to produce the specified offset signal. Additional offset is computed by the DSP to achieve the programmed setting.

To achieve a particular gain or offset chosen by the user, the next lowest available hardware setting is used and the difference is supplied by calculation in the DSP. For example, if the desired gain is 95, the PGIA is set to 10, the second gain stage is set to 7.5, with the DSP multiplying each sample by 1.2. (10*7.5*1.2 = 95). Similarly, a desired offset of 49% is achieved by setting the hardware offset to 35.7% with 13.3% added to each sample by the DSP.

Digital Signal Processor

The ADSP2181 is a highly integrated single chip DSP. [1] The instruction cycle rate is 32 MHz, twice the externally supplied 16 MHz. It contains 16k words of program memory and 16k words of data memory on chip. All instructions execute in a single cycle giving the processor 32 million instructions per second (MIPS) capability at this clock rate. Although the instruction set is optimized for digital signal processing, a rich set of bit manipulation and input/output (IO) instructions, along with multiple sources of interrupts, allow the processor to function as an embedded controller as well as DSP.

The 24-bit wide program memory is loaded from a slower byte-wide non-volatile flash EPROM device, which also stores module specific calibration settings. The program code can be downloaded into the flash memory through the serial connection on the base unit allowing field upgrades to be performed easily. Calibration data is programmed during factory test.

Digital filter applications make extensive use of certain instructions, such as multiply and accumulate operations. Filters also require circular data buffers where the buffer pointer wraps around at the buffer length. The ADSP-2181 has a 16-bit by 16-bit hardware multiplier that produces a 32-bit result. It can fetch both multiplier operands along with performing a multiply and accumulate in a single instruction cycle. The ADSP-2181 has a sophisticated address generator that can advance a buffer pointer by a selectable amount and perform the pointer wrap in the same cycle with the operand fetches and arithmetic operation. After pointers are setup, zero-overhead looping enables each filter tap to be executed in only one instruction. Assembly language

programming is used to fully utilize these functions and optimize the code for execution speed.

The ADSP2181 has a high speed synchronous serial port used to transfer data to and from the FPGA. Data samples from the A/D and processed samples output to the telemetry stream use this mechanism. Configuration settings use I/O port registers mapped in the Input/Output memory space (IOMS) of the DSP.

Digital Processing

The digital filters used in the DSP module are finite impulse response (FIR) using a tapped delay line structure. The output at a given sample time is the weighted sum of the present input sample and a finite number of previous samples. The group delay of an FIR can be constant, providing a flat phase response with respect to frequency. The filter coefficients can be designed so there is no roll-off in the passband as with an analog filter. The FIR coefficients can also be designed to model the response of a prototype analog filter. If this is done, the digital filter will have the same roll-off and group delay characteristics.

Two categories of digital filters are used in the DSP module, one response for the decimation stages and one response for the final output filter. The role of the decimation stage filters is to reject high frequency components to allow a sample rate reduction without aliasing. The role of the final output filter is to reject high frequency components to prevent aliasing with the specific sample rate used in the telemetry frame. The final filter cutoff frequency is determined by the sample rate, which is a user specified parameter. Therefore, it is necessary to program the corner frequency.

The digital filters used for decimation are characterized by the passband ripple and stopband attenuation. They have linear phase response. The transition between the passband and stopband does not follow the straight-line slope of an analog filter when log magnitude is plotted against frequency. The digital filter has a flatter slope extending beyond the passband, and then drops off more rapidly toward the stopband. This allows several stages of filtering to be cascaded with minimal effect on the passband.

All channels pass through a 5:1 decimation filter to reduce the sample rate from 100 ksps to 20 ksps. This filter is a 33 tap FIR with Fpass = 5120 Hz with 0.1 dB ripple and Fstop = 14880 Hz and 72 dB of attenuation. This response provides sufficient attenuation so there is no aliasing into the passband of any of the final filters. Transition band aliasing occurs outside the passband and is suppressed -72 dB by the final filter so that there is no resolvable frequency component in the final output above Fs/2. The response is corrected for the roll-off of the analog anti-aliasing filter.

A linear phase FIR structure is used for the decimation filters. An FIR achieves processing reduction when performing down-sampling because the filter output must only be evaluated for each output sample (at the lower rate) and not for each input

sample. Each input sample must be put in the delay line history buffer of the filter. This is done by the autobuffering process for the serial port receiving the samples and does not require the explicit execution of any instructions beyond initializing the serial port. Each serial port autobuffer cycle "steals" one processor cycle, therefore contributing to the total processor loading. With a processor clock of 32 MHz and an aggregate sample rate of 800 ksps, the serial port autobuffering uses 2.5% of the processor time.

Programmable Decimation and Filtering

Down-sampling is required to realize reasonable length filters at low cutoff frequencies. A programmable multi-stage decimator reduces the input sample rate by passing the sample stream of each channel through a series of low-pass filters and down-sampling operations. Each stage bandlimits the signal and decimates by a factor of two. The overall decimation factor is separately programmed for each channel depending on the final filter cutoff frequency. The input sample rate is used directly for high frequency filters.

The final filter produces the response that bandlimits the signal to satisfy the sampling theorem. The theorem states that a signal must be sampled at a rate at least twice the highest frequency present in the signal [2]. This requirement must be satisfied at any point a sampling operation occurs. The analog filters achieve this goal for the A/D sampling and the decimation filters achieve this goal for the down-sampling operations. These elements are fixed in the module design. It is the responsibility of the user to select a bandlimiting frequency that is proper for the telemetry frame sample rate.

Filter cutoff frequencies are available over a nine-octave range. Each octave has ten filter frequencies from 1.0 to 1.9 times the octave base frequency, providing a 10 Hz to 4864 Hz range. Only ten unique sets of filters coefficients are used. These are stored in the DSP program memory area. The cutoff frequency octave is determined by the setting on the decimator and the frequency within the octave is determined by the coefficient set used.

As a result of the flexible software implementation, any filter response within the available processing limits can be achieved by storing the filter coefficients for the desired filter. A Butterworth response is the default response programmed into the signal conditioning module for the final bandlimiting filter. The attenuation of a Butterworth low-pass filter is expressed as:

$$A_{dB} = 10Log\left[1 + \left(w_x / w_c\right)^{2n}\right]$$

where w_x is a particular frequency, w_c is the 3-dB cutoff frequency, and n is the order of the filter [3]. This response is an approximation to an ideal filter that makes a compromise providing a flat response at zero frequency but gives up steepness in the transition band. The Butterworth response has been the typical filter for bandlimiting in telemetry applications because it provided reasonable component values and sensitivities. Due to the heritage of this type filter response, it has been retained as the

filter choice for this module. The filters implemented are 6th order or higher, depending on the cutoff frequency relative to the octave base frequency.

Output Interpolator

Each channel may be programmed with a different cutoff frequency, and therefore have a different down-sample factor. The output structure and interface between the DSP and telemetry stream requires that all channels operate internally at the same sample rate. Once the signal is bandlimited, down-sampled, and bandlimited again by the final output filter, all channels are up-sampled as necessary to the same rate. The interpolator is used to create samples at a higher sample rate, computing the values in between the available sub-sampled data points. A polynomial interpolator was chosen over a zero-stuff and filter approach because the interpolator is computationally more efficient at high up-sample factors, which can be as high at 128. Additionally, the same interpolator stage is used for sample rate conversion.

The 3rd order polynomial interpolator equations are derived using the Lagrange method with equal sample intervals. N data points have a unique N-1 order polynomial that exactly passes through the N data points. The Lagrange method derives the equation for the polynomial using the x and y values of the N data points available. After computing the coefficients, the polynomial can be evaluated in order to provide the amplitude at any arbitrary point in between the N data points. A new set of polynomial coefficients are computed for each sample produced by the final filter operation, then the polynomial is evaluated one or more times as necessary for up-sampling and sample rate conversion.

The interpolation is evaluated using a factored form as follows:

y = (ax + b)x + c)x + d

where y is the interpolated output value at time instant x. This evaluation requires 6 arithmetic operations. By utilizing the multiply/accumulate function of the DSP and multi-function instructions, only 3 instructions are needed, plus fetching and storing. The more significant effort is computing the coefficients a,b,c, and d from the known sample points.

The Lagrange polynomial is:

$$P_n(x) = \sum_{i=0}^{n+1} y_i L_{n,i}(x)$$

where n is the order of the polynomial, y_i is the sequence of amplitude values, and $L_{n,i(x)}$ is derived from the difference between x values $x_1,...,x_n$ as follows:

$$L_{n,i}(x) = \frac{\prod_{j=1}^{i}(x - x_j)}{\prod_{j=1}^{i}(x_i - x_j)}, \; j \neq i$$

The product is performed for j = 1 to i, except that j=i is not used. For j=i, a term in the denominator ($x_i - x_j$) = 0 would be produced and cause $L_{n,i}(x)$ to be invalid.

After each y_i point is multiplied by the corresponding $L_{n,i}(x)$ polynomial, the terms are combined to algebraically determine $P_n(x)$. The coefficients are then known:

$a = -y_1/6 + y_2/2 – y_3/2 + y_4/6$
$b = y_1/2 – y_2 + y_3/2$
$c = -y_1/3 – y_2/2 + y_3 – y_4/6$
$d = y_2$

Amplitude points y_n are produced by the final output filter at the sub-sampled rate. Points y_1, y_2, y_3, and y_4 are the history of sample values produced at the sub-sampled rate, with y_4 being the most recent. The interpolation is performed between samples y_2 and y_3. Samples y_1 and y_4 influence the slope passing through y_2 and y_3 and help determine the trajectory over the range. Interpolating between points y_2 and y_3, while requiring point y_4 for the computation, introduces a processing delay of one sample time.

The coefficients can be computed in the following manner to minimize the number of computations:

$d = y_2$
$b = (y_3 + y_1)/2 – y_2$
$a = -1/6 (2(b+y_3) – y_4 – y_2)$
$c = -(a + b + y_2 – y_3)$

This requires 12 arithmetic operations, plus fetching data values, storing results, and intermediate register moves. When added to the 6 operations needed for the polynomial evaluation, this compares favorably to the Farrow hardware structure proposed in [4] and [5], which requires 17 math operations plus 8 delay operations. A hardware implementation benefits from translating multiply operations to scaling, addition, and delay operations. In a software implementation all operations consume the same resource (an instruction), so total operations are the focus for efficiency.

Sample Rate Conversion

The DSP functions operate at a fixed sample rate. In general, the sample rate of a channel in the telemetry frame is a different sample rate. The fixed 20 ksps rate of the DSP would mix with the telemetry sample rate to produce frequency terms at the difference and harmonics of the difference. To eliminate this effect, the output processing of the DSP performs a sample rate conversion, where amplitude values are produced at sample intervals corresponding to the telemetry sample rate instead of the

DSP sample rate. The interpolator is used to compute the amplitude at the telemetry sample times, which are time instants in between the computed filter output samples.

The sample rate conversion is part of the up-sample interpolator. A time step accumulator is maintained for the output rate. This is structured as a numerically controlled oscillator (NCO). The phase of the NCO represents the difference between an oscillator operating at the DSP rate and an oscillator running at the desired sample rate. When scaled by the decimation factor it equals the difference between a DSP sample base point and the telemetry sample time instant. With a DSP sample base point defined as 0 phase, the scaled phase is applied to the interpolating polynomial to compute the output amplitude.

The NCO serves a second purpose of controlling the output sample rate. The sample rate conversion is synchronized to the telemetry sample rate of the fastest sampled channel in the module. Each of the other channels is required to be equal in sample rate or an integer factor below the fastest sampled channel. The phase increment applied to the NCO is computed using a proportional-integral control loop that tracks the telemetry sample rate and causes the DSP to produce the exact number of samples needed.

Temperature Compensation

The DSP module performs temperature compensation on measurements by monitoring the temperature of the module and correcting gain and offset values as a function of temperature. Gain and offset are separately corrected using a linear equation in the form of y = Mx + B. The values of M and B are determined during factory calibration. M represents the temperature coefficient and B represents the value of y at the reference temperature, which is selected to be room temperature to make calibration simple. For example, the gain correction equation is:

$$Gx = Kg*(Tx – Tr) + Gr$$

Gx = gain correction at measured temperature
Tx and Tr= measured and reference temperature, respectively
Kg = gain temperature coefficient
Gr = gain correction at reference temperature

The temperature measurement of the module is made using a digital temperature transducer, which outputs a pulse-width-modulated signal representing the temperature. The high-level and low-level intervals are measured using an eight-bit counter in the FPGA. The counter values are read by the DSP and converted to temperature using the equation:

$$C^{\circ}=235-(400*t1/t2)$$

t1 and t2 = high-level time period and low-level time period, respectively

Conclusion

This paper has described some of the requirements and design aspects of a programmable signal conditioning module employing DSP techniques. The results are achieved by using an optimized combination of hardware and software approaches. Flexibility has been achieved by performing many functions in software, which can be factory or field upgraded. The design serves as technology platform, which can be adapted through hardware or software changes for new applications.

References

[1] ADSP-2100 Family User's Manual", Third Edition, Analog Devices, Inc, 9/95.
[2] Stanley, W. D., "Digital Signal Processing", Reston Publishing Company, Inc., 1984.
[3] Williams, A. B., "Electronic Filter Design Handbook", McGraw-Hill Book Company, 1981.
[4] Gardner, F. M., "Interpolation in Digital Modems – Part I: Fundamentals", IEEE Trans. Commun., vol. 41, no. 3, pp. 502-508, Mar 1993.
[5] Erup L., Gardner, F. M., and Harris R. A., Interpolation in Digital Modems – Part II: Implementation and Performance" IEEE Trans. Commun., vol. 41, no. 6, Jun 1993.

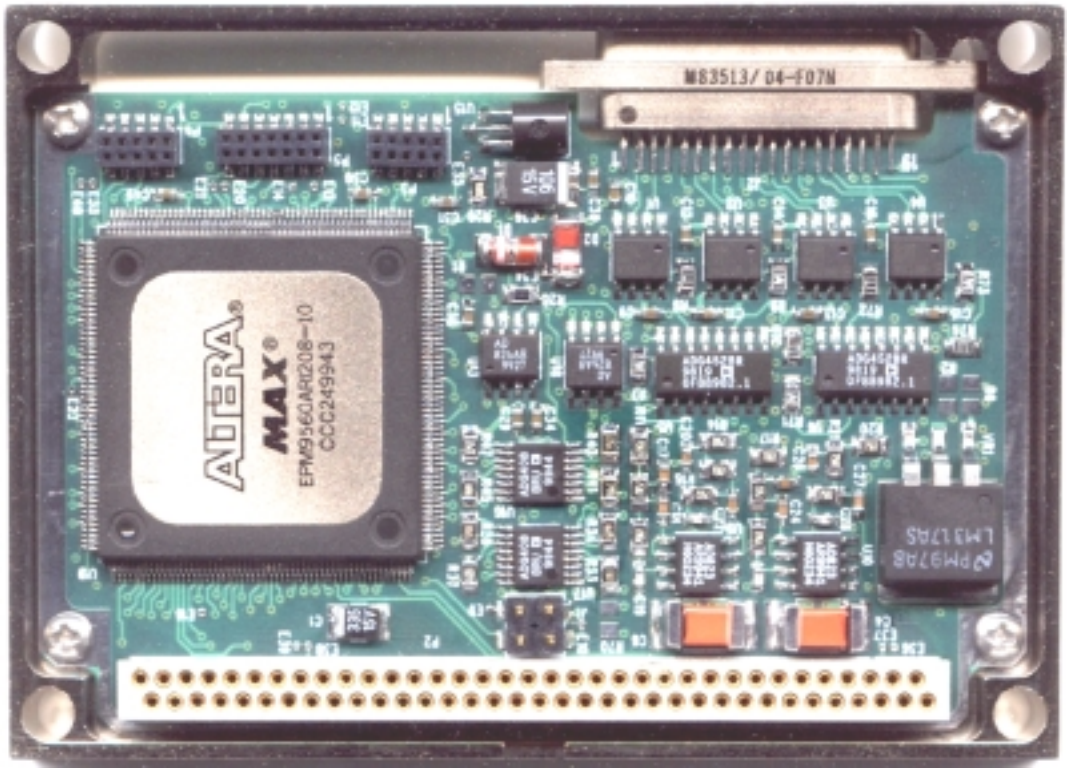
M8351L3/04-F07N
ALTERA
MAX
EPM9560ARQ208-10
CCC249943
LM1742S

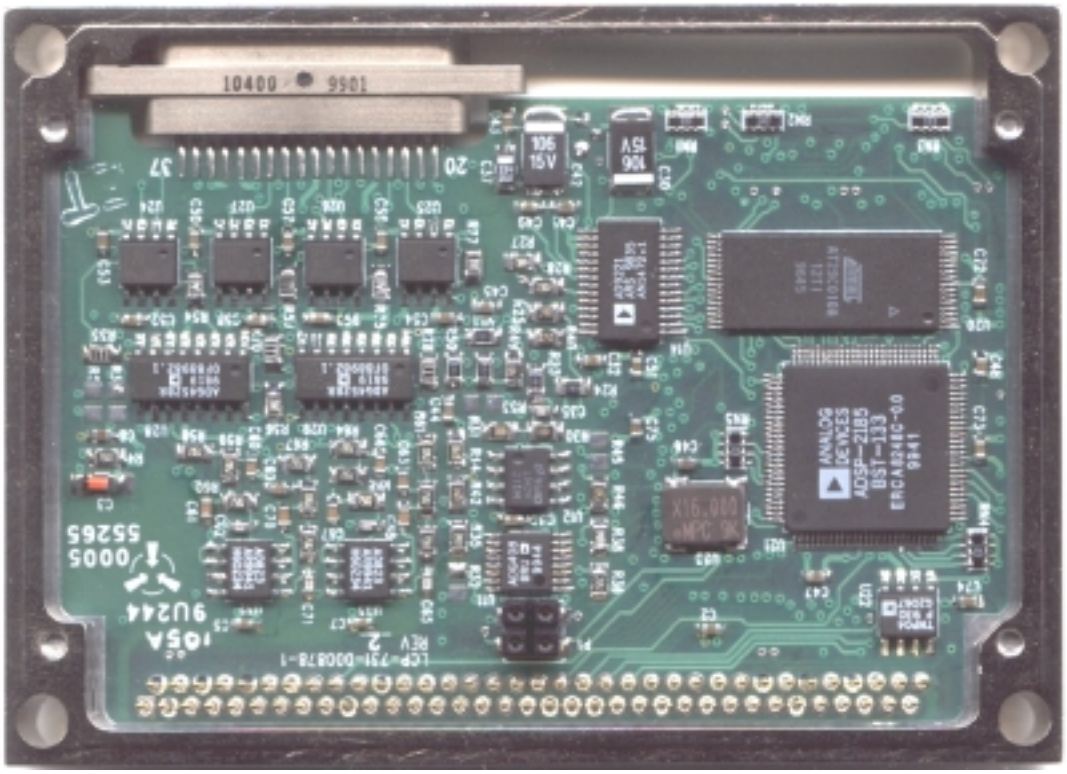
10400
9501
ANALOG DEVICES
ADSP-2185
BST-133

DSP Signal Conditioning Module Block Diagram

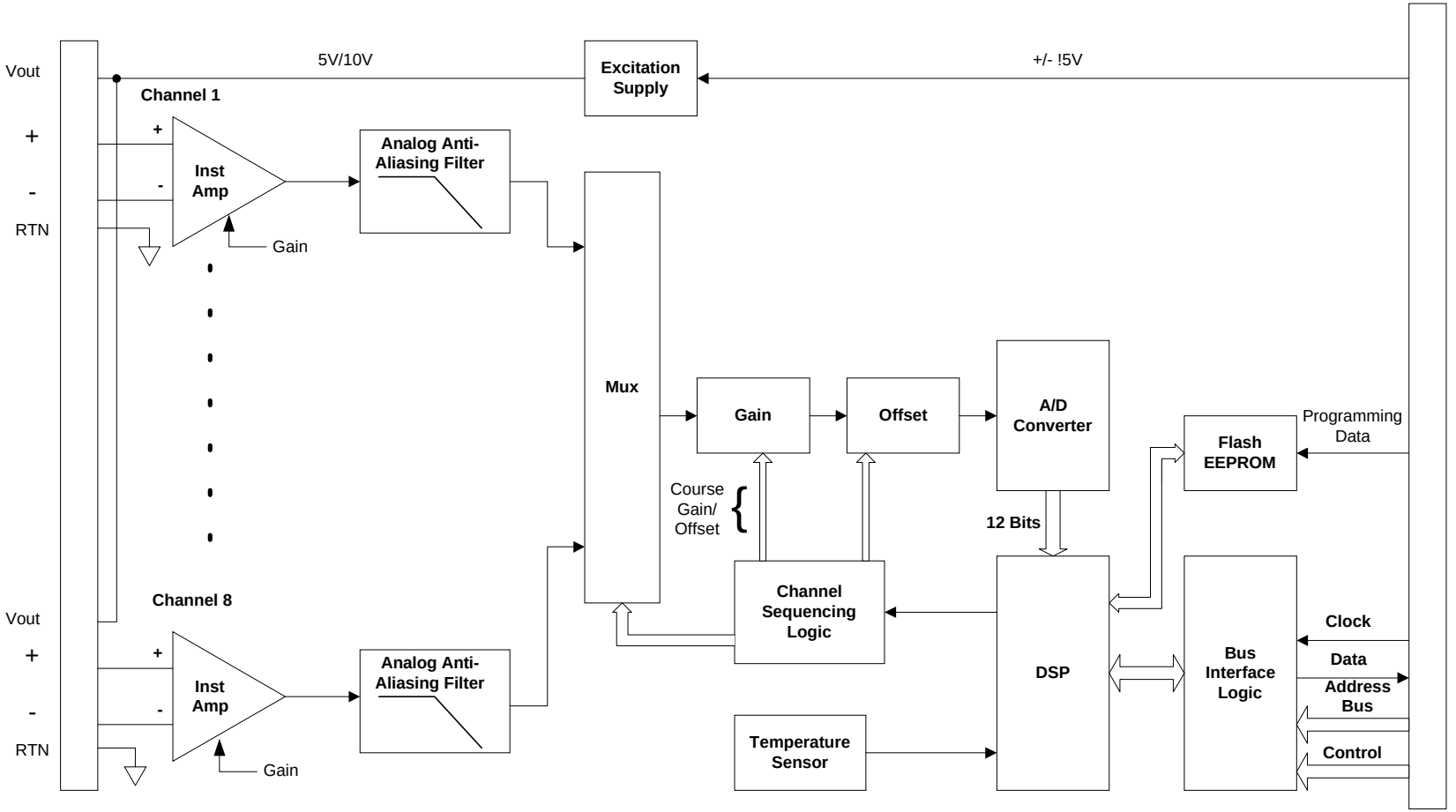

DATA TRANSMISSION, DATA NETWORKS AND CODING TECHNIQUES

The R&TTE-Directive
- Requirements on Radio Equipment -

Dipl.-Ing. Uwe Kartmann
CETECOM ICT Services GmbH
Saarbrücken, Germany

Abstract

By the 8th of April 2000 the European "Directive 99/5/EC [1] of the European Parliament and Council of the European Union on radio equipment and telecommunications terminal equipment and the mutual recognition of their conformity" (R&TTE-Directive) will be into force in all EEA Countries. The new directive will bring about major changes in the routes to market taken by manufacturers seeking to sell radio equipment and telecommunications terminal equipment into European markets.

Introduction

Until the above mentioned date the placing on the market and putting into service of radio equipment was regulated by both, European directives and national law of each Member State. Essential requirements like EMC, TTE, or health and safety requirements were covered by European New Approach Directives. In addition a type approval procedure according to national type approval regulations was required in each Member State. Technical requirements which had to be met were specified in national technical standards, which usually were based on ETSI-standards.
The quantum leap from the closely regulated regimes based on national type approval to a Europe-wide light regime based on manufacturers' declaration as specified in the R&TTE-Directive, opens both, opportunities and risks as perceived by manufacturers and regulators alike. Particular concerns arise over those radio devices using the many non-harmonised radio frequency allocations in the Member States.
The situation will be more complicated as before: On the one hand manufacturers will be fully responsible for meeting all essential requirements defined into the Directive although there are no harmonised standards according the R&TTE-Directive available at the moment. On the other hand, they must find a way for demonstrating compliance with the requirements of the Directive. At the same time they must know details about requirements on interface specifications and frequency allocations in each of the Member States, even if they don’t intend to place the equipment in each of these states into the market. It is important to know that this directive is no frequency harmonisation directive and the spectrum management will remain under

national regulation. National frequency requirements must be fulfilled before the radio equipment is allowed to be operated into the desired Member State.

The New Approach [2]

The R&TTE-Directive is a directive of the *New Approach*. It follows, as all EC-directives of this kind do, the principle of uncompleteness. Here only essential requirements, mainly safety requirements, are specified, technical details are left out. Those are put in concrete terms in the technical specifications, so called *Harmonised Standards*. The advantage of this system consists in the fact that, considering the rapid development of technology, permanent amending of the directive is not necessary. The scope of applicability of New Approach Directives refers to the products. In case of overlaps the manufacturer or his authorised representative established within the Community has to find out according to which directives he has to demonstrate the conformity of his product for CE-marking it and finally, for placing it on the market.
For equipment within the meaning of the R&TTE-Directive, the Low Voltage Directive (LVD) 73/23/EEC [3] and the EMC-Directive 89/336/EEC [4] do not apply. Of course, the protection requirements laid down in these directives are still effective. There is also the possibility to apply defined conformity assessment procedures.

National Implementation

The Member States was given one year for the national implementation of the R&TTE-Directive. As this time frame does not correspond to today's usual duration of legislative processes, the German *Law on radio equipment and telecommunications terminal equipment* (*Gesetz über Funkanlagen und Telekommunikationsend-einrichtungen, FTEG)* might be passed rather late. The FTEG will replace §§ 59-64 (type approval) of the *Telecommunications Act (TKG)* [5]. Today's Tele-communications Type Approval Ordinance *(TkZulV)* [6] which lays down the implementation of these paragraphs of the TKG has also to be replaced. Here, a successive ordinance called *Verordnung über die Anforderungen und das Verfahren für die Anerkennung von benannten Stellen auf dem Gebiet der Funkanlagen und Tele-kommunikationsendeinrichtungen (FTEV)* is being planned. When planning new products, it cannot be expected of manufacturers to wait for the publication of these regulatory frameworks. They have no choice but to work, under consideration of the frame defined by the R&TTE-Directive, and to hope that the national specifications will be close to those of the directive. The transitional period of two years (as of 7 April 1999) allows the application of the regulations valid up to now. But this period is strictly defined: only until 7 April 2000 approvals according to the old regime are possible. With that „old" demonstration of conformity, products are allowed to be placed on the market until 7 April 2001. From 8 April 2001 all equipment placed on the market must meet the requirements of the R&TTE-Directive.

Scope

The regulatory framework established by the R&TTE-Directive refers to all telecommunications terminal equipment and to radio equipment in the frequency

range 9 kHz to 3000 GHz, with a few exceptions (see Fig. 1*)*. Article 1.2, 1.3 specifies the application for medical devices and motor vehicles.

Equipment	*Regulation*
Radio equipment used by radio amateurs	ITU Radio Regulations, Art.1 Def. 53
Marine equipment	Directive 96/98/EC
Cabling and wiring	---
Radio and TV broadcasting receivers	Directive 89/336/EEC
Equipment on civil aviation	Regulation (EEC) No. 3922/91
Air traffic management equipment	Directive 93/65/EEC
Apparatus exclusively used for activities concerning: - public security - defence - state security - activities of the state in the area of criminal law	National Regulation

Fig. 1: Exceptions

Essential requirements

Which *Essential Requirements* does apparatus have to meet within the meaning of this directive? Two requirements are always essential:

- Protection of the health and the safety of the user including the LVD requirements with no voltage limits applying
- Protection requirements with respect to electromagnetic compatibility

For radio equipment the effective use of the allocated spectrum and orbital resources applies additionally. For special equipment the Commission can define additional essential requirements. If this is the case, the Commission determines the date of application of the requirements (Art 6.2). TCAM, the „Telecommunication Conformity Assessment and Market Surveillance Committee“ has agreed not to define any additional essential requirements up to 1 January 2001. Nevertheless, since the second half of the year 1999 there have been efforts to define essential requirements for avalanche beacons and non-SOLAS maritime radio equipment according to Art 3.3.d in order to comply with particular essential requirements. In parallel to this there are attempts to amend the Council Directive on Marine Equipment 96/98/EG for any kind of vessels.

Interface specifications

Interface specifications shall allow manufacturers to meet the essential requirements which apply to the equipment. The Member States notify the interfaces which they have regulated to the Commission insofar as the said interfaces have not been notified under the provisions of the Telecommunications Terminal Equipment (TTE) Directive [7]. So one can conclude that all Member States will notify accurate descriptions of the radio interfaces for any kind of radio equipment whose use is not harmonised in the Community. In general this applies to all radio transmitters except GSM-, DECT-, TFTS- and TETRA-equipment. The Commission establishes the equivalencies between notified interfaces and assigns an equipment class identifier. In a first step TCAM defined two equipment classes: equipment which may be put into service throughout the whole Community and equipment which may only be put into service in certain geographical areas. The latter will be marked with an alert symbol in addition to the CE mark.

Harmonised standards

Harmonised standards according to the New Approach are a possibility for the presumption of conformity. The question is whether new standards will be available on 8 April 2000. This is not so bad as the transitional provisions allow the application of those standards with reference to the Low Voltage Directive and EMC Directive whose references were published in the Official Journal of the EC. Of course, it has to be considered that the lower voltage limit defined in the Low Voltage Directive ceases to apply. The CTRs/TBRs published under the Telecommunications Terminal Equipment Directive whose references were published in the Official Journal of the EC can be used for the presumption of conformity together with the essential requirements specified in Art 3. For radio equipment not within the scope of the terminal directive or for radio equipment without defined harmonised standards according to the previous directive, a *Notified Body* is the only solution.

Equipment Attributes	
A	RE that is unable to transmit before receiving an appropriate enabling signal
B	RE that is able to transmit without receiving an appropriate enabling signal
C	RE capable of receive only
D	Apparatus intended for use in ‘emergency applications’
E	Short range radio transmitting devices
F	RE intended for installation in sites which may be shared with other RE without co-ordination from single operator
G	RE sharing radio spectrum resources with or without operational co-ordination
H	TTE using an electrical interface for communication
I	TTE using an optical interface for communication

Fig. 2: Equipment Attributes

The ETSI task group TC ERM TG 6 worked on a guideline for the development of standards according to the requirements of the R&TTE-Directive, available as draft EG 201 399 [8]. Although it is very much discussed it gives useful hints which phenomena will be decisive for which equipment attributes within the meaning of the R&TTE-Directive.

All standards should have the same modular structure. ETSI published a guidance to the production of harmonised standards for application under the R&TTE Directive [9]. Furthermore, ETSI forwarded two working documents for the alignment of the present TBRs [10] and Radio Standards [11] with the requirements of the R&TTE-Directive. Here all standards for each product class are listed. The technical phenomena are sorted out with the help of the guideline EG 201 339 and the result shows the remaining requirements according to the R&TTE-Directive. Additionally, summaries of existing standards are recommended. For Short Range Devices e.g., which were almost completely covered by the standards EN 300 330, EN 300 220-1 and EN 300 440, only one standard is proposed which encompasses all SRDs within the range 9 kHz to 40 GHz. The required technical phenomena are the following:

Essential Requirement	*Phenomena*	*Equipment Attributes*								
		A	B	C	D	E	F	G	H	I
Art. 3.2 (Transmitting)	Frequency error / stability, and designation of channels	✓	✓			✓		✓		
	Transmitter power	✓	✓			✓		✓		
	Adjacent channel power	✓	✓			✓		✓		
	Spurious emissions	✓	✓			✓		✓		
	Inter-modulation attenuation						✓			
	Release time	✓						✓		
	Transient behaviour of the transmitter	✓	✓					✓		
	Modulation accuracy	✓	✓			✓		✓		
	Duty cycle					✓		✓		
Art. 3.2 (Directional)	Off-axis EIRP density	✓	✓					✓		
	Antenna gain	✓	✓					✓		
	Antenna X-polar discrimination	✓	✓					✓		
	Antenna pointing accuracy/control	✓	✓					✓		
Art. 3.2 (Receiving)	(Maximum usable) sensitivity (inc. duplex)				✓					
	Co-channel rejection				✓					
	Adjacent channel selectivity	✓	✓	✓		✓		✓		
	Spurious response rejection (inc. duplex)	✓	✓	✓		✓		✓		
	Inter-modulation response rejection	✓	✓	✓		✓	✓	✓		
	Blocking or desensitisation (inc. duplex)	✓	✓	✓		✓		✓		
	Spurious emissions	✓	✓	✓		✓		✓		
	Multipath sensitivity				✓					

Fig.3: Phenomena (1)

Essential Requirement	*Phenomena*	*Equipment Attributes* A B C D E F G H I
Art. 3.2 (TDM: CDM: Control and Monitoring Functions for Terminal)	Enabling signalling	✓
	Sharing protocols	✓ ✓ ✓
	Network interface bit errors	✓
	Error control by coding and decoding of logical channels	✓
	Logical channel arrangement	✓
	Control of communication in logical channels	✓
	Correct interpretation of Network control information	✓
	Network interface addressing	✓
	Control of basic link communication	✓
	Control of random access	✓
	Control of radio resource allocation	✓
	Monitoring functions for cell selection	✓
	Control functions for usage of cells	✓
	Control of group attach/detach	✓
	Tx enable/disable control	✓
	Tx call set up control	✓
	Control of call maintenance	✓
	Control of call disconnect	✓
	Authentication control	✓
	Encryption control procedures	✓

Fig.4: Phenomena (2)

Additional requirements

In addition to the *Declaration of Conformity (DoC)*, information about the geographical area where the radio equipment will be put into service is required, as well as information about possible restrictions or conditions attached to authorisation. The reason for this is that despite vehement harmonisation efforts, frequency ranges are allocated nationally. Again and again it must be emphasised that the R&TTE-Directive is no frequency harmonisation directive. The frequency allocation management will remain in national competence in the future. Legal basis in Germany is the Telecommunications Act.
Additional information is also required for telecommunications terminal equipment. Where it concerns those, such information shall be sufficient to identify interfaces of the public telecommunications networks to which the equipment is intended to be connected.
Where to get this information? Authorities of the Member States are helpful in every case. But this way is laborious and time-consuming: in the worst case 18 authorities have to be contacted. Using the consulting service of test houses with their expert knowledge and long-term experience is much more advantageous.

Conformity assessment procedure and marking

The manufacturer's freedom to choose a suitable conformity assessment procedure which automatically leads to a Europe-wide market access of his product, is intended by this directive. The different conformity assessment procedures and their application were presented in detail in [12]; Fig. 5 illustrates a summary.

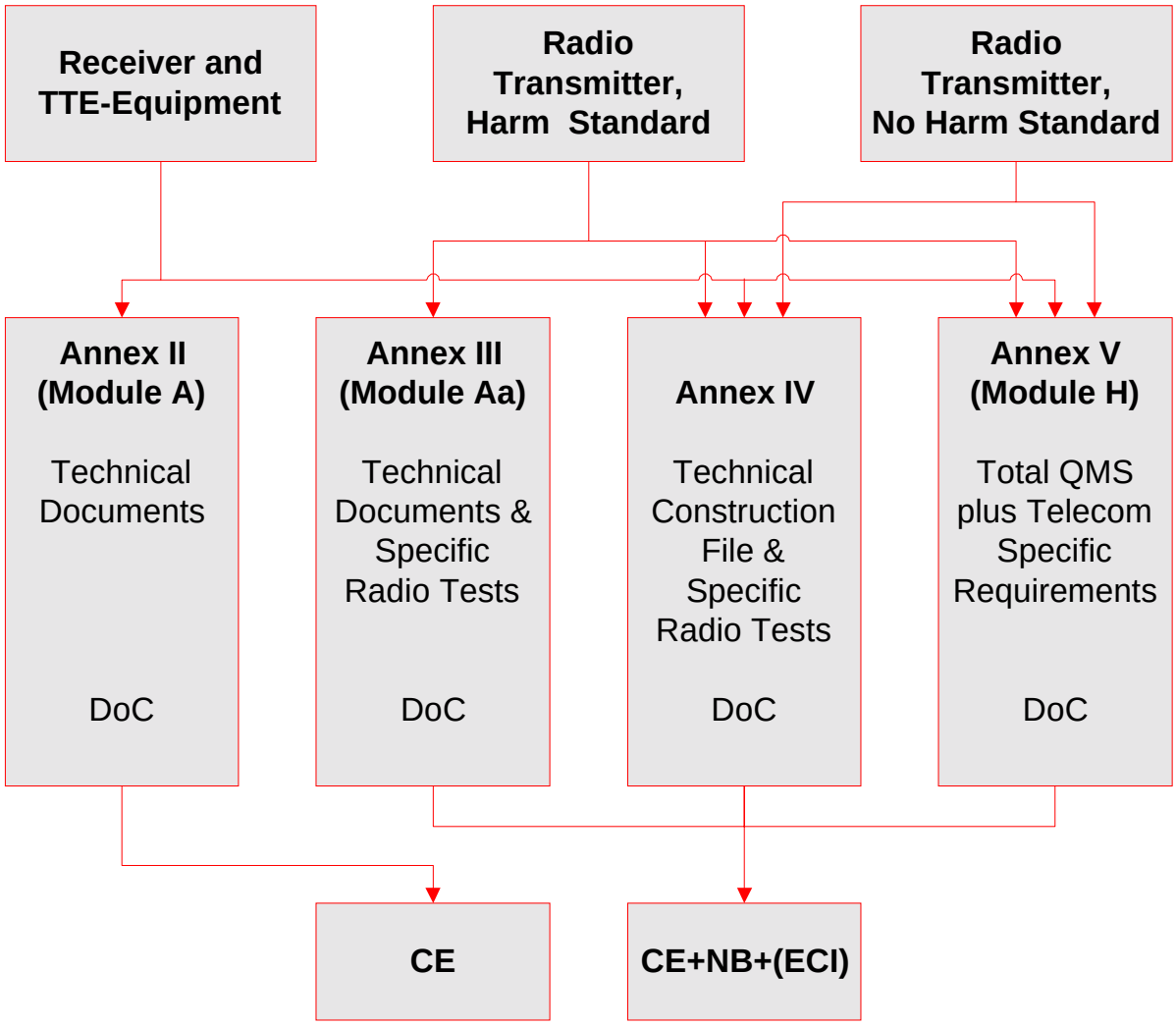

Fig. 5: Conformity assessment procedures

All procedures have one feature in common: conformity has to be demonstrated with the technical documentation containing the description of the product, user's manual, manufacturing drawings and schemes, description of the solutions chosen for meeting the essential requirements etc. and last but not least the test report. At this time at the latest the manufacturer must check whether he has the possibility to run the measurements of his own or whether it might not be more advantageous to address to an accredited test house which handles the measurements and test documentation in a fast and accurate way with efficient tools. Also with regard to issuing the complete documentation set this question is worth thinking about.

It is up to the manufacturers in how far they subject their product to further quality tests, voluntary certification- and marking schemes for improving consumers' confidence. The directive's preamble explicitly says that Member States may support such schemes.

Summary

In the preliminary stages of product development, several observations have to be made in order to fulfil the requirements of the R&TTE-Directive. The following concise overview shall serve as a guideline:

- Is the equipment covered by the R&TTE-Directive?
- Which essential requirements have to be met?
- Which annex of the directive has to be considered for a conformity assessment?
- Do applicable harmonised standards exist?
- If not, no annex V and if radio transmitter, contact Notified Body!
- If apparatus is radio transmitter, pay attention to national frequency allocation!
- If apparatus is radio transmitter, pay attention to national authorisation provisions!
- If apparatus is telecommunications terminal equipment, pay attention to tele-communications network interfaces!
- Decide if tests shall be run in a testing laboratory!
- Decide if documents shall be issued by a testing laboratory!
- Are additional voluntary quality tests and certification appropriate?

Before placing on the market the following points have to be considered:

- Is the documentation for demonstrating conformity complete?
- Is apparatus and packaging marked correctly?
- Is the service of a third party, e.g. a test house, necessary concerning instructions for operating apparatus?
- Were frequency management authorities sufficiently informed?
- Are the requirements concerning authorisation met in every Member State?

The above-mentioned central ideas illustrate that the R&TTE-Directive transfers the full responsibility to manufacturers and distributors. They are fully responsible for following the technical regulatory framework. In most cases these high requirements can only be met with the help of third parties. Nevertheless, placing products on the market is a more and more accelerated process. Time will tell whether this new system will be more economical than it has been until now. Time will also tell whether it will be sufficient as a criterion for placing radio equipment on the market although the European spectrum has not been harmonised yet. Should it fail, then first the users, e.g. network operators or end-users will be the sufferers, and, finally, the manufacturers themselves.

Notes

[1] Directive 99/5/EC of the European Parliament and the Council of 9 March 1999. Brussels: Official Journal of the European Communities L 91, 7 April 1999.

[2] Council Resolution of 21 December 1989 on a global approach to conformity assessment. Brussels: Official Journal of the European Communities C10/1 and 2, 16 January 1990.

[3] Council Directive of 19 February 1973 on the harmonisation of the laws of the Member States relating to electrical equipment designed for use within certain voltage limits (72/23/EEC). Brussels: Official Journal of the European Communities L 77/29, 26 March 1973.

[4] Council Directive of 3 May 1989 on the approximation of the laws of the Member States relating to electromagnetic compatibility (89/336/EEC). Brussels: Official Journal of the European Communities L 139/19, 23 May 1989.

[5] Telekommunikationsgesetz (TKG) vom 25. Juli 1996.
Bonn: Bundesgesetzblatt, Jahrgang 1996 Teil I, Nr. 39, 31. Juli 1996.

[6] Telekommunikationszulassungsverordnung, 20. August 1997.
Bonn: Bundesgesetzblatt, Jahrgang 1997 Teil I, Nr. 60, 28. August 1997.

[7] Directive 98/13/EC of the European Parliament and the Council of 12 February 1998. Brussels: Official Journal of the European Communities L 74, 12 March 1998.

[8] A Guide to the Production of candidate Harmonized Standards for application under the R&TTE Directive: draft F EG 201 399, May 1999 and draft E EG 201 399, March 1999. European Telecommunications Standard Institute.

[9] Guidance to the production of candidate Harmonized Standards for application under the R&TTE Directive (1999/5/EC); Pro-forma candidate Harmonized Standard: SR 001 470 V1.1.1, October 1999. European Telecommunications Standard Institute.

[10] Report on the implication of the R&TTE Directive for existing TBRs; STF 149: Report on TBRs V0.1.2 November 1999. European Telecommunications Standard Institute.

[11] Report on the implication of the R&TTE Directive for existing radio (not EMC) product standards; STF 149: Report on Radio V0.1.2 November 1999. European Telecommunications Standard Institute.

[12] Uwe Kartmann: Die geplante europäische R&TTE-Richtlinie. EMC Kompendium 1999, p. 46

The Fundamental Conceiving of Implementing CCSDS Recommendation in China

Yu Zhijian Fang Hongrui
(Beijing Institute of Technology of Tracking and Telecommunication, Beijing 100094)

Abstract

The researching and implementing of CCSDS recommendation in international has developed rapidly and have been a strong trend in near years. Up today there are 150 space mission have been registered in CCSDS, including not only satellites, space shuttle, orbit stations, but also carrier rockets, such as ARIANE 5(France). How to implementing CCSDS recommendation has been turned into an important question before us. Our fundamental conceiving is: on the basis of the network of tracking and telecommunication having been developed in China, utilizing advanced digital technology, such as reconfiguring technology, the function of the network can be extended to be compatible with CCSDS recommendation and to fit for manifold type of missions in China and international cooperation.
Keywords: CCSDS recommendation, implementing, fundamental conceiving

1 Introduction

CCSDS recommendation has been introduced to China for ten years, but it has not been adopted systemically because of all kinds of reasons. Up today there are 150 space mission have been registered in CCSDS, including not only satellites, space shuttle, orbit stations, but also carrier rockets, such as ARIANE 5(France). How to implementing CCSDS recommendation has been turned into an important question before us. Our fundamental conceiving is: on the basis of the network of tracking and telecommunication having been developed in China, utilizing advanced digital technology, such as reconfiguring technology, the function of the network can be extended to be compatible to CCSDS recommendation and to fit for manifold type of missions in China and international cooperation.

2 Contents of function extension

2.1 Analyzing of today's status

The network of tracking and telecommunication for space research has been developed

gradually together with the researching of spacecraft in China. Today the transition from UHF system to S-band system has completed. A S-band network of tracking and telecommunication has been formed and it will be the main role of the networks of tracking and telecommunication for space research in China.

2.2 Extension contents

2.2.1 Radio frequency, modulation and radio metric

The radio frequency and modulation of the USB(Unified S–Band) systems, which exist in China currently, meet the requirements of "CCSDS 401.0-B-1: Radio Frequency and Modulation Systems – Part 1:Earth Stations and Spacecraft". Its radio metric meet the requirements of "CCSDS501.0-B-1：Radio Metric and Orbit Data". So, these part of hardware and software can be used continue.

2.2.2 Telecommand

For the USB system, packet telecommand can be implemented in the upload sub-carrier. But, the sub-carrier method should be washed out according to CCSDS recommendation. The function of telecommand terminal should be extended with BCH encoding, data protecting, packetization, virtual channel management, in the light of CCSDS 201.0-B-2 , 202.0-B-2, 201.0-B-1 and 203.0-B-1.

2.2.3 Telemetry

Packet telemetry can be implemented in downlink QPSK channel, but the function of telemetry terminal should be extended with channel decoding, de-framing, de-packetization and data dispatching, according to 101.0-B-3, 102.0-B-4 and 103.0-B-1.

2.2.4 Time Code Format

Presently, IRIG-B is used in the USB system in China. It can be used continued or new time code format is chosen and new time terminal is developed, according to "CCSDS 301.0-B-2: Time Code Format"

3 Conceiving of Function Extension

3.1 Aim

The aim of function extension is tuning the existing network of tracking and telecommunication into a network which meets AOS and COS specs of CCSDS recommendation together with our current space data standards.

3.2 Function of the system

a. Packet telecommand;
b. Packet telemetry;
c. Distance measuring;
d. Velocity measuring;
e. Time code;
f. Retaining all the other current functions.

3.3 Compose of the system

a. The current USB(United S-band) system in existence;
b. Packet telemetry real-time transmission sub-system;
c. Telemetry de-packetization and data dispatching sub-system;

d. Telecommand packet incepting and composing sub-system;
e. Time code sub-system.
The diagram of ground device of CCSDS compatible spacecraft TT&C system is illustrated in figure 1.

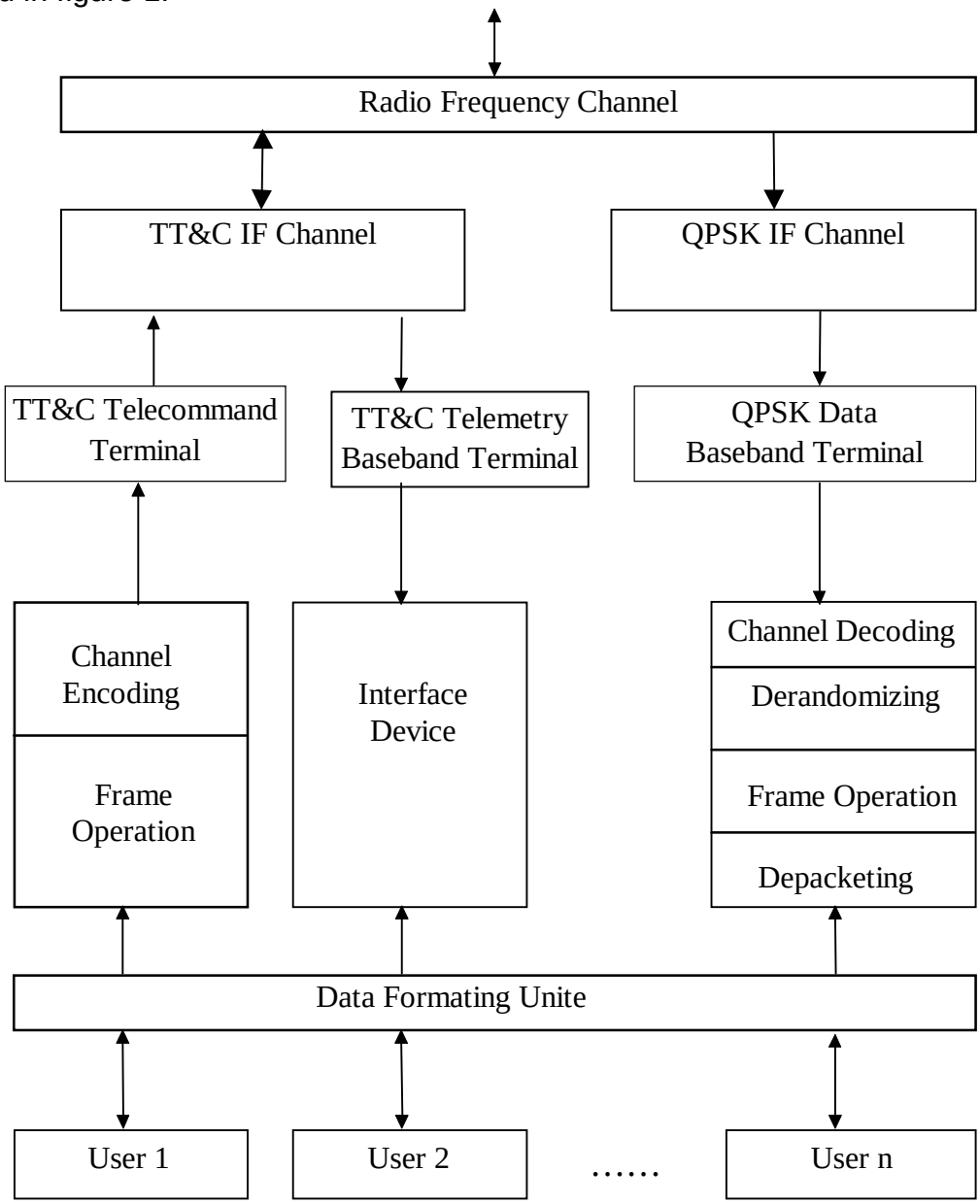

Figure 1 The diagram of ground device of CCSDS compatible spacecraft TT&C system

3.4 Key technical specs upon extension
3.4.1 Carrier frequency
a. One pair of carriers for TT＆C's uplink and downlink, which are correlated with each other and the correlation ratio is 221/240;
b. One carrier frequency for data transmission.
3.4.2 Frequency band
a. Uplink: 2025~2120MHz, step 0.1KHz;
b. Downlink: 2200~2300MHz, step 1KHz.
3.4.3 Working mode

a. The working mode for TT&C is sub-carrier PSK/PM correlatively transmitting, in which telecommand signal and distance measuring tones have modulated onto uplink carrier and telemetry signals and distance measuring tones have modulated onto downlink carrier.

b. Modulation mode for downlink data transmission is PCM-QPSK.

3.4.4 TT&C sub-carrier

a. Telecommand: 8KHz, 16KHz;

b. Telemetry: 5KHz~512KHz, step 1Hz.

3.4.5 Equivalent distance measuring tones

100KHz, 20KHz, 16KHz, 16.8KHz, 16.1KHz, 16.032KHz, 16.008KHz.

3.4.6 Data rate

a. Telecommand: 100bps~4kbps, step 1bps;
sub-carrier/data rate = integer

b. Telemetry: 100bps~64Kbps, step 1bps;
sub-carrier/data rate = integer

c. Data transmission: 64Kbps~1Mbps, step 1bps.

3.4.7 Code type and sub-carrier modulating mode

a. Telecommand: NRZ-L, M, S; PCM-PSK.

b. Telemetry: NRZ-L, M, S; PCM-DPSK.

c. Data transmission: NRZ-L, M, S.

3.4.8 Bit error rate

a. Convention telemetry: $P_e \leq 10^{-5}$ (not including channel encoding)

b. Telecommand: $P_e \leq 10^{-6}$.

c. Packet telemetry: $P_e \leq 10^{-6}$ (not including channel encoding)
$P_e \leq 10^{-7}$ (including channel encoding)

3.4.9 Data format

a. Telecommand

Meets the requirements of “Satellites telemetry and telecommand and data management PCM telecommand, GJB1198.1-91”;

And “CCSDS 202.0-B-2: Telecommunication Part 2-Data Routing Service”;

And “CCSDS 203.0-B-1:Telecommunication Part 3-Data Management Service”.

b. TT&C telemetry

Meets the requirements of “Satellites telemetry and telecommand and data management PCM telecommand, GJB1198.1-91”;

c. Data transmission(Packet telemetry):

Meets the requirements of “Satellites telemetry and telecommand and data management PCM telecommand, GJB1198.1-91”;

And “CCSDS 102.0-B-4: Packet Telemetry”.

3.4.10 Packet telecommand operating procedures

Meets the requirements of “CCSDS 202.1-B-1: Telecommunication Prat2.1-Command Operation Procedures”.

3.4.11 Packet telemetry channel coding

Meets the requirements of “CCSDS 101.0-B-3: Telemetry Channel Coding”.

3.4.12 Data randomization

Meets the requirements of “CCSDS 701.0-B-1: Advanced Orbiting Systems, Networks

and Data Links Architectural Specification".
3.4.13 Time code format
Meets the requirements of "CCSDS 301.0-B-2: Time Code Format".
3.4.14 User number: 64×64.

4 Extension scheme of telecommand sub-system

4.1 Application conceiving

Chinese tracking and telecommunication network should have devices which support routing service and channel service in order to meet the requirements of CCSDS recommendation and support the users of meeting the requirements of CCSDS recommendation. Whether its convention users develop devices which meet the requirements of CCSDS recommendation decided by its circumstance, but if they want to use others network of CCSDS recommendation packetization layer, they should develop CCSDS device correspondingly.

Presently, Chinese ground devices of S-band telemetry and telecommand are only compatible with CCSDS recommendation in physical layer and their users' telecommand data are not compatible with CCSDS recommendation. So, the devices of segmenting layer, transmission layer and coding layer should be developed.

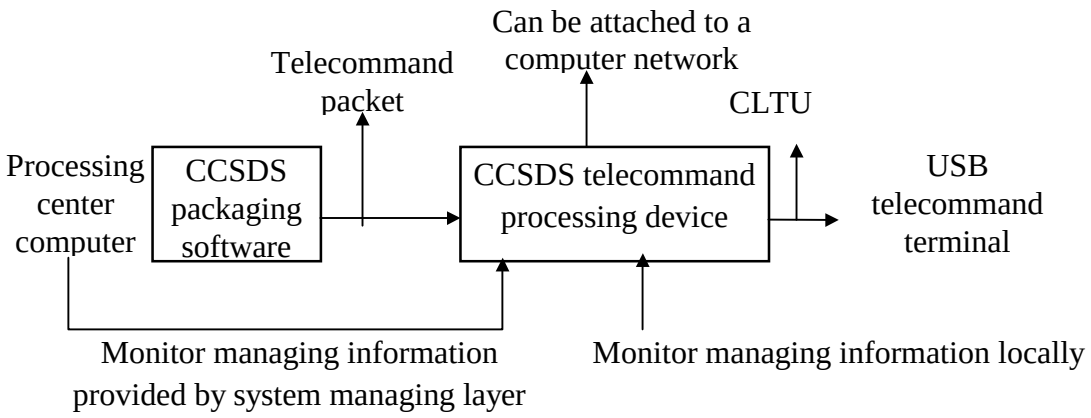

Figure 2 The block diagram of extension CCSDS devices

4.2 Extension scheme

The block diagram is illustrated in figure 2.

The function of the CCSDS packetization device in the processing center is implemented by developing the data format converting in former processing center computer or a new computer, according the requirements of CCSDS 203.0-B-1, chapter 5.

The function of the CCSDS packetization device in the ground station is implemented by adding a CCSDS telecommand processing device which carries out segmenting service and transmission service of CCSDS 202.0-B-2 and 202.1-B-1 and coding operation of CCSDS 201.0-B-1.

The technical specs are as follows:

Modulation mode: NRZM-PSK-PM;

Max bit rate: 8Kbps(32KHz sub-carrier);

Physical channel bit error rate: (Having BCH encoding): 10-7;
Users of ground station: 64×64;
Having data protecting technology.

5 Extension scheme for telemetry sub-system

5.1 Current telemetry of USB device

The USB device has a data transmission channel of PCM-QPSK, which can be used for two 64Kbps~1Mbps data stream and its I channel is for television image and Q channel for telemetry, its physical bit error rate is 10^{-5}(not including channel encoding). The diagram is illustrated in figure 3.

5.2 Extension scheme

Under the condition of the physical cannel of USB not changed, all former function are retained and all the functions of “CCSDS 101.0-B-3: Telemetry Channel Coding” are met.

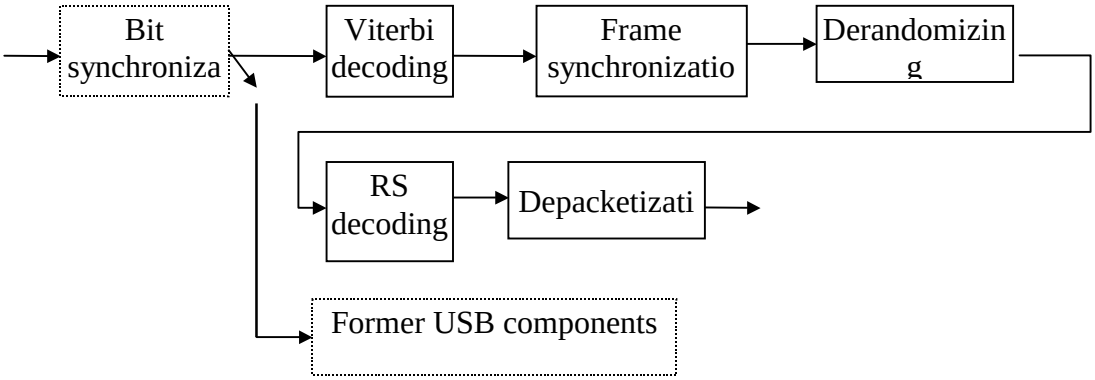

Figure 3 The diagram of telemetry compatible with CCSDS

If bit rate is not changed, the IF QPSK receiver and bit synchronizer of USB system can be used, but a switch is needed to control the data stream according its application. In figure 3, the parts with dashed line are the former component of USB which settings are unchanged and the parts with real line are new components for Viterbi decoding, frame synchronization(including ASM), derandomizing, RS decoding and depacketization.

6 Time code format

There are four time code format: CUC, CDS, CCS and ASCII, which are recommended in “CCSDS 301.0-B-2: Time Code Format”. Their performances are compared in table 1.

Table 1 The four time code format

	CUC	CDS	CCS	ASCII
Grade	1 or 2	1 or 2	1	1
Segments	No segmenting	2~3	5~12	over 6
Coding mode	Binary	Binary	BCD	Character
Coding efficiency	Highest	Higher	Lower	Lowest
Basic time differentiate	1S	1×10^{-3}S	1S	0.1S
Highest time differentiate	6.0×10^{-5}S	1×10^{-5}S	1×10^{-12}S	not limit
Compatibility with UTC	No compatibility	Compatible	Compatible	Compatible
Efficiency for computing	Best	Better	Worse	Worst
Readability	Worst	Worse	Better	Best

According to requirement of “CCSDS701.0-B-2: Advanced Orbiting Systems, Networks and Datalinks” Annex A Addendum on CCSDS Packet Timetagging, a timetag is needed to be added to the secondary header of a CCSDS packet by the spacecraft.

In order to synchronize ground with spacecraft, a new time code format terminal should be added to USB.

Opening up Business Opportunities by Exploiting Mobile Telephone Technologies

Robert Fodor
Product Management Wireless Modules
Siemens AG, Munich / Germany

Abstract

The desire to be mobile while at the same time still being accessible has dramatically increased the use of cordless and cellular telephones all over the world. This has boosted the development of radio technologies covering the markets from residential and business applications to country-wide mobility.

This paper explains how these "telephone" technologies might be used to open up new business opportunities for telemetry and take advantage of the wide base of installed systems. After a short discussion of the available technologies, a series of scenarios is presented to illustrate possible applications. Further on it is explained that an easy way of employing these technologies is by integrating third-party modules. An overview of further possible developments in radio technologies is also included.

1. Introduction

The use of professional mobile or trunked radio systems with data modems has become increasingly popular and accepted for the wireless transmission of telemetry information. On account of the tariff structure, the public GSM mobile telephone systems were absolutely unattractive as an alternative to trunked radio for telemetry applications with large distances to be bridged. In addition, it was not generally possible to combine GSM terminals with telemetry terminals at all or only to a very limited extent.

In the in-house area conventional professional mobile radio or the registration-free and charge-free local-area radio was likewise used almost exclusively for data communication. However, the great disadvantage with this is that radio channels generally have to be used several times by a number of different companies or users and as a result co-channel interference can occur.

At present mobile telephone technologies are becoming established on a very wide basis as a platform for data communication. Thanks to a genuine mass market, appropriate terminals can be produced very economically. GSM terminals are today marketed as consumer products in such enormous quantities that professional mobile radio and trunked radio are loosing more and more of their attractiveness. The same is true of the DECT standard (Digitally Enhanced Cordless Telecommunications) which has also now become very widespread and which, thanks to secure full-duplex communication in the local area, has developed into a real alternative to professional mobile radio.

2. Technologies of the cordless telephone systems

2.1 DECT for professional local-area communication

Although DECT has been in use since 1993 for cordless telephony in the domestic and business areas, this technology was not developed on a somewhat wider front for data transmission until 1999. In addition to in-house voice communication with noise-free quality, the DECT standard also makes possible secure data transmission. DECT operates according to the TDMA principle in the frequency range 1.88 to 1.90 GHz . 2x12 user time slots (12 transmit time slots and 12 receive time slots each) are available in each of 10 simplex radio channels. Every user can operate with a gross data rate of 32 kbit/s in each traffic channel. In addition to that the DECT standard also permits the grouping of several traffic channels in order to obtain higher data rates.

DECT terminals operate with a peak transmit power of 250 mW - as a result of the 2x12 time slots, this corresponds to a mean transmit power of approx. 10 mW. The typical range of DECT systems is approx. 300 meters outdoors and 30 to 50 meters within buildings. In many cases DECT base stations have two antennas for optimization of the transmission quality and operate with antenna diversity. The range of smaller DECT systems from some manufacturers can be considerably extended for relatively small outlay with the aid of repeaters (intermediate repeaters) arranged around a base station at the limit of the range. Thanks to its suitability for cellular structuralization, DECT systems can also be expanded to form multicell radio networks.

Since the DECT frequency band is barred to other radio technologies, other radio systems cannot interfere with DECT links. The dynamic channel selection laid down in the DECT standard prevents neighboring systems or different systems installed on the same site from interfering with each other.

Within a DECT system access by individual users to the communication switching center can be very well ”shielded” against external users. Only terminals previously registered in a registration procedure are accepted by the system. In contrast to professional mobile radio or local-area radio, selective interference of individual communication channels is possible only with considerable effort. Interception of the communication, which as a rule is encrypted end-to-end, is also practically impossible. Because of the full-duplex communication, a DECT data transmission can be protected against transmission errors even during the transmission.

2.2 GSM opens up total mobility

The triumphant progress of the GSM standard worldwide has been well high explosive over last 12 months. In Germany alone a growth in users of over 60 percent to more than 23 million users in the year 1999 was recorded on 1.1.2000. Worldwide there were at that time more than 300 GSM networks in active operation and more than 250 million users.

The GSM standard is available in Europe in the frequency ranges 880-960 MHz (GSM 900) and 1710-1880 MHz (GSM 1800). In the case of GSM 900 a maximum permissible transmit power for vehicular equipment of up to 8 watts is normal nowadays and for mobile phones typically 2 watts. In the case of GSM 1800 the maximum permissible transmit power is 1 watt. In general a step-by-step transmit power reduction is provided in all GSM systems. In large towns in particular it is hardly ever necessary now for a GSM terminal to operate with maximum transmit power. In the vicinity of a base station the transmit power is frequently only 100 milliwatts or even markedly less.

GSM operates according to the TDMA principle on duplex traffic channels at 200-kHz intervals with eight time slots each, which are assigned to the users every 4.6 ms for a period of 577 µs . The digitized voice signal is compressed to 13 kbit/s before transmission and expanded to 22.8 kbit/s with channel encoders to increase the transmission reliability. The corresponding time slots of the receive and transmit frequencies are offset relative to each other.

GSM terminals operating in standby mode continuously monitor the nearest base station. In order to reduce the current drain this monitoring does not take place continuously, but cyclically at regular intervals. In the case of GSM several cells are mostly combined to form a larger cluster via a BSC (Base Station Controller). In the case of a

call to a mobile terminal, the call request is radiated via all cells of this cluster in parallel. As a result of this principle, a terminal within the cluster is not subject to active handover when changing cells. The identifications of the adjacent base stations are radiated via every base station. In this way the terminal can continuously check the received field strength of the adjacent stations. Only when the adjacent cell belongs to another BSC area is it necessary for the terminal to actively notify the system.

2.3 Data transmission via GSM

In addition to voice communication, GSM also makes data transmission possible. At present there are two basic options for this: the SMS short message and end-to-end data transmission. SMS messages (Short Message Service) are handled via the organization channels of the GSM network and can contain up to 160 text characters. As a rule an SMS requires only a few seconds for network-wide transmission from one terminal to the other. If the SMS receiver is not available, the message is automatically buffered in the SMSC (SMS Center) of the network operator until the terminal is accessible again. Because of this mechanism and the otherwise very short transmission time, data transmission via SMSC in the German D networks, for instance, is even recognized by the VdS (Association of Property Insurers) as a safe preventive protective measure.

Data transmission in a traffic channel is likewise very efficient in the case of GSM. As a rule it takes place at not less than 9600 bit/s - in the future GSM systems with a maximum data rate of 13,400 bit/s per traffic channel should also be increasingly implemented.

GSM is a very safe medium as a platform for data communication. On the one hand a multi-level PIN concept (Personal Identification Number) ensures high security against misuse. On the other, communication via GSM is as a rule encrypted between terminal and base station and can even be additionally encrypted end-to-end if required. Finally, on the basis of the directory number transmission integrated into the networks, the connection setup can be safeguarded in that the terminal only through-connects calls from directory numbers previously stored as receive-authorized. As a result, data communication can be carried out very safely.

3. Modules as simple access to radio technologies

Anyone wishing to use DECT or GSM for data communication in telemetry tasks has in principle the option of using digital cordless telephones or GSM mobile telephones with integrated RS.232 data interface. Though, due to the extremely short product cycles in the case of terminals, this involves the great risk, in particular for systems used for long periods, that in the event of system expansions comparable units, data adapters, replacement batteries, etc. are no longer obtainable.

Considerably more useful is the use of special data radio modules for DECT and GSM, such as are marketed by Siemens, for instance, under the names DECT Engines and Cellular Engines. Such mini modules can be much more simply integrated into a system environment than conventional end-user mobile phones. In addition, the modules as a rule comply with considerably more stringent specifications with regard to input sensitivity, operating temperatures, immunity to vibration, etc., than a mobile phone.

By using industry-standard modules, the developer of a telemetry implementation has the great advantage that work can be concentrated on the development of the core

products and it is not necessary to laboriously acquire know-how in the hotly contested telephone terminal market. Product support also calls for a certain amount of know-how. By and large the in-house development of a radio module is very costly and includes a not inconsiderable development risk. In particular, developing products suitable for approval is anything but child's play.

If tried and tested modules from an experienced manufacturer can be used, this results in a considerable reduction in the period of time to market of a complete system. And since a module manufacturer produces in large quantities, the modules are distinctly more favorably priced for the user than those from in-house production with very small quantities.

4. Typical requirements for DECT and GSM modules

4.1 DECT

There are a few very important basic requirements for a DECT data module to give it the maximum possible applicability:
As far as possible, an RS232 interface should be capable of transmitting the data completely transparently for the end-to-end communication, so that it is not necessary to first develop an appropriate driver.
The actual DECT communication (connection setup and release, channel change, protocol execution, etc.) should take place completely automatically. The fact that the data is actually transmitted via an aerial link must be completely concealed from the telemetry system. The optimum arrangement would be the availability of an analog audio interface so that the modules could also be used for voice communication or, for instance, for listening-in in a room.

The antenna should be integrated or plug-in or soldered on.
As far as possible the module should require only one supply voltage and cover a large input voltage range.
The available user data rates should be as high as possible and properly utilize the DECT time slot.
The module should comply with the GAP specification (Generic Access Profile[1]), so that it can also be integrated into existing DECT systems.
The module should be usable both as base station as well as mobile terminal, so that the integration and logistics effort for the application developer is as small as possible.
An antenna diversity circuit could noticeably increase the range and link quality of the DECT system.
The module should be capable of serving several DECT channels simultaneously, in order either to make higher data rates possible or to be able to implement multi-user systems.
The module should also support operation at several base stations, so that it can be used in multicell systems.

4.2 GSM

In the case of data communication via GSM there are likewise a few basic requirements for the corresponding modules which in part, however, differ noticeably from the requirements for DECT modules:
The RS232 interface must be implemented as a hardware interface, so that the data communication and the GSM communication handling can take place as simply as possible via the ”AT Cellular Instruction Set”. This instruction set was standardized by ETSI (European Telecommunication Standards Institute) in imitation of the AT Hayes instruction set known in the PC world.

[1] Profiles are secondary standards of the DECT specification

As far as possible the antenna connection should be designed for standard RF connectors.
The module must have an interface to an external SIM card reader or have an internal SIM card reader.
The entire GSM functionality and protocols must be dealt with autonomously by the module, without the application software having to intervene (e.g. GSM handover).
As far as possible, the input sensitivity should be higher than that of a GSM mobile phone, so that the module also operates reliably when used in-house or in rural regions.
A voice interface would be desirable in addition to the data interface, so that the module can also be used for emergency communication or for the monitoring of ambient noise.
A display interface could noticeably increase the functionality of the GSM module in special applications.
As far as possible the supply voltage should also be designed for use in motor vehicles or heavy goods vehicles, so that the module can be used as the basis for mobile implementations.

5. Use of telephone technologies in telemetry

5.1 DECT modules are optimally suited to in-house telemetry

Due to the large number of existing cordless systems, DECT is outstandingly well suited to the most varied tasks in the area of facility management. Systems for the cordless monitoring of equipment are just as easily implemented as alarm system modules for property protection or flexible access control systems. Medical engineering is conceivable as a further application area for DECT systems. Thanks to compact DECT data modules, for instance, a biometry module for the wireless monitoring of patients

could be implemented for a very acceptable outlay. Incidentally, a mobile in-house data entry system could be set up on the basis of an existing DECT system, for instance for warehouse logistics.

If the modules support the GAP profile (Generic Access Profile as secondary standard of the DECT specification), they can be connected as terminals to existing DECT systems (such as cordless private branch exchanges). The data is then transmitted unprotected in the voice channel of the system, which requires the integration of a modem or an error-protection protocol in the host. In the first case net data rates of 9.6 kbaud max. can be achieved, and in the second case rates of almost 30 kbaud.

If the modules operate with data profiles, markedly higher data rates are possible through channel bundling. In the case of point-to-point operation, two modules quite simply and completely transparently take the place of an RS232 cable. If the DECT modules in terminal mode can log-on to several base stations, complete multicell DECT networks for the coverage of larger buildings or corporate sites can also be implemented in conjunction with a LAN and the server base stations .

5.2 Mobile and widely distributed GSM terminals

GSM is practically ideal for the realization of extensive telemetry solutions. Through the almost explosive growth of the mobile telephone market and through the associated drop in communication costs, the transmission of measured values, telecontrol signals, GPS positional data and other important information via GSM is now becoming extremely attractive for many industrial applications. At the same time the telemetry sector receives further impetus in the direction of new mass-market-relevant marketing structures through system solutions for semiprofessional use. Thus, for instance, remote

control of a heating system in a weekend home or the protection of a boat or a family vehicle are no longer prohibitively expensive dreams.
GSM modules deal with the basic communication sequences for the telemetry application and permit optionally the transmission of short control information via SMS short message service or the transmission of larger volumes of data in the form of an end-to-end data link.

5.3 Combination of DECT and GSM

In principle telemetry solutions can also be implemented in which both GSM as well as DECT are used jointly. Thus it is possible at any time to use DECT modules for flexible on-site data entry in the local area and to relay the collected information to a central measured value recorder via GSM modules. Application areas for this mixed configuration could be, for instance, environmental measurement stations with remote wind, temperature or pH value sensors. The combination of an in-house DECT system for local building protection and a GSM module as wireless contact to an external alarm center is not a very unusual application.

6. Future technological development

Development in the mobile telephone sector is continuing almost unchecked. By the standards customary today the potential for telemetry solutions based on DECT and/or on GSM should be extremely interesting. High-speed data transmission (HSD), in which in each case two to four GSM time slots can be used jointly, has been coming into use in some GSM networks since the end of 1999. By the end of 2000 the new General Packet Radio Service (GPRS), in which up to 115 kbit/s can be transmitted on a packet-oriented basis in a special organization channel, should have been implemented.

In spite of these fantastic possibilities, it is not only GSM and DECT that will play an important role in the future. In the area of short-haul or long-haul applications the first terminals and systems for the UMTS standard, which operates in the range 1900 to 2170 MHz, can be expected from 2002. This Universal Mobile Telephone System will stand out for the very high transmission capacities (in the Mbit/s range) for mobile multimedia applications and will thus form the basis for the widest variety of flexible video surveillance systems. From today's standpoint the transition from GSM to UMTS will not prove to be a big step, but rather take the form of a slow migration. For this reason it is perfectly conceivable that today's GSM will be fully integrated into UMTS.

In the in-house area the Bluetooth standard will also play an important role along with DECT. This new local-area communication standard is intended for data transmission between a very wide variety of equipment and operates in the 2.4 GHz frequency range with a transmit power of 1 mW or 100 mW. A user data rate of 722 kbit/s max. per RF channel is planned. Naturally, the first Bluetooth systems will soon come into use in the telemetry sector too, though DECT should continue to play an important role, particularly since the range that it can cover is markedly greater than is the case with Bluetooth.

Sources:

- Manual of Telecommunications, Springer-Verlag
- MOBILCOM, Information service of Funkschau

RECONFIGURABLE TECHNOLOGY
AN APPLICATION EXAMPLE
RELATED TO A BIT SYNCHRONIZER

Henry Chandran

Navtel Systems SA – 28700 Houville - France

Chandran@navtelreconfig.com

Abstract

Navtel Systems is actively engaged in the research and development of generic reconfigurable hardware for cost-efficient system level applications. Its advanced hardware allows to build various complex systems without changing the underlaying hardware and software architecture.

This paper describes a digital bit synchronizer based on a generic reconfigurable hardware plateform currently under study. This module is part of the Neptune project concerning a reconfigurable generic satellite receiver.

Another module of the Neptune project dealing with turbo code is the subject of another paper.

Keywords

ADC: Analog Digital Converter

DBS: Digital Bit Synchronizer

DTTL: Data Translation Tracking Loop

MAP: Maximum a posteriori

ML: Maximum Likelihood

NCO: Numerical Control Oscillator

1) Introduction

The main objective of the project is to develop a reconfigurable generic satellite receiver able to handle telemetry as well as UMTS based applications. The required embedded core for this application contains the following items:

- A Digital Bit Synchronizer
- A high speed reconfigurable Error Corrector
- Reconfigurable simulator and emulator

It is able to handle various modulation schemes.

A SIPOS real time kernel is used to free the low level programming as well as to handle the dynamic hardware configuration at task level.

2) Choice of a digital bit synchronizer

In a telemetry receiver system, error correctors can function under very low signal to noise ratio but this is not often possible due to the analog bit synchronizer. Using a reconfigurable digital bit synchronizer enable to attain a full performance of the error corrector.

System objectives

1. Low acquisition time
2. Possibility to lock sub signal to noise ratio
3. Open-Closed loop synchronization
4. In closed loop mode : an adaptable filter structure
5. Error corrector status information feedback to improve the tracking performance
6. Algoritms implemented in FPGA, ASIC and DSP

3) Bit synchronizer overview

Digital bit synchronizers are usually divided into two categories: Early-Late or DTTL. Literature describing the theory behind these models are given in references [1 to 4]. The current DBS development is based on a MAP bit synchronizer with iterative reconfigurable structure for NRZ_L and bi-phase formats.

The received PCM stream pulse noise is defined as follows:

$$x(t) = \sum_{k=0}^{K} a_k p_s[t-(k-1)T-\varepsilon] + n(t)$$

where a_k is an antipodal signal for the k^{th} transmission interval and $p_s(t)$ is the basic pulse shape of the signal.

The incoming signal is filtered by a lowpass linear phase filter in order to limit the noise before further processing in the DBS chain.

MAP theoritical basis:

1. Incoming bit period is a known constant, T
2. The bit stream has equal probabilities of “0” and “1”
3. The time shift of the received signal is constant but unknown during the number of bit periods.
3. The noise is white Gaussian

Under the above conditions, it has been shown [2] that the only parameter needing to be estimated is the time shift of the received bit in comparison with the transmitted bit which is observed over M bits with symbol time T.

$$f(x,\varepsilon) = \sum_{k=0}^{k=M} \ln\cosh\left[(2/(No)) \int_{T_k(\varepsilon)} x(t)g(t-(k-1)T-\varepsilon(t))dt\right]$$

The above equation shows that in order to estimate the phase shift of the received bit stream, one requires a N number of parallel match filter structures with V number of clock phases.

In order to have the best phase estimation, the output of the N parallel structure outputs are observed over M bits, compared and then the best estimation is selected. The precision of the estimation depends on the T/V. In a pratical system one needs to take into account two other points.

1. In a match filter it is not the shape of the received bit which matters but its energy. In a real system, the power spectral density of the noise influences the received bit
2. The ISI (Inter Sample Interference) influences the match filter response time.

The pratical implementation requires a closed and open loop structure. Reconfigurable technology provides the necessary flexibility to implement a high performance bit synchronizer with the following features:

1. Fast acquisition time
2. Acquisition under very low signal to noise ratio
3. Open and closed loop switching according to system environment

4. Implementation structure

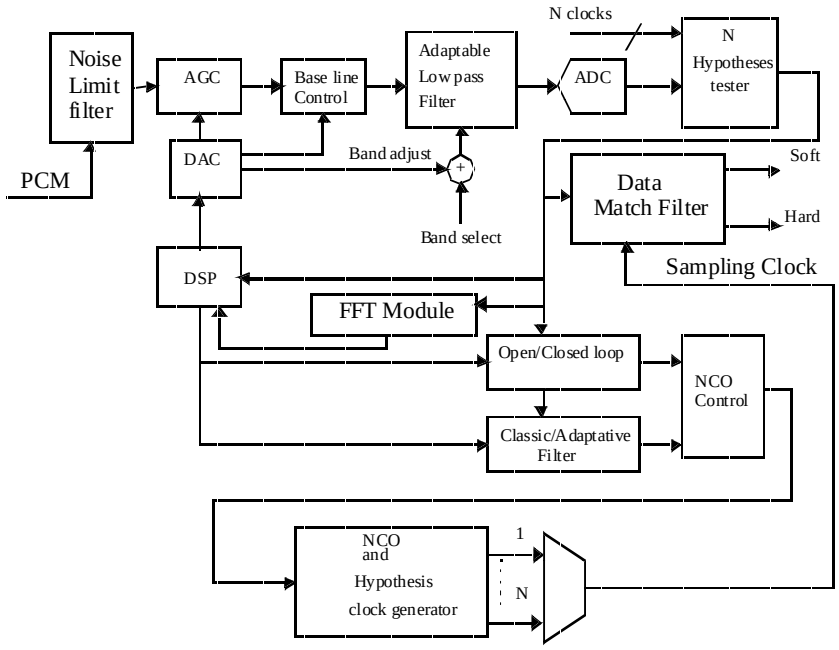

Description

The current implementation focuses on NRZ_L and biphase formats.
The incoming bitstream is band-limited by the input filter and passes through three functional modules: an Automatic Gain Control, a Baseline Control and an Adaptative Low-pass Filter. The Low-pass Filter output is sampled by an ADC and fed to a 4-match filter structure. The ouput of the match filters are accumulated over M bits and the best phase estimation provides a coarse estimation of the phase. This coarse estimation is used by the DSP to shift the NCO phase in the open loop mode and enable the iterative mode. The number of hypotheses selected for the coarse phase estimation depends on the bit rate.

The data match filter output is used by the following front end control circuits:

- Automatic Gain Control
- Base line control
- Input analog fine bandwidth tuning.

Iterative Loop filter

Two modes are under evaluation : one is a classical mode and the other is an adaptative filter. The adaptative filter provides a best estimation but it will be slow to converge (due to matrix operation) and not ideal during the acquisition phase. During the tracking phase, the adaptative filter can be switched on to improve the loop filter performance.

5) Conclusion

The current evaluation uses NRZ_L and biphase formats. Each format requires a different match filter structure which is down-loaded in Soft Core form in the generic hardware.

- The system works under open and closed loop modes. This allows to open the loop under high jitter or lack of transition.
- If the frequency offset gets larger, the steady-state error pushes the phase detector towards its non linear region.The consequence is a bit slippage. In the current bit synchronizer, a small buffer is used to store the samples for bit decisions. This buffer allows us not to lose any bit during the bit slippage.
- Error corrector status information is used to enhance the performance.
- The reconfigurable technology based architecture provides a flexible way to implement the complex Embeded DSP algorithms in the form of soft cores.
- The 2^{nd} phase of this project will consider extending the bit synchronizer to a demodulator by adding a 2^{nd} processing branch. The demodulator will thus have two branches: I (In-phase) and Q (quadrature phase).
- The generic reconfigurable hardware plateform consists of ADSP21060, Virtex from Xilinx and 10KE family from ALTERA.

6. References

1. Synchronization systems in communication and control, 1972 W.Lindsey
2. Telecommunication Engineering, 1973 W.Lindsey and M.Simon
3. Detection, Estimation and modulation theory, H. Van Trees
4. Digital communication , J.G.Proakis
5. Synchronization in digital communication , H.Meyr and G.Ascheid
6. Optimum estimation of bit synchronization IEEE Trans. on AES vol 5 may 1969 by A.P Sage and A.L Mc Bride

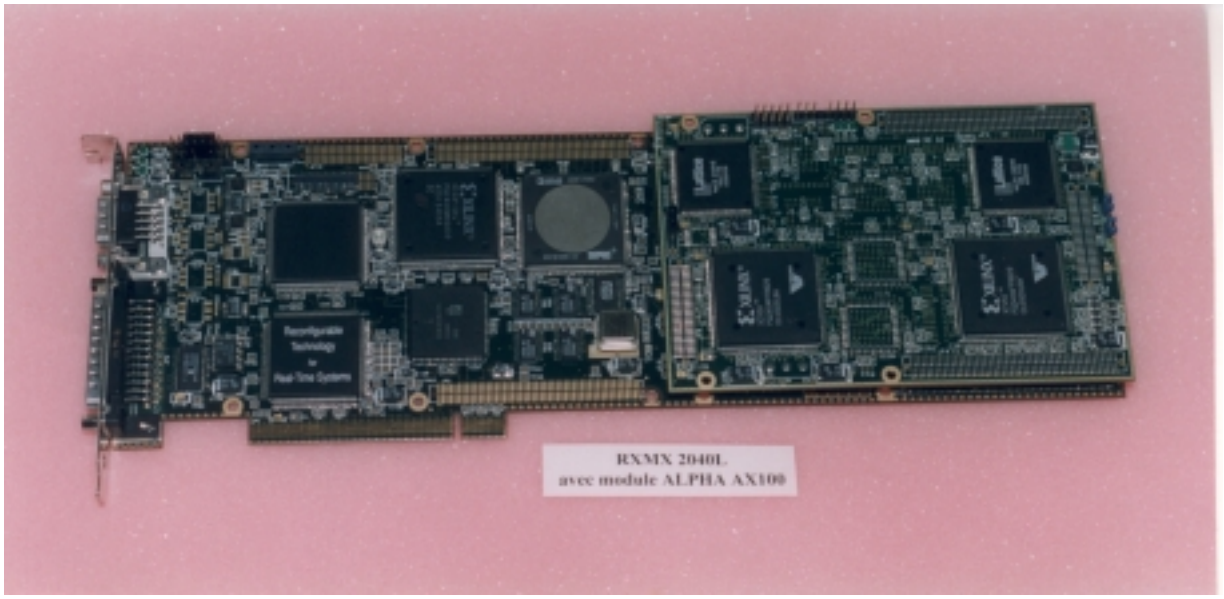

The bit synchronizer for Neptune project will be based on RXMX 2040 generic hardware

MULTI-STANDARD TURBO CODE DESIGN

BASED ON ADVANCED RECONFIGURABLE HARDWARE

Kjetil Fagervik[1] *and Henry Chandran*[2]

[1]Codabit Communications,
fagervik@codabit.com
[2]Navtel Systems SA

ABSTRACT

Due to the near-optimum performance of Turbo Codes, studies are undertaken in order to incorporate these codes into the new standards of wireless communications. Examples here are the Universal Mobile Communications System (UMTS) and the CCSDS standard for telemetry systems. This paper will review the performance of the proposed Turbo Code configurations of the CCSDS telemetry channel coding standard, and we will discuss how this may be implemented in reconfigurable hardware

1.THE CCSDS TURBO CODE STANDARD

As a result of the excellent performance of turbo codes [1], efforts are being made in order to make the codes practically useful, and the standardisation process is of considerable importance in this respect. Currently, turbo codes are being considered for the UMTS standard, applications within digital broadcasting, and not least for the CCSDS telemetry standard, which will be the focus here.

The block diagram of the encoder of the proposed CCSDS telemetry standard is shown in figure 1

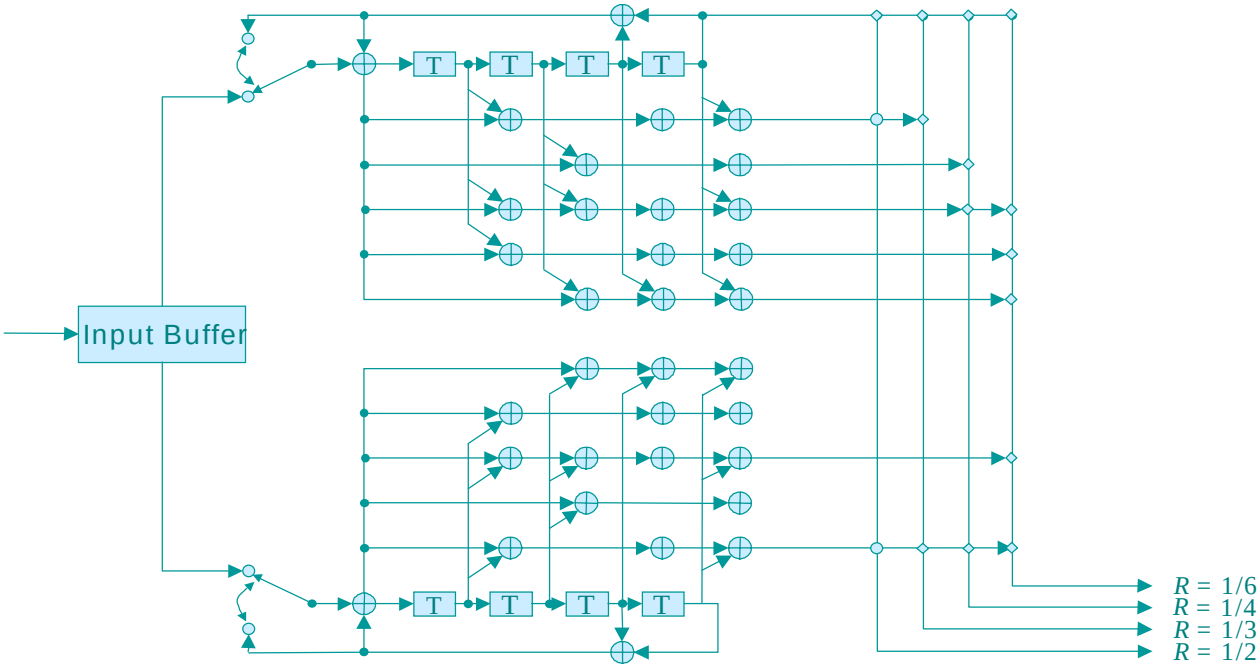

Figure 1. CCSDS Turbo Encoder

The code of figure 1 is highly reconfigurable, and the code rates may vary from as low as R=1/12 to a code rate close to R=1. If we assume that Code B will never transmit the systematic bit, i.e. bit b_0 then the lowest rate possible is R=1/11. In the proposal for the CCSDS telemetry standard, the rates R=1/6, R=1/4, R=1/3 and R=1/2 have been chosen. These different rates are obtained by puncturing the encoder output bits to a varying degree, which is performed by the multiplexer at the code outputs.

In addition, the CCSDS standard have five different block, or frame lengths as options, namely 1784, 3568, 7132, 8920 and 16384 bits.

In order to generalise the code configuration, it is possible to include other code rates by simply changing the puncturing function. This would be of interest for e.g. the UMTS standards. Very low coding rates will most likely not be of interest for this standard, unless it is seen useful to partly undertake the CDMA spreading with the channel encoder before transmission. Hence, in order to preserve spectral efficiency it would be desirable to include even higher rate turbo codes in this standard, possibly R = 2/3, R=3/4 or even higher. In addition, it is probable that the block lengths for the UMTS standard will be of a reduced length compared with the CCSDS telemetry standard, due to the non-stationary mobile radio environment.

2.NOTES ON CODE IMPLEMENTATION

In this section we will briefly consider some implementation issues about the encoder and decoder.

2.1The Encoder

The input buffer accepts input bits on a frame by frame basis, and will work as a ROM for the duration of the encoding process of that frame. The selection of bits for Code A works on a sequential basis, i.e. the encoder input bits follow the same order as that of the input frame.

It should be noted that this configuration could be altered.

The input bits to Code B are permuted before being applied to the input of Code B. The permutation is algorithmic, and may be adapted to different input frame-lengths.

The encoder may be implemented as this particular code only, or one could potentially consider a more general structure, in the sense that the generator polynomials are allowed to vary. This latter case will allow the code to be used in a wider range of scenarios. It should be noted that a trellis of 16 states is needed for both Code A and B, although Code B is a subset of Code A. Since all the codes of the different rates are sub-codes of the overall rate 1/6 code, only the puncturing functionality needs to change between the codes. This puncturing operation could potentially be implemented as a logic unit which is also responsible for the multiplexing of bits before they are passed on to the pulse shaping and modulator, as illustrated in figure 1.

2.2 The Decoder

In this section we will consider the more difficult operation of decoding. Consider Figure 1.

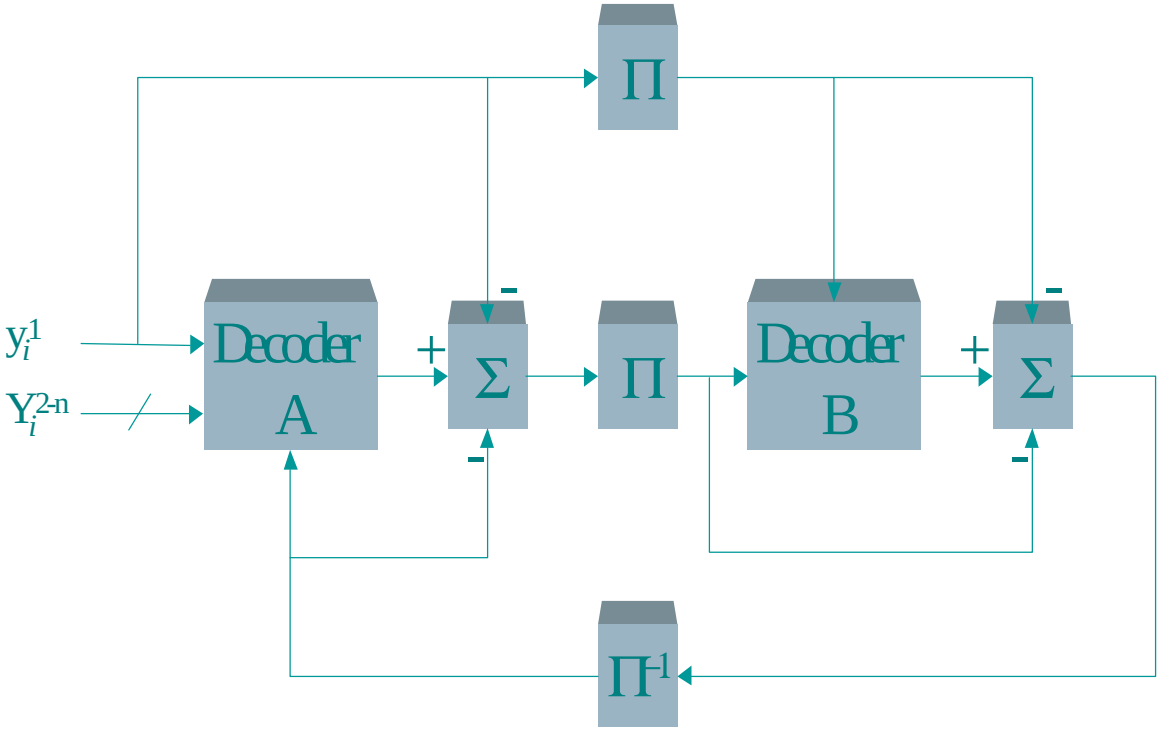

Figure 1. Generic Turbo Decoder

In this figure, the symbol y^1_i refers to the soft channel outputs (from the demodulator) which correspond to the systematic bit from Code A (bit a_0 in previous notation), $y^{2\text{-}n}_i$ refers to the soft channel output of the transmitted bit $a_{2\text{-}n}$ from Code A and Code B, all taken at time *i*.

We shall assume that the decoding stages $D_0(\mathbf{d})$ and $D_1(\mathbf{d})$ operate according to the *Maximum a Posteriori* MAP decoding rule. We shall further assume that the decoder outputs are effectively *proportional to the logarithm of the a Posteriori Probabilities* (APP) of each individual decoded bit. Such an operation is most effectively achieved with the algorithm described in [4], hereafter denoted the BCJR algorithm after the authors. A simplified algorithm may be utilised, with no loss in performance, by operating in the log-domain, as described in e.g. [5] and [6]. The even simpler, albeit sub-optimum, APP algorithm proposed in [7], may also be used. This algorithm is denoted the Soft Output Viterbi Algorithm (SOVA). However, it has been found that roughly 0. e BCJR algorithm (and the SOVA) effectively operate as amplifiers of the signal to noise ratio (*S/N*), in the sense that the *S/N* of the APP outputs is higher than the *S/N* of the demodulated symbols. This imposes a problem on the relative scaling which exists between the demodulated s7dB coding gain is achieved with the BCJR or Log-BCJR algorithm compared with the SOVA [6].

The success of the decoding operations of the code relies on several different factors. Th ymbols and that of the decoded symbols. This again imposes a problem on the type of quantisation of the APP outputs. This is identified as a research area. In addition, it is accepted as a decoding rule in Turbo Codes that every piece of information that is available should only be used once in each decoding operation (each $D_j(\mathbf{d})$ stage). This implies that there will be subtractions taking place at the output of each $D_j(\mathbf{d})$ stage - i.e. a separate logic unit.

In Figure 1 two interleavers, or permuters, are depicted in the forward path. It is possible to reduce this to one, by omitting the uppermost interleaver, and not use the permuted

versions of the y^1_i symbols in the second decoding stage. This, however, must be compensated for by effectively including the y^1_i symbols in the output of the first decoding stage. This will effect the subtraction unit at the output of $D_0(\mathbf{d})$.

The feedback path may be implemented in pipeline. Each iteration then consists of the algorithm depicted in Figure 1 with the exception of the feedback path. This may be a viable solution to the implementation problem.

It is also of importance to consider fast structures of the BCJR algorithm. The BCJR algorithm works with a forward recursion, where the probability of ending up in one of the 16 states of thetrellis is evaluated for every state at every time step throughout the trellis. The same is undertaken in the reverse direction. A final decoding stage is then undertaken in order to compute the state transition probabilities. If the Log-BCJR algorithm is used, the whole operation becomes very similar to the Add-compare-select operation of the Viterbi algorithm, in both the forward and backward direction, however, as described in e.g. [6], a nested look-up operation of a correction term must be implemented in both the forward, backward and final decoding stages for a general code. For this CCSDS binary code, only the final decoding stage needs a look-up operation. With this operation, the decoding operation becomes 2.5-3 times more complex than the Viterbi Algorithm in terms of computation. However, a considerable amount of memory is needed in order to store the forward probabilities for each state for every time state. In addition, we need the same storage of the transition probabilities.

This memory requirement may be somewhat reduced by efficient re-use of information, but is a good guidance. It is possible to reduce this memory requirement by trading memory off with additional processing. The advantage of the decode-while-buffer-loads operation described above, is that we do not need more than these stages in the decoder, hence saving hardware expense, and instead focusing on algorithm generality. Studies currently being undertaken in this respect were presented in [8] and [9].

3. CODE PERFORMANCE

This section will review the performance of the CCSDS coding standard. Figures 3, 4 5 and 6 show the performance of the rate R=1/6, R=1/4, R=1/3 and R=1/2 codes respectively, for a varying number of block lengths. The number of iterations were kept constant at 10 iterations for all these codes. As is seen from all these curves, the higher the block length, the better the performance. A considerable coding gain is obtained by going from a block length of 1784 to 16384, particularly at low BER values. As an example, a coding gain of about 0.5dB is obtained when using a block length of 16384 instead of 1784 for the R=1/2 code, when seen at a BER of 10^{-5}. This coding gain reduces for the lower rate codes, albeit it is still around 0.35dB for the 1/6 rate code.

Figure 7 shows the performance of the R=1/2 code of the CCSDS standard, where the block length is 16384 bits long. A varying number of iterations were used to obtain the curves. It is noticeable from this graph that a substantial coding gain is obtained when increasing the number of iterations from one to four. Furthermore, coding gains are consistently obtained when increasing the number of iterations beyond 4, albeit only minor ones after about 8 iterations. It will depend heavily on the application whether or not increasing the number of iterations beyond 4-8 would be of interest.

Figures 8, 9 and 10 show the performance of the codes in a different light. Here, the block lengths are kept at 16384 bits, 8920 bits and 3568 bits respectively, but the rates have been allowed to vary. Common for all these graphs is that the R=1/2 code is substantially

worse than the others, and that, as expected, the R=1/6 code is superior. More than 1dB asymptotic coding gain is obtained with the R=1/6 code compared with the R=1/2 code for a block length of 16384 bits, which is also consistent with the other block lengths.

It is also of interest to observe the performance of turbo codes when the frames are of a substantially smaller size than that of the frame lengths specified in the CCSDS standard. A potential protocol for wireless data communications would be that of ATM, where the cells are specified to be of a length of 53 Bytes, i.e. 424 bits. This imposes a somewhat reduced performance on turbo codes, but even with such short frame lengths, turbo codes will deliver excellent performance. This may be seen from 11 where a rate R=1/2 turbo code has been simulated for various number of iterations. The reduced performance of this code compared with the CCSDS codes is mainly due to the reduced frame length, as the same framework decoding algorithms were used for this code as in the examples of the CCSDS codes. If turbo codes were to be used in ATM applications, it would be of interest to investigate scenarios where the turbo block length comprises multiple ATM cells.

4. CONCLUSION

In this paper we have reviewed the performance of the CCSDS turbo coding standard. The codes have been presented in general terms, and it has been argued that this standard may easily be used and adapted by other applications, where UMTS and DVB were explicitly mentioned. Some notes about implementational aspects were given. We also gave examples of the performance of turbo codes in which the block length has been set to be very small, i.e. to the size of an ATM cell.
The reconfigurable hardware has been selected for the implementation because it provides a flexible way to implement various standards. The selected architecture similar to Viterbi with finite trellis lengths. Currently , major focus is how to reduce the number of ACS (Add Compare Select) elements and improve their numerical precision.

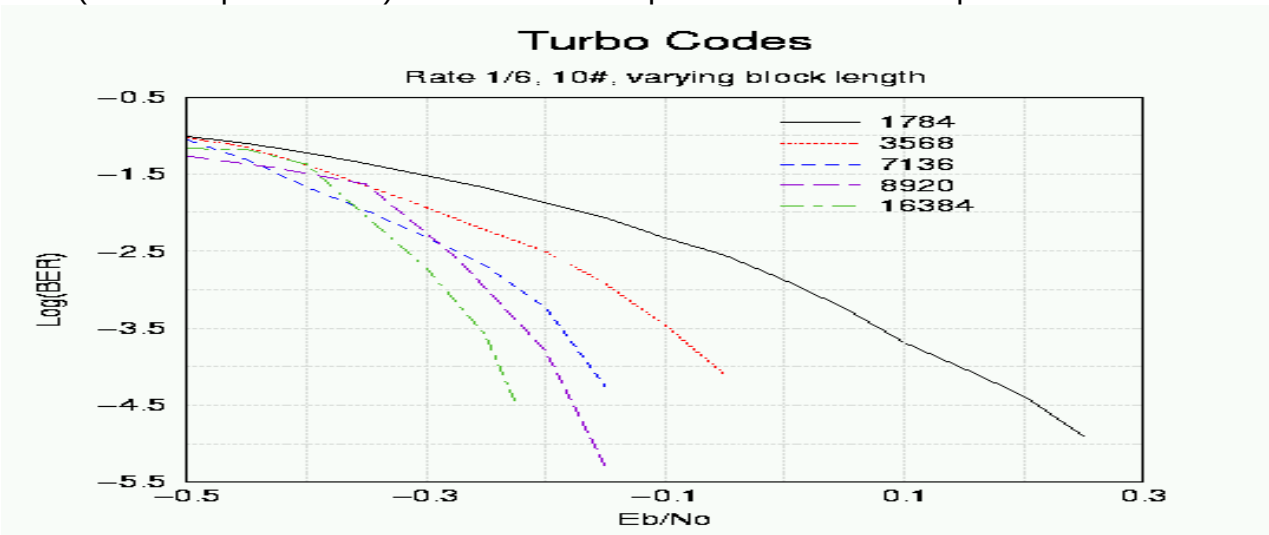

Figure 2. Performance of CCSDS rate 1/6 code for different block lengths. 10 iterations were used for all code configurations.

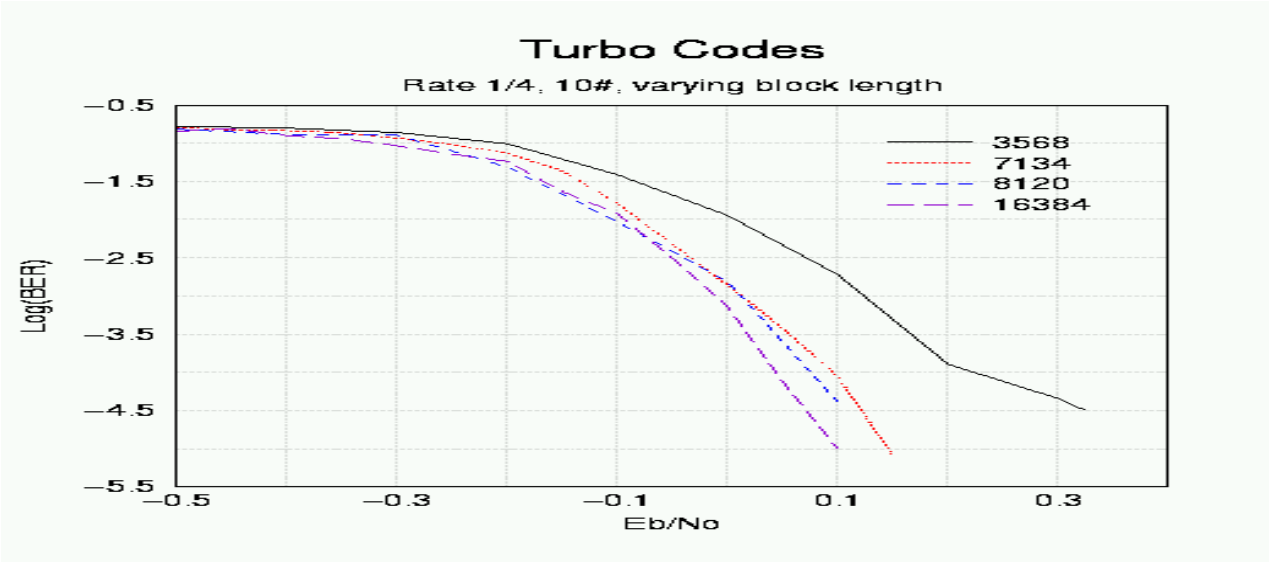

Figure 3. Performance of CCSDS rate 1/4 code for different block lengths. 10 iterations were used for all code configurations.

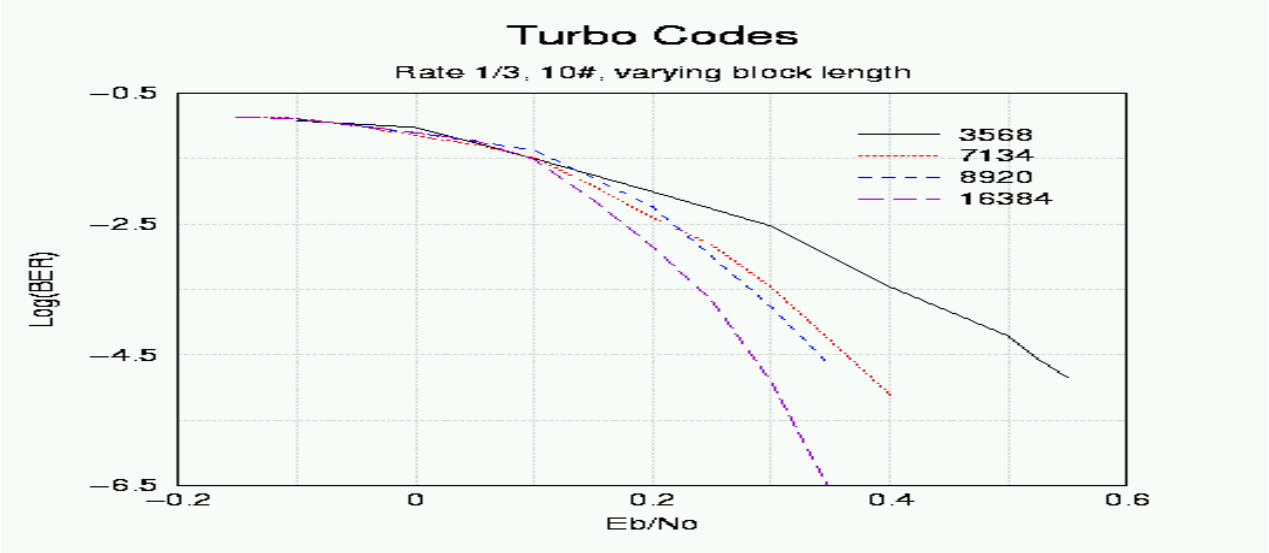

Figure 4. Performance of CCSDS rate 1/3 code for different block lengths. 10 iterations were used for all code configurations.

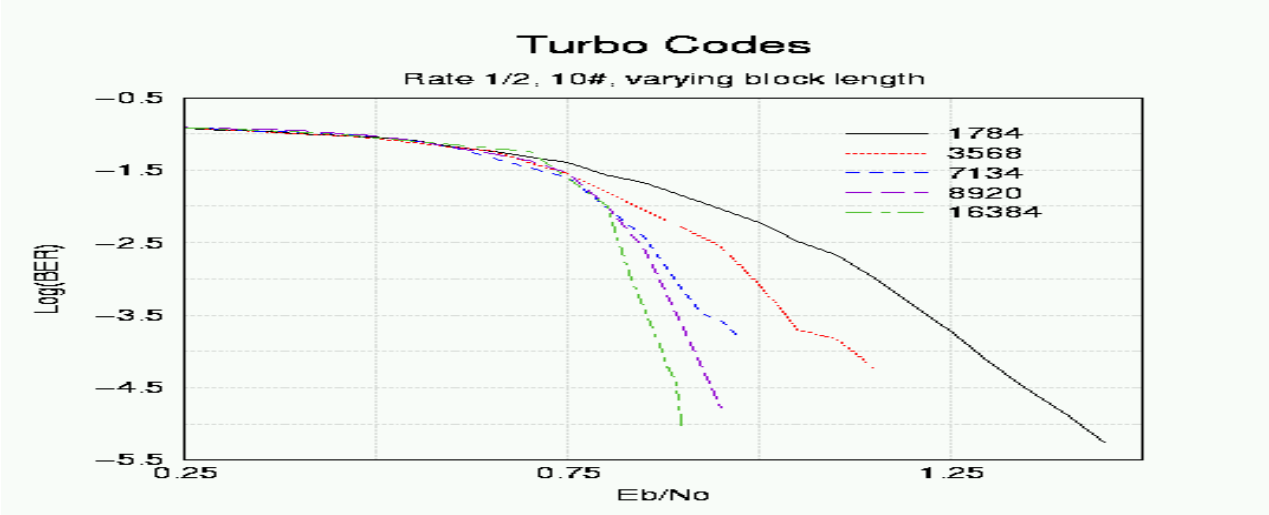

Figure 5. Performance of CCSDS rate 1/2 code for different block lengths. 10 iterations were used for all code configurations.

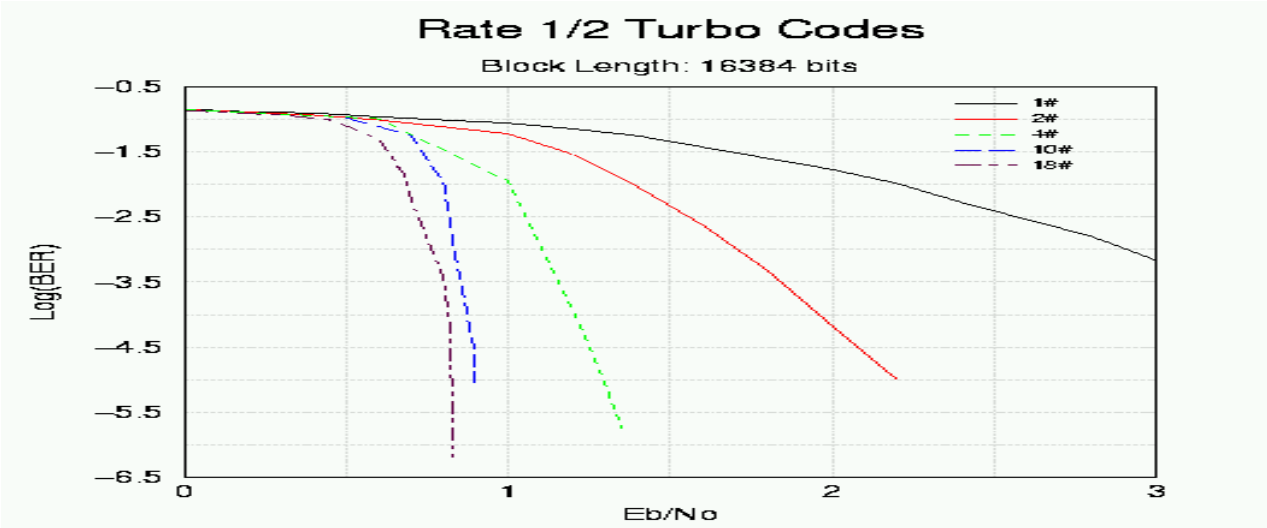

Figure 6. Performance of rate 1/2 CCSDS code of information block length 16384 bits for varying number of iterations.

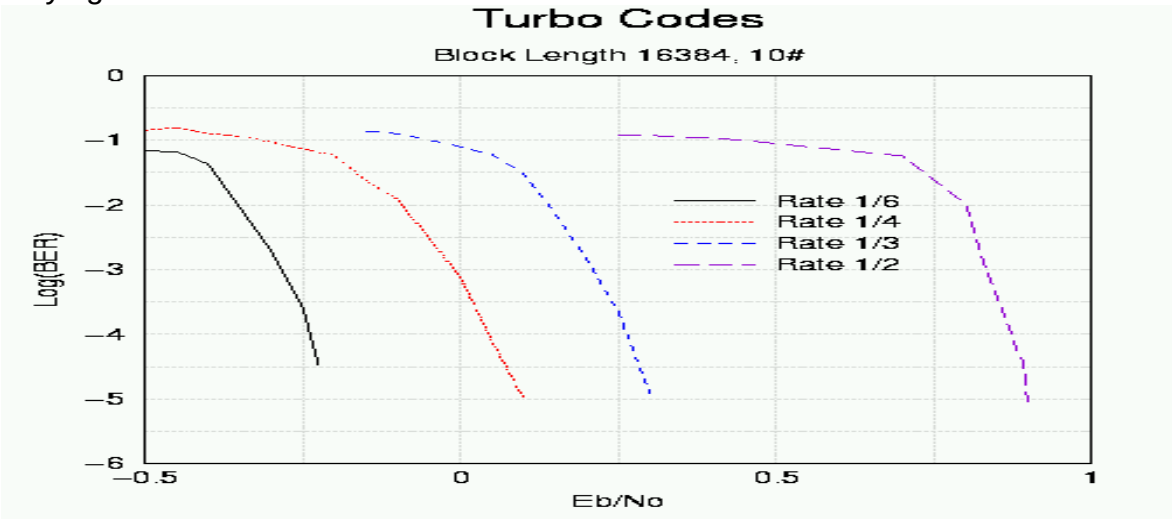

Figure 7. Performance of different rate CCSDS codes of information block length 16384 bits. 10 iterations were used for all code configurations.

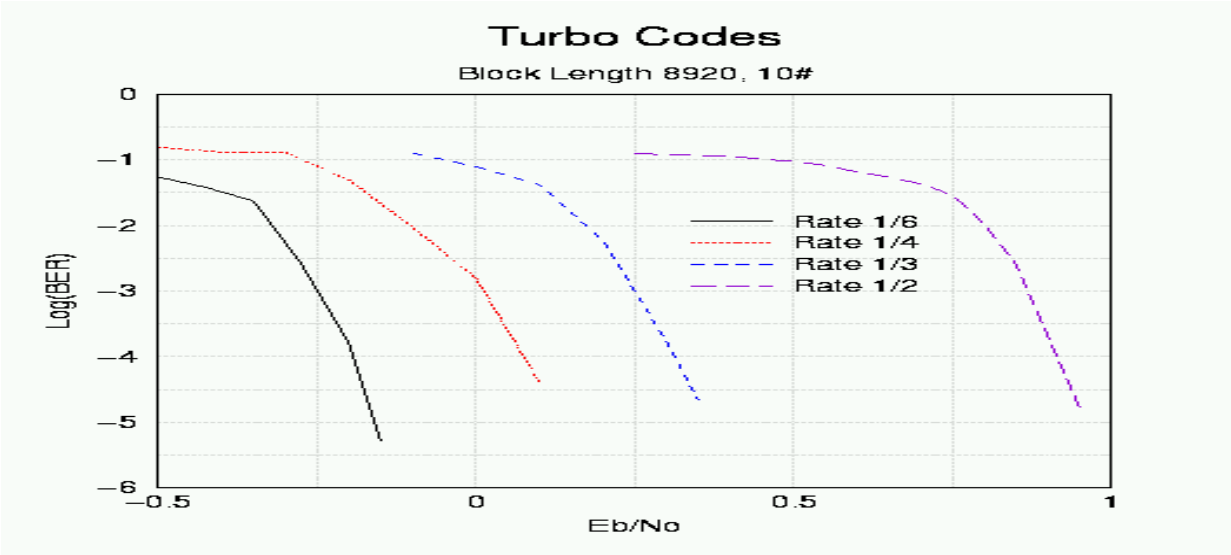

Figure 8. Performance of different rate CCSDS codes of information block length 8920 bits. 10 iterations were used for all code configurations.

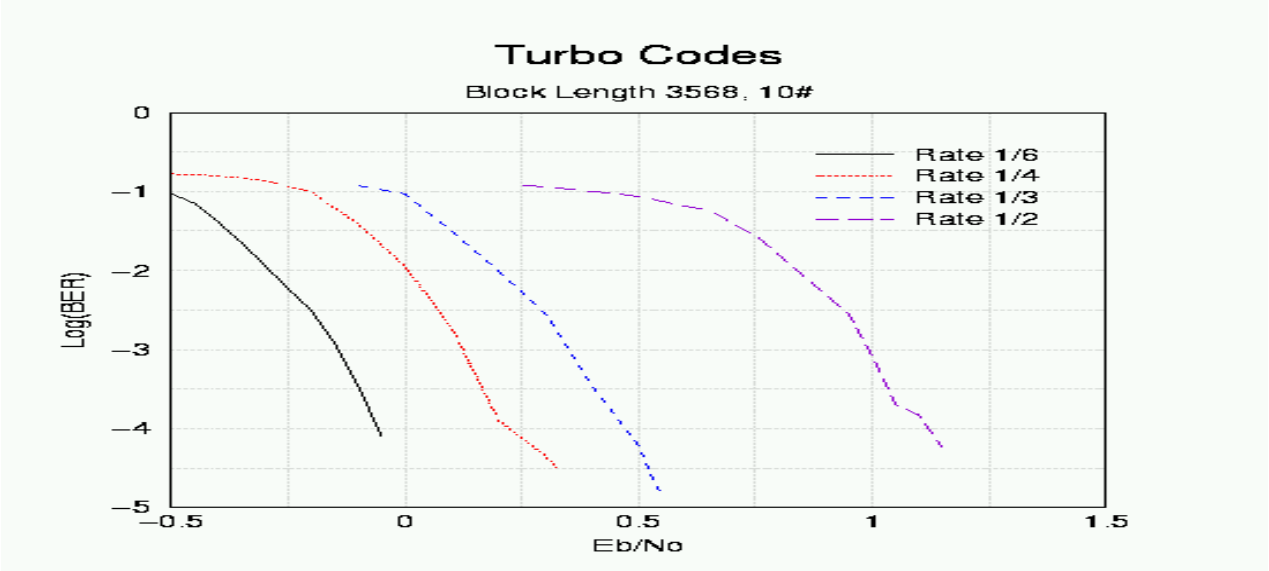

Figure 9. Performance of different rate CCSDS codes of information block length 3568 bits. 10 iterations were used for all code configurations.

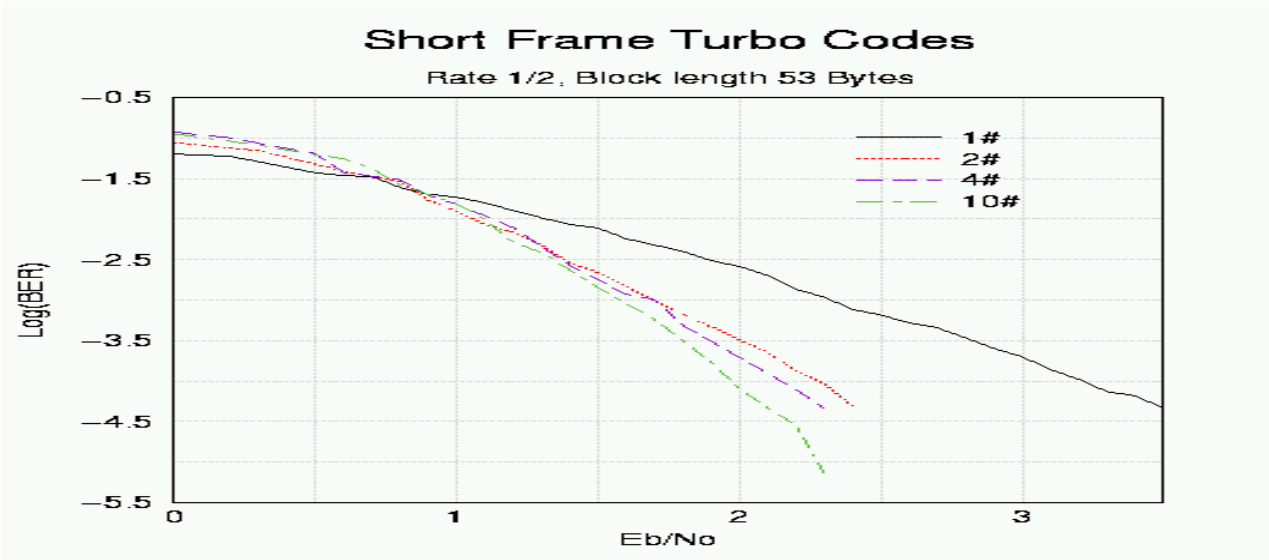

Figure 10. Sample performance of small frame length turbo codes (frame length 53 bytes) using a R=1/2 turbo code.

2. REFERENCES

[1] C. Berrou, A. Glavieux, and P. Thitimajshima, '*Near Shannon limit error-correcting coding and decoding: Turbo-codes*', in Conf. proceedings IEEE ICC '93, (Geneva), pp. 1064--1070, IEEE, May 1993

[2] Consultative Committee for Space Data Systems, '*Draft CCSDS recommendation for telemetry channel coding (updated to include turbo codes)',* tech. rep., CCSDS, May 1998. Pink Paper, Revision 4.

[3] P. T. PT-55V, ETS 300 421, *Digital broadcasting systems for television, sound and data services; framing structure, channel coding and modulation for 11/12 GHz satellite services*. European Telecommunication Standards Institute, Geneva, Switzerland, December 1994.

[4] L. R. Bahl, J. Cocke, F. Jelinek, and J. Raviv, *'Optimal decoding of linear codes for minimizing symbol error rate',* IEEE Transactions On Information Theory, vol. IT--20, pp. 284--287, March 1974.

[5] J. Hagenauer, E. Offer, and L. Papke, *'Iterative decoding of binary block and convolutional codes',* IEEE Transactions on Information Theory, vol. 42, pp. 429--445, March 1996.

[6] K. Fagervik, *Iterative Decoding of Concatenated Codes.* PhD thesis, Centre for Communications Systems Research (CCSR), University of Surrey (UNIS), June 1998.

[7] J. Hagenauer and P. Hoeher, *'A Viterbi algorithm with soft-decision outputs and its applications',* in Conf. proceedings IEEE Globecom '89, pp. 1680--1686, IEEE, 1989.

[8] K. Fagervik and H. Chandran, *'RXMX 2040: A reconfigurable system for high speed signal processing',* in European Test and Telemetry Conference 1999, (Paris), pp. 6.9--6.22, June 1999.

[9] G. P. Galzolari, E. Vassalo, S. Benedetto, G. Montorsi, R. Garello, and P. Pierleoni, *'The ESA experience with CCSDS turbo codes recommendation: From deep space missions to high rate near-earth missions'*, in European Test and Telemetry Conference 1999, (Paris), pp. 6.9--6.22, June 1999.

Future Directions In Packet Telemetry

Colin Douglas
John Douglas Associates / Aurich,Germany

Introduction

The IRIG standards have been with us for many years and have proving a great success in allowing telemetry equipment from many companies to work correctly together.

The Chapter 8 standard was introduced to allow airbus data to be placed within a telemetry frame, this is a requirement if standard telemetry systems are to be used for data recovery. However it seems a shame to have to squash a packet format into a fixed frame to make it useable, wouldn't it be better to be able to transmit a packet format.

In this past this has not been any easy task and despite numerous attempts e.g.CE83, it has not taken off except within isolated sections of the telemetry community. This appears about to change and we are moving rapidly to the situation where many telemetry applications will be a specialist subset of standard telecommunications.

Future trends in Packet Telemetry

It would appear that the telemetry requirements for the future could be split into two distinctly different types.

The first is a high-speed requirement that will for the moment still be required to be sent using traditional techniques, these streams often include aspects off encrypted video or radar information and therefore require a high bandwidth for their transmission. The recovery of such telemetry information requires highly specialized decommutation equipment capable of speeds often in excess of 30 Mbps. Most of the data recovery does not however require to be processed within the decommutation equipment but simply needs to be passed on to an external decoder of some sort. The remainder of the data structure can only be treated as the standard telemetry signal and decoded by a modern telemetry decoder such as the VuSoftNT system.

The second type may be looked upon as a standard telemetry requirement with rates not exceeding 10 Mbps. A traditional telemetry system to deal with this type would consist of an on-board encoder, transmitter and antenna set and a ground based tracking antenna feeding the signal into receivers and perhaps a diversity combiner before sending it to a bit sync and decommutator. The equipment described is traditionally required because in the past there was no

other practical way of recovering the required signals from the test object. Of course this will still be the case for many applications and for flight safety requirements will remain do for the foreseeable future, however with the advent of cable free telecommunication it is possible to imagine a scheme whereby data may be securely transmitted using standard telecommunications technology thus removing the requirement for much of the specialized equipment traditionally used for recovering the telemetry data.

Such a system would require an airborne component that was capable of gathering data from the various data sources available on the test vehicle optionally perhaps providing local display, data distribution capabilities and a flexible intelligent telecommunications interface. The accompanying ground system would consist of a controlling component whose primary data interface would be a high-speed telecommunications input, for example ISDN, and some sort of local network to distribute the data recovered for display and data processing.

This innovative approach to the problem flight test data recovery is now a reality.

John Douglas Associates, a specialist telemetry company based near Bremen in Germany, have been working on such a system for the last two years and are proud to announce the introduction of their new GSM and satellite data recovery system which is an extension to their standard VuSoftNT data recovery and analysis system. The components are based around PC computers running under the Windows operating system.

The VuSoftNT server on board comes in a choice of subminiature, mini or 19 inch rack mounted computers with integrated ARINC 429, 1553b airbus, CAN bus, telemetry, IRIG time and analog/digital I/O. The data gathered by the server is available for immediate distribution over the local Ethernet network for display within the test vehicle on client displays and may also be archived for post flight analysis. The data may also be sent directly out of the VuSoftNt server as a traditional IRIG telemetry stream, however the primary data transfer interface consists of a number of cable free telecommunication devices capable of receiving controlling commands from the VuSoftNT ground station and transmitting data packets based on those commands and local variable.

The system is intelligent enough to apply active data reduction techniques that minimally impact the quality of the data as seen by the ground users but greatly reduces the bandwidth requirements needed when compared with a traditional telemetry system.

On the ground the VuSoftNT server is connected to a standard high speed telecommunications interface via a dial-up or leased line and a local Ethernet network for distribution of data to clients for display and processing. The VuSoftNT server carries out the critical process of controlling the contents of the transmitted packets from the airborne system. This selection of data to be sent is based on the selection of parameters currently active within the complete ground system for the process and display requirements of the connected clients.

Of course there is a requirement for security in regard to transmission data. This is effectively dealt with within the VuSoftNT system by encrypted data packets sent on any of the connected interfaces; these include the open telecommunications interface and the local Ethernet interface. The encryption utilizes a 100-bit recycling crypt2 algorithm that is more than adequate for most users and meets the stringent requirements for bank and money transfers over open telecommunication links. However as the encryption process is carried out in a separate library, it is possible for the user to replace it with other encryption routines that are qualified by the user for high security requirements.

It is possible with this new approach to extend the test envelope by allowing users to carry out flight testing where and when required. This can be done without the need to send critical ground staff and equipment to often far-flung and inhospitable test environments. As the data from the test object is send via standard telecommunications links and the VuSoftNT server can send its clients information securely even over open networks flight test can in the future be truly physically distributed precluding the requirement for all the test engineers to be physically near each other.

Of course test engineers need to communicate during a test so the VuSoftNT system includes another innovation, the intercom system. This is a John Douglas Associates software product that may be installed on each VuSoftNT server or client and allows the users to form audio-visual subgroups. Within each subgroup the users may speak freely in full duplex to one another and even share visual and whiteboard information, all the communications are sent as encrypted packets over the same network on which their data is transported, by using GSM compression technology for the audio and MPEG for the video the network bandwidth requirement for this unique feature is minimal and no special requirements are need for the network in this respect.

Another use for this new technology is the ability to communicate with a fleet of in service aircraft to simplify the tasks involved with maintenance. If each aircraft were fitted with a VuSoftNT server then they could be called at any time and instant or statistical information gathered from the aircrafts buses, also a complete GPS log can be maintained within the VuSoftNT server as a confirmation of air space charges imposed on commercial airliners.

Conclusions

The VuSoftNT GSM and satellite data recovery system offers a new approach to solve many of the problems inherent in flight test. By developing on the back of innovations in the telecommunications industry and using standards when they are available a flexible and expandable system has been constructed that will expand the flight test envelope and assist in service maintenance.

BIOTELEMETRY

NOXIOUS EFFECTS OR SIGNAL DETECTION - ? EXAMPLES OF INTERACTIONS BETWEEN ELECTROMAGNETIC FIELDS AND BIOLOGICAL SYSTEMS

Michael Bornhausen[1] and Herbert Scheingraber[2]

[1]Institut für Toxikologie, GSF-Forschungszentrum für Umwelt und Gesundheit, München-Neuherberg
and
[2]Max-Planck-Institut für extraterrestrische Physik, München-Garching, Germany

Summary

In recent years, a variety of biomedical phenomena - from headache to cancer promotion - were mentioned in the literature (Bernhardt et al. 1997) to be the consequence of the allegedly noxious influences of low-level, pulsed, high-frequency electromagnetic fields (EMFs). GSM (Global System of Mobile communication) and DECT (Digital Enhanced Cordless Telecommunication) telephone systems use high-frequency EMF-pulses to assure hand-held mobile communication almost world-wide. Their impact on modern life style is high and still increasing. Although science has failed so far to prove a dose-effect relationship, exposure duration and pulse characteristics of these EMFs are suspected to be potentially capable of disturbing the inter-cellular communication of a living organism.

Cognitive functions of the mammalian Central Nervous System (CNS) are particularly sensitive during prenatal development. To assess an eventual risk of low-level, pulsed high-frequency EMFs to the developing CNS, a group of 12 pregnant Wistar rats was continuously exposed during the 20 days of pregnancy to an EMF of 900 *MHz*, 217 *Hz* pulse modulation, and 0.1 mW/cm^2. This energy flux density corresponds to that of base antennas of the European digital GSM standard of hand-held mobile telecommunication devices. Another group of 12 rats was simultaneously sham-exposed. Specific absorption rates (SARs) for models of exposed freely roaming rats was measured to range between 17.5 and 75 *mW/kg*.

The coded male and female offspring of both groups were automatically trained when adult to lever press for food reinforcement by a *DR0* schedule and then tested during consecutive night-sessions in a battery of 10 simultaneously operated lever chambers (Skinner boxes). The rats were challenged by a sequence of 9 different contingencies of *Differential Reinforcement of High* resp*. Low Rate* (*DRH* resp. *DRL*)(Ferster and Skinner 1957) with increasing performance requirements. Individual data of activity (lever presses), performance (reinforcements), and relative performance (reinforcements relative to test requirement) were normalized with respect to group means and then mutually correlated.

Operant test performance scores of the offspring was further validated by a correlation analysis of behavioral microstructures, i.e. inter-response intervals between consecutive

lever presses. The analysis revealed time pattern changes which were characteristic for "learners" and "non-learners" in the *DRH* and *DRL* tests.

A systematic analysis of results obtained in a total of 80 rats focusing on normalized activity, performance, and rel. performance, and their mutual correlation did not reveal any changes relative to controls. EMF-induced changes of behavioral microstructures were not found. The prenatally exposed group did not demonstrate a deficit in the occurence of "learners" relative to the control group. Further systematic experimental and epidemiological studies are needed to prove the alleged risk of exposure to pulsed high-frequency EMFs during prenatal development.

Introduction

Functions of the central nervous system are particularly vulnerable during development. In teratology, conventional screening procedures - besides checking for structural anomalies - assess changes in fertility, growth, and the timely development of morphological signs and reflexes. Results are summarized as "developmental landmarks" (Jensh 1983). Obviously, many pups have to be handled and examined to collect statistically relevant data.

A computer-controlled operant behavior test system was designed to overcome some of these personal bias-prone methodological difficulties. It features 10 standardized test cages ("Skinner boxes") in which 10 rats can be tested simultaneously. Tests are run automatically during night.

Earlier studies demonstrated that this system reliably detects the neurotoxic consequences of a prenatal exposure (0.01 *mg/kg* bodyweight/day, days 6-9 post conception) to very low doses of methylmercury chloride in rats (Bornhausen et al. 1980). In fish, the WHO-defined tolerance limit of that well known human teratogen is 0.5-1.0 *ppm*.

Therefore, the eventual risk presented by an EMF of 0.1 mW/cm^2 to the developing central nervous system was aimed to be assessed by measuring cognitive functions in the adult offspring of exposed rat dams.

Material and Methods

12 pregnant Wistar rats were continuously exposed during 20 days under far-field conditions in exposure chambers provided by the Deutsche Telekom AG. Another group of 12 pregnant rats was simultaneously sham-exposed. Specific absorption rate (SAR) for the unrestraint, pregnant animals was measured in models to range between 17.5 and 75 *mW/kg*. SARs for the pups *in-utero* were not available. The offspring of exposed and sham-exposed rats were coded and tested when adult in groups of 10 subjects each. Each group was made of 5 exposed and 5 sham-exposed and coded rats. A total of 40 male and 40 female animals were trained automatically to press a lever for food reinforcement by a *Differential Reinforcement of Zero Rate (DR0)* schedule. All subjects

reached the criterion of successful training. Subsequently, all 8 groups were tested by a sequence of 3 sets of the contingency *Differential Reinforcement of High* resp*. Low Rate* (Ferster and Skinner 1957) with increasing performance requirements (Fig. 1):

(1) *DRH 2/1, DRH 4/2, DRH 8/4* where 2, 4, or 8 lever presses were required within a time lapse of 1, 2, or 4 *sec*;

(2) *DRL 1/8, DRL 1/16, DRL 1/32* where a blocking interval of 8, 16, or 32 *sec* had to be respected after each reinforcement;

(3) In the final test set, the previous three *DRH*- and three *DRL*-contingencies were combined (*COM*) in ON-periods of 45 *min* with alternating test requirements:
COM 1 (DRH 2/1-*DRL* 1/8),
COM 2 (DRH 4/2-*DRL* 1/16),
COM 3 (DRH 8/4-*DRL* 1/32).

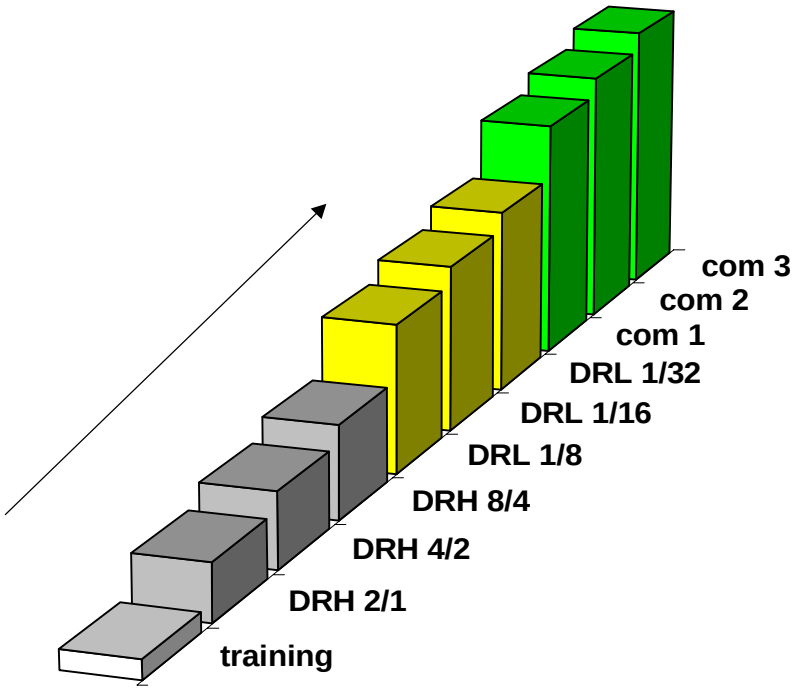

Fig. 1
Test sequence

The schedules of reinforcement and their sequence were chosen to differentiate between eventual cognitive and motor deficiencies and to challenge the animals while preserving their lever pressing activity. Nocturnal test sessions lasted 15 hours (16:00-07:00 CET). To minimize early satiation of the animals, sessions were subdivided into 30 *min* ON- and 60 *min* OFF-periods. Reinforcements (food pellets à 45 *mg*) were available during ON-periods only.

Operant test performance scores of the offspring was validated by a correlation analysis of the inter-response intervals between consecutive lever presses during ON-periods. This analysis of behavioral microstructures (Weiss et al. 1989) revealed time pattern changes which were characteristic for "learners" and "non-learners" in the *DRH* and *DRL* tests.

The following parameters of operant behavior test performance were measured in all subjects during the 9 consecutive test sessions:

(1) Activity (number of lever presses in ON-periods),
(2) Performance (number of reinforcements in ON-periods), and
(3) Relative Performance (number of reinforcements in ON-periods relative to specific test requirements).

Results and Discussion
Operant behavior performance of 80 coded animals in 9 nocturnal test sessions was measured and analyzed by two different approaches:

(1) Ratios of reinforcements vs. lever presses and
(2) Microstructures of operant behavior (Weiss et al. 1989), i.e. inter-response interval patterns.

Results of the first analysis are summarized in Fig. 2

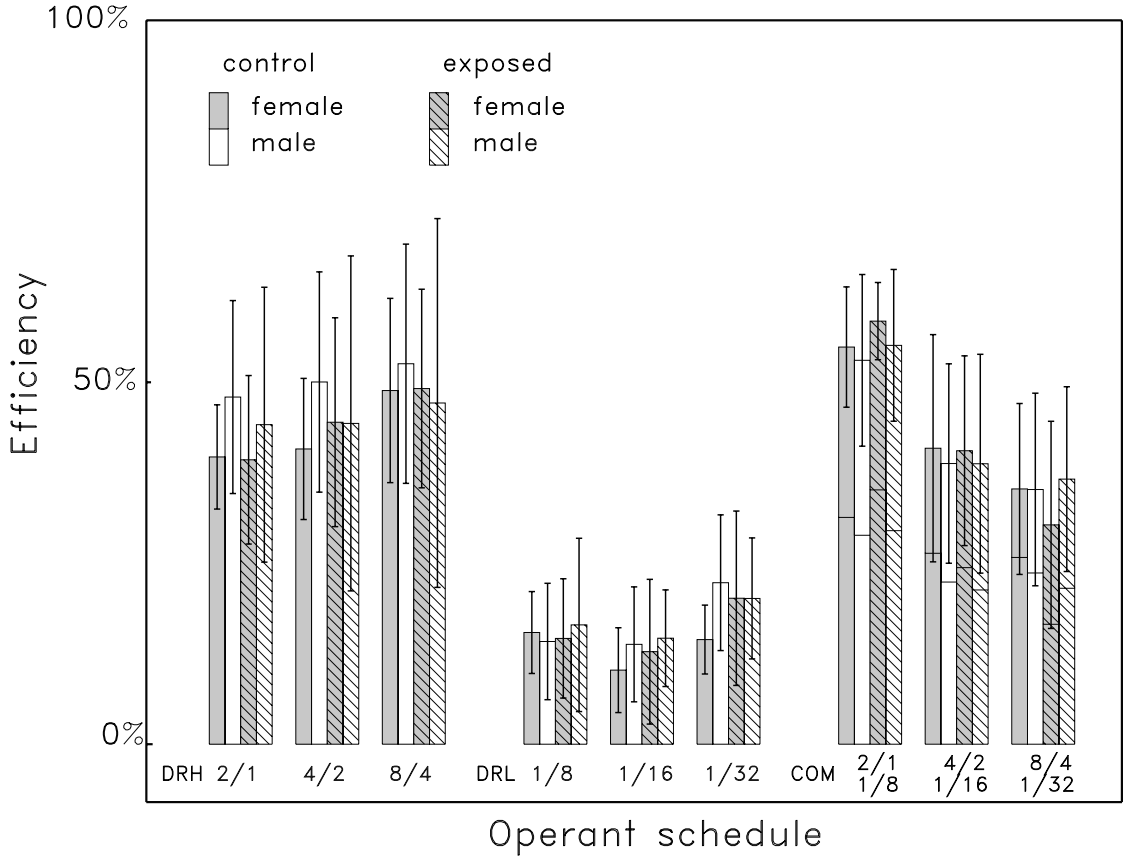

Fig. 2
DRH, *DRL*, and *COM* test performance

Thu Dec 09 14:21:50 1999
c:\pro\gsf\gsf_lp7s.pro

Individual scores of activity, performance, and relative performance were normalized with respect to group means and then mutually correlated in order to detect exposure-induced changes that might have been obscured by the inter-individual variability within groups.

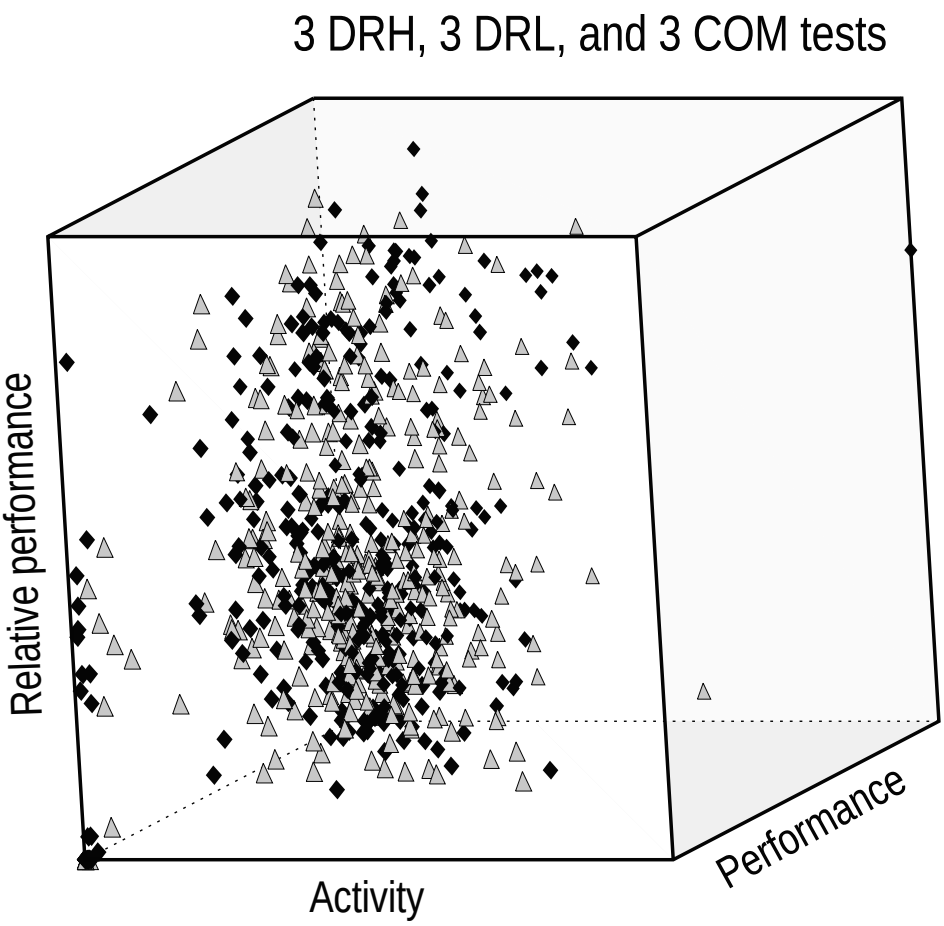

Fig. 3
Activity vs. Performance vs. Rel. Performance

Thu Dec 09 14:37:43 1999
c:\pro\gsf\gsf_cube.pro

Examples of the second analysis are given in Fig. 4.

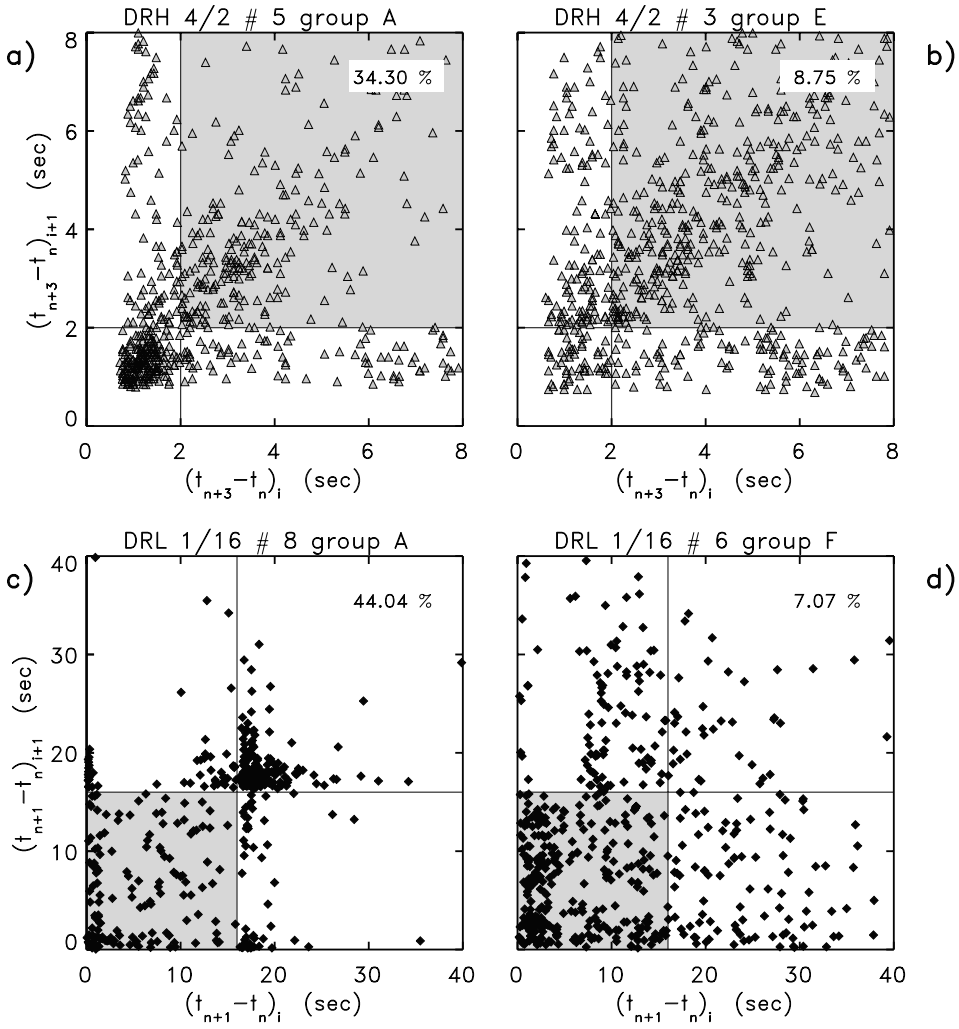

Fig. 4

Behavioral microstructures, examples of inter-response interval patterns in the *DRH* and *DRL* tests

EMF-induced changes of the incidence of "learners" vs. "non-learners" relative to controls were not observed.

The analysis of the results of both systems concurred: Prenatal exposure of Wistar rats to low-level, high-frequency EMFs did not produce deficient operant behavior and did not induce overt microstructural changes of that behavior.

These negative findings were validated by the absence of observable changes of developmental landmarks in litter mates of the operant behavior test subjects.

Conclusion

Neither male nor female rats that had been exposed prenatally to EMFs typical of the European GSM telecommunication system demonstrated any operant behavior performance deficits relative to controls. The incidence of specific inter-response patterns between experimental and control subjects was compared and confirmed the results obtained by conventional analysis of performance scores.

Our automated operant behavior test system proved to be a powerful tool for the assessment of neurotoxic risks in rats, especially after prenatal exposure. It requires only a relatively small number of test subjects. Furthermore, it offers perspectives for routine neurotoxicity tests in epidemiological surveys also of human subjects without the help of specialized personnel.

Acknowledgement

'The technical help of Mrs. B. Semder is gratefully acknowledged. Part of the work described here has been supported by Deutsche Telekom AG.

References

Bernhardt J.H., Matthes R., Repacholi M.H. (eds.): Non-thermal effects of RF electromagnetic fields. Proceedings of the International Symposium on Biological

effects of non-thermal pulsed and amplitude modulation RF electromagnetic fields and related health hazards. München-Neuherberg, November 20-22, 1996. ICNIRP 3/97

Bornhausen M., Müsch H.R., Greim H.: Operant behavior performance changes in rats after prenatal methylmercury exposure. Toxicol. Appl. Pharmacol. 56:305-310, 1980

Ferster C.B. and Skinner B.F.: Schedules of Reinforcement. Appleton-Century-Crofts, New York, 1957

Jensh R.P.: Behavioral Testing Procedures: A Review. In: Johnson E.M. and Kochhar D.M. (eds.): "Handbook of Experimental Pharmacology", Vol 65. Teratogenesis and Reproductive Toxicology. Springer Verlag, Berlin, Heidelberg, New York, 1983

Weiss B., Ziriax J.M., Christopher Newland M.: Serial properties of behavior and their chemical modification. Animal Learning & Behavior 17 (1):83-93, 1989

Legends to Figures

Fig. 1
After a *DRO*-training session, 8 groups of 10 coded animals each were challenged by a sequence of 9 different operant behavior test sessions with increasing requirements (see Material and Methods).

Fig. 2
Performance of male and female offspring is shown in percent of possible performance during the 3 steps of the *DRH*, *DRL*, and *COM* tests. Vertical brackets indicate standard deviations.

Fig. 3
The 3-dimensional cube correlates and summarizes the levels of activity vs. performance vs. rel. performance of 80 subjects as revealed by inter-response interval occurences during 9 test sessions. Note that there is no separation between the accumulated dots of exposed (diamonds) and sham-exposed (triangles) subjects.

Fig. 4
Examples of the correlation analysis of inter-response interval occurences are given for "non-learners" (right) and "learners" (left) in the test steps *DRH* 4/2 (above) and *DRL* 1/16 (below). The "forbidden" areas of the 2 different tests are shaded. Note that subjects # 3 and # 6 of groups E and F, respectively, have not acquired the specific test requirement. To the contrary, subject # 5 of group A has obviously learned the *DRH* 4/2 requirement. 34.30 % of all inter-response intervals are situated beyond the shaded area. Subject # 8 of group A is an example of a typical "learner" in the *DRL* 1/16 test. Here, 44.04 % of inter-response intervals are situated beyond the blocking interval of 16 *sec* (shaded area).

Interaction of RF Fields with Biological Systems

F. Feiner, J. Brix
Institute of Radiation Hygiene, Federal Office for Radiation Protection
Oberschleissheim, Germany

Abstract
This paper describes the fundamentals of the interactions of radiation in the radio frequency (RF) part of the electromagnetic spectrum. Especially in relation to hand-held mobile telephones the significance of this topic can be assessed by its almost continuous presence in the news media and the heated debate conducted in the public. To understand the mechanism underlying the biological consequences of RF-exposure to biological systems, the pronounced influence of the content of bound and free water within tissues and biological relevant substances is of crucial importance. On a cellular level, the high capacity density (0.01 F/m^2) of the cell membrane acts as a high-pass filter and enables high frequency currents to develop within the cell.
A special focus must be placed on the ability of living tissues to conduct heat via the nonlinear behavior of the blood circulation, which alters the heat distribution within tissues drastically. But also the direct coupling of high intensity electric fields to cells and organelles evokes interesting phenomena like “pearl chain” formation. On the other hand, the often discussed possibility of a nonthermal influence of low intensity electric fields on cells and tissues is backed by little or no evidence.

1. Motivation

In recent years the debate on health consequences of the increased utilization of electric and magnetic fields in a modern society has penetrated almost every newspaper and TV-magazine. Special concern is given by the public to the effects of the radiation emitted by hand-held mobile telephones and their base stations on sleep and mental processes as well as on more subtle alterations of inter- and intracellular interaction.

In the case of radio-frequency (RF) emissions this script attempts to describe the basics of the interaction of electric fields on biological systems. Information about the dielectric properties of biological systems is essential to understand their interaction with electromagnetic fields.

2. Electrical Properties of Biological Systems

Because of their importance the two electrical properties that define the electrical characteristics of tissues are summarized, namely, the permittivity (ε) and the specific conductivity (σ). Both properties change with temperature and, strongly, with frequency. As a matter of fact, as the frequency increases from a few hertz to gigahertz, the permittivity decreases from several million to only a few units; concurrently (Kramers-Kronig relation), the specific conductivity increases from a few hundred millisiemens per meter to nearly a hundred siemens per meter.

Biological tissues exhibit three strong relaxation phenomena (the α-, β-, and γ-dispersion) and one weak (the δ-dispersion). Figure 1 indicates the dielectric behavior of practically all tissues. Two remarkable features are apparent: exceedingly high permittivitys at low frequencies and three clearly separated relaxation regions – α, β, and γ – of the permittivity at low, medium, and very high frequencies. Additionally a fourth dispersion (δ) in between of the β- and γ-dispersion can be found. The mechanisms responsible for these four relaxation regions are indicated in Table 1.

The **α-dispersion** occurring between 10 Hz and 10 kHz (blood: 2 kHz, muscle: 100 Hz), may be considered as to be a dipolar relaxation that concerns the large dipole formed by the cell due to the accumulation of charges of opposing polarities (counter-ions) on either side of the cell membrane under the influence of the electric field. It is therefore a surface phenomenon.

The **β-dispersion** takes place in the RF-range between 10 kHz and 100 MHz (blood: 3 MHz, muscle: 100 kHz). It is mostly due to the capacative charging mechanism of cell membranes, which separate regions having different permittivities and electrical conductivities, resulting in an interfacial polarization causing the Maxwell-Wagner type relaxation. Smaller contributions result from the relaxation of proteins.

Another contribution to the high-frequency part of the β-dispersion is caused by the dipolar reorientation of smaller subcellular structures (mitochondria, cell nuclei, other organelles). Since these structures are smaller in size than the surrounding cell, their relaxation frequency is higher.

The **γ-dispersion** is most pronounced in the microwave region of the electromagnetic spectrum centered at about 20 GHz and has its origin in the reorientation of the dipoles of *free* tissue water molecules (80% of the soft-tissue volume).

The **δ-dispersion**, which occurs somewhere between 300 MHz and 2000 MHz, results from relaxation of *protein-bound* water, rotation of amino acids, partial rotation of charged side groups of proteins.

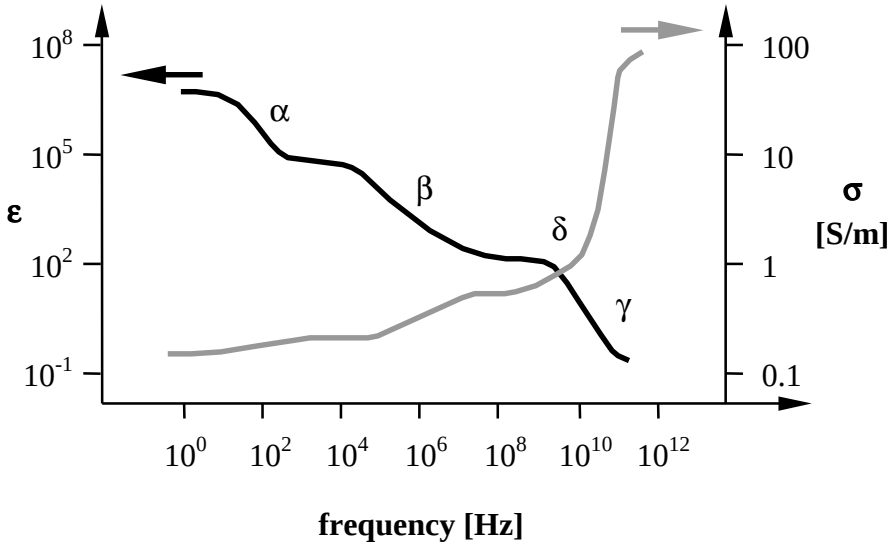

Figure 1. *Frequency dependence of the permittivity ε (black curve) and specific conductivity σ (gray curve) of typical biological tissue (Schwan, 1985, modified). Dominant contributions are responsible for the α-, β-, and γ-dispersions. They include for the α-dispersion, the acting of the whole cell as dipole and counter-ion effects; for the β-dispersion, cell membrane behavior; for the δ-dispersion, the rotation of specific sub groups; and for the γ-dispersion, the properties of the water molecules.*

Table 1. *Range of characteristic frequencies observed with biological material for α-, β-, δ- and γ-dispersion effects and their electrical relaxation mechanisms.*

Dispersion effect	Frequency Range [Hz]	Electrical relaxation mechanism (Schwan, 1975)
α	$10 - 10^4$	cell acting as dipole, counter-ion relaxation
β	$10^4 - 10^8$	charging of cell membranes, dipole rotation
δ	$3 \cdot 10^8 - 2 \cdot 10^9$	rotation of amino acids, charged side protein-groups, and protein-bound water
γ	$\approx 2 \cdot 10^{10}$	dipole rotation of free tissue-water

The dielectric properties of liquid pure water have been well established from dc up to microwave frequencies approaching the infrared (Afsar and Hasted, 1977). For all practical purposes, these properties are characterized by a single relaxation process centered near 20 GHz at room temperature. Static and infinite frequency permittivity values are close to 78 and 5, respectively, at room temperature. The dielectric properties of water are independent of field strength up to fields of the order 10 MV/m. Figure 2 shows that the dielectric behavior of typical biological materials in the RF-region can readily be explained by their content of free and bound liquid water.

The relatively simple geometrical shapes of cells in suspensions facilitates the understanding of the role of cell membranes in the polarization processes of biological media in the RF-range (Figure 3). The principal mechanism for dielectric polarization at RF-frequencies is the accumu-

lation of charges at membranes from extra- and intracellular fluids (usually, the membrane conductance can be neglected).

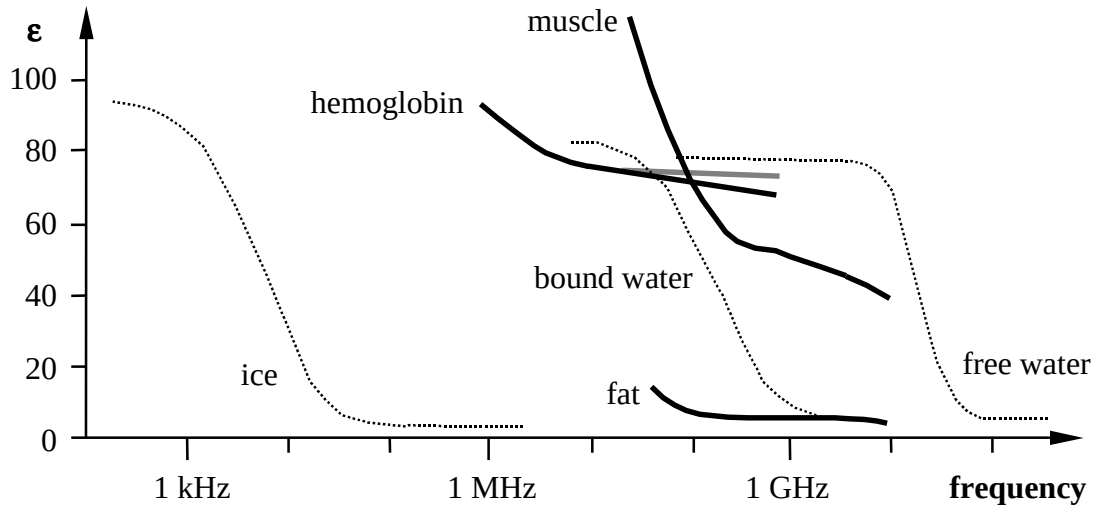

Figure 2. *Permittivities (ε) of ice, bound and free water (dashed) compared to the permittivities of hemoglobin, muscle and fat. The gray line (hemoglobin) indicates the behavior when omitting the δ-dispersion (Schwan, 1974, modified).*

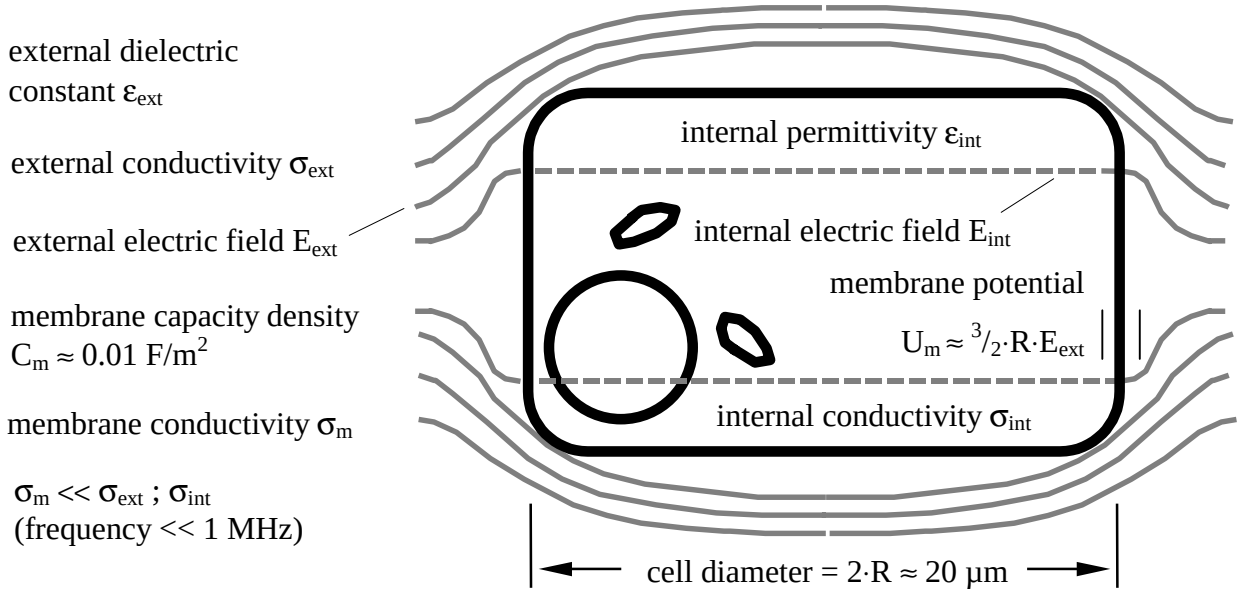

Figure 3. *Electrical properties of a typical cell in an external electric field. The gray lines represent the external and the dashed gray lines the internal electric field. The cell membrane is shown and internal structures are depicted in black.*

All evidence taken together justify the important conclusion that the capacitance density of all biological membranes, including cellular membranes and those of subcellular organelles such as mitochondria, is of the order of 0.01 F/m^2. This value is apparently independent of frequency in the total RF-range (Schwan, 1974).

From the membrane capacitance, values for the transmembrane potentials induced by RF-fields can be estimated. At frequencies well above 1 MHz, the membrane-capacitance impedance becomes very small by comparison with the cell-access impedance and the membrane behaves electrically like a short circuit. Since intracellular and extracellular conductivities are comparable, the average current density through the tissue is comparable to that in the membrane.
If the frequency is much lower than 1 MHz, the total potential difference applied across the cell is developed across the membrane capacitance. In this limit, the induced membrane potential U_m, across a spherical cell is approximately $U_m = 1.5 \cdot E \cdot R$, where E represents the applied external field and R the effective cell radius. Thus the cell samples the external-field strength over its dimensions and delivers this integrated voltage to the membranes, which is a few millivolts at these low frequencies for a cell radius greater than 10 µm and external fields of about 100 V/m.
In comparison, the propagation of action potentials along nerves is initiated or interfered with by pulses or low-frequency potentials of roughly 10 mV across the membrane. Corresponding current densities and field-strength values in tissues and the medium external to the affected cell are of the order of 10 A/m² and 100 V/m (Schwan, 1972; National Academy of Sciences, 1977; Schwan, 1971).

3. Thermal RF-Absorption in Biological Tissue

The most important effect of RF-frequency radiation on tissue is the deposition of heat due to the relaxational effects described in section 2. If one considers a simple system (as shown in Figure 4) consisting of an indefinitely thick layer of muscle tissue covered by a layer of fat tissue of a certain depths, the rate of absorbed energy in the fat layer varies firstly with its thickness and secondly with the frequency of the incident radiation. The reason for the pronounced pattern at 3 GHz and 10 GHz are the different factors for transmission and reflection on the surface between fat and muscle tissue. These factors in turn are a direct consequence of the different permittivities and conductivities.
The temperature rise evoked by RF-radiation in a given medium is directly proportional to the specific heat capacity of this medium, so if the incident power of RF-radiation is constant, the resulting temperature difference is linearly connected to the time the radiation is applied to the medium.
The complexity of the situation is increased dramatically if the effects of heat conduction and blood circulation are taken into account (Figure 5). Now there exists a steady state temperature, which will not change even if the radiation is applied for an infinitely long duration. Figure 6 visualizes the importance of heat conduction in different locations within the tissue.
It can be seen that especially at high frequencies the radiation heats up thin layers of tissue with poor heat conduction properties such as the uppermost layers of skin. Under those conditions, the influence of the penetration depths, which becomes evident in Figure 4, is overwhelming. In tissues with a highly developed blood supply, the influence of blood circulation is paramount because of its nonlinear behavior.
Summarizing all those dependencies, the concept of a specific absorption rate (SAR) for each type of tissue is a helpful tool to determine which incident RF-radiation power leads to a certain rise in temperature for each and every tissue under consideration (International Commission on Non-Ionizing Radiation Protection, 1998).
Another way to look upon the thermal effects of RF-radiation on biological systems – especially if the whole body of a certain animal is exposed to the radiation – is to relate the incident radiation power to the rest heat production of this system (Tell, 1999), which can be approximated by its black-body-radiation with the law of Stefan and Boltzmann (examples in Figure 7). If the incident RF-radiation power is only a small fraction of the heat production, then the temperature

rise for the whole body is negligible. In the case of local irradiation or highly inhomogenous power densities, the information about the local SAR values is much more reliable.

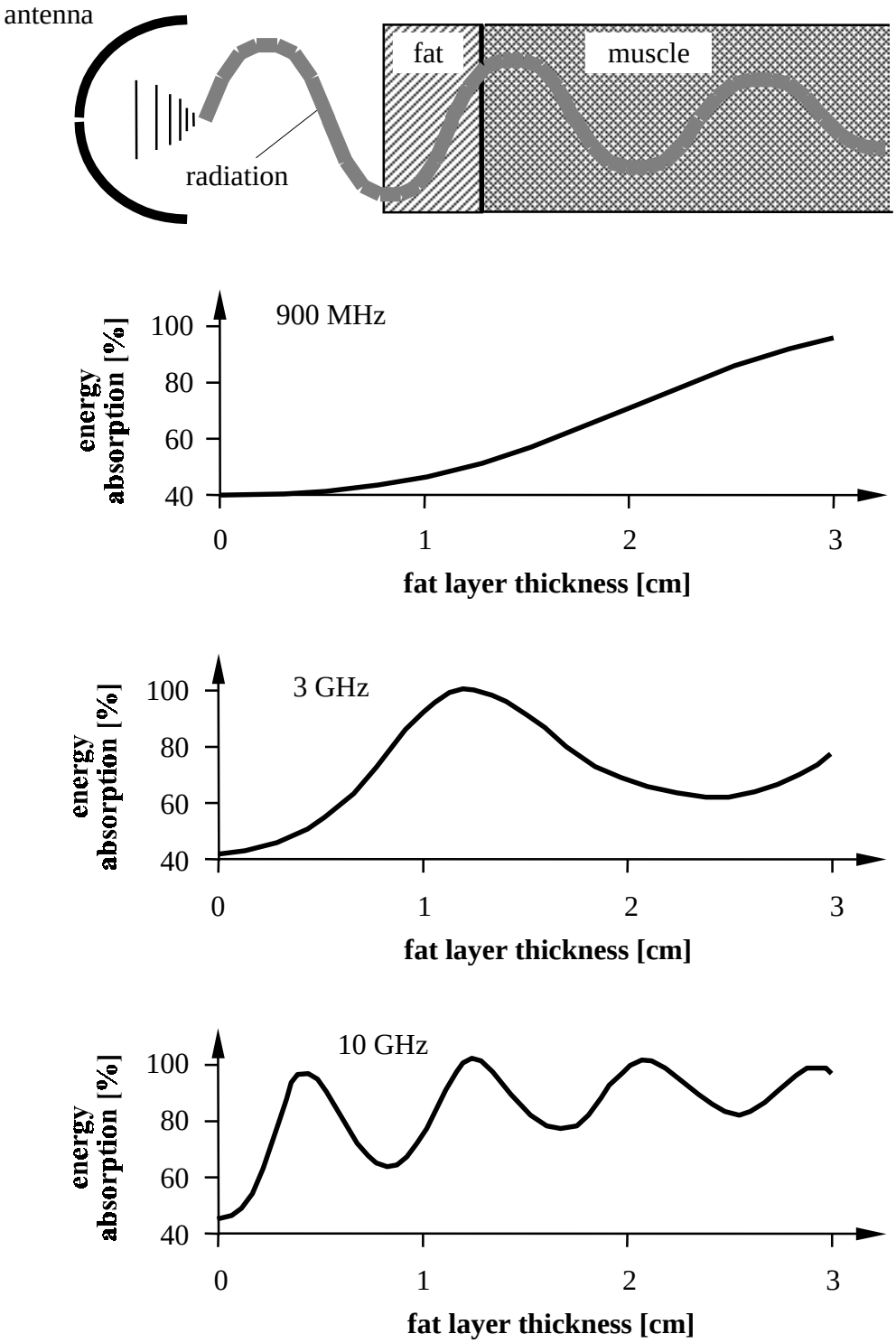

Figure 4. *RF-radiation hits a layer of fat tissue in front of an infinitely thick layer of muscle tissue (top). The variation of energy absorption within the fat layer dependent on frequency and thickness of the fat layer is shown below (Schwan, 1974, modified).*

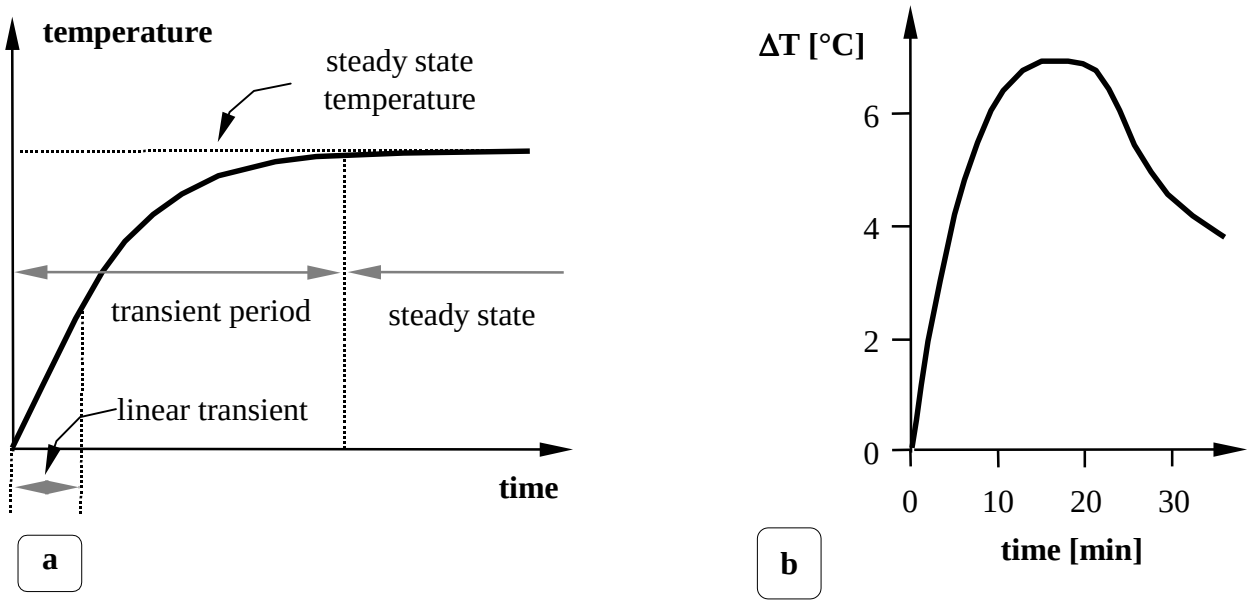

Figure 5. **a)** *Temperature versus time in irradiated tissue taking into account heat conduction. Only in the first short time interval the rise in temperature is directly proportional to the irradiation time (linear transient). With the end of the transient period, the temperature approaches its steady state value (Schwan, 1974, modified).*
b) *The influence of blood circulation on the temperature rise (ΔT) in tissue is nonlinear, which makes the process more complex. At a certain increase in temperature, the diameter of blood vessels widens, enhancing the blood flow which in turn leads to a decrease in tissue temperature (Schwan, 1974, modified).*

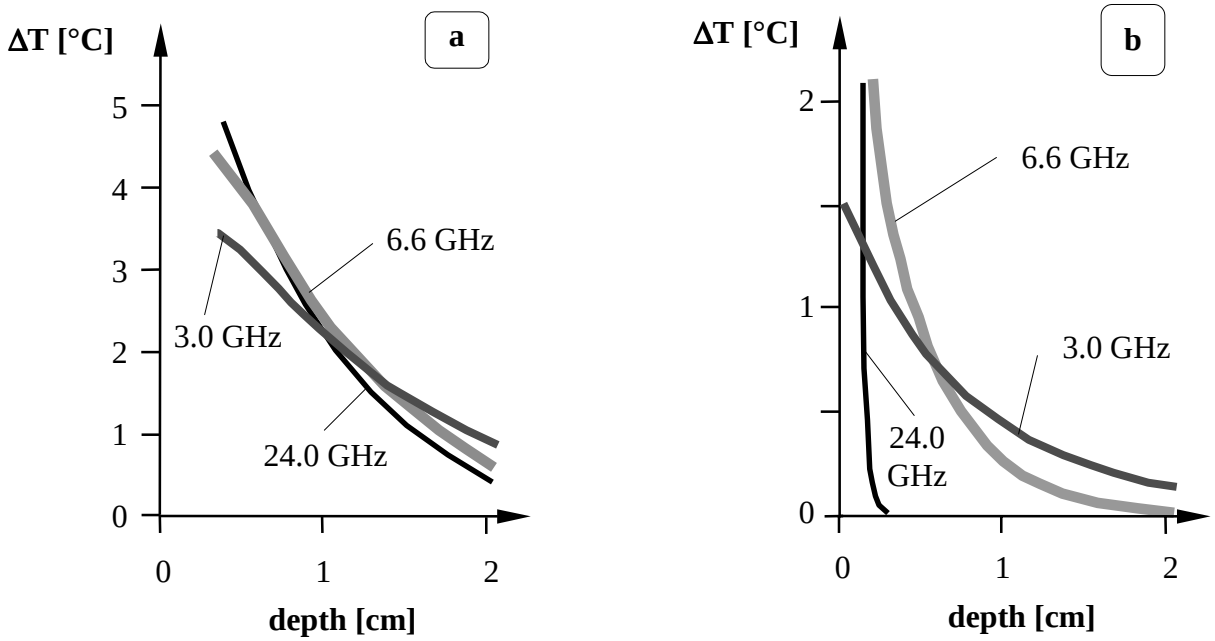

Figure 6. *Comparison of the rise in temperature (ΔT) at different depths of tissue (containing a high proportion of water, surface at 0 cm) with* (**a**) *and without* (**b**) *heat conduction at three frequencies. A linear model of heat conduction into the depth of the tissue was assumed. This shows that at frequencies above 4.6 GHz the temperature increase is determined by heat conduction and not by the frequency dependent penetration depth (Schwan, 1974, modified).*

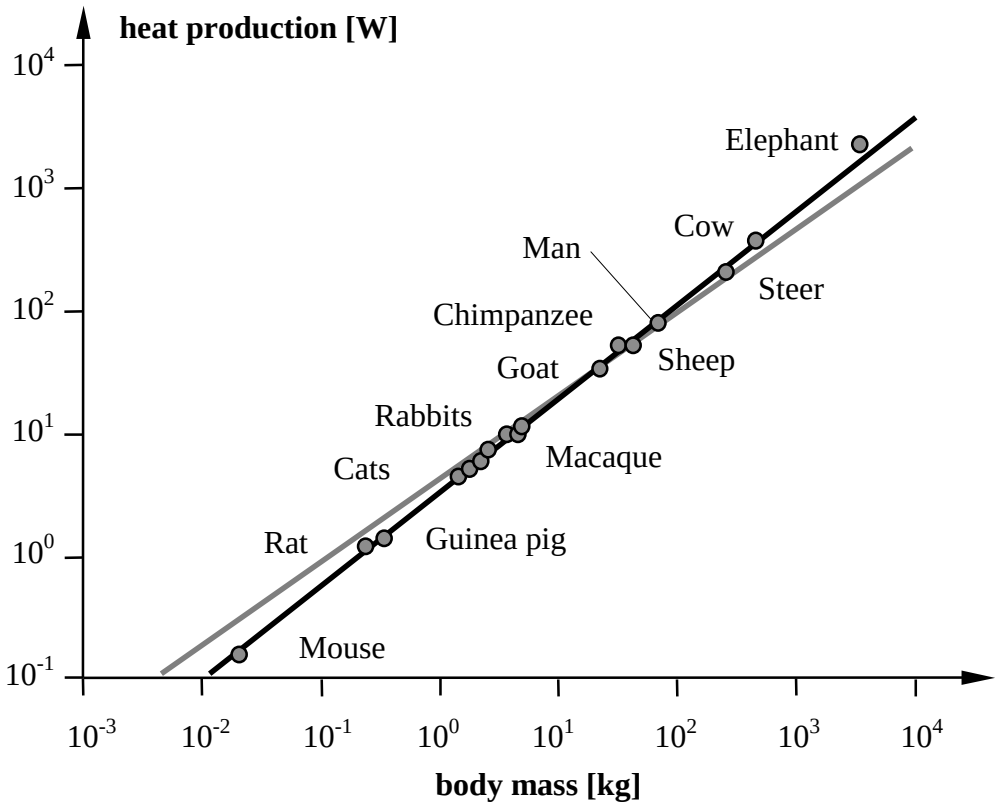

Figure 7. *According to the law of Stefan-Boltzmann, the heat production of mammals can be related to their body masses by a power law. This theory predicts a power of $^2/_3$ (gray line) but the observed value is $^3/_4$ (black line). The gray dots show the measurements for certain mammals (Schwan, 1974, modified).*

4. Field-Generated Force Effects

Electric fields can also create forces that act directly on molecules as well as on cellular and larger structures. Most of these interactions are reversible and do not necessarily have demonstrable biological effects. An example is the movement of ions in an ac field, which is inconsequential if the field is weak enough to prevent undue heating from molecular collisions (e.g., below about 100 V/m, corresponding to 10 A/m^2 in a physiological medium). Another example is the orientation of polar macromolecules. For low field-strength values, only a very partial, preferential orientation with the field results. Complete orientation and consequent dielectric saturation requires field strengths of some hundred thousands of volts per meter.

Electric fields can interact just as well with nonpolar cells and organelles in the absence of any net charge (Figure 8). These “ponderomotive” forces are well known and understood. Any system exposed to an electric field will tend to minimize its electric potential energy by appropriate rearrangement. This statement is equally true for dc and ac fields because the potential energy is a function of the square of the field strength. Pohl (1973) developed “dielectrophoresis” as a tool of separating cells in inhomogeneous fields, and Elul (1967) observed cell-destruction phenomena and cell-shape changes.

The field effects may manifest themselves as an orientation of particles in the direction of the field or perpendicular to it, or “pearl chain” formation which describes the alignment of particles in the field direction may occur (Figure 9).

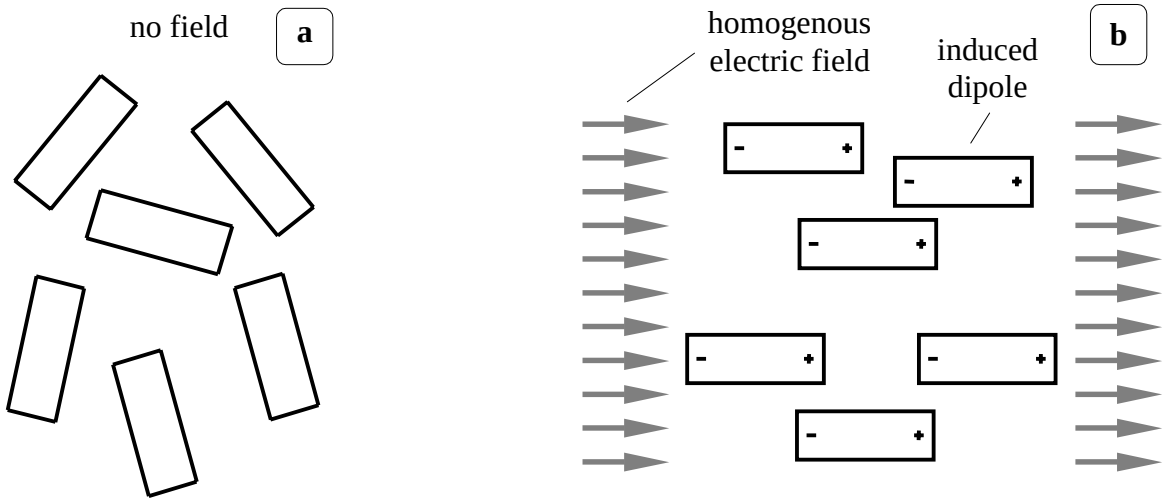

Figure 8. *In solution and with no electric field applied the orientation of cells is usually inhomogenous* (**a**). *If a very intense homogenous electric field is applied, the field induces dipole moments in the cells and the induced dipoles orient themselves in the direction of the applied electric field* (**b**) *(Schwan, 1974, modified).*

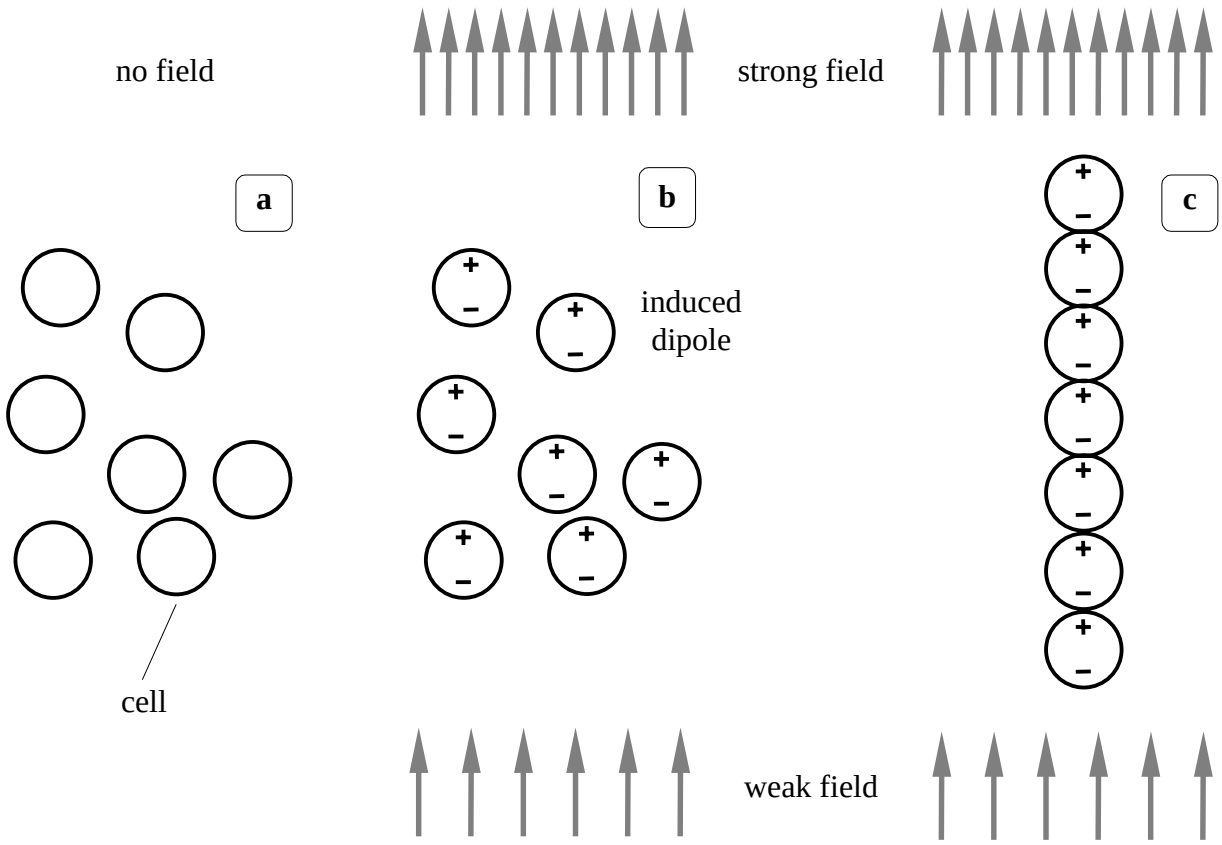

Figure 9. *The forces exerted on the induced dipole moments of the cells (dielectrophoresis) in a large field gradient line up the cells to form so called "pearl chains". Depending on the cell size and the suspending fluid, the optimum frequency is usually in the range of 10 kHz to 100 MHz. As shown in* **a**) *the cells are under no field influence. But when an electric field is applied* (**b**) *dipole moments are induced in the cells. Dipole-dipole interaction leads to the formation of "pearl chains"* (**c**) *(Schwan, 1974, modified).*

A theory worked out by Schwan (1969) and Hu (1975) shows that particles in solution take on the lowest energy configuration in an alternating electric field. Schwan (1974) could also show, that the threshold electric field strength for "pearl chain" formation is within a large range of frequencies independent of the frequency of the applied electric field and in very good agreement with theory (Figure 10). Zimmerman et al. (1974, 1982), Benz et al. (1980), Vienken et al. (1982), proved that cells lined up in "pearl chain" formation can be fused.
Neumann and Rosenheck (1972) studied the effects of fields on chromaffin vesicles. Friend et al. (1974) as well as Goodman et al. (1975, 1976) examined the influence of fields on fairly large cellular organisms. Orientation effects have been observed by Teixeirra-Pinto et al. (1960), Sher (1963), and Novak and Bentrup (1973).
Some of these field-generated force effects can be very startling and dramatic, especially near the tip of small electrodes. Of a similar nature is the movement of magnetotactic bacteria, reported by Blakemore (1975), in magnetic fields of fairly low intensity. Apparently these bacteria are equipped with magnetic properties and are therefore significantly oriented by the magnetic field and motivated to move in the field direction.
Experimental and theoretical evidence indicates that pulsed fields cannot have greater effects than continuous fields of the same average power (Sher et al., 1970). Modulation is therefore not expected to have special effects.

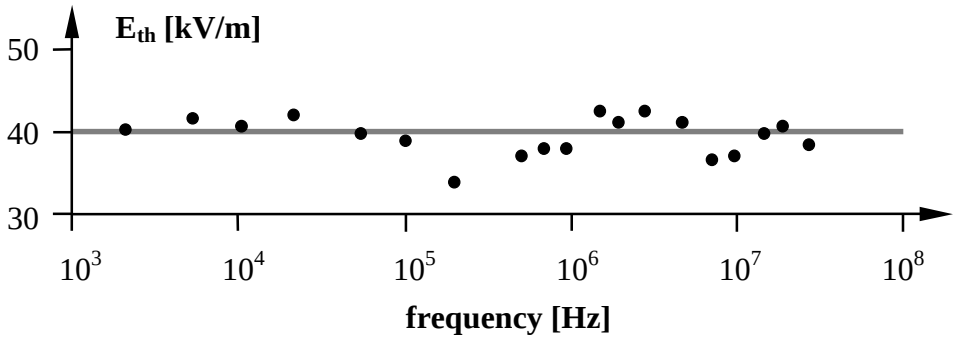

Figure 10. *Measured threshold field strength E_{th} (black dots) for "pearl chain" formation in an emulsion of silicone particles with a diameter of (0.6 ± 0.1) µm. The theoretical value of 40 k V/m (gray line) is independent of frequency (Schwan, 1974, modified).*

4. Possibility of Weak Nonthermal Interactions

The considerations presented above do not suggest any weak nonthermal mechanism by which biological systems could react to low-intensity microwave fields. Fields of the order of a few hundred kilovolts per meter are needed to orient long biopolymers, and still higher fields to excite internal vibrations or produce submolecular orientation. External fields acting on biopolymers must further overcome strong local fields, which are 150 kV/m at a distance of 10 nm from a monovalent ion and 180 kV/m at the same distance from a hemoglobin molecule. Microwave frequencies are well above those corresponding to significant rotational diffusion times, excluding orientational effects. Transmembrane potentials induced by typical nonthermal microwave fields are vanishingly small relative to potentials required for stimulation and compared with membrane noise. Field-induced force effects are unlikely to be significant on a single molecular

or cellular level because the threshold field strengths necessary to overcome thermal disturbances are too high (Schwan, 1977).

The large dimensions necessary for biological responses to weak microwave fields might be achieved by a cooperative reaction of a number of cells or macromolecules to the microwave stimulus, which increases the effective size of the structure and correspondingly reduces the threshold required for an effect. Bawin and Adey (1976) suggested that such cooperation might be induced in the counter-ions loosely bound near membrane surfaces which contain a loose framework of charged polysaccharides.

Froehlich (1973, 1975) suggested that giant dipole moments may be formed during enzyme substrate reactions and that the corresponding dielectric absorption processes might channel energy into lower frequency modes of vibration. He also considered the membrane as a likely site of resonant electromagnetic interactions; and from the velocity of sound and the membrane thickness, he derived an estimate of the resonant frequencies to be of the order of 100 GHz. Acceleration and deceleration of a variety of biological responses that suggest resonances in the millimeter wave range have been reported by Webb and Booth (1971), by Devyatkov (1974), and by Grundler et al. (1977). But some of these studies have been criticized on technical grounds. Gandhi et al. (1979) conducted continuous dielectric spectroscopy measurements at millimeter-wave frequencies with no indication of any resonance processes. Also, on a variety of cellular processes they found no effects of millimeter-wave radiation that were not attributable to sample heating. But the resonance phenomena reported by Grundler et al. and postulated by Froehlich may only involve a minor fraction of the total cellular entity and thus not demonstrate itself strongly enough to be observed in the bulk dielectric data.

REFERENCES (in alphabetical order)

Afsar, M. N., and J. B. Hasted. Measurements of the optical constants of liquid H_2O and D_2O between 6 and 450 cm^{-1}. J Opt Soc Am 67:902-904 (1977).

Bawin, S. M., and W. R. Adey. Sensitivity of calcium binding in cerebral tissue to weak environmental electric fields oscillating at low frequency. Proc Natl Acad Sci USA 73:1999-2003 (1976).

Benz, R., Zimmerman, U. Pulse length dependence of the electrical breakdown in lipid bilayer membranes. Biochem. Biophys Acta 597:637 (1980).

Blakemore, R. Magnetotactic bacteria. Science 190:377-379 (1975).

Devyatkov, N. D. Influence of millimeter-band electromagnetic radiation on biological objects (transl). Sov Phys USPEKHI 16:568-579 (1974).

Elul, R. Fixed charge in the cell membrane. J Physiol 189:351 (1967).

Friend, A. W., et al. Low-frequency electric-field-induced changes in the shape and motility of amoebae. Science 187:357-359 (1974).

Froehlich, H. Collective behavior of nonlinearly coupled oscillating fields. J Collective Phen 1:101-109 (1973).

Gandhi, O. P., et al. Millimeter wave and raman spectra of living cells – some problems and results. Workshop on Mechanisms of Microwave Biological Effects, University of Maryland, College Park, MD, 14-16 May 1979.

Goodman, E. M., et al. Effects of extremely low frequency electromagnetic fields on growth and differentiation of Physarum polycephalum. Technical Report Phase I (Continuous Wave). University of Wisconsin-Parkside, Kenosha, WI, 1975.

Goodman, E. M., et al. Effects of extremely low frequency electromagnetic fields on Physarum polycephalum. Technical Report, office of Naval Research, Contract N-00014-76-C-0180, University of Wisconsin-Parkside, Kenosha, WI, 1976.
Grundler, W., et al. Resonant growth rate response of yeast cells irradiated by weak microwaves. Phys Lett 62A:463-466 (1977).
Hu, C. L., Barnes, F. S. A simplified theory of pearl chain effects. Radiat. Environ. Biophys. 12 (1975).
International Commission on Non-Ionizing Radiation Protection. Guidelines for Limiting Exposure to Time-Varying Electric, Magnetic, And Electromagnetic Fields (up to 300 GHz). Health Phys. 74(4): 494-522 (1998).
National Academy of Sciences-National Research Council. Biological Effects of Electric and Magnetic Fields Associated with Proposed Project Seafarer. Washington, DC, 1977.
Neumann, E., and Y. Rosenneck. Permeability changes induced by electric impulses in vesicular membranes. J Memb Biol 10:279-290 (1972).
Novak, B., and F. W. Bentrup. orientation of focus egg polarity by electric ac and dc fields. Biophysik 9:253-260 (1973).
Pohl, H. A. Biophysical aspects of dielectrophoresis. J Biol Phys 1:1-16 (1973).
Schwan, H. P., and L. D. Sher. Alternating current field induced forces and their biological implications. J Electrochem Soc 116:170-174 (1969).
Schwan, H. P. Interaction of microwave and radiofrequency radiation with biological systems (invited paper). IEEE Trans MTT-19:146-152 (1971).
Schwan, H. P. Biological hazards from exposure to ELF electrical fields and potentials. NWL Tech Report, TR-2713, US Naval Weapons Lab, Dahigren, VA, 1972.
Schwan, H. P. Biophysical foundations of protection measures regarding non ionizing radiation. Lecture at University of Erlangen, Germany, January 1974.
Schwan, H. P. Dielectric properties of biological materials and interaction of microwave fields at the cellular and molecular level. In: S. M. Michaelson and M. W. Miller (eds.). Fundamental and Applied Aspects of Nonionizing Radiation. New York: Plentnn Publishing Co., 1975.
Schwan, H. P. Field interaction with biological matter. Ann NY Acad Sci 303:198-213 (1977).
Schwan, H. P., and K. R. Foster. Biophysical principles of interaction and forces, pp. 243-271. In: Grandolfo, M., Michaelson, S. M., and Rindi, A., ed. Biological effects and dosimetry of static and ELF electromagnetic fields. New York, London, Plenum Press, 1985.
Sher, L. D., et al. On the possibility of nonthermal biological effects of pulsed electromagnetic radiation. Biophys J 10:970-979 (1970).
Sher, L. L. Mechanical effects of ac fields on particles dispersed in a liquid: Biological implications. Ph.D. Thesis, University of Pennsylvania, Philadelpha, PA, 1963.
Teixeirria-Pinto, A. A., et al. The behavior of unicellular organisms in an electromagnetic field. Exp Cell Res 20:548-564 (1960).
Tell, R. Overview of several large scale RF projects in the US In: Effects of electromagnetic Fields on the living Environment. ICNIRP-Seminar, Ismaning, Germany, October 1999.
Vienken, J., Zimmerman, U. Electric field-induced fusion: Electro-hydraulic procedure for production of hetrokaryon cells in high yield. Federation of European Biochemical Societies Letters 137:11 (1982).
Webb, S. J., and A. D. Booth. Microwave absorption by normal and tumor cells. Science 174:72-74 (1971).
Zimmerman, U., et al. Dielectric breakdown of cell membranes. Biophys J 14:881-889 (1974).
Zimmerman, U., et al. Electric field-mediated fusion and related electrical phenomena. Biochimim. Biophys Acta 694:227 (1982).

WIRELESS AMBULATORY ACQUISITION

OF HIGH RESOLUTION PHYSIOLOGICAL SIGNALS

N. Noury[1], T. Hervé[1], V. Rialle[1], G. Virone[1], C. Cingala[2], E. Gouze[2], E. Mercier[2]
(1) TIMC-IMAG, Team Microsystems – UMR CNRS 5525 – Domaine de La Merci
F-38700 La Tronche
(2) Thomson-CSF Semiconducteurs Spécifiques (TCS) – avenue de Rochepleine
BP 123 – F-38521 St Egrève

Abstract: The purpose of this paper is to describe a method for the remote surveillance and condition monitoring of patients while in the home. The use of miniaturised sensors and wireless data transmission allows the subject greater freedom of movement, as well as faster identification of pre-defined symptoms. We shall explain the particular needs required by the sensors and the use of a Radio Frequency(RF) Transceiver for the transmission and reception of this medical data.

1 Introduction

'Telemedicine' is concerned with combining computers and telecommunications to improve the quality of health care, currently available, by linking remote patients with centres of medical expertise via a wireless data link. Telemedicine has drawn increasing attention as one of the fastest emerging solutions to face health reform initiatives and to generally improve health care access, thereby reducing the government healthcare costs. Currently this accounts for approximately 10% of the GDP (Gross Domestic Product), for industrialised countries.

The top clinical specialists utilising Telemedicine, for instance are: cardiology, obstetrics, paediatrics, radiology, dermatology, psychiatry and emergency medicine, with more than 1000 clinical systems currently in use in the USA. European countries are still trying to implement such solutions, mainly for legislation and cost reasons.

The acquisition of human physiological data, in normal situations of activity, is very interesting for the purpose of long term data-storage for later diagnosis[1,2], or for the purpose of medical exploration. To allow the person free motion it would be necessary either to resort to the technique of Holter; according to which one records the signals over a long period with processing later or to establish a wireless communication link with a fixed station. This second type of connection authorises 'real time' signal processing on a distant fixed computer and it makes it possible to reduce the volume and consumption of the embarked part. Oviously, it is also important to be able to send back result of the diagnoses, in real time, to the patient. Implementing a backward link also paves the way to more effective communication protocols and other useful functions from a medical point of view, for instance: to alert the patient that it is time to take a pill.

Even though most applications do not need high data rates, areas like cardiology may require a higher than normal data rate in order to include heart beat information and also the actual shape of the electrocardiogram. Furthermore the ambulatory, or mobile, nature of the signal implies that one should consider the activity of the person in order to take the actimetric events into account for the signal reception and processing (signal blanking or restoration).

We have developed an ambulatory system intended for high resolution acquisition of 4 physiological signals recorded from surface electrodes. The signals are converted into digital values, then fed to a micro controller which controls the serial communication of the data through a bi-directional RF link, maintained by the TRX01 RF Transceiver from TCS. In addition to the functional signals the actimetry information on the person is transmitted for data marking and fusion functions.

This device is intended to be used in telemedicine for the monitoring of physiological parameters in the home. The first application in sight is the ambulatory continuous monitoring of the fœtal's heartbeat rate, for certain high risk pregnancy cases[3].

2 Wireless Communications Hints

2.1 The communication requirements.

The amount of data to be transferred at a time is typically in the range of 10 to 100 bits, with a maximum transmission cycle frequency is 1 Hz. With an occupation time of about 1/20, this induces a transmission duration of 50 ms, which means that a data rate of 2400 bits per second (bps) is suitable.
A simplex communication link would be inadequate as we 'd better be able to re-adjust its operation parameters (amplifier gain, filtering frequencies, levels of detection, etc.), so the obvious choice is for a half duplex communication system, with either a balanced or unbalanced data rate.

2.2 The technology for wireless communications.

Two main techniques can be considered for short range communications in the home. The optical IR(Infra-Red) communication link and the RF communication link.

- The optical link requires an unrestricted, line-of-sight, view in order to communicate effectively between devices. This is of course a real limitation for the free motion of the person around the home.
- The RF link enables non-line-of-sight communication and better suits an indoor mobile task. The choice for the carrier frequency naturally falls to one of the free ISM bands, 434 MHz or 868 MHz bands (European countries), with 915 MHz for the USA. It is also advantageous to use the low cost equipment and the low power consumption associated with these bands.

2.3 The physical limitations of a RF data transmission link in the home.

There are 2 physical effects to be taken into account for a data communication with a "human mobile" in a building[4].

- The first one is the Doppler effect, which induces a frequency shift due to the motion of the transmitter embarked on the person. A transmission carrier of frequency **F** is associated to a wavelength λ with $\lambda = c/F$ (where **c** is the velocity of light). If an object moves along with a speed **v**, it will take the time $\tau = \lambda/v$ to move along the wavelength λ, this will introduce a corresponding frequency shift **Fdi = F * v/c**. If the angular direction between the electromagnetic waves alter direction and the direction of the movement is α, then this shift becomes $Fdi = F*v*\cos\alpha / c$. In any case the maximum frequency shift is obtained with $\alpha = 0$. For **F = 433 MHz (λ = 69 cm)**, if we consider a maximum movement of **2 m/s (7.2 km/h)**, we obtain a negligible shift of **about 3 Hz** maximum value.
- The second effect is the Rayleigh fading[5] which introduces an amplitude variation of the electrical field with space due to the different interferences of the reflected. The spatial frequency of such interference is $\lambda/2$, for a monochromatic wave, so for the same mobile speed, **v**, the frequency of the interference is $Fr = 2 * v/\lambda$ that is
- **Fr = 2 * Fdi**, twice the Doppler shift frequency. This phenomenon introduces blanks in the transmission which can be disastrous for any digital link. For the same ISM carrier **(F = 433 MHz)**, the fading duration is about **30/v**, that is **15 ms** for **v = 2 m/s**; but it increases if the mobile remains in the blank region. There are two ways to reduce this effect:
- The first, Spatial Diversity, consists of receiving the same signals on multiple antennas spatially distributed. The cost of such a solution increases with the multiplication of the receivers.
- The second, Frequency Diversity, consists of using multiple carriers[6] which leads to different spatial repartition of the Rayleigh fading issue. We usually have two options to implement this strategy:
  - the carrier frequency is changed only when a transmission error occurs, the Multi-Channel option.
  - the carrier frequency is changed at a regular pace, whatever the propagation conditions, the Frequency Hopping Spread Spectrum option (FHSS).

With a simplex link it will be needed to operate with a good error correction encoding system[7]. If the transmitter has a bi-direction link, it can also receive an acknowledgement in return, so it may be possible to put to work a very simple "ACK-NACK" kind of communication protocol.

3 The Radio Transceiver

TRX01 is a low power, half duplex, RF transceiver based on a 0.5µm BiCMOS technology and combines both RF performance with numerous digital functions to make it a very simple-to-use product.

TRX01 makes a cost-effective way of implementing a basic communication protocol. With the increasing number of applications requiring a two-way communication path, the TRX01 not only allows the system to check whether a message has been correctly received it can also reprogram a remote unit or even select and interrogate a device among several remote units.

An external µC manages the TRX01 and controls the communication protocol and frequency hopping operations, if required. TRX01 covers the ISM bands 433 MHz, 868 MHz and 915 MHz, therefore, any application can easily be adapted to meet European and American Standard Regulations.

Our ambulatory signal acquisition system involves some specific requirements needed for RF transmission :

- Secured Transmission

It is possible to choose among three strategies to secure the transmission and adapt the protocol complexity to the varying propagation conditions:

- Narrow Band Operation: TRX01 provides a fine digital tuning capability of the carrier central frequency (200 Hz resolution), from a commonly used reference crystal typically operating at 10.245 MHz. Narrow band operation means a lower sensitivity to out-of-band interferences and a better throughput over the ISM frequency, several transmissions can be safely completed in neighbouring channels.

- Multi-Channel Operation: The system can select a new channel when the error rate in the current channel turns out to be higher than the correction code recovery capability.

- Frequency Hopping Operation: TRX01 needs less than 100µs to shift the carriers central frequency by several hundreds of kHz, so that Frequency Hopping systems no longer waste time waiting for a new frequency to become stabilised.

- Indoor Environment

TRX01 is the first highly integrated transceiver whose output power can be adjusted up to the maximum power authorised by the regulations. In an indoor environment where a high signal loss is expected having the extra power capability is then vital, in order to reduce the design constraints and therefore the cost, of the receiving part of the system.

- Small Size

To build a full transmission system can prove costly. The TRX01 has been designed so it connects to the minimum amount of external components as possible. In particular, no external synthesizer or VCO is required. The full layout of a PCB (Printed Circuit Board) needs less than 30*40mm (see photo).

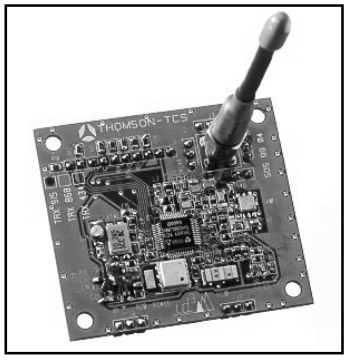

- Low Power Consumption

TRX01 switches automatically to and from “sleep” mode (with a current consumption lower than 3µA), to a receive or “wake” mode, in which it can check the arrival of a predefined message without any action from the external µC.

As our application refreshes the information at 1 Hz, the TRX01 can be set to sleep mode between transmissions, with an average sleep/wake ratio of 200/1. The transmitter output power can be digitally adjusted, to continuously set its value to the minimum power level required, based on the actual propagation conditions.

- High Data Rate

The application today requires a transmission data rate of 2400 bps. Since the TRX01 can achieve up to 50000 bps, the transmission duration and therefore the power consumption, can be greatly reduced. When more sensors and consequently a higher volume of data is needed, the TRX01 will easily be able to handle the load increase required by any future application.

4 Integration Of The Ambulatory Device

This device is intended for the acquisition of 4 analogue levels recorded from body surface electrodes, along with information on the person's actimetry. This data is digitally converted, then written into a data message format which is then sent to a central computer via the RF link :

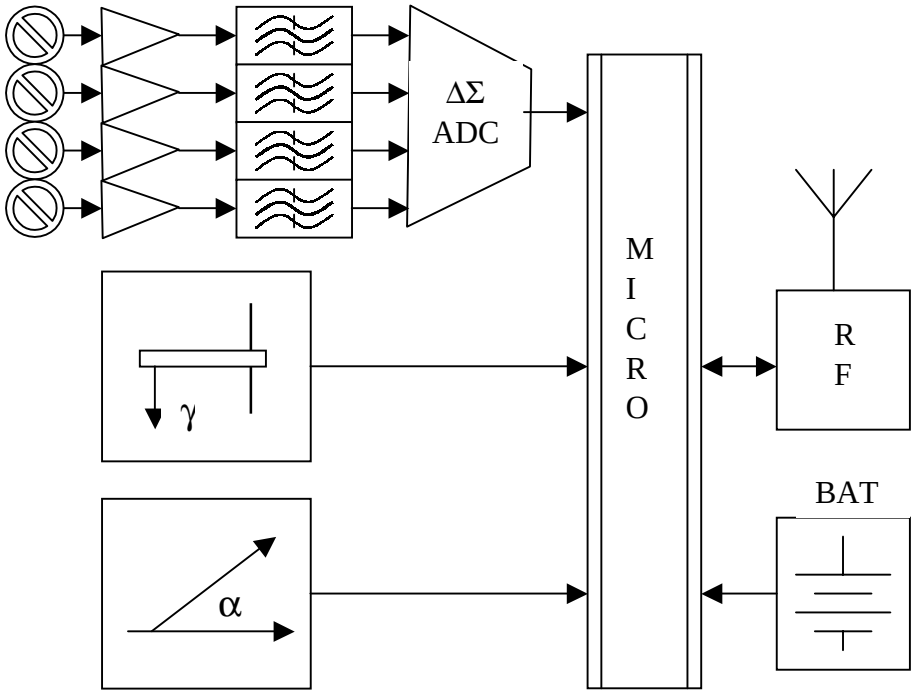

The surface electrodes are standard AgCl disposable electrodes from 3M. The analogue signals are initially conditioned with a high impedance buffer amplifier with a programmable gain (10, 100, 1000). The bandwidth is further reduced in the range of 0.1 Hz to 125 Hz with a 1st order High pass discrete filter followed with a 7th order active low pass filter. A 50 Hz and 100 Hz rejection of the frequencies is obtained from a comb rejection filter. Eventually the signals are converted into a 24-bit digital value via a Delta-Sigma converter. The converter is driven from a micro controller which oversees the serial communication of the data. The micro controller also receives two other pieces of information on the activity of the person; the vertical acceleration level obtained from a piezoelectric sensor and the "body orientation", standing or lying, from a position switch. The transmitted message is made of the device 'identity' code, the 4 analogue levels with

the amplification gain value and the Boolean information of position and acceleration. The bi-directional wireless communication is carried out with the TRX01 radio transceiver.

5 Conclusions And Perspectives

The first prototype of the system was completed last year with a single 433 MHz RF transmitter with no possibility of frequency hopping and no two-way link. Although its transmission rate of 2400 bps showed to be enough for the technical validation of the four channel analogue acquisition and for the actimetric module set-up. Nevertheless, it showed the need for a Half-Duplex RF transceiver, with enough flexibility to switch from one carrier to another for FHSS purposes and to quickly toggle between transmit and receive modes.

A new system has been developed and is currently under test. The next task is to optimise the power supply management of the device to reduce the total consumption of the system. This will be obtained through correct control of the 'sleep' mode which is possible using the micro controller and the TRX01 Transceiver. The goal is to have a 24-hour power autonomy at one's disposal, in order to follow up in real time the signals coming from the 4 electrodes placed on the *pregnant mother's* body, for example. Future versions may be optimised thanks to the use of a custom ASIC.

References

[1] Johnson P, Andrews DC (1996). Remote continuous physiological monitoring in the home. *J Telemed Telecare* 2(2): 107-113.

[2] Rodriguez MJ, Arredondo MT, Del Pozo F, Gomez EJ, Martinez A, Dopico A (1995). A home care management system. *J Telemed Telecare* vol 1 : 86-94.

[3] Horio H, Murakami M, Chibe Y, Inada H (1998). Fetal Monitor for Non-Stress-Screening at home. *Biomed Instr & Techno*, 39-47.

[4] Remy JG, Cueugnet J, Siben C (1988). Systèmes de radiocommunications avec les mobiles. *Eyrolles CNET-ENST.*

[5] Rice SO (1944). Statistical properties of sine waves plus random noise, *Bell Syst Techn J*, vol 23: 282-232.

[6] Muammar R, Gupta S (1982). Performance of a frequency-hopped multilevel FSK spread-spectrum receiver in a Rayleigh fading and lognormal shadowing channel. *ICC 1982, session B*.

[7] Battail G, Cohen G, Codlewski (1975). Théorie de l'information et codes correcteurs d'erreur. *ENST Paris 1975*.

Hospital-based Recording and Characterisation of Impulsive VHF Noise

A.I. Riemann
CETECOM GmbH
Im Teelbruch 122
45219 Essen
Germany

N.E. Evans
School of Electrical & Mechanical Engineering
University of Ulster at Jordanstown
Newtownabbey, Co Antrim
Northern Ireland, BT37 0QB

Tel: +49 2054 951943, FAX: +49 2054 951913, e-mail: AI.Riemann@iee.org
Key Words: impulsive radio noise, radio interference, pulse energy distribution

Abstract

This paper reports on the measurements of incidence and level of man-made electrical impulse noise capable of causing interference to low-power, ASK and FSK radio biotelemetry links. Measurements were made at two acute hospitals, one in a residential area of Belfast, Northern Ireland (i) and the other in an industrial part of Berlin, Germany(ii). At both locations hospital staff had reported patient ECG-telemeter malfunctions that were subsequently associated with interference from man-made impulsive noise: these observations [1,2] indicated that further investigations into the nature of the interference sources were required.

Initial findings

For the initial measurements a standard communications (IC-R7000) receiver was modified to produce unbiased pulse information by disabling the AGC line. Its post AM-detection baseband signal was extracted and fed into a PC-based logger which counted the detected pulses above a

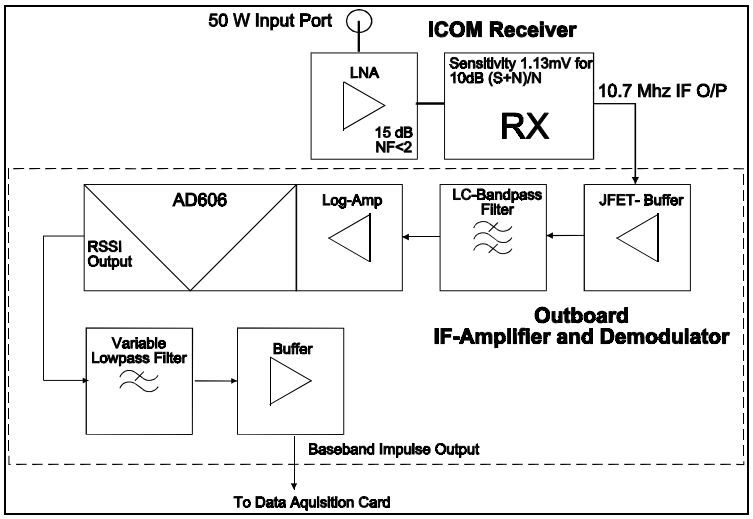

Figure 1: block diagram of updated receiver

set threshold level and stored the count per minute in a file on disk. The RF bandwidth of the receiver was 20 kHz and a rotatable folded-dipole receiving antenna was used.
The equipment was deployed close to the existing telemetry receiver of each measurement location and set to a previously monitored vacant frequency in the 450 MHz band.
For the initial work, data were collected continuously over a six-week period, for both horizontal and vertical polarisations at each of the hospitals.
An example of the average impulse occurrence is plotted in Figure 2; this shows that interference

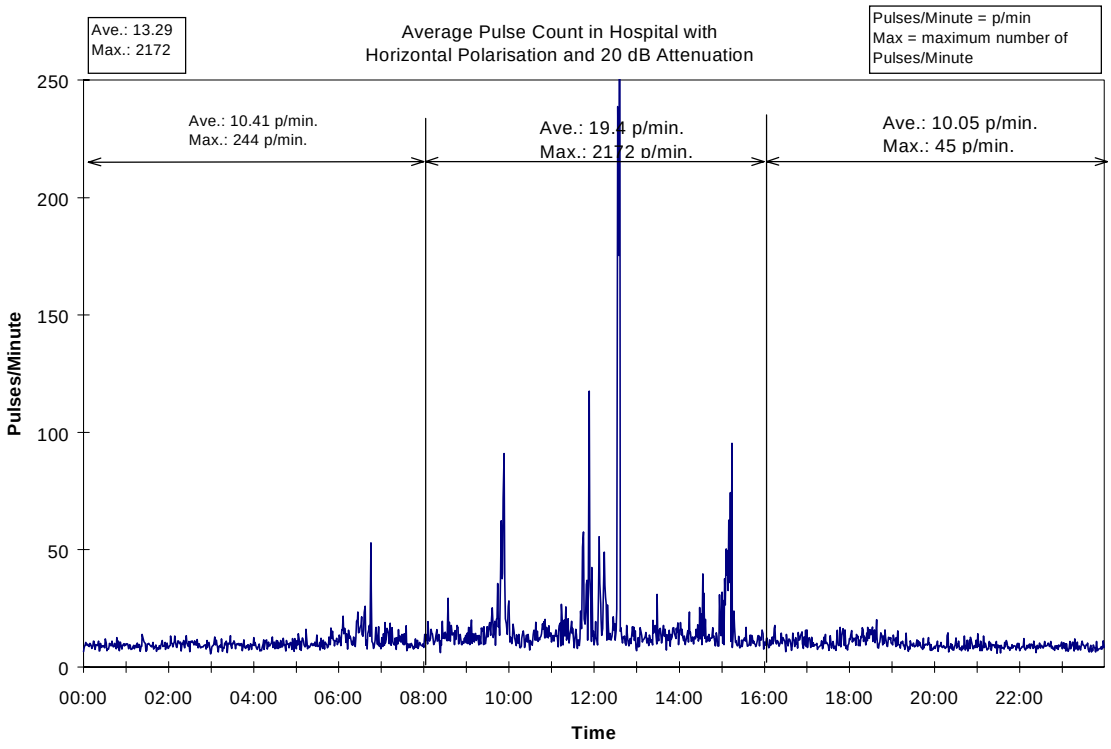

Figure 2: average impulse occurrence as noted over a 7-day period, for horizontal polarisation, in Berlin.

generation follows the working shift pattern, a feature noted at both measurement locations. Seven-day impulse counts were recorded at each location, for separate RF input thresholds of -100, -110 and -120 dBm and a common trigger window of 10 µs - 10 ms. Histograms depicting the average pulse count per minute are presented; values range from a maximum of 55 x 10^3 / min. for –120 dBm sensitivity in Berlin, to a minimum of 1.2 / min. for –100 dBm sensitivity in Belfast, both with vertical polarisation. In general, maximum pulse counts were recorded during noontime, when pulse amplitudes above –80 dBm were noted.
Noise impulses were recorded at levels sufficient to interfere with current, low power (<10 mW) radio telemetry links dedicated to the acquisition of human physiological data.

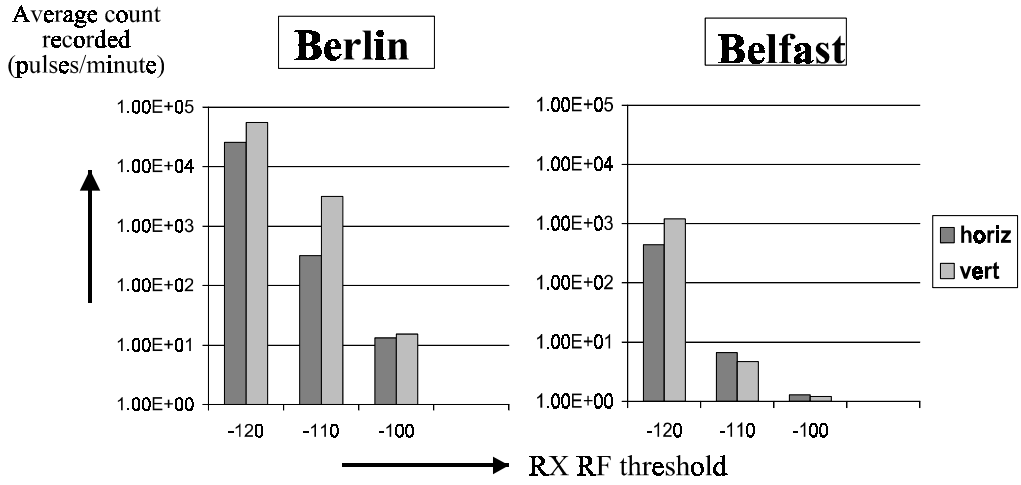

Figure 3: Histogram of pulse count for Berlin and Belfast

Extended Measurement Procedure

To produce detailed characteristics of the impulsive noise present at each hospital a specialist recording device was devised, using an IF-pulse-amplifier and logarithmic demodulator built around an Analog Devices AD 606: see Figure 2. The IF-signal extracted from the receiver's front end mixer was passed through Gaussian filters before being amplitude demodulated. The bandwidth of the filter network was set to 120 kHz to match the CISPR recommendations [3]; the design employed restricted ringing to below 1 dB for an 8μs-wide input RF test pulse. This system produced a receiver-independent impulsive noise signal that was fed into a high-speed A/D conversion data acquisition card (750k samples/s @ 12 bit).

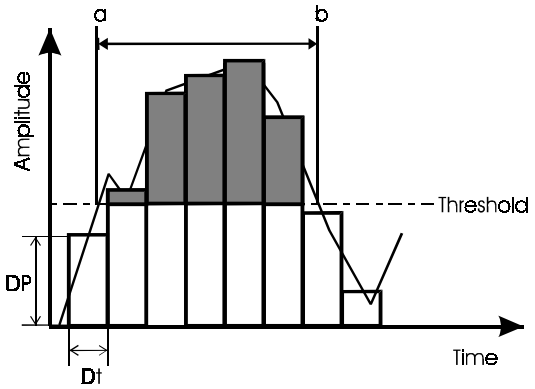

$$W = \int_a^b P \cdot t \, dt$$

Figure 4: method of obtaining Pulse Energy Distribution, using recordings of the complete noise envelope

Measurements were again effected in the hospitals i) and ii) previously monitored, at times established as returning high and low pulse counts. The λ/2 dipole was again mounted in both horizontal and vertical planes and six spot measurements were carried out for a series of twelve minute experimental sessions. Recorded data from each site were stored on CD-ROM. From

these data various cumulative distributions were extracted, notably the amplitude probability (APD), pulse width (PWD), pulse interarrival (PID) and noise amplitude distributions (NAD). A new parameter was also derived for study, namely the pulse energy distribution (PED): see Figure 3.

Results

Figure 5 presents the APD recorded at the sites during active and quiet periods, and also the overall minimum and maximum values noted for horizontal polarisation. The plot suggests that the impulsive noise present has little variation between locations. This trend was also observed for measurements carried out with vertical polarisation. On the other hand, the PWD and PID plots confirmed the necessity to obtain more than one parameter to characterise impulsive noise, as these particular plots greatly varied between locations. In Belfast there was 1 % probability that the pulse interarrival time was >18.2 μs: the corresponding figure in Berlin was >221 μs. For the PWD the 1 % probabilities were 14 μs and 23 μs at the respective sites. Further study of the data also showed that it is inadequate to linearly correlate the PWD with the PID to obtain the PED. With the equipment used, it was for the first time possible to accurately measure the pulse energy of low-power UHF impulsive noise, independent of a specific receiver system. Figure 6 presents the PED plots extracted from the datasets as noted for horizontal polarisation.

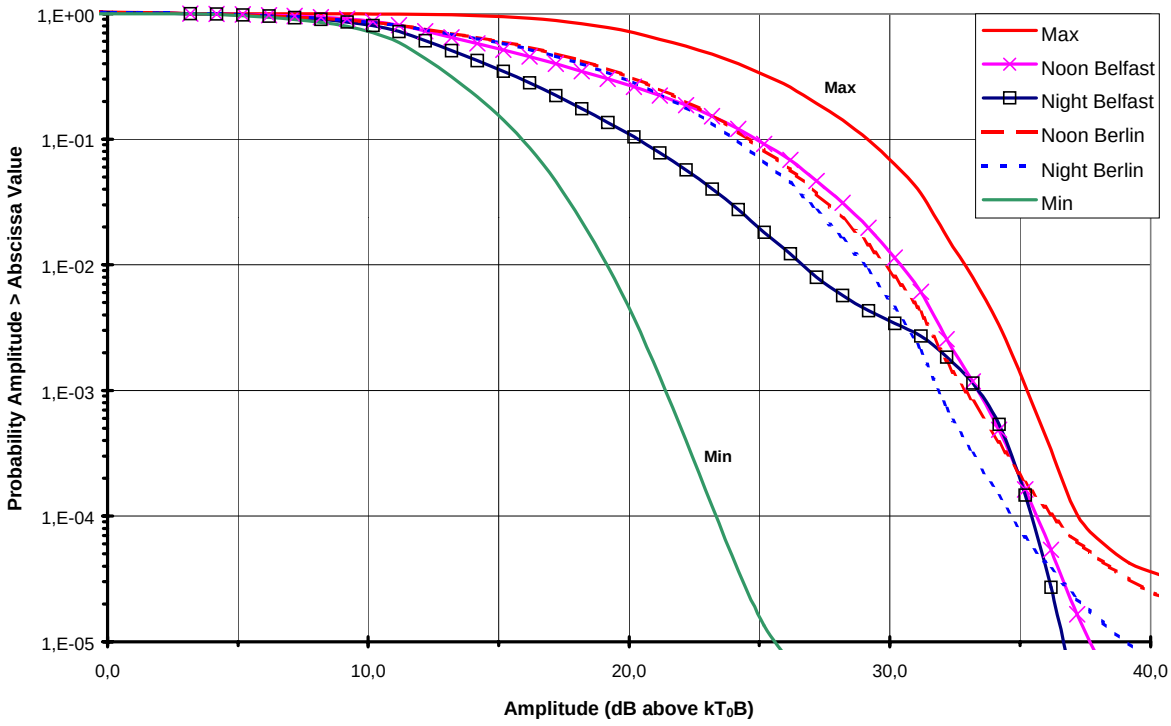

Figure 5: APD noted for horizontal polarisation

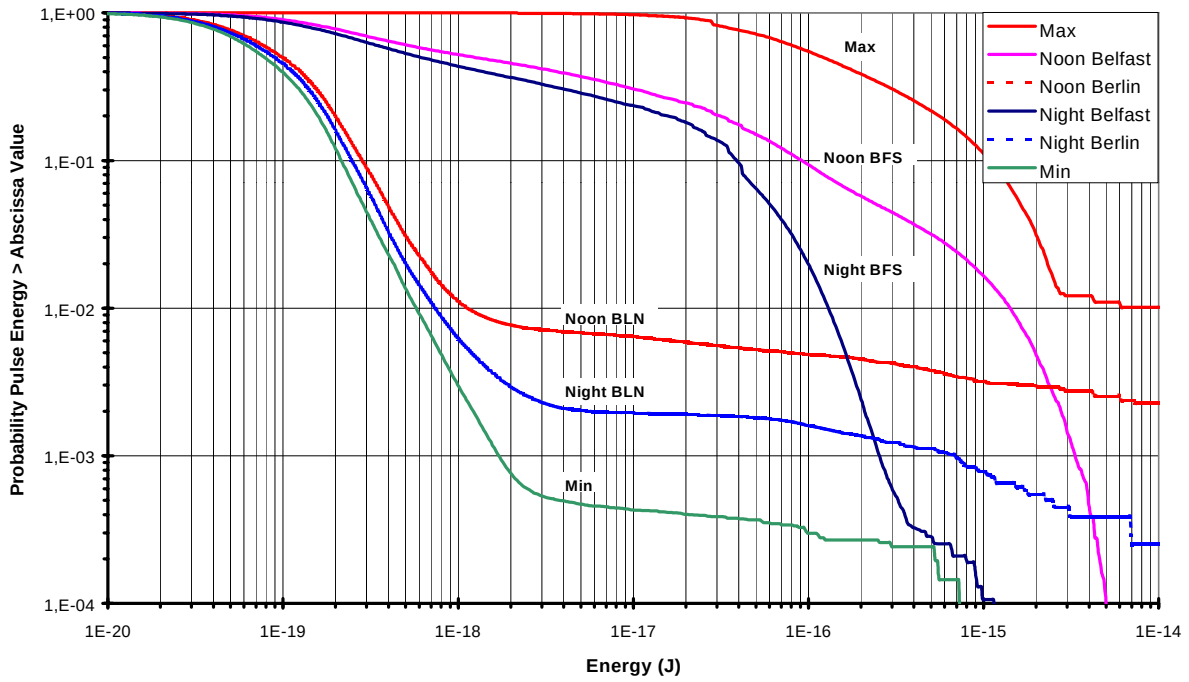

Figure 6: PED noted for horizontal polarisation

Conclusions

The data obtained and analysed to date prove that the defining characteristics of impulsive noise in hospital buildings are strongly dependent upon the measurement location selected, and no generalisation is possible. Further investigations are necessary in both hospital and domestic environments; a full characterisation of the latter locations is essential prior to the widespread use of portable VHF/UHF bio-telemeters built into telemedicine reporting systems.

References

[1] Riemann, A.I. and Evans, N.E. Man-made impulsive noise measured at 450 MHz in a hospital environment, *14th International Symposium on Biotelemetry*, Marburg, Germany, p. 77, 1997.

[2] Riemann, A.I. and Evans, N.E. Hospital-based recording and characterisation of impulsive RF noise, *Medical Engineering and Physics*, in press, 1999 I will try to find out page numbers before the abstracts go in.

[3] CISPR 16-1: Specification for Radio Disturbance and Immunity Measuring Apparatus and Methods, Part 1, First Edition, 1993.

An Improved Voltage-to-Frequency Converter Using a Switched Capacitor Topology Dedicated To Long Term Monitoring of Strain Gage

K. Salmi O.Chevalerias F. Rodes P.Marchegay
ENSERB – IXL
351 Cours de la Libération 33405 TALENCE – France
salmi@ixl.u-bordeaux.fr

Abstract

An improved switched capacitor V/F converter, made in 1.2µm BiCMOS technology, is described. It takes the output directly from a strain gage bridge and performs a signal-conditioning with high-resolution (9 bits). The converter is insensitive to the temperature and the offset drifts as the offset is automatically cancelled. Thus, the transfer function is ratiometric. Compared to our earlier three-phases switched capacitor converter, the power consumption is reduced by 30%. Furthermore, the new converter is an optimized version in terms of external components count and size minimization (the die occupies only $3mm^2$). A contactless inductive power supply has been used to power the intracorporal circuitry. The inductive link is achieved by means of weakly coupled resonant coils (k^2 <0.1) associated to a MOSFET low drop-out (LDO) regulator. This improved regulator respects temperature, size and powering limitations. Thus, this system is suitable for long term monitoring of stainless orthopedic implants.

I. Introduction

Nowadays, improving diagnostics and therapy in medicine calls for long term monitoring systems. The converter we describe in this paper is developed for a telemetric implant for mechanical strain monitoring in femoral nailplates. Thus, the main design constraints for such a system consist in minimizing size, components count, temperature drift and power dissipation. To deal with the very weak strain gage bridge signal, a V/F converter with integration is used. The PPM coding, double-phase switched-capacitor version chosen provides an automatic offset cancellation capability, a well drift characteristic, the best rejection of the input noise and a small consumption. In this new topology, the data conversion cycle takes only two clock periods instead of the three clock periods cycle needed by our earlier topology[1]. Hence, power consumption is reduced.

Inductive powering, we used in this system, is a widely accepted solution to replace implanted batteries. By means of weakly coupled inductive links, a good optimization of the power efficiency is achieved, a bi-directional information exchange is offered and last but not least, a locking loop is created to adjust frequency and power. So, the converter clock is directly provided by the inductive powering as described below.
This paper presents a strain gage bridge-to-pulse position modulation (PPM) converter, using an improved two-phases switched capacitor topology. It is realized in a 1.2µm BiCMOS technology. The switched-capacitor V/F converter theory is developed in section II. The section III is dedicated to the inductive powering description. The circuit design and the results are given in section IV.

II. The V/F Converter

The telemetry system combines the typical instrumentation amplifier function required to condition the strain-gage bridge with a PPM generator [2]. Stretching the strain-gage causes a Δl deformation which in turn, produces differential output voltages.

A. Principle of switched-capacitor integrator

The switched-capacitor structure (Fig.1) uses a capacitor C_1 associated with some switches driven at a frequency f_H to realize the classical integrator resistance R. With such an arrangement, the resistor R is given by $R=1/(C_1 f_H)$ [3], hence the time constant expression : $C_2/(C_1 f_H)$ (C_2/C_1value is more accurate than RC_2 due to the one-chip realization).

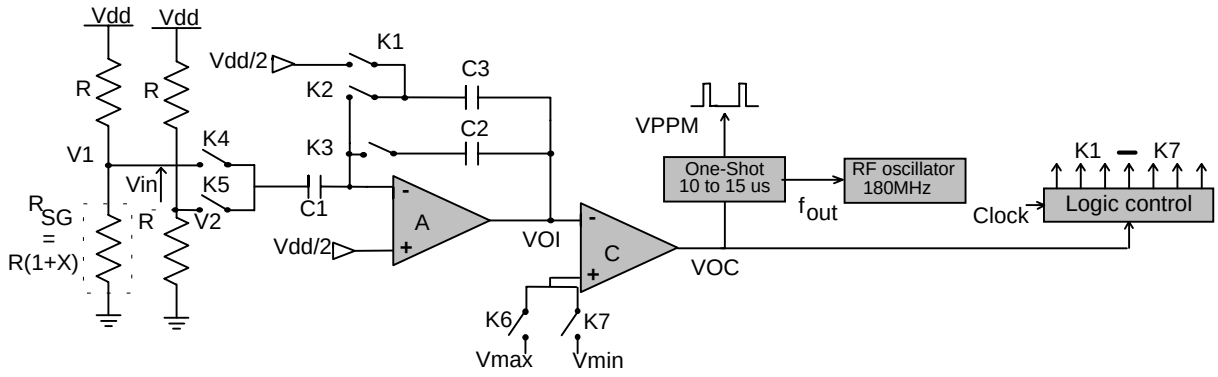

Fig. 1.Schematic of the switched-capacitor voltage-to-frequency converter

The SC integrator made with A, C_1-C_3, K_1- K_5 has been associated in such a way that the input voltage V_{in} is converted to an output PPM frequency f_{out}. So, the transfer function of the V/F converter is:

$$f_{out} = \frac{V_{in} \cdot f_H}{V_{max} - V_{min}} \cdot \frac{C_1}{C_2} \text{ where : } V_{in} = \frac{R_{SG}}{R + R_{SG}} \cdot V_{dd} - \frac{V_{dd}}{2} \cong \frac{X}{4} \cdot V_{dd} \qquad (1)$$

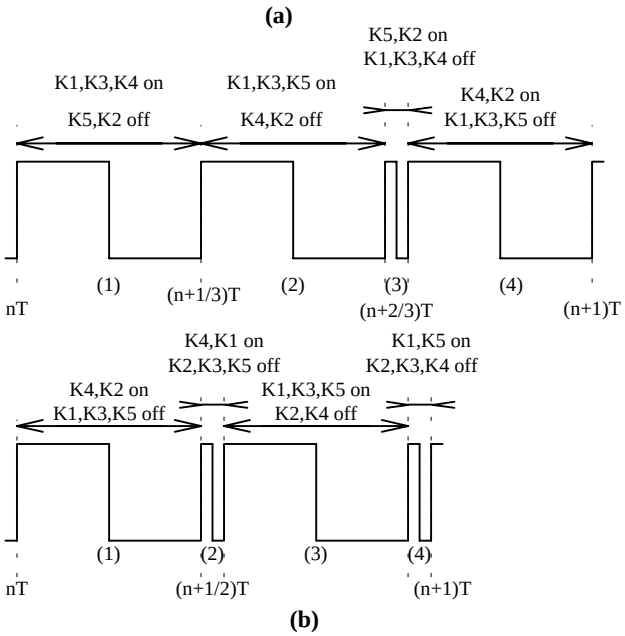

Fig.2. Nonoverlapping clock :
(a) for the 3 phases-cycle
(b) for the 2 phases-cycle

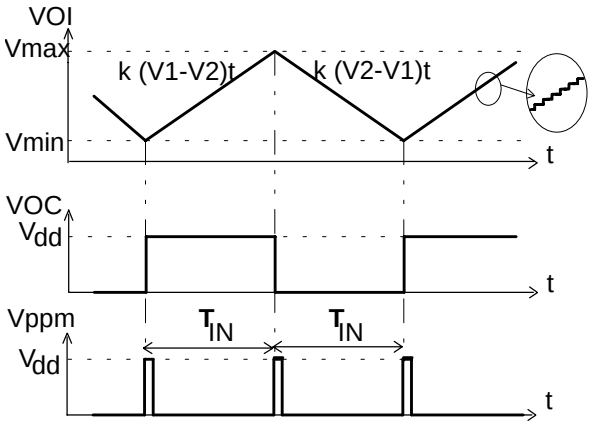

Fig.3. Waveforms of the voltage-to-frequency output signals

In our former three-phases topology [1], the switches are driven by a non-overlapping four-phases clock presented in Fig.2-a. The charge transfer was done during phase1 and 3 when the remaining phases (2 and 4) were required to cancel the integrator offset voltage and to respect the driving chronology. The new SC converter uses a four-phases-clock cycle too. However, the second phase is reduced to permit a lower power consumption (Fig.2-b). Consequently, the output voltage is given by:

$$V_{OI}((n+\frac{1}{2})T) = V_{OI}((n-\frac{1}{2})T) + \frac{C_1}{C_2}\left[V_1(nT) - V_2((n+\frac{1}{2})T)\right] \qquad (2)$$

V_1 is the strain-gage divider voltage and V_2 equals $V_{dd}/2$. The capacitor C_3, required to perform cancellation of both the offset and the charge injection, equals C_1.

B. Qualitative Analysis

The whole cycle of the double-slope converter is divided into two identical periods T_{IN}. The first slope is generated with the integration of the positive input voltage V_{in} and the second slope with $-V_{in}$. Let assume that V_{in} is constant, which is true over a converting cycle, and that the input voltage V_{in} is integrated. The comparator reference voltage is connected to V_{max} by means of K_6 (K_7 open). The other switches (K_1-K_5), driven by the clock shown in Fig.2-b, perform the integration cycle, in accordance with the principle of [3]. Thus, the integrator output V_{OI} ramps up towards the comparator threshold V_{max}, according to the following expression :

$$V_{OI}(t) = \frac{C_1}{C_2}.f_H.V_{in} \cdot t + V_{min} \qquad \textbf{(3)}$$

When the ramp reaches V_{max} , the comparator output goes low, and triggers a one-shot which turns on the 180MHz RF transmitter during 10 to 15µs. K_4 and K_5 switches force the polarity of the input to $-V_{in}$. That is, the comparator output V_{OC} settles to its

low value while the integrator's output V_{OI} ramps down towards the comparator low-level threshold Vmin (Fig.3).

Then, the total duration T_{IN} of this slope is :

$$T_{IN} = \frac{V_{max} - V_{min}}{\frac{C_1}{C_2} \cdot f_H \cdot V_{in}} \qquad (4)$$

According to expression (4), the PPM signal frequency f_{out} ($f_{out} = 1/T_{IN}$) is a ratiometric function of the output voltage of the bridge and is independent of the time of either ramp.

III. Inductive powering

As shown on Fig.4, the implantable telemetry, including the V/F converter, is hermetically sealed inside a 5mm diameter and 14mm length cavity done in the prosthesis. Unfortunately, neither batteries nor wire feedthrough can be used, due to the infection risks and to power supply limitations. Consequently, a contactless inductive power supply has been used to power the intracorporal circuitry. The inductive powering is achieved by means of weakly coupled resonant coils. The cavity dimensions drive us to fix the internal coil diameter to 9.2mm. The theory to maximize the coupling factor, developed in appendix1, makes possible the design of transcutaneous links of simultaneously high overall efficiency and good displacement tolerance while keeping the implanted receiver simple.

A Principle of the inductive powering

Inductive powering is based on the magnetic coupling between an external coil driven by an alternating current I_p and an internal coil [4]-[6] (Fig.4).
Both coils form a closely coupled coreless transformer. Inside the implant, power receiving circuit consists of a small coil (L_s) with a parallel resonant capacity(C_s), a bridge rectifier and a low drop-out regulator (Fig.5). This series-pass regulator, based on a new topology [7] provides a constant 4V output voltage with regard to the coil movements and to the load variations.

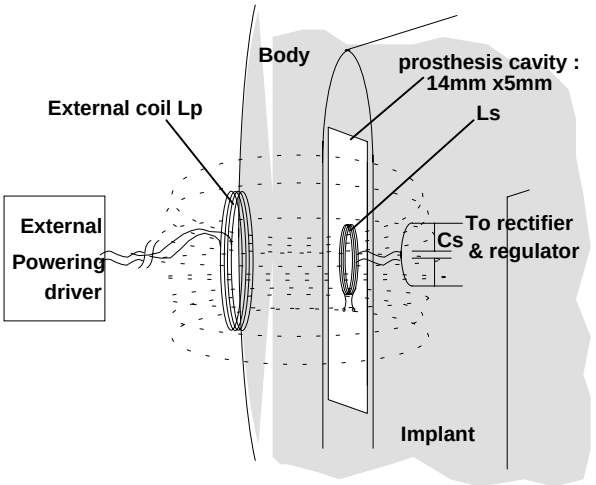

Fig.4. The principle of inductive powering

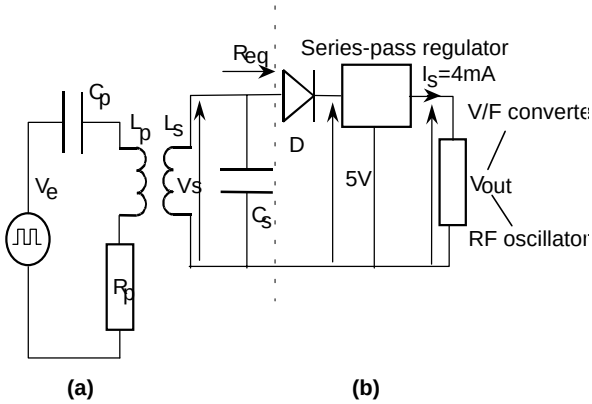

Fig.5. Series-tuned transmitter coil (a) magnetically coupled to the shunt-tuned receiver coil with load (b)

Both medical safety considerations and distance between the transformer coils limit the coupling coefficient k. Thus, the external driver must be exactly tuned to the implanted circuit to obtain a precise optimization of the power efficiency. To achieve this, an automatic search for the resonance frequency is systematically performed. Using a micro controller, the power link optimization is obtained in two steps. **During the first step**, the principal loop adjusts the level of the boost switching supply and the frequency of excitation in the [100KHz, 150KHz] range.
The driver frequency is swept until a maximal value is reached for the internal voltage V_{out} (Fig.6). During this step, the *"fine-and-find"* auto-tuning is performed by a feedback loop including a pulse position modulator which converts the DC-output V_{out} of an internal regulator into a low duty cycle pulse. At each pulse, a switch S short-circuits the coil L_s.
In the second step, the V_{out} information controls the driver power to maintain a 4V value at the regulator output. To do this, a variable inductance is added to the transmitter coil to keep the resonance conditions, even if the frequency varies between 100KHz and 150KHz.

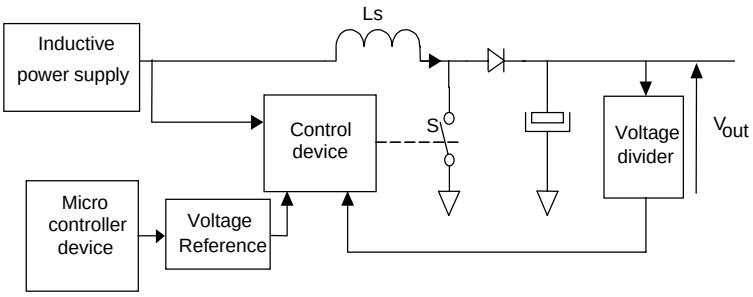

Fig.6. Auto-tuning inductive powering system design

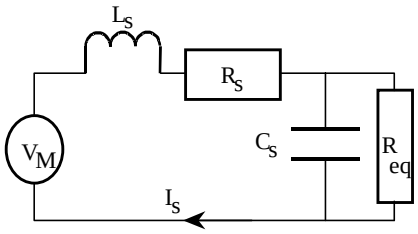

Fig.7. The internal coil losses and the steady-state AC equivalent of the actual load

B. Detailed Analysis

The induced voltage V_M expressed in (5), depends mainly on the primary coil spire number N_p, the coupling coefficient k and the mutual inductance M :

$$\left|V_M\right| = M_0 \times N_P \times N_S \times \omega \times \left|I_P\right| \qquad (5)$$

Power efficiency relies on high Q resonant tank circuits. However, a compromise must be found, because high-Q devices cause low bandwidth capabilities. Temic engineers researches showed that the resonant factor Q must be about 12. Thus, the Q factor of both primary and secondary coils is given by expression $Q/\sqrt{2}$. The corresponding bandwidth, given by (6), equals 9.5KHz (see appendix2).

$$Bp = \frac{f0\sqrt{\sqrt{2}-1}}{Q} \approx 0.64 \cdot \frac{f0}{Q} \qquad (6)$$

The waveform appearing across the internal tuned circuit is rectified by the diode D which is connected to the load resistor R_L, as shown in fig.5. To analyze the coupled circuit, a linear equivalent to D and R_L is needed. KO and al. (1977) demonstrated

that these components act as a perfect peak rectifier so that the peak value of voltage across C_s appears as a direct voltage across R_L (Fig.7). The resulting equivalent resistor is then:

$$R_{eq} = \frac{R_L}{2 \cdot \left(1 - \alpha \cdot \frac{V_D}{V_{Mpk}}\right)2} \approx \frac{R_L}{2} \qquad (7)$$

The secondary coil diameter is fixed by the cavity dimensions. The Q factor depends of both the secondary inductance and capacitor values and is given by expression (8).

$$Q_S = \frac{\sqrt{L_S C_S}}{r_S C_S + \frac{L_S}{R_{eq}}} \qquad (8)$$

With regard to the desired value of Q, performed iterations to find the optimal value of C_s give 33nF for C_s and 49.1µH for L_s. The resulting Q_s value is 8.24. Furthermore, the primary inductance value is given by the Wheeler formula (9) and equals 27.1µH.

$$L = \frac{0{,}0788 d^2 n^2}{3d + 9l + 10r} \qquad (9)$$

The corresponding capacitor value (60nF) is deduced from the resonance expression.

C. The NMOS series-pass regulator

For the classical NPN or MOSFET series-pass regulator, the input to output drop-out voltage can not be lower than V_{BE} or V_{TH}. Consequently, practical series-pass regulators exhibit minimum drop-out voltage in the range of 0.8V to 2V, which yields a poor efficiency for low output voltage. The drop-out voltage of a FET-based regulator is very low since FETs act like variable resistors. The minimum drop-out is simply the product of load current and FET's on-resistance (10).

$$V_{out} = V_{in} - R_{on} \cdot I_{Load} \qquad \text{where :} \qquad V_{out} = V_{bg} \cdot \frac{R_1 + R_2}{R_2} \qquad (10)$$

The contactless inductive supply provides less than a 6V voltage in the intracorporal circuit. The MOSFET-based LDO needs to drive the gate of the n-channel MOSFET to reach 10V to achieve minimum on-resistance. This higher drive voltage requires additional circuitry in the form of a "voltage doubler", as shown in Fig.8. This structure provides a 10V voltage necessary to run the error amplifier and a 5V voltage to drive other devices.

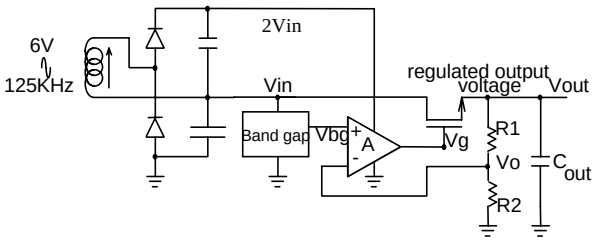

Fig.8. MOSFET-based voltage regulator

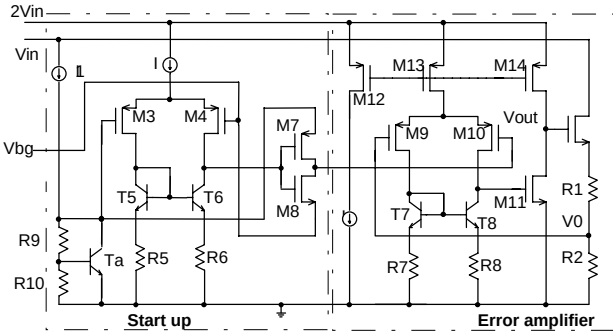

Fig.9. Error amplifier associated to start up circuit

The threshold voltage of n-channel pass device is roughly 1.5V. The error amplifier output voltage must extend from the lowest possible value to the point where the pass device is shut off ($Vg \leq Vout + V_{TH}$). The upper limit must provide maximum gate drive for the pass device. Thus, the amplifier topology consists of a two-stage buffer which second stage is an emitter follower (see Fig.9). The reference is a 1.22V Brokaw bandgap [8].
The load regulation (11) can be kept small by lowering the output resistance, which value, expressed in (11), depends on the invert of the amplifier gain.

$$\frac{\Delta V_{out}}{V_{out}} = \frac{\Delta I_{Load} \cdot R_{out}}{V_{out}} \approx \frac{\Delta I_{Load} \cdot R_{out}}{A \cdot V_{bg}} \qquad \text{where : } R_{out} \approx \frac{R_{on}}{A} \cdot (1 + \frac{R_1}{R_2}) \qquad (11)$$

If A and $(1+R_1/R_2)^{-1}$ are fixed to respectively 10000 (80 dB) and 0.33, the output resistance would not exceed a few milliOhms.

IV, Circuit design

The clock frequency f_H directly extracted from the inductive powering by means of a clock regenerator [9] is set to 125KHz. Measurements performed on the strain gage bridge showed that the output period T_{IN} varied between 2.5ms and 6.66ms. So, to keep the output frequency value within the range 150Hz-400Hz, we set C_1/C_2=0.56.
Both integrator and comparator, used for the V/F converter, are represented in Fig.10. The opamp integrator uses large PMOS front-end transistors to minimize the input noise. To reduce the error induced by the power supply ripple, a cascoded topology is used [10]. Moreover, the associated current source is independent from the power supply voltage.

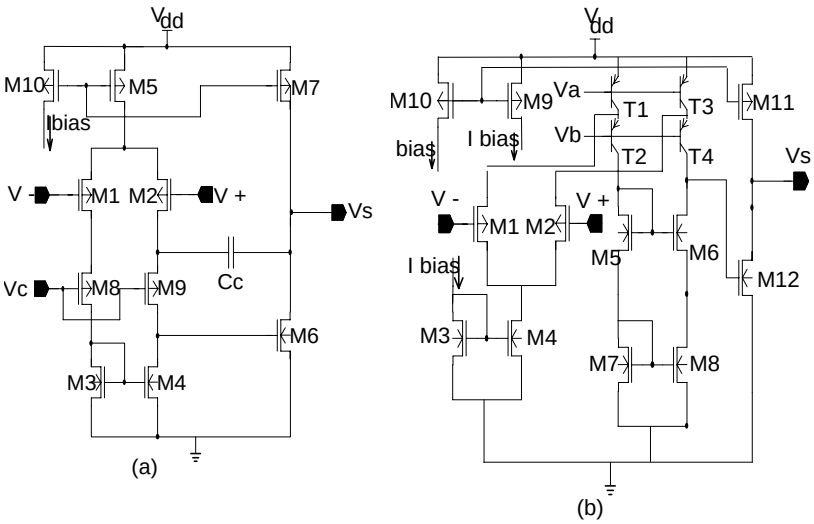

Fig.10. Schematic of the integrator (a) and the comparator(b)

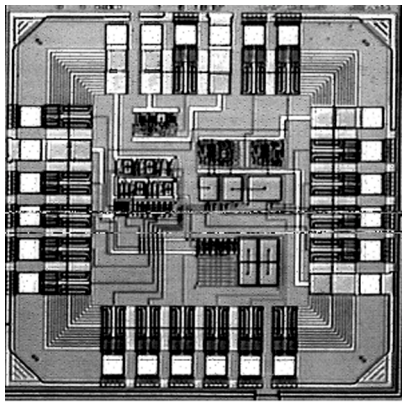

Fig.11. Microphotography of the V/F converter

The main characteristics of these two devices are given in Table 1.

Table 1: Integrator and Comparator characteristics

Parameter	Integrator	Comparator
DC Gain	79.5 dB	80 dB
GBW	7.2MHz	7MHz
Power Consumption	106µW	240µW
Output Swing	152mV to 3V	
PSRR	87 dB	90 dB
CMRR	91 dB	70 dB
Phase Margin	43.2°	23°

A. Experimental results of the V/F converter

The entire converter has been designed in a 1.2µm BiCMOS technology (Fig.11). The die surface does not exceed 3mm^2. Both the input stage transistors and the integrator capacitor are formed from cross-connected segments of an elements quad. This topology, called "common centroid geometry"[11,12], is very useful to achieve a low offset voltage and a low integration dispersion.

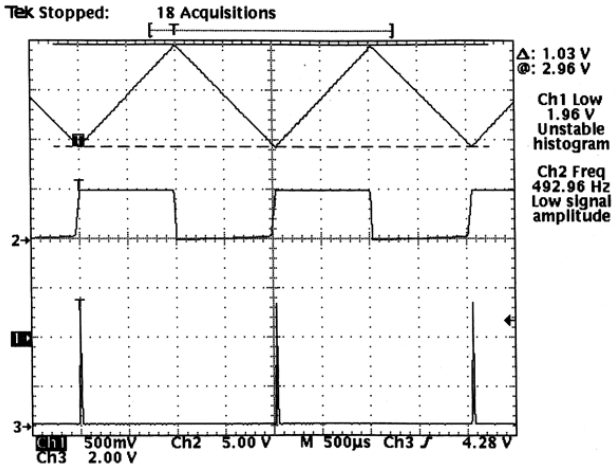

Fig.12. Experimental measurements of the switched-capacitor converter

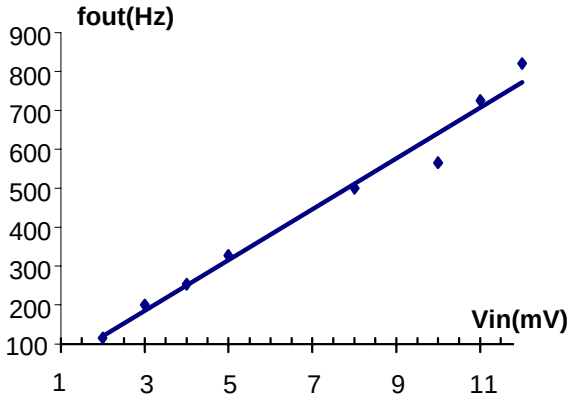

Fig.13. Transfer function of the SC V/F converter

The converter current consumption is only about 2mA. Fig.12 depicts the experimental result of this converter. It is an oscilloscope screen plot of respectively V_{OI} (chart1), V_{OC} (chart2) and the PPM output signal (chart3). We can see that these waveforms are very close to the theoretical ones represented in Fig.3.

By applying an input voltage V_{in} of 20mV under 37°C, we observed a PPM signal period T_0 of 1490µs. So, T_{IN} equals 745µs. Thus, the corresponding accuracy was roughly 3%. Even though the die temperature varied from 37°C to 40°C, the inherent accuracy remained at 4%. Fig.13 plots the transfer function of the V/F converter.

Over the whole operational zone ($1.9mV<V_{in}<5.9mV$) corresponding to ($4980\Omega<R_{SG}<5020\Omega$), f_{out} was linearly proportional to the input signal V_{in}. As expected, this frequency remained between 150Hz and 400Hz while the error was less than 3%.

B. Experimental results of the low-drop-out regulator

All the LDO characteristics are summarized in Table 2. Compared to classical regulators, ours responds fully to intracorporal constraints as the output temperature variation is only around 90ppm/°C, which corresponds to a 170% improvement over the classical regulator.

Table 2: Regulators performance summary

	LDO	Classical regulator
Vs	4V	4V
Line Regulation	49mV/1V	60mV/ 4V
Load Regulation	22mV/7mA	100mV/1A
$\Delta V_{out}/\Delta T$	90ppm/°C	250ppm/°C
V_{in}-V_{out} @ I_{load}=5mA	245mV	2V
I_{cond}	240µA	1mA
Ripple Rejection	56dB	65dB
ΔV_{out} for I_{load}=pulse(0 to 12mA)	140mV	200mV

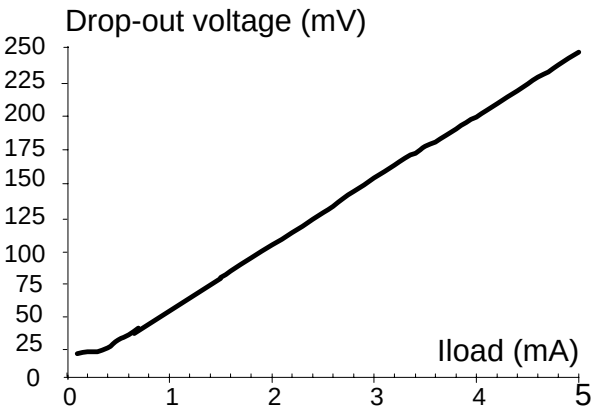

Fig.14. Drop-out versus load current

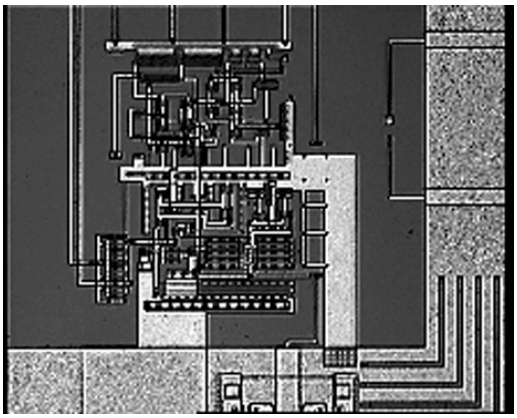

Fig.15. Microphotography of the low-drop-out regulator

IV. Conclusion:

We have designed and tested a new switched capacitor V/F converter. This converter, powered by an inductive system, uses only two clock periods converting cycle. It is more performant than the three-phases we had designed earlier. As a result, The power consumption is reduced by 30% while the noise rejection capability is maintained. The number of external components is also reduced as no voltage reference V_{ref} is used in this new topology. Finally, the relative error is kept under 3% over the input operational zone when the temperature varies within the [27°C,47°C] range. Consequently, the converter proposed is particularly appropriate for data conversion applications requiring extreme level of miniaturization like in intracorporal biotelemetry.

References

[1] J.B. Begueret, M.R. Benbrahim, Z. Li, F. Rodes, and J.P. Dom, “Converters Dedicated to Long-Term Monitoring of Strain Gage Transducers”, IEEE J. Solid-State Circuits, vol. 32, no 3, March 1997, pp.349-356.

[2] F. Goodenough, “Mixed-Signal IC Developments Highlighted at the CICC”, Electronic Design, May 1996, pp.102-108.

[3] F. Baillieu, Y. Blanchard, “Signal Analogique- Capacités commutées”, dunod Paris, 1994, pp.149-152.

[4] N. de N. Donaldson and T.A.Perkins :"Analysis of resonant coupled coils in the design of radio frequency transcutaneous link", Medical & Biologica Engineering & Computing, September1983, pp.612-627.

[5] P. Benedetti and al. :"Overview of telemetry systems with inductive links and variable coupling distances", Biotelemetry XIII, March26-31,1995, Williamsburg, Virginia, pp.57-62.

[6] K. Van Schuylenbergh, R. Puers : "A computer assisted methodology for inductive link design for implant applications", Biotelemetry XII, August 31-September 5,1992, Ancona, Italy, pp.392-400.

[7] K. Salmi and al. :“A 4V-5mA low drop-out regulator using a series-pass n-

channel MOSFET", Electronic Letters, vol. 35, no 15, July 1999, pp.1274-1275.

[8] A.P. Brokaw: " A simple three-terminal bandgap reference", IEEE J. Solid-State Circuits, vol. 9, no 6, December 1974, pp.388-393.

[9]U. Kaiser, W. Steinhagen: "A low-power transponder IC for high-performance identification systems", IEEE J. Solid-State Circuits, vol. 30, no 3, March 1995, pp.306-310.

[10] A.B.Grebene, "Bipolar and MOS analog integrated circuit design", Wiley&Sons, New York, pp.348.

[11] P.R. Gray, R.G. Meyer, "Analysis and Design of analog Integrated circuits", 3rd Ed., Wiley&Sons, New York, 1993, pp.451-465.

[12] P.M. BROWN: " A guide to analog ASICs", Academic press, 1992, pp.161-163.

Appendix 1

Mutual inductance optimization in the case of a weakly coupled resonant coils

REFERENCE

F.W. GROVER: "Inductance calculations", chapter11, pp77.

Both primary coil and secondary coil of the transformer are circulars. We suppose that the diameter 2*r* of the secondary coil and the distance *d* between the two coils are fixed to9.2mm and 6cm respectively (Fig.1).

For weakly coupled resonant coils ($k^2 \leq 0{,}1$), the mutual inductance is expressed as:

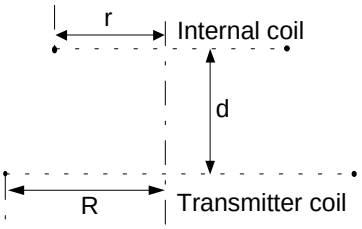

Fig.1.Simplified schematic of the coupled coreless transformer

$$M_0 = f\sqrt{rR} \qquad (1) \qquad \text{where :} \qquad \log f = -2{,}60776 + \frac{3}{2}\log {k_1}^2 \qquad (2)$$

Noting that : $${k_1}^2 = \frac{4Rr}{(R+r)^2 + d^2} \qquad (3)$$

So, developing expression (2) and substituting (3) into (2) gives :

$$f = 0{,}0024674 \cdot \left[\frac{4Rr}{(R+r)^2 + d^2}\right]^{\frac{3}{2}} \qquad (4)$$

Substituting (4) into (1) leads to:

$$M = 0{,}0024674 \cdot \left[\frac{4Rr}{(R+r)^2 + d^2}\right]^{\frac{3}{2}} \cdot \sqrt{Rr} \qquad (5)$$

Then:

$$\frac{dM}{dR} = 0{,}0024674 \cdot \left\{12 \times (r\left[(R+r)^2 + d^2\right] - 2rR(R+r)) + 4a \cdot \left[(R+r)^2 + d^2\right]\right\} \cdot \frac{Rr}{\left[(R+r)^2 + d^2\right]^{\frac{5}{2}}}$$

So : $$\boxed{\frac{dM}{dR} = 0{,}0024674 \cdot \left\{-8r \cdot \left[r^2 - Rr - 2d^2 - 2r^2\right]\right\} \cdot \frac{Rr}{\left[(R+r)^2 + d^2\right]^{\frac{5}{2}}}}$$

The optimum value of M is set by the resolution of $\frac{dM}{dR} = 0$.

This second order equation has for solution :

$$\boxed{R = \frac{r + \sqrt{9r^2 + 8d^2}}{2}}$$

From the foregoing analysis, it is seen that if d =6cm and r =4.6mm, the ideal value of R is 7.34cm which allows an optimal M_0 value of **262pH**.

Appendix 2

The LC bandwidth expression

LC circuits gain is often expressed as: :

$$A = \frac{n \cdot Q}{1 + n^2 - X^2 + 2jX} \quad (1) \quad \text{with} : X = 2 \cdot Q \cdot \frac{f_c - f_0}{f_0}, n = k \cdot Q, k = \frac{M}{\sqrt{L_p \cdot L_s}} << 1$$

From the foregoing results, we can deduce k value:

$$k = \frac{M}{\sqrt{L_P \times L_S}} = \frac{262 \times 10^{-12}}{\sqrt{28 \times 10^{-6} \times 49 \times 10^{-6}}} = 7{,}07 \times 10^{-6}$$

and: $n = k \cdot Q = 7{,}07 \times 10^{-6} \times 12 \approx 8{,}5 \times 10^{-5}$

So : $A = \frac{A_{max}}{1 - X^2 + 2jX}$ with : $A_{max} = n \cdot Q$ (2)

At f_c, the gain value is expressed as : $$|A| = \frac{A_{max}}{\sqrt{2}} = \frac{A_{max}}{\sqrt{\left(1 - X^2\right)^2 + 4 \cdot X^2}}$$

which leads to: $\left(1 - X^2\right)^2 + 4 \cdot X^2 = 2 \Leftrightarrow X^4 + 2X^2 - 1 = 0$

Using $Y = X^2$ gives the second order equation: $Y^2 + 2Y - 1 = 0$

Only $Y_1 = -1 + \sqrt{2} > 0$ is a suitable solution. So:

$$X = \pm\sqrt{Y_1} \Rightarrow \begin{cases} X_1 = \sqrt{\sqrt{2} - 1} \approx 0{,}64 \\ X_2 = -\sqrt{\sqrt{2} - 1} \end{cases}$$

Applying the bandwidth definition gives:

$B_P = 2 \cdot \left(f_c - f_0\right) = X_1 \cdot \frac{f_0}{Q}$ (3) according to expression (1).

Substituting the X1 value into (3) gives:

$$\boxed{B_P = \frac{f_0 \cdot \sqrt{\sqrt{2} - 1}}{Q} \approx 0{,}64 \cdot \frac{f_0}{Q}}$$

Biotelemetry on Birds: New Technics for New Ethological as well as Ecological Results

Hans-Wolfgang Helb
University of Kaiserslautern,
Dept. of Biology, Div. of Ecology
Kaiserslautern, Germany

Abstract

This paper describes two examples of applied researches in ethological as well as ecological questions to birds as important bio-indicators using biotelemetry technics:

a) To get new insights into the behavior of the European blackbird we constructed two types of small radio transmitters to show and to analyse the heart rate in various natural as well as cultural situations. After earlier observations and experiments with the song and call behavior we tested now whether there is an influence of a 50 Hz alternative electromagnetic field to the heart rate of this bird species. First experiments showed no changes of this physiological parameter.
b) We studied the ecology and the behavior of carrion crows using commercial radio tracking telemetry and behavioral observation in order to determine wether they cause damage in agricultural systems and amongst the fauna. During the breeding season the flock is devided in two groups, paired crows and a flock of solitary non breeders. Outside the breeding season the paired couples join the flock. In neither group aggressive behavior against other animals, small birds or small game was observed.

Introduction

Birds are world-wide a favourite and interesting group of animals and there is often an emotional relationship between humans and birds. However, they may also function as important bio-indicators used to support nature conservation schemes.
One way to use them is in telemetric studies. With the help of this technique, in which birds are monitored using small radio transmitters or transponders, we can gain detailed insight in the physiology, behaviour and ecology of the birds in the laboratory, but also in the wild like in the vicinity of settlement as well as in remote areas such as forests, lakes, mountains and the sea.

1. Ethological studies on European blackbirds using heart rate

In the presence of a rapid increase of electromagnetic fields in the biosphere with the possibility of health risks it is necessary to investigate possible influences on animals. Particularly free living birds are confronted with that problem in the wired landscape. In continuation of our many experiences in research with songbirds [4-15, 18-20, 23-25, 27] we are interested in analysing whether electromagnetic fields influence the behavior of songbirds on the basis of the very sensitive physiological parameter of heart rate measured by means of radiotelemetry.

Methods

In addition to our earlier type of miniaturized radiotransmitter [14] we constructed a new transmitter using a miniaturized microphone to measure the heart rate of European blackbirds (*Turdus merula*) with and without an artificial electromagnetic field generated by an alternating current (50 Hz, induction B = 1,3 mT) [28, 37-39]. The observations and experiments were performed on birds in cages standing in a laboratory. The heartbeats were transmitted by radiotelemetry to a personal computer in the first part of the night while the birds were sleeping. The stored data were evaluated and compared by means of a specially developed body sound analytic program [39].

Results

The research didn't show any significant differences in the heart rate of European blackbirds when we compared the values in the absence and in the presence of an alternating electromagnetic field of 50 Hz (B = 1,3 mT).

Two examples show these results:
Figure 1 presents the "experiment 4" with a male (m) European blackbird, for individual identification tagged with a red ring on its one leg. During 12 measure sequences (1 to 12) with differential times between 4 and 56 minutes there were no differences between the heart rate during measure sequences without electromagnetic field (1-3, 8-11) and with electromagnetic field (4-7 and 12). In all test situations the individual specific heart rate was very slow and constant with a mean value of 5,15 beats per second.

Figure 2 presents the "experiment 6" with a female (f) European blackbird, for individual identification tagged with a green ring on its one leg. During 11 measure sequences (1 to 11) with differential times between 1 and 41 minutes there were no significant differences between the heart rate during measure sequences without electromagnetic field (1-3, 9-11) and with electromagnetic field (4-8). In all test situations the individual specific heart rate was very high and constant with a mean value of 7,85 beats per second.

2. Ecological studies on carrion crows using radio tracking

The carrion crow *(Corvus corone corone)* is a resident bird in Central Europe, present in a wide spectrum of habitats [1-3, 16-17, 30-31, 40] . In general this euryoecios species prefers open sites with individual or small groups of trees, shrubs and areas with low ground cover. They generally avoid dense forest but increasingly got adopted to settlements. Their preferred nest sites are in general at a height of approximately 5 m. The tree species underlies regional variations. Occasionally nest can bee found in rock formations if no suitable trees are available. Carrion crows are typical omnivorous birds as adults, but nestlings are mainly fed on food of animal origin. The female produces three to six eggs that are usually laid in April. The breeding duration ranges between 17-22 days, followed by a nestlings stage of 30-35 days. During breeding season it is possible to observe two different behavioral societies:

- Territorial pairs, that are involved in reproduction and
- Flocks of solitary individuals that do not breed.

measure sequence	1	2	3	4	5	6	7	8	9	10	11	12
time*	0	10	19	10	21	56	27	4	6	25	17	14
field	without	without	without	with	with	with	with	without	without	without	without	with
heart rate	4,3	5,0	4,9	4,9	5,2	5,5	5,4	5,3	5,2	5,3	5,4	5,4
standard deviation	0,1	0,30	0,30	0,05	0,15	0,36	0,30	0,23	0,00	0,26	0,25	-
standard deviation	-0,1	-0,3	-0,3	-0,05	-0,15	-0,36	-0,30	-0,23	0,00	-0,26	-0,25	-
relation	0	0	0	0	0	0	0	0	0	0	0	0

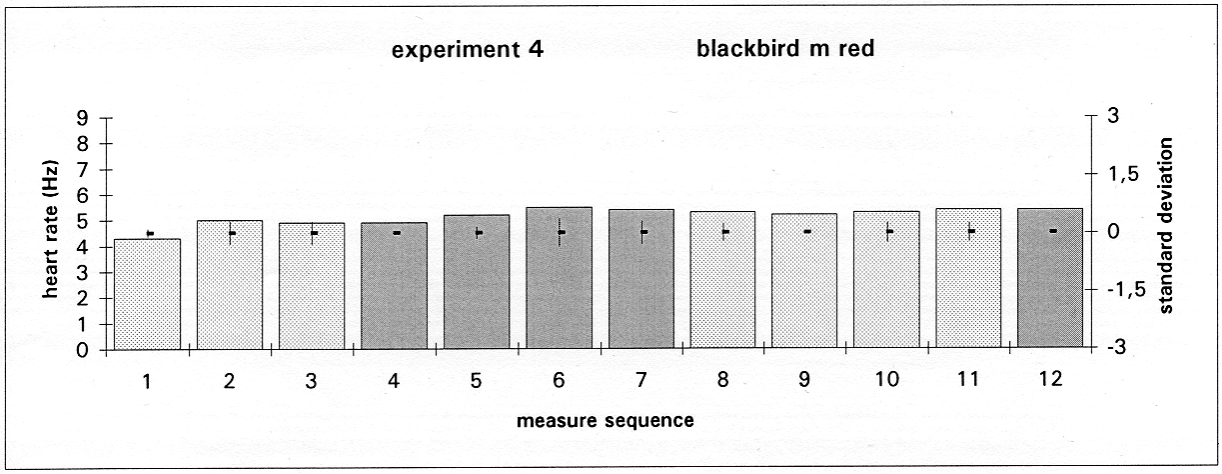

* differential minutes

Figure 1: Results of the "experiment 4" with male European blackbird (more see text).

measure sequence	1	2	3	4	5	6	7	8	9	10	11
time*	0	41	18	17	9	19	1	13	26	5	39
field	without	without	without	with	with	with	with	with	without	without	without
heart rate	7,3	7,5	7,6	7,8	7,7	8,2	7,8	8,0	7,9	8,1	8,4
standard deviation	0,32	0,62	1,35	0,24	0,52	0,15	0,15	0,25	0,31	0,27	0,37
standard deviation	-0,32	-0,62	-1,35	-0,24	-0,52	-0,15	-0,15	-0,25	-0,31	-0,27	-0,37
relation	0	0	0	0	0	0	0	0	0	0	0

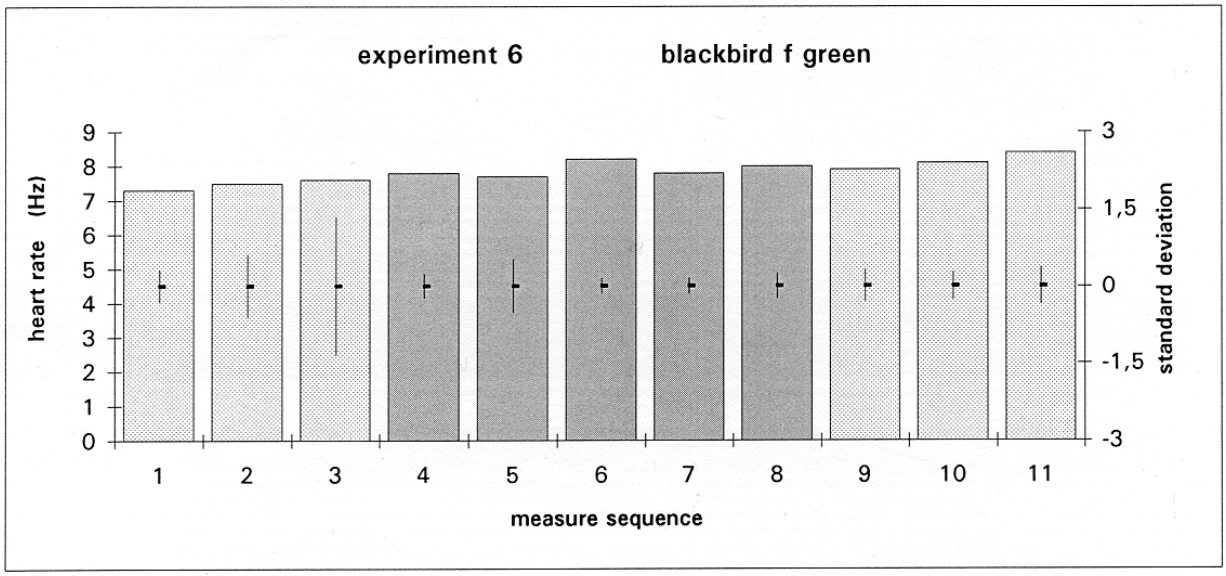

* differential minutes

Figure 2: Results of the "experiment 6" with female European blackbird (more see text).

Outside the breeding season the paired crows join the flocks.

The carrion crow has repetitively been made responsible for significant damage in agricultural systems and amongst the native fauna, especially small birds as well as small game. As the main areas of damage are known destruction of seeds and seedlings. This is especially the case when larger flocks invade agricultural systems. In addition carrion crows have been made responsible for puncture of the plastic foil used to cover silage systems, which may cause substantial damage due to the fermentation initiated by the exposure of the stored product to air. Predation of eggs and young birds or juvenile hares and rabbits have been listed as one of the problems caused by crows. For that reason the Ministry for Environment and Forestry initiated a study with the aim to determine the actual dimension of the damage caused by carrion crow. On the basis of these findings the decision was to be made whether regulatory mechanisms are required (e.g. hunting) to control/reduce the population density of the carrion crows in Rhineland Palatinate. For this purpose behavioral observation and radiotelemetric studies were carried in order get gain new insight into the ecology and behavior of the carrion crow [21-22, 26].

Methods

Observations took place from fall 1996 to spring 1998. The population of carrion crows were monitored on three sites near Kaiserslautern, Germany. The sites had an approximate size of 15 km².

Figure 3: The territory of a breeding pair of carrion crow near Kaiserslautern, Germany.

Radiotelemetry

The equipment for radiotelemetry was supplied by BIOTRACK Ltd. UK.
The model of transmitters used were 20 transmitters TW-3 emitting pulses of 20 ms duration at approximately 1 Hz. The frequency band ranges between 150,050 and 150,240 MHz. The frequencies of the 20 individual transmitters were separated by 12.5 kHz frequency band allowing individual identification of each transmitters. The radiation output of the transmitters was limited to 0,2 mW (ERP).
The weight of the transmitters was below 5 % of the body weight of the crows, which was shown to not alter/influence the behavior of the animals.
The receiver used of the type Mariner-57, which allowed acoustic as well as optical identification of the individual transmitters (respectively bird).
The birds were tracked using two antennae (YAGI-type with five elements, trimmed to the 150 MHz range)
The transmitters were attached to the back of the crows with the help of teflon ribbon harness (glue mounted backpack style attachment) [29].

Field observation

The paired crows are very stationary during the breeding season. Most of the observations in that stage did not require the application of radiotelemetric equipment. The parameters recorded here were: the development of the population densities (number of individuals) during the research period, flock typical behavior, mate finding, territorial behavior, choice of biotop/habitat, size of the home range, spatial and temporal distribution and their food spectrum.

In addition 19 carrion crows were observed individually during winter (i.e. outside the breeding season). They were equipped with radio transmitters (range ca. 40 km) and tagged with color rings for identification.

Behavioral observations (radiotelemetric and visual) of individuals were carried out on 240 days partly over entire days (during their entire activity). Their behavior was classified and recorded. Their behavior was monitored continuously and the behavior displayed recorded every minute.

Results

The distribution of different behavioral patterns displayed by paired crows during breeding season is presented in Table 1.

Behavior	**%**
Feeding and foraging	36
Resting outside the nest area	20
Near the nest area	9
Preening	5
Others	30

Table 1

The data derived from 4 different pairs, which were observed for 86 hrs on several days.

The behavior of the four individual pairs showed variations in absolute numbers. However there was similarity in the distribution of the behavior of those pairs. During

breeding season the carrion crows spend most of their time feeding, foraging and resting. This is also true when comparing different days.

The distribution of different biotop types used by paired crows during breeding season is presented in Table 2.

Biotop type	**%**
Freshly mowed greenlands	24
Shrubs and hedges	19
Pasture	16
seeded land	3
Others	38

Table 2

The observed crows spend 40 % of their time in areas with low groundcover (24% & 16%) were they were obviously feeding on ground arthropods. The mean time spend for foraging (collection of food) was approximately 20 minutes after which the adults returned to the nest (for approximately 4 minutes) to feed the nestlings.
Intake of vegetation (grass or grain) could not be observed. Other agricultural habitats such as seeded land, summer and winter grain field were hardly used.
The time spend in shrubs and hedges was mainly used for resting.

The distribution of different biotop structures used by paired crows during breeding season is presented in Table 3.

Biotop structure	**%**
Open land	61
Forest edge	15
Partly open land	14
settlements	1
Others	9

Table 3

61% of their entire activity took place on open sites, followed by activity in the edge of forests (15%) and in partially open land (14%).
Although carrion crows can be found in very different habitat types it is known that they prefer open landscape structures. Our results confirm those earlier findings.

Time of activity
Our observations showed that the daily activity of the carrion crows can start as early as 4:30 h CEST (= 3:30 h CET) often starting with calling behavior. At around 21:45 h the activity of the crows was starting to cease.

Home-Range
When breeding carrion crows are rather stationary. The mean home ranges of the paired crows during the breeding season ranged from 215.000 m² to 369.000 m². Outside the breeding season the home-ranges are significantly larger. It was impossible for us to determine the absolute extension due to the immense distances that the crows flew and the limited range of the transmitters in uneven habitats.

Conclusion

Radiotelemetric methods offer a very effective strategy to obtain biological data in animals without the usual disturbances due to the experimenter and to the experiment apparatus. Therefore, a large variety of systems has been developed, ranging from transmitters attached to the back like a rucksack to implantable systems measuring several physiological parameters sometimes at the same time, for example motion, activity, body-temperature, respiration, oxygen consumption, blood-flow, blood-pressure and at last heart rate.

Heart rate of birds is affected by quite a number of physiological influences. Yet an even more interesting aspect of this field are heart rate alterations due to „emotional“ effects, social relations and fear, mainly as experienced during the approach of a predator.

From this more basic level of stimulus processing we can get a lot of new informations on the birds spatial distribution and habitat, on their diurnal activity pattern (feeding, preening, singing, sleeping etc.) and also on their interaction with their pair partner and neighbours. Very important and up today not used enough are also new insights by telemetry for the wide field of nature conservation [21-22, 25-26, 32].

By measurement of heart rate alterations after playback experiments in songbirds it is possible to study reactions to single conspecific or heterospecific song strophes or calls not only in males, as with more traditional methods, but also in females and young birds, for example on European blackbirds and yellowhammers (*Emberiza citrinella*) [19, 27, 36]. In contrast to the absence of behavioural responses to playback of vocalizations often the heart rate shows a dramatic reaction of the bird tested and by it an important function never analysed and seen before.

Acknowledgments

I would like to thank the Ministry for Environment and Forestry of Rhineland-Palatinate for its financial support of the research project two. I am also grateful to my coworkers Dr. P. Diehl, H. Vogt, H.-M. Helb, M. Helb, J. Jeblick, K. Müller, K. Nagel, L.-G. Otto, M. Stremmel and T. Vicinus for their engaged support in the laboratory as well as field.

Literature

[1] Bezzel, E. (1993): Kompendium der Vögel Mitteleuropas. - Bd. 2: Passeres - Singvögel. Aula Wiesbaden.

[2] Bezzel, E. (1995): Anthropogene Einflüsse in der Vogelwelt Europas. Ein kritischer Überblick mit Schwerpunkt Mitteleuropa. - Natur und Landschaft 70/9: 391-411.

[3] Dick, H. (1995): Randeffekt - Problematik durch generalistische Beutegreifer am Beispiel von Rabenkrähe (*Corvus corone corone* LINNAEUS 1758) und Wurzacher Ried (Süddeutschland). - Ökologie der Vögel 17: 1-128.

[4] Diehl, P. (1984): Radiotelemetrische Herzfrequenzmessungen an Amseln (*Turdus merula*) - Reizexperimente mit Verhaltensstudien. - Diplomarbeit, Universität Kaiserslautern.

[5] Diehl, P. (1988): Die Herzfrequenz von Amseln (*Turdus merula*) beim Singen und nach Tonbandvorspiel von Rufen und Gesangsstrophen - eine radiotelemetrische Untersuchung. - Dissertation, Universität Kaiserslautern.

[6] Diehl, P. (1990): Herzfrequenzänderungen bei Amseln (*Turdus merula*) nach Vorspiel von Alarm- und Erregungsrufen - eine radiotelemetrische Untersuchung. - In: R. van den Elzen, K.-L. Schuchmann & K. Schmidt-Koenig (eds.), Proc. Int. 100. DO-G Meeting, Current Topics Avian Biol., Bonn 1988, 195-200.

[7] Diehl, P. (1992): Radiotelemetrische Untersuchungen der Herzfrequenz singender Amseln (*Turdus merula*). - J. Ornithol. 133: 181-195.

[8] Diehl, P. & H.-W. Helb (1985a): Vogelgesang und Herzfrequenz - radiotelemetrische Messungen zum Subsong bei der Amsel (*Turdus merula*). - J. Ornithol. 126: 281-286.

[9] Diehl, P. & H.-W. Helb (1985b): Radiotelemetrische Herzfrequenzmessung zur Verbesserung der Analyse von Reiz-Reaktions-Tests. - Verh. Dtsch. Zool. Ges. Wien 78: 178.

[10] Diehl, P. & H.-W. Helb (1986): Radiotelemetric monitoring of heart-rate responses to song playback in blackbirds *(Turdus merula)*. - Behavioural Ecology and Sociobiology 18: 213-219.

[11] Diehl, P. & H.-W. Helb (1987): Heart rate of songbirds: radiotelemetric measurement during playback experiments. - Biotelemetry 9 (Dubrovnik 1986), 335-338.

[12] Diehl, P. & H.-W. Helb (1989): The influence of alarm calls on heart rate of free-ranging songbirds: a radiotelemetric study. - Biotelemetry 10 (Fayetteville, Ark., 1988), 332-338.

[13] Diehl, P. & H.-W. Helb (1992): Seasonal variation in heart rate response to song playback in blackbirds (*Turdus merula*). - 12th Symposium of the International Bioacoustics Council, Osnabrück 1991. Bioacoustics 4: 71.

[14] Diehl, P., H.-W. Helb, U.T. Koch & M. Lösch (1986): A radiotelemetry system for analyzing heart rate responses during playback experiments in blackbirds (*Turdus merula*). - Behav. Processes 13: 311-325.

[15] Diehl, P., H.-W. Helb & H. Vogt (1988): Fortschritte in der radiotelemetrischen Herzfrequenzmessung an Singvögeln. - Proc. European Telemetry Conf. Garmisch-Partenkirchen 1988, 307-316.

[16] Epple, W. (1996): Rabenvögel, Göttervögel - Galgenvögel. Ein Plädoyer im „Rabenvogelstreit“. - G. Braun Karlsruhe.

[17] Glutz von Blotzheim, U. N. (Hrsg., 1993): Handbuch der Vögel Mitteleuropas. Bd. 13. Passeriformes. Teil 3. Corvidae-Sturnidae. - Aula Wiesbaden.

[18] Helb, H.-W. (1982): Ethometrie - Einsatz und offene Probleme der Telemetrie in der Verhaltensforschung bei Tieren. - 6. Telemetriekonferenz Garmisch-Partenkirchen, 369-381.

[19] Helb, H.-W. (1992): Song dialects in the yellowhammer (*Emberiza citrinella*): current situation of research in Central Europe, and heart rate response to song playback measured by means of radiotelemetry. - 12th Symposium of the International Bioacoustics Council, Osnabrück 1991. Bioacoustics 4: 63.

[20] Helb, H.-W. (1998a): Telemetry of physiological data of birds. - Proceedings of the 26thGöttingen Neurobiology Conference 1998, Vol. I: 169.

[21] Helb, H.-W. (1998b): Radiotelemetrische Untersuchungen zur Raumnutzung,

Zeitnutzung und Nahrungswahl bei Rabenkrähen (*Corvus c. corone*). - Wissenschaftliche Begleituntersuchungen im Auftrag des Ministeriums für Umwelt und Forsten Rheinland-Pfalz 1996-1998, Endbericht (235 S.).

[22] Helb, H.-W. (1999): Wissenschaftliche Begleituntersuchungen an Elster *(Pica pica)* und Rabenkrähe *(Corvus c. corone)* in Rheinland-Pfalz: "Rabenvögel-Gutachten" der Universität Mainz (Prof. Dr. J. Martens) und der Universität Kaiserslautern (PD Dr. H.-W. Helb) 1996 - 1998. - POLLICHIA-Kurier 15 (1): 6-10.

[23] Helb, H.-W. & P. Diehl (1986): Radiotelemetric monitoring of heart-rate in behavioural studies of songbirds. - Proc. European Telemetry Conf. Garmisch-Partenkirchen 1986, 62-71.

[24] Helb, H.-W. & P. Diehl (1987): Heart rate of songbirds: radiotelemetric monitoring of spontaneous alterations. - Biotelemetry 9 (Dubrovnik 1986): 331-334.

[25] Helb, H.-W. & O. Hüppop (1992): Herzschlagraten als Maß zur Beurteilung des Einflusses von Störungen bei Vögeln. - In: Bezzel, E., P.H. Barthel, H.-H. Bergmann, H.-W. Helb & K. Witt (Hrsg.): Ornithologen-Kalender 1992. Aula Verlag Wiesbaden, 217-230.

[26] Helb, H.-W. & G. Karg (1999): New insight into the behavior and ecology of the carrion crow using radio telemetry. - 15th Intern. Symposium on Biotelemetry I.S.O.B., May 9-14, 1999: Juneau, Alaska USA (in press).

[27] Helb, H.-W., H. Vogt & P. Diehl (1989): The cardiac response of small songbirds to different song dialects measured by means of radiotelemetry. - Biotelemetry 10 (Fayetteville, Ark., 1988), 345-351.

[28] Helb, H.-W. & J. Wilbert (1995): The influence of the electromagnetic field on the heart rate of songbirds measured by means of radiotelemetry. - Biotelemetry 13 (Williamsburg, Virginia, 1995), 263.

[29] Kenward, R. (1987): Wildlife radio tagging, Equipment, Field Techniques and data Analysis. - Academic Press London.

[30] Mäck, U. (1998): Populationsbiologie und Raumnutzung der Elster (*Pica pica*) in einem urbanen Ökosystem - Untersuchungen im Großraum Ulm. - Ökologie der Vögel 20: 1-215.

[31] Richner, H. (1989): Habitat-specific growth and fitness in Carrion Crows *(Corvus corone corone)*. - Journal of Animal Ecology 58: 427-440.

[32] Stock, M., H.-H. Bergmann, H.-W. Helb, V. Keller, R. Schnidrig-Petrig & H.-C. Zehnter (1994): Der Begriff Störung in naturschutzorientierter Forschung: ein Diskussions-beitrag aus ornithologischer Sicht. - Z. Ökologie u. Naturschutz 3: 49-57.

[33] Szymczak, J.T., H.-W. Helb & W. Kaiser (1991): Sleep and wakefulness rhythms in the blackbirds. - VII. Meeting of the European Society for Chronobiology, Marburg/Lahn 1991. - J. interdiscipl. Cycle Res. 22: 194.

[34] Szymczak, J.T., H.-W. Helb & W. Kaiser (1993): Electrophysiological and behavioral correlates of sleep in the blackbird (*Turdus merula*). - Physiology & Behavior 53: 1201-1210.

[35] Szymczak, J.T., W. Kaiser, H.-W. Helb & B. Beszczynska (1996): A study of sleep in the European blackbird. - Physiology & Behavior 60: 1115-1120.

[36] Vogt, H. (1989): Radiotelemetrische Herzfrequenzmessungen an Goldammern (*Emberiza citrinella*): Verhaltensstudien und akustische Reizexperimente zur Bedeutung von Gesangsdialekten. - Diplomarbeit, Universität Kaiserslautern.

[37] Wilbert, J. (1993): Konstruktion eines Herzfrequenzaufnehmers. - Studienarbeit im Fachbereich Elektrotechnik, Universität Kaiserslautern.

[38] Wilbert, J. (1994): Digitale Analyse eines im magnetischen Wechselfeld aufgenommenen Körperschalles. - Diplomarbeit im Fachbereich Elektrotechnik, Universität Kaiserslautern.
[39] Wilbert, J., H.-W. Helb & P. Weiß (1994): Körperschallanalyse - Software 2.0. Windows-Programm zur Bestimmung der Herzfrequenz.
[40] Wittenberg, J. (1968): Freilanduntersuchungen zu Brutbiologie und Verhalten der Rabenkrähe (*Corvus c. corone*). - Zoologisches Jahrbuch für Systematik 95: 16-146.

Address:
PD Dr. Hans-Wolfgang Helb,
University of Kaiserslautern, Department of Biology, Division of Ecology, P.O.Box 3049, D-67653 Kaiserslautern, Germany

Tel. + Fax: ++49-(0)631-2017-416
Email: hhelb@rhrk.uni-kl.de
Homepage: http://www.rhrk.uni-kl.de/~hhelb/

The GPS Flight Recorder for Homing Pigeons Works: Design and First Results

Karen von Hünerbein, Hans Joachim Hamann, Wolfgang Wiltschko

Zoologisches Institut
University of Frankfurt
Siesmayerstr. 70
Frankfurt, Germany

Eckhard Rüter

Rüter EPV Systeme GmbH
Sandtrift 87
Minden, Germany

Abstract:

This paper describes a first version of the GPS flight recorder for homing pigeons. The GPS recorder consists of a hybrid GPS board, a patch antenna 19*19 mm, a 3 V Lithium battery as power supply, a DC-DC converter, a logging facility and an additional microprocessor. It has a weight of 33g. Prototypes were tested and worked reliably with a sampling rate of 1/sec and with an operation time of about 3 h. In first tests on homing pigeons 9 flight paths were recorded, showing details like loops flown immediately after the release, complete routes over 30 km including detours, rest periods and speed.

Introduction:

For several years we have tried to develop a GPS flight recorder, specifically designed for homing pigeons in order to accurately measure flying positions and record their flight paths [2].

Homing pigeons are able to home from places where they have never been before and the mechanism of navigation is not yet completely understood [6,9]. For this reason, it may be helpful to record the flight paths of homing pigeons, in order to correlate them with the topografical structure of the area and other factors that are suspected to be involved in their navigation.

The technical reason for developing a new type of flight recorder is that the other methods used so far for measuring the flight paths of birds like ARGOS, conventional radio tracking, aircrafts and a magnetic direction recording device have major disadvantages. These are either small range, low resolution in time and space and lack of accuracy or a lot of effort to carry out measurements or high operation costs.

For a detailed description of navigation technologies which can be used for measuring and recording flight paths, their advantages and disadvantages see our former publications [3,4].

We are here describing the first version of the GPS flight recorder. Giving examples of the flight paths of homing pigeons from a site 30 km from the home loft, we demonstrate its effectiveness.

Requirements

There are several challenges to measuring the flight paths of pigeons. The birds are rather small, 300-500g, and should not be burdened with more than 10% of their body weight. Orientation experiments are performed within a medium range of 10-200 km. The pigeons move fast with an average speed of 70 km/h. They come home within 0.3 - 24 h after release (= take off). The advantage of this short duration of flight is that the flight recorder needs to work only for several hours, the disadvantage is that a high sampling rate is necessary in order to get a good resolution of the flight path. For tracking experiments a big advantage of pigeons in contrast to other animals is that they return to their home loft on their own and can easily be recaptured. They need not be trapped outdoors, so that the data can be logged and need not be retransmitted. Pigeons' backs have a free access to the sky as long as they fly. Thus satellites can be received with no obstruction.

These conditions lead us to set up the following major requirements for a flight recorder:

- Recording of position and speed with a good accuracy (100-300 m)
- Small dimensions (70*40*30 mm)
- Low weight: about 30 g (with antenna and power supply)
- Sampling rate 5 sec - 5 min
- Operation time: 3 - 12 h

We decided that GPS, Global Positioning System, [3] is the best technical system to fit these requirements.

Advantages and disadvantages of GPS

GPS offers:
- high accuracy of position
- possible sampling rate of once per second
- no transmissions in flight
- worldwide availability

Major disadvantages of GPS for this application are:
- size and weight of components
- power consumption
- high cost of devices
- animals have to be recaptured to retrieve the data, the GPS recorder and all the data may be lost, if the animal does not return to the loft
- residual magnetic field

Design of the GPS recorder:

The GPS recorder (Fig. 1) measures the position of the pigeon during its flight and records these positions in internal memory. At the end of the pigeon’s flight the position

data are downloaded to a computer. Then the flight paths or parts of it can be calculated or displayed on a map.
Data protection in case of power failure is achieved, because the positions are stored on a flash RAM. Data can be downloaded as NMEA (standard defined by the National Marine Electronics Association, USA), in a company owned format or as ASCII text. NMEA data are converted by a Visual basic program to allow processing by standard PC software.

The GPS recorder consists of a GPS antenna, a GPS receiver board, a datalogger, a power supply, a DC-DC converter, a connector and a display of status. It has a weight of 33g and a physical size of 8.5 * 4 * 1.5 cm. The GPS recorder has a sampling rate of 1/sec and operates for approximately 3 hours.

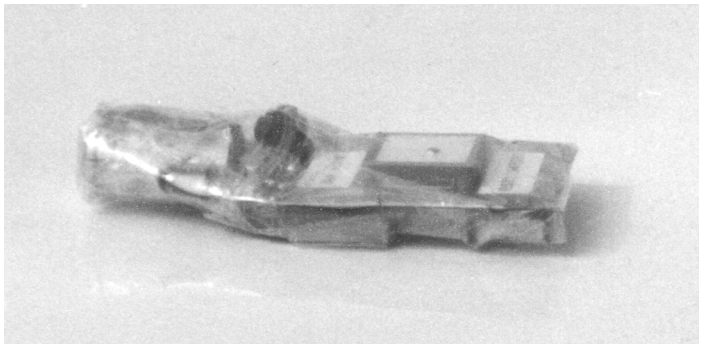

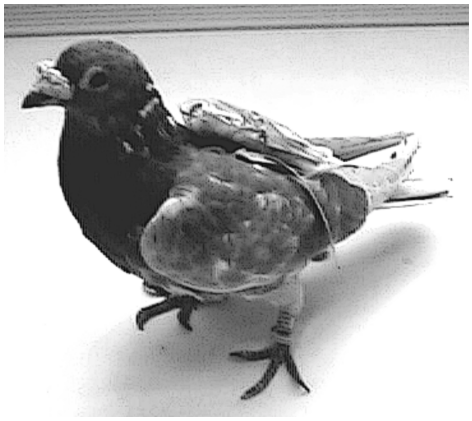

Figure 1: GPS recorder stand alone (left) and on a pigeon (right)

Components

Antenna: Passive patch antenna with a size of 19*19 mm
GPS board: 1 hybrid board with a size of 30*30 mm -weight: 6.2 g measuring position with the standard positioning service SPS.
Datalogger: A logging facility storing the GPS positions directly on the receiver board, external logging is also possible
Power supply: A primary lithium battery of 11 g.
DC DC converter: The voltage of the battery is adapted to the voltage of the GPS receiver
Connector: for the PC interface
Indicator: The internal status of the device is indicated.
External microprocessor.M. Riechmann and the fourth author wrote a program for the microprocessor to control the mode of the device. In the measuring mode it correctly starts up the GPS receiver and initializes it with the desired parameters.

Hardware interface between the GPS flight recorder and the PC:
built by H.J. Hamann and M. Riechmann allowing transfer of the data between PC and GPS recorder.

Casing In this first version the GPS recorder was packed in thin plastic foil and attached to a the pigeon with velcro on a harness (after a design by Kenward *et al.* [5]). The harness consists of an epoxid back plate with a strip of velcro on it, an epoxid breast plate and Teflon ribbon. It has a weight of 7 g.

Software:

1. Software to download the data from the GPS recorder and to watch the GPS receiver sending messages while operating.
2. Software to convert NMEA to other formats. It was written by the first and second author.
3. Software to plot GPS data. The programs: Fugawi, Sigma plot, Top50 Hessen are available commercially.

Experiments:

Training of the pigeons:

We used adult, experienced pigeons to test the GPS recorder. 10 pigeons were trained for 3 months carrying the harness and increasing weights. They were released from increasing distances and different directions to get used both to carrying the harness and the additional weight.

Test flights:

Experiments were done on Septembre 27th and 28th in Obermörlen, a release site approximately 30 km North of Frankfurt, home direction: 185°. The release site was chosen, because there pigeons often showed considerable deviations to the east of the home direction in the very first part of the flight in previous experiments [e.g. 8]. GPS flight recorders were switched on 7-30 min before the test. The early switch on served to let the GPS receiver find satellites and acquire a first fix and to check whether the GPS recorder operated. 10 pigeons were released with a GPS flight recorder, 9 tracks were obtained. Every recorded track contains approximately 10 000 recorded positions. Homing times could be measured from all 10 pigeons carrying GPS recorder.

Results:

Observations of flying behaviour

We carefully observed the pigeons, to find out whether there were differences between pigeons carrying the GPS recorders and pigeons not carrying anything, called controls. Pigeons flew well with the GPS recorder, but they tended to fly lower and their wing beat frequency seemed to be higher. Furthermore, some birds carrying GPS disappeared behind obstacles before giving a normal vanishing bearing.

Examples of flight paths:

Most pigeons flew extensive loops immediately after starting their flight (Figure 2). Surprisingly, all the flight path positions beyond a few hundred meters south of Obermörlen village are situated east of the direct line between the release site and the loft. Pigeons deviated as much as 9.3 km to the East of the direct route.

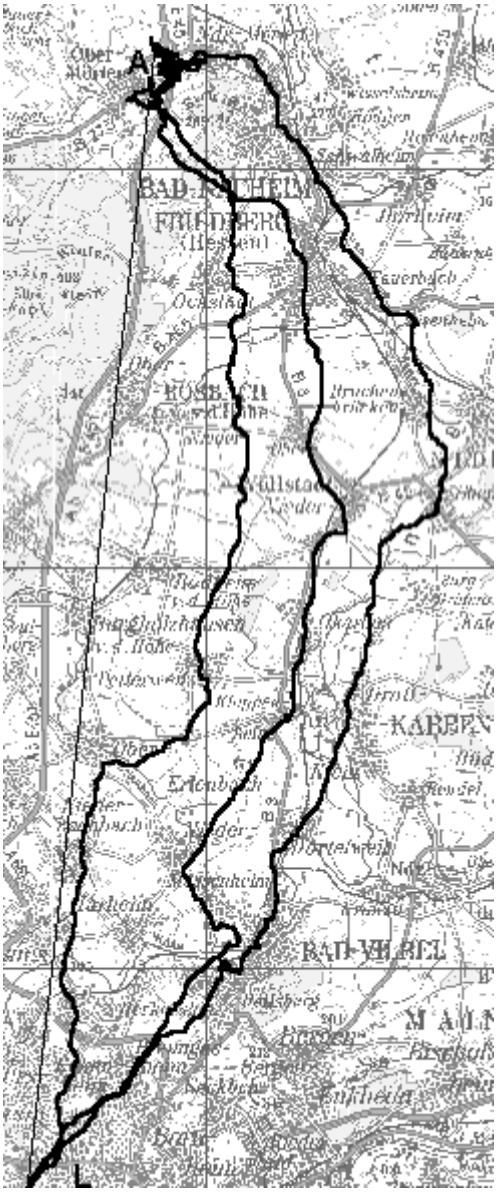

Figure 2: Examples of three complete flight paths, A = Auflaßort = release site = start of flight, L = loft = pigeons' home. The thin, straight line is the direct route between the release site and the loft.

The release site has a special topography. There are two mountains connected by a ridge almost perpendicular to the direct route home, presenting an obstacle on the first few km of the homing flight. The ridge is 70 m higher than the release site and 80 m higher than the valley. The one pigeon flying 90° eastward at the beginning of its flight in Figure 2 circumnavigated the mountain. The other two chose to climb 70 m and to fly over the ridge.

Speed profiles:

The GPS recorder also measures speed, which allows us to determine where and when a pigeon stopped flying. Most pigeons took several breaks during their flight home, ranging from 1 min to 3 h.

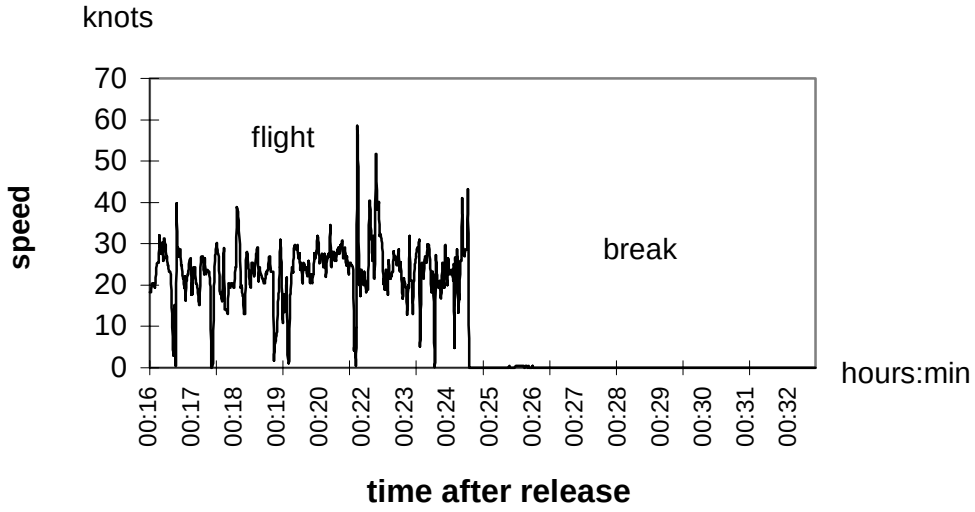

Figure 4: Speed values no. 1000 - 2000 of pigeon no. 356

The GPS recorder's Accuracy of Position :

At the very beginning of the operation of the GPS recorder, some major errors in position occured. Some initial positions deviated by as much as 2.9 to 5.6 km from the true position for several seconds. The reason for these errors is that the GPS receiver had not yet acquired all satellites in view. This type of „switch on“ error was already observed during the development of the GPS recorder. Therefore we took care during the experiments to switch on the GPS recorders at least 7 min before the animals were released. During the flights themselves no sudden big jumps of position were observed.

Several pigeons landed for more than 15 min. This gave us the opportunity to check whether the error in a series of measurements is the one defined by SA, Selective Availability, the standard error built into civilian GPS. We analysed the shift of positions during pigeons' breaks and measured on a map the maximum distance between two positions. In 14 out of 16 long breaks we found that the maximum difference in positions is 100 m.

In the two remaining cases the maximum differences were 110 and 130 m. The last two values are from the two pigeons who made very long breaks. This analysis shows that the positions measured by the GPS recorders are consistent within themselves and that the error is well within the range of 300 m, the error defined by SA: 100m 95% of positions and 300 m 99% of positions.

Sampling rate:

The high sampling rate of one value per second makes possible a clear resolution of the loops flown (Figure 3). In contrast the same loops are hardly visible anymore with a sampling rate of 1 value every 30 sec. At this resolution it is still possible to see that the flight path deviates from a straight course, but the nature of this deviation cannot be clearly identified.

Figure 3: Examples of the initial part of flight path of the same pigeon, with a sampling rate of 1/sec (left) and a sampling rate of 1/30sec (right), right flight path simulated by drawing every 30th value only.

Homing times:

Pigeons carrying GPS took significantly longer to home than two out of three groups of controls of previous experiments. The median value of the GPS pigeons was 133 min, compared to 52, 91 and 56 min of three controls from previous years. In our experiments the fastest pigeon carrying GPS flew without a break and took 52 min to home. The slowest pigeon took a very long break lasting at least 3 hours and came home after 6 hours and 40 min. During the long break the GPS recorder stopped operating.

Discussion:

We have now achieved our main aim of developing a GPS application sufficiently miniaturized to put it on homing pigeons, have them fly with it and obtain accurately measured flight paths.

But there are also two grave limitations of the device with regard to homing pigeons: weight and a residual magnetic field.

The physical size of the device suits the pigeons well, it has been constructed to be more narrow towards the head so that the wings are not obstructed flapping. We are also satisfied with the harness, except for its weight. It fits on the pigeons very well and does not fall off, even though pigeons pick at it with their beaks. The teflon ribbons caused no damage to feathers and skin. The devices stuck very well to the back plate and never fell off in experiments.

Compared to our initial requirements two properties of the GPS recorder are far better than we dared to expect at the beginning of the project: the sampling rate is even higher (1/sec) than our minimum value of 1/5sec and the amount of positions that can be stored is also much higher than the minimum of 1000 we defined at the beginning. We can now store 10 000 positions and would be able to store about 90 000, if the battery lasted that long.

The operation time of 3 hours is the minimum time we wanted. At the moment there is only one battery on the market that has the right combination of very low weight, high capacity and high output current to suit the GPS, so those 3 hours is the best that can be done right now. There is an alternative solution that lasts 30-45 min longer, but that battery weighs several gram more. It could be included into an application for larger animals.

The two major disadvantages of the device remain the weight and the residual magnetic field.

The weight is 33 g plus 7 g for the harness. With the electronics there is no room for further saving of weight at the present state of the art of the components. The 7g for the harness might be reduced by omitting the breast plate or we might use a different technique for attachment.

40 g is still a high weight for a pigeon representing about 10% of its body weight. There is an influence on the pigeon's flying behaviour as can be seen in the long homing times and we also saw from our observations that pigeons lost their ease of flight and flapped their wings with a higher frequency. The long breaks many of pigeons took also indicate that the GPS recorder caused them an additional effort. A study by Gessaman and Nagy 1988 [1] showed that pigeons can be influenced very much by transmitter loads with a weight of 2.5% and 5%. The birds slow down by 15%-28% on 90 km flights and their CO_2 production increases by 41%-50%. Nevertheless we think that the weight of the device is within the physiological range, because the weight of the device is about the same as the weight of the food the pigeons carry after feeding and because all of our birds returned from the homing flight on the day of the release, which implies that the impairment is not too great. Also the orientation may not have been influenced by the additional effort, nor the flight path significantly altered. But it is necessary to further decrease the weight in future versions and the weight is such that the GPS

recorder cannot be considered an ideal solution for measuring the flight path of homing pigeons yet.

The device produces a residual magnetic field with a strength of 1,500 nT. This is ~3% of the intensity of the earth‘s magnetic field. In previous work it was shown that very small differences in field intensity of about 0.2% of the strength of the field can make a difference in pigeons' initial orientation [7]. This means that in studies with the GPS recorder the possible magnetic influence needs to be considered as a part of the experimental condition.
The residual magnetic field can be reduced only after more progress in battery technology has been made, since at this moment there is no Lithium battery capable of both supplying the high output current and the right voltage to suit the GPS receiver board.

Conclusion:

Despite its disadvantages the GPS recorder greatly extends the possibilities of measuring flight paths on birds. The GPS recorder has now made it possible to accurately measure, record and plot details of the flight paths with a so far unequalled temporal and spatial resolution, a range of measurement limited only by the power of the battery and a comparative ease of experimental procedure requiring little manpower. It represents a significant advance in measuring technology on animals. Many more species can now be tracked with GPS. When tracking animals with our GPS recorder the animals need to have a weight of at least 500g, travel under the free sky and have to be be recaptured.

Acknowledgements:

This project has been **financially supported** by the Deutsche Forschungsgemeinschaft DFG (grant to W.W.) and the German Society of Telemetry (Arbeitskreis Telemetrie, grant to K.v.H.). **Partners in cooperation** building and testing of hardware and software: Frank Joest and Dr. Stefan Wolff, University of Darmstadt, Germany; Rainer Hartmann, Prof. Klinke, Ralf D. Müller, B. Klauer (last 4 from the University of Frankfurt, Germany), Stefan Werffeli and Clemens Buergi, ETH Zuerich. Switzerland. For **tests on pigeons:** Harald Schuka, Minden, Germany. For **supplying samples** of components at no cost and for being very helpful with information we thank the following companies: WiSi, Rockwell (now Conexant), Murata, Bosch, Varta, Eagle Picher. For **helpful comments to the manuscript**: R. Wiltschko, University of Frankfurt, Germany, Prof. Joe Riley and Ann Edwards, NRI Radar Unit, UK. For **encouragement and interest in cooperation**: God, Dr. Sandra Woolley and Dr. Anthony Woakes, University of Birmingham, UK; Mohamed al Bowardi, NARC, United Arabic Emirates; Stan Tomkiewicz , Telonics, USA; Dr. Wolfgang Lechner, Germany.

References:

[1] GESSAMAN, J., NAGY, K. (1988). Transmitter loads affect the flight speed and metabolism of homing pigeons. The Condor 90:662-668.

[2] HÜNERBEIN, K., WILTSCHKO, W., MÜLLER, R. AND KLAUER, B. (1997). A GPS Based Flight Recorder for Homing Pigeons. In: Conference Proceedings of the GNSS 97 (ed.: Deutsche Gesellschaft für Ortung und Navigation) April 21st-25th,1997. Bonn. Volume II: 561-570.

[3] HÜNERBEIN, K. AND MÜLLER, R. (1998). Development of a GPS Flight Recorder for Birds. Arbeitskreis Telemetrie e.V. (ed.) In Conference Proceedings of the European Telemetry Conference 98, Braunschweig: 86-98.

[4] HÜNERBEIN, K., HAMANN, H.J. AND WILTSCHKO, W. (in press). Progress With the Development of the GPS Based Flight Recorder for Homing Pigeons. In: Conference Proceedings Biotelemetry XV. May 10th-15th, 1999 Juneau, Alaska.

[5] KENWARD, R.E., PFEFFER, R.H., AL-BOWARDI, M.A., FOX, N.C., RIDDLE, K.E., BRAGIN, Y.A., LEVIN, A.S., WALLS, S.S. & HODDER, K.H. (in press). New techniques for demographic studies of falcons. Journal of Field Ornithology.

[6] SCHMIDT-KOENIG, K. (1991). Über Karten und Kompasse bei Brieftauben. Verh. Dtsch. Zool. Ges. 84: 125-133

[7] WILTSCHKO, W., NOHR, D., FÜLLER, E. and WILTSCHKO, R. (1986). Pigeon Homing: The Use of Magnetic Information in Position Finding. In: G. Maret, J. Kiepenheuer, N. Boccara (eds.) Biophysical Effects of Steady Magnetic Fields. Proceedings of the Workshop Les Houches France, Springer Verlag, Berlin: 154-162.

[8] WILTSCHKO, R. (1993). Pigeon Homing: Release Site Biases and Their Interpretation. In: Orientation and Navigation - Birds, Humans and other Animals. Proc. Conference Royal Inst. Navigation. Oxford 1993, Paper No. 15.

[9] WILTSCHKO, W., WILTSCHKO, R. (1994). Avian orientation: Multiple Sensory Cues and the Advantage of Redundancy. In: Davies MNO and Green PR (eds.) Perception and Motor Control in Birds: 95-119. Springer Verlag, Berlin, Heidelberg.

COMPUTERS, INTERFACING, TIMING AND BUS SYSTEMS

Timing in the Upcoming Century
- An Overview

Werner R. Lange
Lange-Electronic GmbH, Ganghoferstr. 29, 82216 Gernlinden

Abstract:

Distributed and more complex systems, higher data rates, new telemetry formats and the advances in processing telemetry data lead to higher demands using timing systems. Two decades ago a time resolution of 1 ms was sufficient for most of the timing units used in the area of telemetry, now resolutions of 100 nsec are available and are used in increasing numbers of systems.

The paper will give an overview of the ways next generation timing units, as well as instruments as well as board level products, can help the telemetry engineer solve his time tagging and synchronisation problems.

Introduction:

At TC 78, the first German telemetry conference held at Garmisch-Partenkirchen, I presented a paper about “The Special Possibilities of Time Codes at Data Recording”. The paper was presented in German language and we still have a few reprints, which we some times mail to a potential customer if he asks questions about IRIG time codes.

Some of the statements made in this paper are still valid, off course – IRIG B is still IRIG B, with all its advantages and limitations, but the use of time codes is merely completely different now than it was 22 years ago. At that time we sold a lot of time code systems to customers using magnetic tape recorders and just a very few systems have been used as synchronisation units. Today I have a hard time to remember the last order we received for a time code system used in the “classical” way – most of the systems and units our customer use are more related to time tagging and synchronisation.

In this paper I try to make some “prophecies”, and as it is with all prophecies, they are very hard to make and uncertain because we are talking about the future.

Time:

The following chart illustrates the differences as I see them in data acquisition and telemetry in the years of 1980, 2000 and 2020. The second chart shall show how the proposed changes relate to time and frequency.

	1980	**2000**	**2020**
time resolution	1 ms	1 µs/100 ns	100ns/10 ns
synchronisation error	20 - 50 µs	5 µs	< 1 µs
accumulated time error (mission time 3 - 4 hrs.)	500 ms	500µs	1 - 10 µs
Signals	analog (few digital) no bus data separate video	digital (few analog) incl. Video, some data pre-processed	digital bus data, video, (almost) no analog data, mostly pre-processed
signal frequencies	mHz ... kHz		
Tx bandwidth	100 kHz...5 MHz	to 6.. 8 MHz	to 20 MHz

Chart 1

What impact do these assumptions have in time and frequency?

If we look at a typical telemetry ground station, there are other types of oscillators in use. A time resolution of 100 ns requires an oscillator frequency of 10 MHz, a resolution of 10 ns requires 100 MHz. Besides this self clocking time codes will be widely used to synchronize the different places where time is essential.

We presently see the necessity to synchronize data acquisition systems and control units to different levels of accuracy. Computer networks require synchronisation, too, but usually the processes inside of a computer are not very precise, so the level of synchronisation can be much lower as in data acquisition or time tagging units. We may use the synchronisation processes in a large optical observatory as an example, where the computer network for data processing is synchronized to some milliseconds, while another cluster of computer controlling the mirrors have to be synchronized to a few microseconds in order to achieve the optical precision necessary to have the resolution the system is designed for.

In 20 years the synchronisation within a computer network will be in the range of better than 100 microseconds or about 10 to 1000 times better than it is today. This will be necessary due to the higher processing speeds.

Frequency:

	1980	2000	2020
Oscillator frequency	1 MHz	1 ...10 MHz	10...100 MHz
Oscillator aging rate	5x10E-6	3x10E-8	5x10E-10
Time resolution	1 ms	1 µs	10 ns
Data transfer into system - mode	BCD parallel 16 bit GPIO	RS232, Ethernet, plug-in board	fiber-wire type, plug-in board
-latency	0 to ms	0 to ms	0 to µs

Chart 2

So, what about frequency ?

In the "standard" stand alone or mobile timing systems there will be no dramatic change, off course, the oscillator frequency will be higher due to the higher resolution. There will be two side effects which shall warrant that two independent timing systems remain in quasi-synchronisation for a longer period of at least several hours: First of all the power consumption of high quality oscillators will be reduced, so that oven controlled oscillators can be used also in battery backed up units and secondly there will be some synchronisation mechanisms during missions, perhaps by using GPS or its successors.

There will be some differences at the ground stations – the transmission frequencies will be higher and the use of the also higher data rates will be enhanced by using precise external frequencies for the down converters in the receivers. Presently the frequency sources used in receivers are of “moderate” quality, this is enough for the present requirements of today. But in the future techniques presently used in high data rate satellite communication systems will also be used in receiving stations. Therefore the receivers will have a 10 or 100 MHz external input. The signal used will be sine wave, with special aim of low signal distortion and little phase noise. This will enhance the signal to noise ratio and the bit error rates.

Telecommunication will have a much higher influence in telemetry than it has today. We see the use of GSM and DECT techniques today; we will see much more use of these cellular radio like techniques in the future when the transmitted data rates will be in the Mbps range. I can easily imagine a civil aircraft transmitting their data via satellite or terrestrial communication links. But there are also very high requirements for synchronisation of data links, which have to be settled by the telecom companies. Nevertheless will there be a constant “time update” with algorithms derived from NTP or similar protocols – as soon as we go online with our computer (which may be in

our wristwatch or we will wear it on a chain around our necks like a piece of jewellery) his internal clock will be synchronized.

Conclusion:

There will be no “revolution” in the next two decades, but there is some space for improvements. And if you select a new timing system, take care that it is a little bit ahead of today.

Key words: Time, frequency, synchronisation, IRIG codes, resolution, µs, ns, latency, NTP,GPS, signal distortion, phase noise, GSM, DECT, telecommunication, Ethernet

Common Platform Design of Telemetry Software

MiaoLiucheng Zhaojun

Beijing Institute of Tracking &Telecommunication Technology

Beijing, PR China

Abstract

At present, telemetry technology has been used in many important fields. Commonly, the hardware and software in all system are used for a special purpose. But in view of the trend of telemetry technology development in the world, telemetry system will adopt modularization, standardization, universalizes technologies widely in hardware, and therefor the software platform will be developed like the hardware too. In other words, hardware-independent and software-independent will be the trend for next generation telemetry system. So, a common software platform should be built in the future. In this paper, the following question will be discussed: What's the meaning to build a common soft platform for telemetry system? How to build it? What is the key technology to built it? How is the application prospect?

Introduction

Telemetry systems are used for acquiring important test data in many fields. For example: airplane test, environment measurement and software to accomplish certain different mission. The reason for this is that different hardware is used for different system, different data acquiring method and processing method will be asked in different system. Today, advanced computer technology is being adopted more and more widely with telemetry system, especially with data acquiring, data processing, protocol controlling and hardware controlling. In view of the development direction of telemetry technology and computer technology and control technology, we will need a common software platform (platform-independent) to accomplish all of these functions in almost all of telemetry system. The result to do so should reduce the cost of telemetry system, and enhance the commonality and maintainability of the telemetry system.

Presently, the degree of automation has been getting higher and higher, the method to build common software for telemetry system should be relatively easier. In this paper, we shall discuss how to build a common software platform that is standard and applicable.

The Meaning to Build a Common Software Platform

As we have elucidated in the introduction, the significance is very clear to build a common software platform.
First of all, the cost and periods of development about system could be reduced greatly. The description of main software for a telemetry system can be described as Fig.1.

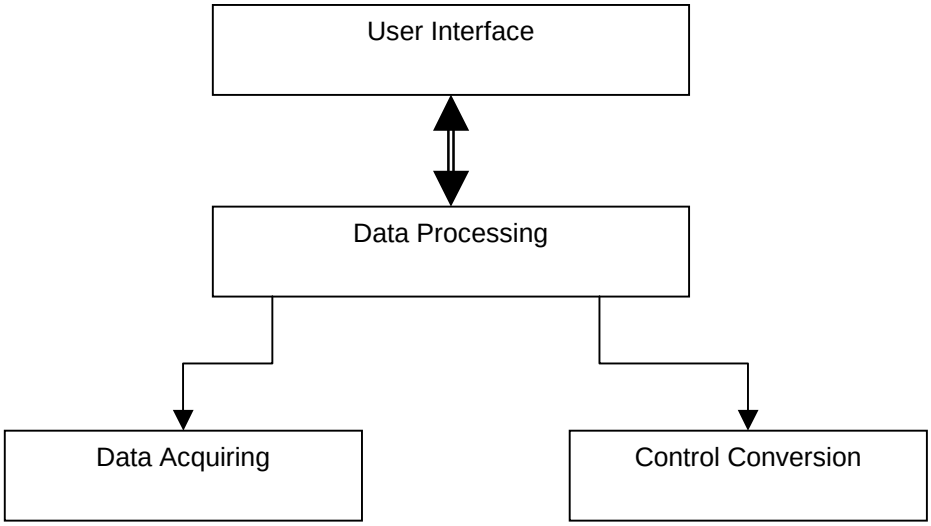

Fig.1 Description of Software for Telemetry

Seeing Fig.1. The user interface is needed in almost all system. The interface can be designed as uniform format, but its contents can be different for different application. Data processing unit will complete general data processing of engineering parameter, and translate user command to different control command. For Data acquiring Unit, it will exactly accept data according to the user's setting, and transmit the data to data processing Unit. Control Conversion Unit will transmit the control command to different format for different function unit in different hardware unit. Generally, the Control Unit and Data Acquiring Unit are connected closely to certain hardware system. Relatively, User Interface and Data Processing Unit are independent in most system. If they could be separated from the whole software design, the cost and periods will be greatly reduced, and the maintainability will be very good. At the same time, the reliability of the system will be increased greatly, and we can do it better and best.

How to do it?

In order to build the common platform of software referred above, the preliminary analysis of demand must be completed, and then the software unit could be designed and built. As a sample in this paper, we will discuss the User Interface Unit.
The function of User protocol (or communication interface) with the Data Processing Unit and all of peripheral equipment (magnetic-tape units, and high- speed printers

etc.). In general, the manufacturer has completed interfaces of peripheral equipment as standard driver software. The work that must be done is to unify the interface between different unit.

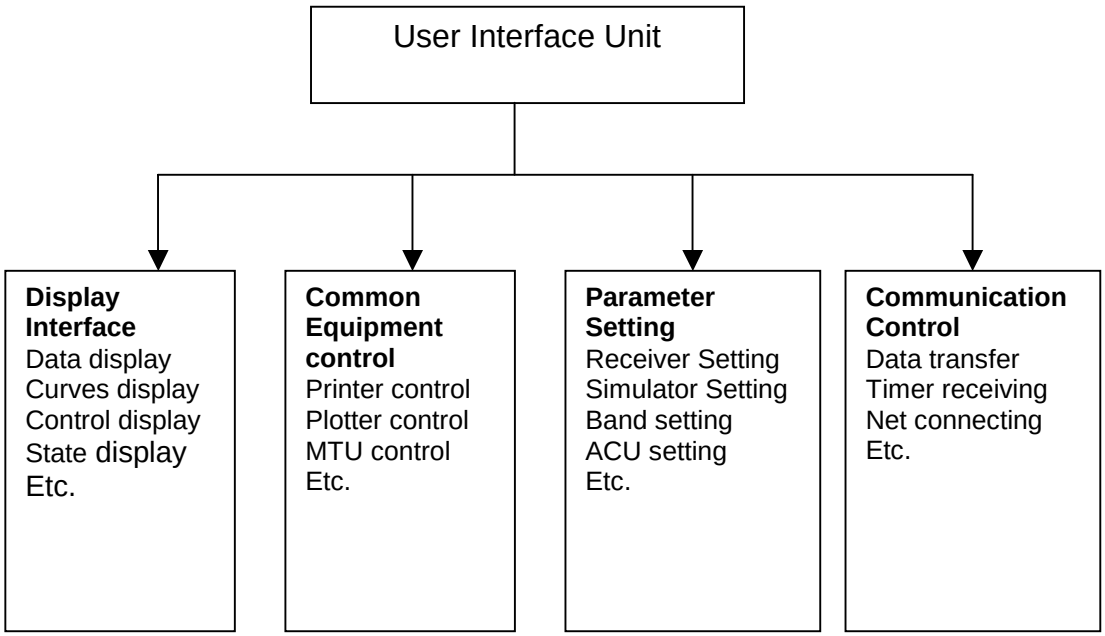

Fig.2 the Function of User Interface Unit

The Key Technology

In order to build the common software platform between different system, there are some technical problems must be solved.

a. To Uniform Software Interface between different products
   Up till to now, the software interface in hardware system is different between different hardware producer. So, it is not easy to build the uniform software interface in different products.
b. Open software interface
   Technology of open OS platform and Unit interface are required in Open Software Interface. Now, most of software has been developed with Windows 9x or Windows NT. So it is a comparatively easy job to build an open software interface than others.
c. How to build the standard of unit control and communication?
   The hardware interface standard is easy to be unified. The key technology is to unify the software interface of control and communication between different hardware made by different company.

Conclusion (Application Prospect)

Today, telemetry systems have been used in many important fields and have been produced in many companies all over the world. If the technology of common software platform has been built, it may be a new technology, and the system function will be greatly enhanced. The function of user Interface will be greatly enlarged.
From the commercial standpoint, this should be a chance of market. From the user standpoint, the system should be easy to be used and be redeveloped. Making a comprehensive view of the next generation telemetry system, hardware-independent and software-independent must be the direction for the future. Common platform of telemetry software must be a part of the telemetry system.

Acknowledgement

Many people have given me many help and support in the completion of this paper. I shall especially thank my friend Dr Su-ZengLi for checking up and suggestion in writing of this paper.

References

1 LiuYunCai, Telemetry System, in "Systems engineering of missile & satellite control", China National Defense Industry Publishing Company.

2 O.J.Strock, US, "New Generation Computer Telemetry System"

KEY WORDS

Software, Telemetry system, Application.

Why Trial and Error with ASICS if there is Software?

Hans van Leeuwen
Peter van Leeuwen
Kees de Nie
Smart Telecom Solutions (STS)
Amsterdam / The Netherlands

Abstract

STS is an organization specialized in the development of digital wireless communication products. The outline of the paper is as follows. We will start with an introduction of a general overview of chip design and new developments in the field of system simulation, digital simulation and circuit simulation software and tools. In this paper we will publish the results of an application experiment of software and simulation tools to upgrade and enhance the STS design cycle in producing digital wireless communication products. The experiment was held in 1996/1997. In this paper we will discuss the results of this application experiment. Part of the experiment was to build and evaluate a Spread Spectrum WLAN transceiver. STS reflected on software and simulations techniques on the market and evaluated the cost and benefits of each tool. The system software tested are Omnisys, Success, PV Wave, SystemView, C++ math-module, Mathematica. Circuit software tools tested are MDS, Harmonica, Spectre/XL, Genesis. Software tested for digital hardware is Leonardo, Galileo. Results of this application experiment and an analysis of the advantages and disadvantages of the software and tools will be presented. The paper concludes with the results of the evaluation and an overview of development projects in which these tools proof to be of some value.

Introduction

Smart Telecom Solutions is a young-engineering company specialized in digital wireless communication solutions. The mission of STS is to meet the global demand for information transfer systems based on the best available digital wireless technology. To complete this mission STS has four major research programs. As a commercial enterprise the point of departure for any program is product development of wireless audio, video and data transfer systems for our principals. In the conceptualisation of the wireless solution, STS uses the output of four technological research programs. The first program is the product development program. The second is spread spectrum technology at 2,4 GHz and 868 MHz. The third program is to implement Radio Frequency on CMOS. This program is targeted at realising low cost ASIC's with RF capability. The fourth program aims at realising digital wireless transceiver on a single ASIC (system on chip). These research programs makes STS a technology partner that enables principals a fast route to market with state of the art wireless technology.

STS was founded in 1993 and is a fast growing engineering company ever since. Starting from scratch STS had the qualified engineers but had a pretty basic design cycle. System definition and system specification was performed largely manually, supported with simple tools such as a spreadsheet. Holes in the design cycle were contracted out, tools rented and critical tools were in house developed and some were bought. Technology partners that filled the holes and served as subcontractors were the Technical University of Delft, the Center for Microelectronics, Hewlett Packard, Compact and Translogic. The European Esprit-subsidy gave STS the opportunity to do an application experiment to optimize the design cycle with state of the art simulation software thus giving an impulse in the infrastructure of the company it is today. The central question of the application experiment was: How can the STS design cycle be optimized with state of the art simulation software especially designed for PC?

The experiment enabled and empowered STS engineers with the necessary tools and equipment. In the remaining of this paper we will discuss the methods used to select the simulation software and the indicators at which we processed the evaluation. In the second part we will present the results of the evaluation. We conclude this paper with the impact of this experiment for further scientific and product development research.

Reasons and timing of the experiment

In 1996 the management signaled various trends that an experiment of simulation software would be favorable. STS had skilled engineers and STS was granted governmental support by the Ministry of Economic Affairs for developing a Wireless Local Area Network transceiver. The support was the development of a device for wireless RF communication between computers in the 2,4 GHz ISM-band (Industrial, Scientific, Medical). The application has been denoted as the '*SmartLink*™*.* The *SmartLink*™ project served as a perfect application for the simulation software in the evaluation experiment. STS had to improve its technical infrastructure to level design capacity and to meet its targeted technical goals. In the experiment the strategic choice was made to focus on software that was especially designed for Personal Computers (PC). Arguments for this choice were the following. In the mid-nineties Intel introduced the Pentium thus enhancing calculation power for personal computers considerably. As a consequence, the investments in hardware decreased by 30 of 40 percent compared to the costs of high-end systems. An additional benefit was that interaction between various systems is less complicated with PC's (e-mail of data) than workstations. The interpretation of these trends resulted in the choice to verify the released simulation software for PC's.

Method

In preparation of the experiment a pilot study was held to analyze the definition of the wanted design cycle in order to realize the *SmartLink*™*.* Each phase technical challenges and milestones were defined. After the definition phases in the design cycle a market study was held to see what software was available and which companies were willing to be part of the experiment. By matching software

and the design cycle within the constraints of the budget, the final design of the experiment was concluded.

General overview of the application experiment
In the article we will present the STS design cycle and the various steps we use to realize our designs of the *SmartLink™.*

Conclusion
In our paper/presentation we will show the benefits of our designcycle and methods with state of the art simulations tools in realizing other concepts like Bluetooth, Hyperlan, 868/917 MHz and 2,4 GHz devices.

AEROSPACE TELEMETRY AND FLIGHT TEST INSTRUMENTATION

CONCEPTUAL DESIGN OF AN INTEGRATED OPERATING ENVIRONMENT FOR FLIGHT TESTING

Sergio D. Penna, Engineer - Felipe E. Fernandez, Engineer
EMBRAER Flight Test Division
São José dos Campos, Brazil

Abstract

In organizations with tradition in flight testing aircraft for Type Certification under FAA or JAA regulations, the use of one or more computer-based systems is often mandatory. Any such system acting as a repository for storage and retrieval of valuable flight test *Information* can be seen and treated as an *Information System*. *Information* in this context can be anything from a mere transcription of FAR or JAR chapters to post-processed flight test data.

In many cases, *Information Systems* found in flight test organizations were not conceived together, rather the contrary, they were built in response to new operational requirements raised in different times, making querying, joining or consisting *Information* stored in two or more repositories very inefficient. A tentative reduction of this inefficiency can be identified when the same *Information* is found replicated in more than one repository.

This paper intends to lay out a conceptual design of an Integrated Operating Environment, where *Information* is validated, stored once and shared among users through an interface that can provide transparent access to one or more *Information Repositories* in a standard way. In a Flight Test environment, it shall store and maintain correlation of all that is needed to an efficient conduction of a large Flight Test Program, including compliance check-lists, test proposals, parameter lists, on-board instrumentation configurations, flight test schedules, flight-cards, flight test data visualization screens, data processing algorithms, flight test results, time-history files and prototype configurations.

As a result of being conceptually integrated, storage or retrieval of generic flight test *Information* is expected to be greatly improved under such environment, where consistency is promoted, redundancy is eliminated, and an uniform interface for all users is provided.

Introduction

Database Engineering is seldom seen as a necessity in a Flight Test environment.

Information is normally organized and stored in any possible format. Sharing it is often difficult, as it is any cross-correlation between two different table formats. This phenomenon is quite common because most organizations emphasize creating a *tool* rather than dealing with *processes*. Someone expresses a need and a *tool* that serves momentarily the purpose of bringing some order to tabulated *information* is build up. Once this small requirement is fulfilled, everybody seems to be satisfied. The *process* itself, producer or consumer of *Information* and eventual beneficiary of this *tool*, is neglected, never reviewed, never improved.

In smaller flight test campaigns, speaking of *Database Engineering* may be seen as an exaggeration. In larger ones, it can draw a path to success or failure.

Flight Test organizations that early recognize that a professional *Database Engineering* work can not only make gathering and sharing information more meaningful, but can also speed up a few of their processes, may become quickly much more efficient.

Definitions

Any means used to contain *Information* can be qualified as an *Information Repository*. In the context of this paper, *Information Repository* will be a computer-based system were a *Database Engine* is installed and used to populate a *Database* with useful *Information*. A *Database Engine* is an application program capable of orderly store and retrieve *Information* in and out of a *Database* as a result of a coded command called *query*. *Databases* are collection of *tables*. *Tables* are structures organized in *rows* and *columns* to hold general data.

Two or more *Information Repositories* working together to complement each other will be called here an *Information System*. Organizations may be using one or more *Information Systems* in any given point in time.

The discipline that studies such entities [and many others] is called *Database Engineering*. The software engineering activity conducted during a database design and implementation is called *Data Modeling* [1] [2] [3].

Information Repositories in a Flight Test Environment

It is useless to re-state how the development and certification of a new aircraft affects everybody's life. For the purpose of this paper, five areas will be focused: *Certification* [coordinates the certification process], *Coordination* [coordinates flight test activities], *Maintenance* [coordinates prototype configuration and maintenance], *Instrumentation* [coordinates installation and configuration of data acquisition systems] and *Ground-Station* [processes and stores flight test data].

These areas have major roles in the certification process and they interact before and after the new aircraft is formally certified. Each of these areas conduct internal *processes* and tries to keep them under control. Each *process* consumes and produces *Information*, and very frequently information produced by a process in one particular area is consumed by other process in a different area. How this information flow is maintained is the key factor for the efficient use of *Database Engineering* solutions.

Certification Repository (Figure 1)

Certification interprets FAR and JAR requirements and lists which ones are applicable to the new aircraft. These specific requirements need to be verified by one or more Means of Compliance, one of them can be Flight Testing. *Coordination* needs access to specific requirements selected by *Certification* that are to be verified by means of a test flight.

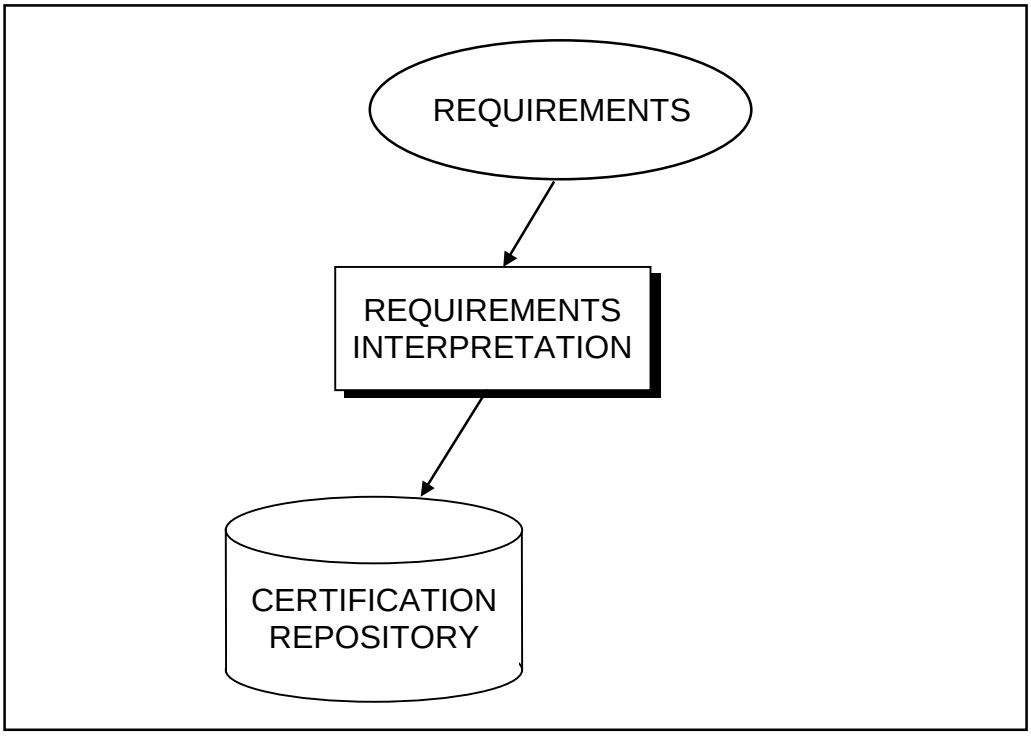

Figure 1

Coordination Repository (Figure 2)

Coordination can draw lots of useful Information from *Certification Repository* and plan the Flight Test Campaign over time. It can break down flight test requirements into small tasks and assemble them into flight scripts that will be carried out in a series of test flights.

Coordination can also determine what parameters will be measured and what aircraft prototype configuration will be required to produce proper flight test results for later compilation. Flight test results are the most basic substance used to produce reports for the Certification Authority.

During a test flight, information about every task performed -- perhaps initial and final test conditions and associated mission time -- is gathered and stored in *Coordination Repository* for future reference.

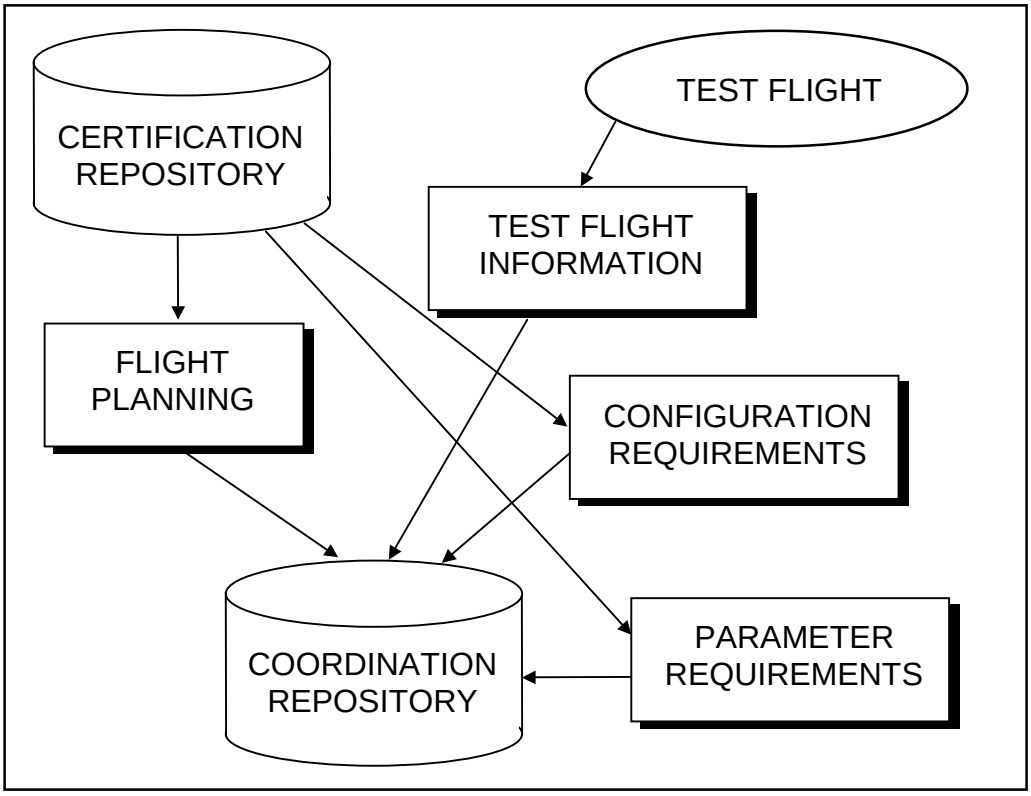

Figure 2

Instrumentation Repository (Figure 3)

Instrumentation needs to plan the installation and calibration of transducers, which will be wired to one or more data acquisition systems designed to match parameter measurement requirements stored in *Coordination Repository*.

It also needs to account for changes in the Instrumentation Configuration and keep a historic record for future reference. These changes need to be reported back to *Coordination*, giving them a chance to modify or adapt measurement requirements as the Flight Test Campaign progresses.

Maintenance Repository (Figure 4)

Similarly to *Instrumentation*, *Maintenance* needs to incorporate engineering changes to the new aircraft prototype as they get released and report them back to *Coordination*, which in turn has to account for any possible change in aircraft behavior.

To incorporate changes in the new aircraft efficiently, as well as to assure that the configuration needed for any particular flight will be ready in time, *Maintenance* needs to access *Coordination Repository* looking for Flight Planning information.

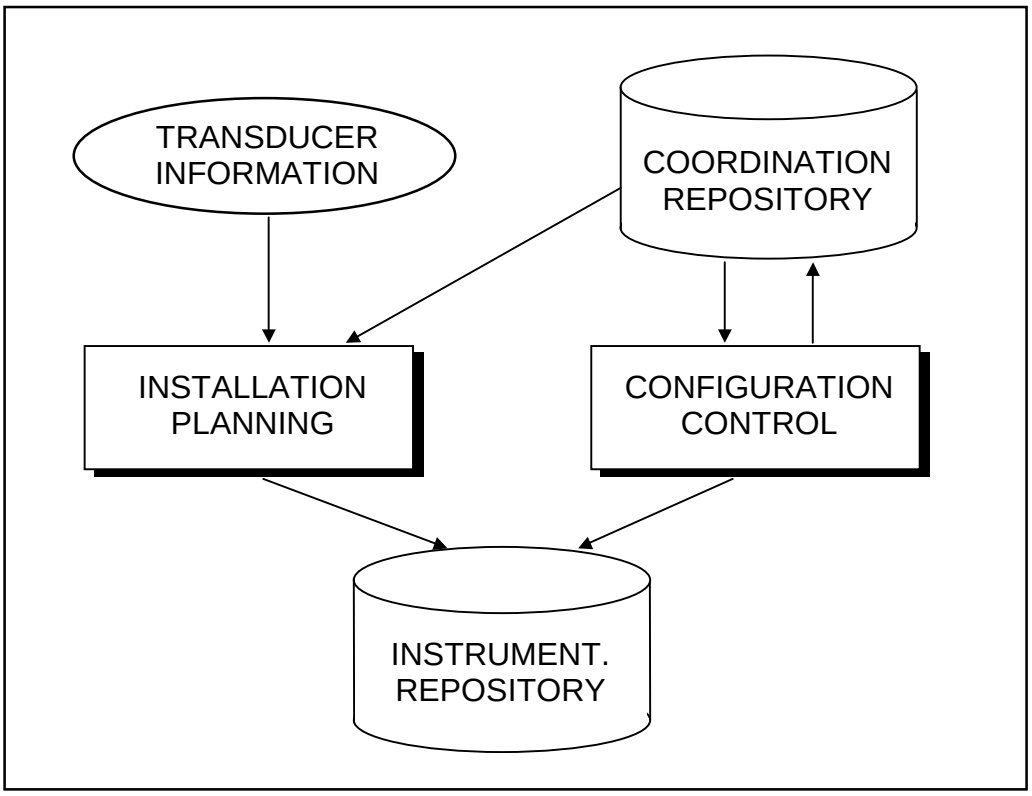

Figure 3

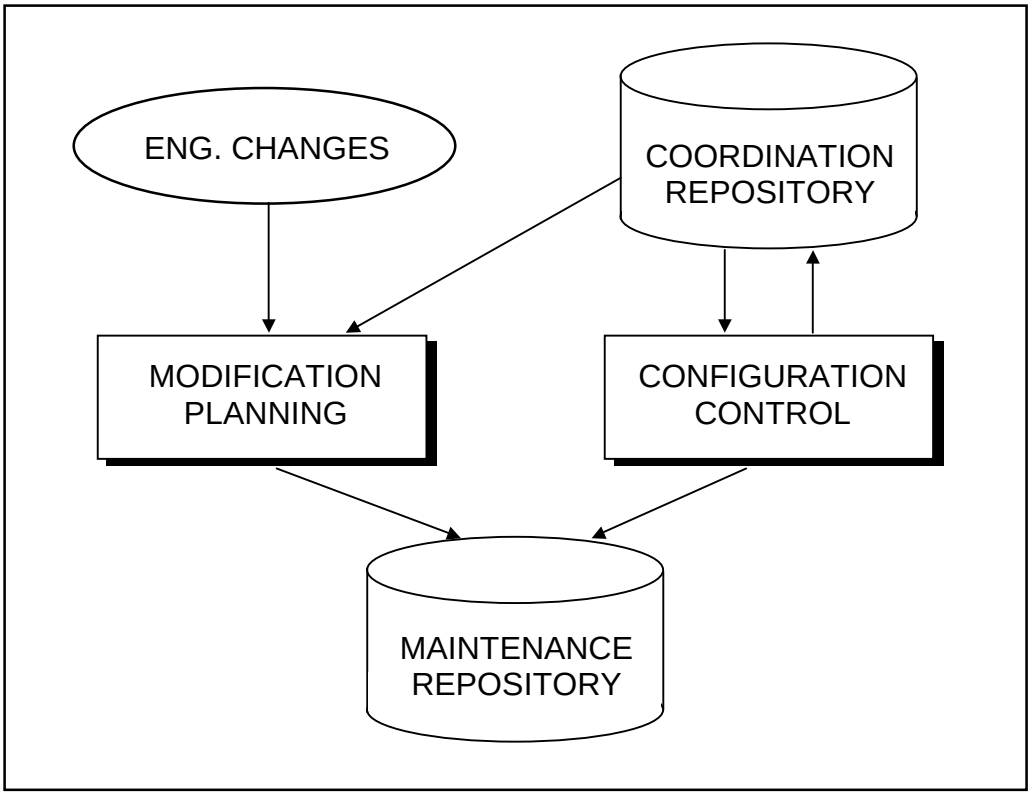

Figure 4

Ground-Station Repository (Figure 5)

Ground-Station stores and preserves all test data collected by every data acquisition systems installed in the new aircraft for all flights. It needs eventually to access the *Coordination Repository* looking for Flight Information to retrieve specific portions of a particular flight.

Since most of test data processing -- specially raw-to-EU data conversion -- is prepared in the *Ground-Station*, it also needs access to *Instrumentation Repository* looking for transducer calibration and other related data acquisition information.

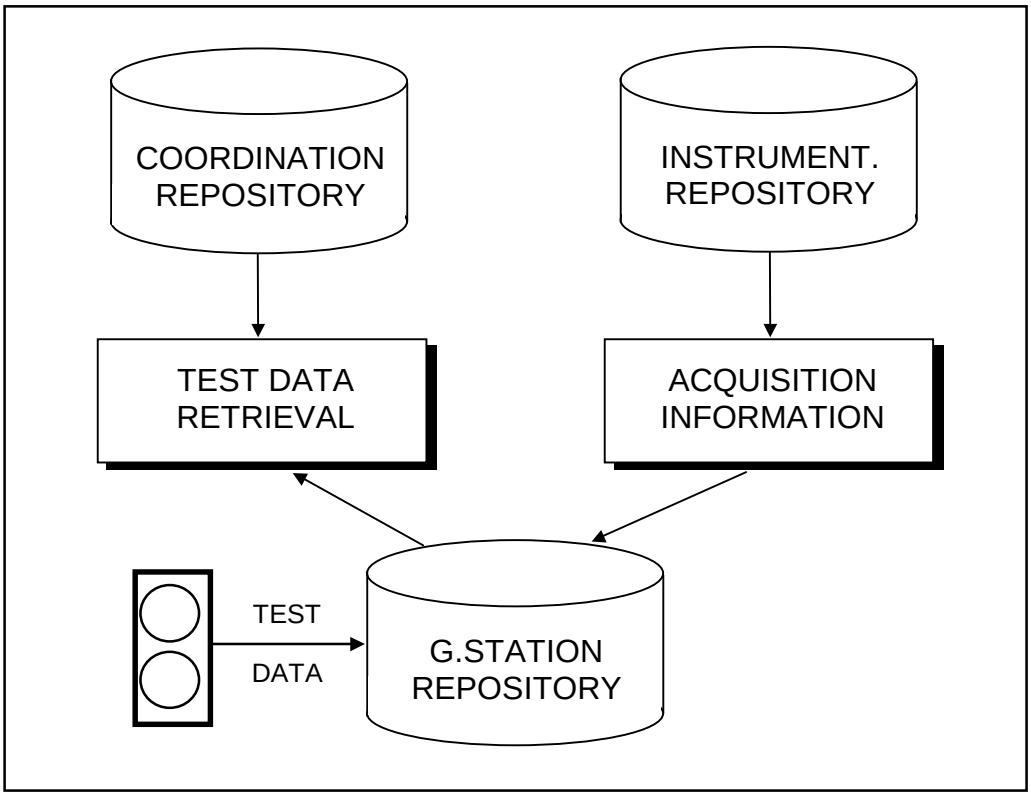

Figure 5

It may now become apparent how complex the interaction among these five areas tend to be, even if observed exclusively from a *Database Engineering* perspective.

It also suggests that dealing with this complexity is something that would require a qualified professional with skills not commonly found among Flight Test professionals.

The next paragraph will tell how much this environment can benefit from being integrated.

Building up an Integrated Operating Environment

For a regular client, a Hydraulic Systems Engineer for instance, it would be best if he does not have to know about *Flight Test Repositories*. To the manager of *Flight Test Information Systems* it is also good that the client knows little about how *Information* is actually distributed in *Repositories*, so he can maintain it transparently.

Here is where integration starts playing an important role. It is easier to "hide" a complex network of *Information Systems* if it appears to a client as coming from one system (Figure 6). This is the key feature of an *Integrated Environment*: a client can access *Information* with little or no knowledge of how it is stored or manipulated before being delivered to him.

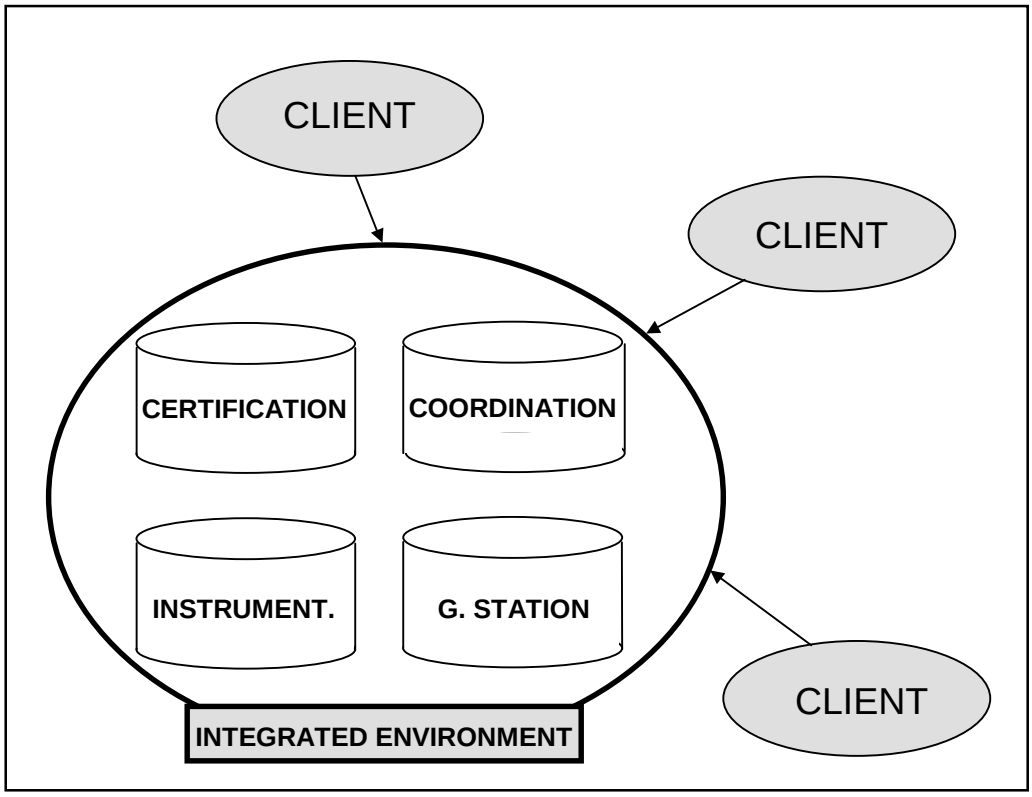

Figure 6

The first step for building up an *Integrated Environment* is to assure that all *Repositories* share a common database architecture. Most *Database Engines* respond to *queries* more or less the same way, but if all *Repositories* are created by the same *Database Engine* other benefits will appear. A somewhat larger computer system -- the *Database Server* --can be configured to hold all *Repositories* under a single *Database Engine*.

The second step is to provide a single interface to potential clients for accessing *Information* in any *Repository*. This interface can be implemented in a specialized computer system -- the *Information Server* -- which can de configured to hide information distribution to an external client. Rules for accessing and combining *Information* residing in different *Repositories* can be stored and maintained in this system, offering a single point of management of all client *queries*.

The third step is to provide every client with a tool that will handle all communication between his own computer system -- normally a desktop computer -- and the *Information Server*. In modern times, the tool most frequently found in a desktop computer is what we currently know as a *Browser*.

These three components -- *Database Server*, *Information Server* and *Browser* -- acting together in one Integrated Operating Environment (Figure 7) build an infrastructure that makes possible almost any way of storing, combining and retrieving *Information* from one or more *Information Repositories*.

The development effort required to design, implement and integrate these three components is currently facilitated because most key features (application programs and communication protocols) are commercially available. Unfortunately, customizing a graphic user interface -- and using a *Browser* makes no exception to the rule -- still needs to be done by hand, although there are many commercial tools that would do most of the hard work for the programmer.

The only design task required from a potential user of this concept is the modeling of all intended interaction between producers and consumers of *Information*, activity best conducted by skilled professionals working in tight integration with the group that wants to benefit from this Integrated Operating Environment.

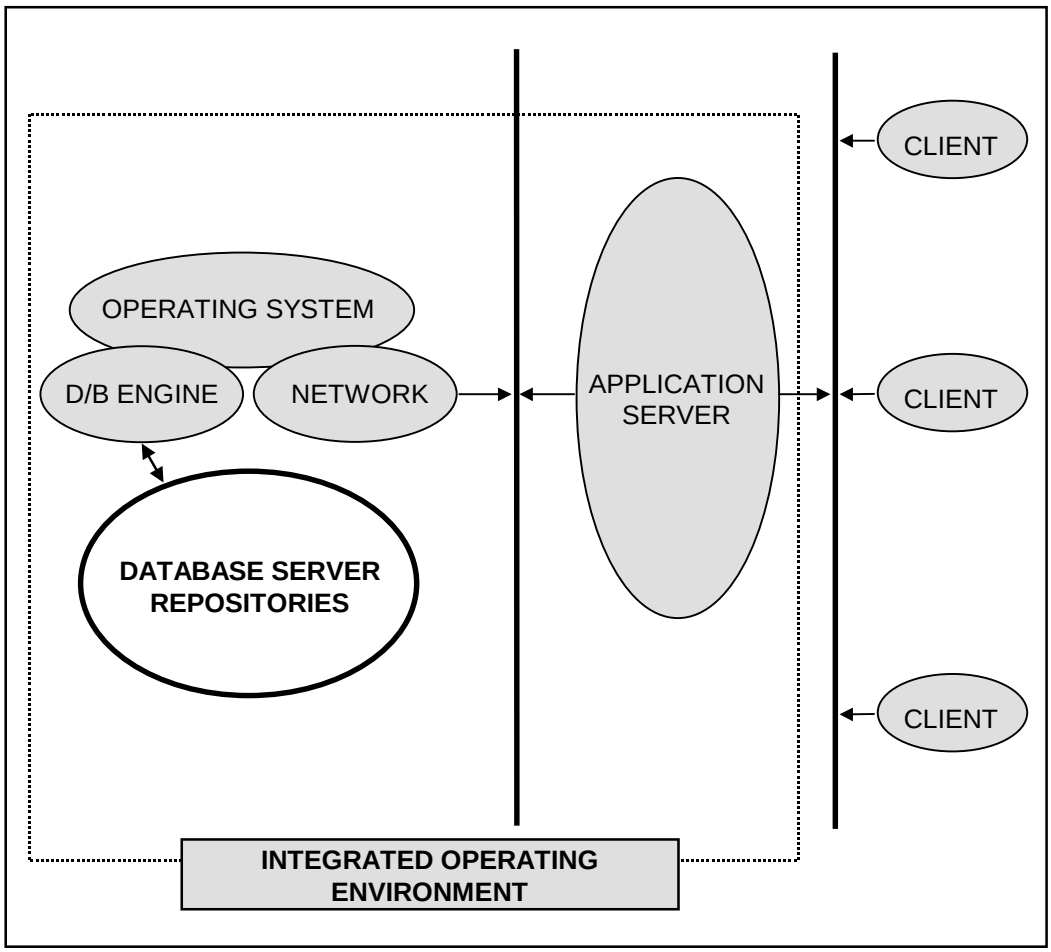

Figure 7

Benefits

Integrating *Information Systems* in a Flight Test environment can result in a number of benefits:

- *Information* can be stored once and propagated to all potential consumers automatically. For instance, a measurement parameter created as result of a Requirements Interpretation done by *Certification* may first appear to *Instrumentation* as a request for purchasing a new transducer.

- *Information* can be checked for consistency before it is permanently stored. For instance, *Instrumentation* cannot use the same transducer for two different measurements in the same flight.

- *Information* can be combined and merged into "new" Information. For instance, combining Information stored by *Coordination* and *Instrumentation*, a table of measurement parameters which were less frequently requested during the Flight Test Campaign can be built and used for *Instrumentation* cost trimming in the next campaign.

Further, this Integrated Operating Environment can help making the Type Certification process more consistent, forcing areas involved to plan ahead and understand each other's part deeper in detail.

Conclusion

In the previous paragraphs it was said that *Coordination* benefits from Information stored in *Certification Repository* when planning the Flight Test Campaign over time. Let us assume that now *Certification* wants *Coordination* to update the *Certification Repository* marking all requirements that had been already covered by test flights, so progress can be more easily reported to the Certification Authority.

To implement such request a certain amount of computer programming hours must be spent in reconfiguring database tables and redesigning user interfaces. In an Integrated Operating Environment implementing new client requirements can be facilitated, but the spending of manpower under these circumstances will never be eliminated.

Correct understanding of how *Information* is manipulated by areas involved in any particular process should be sufficient for avoiding most non-planned computer programming activities. It is important to recognize that a superficial study of processes will never provide subsidies for a good *Data Modeling* and will seldom result in benefits to the organization.

The concept of an Integrated Operating Environment applied to Flight Testing can be used to maintain control over the Type Certification process, specially if having it completed on schedule means more aggressive time-to-market for the new product.

References

[1] Pressman, R. S., *Software Engineering - A Practitioner's Approach*, McGraw-Hill, 1992

[2] Date, C. J., *An Introduction to Data Base Systems*, Addison-Wesley, 1986

[3] Chen, P., *The Entity Relationship Model - Toward a Unified View of Data*, ACM Transactional Data Base Systems, March 1976

Keywords

Flight Testing, Type Certification, Information System, Information Repository, Database Engine, Database Query.

Airborne network system for the transmission of reconnaissance image data

Dirk-Roger Schmitt[a], Heinrich Dörgeloh[a], Ingo Jessen[a], Kai Giese[a], Jürgen Tetzlaff[a]
Jochen Fries [b], Siegfried Kleindienst [c],

[a] Deutsches Zentrum für Luft- und Raumfahrt (DLR)
Institut für Flugführung
Braunschweig, Germany

[b] Deutsches Zentrum für Luft-und Raumfahrt (DLR)
Institut für Methodik der Fernerkundung
Weßling, Germany

[c] Forschungsinstitut für Optronik und Mustererkennung (FOM),
Tübingen, Germany

Abstract

Airborne network systems to transmit reconnaissance data from UAVs have been investigated. An airborne experimental system has been developed as testbed to investigate different concepts of the communication between UAV sensor platform, relay platform and ground station. It is based on an Eurocopter BO 105 helicopter and a Dornier DO 228 aircraft. The helicopter is utilized as sensor platform and is equipped with an IR video sensor. It has been demonstrated that video reconnaissance images can be transmitted through a distance of 500 km using the relay platform.

Introduction

There is an increasing demand to develop reconnaissance systems which are based on Unmanned Aerial Vehicles (UAVs) with online data transmission [1]. An UAV as used in a reconnaissance task gathers information from a hostile area and transmits it to a ground station, possibly under jamming conditions. The information is collected by different types of systems, i.e. infrared (IR), electrooptical (E/O) [2] or for example synthetic aperture radar (SAR) sensors. Also multispectral sensor suites are used. Transmitted images are processed and displayed for military reconnaissance observers for evaluation and target detection. Especially networks of Unmanned Airborne Vehicles (UAVs) with realtime jam resistant data transmission capabilities are of high interest to support the battlefield surveillance. The networks consist of sensor platforms as well as of transmission platforms which are used as relay stations for the information distribution.

System Overview

Objective of the developed airborne experimental system is to investigate a network consisting of a reconnaissance UAV and an UAV relay for data transmission. It should be capable for the study of different concepts of the communication between sensor platform, relay platform and ground station. The principle is shown in Fig 1.

The flying platforms are based on an Eurocopter BO 105 helicopter and a Dornier DO 228 aircraft. In this case both are used to simulate the operations of UAVs. The technology has been described earlier [3]. The helicopter is utilized as sensor carrier and is equipped with the Heli Tele sensor platform. It consists of an IR sensor which is mounted on a two axis stabilized platform. The sensor itself delivers images in CCIR format. The image data are coded and compressed using a wavelet codec. After that, canal coding is done using phase shift keying (PSK) modulation. The RF is then transmitted through the directional antenna 1 from the helicopter to the aircraft, which is used as relay. The band used for this transmission is in the 2.3 GHz range. Reception of data at the aircraft is also done through a directional antenna. In the aircraft receiver the PSK signal is demodulated.

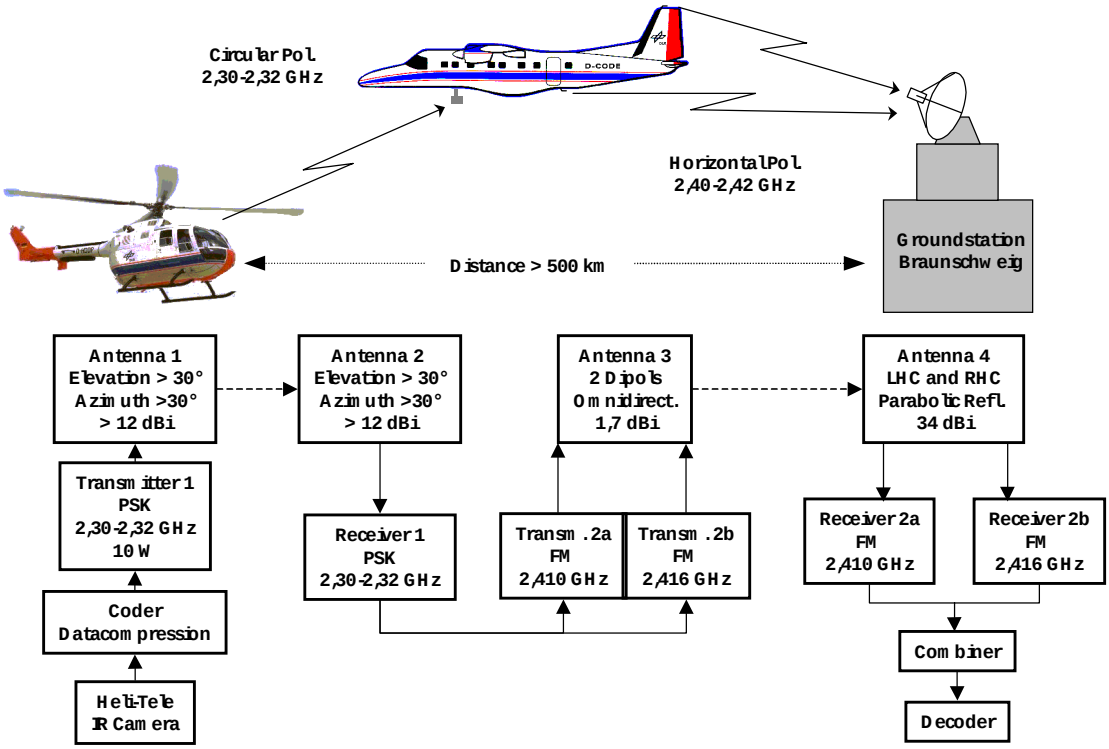

Fig 1: Principle of the relay based UAV reconnaissance network

The transmission from the aircraft to the ground station is performed by two omnidirectional antennas in frequency diversity. I.e. the signal is split to two transmitters which modulate in FM and which operate at 2.38 GHz and 2.40 GHz, respectively. The omnidirectional antennas are used instead of a directional type for cost reasons. By use of two antennas in frequency diversity it is possible to overcome problems of the non homogeneous antenna radiation pattern which is due to the influence of aircraft geometry.

The helicopter transmitter power is 17 W, where the two transmitters of the aircraft have 10 W each.

At the groundstation the signal is detected by a directional parabolic antenna. To be able to receive signals independently from the polarization which is influenced by the aircraft orientation, left hand circular (LHC) and right hand circular (RHC) polarization

components are detected. Afterwards both channels are demodulated and then processed by a combiner to one signal again which is decoded to the IR video image.

The position of the two flying platforms is determined by differential GPS systems which also transmit the position data via a data link (Global Position & Communication System, GP&C) [3]. Using this information the directional antenna of the aircraft and the helicopter are tracked.

The IR image data of the helicopter platform have been compressed to a rate of 1 Mbit/s. Taking the data stream of the original video image of 80 Mbit/s into consideration, the compression ratio comes to a value of 80. After that 1 Mbit/s was added again to the data stream for forward error correction. So totally a rate of 2 Mbit/s was transmitted by the system.

Experimental Results

To determine the performance of the system, several flight tests have been conducted. The relay aircraft was flying at an altitude of 25,000 feet, whereas the helicopter was hovering between 300 feet and 3,000 feet and was gathering IR video images.

The bit error rate (BER) versus the distance was measured by the way that the aircraft was flying outbound from the helicopter platform until the data link was nearly interrupted, then turned and flew inbound back. The results are shown in Fig 2 separately for outbound and inbound flight. It clearly can be seen that the BER remains very stable in the range of less than 10^{-7} with some peaks up to 10^{-6}. At a distance of 250 km the rate jumps up to 10^{-2} until the link is interrupted. This is clearly due to the loss of the line of sight condition between the platforms. This experiment shows that the data links between helicopter and aircraft as well as between aircraft

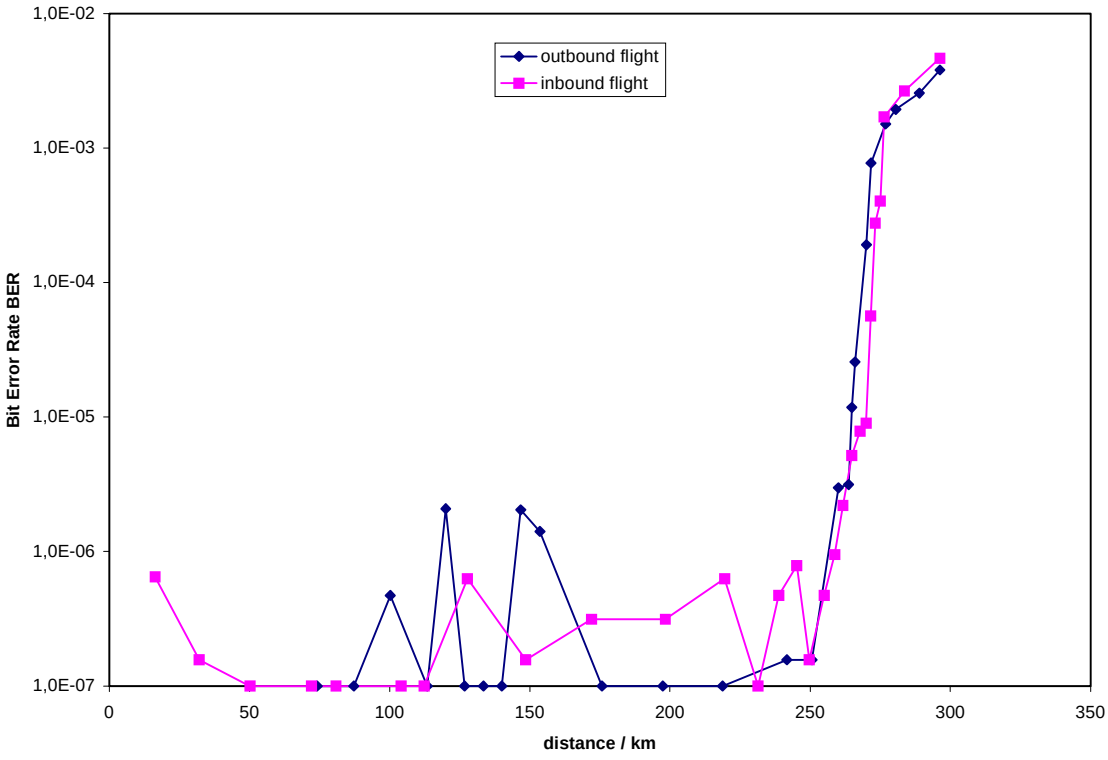

and ground station perform very well up to a distance of 250 km which is the line of sight limit. This gives the whole system in total an operating distance of 500 km.
Fig 2: Measurement of the bit error rate (BER) vs. distance

Conclusions

It has been demonstrated that it is possible to handle the operations for a relay based reconnaissance system for real time image data transmission up to 500 km distance. The operational scenario as well as the subsystems of sensors, coders, directional antennas, and ground station performed very well. The IR image was transmitted with a bitstream of 2 Mbit/s which gave acceptable results. The tested equipment is qualified for implementation to future UAV reconnaissance systems as well as the test suite demonstrated the feasibility for the validation of upcoming UAV and reconnaissance technologies.

Acknowledgements

Part of the work was funded by the German Ministry of Defense. Special thanks to the DLR flight test crew for their work under harsh experimental conditions.

References

[1] J. Wilson, "A bird's eye view", *Aerospace America* **34,** pp. 38-43 (1996)

[2] R. Sandau, D. Oertel, H. Jahn, I. Walter, “Weitwinkel-Stereokamera WAOSS – Konzept und Arbeitsweise” *Bild und Ton* **45**, pp. 224-230 (1992)

[3] D.-R. Schmitt, H. Dörgeloh, H. Keil, Wilfried Wetjen, “Airborne system for testing multispectral reconnaissance technologies” in: *Acquisition, Tracking, and Pointing XIII*, M. K. Masten, L. A. Stockum, eds., Proc. SPIE **3692**, pp.51-63 (1999)

An Object-Oriented Software Tool for Instrumentation System Setup and Configuration

Daniel M. Dawson
Thomas B. Grace

Veridian Systems Incorporated
CAIS Program Office, NAWC
California, Maryland, U.S.A

Abstract

Object-oriented software development techniques have become accepted throughout the commercial software development industry over the past several years. As a result, these techniques are starting to become visible within the military and commercial flight test markets. This paper addresses the development of a software system that is specifically designed to exploit the inherent technologies and benefits behind object-oriented software. It also discusses how a component-based software system can support various vendor hardware platforms while providing a common graphical user interface and permitting continuous additions of new hardware elements at installed sites.

Introduction

The Department of Defense (DoD) has developed a Common Airborne Instrumentation System (CAIS) through a Tri-Service Program office to promote standardization, commonality, and interoperability among aircraft test instrumentation systems. The CAIS architecture provides a standard interface bus that can be supported by multiple vendors. The use of CAIS allows the government to maximize the use of existing inventory, minimize investment costs, reduce operational costs, and provide the ability to maximize productivity. The DoD has completed the CAIS hardware development phase of the project. Multiple hardware vendors now provide CAIS-compliant hardware products, and the U.S. Navy has formally selected CAIS as its core instrumentation architecture.

In 1999, the U.S. Navy selected Veridian Systems' OMEGA-IES software as the baseline software environment to provide the setup and control of its CAIS systems. OMEGA-IES software provides customers with the ability to incorporate the hardware from multiple CAIS vendors into a single installation while utilizing a common support tool. Prior to OMEGA-IES, meeting test article requirements was defined and limited by vendor hardware. As a software tool, OMEGA-IES eliminates this restriction and enables the user to design an instrumentation system that best meets the requirements of the test article regardless of the hardware vendor.

OMEGA-IES is an object-oriented software tool that provides users with a platform for configuring and controlling CAIS hardware. Developed under a joint venture between Veridian Systems and Teletronics Technology Corporation (TTC), this software tool was initially designed to support TTC's line of instrumentation hardware; however, the component-based design of OMEGA-IES facilitated the inclusion of software components to program other vendor hardware. In addition, this software seamlessly integrates with Veridian's OMEGA-NT telemetry acquisition, processing, and display software and Series-3000 PCI-based telemetry processing systems. The combined systems offer the airborne instrumentation engineer a single software/hardware environment for end-to-end development of instrumentation configurations and ground checkout and processing.

Component Object Module

Microsoft's Component Object Model (COM) provides a software architecture that allows components from different software vendors to be combined in a variety of applications. COM defines a standard for component interoperability that is not dependent on any particular programming language and is supported across multiple platforms. The COM approach can also be extended to a distributed COM environment to support communications among objects on different platforms; e.g., local area networks. In a COM environment, applications interact through a system of interfaces. The interface system is simply an agreement between software components based on a set of methods, which are a set of semantically related operations used to define the expected actions and tasks of the interface.

The advantage of the interface is that it facilitates a spiral development process that rapidly demonstrates the functionality within an application. This enables both vendor and customer to benefit by the early validation of requirements and thereby reduces the risk of missing capabilities and integration difficulties associated with the new functionality. This compels the developer to not limit the choices in component designs and to remain flexible in trading off functionality across components until the components are verified and integrated. The component approach allows customers and vendors to add additional functionality from other component developers as well. This ability to plug-in components offers a significant advantage to the user.

OMEGA-IES Software Description

The OMEGA-IES software consists of a Configuration Manager window that enables users to select CAIS chassis and associated I/O modules to create a mission-specific hardware configuration. Figure 1 shows the initial (blank) screen that a user sees when instantiating the OMEGA-IES software. Note that in this case, the user has registered chassis and card-level components produced by Teletronics Technology Corporation.

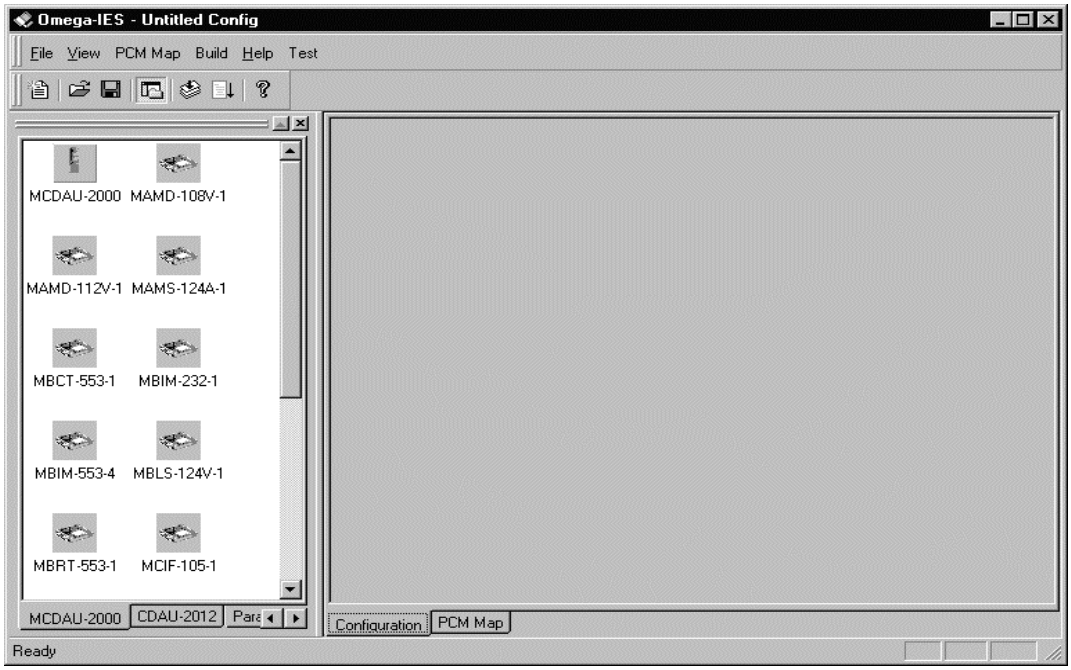

Figure 1. Initial Screen

In figure 2, the user has selected a master chassis. This is accomplished by dragging and dropping the icon that represents the chassis (in this case an MCDAU-2000) onto the configuration manager's workspace.

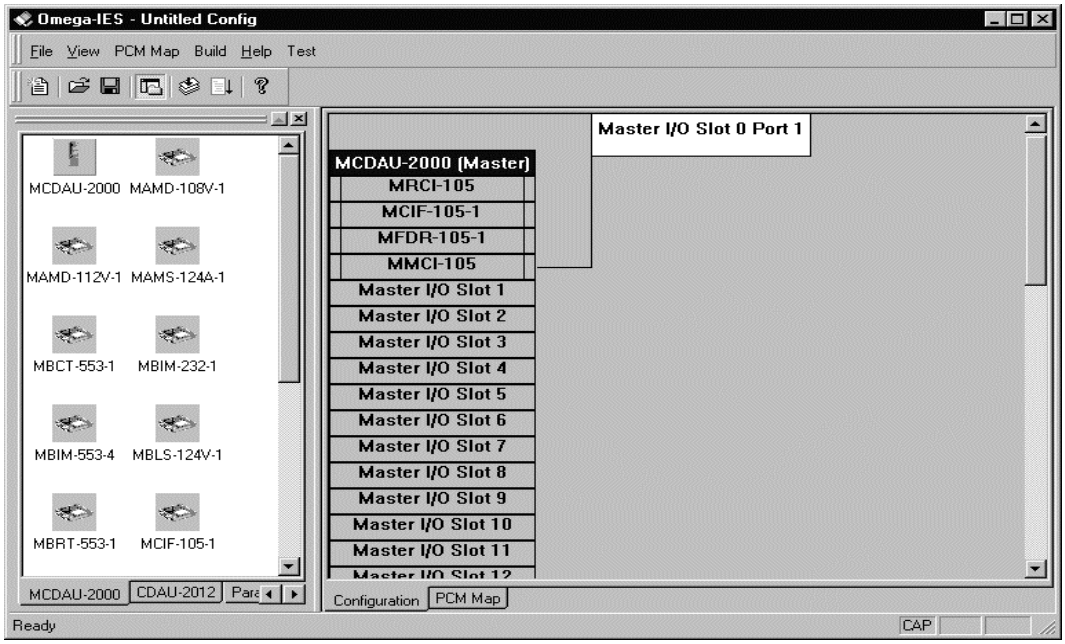

Figure 2. Example Showing Master Chassis Selection

When all master and remote chassis have been added to the configuration workspace, the user selects individual card-level components and adds them to the appropriate chassis, again using the drag and drop method. Figure 3 shows the master chassis populated with several I/O cards.

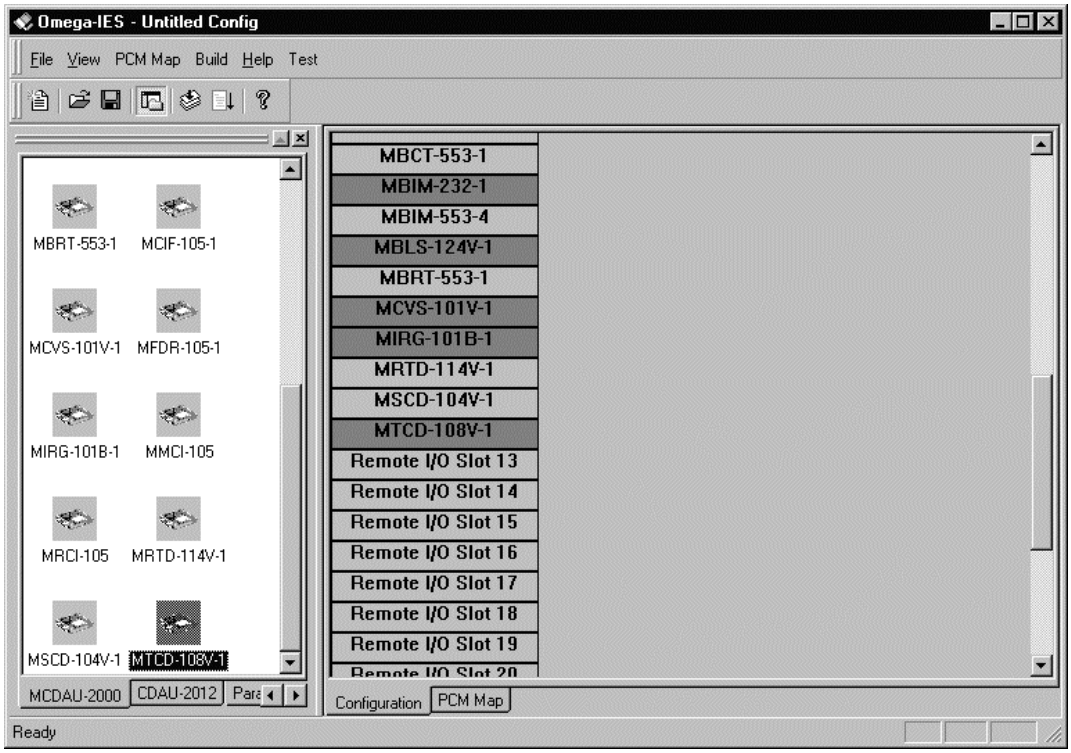

Figure 3. Master Chassis Screen Populated with I/O Cards

Individual I/O card components include their own setup forms. The user selects individual cards to access their setup forms by right clicking the mouse. An example of a typical card-level setup form is shown in figure 4.

After all I/O cards are configured, the OMEGA-IES software allows the user to create a PCM map and to populate the MAP with previously created parameters. Figure 5 shows the OMEGA-IES Configuration Manager exposing the parameter explorer and the PCM map template. The user simply drags and drops parameters into the PCM map in the appropriate location. This manual process is complimented by an automatic PCM format generation capability. When the PCM map has been created, the OMEGA-IES software automatically produces the setup files for Veridian Systems' Series-3000 Telemetry Ground Processing system as well as an IRIG-compliant Telemetry Attributes Transfer Standard (TMATS) setup file.

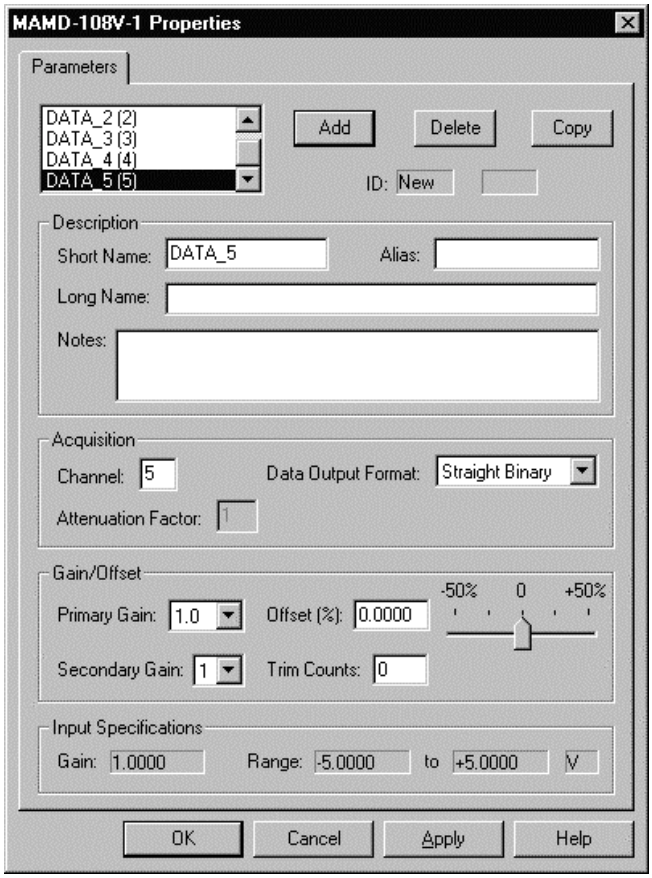

Figure 4. Example of a Card-level Setup Form

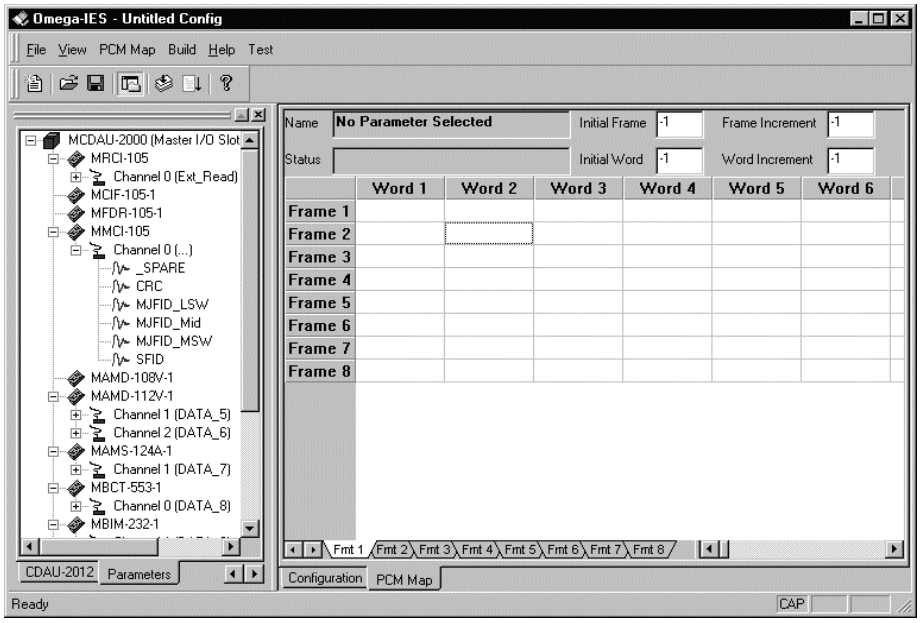

Figure 5. OMEGA-IES Configuration Manager Screen

OMEGA-IES Calibration Capability

The OMEGA-IES tool provides an integrated end-to-end calibration capability that uses the decommutation and processing capabilities of Veridian Systems' Series-3000 Telemetry Ground Processing system to acquire samples of parameters and to calculate polynomial coefficients. The calibration software provides polynomial order minimization, generates ACSI files and graphical transducer calibration curves, and automatically updates the project database. Figure 6 shows the main OMEGA calibration form.

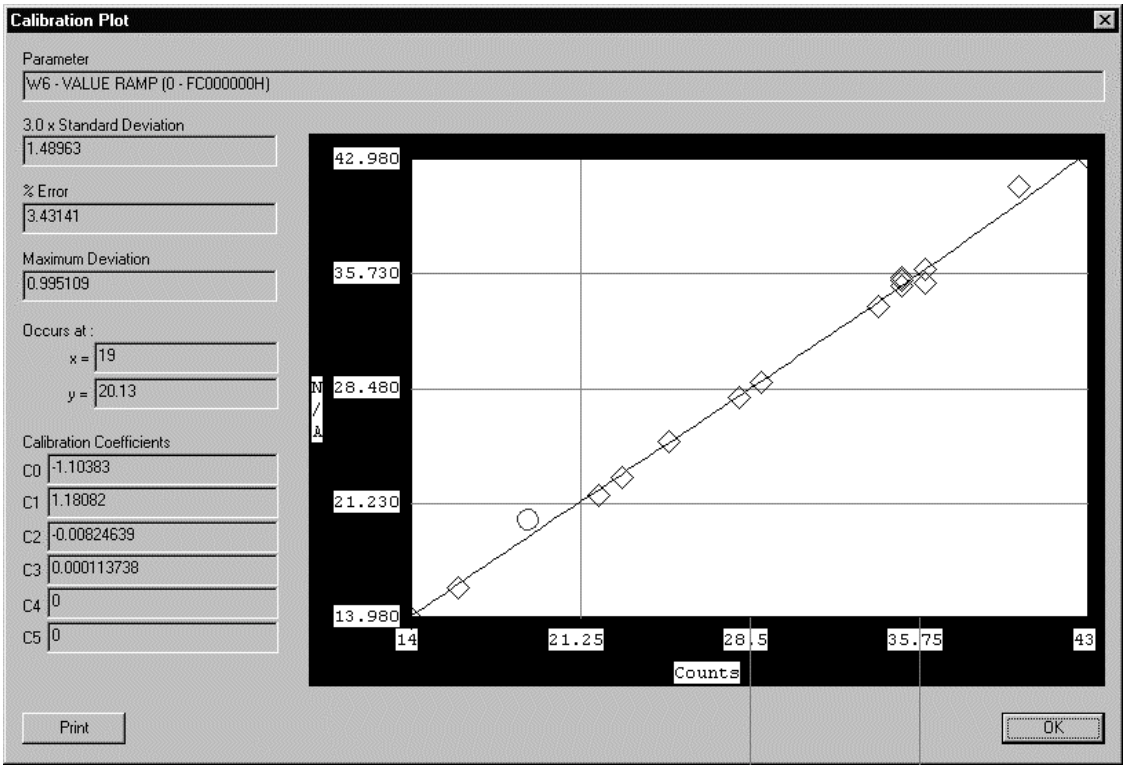

Figure 6. Main OMEGA Calibration Form

Component Standard

The OMEGA-IES product provides a common software platform for configuring CAIS modules developed by multiple vendors. Veridian Systems' decision to publish the component developer's specification provides an open environment that enables any CAIS hardware provider to develop software components that will install and operate within the OMEGA-IES environment. This allows a user to select hardware based on capability rather than being limited in hardware selection based on the user's limited support environment. This places the responsibility on the hardware vendor to provide

the software component for the items being procured. This means that when DoD procures a specific hardware instrumentation product, the software component/driver will be delivered with the hardware, which effectively guarantees rapid integration and minimizes startup costs.

Conclusion

OMEGA-IES software gives users an intuitive graphical user interface that remains unchanged as new signal conditioning modules are developed and added to their systems. A corresponding software component that provides all required setup and control interfaces must accompany each new hardware module (card or chassis). Under this scheme, OMEGA-IES software acts as a fixed framework that compliments the development of CAIS hardware modules.

MOdular Networked TArGet control Equipment

(MONTAGE)

A New Generation of Target Control Systems

Peter Austermann

Micro Systems, Inc.
35 Hill Avenue
Fort Walton Beach, FL 32548

ABSTRACT

A New Generation of Target Control Systems

MONTAGE is a new 'building block' approach to target vehicle command and control systems. With MONTAGE a user can custom configure a target control system based upon his specific needs and requirements. MONTAGE can be easily upgraded in the field to meet new requirements.

Montage uses a modular, open architecture allowing multiple independent data links, multiple target vehicles, and tracking pods to be used simultaneously. A system can be configured for a single target and data link, and later upgraded in the field to simultaneous multiple targets and data links.

MONTAGE system components include a System Controller, one or more Target Control Consoles, one or more RF Modules, and one or more Range Interfaces. Additional components can be added to the system and are automatically recognized by the System Controller in a 'Plug and Play' environment.

MONTAGE is currently available configured for the BQM-34, BQM-74, MQM-107, and QUH-1 aerial targets. Other targets can be accommodated with minimal effort.

MOdular Networked TarGet Control Equipment
System Description

1.0 INTRODUCTION

This paper describes the MOdular Networked TarGet Control Equipment (MONTAGE) aerial target command and control system. MONTAGE represents a modular systems approach to aerial target command and control using distributed processing functions to allow the user to configure the required capabilities of the system by adding 'building blocks.' Use of such building blocks enables the user to configure a system to meet his specific needs, yet is expandable in the field to meet new requirements. MONTAGE is target, data link, and range independent.

2.0 GENERAL DESCRIPTION

MONTAGE is a multiprocessor network as shown in Figure 1.

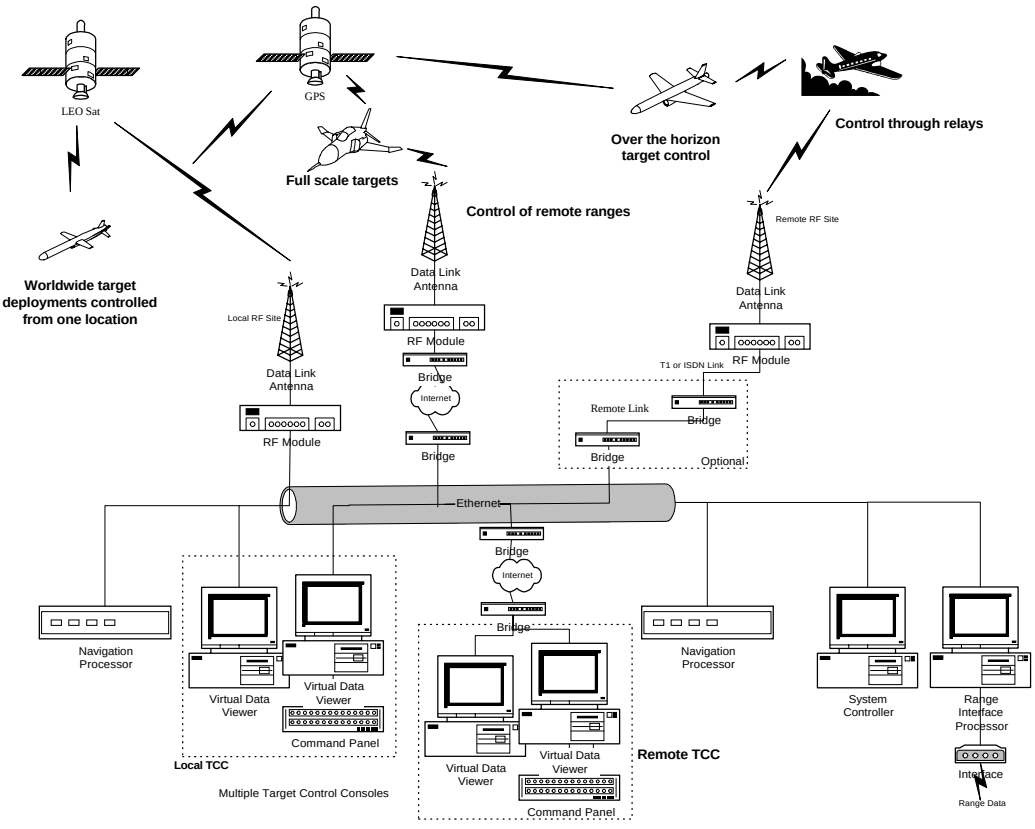

Figure 1. MONTAGE System Diagram

As shown in the figure MONTAGE is a local area network of distributed processing functions. Available functions include:

- System Controller
- Target Control Console(s)
- Radio Frequency (RF) Module(s)
- Navigation Processor(s)
- Range Interface Processor(s)

All processors interconnect on a common Ethernet bus using the open Transmission Control Protocol/Internet Protocol (TCP/IP) protocol. This open architecture design readily accommodates the addition of new, yet to be defined modules in the future as well as additional Target Control Consoles, RF Modules, Navigation Processors, and Range Interface Processors. Each processor registers itself to the System Controller as an available resource as it comes on line.

MONTAGE offers several unique advantages including:

- True open architecture design
  - Reliable Windows NT Operating System
  - TCP/IP communications between units
- Ability to physically remote consoles and modules via a bridge or router
- No major development efforts (low risk)
- Current design in service with U.S. Navy
- Upgrades performed for U.S. Navy readily incorporated into other MONTAGE stations
- Ability of a target to function as a relay
  - Decreased dependence upon manned aircraft to support missions Ability for relay to fly into lethal zone
- High performance
  - 10 Hertz (Hz) Command and Control Rate (Direct Mode)
- Substantial growth capabilities
  - Open Architecture of MONTAGE easily accommodates additional nodes to network
  - Substantial spare processing capacity in computers for functions such as waypoint navigation
  - Substantial spare processing capacity in airborne transponders for future capabilities such as autonomous waypoint navigation.

Hot Backup Target Capability

Ability of system to have a backup target ready to launch during a mission

Improved probability of mission success

Multiple Redundancy

Any Target Control Console can function as a backup for another Multiple RF Module Capability

System can accommodate multiple RF Modules

RF Modules can be used simultaneously

User selectable operating frequency

Fully synthesized data link transceivers

User can change operating frequency for different locations

2.1 Detailed Description

2.1.1 System Controller

The System Controller (SC) coordinates and controls all system functions. As the other consoles come on line the 'register' themselves with the SC as an available resource, in a 'Plug and Play' fashion. The SC can then assign a Target Control Console to a particular target vehicle through a selected RF Module, and even a selected transceiver within a selected RF module. This flexibility allows the SC to use available Target Control Consoles and RF Modules as backups for redundancy. A second SC can be added for full system redundancy.

The System Control Console (SCC) interfaces with the other computers of the system via the Ethernet interface. This processor performs the communications with the target vehicles (through the RF Module), then collects/disseminates the data to/from the appropriate consoles at a 10 Hz rate. The console Cathode Ray Tube (CRT) displays the status of the data link to/from each target, as well as the general status and health of the transceivers in the RF Module.

The following data is displayed on the System Control Console:

- Transmit power status (GO/NO-GO)
- Relay/Direct Mode switch status

  Direct to target or through relay to target
- Results of RF link monitor

  A low power RF Radiation Monitor samples the RF transmitted by the system and verifies proper power output. It is also capable of transmitting a time delayed downlink to simulate a vehicle to verify RF link integrity.

- Loss of carrier indication for each controlled target and relay
- Address and type of each target

The SCC processor sets the mode of the system as pre-mission, operate, playback, or diagnostics. It also performs the data reduction and analysis task. All data is recorded by the SCC, time tagged with Global Positioning System (GPS) data. All uplinks are synchronized to GPS time.

2.1.2 Target Control Console

Each Target Control Console (TCC) consists of two Pentium computers and color graphics monitors. One computer is dedicated to display of the target vehicle on a range map. The other computer is dedicated to telemetry display and command encoding. All interconnected via Ethernet. A Micro Systems, Inc., produced command panel with an electronically pitch-locking joystick is provided for target operator inputs (pitch, roll, throttle, payloads, etc.).

2.1.2.1 Map Display Processor

The map display is based on a Pentium processor executing Commercial Off the Shelf (COTS) Intergraph MicroStation software. The MicroStation software package supports custom application programs which facilitates adaptation of MicroStation for specific applications. In this case a Micro Systems, Inc., produced program provides the functionality to operate as a map display. This package is currently in use with the C-Band Target Tracking Control System (TTCS) at North McGregor Range, Ft. Bliss, TX where applications programs have been developed, tested, and placed into day-to-day operation to support real-time map display and target position plotting. It is also currently being used in the Over The Horizon Target Control System (OTHTCS) system at Atlantic Fleet Weapon Training Facility (AFWTF). The map display provides the following features and capabilities:

- Display of multiple vehicle tracks and plans
  - Four tracks from MONTAGE and up to 24 external tracks as input from range
- Stationary or moving map display
- User selectable target icon size
- Heading display (using delta position) indicated by icon direction
- Real-time zoom (scale factor changes) with on-screen mileage scales
- User selectable target trail options
- User specified event and waypoint markers
- On-screen range and bearing indicator between user-specified points

- Real-time element (planned track) move and rotation
- On screen display of altitude, ground speed, total mileage flown, and) bearing/range to target from specified point (similar to range displays
- User definable attributes such as:
  - Color
  - Line width
- User entered or computer scanning of maps
  - Coastlines
  - Elevation contour lines
  - Map cultural data
  - Range boundaries
- 10 Hz display update rate
- User entered planned tracks
  - Waypoints
  - Target vehicle
  - Selected participants

2.1.2.1.1 Map Entry

Maps can be readily input to the system through several sources. The most straightforward method is to enter the map manually, using the touchpad to manipulate the cursor and apply attributes (color, width, layer selection) as appropriate. Another method includes scanning of monochrome maps using a blueprint type scanner, then performing raster to vector conversion using the software package Mapping Office from Intergraph.

The final output product of either of the above methods is a MicroStation Design (DGN) file. This is the file used for map display. This flexibility for map entry enables the user to quickly deploy to a site and enter a simple map (range boundaries, points of interest, etc.) in the event professional maps are not readily available.

2.1.2.2 Telemetry Display Processor

The Telemetry Display Processor is based on an identical (to the Map Display processor) Pentium computer. An off-the-shelf software package from Global Magic Software, Inc. is used to display the aircraft telemetry using realistic appearing instruments.

The aircraft instrument displays are augmented by indicator displays (On/Off) and bar graph displays which indicate the values of discrete and proportional telemetry, respectively.

All displays are fully programmable as to labels, appearance, scale, and offset using the ‘Active-X’ capabilities of the Global Majic software package.

2.1.2.2.1 Telemetry Display Manipulation

The telemetry displays can be changed (prior to a mission) by the user for meter type (thermometer, dial, or aircraft instrument) label, scaling, and offset (proportional) or sense (discrete). Positions are provided on the display for several spare discrete channels.

Available indicators include:

- Airspeed
- Revolutions per Minute (RPM)
- Baro and Radar Altitude (scale below 50,000/5,000/500 feet controlled by discrete telemetry bit and an invalid indicator)
- Pitch and Roll on a aircraft style artificial horizon display
- Heading
- Estimated Fuel Remaining
- Transmit Power
- Relay Mode Switch Status
- Data Link Status
- Radar Altimeter Valid/Invalid

2.1.2.2.2 Command Panel

A command panel is incorporated into each TCC. The command panel is the target controller's interface with the target vehicle, and consists of a collection of environmentally sealed switches, rotary controls, and a joystick with an electrically enabled pitch lock. The command panel and telemetry display are optimized to minimize operator workload and piloting skills.

This panel addresses the human engineering aspects, and appears to the operator very similar to that of the Integrated Target Control System (ITCS) command panel. All controls are grouped according to function. An interchangeable overlay allow configuring the command panel for different vehicle types.

2.1.3 RF Module

A separate RF Module controls the data link to the target vehicles. This RF Module also houses the GPS reference receiver and the RF monitor/test transceivers. An embedded processor provides the communications link with the System Controller processor via thin-net (RG-58 coaxial cable) Ethernet. The RF Module is housed in a rugged RF sealed NEMA-4 chassis to protect the electronics. This NEMA-4 chassis can withstand severe weather and direct water hose-down while protecting the contents.

2.1.3.1 Embedded Processor

A Ruggedized PC compatible COTS embedded processor provides control of the data link functions. This processor uses a solid-state disk for reliable operation in harsh environments. The RF Module uses the PC/104 form factor LBC-Plus embedded processor from WinSystems. This processor module combines a 133 Megahertz (MHz) Pentium processor with an Ethernet interface, solid state disks, serial and digital Input/Output (I/O) into a single highly integrated module. A highly deterministic real-time operating kernel from Phar-Lap provides all required Ethernet and solid-state disk functionality. The RF Module functions to isolate the balance of the system from the details of the RF data link. This allows the system to operate multiple RF Modules with different data links simultaneously.

2.1.3.2 UHF Data Link Configuration

A COTS Ultra High Frequency (UHF) transceiver is used for all RF communications. The receiver is a dual-conversion superheterodyne design, with a final IF bandwidth of 20 KiloHertz (KHz), and a sensitivity of -117 decibel referenced to 1 milliwatt (dBm). The transmitter is frequency modulated and outputs 5 watts to the antenna ports. This is the same transceiver as used in the airborne transponders. For the RF Module the output is boosted by a Power Amplifier to 50 watts.

This transceiver is well suited to the intended operating environment. This transceiver is designed specifically for Gaussian Minimum-Shift Keying (GMSK) data communication by featuring extremely low group delays. It is not a converted voice transceiver. The transceiver is Federal Communication Commission (FCC), Industry Canada, and European Telecommunication Standards Institute (ETSI) compliant for data applications. This transceiver is, in fact, the only synthesized unit which meets the stringent ETSI 200.113 high-level data transmission specification.

The transceiver is a new technology transceiver with fast attack synthesizers for very fast lock times, minimal key up/down sideband noise, and superior frequency stability. The operating frequency is fully synthesized, and is selectable by the system operator. The standard operating frequency range is 435 to 450 MHz. Other frequency ranges can also be accommodated.

The transceiver is coupled to a new technology 19,200 bps GMSK modem. This modem, designed for use specifically with the transceiver, allows transmission of data with a minimum of overhead and delay, making it well suited for aerial target command and control applications.

A total of four transceivers are used in the RF Module. Two are the primary data link transceivers (one for expansion to four targets) and two are for data monitoring purposes. The monitor transceivers can also function as reply transponders to support data link integrity checks prior to a mission.

2.1.3.3 Other Configurations

Other configurations of the RF Module are available including Gulf Range Drone Control System (GRDCS) (L-Band Spread Spectrum). Future configurations will become available as new command and control data links are defined.

2.1.3.4 UHF Data Link Interface

The data link is described, in detail, in the ensuing paragraphs. The MONTAGE is designed with a maximum of flexibility, as demonstrated by the following data link discussion. Please note that the data format readily accommodates an extra target for 'hot standby' operation.

2.1.3.4.1 Uplink

The uplink is encoded and transmitted by the Ground Control Station (GCS) at a maximum rate of 15 Hz and no less than 4 Hz. The Uplink Format provides the following capabilities.

- 10 bits/byte (8 data bits + 1 start bit + 1 stop bit)
- Alternate start byte sequence allows for uplink to dedicated relay unit
- Uplink can specify a target address (0-7) to signal a transponder to act as a relay unit for the next downlink cycle
- Uplink can interrogate between zero and four targets at any time from a group of eight possible targets per frequency.
- Six bytes of command data per target
- Antenna Select Command per target
- Command Error Bit (to simulate uplink errors) per target
- GPS Radio Technical Commission for Maritime (RTCM) SC-104 Differential Corrections
- Checksum Error Detection on each message component

2.1.3.4.1.1 Uplink Processing

2.1.3.4.1.1.1 Uplink Header Qualification

In order for the airborne system to accept and decode an uplink message, the uplink message must be preceded with a valid Header. The Header (bytes 1 - 4) of the uplink message consists of the start bytes and header data (i.e., Number of Targets, Target Relay Address, and Target Relay bit) followed by the Header Checksum. The Airborne system uses the Start Bytes to synchronize to the beginning of the uplink message. In order for the Airborne system to qualify a Header (and uplink message) the following criteria must be met when reading the Header.

The start bytes = CAH, 53 Hexadecimal (H), respectively

The Header checksum (byte 4) is equal to the calculated header checksum.

If a valid Uplink Header is not qualified within 1 second the airborne system will enter Loss of Interrogation (LOI) mode.

2.1.3.4.1.1.2 Uplink Command Data Qualification

If the airborne system qualifies a valid Header, it will read the *n* Command Blocks within the uplink message (*n* = “No Of Targets” field in the Message Header). In order for the Airborne system to qualify and decode a Command Block the following criteria must be met when reading the Command Data.

The target address field of the block is equal to the target address that is set in the transponder.

The Command Checksum is equal to the calculated command checksum.

2.1.3.4.1.1.3 Uplink Command Decoding

If a Header and the following Command Data are successfully qualified, then the airborne system will decode the message only if the following condition is met:

a. Command Error bit (in the Header) is 0. NOTE: If the Command Error bit is 1, then the Command Error bit in the next downlink message is set to 1.

If the above condition is met, then the airborne system performs the following functions:

a. Command the UHF antenna switch based on the “Antenna Select” field in the uplink message.
b. Decode the Discrete Commands and command the corresponding discrete outputs to the target vehicle. The airborne system offers provisions for debouncing the selected discrete commands (i.e. Engine Kill, Drogue Deploy, etc.) for up to three messages.
c. Decode the Proportional Commands and command the corresponding analog outputs to the target vehicle.

If the airborne system does not decode valid Command Data within the time selected on the Recovery Time Out switch (1, 2, 4, 8, or 16 seconds), then the Airborne system will enter Loss Of Command (LOC) mode.

2.1.3.4.1.1.4 GPS Differential Corrections Qualifying

If the airborne system qualifies a valid Header, it will read 9 bytes of the Differential Corrections (DC) Message within the uplink message. The beginning of this block will follow the end of the last command block. In order for the Airborne system to qualify and decode the DC Message the following criteria must be met when reading the DC Message.

a. The RTCM Checksum is equal to the calculated RTCM checksum.

2.1.3.4.1.1.5 GPS Differential Corrections Processing

RTCM SC-104 Differential Corrections are read from a GPS base receiver located in the GCS and transmitted to the Airborne system in the Differential Corrections block (only 7 bytes containing DC data) of the uplink message in successive uplink messages. The maximum length of an entire DC message is 104 bytes (for 12 satellites). Therefore, up to 15 uplink messages may be required to send a single DC message. The first byte of the Differential Corrections block contains the start bit and message length of the DC message. When the first byte of a DC message is being transmitted the start bit is set to a logic 1 and the message length contains the total number of the bytes that are in the entire DC message. For each successive uplink message (till the entire DC message is transmitted) the start bit will be set to a logic 0 and the message length field will be replaced with the DC message byte number that is being sent in the first byte of the 7 byte block (Byte 2 of the Differential Corrections block) contained within the Differential Corrections block. Therefore if the DC message length is 50 bytes, then 8 uplink messages will be required to transmit the entire DC message. If a received uplink message does not qualify, then the airborne system will discard the current DC message being buffered, and wait for the next occurrence of Start Bit = 1 before buffering the next DC message. If at anytime the Start Bit is set to one before the complete DC message is read, the airborne system will discard the current DC message and begin buffering the next DC message beginning with the current uplink.

2.1.3.4.1.2 Loss Of Interrogation Mode

If a message is not qualified within 1 second the airborne system will enter LOI mode and begin switching the UHF antennas at a 1 Hz rate until it receives and successfully qualifies a message. At this point it will stop switching antennas (and remain on the current antenna) and resume normal command and control operations. NOTE: If the airborne system is in LOI mode then it is also in LOC mode. However, if it is in LOC mode it is not, necessarily, in LOI mode.

2.1.3.4.1.3 Loss of Command Mode

If the airborne system does not decode an uplink message within n seconds (where *n* is 1, 2, 4, 8, or 16 seconds as defined by the Recovery Time Out switch) then the airborne system will enter LOC mode. In this mode all outputs will remain at their last commanded state and initiate target recovery.

2.1.3.4.2. Downlink

The downlink is transmitted by the Airborne system within the appropriate downlink time slot. The downlink time slot start time is computed by the airborne unit based on the position of its corresponding command block in the uplink message. (If its command block is the first command block in the message then its downlink time slot is 1; if its command block is the second command block in the message then its

downlink time slot is 2; etc.). The duration of the downlink time slots is a function of the time required to transmit a downlink message (20.8 milliseconds (ms)) and the maximum propagation delay of the downlink transmission between the target and the GCS and/or Relay. This scheme allows all targets that were interrogated during the last uplink cycle to respond, one at a time, in their unique downlink time slot on the same frequency.

The analog and discrete telemetry encoded in the downlink message are less than 20 ms old while the GPS data is the most recent GPS position data received from the airborne GPS receiver. This guards against the receipt of 'stale' data in the event of a momentary loss of downlink.

The Downlink Format provides the following capabilities.

- 40 byte downlink message
- 10 bits/word (8 data bits + odd parity + 1 start bit + 1 stop bit)
- Relay/Direct bit
- Power on Reset, Command Error & Antenna Pos. Indication
- Receive Signal Strength Indicator (RSSI)
- GPS Time, Position, Status, Position Dilution of Precision (PDOP)
- Error Detection

2.1.3.4.2.1 Downlink Qualification

The GCS receives the message and calculates a checksum on the message bytes. The message is qualified by the system only if the following conditions are met:

a. The start bytes = ACH.
b. The relay bit corresponds to the mode of the last uplink sent. i.e. If last uplink sent was a relay uplink then this bit must be set, and vice versa for direct mode.
c. The target address of the downlink matches the target address of a target that is known to the GCS.
d. The received checksum is equal to the calculated checksum.

2.1.3.4.2.2 Downlink Decoding

If the message qualifies, then the GCS performs the following functions:

a. Decode the proportional and discrete telemetry channels.
b. Decode the GPS Time, X, Y, Z position, and PDOP/Status.

2.2 Physical Configurations

Montage is available in three configurations including fixed, transportable, and portable.

TABLE OF CONTENTS

LIST OF FIGURES

ACRONYMS

AFWTF	Atlantic Fleet Weapon Training Facility
COTS	Commercial Off the Shelf
CRT	Cathode Ray Tube
dBm	Decibel referenced to 1 milliwatt
DC	Differential Corrections
DGN	Design
ETSI	European Telecommunication Standards Institute
FCC	Federal Communication Commission
GCS	Ground Control Station
GMSK	Gaussian Minimum-Shift Key
GPS	Global Positioning System
GRDCS	Gulf Range Drone Control System
H	Hexadecimal
Hz	Hertz
I/O	Input/Output
IP	Internet Protocol
ITCS	Integrated Target Control System
KHz	Kilohertz
LOC	Loss of Command
LOI	Loss of Interrogation
MHz	Megahertz
MONTAGE	MOdular Networked TArGet Control Equipment
ms	millisecond
OTHTCS	Over The Horizon Target Control System
PDOP	Position Dilution of Precision
RF	Radio Frequency
RPM	Revolutions Per Minute
RSSI	Receive Signal Strength Indicator
RTCM	Radio Technical Commission for Maritime
SC	System Controller
SCC	System Control Console
TCC	Target Control Console
TCP	Transmission Control Protocol
TTCS	Target Tracking Control System
UHF	Ultra High Frequency

Embedded System Design with a Design Tool

Matthias Bodenstein, Klaus Alvermann, Stephan Graeber, Henrik Oertel, Lothar Thiel
DLR Institute of Flight Research
Braunschweig, Germany

Abstract

The Institute of Flight Research of the German Aerospace Center (DLR) develops software intensive real-time systems for embedded airborne systems. Based on the current development of an experimental on-board equipment for a new helicopter testbed, the Process Improvement Experiment 27751 ICARUS aims at reducing the development and maintenance effort for this embedded system. For this purpose the design tool ObjecTime was introduced. The paper describes the experiences with this software process improvement and tries to provide a base for a decision for or against the usage of a design tool in the embedded world.

1 Introduction

The Institute of Flight Research of the German Aerospace Center (DLR) operates real-time systems for on-board experiments and ground support of research aircraft. In this context, the Active Control Technology / Flying Helicopter Simulator (ACT/FHS), an EC135 helicopter, is presently being modified by DLR, Eurocopter Deutschland and Liebherr Aerotechnik to enable fly-by-wire / light operation. The objective of the ACT/FHS project is to develop an airborne helicopter testbed, which will serve the various demands of research establishments, industry, and national flight test centers. Detailed description of the baseline helicopter project and the experimetal on-board equipment from DLR can be found at [1] and [2].

The software development for the experimental on-board computers needs to meet the following criteria:

- All components of the experimental on-board computer system have to fulfil hard real-time requirements with cycle and latency times in the magnitude of 1 to 5 milliseconds and an average data throughput of about 1 MByte/s.
- Following the hardware decision for a VMEbus based system and PowerPC processors the VxWorks real-time operating system (Wind River Systems Inc.) was chosen for most computers. The software for the target computers is programmed in C. Software from external companies needs to be incorporated.
- While the hardware of the experimental system has to be qualified to match the requirements of flight approved systems, this does not apply to the software for the

experimental system, which is - due to the safety concept of ACT/FHS - not considered to be flight critical. Although the software is not safety critical, it must be highly reliable.

- The experimental system has to be designed to provide the user with the flexibility to modify, add, and upgrade experimental software and hardware. Parts of the software will change significantly over the years, there is no final product. Instead the experimental use will produce a tree of parallel software versions rather than a linear line of versions with one actual valid version.

- The software is developed and maintained by several people over several years.

Although the software is not safety critical the RTCA DO-178B standard [3] for development of certified airborne systems was chosen as guideline for the software development. All procedures are observed, with the exception of writing the documents only needed for certification. Additional criteria were taken from the internal software development standards of DLR [4] and the software engineering standards of the ESA [5] for the requirements phase. However, the method had to be adapted, since no final product is delivered. Detailed information concerning our main software development process can be found at [6].

This project is a Process Improvement Experiment (PIE) funded by the Commission of the European Communities within the European Software and Systems Initiative (ESSI). Within this project we integrated the usage of the design tool ObjecTime into our software development method. This paper will focus on the results and experiences of this approach.

2 Objectives and Expectation

Aiming at a high maintainability as well as an efficient portability to new hardware coming up during the course of the software life cycle, we started the Process Improvement Experiment 27751 ICARUS in order to better utilise our research helicopter in terms of reducing the time-to-experiment, i.e., the time needed to prepare and execute an experiment. This permanent and effective adaptation of software to different user requirements without sacrificing software quality issues is vital to achieve our business objectives.

Thus, the objectives of the Process Improvement Experiment are to significantly reduce the development time and maintenance effort for the complex, embedded helicopter system via the definition and introduction of an analysis, design, and implementation process based on software best practice methods and tools as well as on the ESA [5] and DO-178B [3] software engineering standards. In addition, significant quality improvements in software verification and documentation were envisaged by the use of a corresponding design tool suitable for embedded real-time system specification and simulation. In detail we expected the following improvements of the software development process:

- Easier and faster design with the aid of the tool.

- Achieving a good documentation of the design which can be used for coding and explaining system behaviour.

- Using simulation to prove system behaviour.
- Merging the steps *(Requirements, Design, Code Generation* and *Testing)* of the software development process in one user interface.
- Improving maintainability by having everything in a consistent user interface.
- Achieve complete software traceability between requirements, design, and source code as well as test functions.

3 The Design Tool ObjecTime

3.1 Decision for ObjecTime

In order to select the best tool and methodology for our software development, several tools were evaluated within an analytical decision making process. The comparison was done by checking each tool against a number of evaluation criteria, which were derived from the requirements for the ACT/FHS project. For each evaluation criterion a mark ranging from -2 (very poor) to 2 (very good) was given to each design tool. Additionally the marks were weighted with a weight factor for each criterion, which was derived from the importance of the criterion for the project. The weighted marks were added for all tools and then the tool with the highest sum - ObjecTime - was chosen. A more detailed description of the evaluation process can be found in [7].

3.2 ObjecTime Overview

The design tool ObjecTime [8] was developed by the Canadian company ObjecTime Limited with the first version dating from 1992. For the ACT/FHS project first the C version 5.2 and later the C++ version 5.2.1 was used. ObjecTime provides a kind of visual programming language. Structures and substructures of a particular design can be represented and modified in a graphical way. The methodology and language of ObjecTime are closely related to the ROOM (Real-Time Object Oriented Modeling) methodology. A detailed description of ROOM can be found in [9], the main features of ObjecTime are as follows:

- Requirements, Design and Source Code are integrated in one Graphical User Interface.
- Object oriented concepts are applied within the tool.
- It is possible to simulate the complete design or parts of it, including animation of data flows and dynamically changing system states.
- The binary code for the target system can be generated within the tool, without the need for a separate source code implementation.
- A hierarchical documentation of the design in HTML can be done automatically.
- ObjecTime uses the ROOM methodology.

3.2.1 ROOM Methodology

In the ROOM methodology a design or model consists of a number of actors, which are connected with links. An actor can be imagined as an independant entity, which is sending and receiving messages. An actor is represented as a rectangular box with several ports on his outside being used to exchange messages with other actors. This is done by connecting a port of the actor with a port of another actor with a link. An actor may be compounded of other actors in a hierachical way, or it is a leaf actor. This view of actors as message exchanging entities is called the *Structure View*, because it shows the structure of a system with its components and subsystems. Examples for a compounded and a leaf actor are shown in Figure 1 and 2.

An actor behaves like a state machine. It has a finite number of possible states and starts in an initial state when the Model is run. Each state of an actor is represented as a rounded box in ROOM, with transitions coming from or leading to other states. Each transition is represented by an arrow. A transition is a possible switch from one state to another, when the actor receives the triggering message. The triggering message can be set individually for each transition and may be any message, which the actor is able to receive on his outside ports. Additionally a transition may go to the same state from which it originates (being called a self transition).

Normally an actor waits for incoming messages from other actors. If it receives a message, which triggers a transition leading away from the current state, it changes his current state and executes a piece of specific code. The executed code may include the sending of messages to other actors and hence trigger more transitions. Thereafter it will again wait for incoming messages. This view of an actor as a state machine is called the *Behaviour View*. An example for such a *Behaviour View* is shown in Figure 3.

3.2.2 Using ObjecTime

The usage of ObjecTime is a bit like using a drawing program. The graphical ROOM elements can be assembled quickly using a mouse. For the nongraphical settings, appropriate editor or setting windows are used, which will open when the appropiate graphical element is clicked. If for example a transition in the *Behaviour View* of an actor is clicked, an editor window for the triggering messages and the code, which will be executed when the transition is triggered, will open.

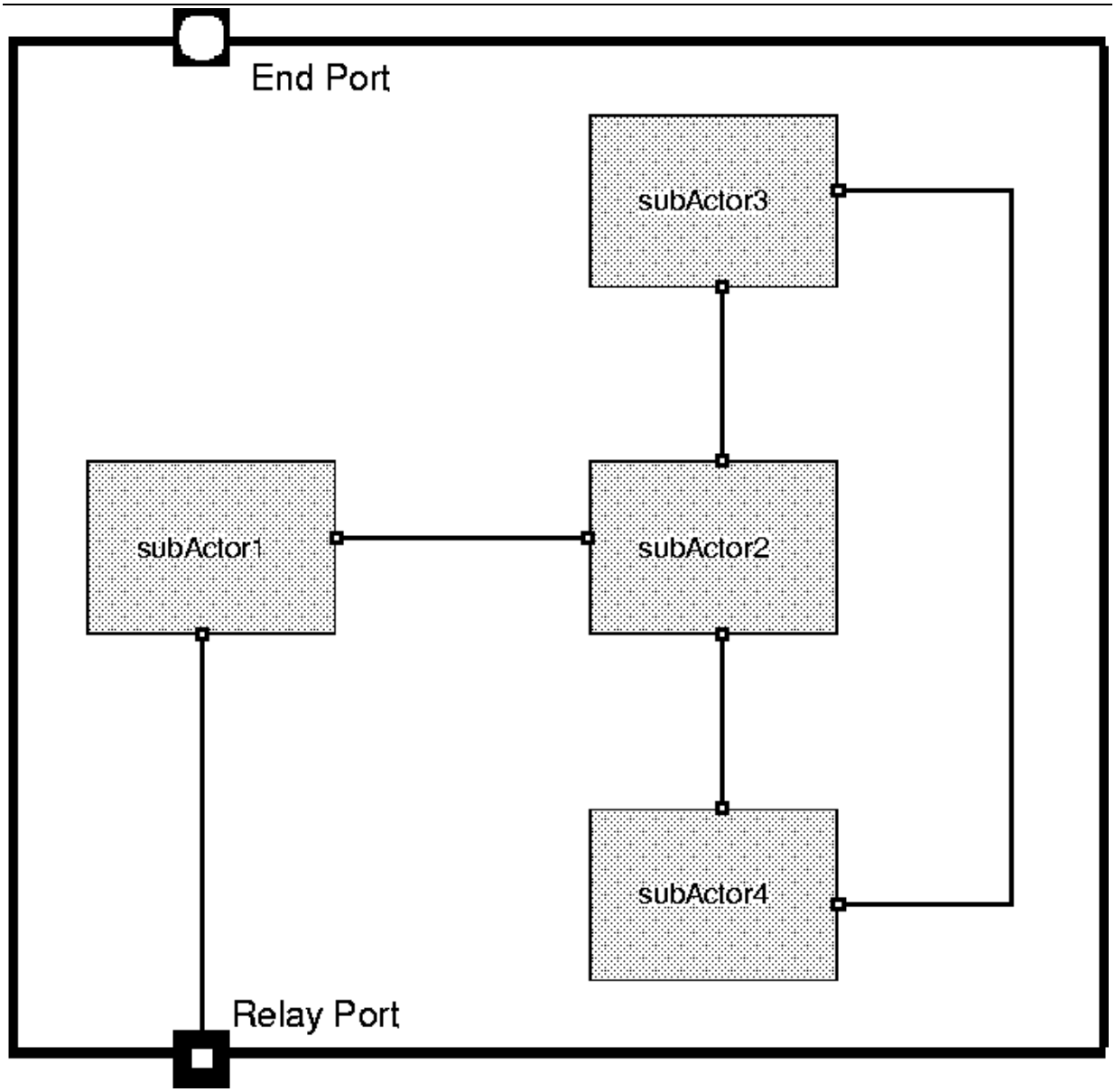

Figure 1: An example actor, which is compounded of several subactors. The ports on his outside may be end ports or relay ports connected to subactors.

4 Designing the Software

Besides designing our system with ObjecTime, we also designed the system with our traditional pencil and paper methodology. For doing this, we had the following reasons: We did not want to rely upon the successfull introduction of ObjecTime. The usage of ObjecTime was part of the Process Improvement Experiment ICARUS. Such an experiment needs a fall-back solution in case that it fails and additionally this enables a better evaluation of the benefit gained.

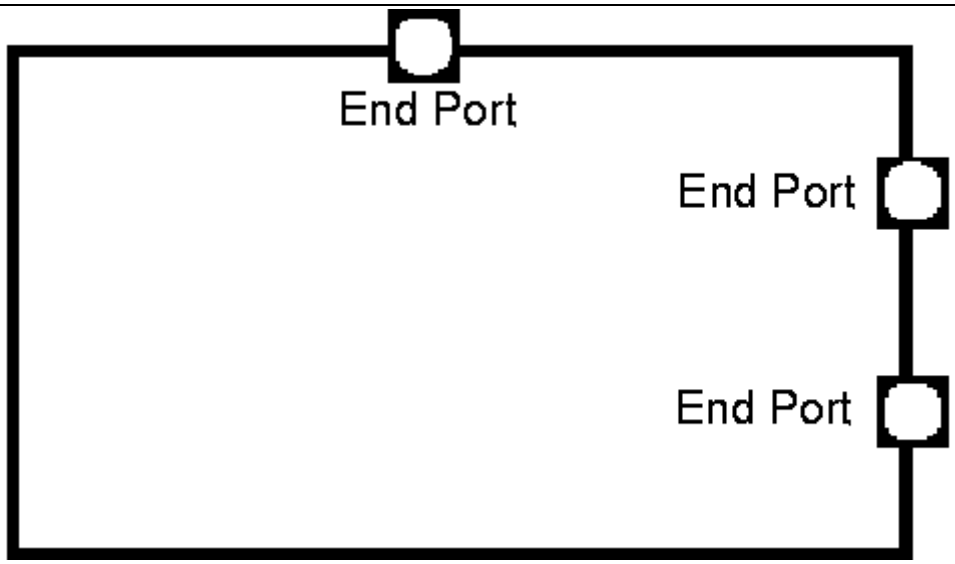

Figure 2: An example leaf actor with 3 ports on his outside, whereby all ports have to be end ports.

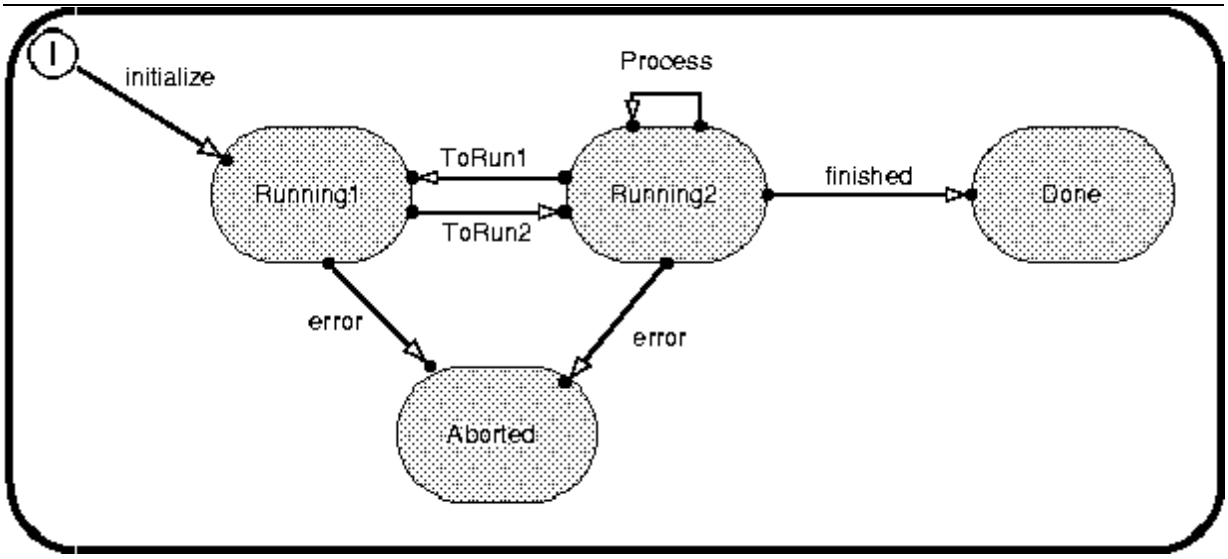

Figure 3: An example *Behaviour View* of an actor with 4 states.

Corresponding with the baseline project we handled the design within successive phases. For the external interfaces the first design dealt only with dummy signals, containing system control information but no real data. Within successive designs these dummy signals are replaced by real signals. This approach simplified the learning process with ObjecTime.

4.1 Advantages of using ObjecTime

The tool allows an easy access to information originating from different software development steps, because the corresponding information is automatically linked: E.g. the *Structure View* of a system enables to see the requirements for a subpart or the source code implementation of another through just one or two mouse clicks.

Without a design tool it would be necessary to browse the requirement documentation or the source code manually.

A second advantage is a better maintainability of the consistence between the software development steps. If for example the design is changed without a tool, one could easily forget to change the corresponding source code. This would result in an inconsistency between design and source code. Using ObjecTime it will not be possible to successfully compile a model with a changed design without adjusting the source code as well.

Another advantage is gained through the possibility to simulate the model or parts of it within the development environment. ObjecTime enables several methods to visualize the data flow during a Simulation. E.g. the current states of *Behaviour Views* are graphically highlighted during changes and thus can be easily observed. Another feature results from the possibility to observe the exchanged messages between actors and to generate a graphical view of the exchanged ones, called MSC (message sequence chart). A MSC example is shown in Figure 4.

The simulating ability can be used for debugging, testing and is also helpful for presentations and reviews of the completed product.

Another more specific feature of ObjecTime is the possibility to automatically generate a HTML-filetree from a model, which is a very efficient way to present the results of the software development process.

Another feature of using a design tool is the combination of otherwise different software development steps in one environment and one model. The software development process can be roughly separated into the steps *Requirements, Design, Code Generation* and *Testing*. Traditionally each step has its own tools (e.g. editors, drawing programs etc.) and therefore the data exchange between the steps is slow and clumsy. In ObjecTime the same steps have to be done, but they are all done in the same environment with the same model. This model includes the requirements, the design and the source code. This approach leads to a number of advantages.

4.2 Disadvantages of using ObjecTime

On the other hand we encountered a number of disadvantages using the design tool. Some of them are valid for design tools in general and others are more specific to ObjecTime:

Licenses for design tools are not cheap. This is a very simple argument, but using a design tool should provide more than a marginal improvement of the software developing process in order to compensate the expenditures for it. A similar point is the need to first become familiar with such a tool. Design tools are very complex software, requiring a lot of training. A learning time of several months up to a year should be projected, before a design tool can be used in an efficient way. Training courses are also sensible which will increase the total cost for a tool.

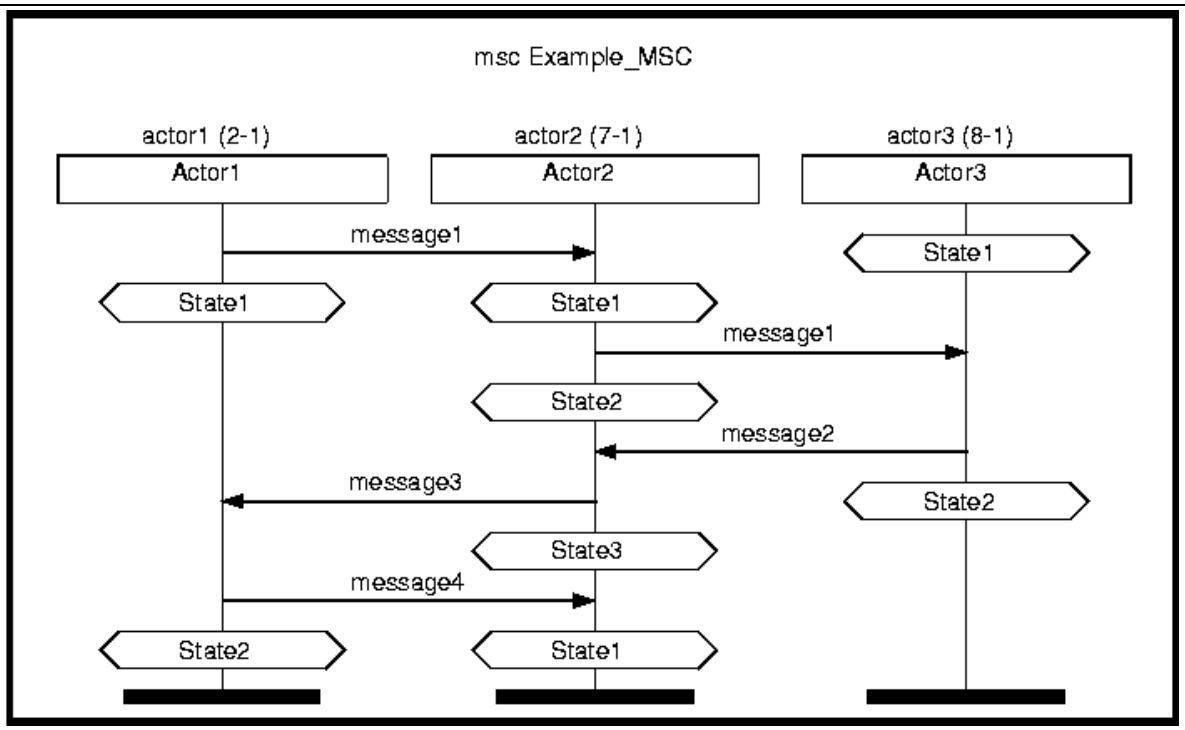

Figure 4: A MSC example with 3 actors. It can be seen how messages are exchanged, and how the states of the actors are changing.

Perhaps the biggest restriction is, that the design must fit into the underlying methodology of the design tool, which may restrict the design in an unpleasant way. It can be expected, that the design has to be done in another way than without a tool. In worse cases there may be no way at all to do the design for a software project with a specific design tool. In ObjecTime for example, the design has to fit the ROOM methodology. This will be explained in detail on behalf of some examples in the next two paragraphs:

One problem with ROOM is the lack of broadcasting. If a message should be sent to more than one receiver, there is no elegant way in ObjecTime to do this. There are some different workarounds to implement broadcasting, but all of them include special drawbacks.

ROOM only allows the execution of a code fragment, when the corresponding state of an actor changes. In some cases it is not possible to implement special tasks with this concept. An example may be a bus receiver, which either has to poll the bus permanently for new data or gets notified through an interrupt. There are ways in ObjecTime to solve this problem too, but they are not very well documented and difficult to implement.

Another drawback with design tools is, that problems with other previously used tools and programs may occur. Because everything is done in one development environment, everything has to be done with the tools provided from the environment belonging to the design tool. Additionally the use of external programs may result in a difficult configuration work or may be entirely impossible. Such tools are for example

editors, drawing programs or configuration management programs.

When a design tool is used, everything is compounded into a single model. It may cause problems to separate the steps of the software development process from each other. This is mainly needed for the handling of source code, which should be modifiable without using the development environment from the design tool. In ObjecTime for example the separation of the source code is problematic. If a model is compiled in ObjecTime, it will be done in two steps. In the first step the 'real' source code is generated from the model and in the second step the generated source code is compiled by an arbitrary compiler. It is possible to take the generated source code and modify it by hand, but this code is too cryptic to be useful. Moreover the manual changes would be overwritten, when the model is compiled again. This may lead to a lack of flexibility for quick changes in the source code and to a diminishment of the control of the source code.

Related to the previous problem is that difficulties may be encountered, when the work should be shared with other groups or facilities. It cannot be expected that they are using the same design tool and therefore they are not capable to use the specific models originating from the design tool.

Another problem may occur with time critical real time applications: The target code being generated with ObjecTime contains the mechanisms, which do the administration for message exchanges and state changes, etc. of the ROOM model. This mechanism consumes CPU resources, which may be needed by very time critical parts.

The simulation ability in ObjecTime surely is a neat thing to have. Nevertheless there are some weak points which decrease its value significantly: The simulation is running in one thread only and therefore cannot be used to simulate multi-threaded models. The simulation cannot be used to simulate performance critical parts of the model, because the extra administrative effort for the simulation will falsify the results.

The GUI also has some drawbacks, which slows down the speed of work and may lead to unnecessary errors. They are too many to mention them all explicitly in this paper. Most of them could be removed without big programming effort. Hopefully they will be eliminated in further versions of ObjecTime.

There are two different versions of ObjecTime, one for C and one for C++. When the design for our experimental system was started, first the C version of ObjecTime was used. In this version some features of ObjecTime are not supported which caused many extra problems. Therefore we switched to the C++ version later, which was much better to work with. Summarizing, the C version makes an unfinished impression and the C++ version should be preferred if possible.

5 Conclusions

The introduction of ObjecTime resulted in a mixed impression. Some parts of the software development process are improved, while other parts suffered significant drawbacks. Concerning our overall objectives we summarize:

- In contrary to the past, we today have an automatic tracing of requirements.
- In contrary to the past, we today can prove the designed system behaviour through simulation.
- The automatic generated HTML documentation is a magnitude better than the pencil and paper documentation from the past.
- The overall development effort was not reduced but the overall quality of the software was improved. The effort saved for maintenance can only be evaluated after the helicopter has been put into operation.
- The tool ObjecTime has shown to be well suited for the design, but for the target code generation we could not use it effectively. We encountered too many problems.

A general recommendation for or against design tools in common or ObjecTime in special cannot be given, because the successful usage of such a tool depends on many individual application specific factors. Instead some hints are given, which may help to come to a decision pro or against a design tool:

- Design tools are complex products requiring a long introduction time.
- The project, in which a design tool is used the first time, should be a small project.
- Care and attention should be paid to the underlying methodology of a design tool, because it may restrict the designing process. It is not a good idea to do the design in the same way than before a design tool was introduced. In ObjecTime for example the ROOM methodology must be used. In many cases there will be an efficient design using ROOM, but there are also cases in which a design is very difficult to do with this methodology. Instead it would be better to use another tool or no tool at all.
- If the design tool will be used for target code generation, it should be observed, whether the design tool supports the specific target with a reasonable configuration work and whether the generated source code meets the expectations.
- Before a design tool is used, at least a coarse predesign with pencil and paper should be done. In the beginning of the design phase we had the expectation, that we could start the design from scratch, but this proved to be fruitless. A design tool cannot do the creative work in a design, it can only help to organize and structurize and to connect otherwise separated parts of the software development process.

For the future it can be expected, that the design tools will improve and the disadvantages using them will decrease. A wider distribution and a formation of

common standards may also help to increase the efficiency of design tools. In any case the underlying ideas of design tools look very promising for the future, and probably will win recognition in some way.

References

[1] ACT/FHS - A New Fly By Light Research Helicopter
Bernd Gelhaar, Heinz-Jürgen Pausder, Ulrich Butter, Manfred Dion
etc98 (European Telemetry Conference), May 1998

[2] ACT/FHS On Board Computer System
Klaus Alvermann, Rüdiger Gandert, Bernd Gelhaar, Stephan Graeber, Henrik Oertel etc98 (European Telemetry Conference), May 1998

[3] Software Considerations in Airborne Systems and Equipment Certification.
RTCA DO-178B, December 1992

[4] Software Quality Standards für kleine Projekte
DLR, Hauptabteilung Qualität und Sicherheit, April 1997

[5] Software Engeneering Standards:
European Space Agency. ESA PSS-05-0, Issue 2, February 1991

[6] Developing Embedded Software for a Helicopter Testbed
Henrik Oertel, Klaus Alvermann, Stephan Graeber, Lothar Thiel
QWE 99 (Quality Week Europe), 1999

[7] Model Based Quality Improvement for Embedded Software
Klaus Alvermann, Stephan Graeber, Henrik Oertel, Lothar Thiel
CONQUEST'99 (Conference on Quality Engeneering in Software Technology), 1999

[8] ObjecTime Website:
http://www.objectime.com

[9] Real-Time Object-Oriented Modeling
Bran Selic, Garth Gullekson, Paul T. Ward
New York 1994, John Wiley & Sons, Inc.

SATELLITE NAVIGATION SYSTEMS AND TARGET TRACKING

Capability of the SW simulation system developed by the DLR in the project NavSim

Evelin Engler et.al.
DLR, Institute of Communication and Navigation,
Oberpfaffenhofen / Neustrelitz, Germany

ABSTRACT

The development of future navigation systems like **GALILEO** and the continually increasing application of satellite navigation systems (e.g. traffic control and management, position related information systems) are the cause, that the need of suitable software simulation tools is increased. Since 1997 the DLR has intensified its activities to develop a GNSS end-to-end software simulation system for validation and consultation purposes.

The **NAVSIM** software simulation system consists of two levels: the signal simulation level (SSL) and the application simulation level (ASL). Both levels are necessary to determine the positioning performance of a global navigation satellite system (GNSS) under consideration of nearly realistic conditions. The subdivision in two levels is the base to gather a suitable handling of the system complexity based on reproduced transmission processes with the serious different bandwidths and time scales (e.g. like signal generation, spatial and temporal variation of propagation errors and receiver type dependent derivation of range and phase measurements). A short description of the architecture of the simulation system and the corresponding signal and parameter flow will be given.

The basic system can operate in several modes:

- estimation of signal states at the receiver input described by range and phase delays, the corresponding rates and the carrier to noise ratio inside a temporal and spatial window
- composition of GNSS observations (ranges & phases) and corresponding estimation of the accuracy and availability of positioning
- extended composition of GNSS observations (range & phases) including an error generator model (receiver type dependent accuracy of range and phase measurements) and corresponding estimation of the accuracy and availability of positioning
- estimation of GNSS reliability by evaluation of several simulation runs with different spatial and temporal windows for typical static and dynamic applications

For each mode a simulation example will be given, based on a well-defined specified simulation task.

1 INTRODUCTION

The need of suitable software simulation systems as design, investigation and verification tools has greatly increased in the last few years. The problem of simulating navigation systems is the GNSS complexity considering on one hand the component and parameter variety in the space and user segment and on the other hand the spatial and temporal variation of natural impacts during signal transmission and reception. The projection of all processes into a simulation system contains a time-scale conflict resulting from the large physical transmission bandwidth (therefore high sampling frequencies of several 10 MHz) and from the comparatively slowly changing scenario determined by satellite tracks, user movement, ionospheric and tropospheric influences, clock drifts and others. This conflict normally result in excessively long simulation times and in the demand of large data storage capacities. To avoid this detected problem and to

achieve a suitable handling of the GNSS software simulation system, the project **NAVSIM** uses a multi-layer architecture.

The so-called signal simulation layer (SSL) is responsible for the estimation and modelling of the signal specific ranging performance. This process divides into 3 steps:

In the first step the simulation scenario is composed by specification of the used signal structure (code, pulse shape, chip rates...) and the selection of the considered transmission and reception components (power amplifier, filter, type of multipath channel, PLL/DLL...). As the next step 30 second long signal-sections are simulated for a reasonable number of carrier to noise ratios C/No to estimate the tracking error of the receiver loops. Due to the highly detailed simulation at sampling frequencies of several 10 MHz and the high computational complexity of interpolation and correlation, each of these simulations takes about one day on a high performance workstation. For each recorded tracking error the variance, mean and the spectrum are extracted. As the last step these data sets and the noise free dynamic behaviour (tracking error) of DLL and PLL are used to establish an error generator model, which reproduces the physical signal processing behaviour for the composition of disturbed range and phase measurements inside the system layer.

The so-called system or application simulation layer (ASL) models the slowly changing system aspects such as satellite tracks, user movements, ionospheric and tropospheric propagation errors, antenna effects, satellite and system time behaviour and importantly the on-line solution of the navigation equation.

On one hand the ASL is used to estimate the GNSS signal states described by C/No, range, phase and corresponding rates and to deliver representative samples for the signal simulation. On the other hand in this layer the corresponding delay measurements are composed (adding technical and natural/physical parts) and used for positioning. This can be done for a specified number of dynamic and/or static user inside a specified temporal and spatial simulation window using one or several satellite systems. Therefore here the capability is given to test new algorithm or components such as navigation equation solvers, ionospheric estimation algorithm, intelligent directive antennas, clock models etc. Effectively, the operation mode of the ASL is determined by the selected optional modules.

Both layers are developed using a flexible software and block based design. This ensures, that the simulation system can quickly adapt to changes resulting from the definition phase of GNSS2. Additional, for further applications it is possible to substitute single modules by improved realisations or to compose extended simulation systems.

The paper is organized as follows: we begin by presenting the architecture of the simulation system and the interaction of both layers for an end-to-end simulation to assess an system constellation by measuring the accuracy, availability and even the reliability. Than preliminary simulation results are shown to demonstrate the capability of software simulation system. At the end the main results are summarized in a brief conclusion.

2 ARCHITECTURE OF THE SIMULATION SYSTEM

The functional diagram of the GNSS end-to-end simulation system is shown in Fig. 1. and consists of two simulation layers: the signal simulation layer (SSL) and the application simulation layer (ASL). If the positioning performance of a global navigation satellite system should be assessed, both layers are necessary to consider all significant natural, technical and physical impacts during signal generation, transmission, signal reception and data processing and to estimate the navigation accuracy under nearly realistic conditions.

The ASL is responsible for the specification of the global simulation parameter like start and end point of the simulation, considered region and sampling frequencies. Further the system composition and therefore the operation mode is specified by the selection of the optional modules. The next steps are the

initialisation of each selected module and if used of the simulation subsystem SSL. At the end of the simulation setup the geometric scenario (satellite constellation, user dynamics), the considered components (e.g. models for signal generation, propagation channel, receiver hard- and firmware) and the aimed results(e.g. signal states, navigation solution) are defined.

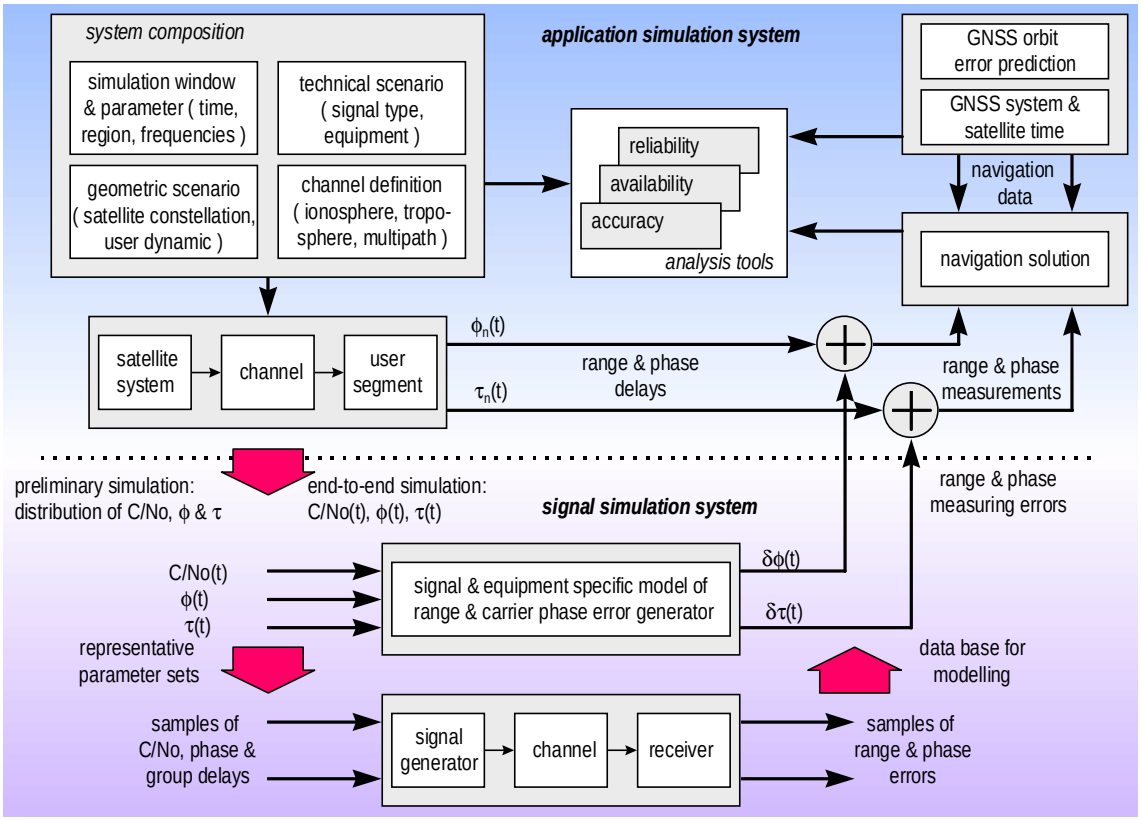

Fig. 1 Functional diagram of the GNSS end-to-end simulation system

The whole system initialisation is realised by several dialog windows. The first window (Fig. 2) defines the global simulation parameter and the system composition (selection of optional modules). In dependence on the composed system now a sequence of dialog windows follows (a further example is given in Fig. 3: initialisation system and satellite time). The controlled chronological order of the used dialog windows guarantees the parameter flow and consistency. Each dialog window enables to work with default parameters or with the setup of the previous simulation. The plausibility and therefore the system consistency is checked under consideration of parameter dependencies of the whole simulation system. A successful initialisation is achieved, if all

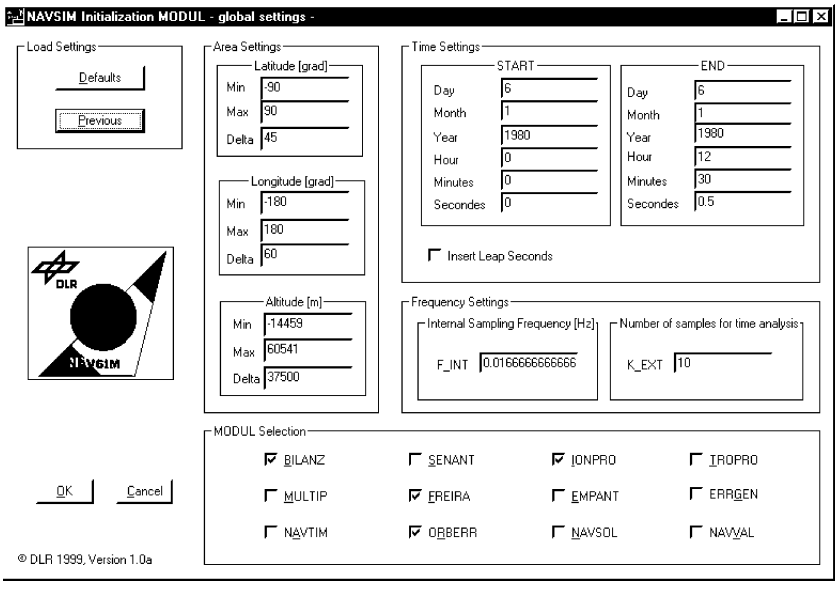

Fig. 2 Initialisation of basic simulation parameters and system composition

dialog windows have been closed with the “okay” buttons. The following simulation run will be started, only if this basic condition is fulfilled.

In dependence on the composed system several modes of the simulation system and its layers can be realised:

- estimation of signal states at the receiver input described by range and phase delays, the corresponding rates and the carrier to noise ratio inside a temporal and spatial window (ASL run mode 1)
- estimation of signal, receiver and channel type specific ranging performance using sets of receiving conditions (SSL run mode 1)

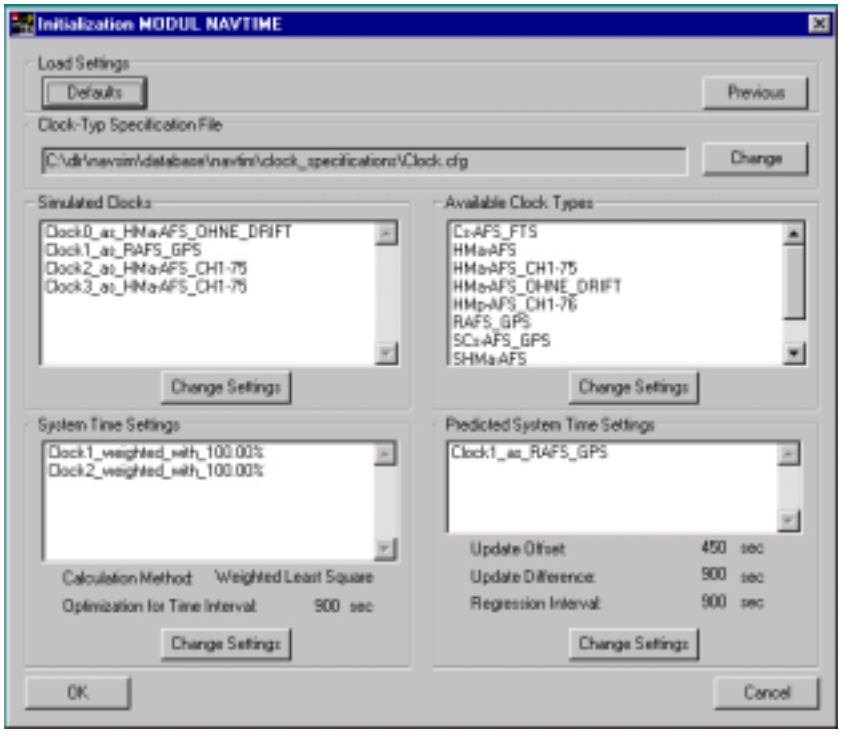

Fig. 3 Initialisation of system and satellite time generation module

- composition of GNSS observations (ranges & phases) and corresponding estimation of the accuracy and availability of positioning (ASL run mode 2)
- derivation of equipment specific models to describe the ranging performance, it’s verification and implementation in a model library (SSL mode 2)

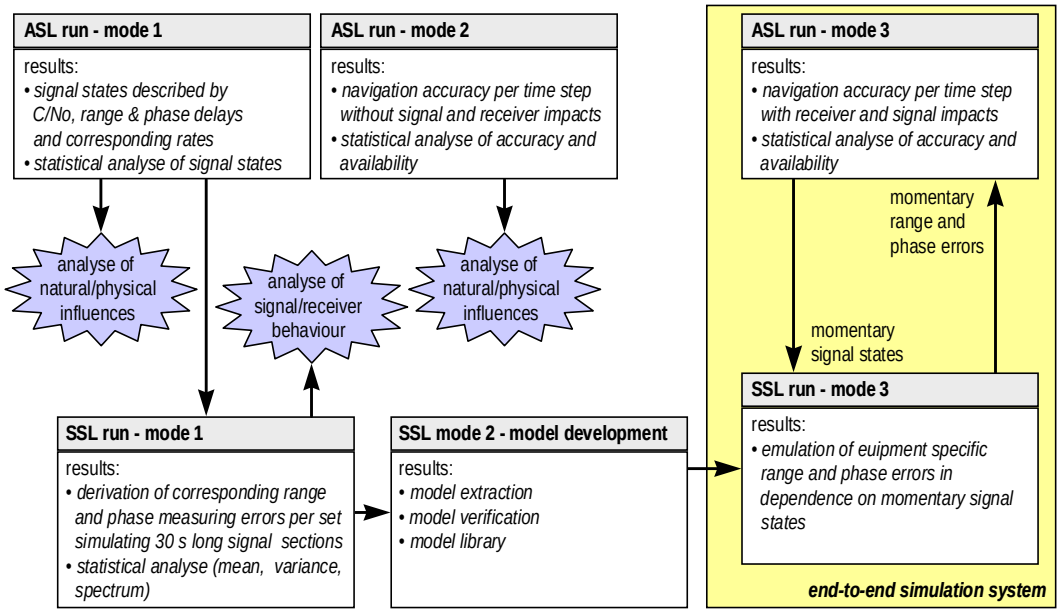

Fig. 4 Data flow to establish the GNSS end-to-end simulation system

- extended composition of GNSS observations (range & phases) including an error generator model (receiver type dependent accuracy of range and phase measurements) and corresponding estimation of

the accuracy and availability of positioning (ASL and SSL run mode 3)

- estimation of GNSS reliability by evaluation of several simulation runs with different spatial and temporal windows for typical static and dynamic applications

The corresponding data flow to establish an end-to-end simulation system based on preliminary ASL and SSL simulation runs is summarized in Fig. 4.

The capability of the whole system is specified by the implemented models and algorithm, which are used for the determination of the signal states, for the estimation of the ranging performance and for the derivation of the navigation solution. The modular design allows to substitute each module by an improved version or to arrange extended simulation systems. A short summary of the main components, which will be implemented in the project **NAVSIM** up to the end of 2000, are given in Tab. 1.

Tab. 1 Potential of main simulation components

Geometric Scenario	
• *satellite position(s)*	*almanac/ephemerides based calculation for GPS, GLONASS, GALILEO; combined GNSS systems and all other satellites with specified orbit parameters (e.g. International Space Station)*
• *user position(s)*	*by definition of start and way points per user or by automatic equipartition in a specified region*
• *geometric availability*	*elevation controlled geometric availability*
System equipment	
• *satellite system*	*each satellite has its own set of technical parameters (number and values of carrier frequencies, EIRP, polarisation, ...), but also GNSS standard values can be used*
• *signal structures*	*generation of several CDMA signal types (spreading code, pulse shaping, chip rates, carrier frequencies...)*
• *nonlinearities & filtering*	*reproduce impact of nonlinearities caused by HPA's (solid state power amplifier, traveling wave tube amplifier) and bandpass filtering (cheby, butterworth...)*
• *ranging performance*	*reproduce ranging performance using standard PLL and DLL, "Maximum Likelihood" receiver, "Closed loop" receiver*
• *antennas*	*described by models of omnidirectional and directional antennas and by measured directional pattern of commercial available GNSS antennas*
• *satellite time*	*generation by flexible specified clock types*
• *system time*	*composition by selection of used clocks, its weighting and the calculation method ("Weighted Least Square" und "Kalman Filter")*
• *clock correction*	*generation of clock correction terms using quadratic regression*
• *orbit prediction error*	*random model*
• *navigation solver*	*GDOP controlled solution, all in view solution, with/without smoothing*
Channel	
• *ionosphere*	*regular behaviour can be calculated by IRI95 or BENT, GIM is used as base to generate amplitude fading and phase scintillation*
• *troposphere*	*clear atmosphere described by vertical standard profiles, rain effects alternatively calculated by ITU-, stratiform or cylindrical rain model, refraction index derived from MPM89*
• *multipath*	*4 stochastic models are used in SSL (en route, final approach, urban, rural), a topographic map based deterministic model can be used for multipath investigations in ASL*
Analysis / modelling	
• *signal states / navigation accuracy*	*recorded per time step, statistical analyse (mean, rms, maximum, distribution) supported for time series, for regional distribution and for equal weighted postprocessing,*
• *ranging performance*	*recorded per time step, statistical analyse (mean, variance, spectrum) supported for*

	measured range and phase errors; development of system equipment specific error generator models

Though the outlined components in Tab. 1 are insufficient to assess all GNSS aspects, the developed software allows to analyse GNSS navigation performance under consideration of prioritized natural/physical impacts and the used software architecture makes possible to arrange problem-orientated or extended simulation system in dependence on topical tasks.

3 SIMULATION EXAMPLES

The number of tracked GNSS signals used for positioning depends on the used satellite system (number of healthy satellites in the orbit) and on the user location and environment.
The global distribution of available satellites is given in Fig. 5 for GPS and GLONASS for an elevation mask of 10° and is derived with a sampling frequency of 1/60 Hz. Because GLONASS operates without the full satellite constellation, only 30% of the time points have 4 or more signals for positioning. GPS with the full satellite constellation offers, that all the time 4 or more signals are geometric available. Which signals are ultimately used for positioning depends on the occurred disturbances during transmission and on the tracking performance of the used receiver equipment. Therefore one important task is the estimation of the signal states at the receiver input described by attenuation, noise, group and phase delay and corresponding rates. In this case, the essential impacts must be reproduced under consideration of it's spatial and temporal variations (e.g. ionosphere, troposphere, multipath, shadowing, antenna). During the simulation each activated channel module calculates its contribution to the signal states. The distribution of the free space attenuation at the Greenwich meridian (longitude=0°, 32 well-distributed station at the meridian) is given in Fig. 6 for GPS and GLONASS assuming the same transmission power of 0dBW. Additional in Fig. 7 the corresponding distribution of geometric induced ranges and range rates are shown. To simulate the impact of regular and irregular ionospheric effects on radio propagation three models are implemented: IRI95 [BIL90] , BENT [LLE73] and GIM. Whereas IRI95 and BENT allow the reproduction of regular or mean ionospheric behaviour, GIM gives the basis for modelling amplitude fading and phase scintillation caused by small scale electron density irregularities in the ionosphere.

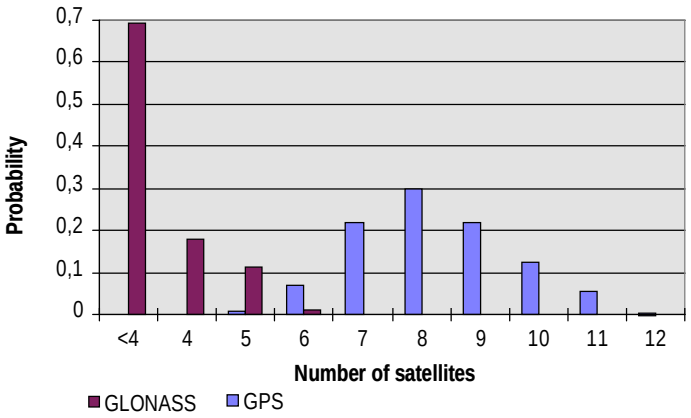

Fig. 5 Global distribution of available satellites (22nd May 00, elevation 10°, 32 well-distributed reference stations, almanac week 1047)

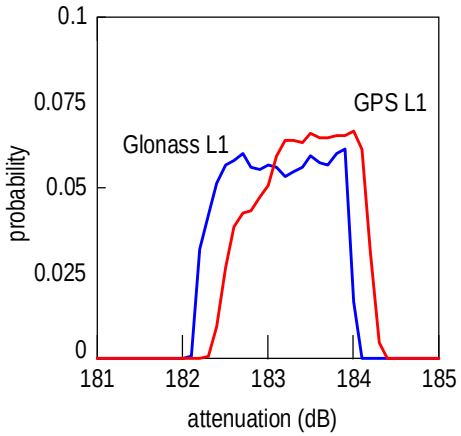

Fig. 6 Distribution of free space attenuation at GNSS signals (Greenwich Meridian, 22nd Mav 2000)

Included tropospheric propagation errors are delay, attenuation and thermal noise by the clear atmosphere and rain clouds. For the clear atmosphere vertical profiles of temperature, pressure and water vapour density for different regions and seasons are implemented. Additionally, rain effects can be included either for a preselected system availability utilising the ITU-R rain model [ITU94] or for a user defined rain rate

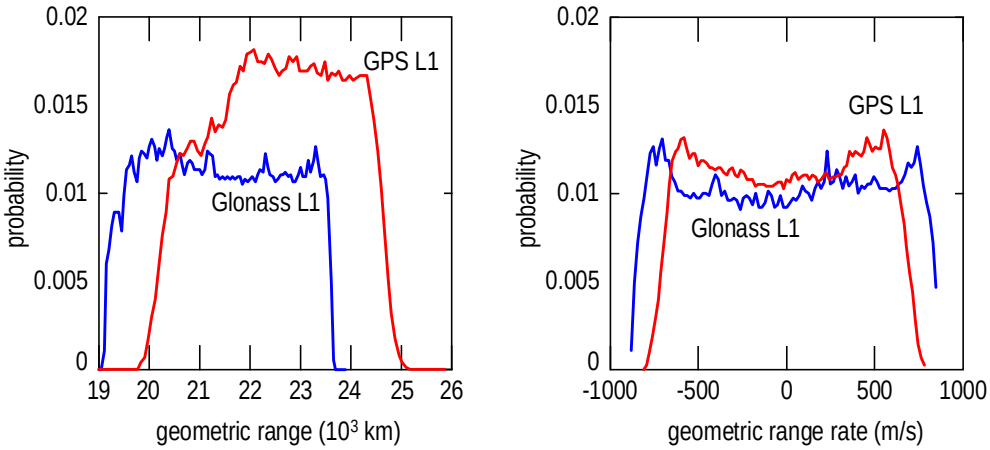

applying a stratiform or cylindrical raincell model. For the computation of the specific delay due to rain the

Fig. 7 Distribution of geometric range and range rate of GPS L1 and GLONASS L1 signals for user at the Greenwich Meridian

real part of the refraction index is calculated with the MPM89-model [LIE89].

As an further example the contributions of the ionosphere (regular by BENT) and of the troposphere (clear atmosphere and ITU rain model) to the noise and to the range are given in Fig. 8 for 3 specified stations.

Based on all delivered contributions tthe C/No, the group and phase delay and its rates will be calculated for each available signal at the receiver input as a function of time.

The estimation of the ranging accuracy is realised inside the SSL for a specified system equipment, which is determined by the used signal structure (code, pulse shape, chip rate, carrier frequency), by the considered transmitter components (amplifier, filter), by the assumed statistical multipath channel (en route, final approach, urban, rural) and by the receiver type (Maximum Likelihood Estimation, Closed loop receiver). For a well-defined set of signal states presimulations (30s signal duration) are realised to determine the ranging performance with an acceptable expenditure of processing time and storage capacity.

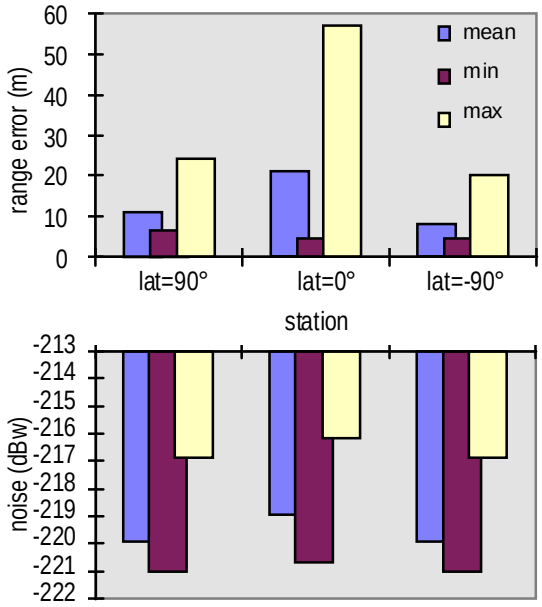

Fig. 8 Ionospheric and tropospheric range error and corresponding noise (included thermical noise) at 22nd May 2000 (longitude 0°, elevation 10°)

Using a non coherent DLL and an AWGN channel shows (Fig. 9), that the use of a SRC pulse shape (square root cosine, β=0.2) results in an improved ranging performance in comparison to rectangular pulses with a lower chip rate. For an assumed C/No of 35 dB the accuracy gain of the SRC (described by the standard deviation σ) is in the order of 1 up to 2 meters. A more realistic estimation of the ranging performance can be realised considering different multipath scenarios, which are specified by the direct path, the number of echos and it's characteristic (delay, power, fading bandwidth). In Fig. 10 the estimated σ in dependence on the C/No is given for 5 different multipath scenarios. In principle, each scenario results in an accuracy loss. For each example exists an optimum, where an increasing C/No result in no further

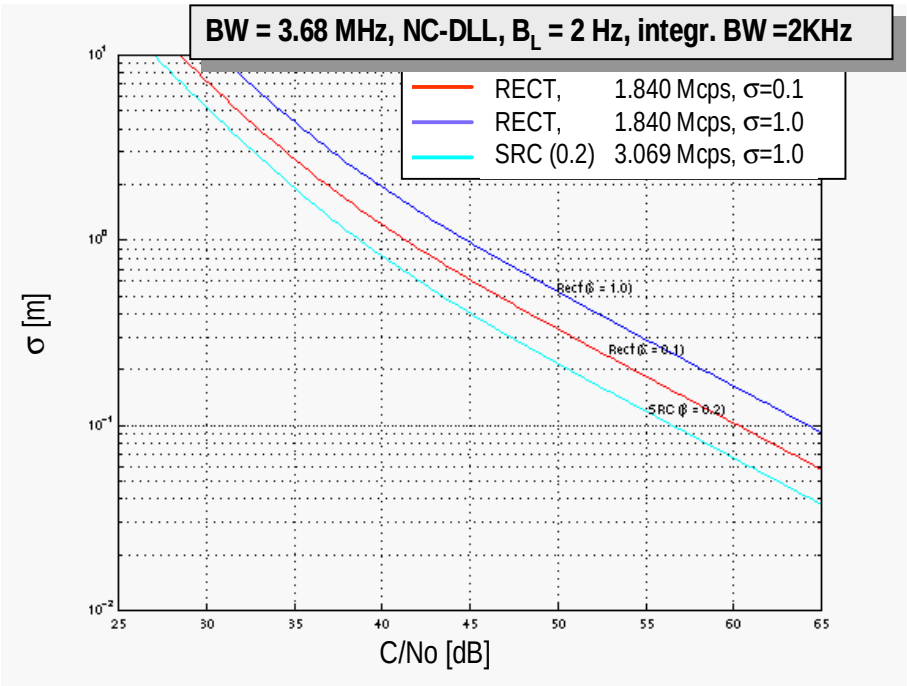

Fig. 9 Estimated ranging performace for 3 specified navigation signals considering an AWGN and using a NC-DLL

important improvement of the accuracy. For low C/No the observed difference to AWGN is in the most cases very small, so it's acceptable to simulate with the easier handled AWGN model.
Based on such presimulations an more time efficient operating error generator model will be created to compose together with the above mentioned ASL components the range and phase measurements in its spatial and temporal variation. Additional to these composed disturbed range and phase measurements it's necessary to provide the predicition error of the satellite position (difference between real and predicted satellite position) and of the deviation between satellite time and GNSS system time. Both results from the used navigation data to determine the satellite position and the clock error correction during the solution of the navigation equations.

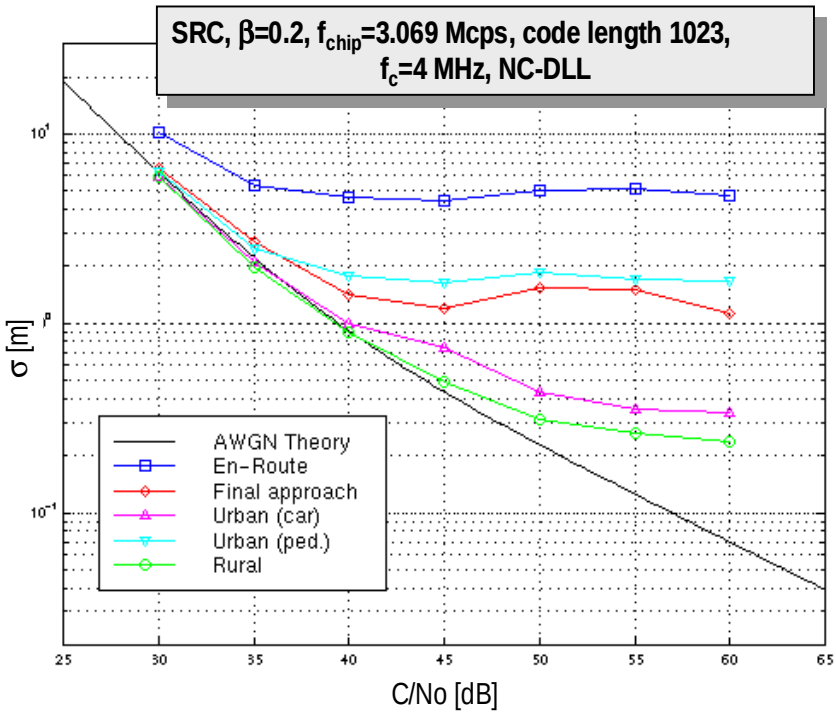

Fig. 10 Influence of different multipath scenarios on the range performance of a SRC signal

Up to the end of the project two standard algorithm will be implemented to solve the navigation equation. An example is given for a point nearly Garmisch-Partenkichen (latitude 47°, longitude 11.16°, altitude 850 m) in Fig. 11. There the ionospheric and tropospheric induced 2D positioning error at the 22nd May 2000 is given for an elevation cut-off of 10° and 20°.

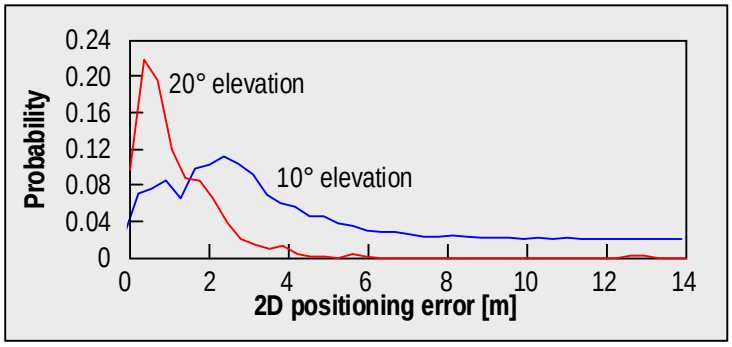

elevation:	10°	20°
mean satellite availabilty:	7.5	5.9
mean horizontal error [m]:	2.8	1.4
mean 3D error [m]:	16.8	12.2
no solution [%]:	0	0.3

Fig. 11 Estimated influence of ionospheric and tropospheric propagation errors on positioning in Garmisch-Partenkirchen at 22nd May 2000 (BENT, clear atmosphere, ITU rain model)

Working with a low elevation mask results in a higher availability of GNSS signals for ranging and positioning. But tracking with low elevation is connected with longer path length through the ionosphere and troposphere and therefore with increased propagation errors. A higher elevation mask reduces the influence of propagation errors (also multipath), but results in a reduced redundance, sometimes in a worse DOP (dilution of position) or in a loss of positioning capability (less than 4 ranging signals). Therefore for each user position and environment a specifc optimum can be found.

4 CONCLUSIONS

The software simulation system developed in the project **NAVSIM** (sponsored by the German government) is considered as a suitable environment to develop and to evaluate models, algorithms and technical components in the navigation area under nearly realistic conditions. One example is the “signal and equipment specific model of range and phase errors” based on gathered data by partial simulations in the SSL. An other example will be the “ionospheric scintillation model” to investigate the impact on amplitude and phase of the transmitted GNSS signal. Such models are important to lab-generate disturbed range and phase measurements in real time or to build up suitable signal simulators for receiver certification.

The GNSS end-to-end simulation capability is achieved by connecting the modules arranged in two layers – the so-called signal simulation layer (SSL) and the application simulation layer (ASL). The two layer concept was used to successfully tackle the problem of different time scale respectively bandwidths. This problem occurs, if signal transmission , ranging and navigation processes are considered together to estimate the GNSS performance.

Last of all the members of the project team should be mentioned: Michael Angermann, Johann Furthner, Jörg Hahn, Achim Hornbostel, Rainer Krämer, Hans-Peter-Müller, Helmut Nickl, Thoralf Noack, Patrick Robertson, Stefan Schlüter, Jesus Selva and Alexander Steingass. The success of the project is mainly carried by their expertise and engagement.

5 REFERENCES

[ITU94] ITU-R Recommendations PN.837-1 and 838, PN Series Volume "Propagation in Non-Ionized Media", ITU-R, Geneva, 1994.

[LIE89] Liebe, H. J: " MPM-An Atmospheric Millimeter Wave Propagation Model, Intern. Journal of Infrared and Millimeter Waves, Vol. 10., No. 6, 1989, p. 631-650.

[LLE73] Llewellyn, S.K. et. al.: “Documentation and Description of the BENT ionospheric model”, AD-772 733, Atlantic Science Corporation, prepared for Air Force Cambridge Research, distrbuted by NTIS, July 1973

[BIL90] Bilitza (ed.), International Reference Ionosphere 1990, NSSDC 90-22, Greenbelt, Maryland, 1990

[KLEU94] Kleusberg, A.: “Die direkte Lösung des räumlichen Hyperbelschnitts”, Zeitschrift für Vermessungswesen, 1994, pp. 188 – 192

[BANC85] Bancroft, S.: “An Algebraic Solution of the GPS Equations”, IEEE Trans. Aerosp. and Elec. Systems, 1985, AES-21, pp. 56 – 59

[EC99] European Commission Communication: „Galileo – Involving Europe in a New Generation of Satellite Navigation Services”, Brussels, 09.02.99

[GML93] R. de Gaudenzi, M. Luise, and R. Viola: „A Digital Chip Timing Recovery Loop for Band-Limited Direct-Sequence Spread-Spectrum Signals“, Trans. on COMM, vol. 45, no. 11, pp. 1760-1769, Nov. 93.

[PAR96]. B.W. Parkinson and J.J. Spilker: „GPS: Theory and Applications Volume I“, Progress in Astronautics and Aeronautics, Vol. 163, 1996

[SDS98] R. Schweikert and T. Woerz: „Final report“, Document No SDS-REP-DLR/NT-02/99, Issue 1, Signal Design and Transmission Performance Study for GNSS-2, ESA Ref. 12182/96/NL/JSC, 30.10.98.

[SFE99] A. Steingass, J. Furthner, E. Engler et al: “Modular end-to-end software simulator for navigation systems”, GNSS 1999, Genua, 8.10.1999

[KHSE99] S. Schlüter, E. Engler, “Reproduction of Regular and Irregular Ionospheric Effect for GNSS Simulation”,
Kleinheubacher Tagung, Kleinheubach, 27.09.-1.10.1999

[ESSE99] S. Schlüter, E. Engler, “Simulation of Ionospheric Corrections Regarding of Solar Activity on GNSS”,
ETT /SATNAV 99, Potsdam, 10.11.1999

Simulation of Scintillation Effects in NavSim

Stefan Schlüter, Thoralf Noack
DLR, Institute of Communication and Navigation,
Neustrelitz, Germany

Abstract

Goal of the NavSim project is the development of a modular end-to-end software simulator for satellite based navigation systems. The simulator shall give future users the opportunity to determine the positioning performance of a global navigation satellite system (GNSS), considering nearly realistic transmission conditions for a variety of signal structures and corresponding receiver types.
One task of the simulator is the reproduction of regular and irregular ionospheric effects on radio propagation and their influence on position accuracy and system integrity.
This paper focuses on the modelling of ionospheric scintillations. These rapid variations in the amplitude and phase of radio signals result from density irregularities in the ionosphere. Even if in the range of GPS frequencies and in mid-latitudes, scintillation effect are generally negligible, these effects have to bee taken into account to ensure a high level integrity of global satellite navigation systems and their applications.

Introduction

The purpose of the NavSim project is the development of a modular end-to-end software simulator for satellite based navigation systems [SFEo99]. To give the simulator the capability to reproduce nearly realistic transmission conditions also natural impacts as multipath, tropospheric and ionospheric effects have to be modelled and implemented. For the reproduction of the ionospheric influence on signal transmission the current versions of the BENT and IRI95 models are used, which give the ability to estimate the ionospheric impact in the absence of storms, scintillations or other irregular effects (a description can be found in [SE99]. Fig.1 shows the user interface of the ionospheric module of the simulator. Here we focus on the part of the simulator, responsible for the generation of ionospheric scintillations.
Scintillation of radio signals due their propagation through ionospheric irregularities is becoming an important issue for GPS receivers operating in especially equatorial and Polar Regions. Scintillation is a rapid, usually random variation in signal amplitude and/or phase. It is a result of abrupt

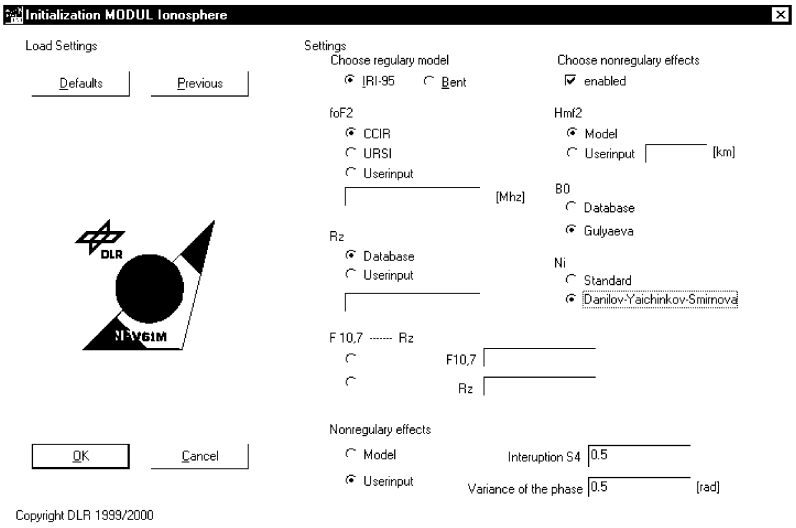

Figure 1: User interface of the ionospheric module in the NavSim simulator

variations in electron density along the signal path which produce rapid signal path variations and defocusing over a period last from 20 minutes up to 2 hours for a given location. While variations over the entire path are important, the most significant variations occur near the F2-peak between 225 and 400km. Scintillation cause both, enhancement and fading in the radio signals. Whenever the signal fades exceeds the receiver's fade margin and the signal is temporary lost.
Our approach used for the scintillation modelling follows the methods published by Hegarty et al [HB099] and Pullen et al [Po99]. Statistically characterisations of scintillations are used to produce realisations of the data, which conform to that statistical description. As a background model the GIM model of global scintillation activity is used to generate parameters describing the scintillation intensity (amplitude: S4; ⑨$_{❷}$) and the time and geographical dependencies.

Generation of Scintillations

As mentioned above several considerations have to be taken into account for the modelling of scintillation time series:

1. The amplitude and phase data must have appropriate probability density functions (PDF),

2. Amplitude and phase must be appropriately correlated in a way that large phase variations are observed when deep amplitude fading occurs (⑧ = -0.6),

3. The time correlation of the data must match the experimentally observed power spectral densities.

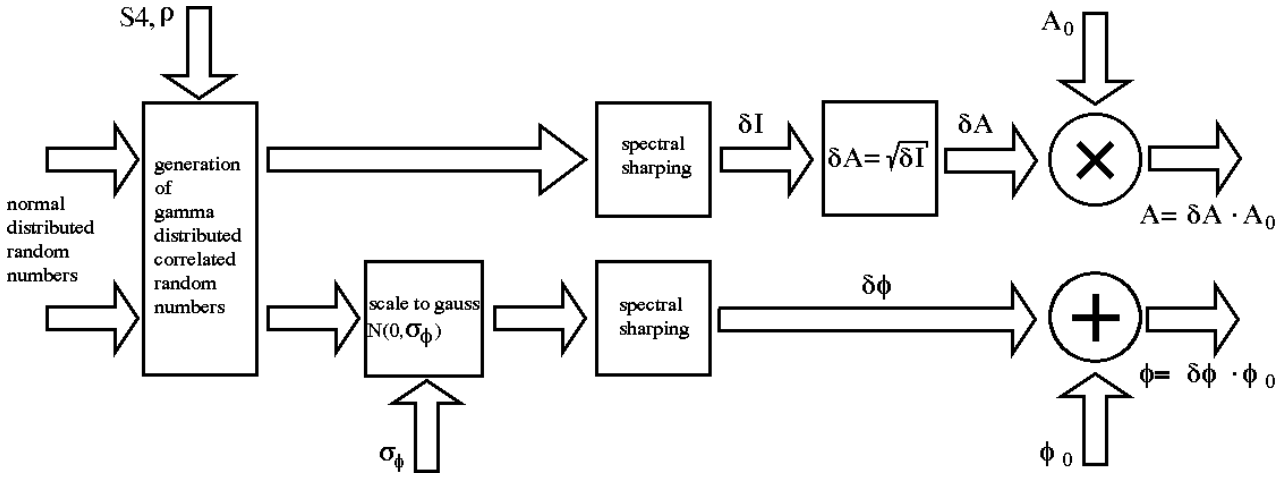

Figure 2: Modeling of scintillation signal

On base of this we have implemented a signal generator as shown in Fig.2 in the NavSim simulator. Feed by S4 and ⑨❷ values from the global GIM model and normal distributed random numbers it is generating scintillations as described in detail in the following.

Signal Generation

A signal of a navigation satellite can be written in a general form as:

$$E = A_0 e^{j\Phi} = A_0 \cos\phi_0 + jA_0 \sin\phi_0 \tag{1}$$

where A_0 is the amplitude and ❷$_0$ is the phase of the signal. To include scintillations these parameters are modified by the additional parameter ☙A and ☙❷:

$$A = A_0 \delta A$$
$$\phi = \phi_0 \delta\phi$$

The intensity (I=A^2) of the scintillation signal ☙I can be modelled as Nakagami-m distribution and the phase ☙❷ as zero mean Gaussian distribution according to Cervera and Knight [CK98]:

$$P_{Nakagami}(\delta\Phi) = \frac{m^m \delta I^{m-1}}{\Gamma(m) < \delta I >^m} e^{-m\delta I/\delta I^2} \tag{2}$$

$$P_{Gauss}(\Phi) = \frac{1}{\sqrt{2\pi\sigma^2}} e^{-\Phi/\ 2\sigma^2} \tag{3}$$

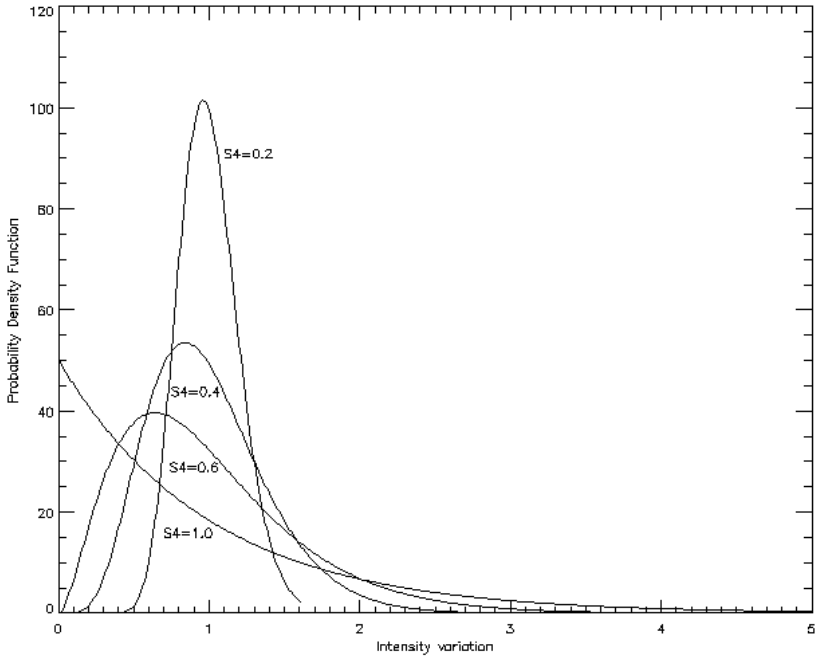

Figure 3: Probability density functions of intensity variations

where Γ is the gamma function, and ⑨ is the standard deviation of the phase fluctuations.
The relation of the m parameter in the Nakagami-m distribution and the S4 index is given by $m = 1/S4^2$ [WAAS72]. For small values of the S4 index the Nakagami-m distribution approaches the Gaussian distribution and tends to the Rayleigh distribution if we increase the S4 index (see Fig. 3).

For the generation of the correlated intensity and phase of the scintillation signal we used the inversion-free method for generation of bivariate gamma random vectors known, as trivariate reduction method[1] [Dev86]. Here two dependent random variables are constructed from three independent gamma distributed random variables:

[GENERATOR]
Generate a gamma ($\alpha_1 - \rho\sqrt{\alpha_1\alpha_2}$) random variate G1
Generate a gamma ($\alpha_2 - \rho\sqrt{\alpha_1\alpha_2}$) random variate G2
Generate a gamma ($\rho\sqrt{\alpha_1\alpha_2}$) random variate G3
RETURN (G1+G3, G2-G3)

[1]With a small modification because of negative correlation

with a correlation coefficient p of:

$$-\frac{\min(\alpha_1,\alpha_2)}{\sqrt{\alpha_1\alpha_2}} \le \rho \le 0$$

The gamma density function of this process has the following form:

$$f_i(x_i) = \frac{\left(\frac{x_i}{\beta_i}\right)^{(\alpha_i-1)}}{\beta_i\Gamma(\alpha_i)} e^{-\frac{x_i}{\beta_i}},\ x_i \ge 0,\ \beta_i > 0,\ i = 1,2 \qquad (4)$$

where x_1 represents the intensity and x_2 the phase of the scintillation, with a relationship between gamma and Nakagami-m distribution of [Po99]:

$$\alpha = m = \frac{1}{S4^2},\quad \beta_1 = \frac{1}{m} = S4^2 \qquad (5)$$

In case of the phase the α_2 is set to a constant high and β_2 to a constant low value to obtain Gauss distributed random variables, which is then scalable to N(0, ⑨₂) without lost of correlation.
For the generation of G1, G2 and G3 we used Berman's gamma generator (in case α < 1.0), best rejection algorithm (in case α > 1.0), and an exponential random variate (in case α = 1.0). The detailed description of these generators can be found in [Dev86].

Spectral Shaping

The irregularities in the ionosphere generally show a power law spectrum of the form ①$^{-p}$ [Har92], where ① being the wave number 2⑥/②$_i$ in which ②$_i$ is the spatial wavelength of the irregularities. In our simulation a combination of a butterworth band-pass filter and 1st-order high-pass and low-pass filters (according to [P099]) are used which approximately match experimentally observed power spectral densities [BM087] (see Fig.4):

$$|H|^2 = K\frac{f^{2m_h}}{f^{2m_h}+c^{2m_h}}\frac{f^{2m}}{f^{2ml}+c^{2m_l}}\frac{f^2+a_0^2}{f^2+b_0^2}\frac{f^2+a_1^2}{f^2+b_1^2}\cdots\frac{f^2+a_n^2}{f^2+b_n^2} \qquad (6)$$

Where the gain K is selected to scale the frequency response such that the desired S4 and ⑨₂ are not changed [Po99]. With the following parameter for strong amplitude scintillations:

c (high-pass corner frequency) = 0.08 Hz
d (high-pass corner frequency) = 0.08 Hz
m_h (high-pass order) = 2
m_l (low-pass order) = 2
a_0 = 1.75 Hz b_0 = 1.25 Hz
a_1 = 2.75 Hz b_1 = 2.25 Hz
K (normalising constant) = 0.3765

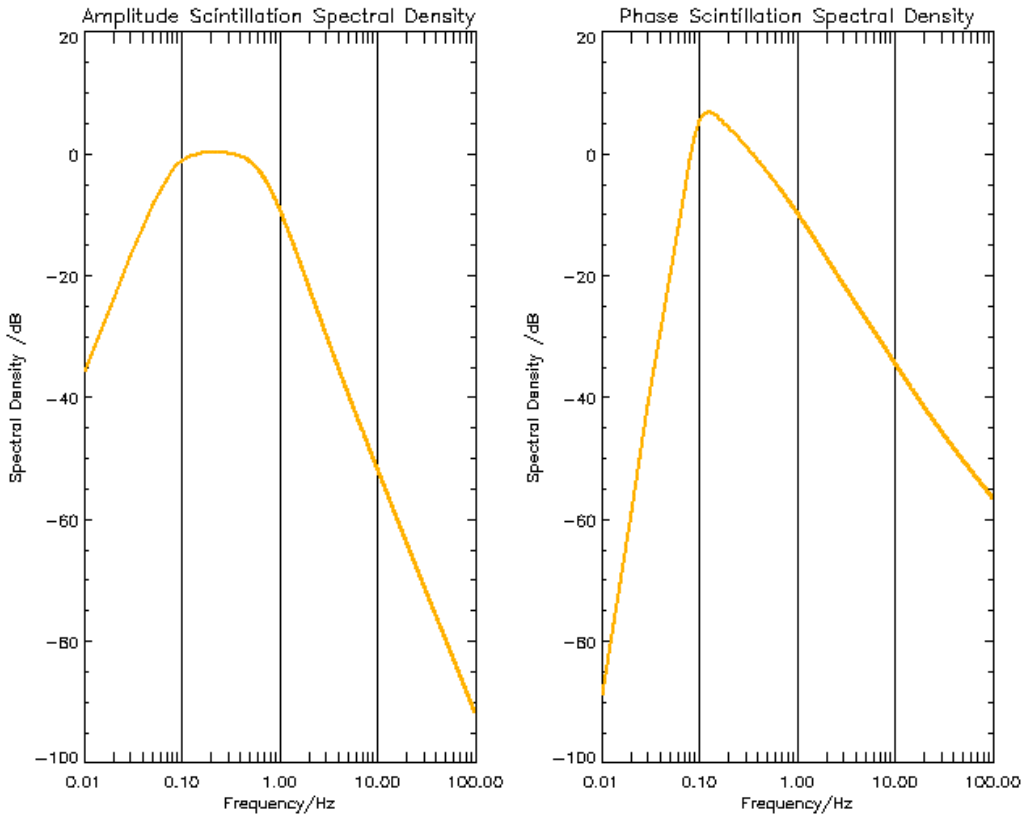

Figure 4: Transfer function of the model-filter used for spectral shaping

and for moderate phase scintillation:

c (high-pass corner frequency) = 0.1 Hz
d (high-pass corner frequency) = 0.1 Hz
m_h (high-pass order) = 5
m_l (low-pass order) = 1
a_0 = 2.5 Hz b_0 = 1.5 Hz
a_1 = 15.0 Hz b_1 = 10.0 Hz
K (normalising constant) = 2.2244

Results

As a result only two examples of the signal generation are shown.
Fig.5 shows the resulting amplitude and phase variations that are used to modify the signal of the simulated satellites. The simulation was done for a scintillation index of S4=0.5, ⑨₂=0.15 rad and a correlation coefficient of ⑧ = -0.6 for 1000 samples, or 20 seconds at an update rate of *50* Hz.

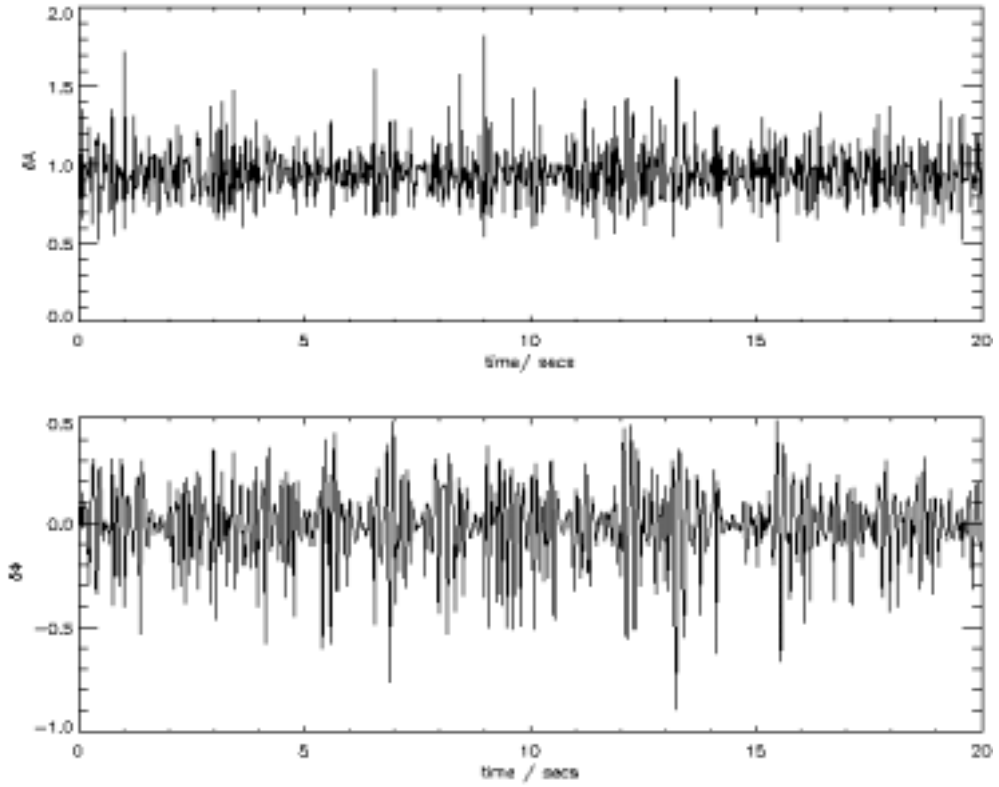

Figure 5: Amplitude and phase variations

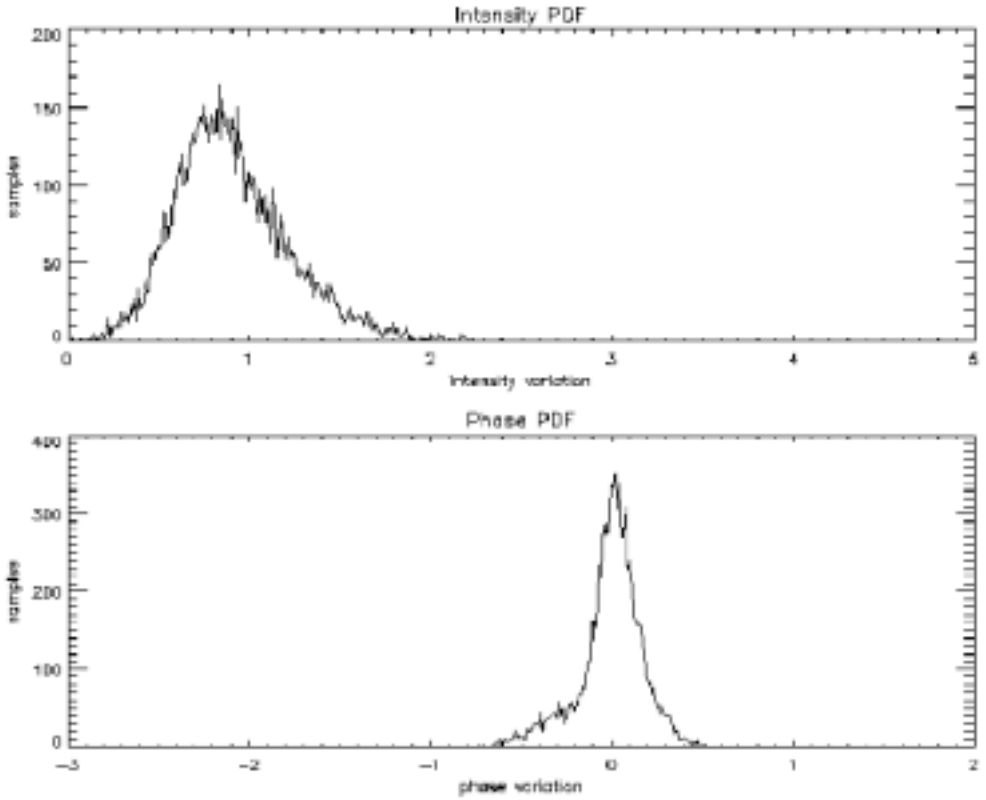

Figure 6: Probability density function of simulation

Summary

This paper shows the first attempt of a scintillation signal generator for the NavSim simulator, based on statistical descriptions of the characteristics of ionospheric scintillations and the GIM model for global distributions of the scintillation strength. Along with the implemented models for the regular ionosphere, even at this early stage of the project users of the simulator will be able to reproduce all major effects of ionospheric influence on radio signals.
Future work will concentrate on the improvement and optimisation of the shaping filters, as mentioned in the paper, the filters used here for all scintillation cases are merely samples of observed data.

References

[BM087] S. Basu, E. Martin, and other. 250 MHz/GHz Scintillation Parameters in the Equatorial, Polar, and Auroral Environments. IEEE Journal on selected areas in communications, SAC-5(2):102-115, February 1987.

[CK98] M. A. Cervera and M. F. Knight. Time series modelling of intensity andphase scintillation at GPS frequencies. In Acta Geod. Geoph. Hung., volume33(1), pages 25-40,1998.

[Dev86] Luc Devroye. Non-Uniform Random variate Generation. Springer_Verlag, New York, 1986.

[Har92] J.H. Hargreaves. The solar-terrestrial environent. Cambridge University Press, 1992.

[HBo99] C. Hegarty, M. Bakry El-Arini, and other. Scintillation Modeling for GPS/WAAS Receivers. In ION GPS, pages 799-807, January 1999.

[Po99] S. Pullen, and other. A preliminary study of the effect of ionospheric scintillation on WAAS user availability in equatorial regions. In ION GPS, September 1998.

[SE99] S. Schlüter and E. Engler. Simulation of ionospheric corrections regarding of solar activity on GNSS. In ETT99 / SATNAV 99, pages 321-324, Potsdam, 08-12 November 1999.

[SFEo999 A. Steingass, J. Furthner, E. Engler, and other. Modular end-toend software simulator for navigation systems. In GNSS, Genua, October 1999.
B.

[WAAS72] H. E. Whitney, J. Aarons, R. S. Allen, and D. R. Seeman. Estimation of the cumulative amplitude probability density function of ionospheric scintillation. Radio Science, 7:1095-1104, 1972.

High Precise Clock Simulation Included in the Modular Software Simulator for Navigation Systems NavSim

Rainer Krämer
DLR Institute of Communication and Navigation
Wessling, Germany

Abstract

The paper presents the time simulation modules for the end-to-end simulator for satellite navigation systems (project: Modular Software Simulator for Navigation Systems NavSim), which simulates the clock errors on satellites and ground stations as well as the resulting system time error. The paper describes the used models and algorithms and shows some simulation results.

Introduction

The German Aerospace Center (DLR) is developing an end-to-end simulator for satellite navigation systems (project: Modular Software Simulator for Navigation Systems NavSim), which is proposed as a suitable environment to develop and to evaluate models, algorithms and technical components in the navigation area under nearly realistic conditions. An example is the derived ”signal and equipment specific model of range and phase errors” based on the gathered data by partial simulations in the signal simulation level. For example, such models are important to lab–generate disturbed range and phase measurements in real time or to build up suitable signal simulators for receiver certification. To fulfil the requirements of an end–to–end simulation system the developed system consists of connected modules arranged in two simulation layers – the so–called signal simulation level and the application simulation level. This is necessary to achieve an acceptable computational complexity and to be open for further developments inside the simulator and its application as a tool. For further information about the whole simulator see [1] and [2]. This paper will describe the complete time simulation modules, which are included in the simulator.

The high precise synchronisation of the satellite clocks to a common time scale, called system time, is an important requirement for all satellite navigation systems like GPS, GLONASS and the planned new European system Galileo. The deviations of the satellite clocks from this system time directly impacts the accuracy of the navigation solution. Thus for the improvement of an existing, or the development of a new satellite navigation system, the choice of the right clock concept is very important. This comprises the selection of the used clock types (H-maser, caesium, rubidium, quartz) in the space and ground segment as well as the optimisation of the generation method for the system time.

Overview of the Time Modules in NavSim

There are three time specific modules implemented in the simulator - the clock module, the system time module and the predicted system time module.

The clock module simulates the error effects caused by real physical clocks. For that the stochastic errors of all used clocks, for the space segment as well as for the ground segment, are simulated by using a so called power-law model. With this model, which describes all five stochastic clock noise types ["random walk frequency modulated noise (RWFM)", "flicker frequency modulated noise (FFM)", "white frequency modulated noise (WFM)", "flicker phase modulated noise (FPM) and "white phase modulated noise (WPM)], it is possible to simulate any kind of high precision clock. Additionally, the deterministic clock errors like clock offset, frequency rate, and drift are modelled too.

The necessary parameters are calculated from the Allan variance information, which is normally available in the data sheet of a real clock. Thus the user can individually simulate each existing real clock (according to its data sheet) or design new clocks. Furthermore, the program allows the user to choose clocks from a large list of predefined clocks, which contains different H-masers, rubidium, caesium and quartz clocks. With this, the user can individually define the clocks for each satellite and each ground station in the simulation.

With these simulated physical times of all clocks, the software calculates the system time with different algorithms.

For the system time generation, the user can individually specify which clocks should be used. Additionally, the influence of each clock can be adjusted by a weighting factor. The first version of the simulator implements a weighted least square algorithm for the system time generation. For the future an additional implementation of a Kalman filter is planned. Furthermore, a possibility exists to implement later more algorithms due to the modular design of the simulator. Thus the effects of the clock errors of different clock types, as well as the algorithms used for calculating the system time or the clock correction coefficients, can be analysed.

Besides, in the predicted system time module the clock correction coefficients A0, A1, A2 will be calculated for each satellite by using a quadratic regression.

Clock Simulation

The model of the time error of a physical clock $x_e(t)$ can be divided into a deterministic and a stochastic component.

$$x_e(t) = x_d(t) + x_s(t) \tag{1}$$

The deterministic part can simply be modelled with the second order polynomial

$$x_d(t) = a_0 + a_1 \cdot (t - t_0) + a_2 \cdot (t - t_0)^2 \tag{2}$$

where a_0, a_1, a_2 and t_0 are the parameters, which describe the deterministic clock behaviour.

For defining a model for the stochastic part of the clock phase error we can use as a starting point the well known power law model for the output of an oscillator. This

model, which is for example described in [3], says that the stochastic error signal of an oscillator $y_s(t)$ can be represented most suitably by means of the following spectral density

$$S_{y_s}(f) = \begin{cases} \sum_{\alpha=-2}^{+2} h_\alpha \cdot f^\alpha & f \le f_h \\ 0 & f > f_h \end{cases} \quad \text{for} \quad , \tag{3}$$

where f_h is the cutoff frequency and h_α is a coefficient. This model covers all actually known stochastic noise types of an oscillator, which are:

α = -2: Random walk frequency modulated noise (RWFM)

α = -1: Flicker frequency modulated noise (FFM)

α = 0: White frequency modulated noise (WFM)

α = 1: Flicker phase modulated noise (FPM)

α = 2: White phase modulated noise (WPM)

With the connection between normalised frequency $y_s(t)$ and the so called phase-time $x_s(t)$

$$y_s(t) = \frac{d}{dt} x_s(t) \tag{4}$$

we get from (3) the power spectral density for the clock phase-time error:

$$S_{x_s}(f) = \frac{1}{(2\pi)^2} \sum_{\alpha=-2}^{+2} h_\alpha \cdot f^{\alpha-2} \quad \text{for} \quad f \le f_h \tag{5}$$

As we can see, the power spectral density can be decomposed into five parts and so the stochastic clock time error can also be described as a sum of five different noise error signals.

$$x_s(t) = \sum_{\alpha=-2}^{+2} x_\alpha \tag{6}$$

This five noise error signals can be generated by means of convolutions of white Gaussian distributed noise signals $w_\alpha(k)$ with the discrete impulse response functions $g_\alpha(k)$, as it is shown in figure 1. For simulating the clock error we now need two calculation specifications, one for the impulse response functions $g_\alpha(k)$ and one for the covariance values for the white Gaussian noise signals $w_\alpha(k)$.

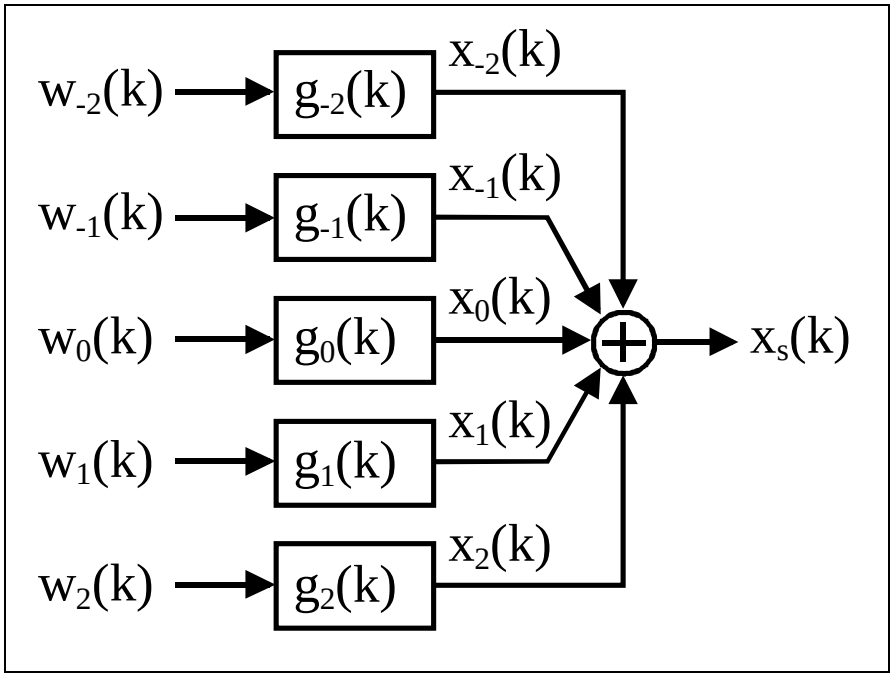

Fig. 1: Principle generation of $x_s(k)$

As a starting point for calculating $g_\alpha(k)$ we can use the following model for the corresponding discrete transfer function

$$G_\alpha(z) = \left(1 - z^{-1}\right)^{\frac{\alpha}{2}-1}, \tag{7}$$

which was first proposed by Hosking [4] and called fractional differencing. If we now calculate the power series expansion of (7) we get

$$\begin{aligned} G_\alpha(z) = 1 + \frac{\left[1-\frac{\alpha}{2}\right]}{1!}\cdot z^{-1} + \frac{\left[1-\frac{\alpha}{2}\right]\cdot\left[2-\frac{\alpha}{2}\right]}{2!}\cdot z^{-2} + \\ + \frac{\left[1-\frac{\alpha}{2}\right]\cdot\left[2-\frac{\alpha}{2}\right]\cdot\left[3-\frac{\alpha}{2}\right]}{3!}\cdot z^{-3} + \ldots \end{aligned} \tag{8}$$

which discrete pulse response function belonging to it results:

$$\begin{aligned} g_\alpha(k) = 1\cdot\delta(k) + \frac{\left[1-\frac{\alpha}{2}\right]}{1!}\cdot\delta(k-1) + \frac{\left[1-\frac{\alpha}{2}\right]\cdot\left[2-\frac{\alpha}{2}\right]}{2!}\cdot\delta(k-2) + \\ + \frac{\left[1-\frac{\alpha}{2}\right]\cdot\left[2-\frac{\alpha}{2}\right]\cdot\left[3-\frac{\alpha}{2}\right]}{3!}\cdot\delta(k-3) + \ldots \end{aligned} \tag{9}$$

With (9) we can find the following calculation specification for the discrete impulse response functions $g_\alpha(k)$:

$$g_\alpha(0)=1$$
$$g_\alpha(n)=g_\alpha(n-1)\cdot\left(1-\frac{\alpha}{2\cdot n}\right) \tag{10}$$

In the next step the variances

$$Q_\alpha = E\left\{w_\alpha(k)^2\right\} \text{ with } E\{w_\alpha(k)\}=0 \tag{11}$$

of the white Gaussian distributed noises must be calculated. For that we calculate the power spectral density $S_{x\alpha}(f)$ for the given transfer function (7) and the input signal $w_\alpha(k)$ with the variance (11). As described in [5], we get

$$S_{x_\alpha}(f)\cong 2\cdot Q_\alpha\cdot\tau_0{}^{\alpha-1}\cdot(2\pi\cdot f)^{\alpha-2} \tag{12}$$

which is an approximation for frequencies well below the Nyquist frequency $\left(\frac{1}{2\cdot\tau_0}\right)$.

Comparing (12) with (5), we get for the searched variance

$$Q_\alpha=\frac{h_\alpha}{2\cdot(2\pi)^\alpha\cdot\tau_0{}^{\alpha-1}} \tag{13}$$

which depends on the noise coefficient h_α. Normally in the data sheet of time and frequency standards the stability is given by a list of typical Allan deviations depending on τ and not the noise coefficients h_α. Thus if we want to simulate a given clock, the noise coefficient must be calculated from the given Allan deviations. For that we can use the following relations adapted from Barnes et al. [6]:

$$h_2={}^A\sigma_y^2(\tau_2)\cdot\frac{4\pi^2}{3\cdot f_h}\cdot\tau_2{}^2$$
$$h_1={}^A\sigma_y^2(\tau_1)\cdot\frac{4\pi^2}{6+3\cdot\ln(2\cdot f_h\cdot\pi\cdot\tau_1)-\ln(2)}\cdot\tau_1{}^2$$
$$h_0={}^A\sigma_y^2(\tau_0)\cdot 2\cdot\tau_0 \tag{14}$$
$$h_{-1}={}^A\sigma_y^2(\tau_{-1})\cdot\frac{1}{2\cdot\ln(2)}$$
$$h_{-2}={}^A\sigma_y^2(\tau_{-2})\cdot\frac{6}{4\pi^2}\cdot\tau_{-2}{}^{-1}$$

where τ_α with $\alpha=\{-2,-1,0,1,2\}$ has to be chosen in a way, that the Allan variance ${}^A\sigma_y^2(\tau_\alpha)$ mainly represents the noise type belonging to the h_α coefficient.

Summarising, the following steps must be taken for the calculation of the clock error signal:

1. Calculation of the noise parameters $\{h_{-2}, h_{-1}, h_0, h_1, h_2\}$ by using the information of given typical Allan variance values according to (14).
2. Calculation of the covariance values $\{Q_{-2}, Q_{-1}, Q_0, Q_1, Q_2\}$ with (13).
3. Generation of five white Gaussian noise signals $\{w_{-2}, w_{-1}, w_0, w_1, w_2\}$ with the covariance values $\{Q_{-2}, Q_{-1}, Q_0, Q_1, Q_2\}$.
4. Generation of the impulse response functions $\{g_{-2}, g_{-1}, g_0, g_1, g_2\}$ according to (10).
5. Convolution of the white Gaussian noise signals with the impulse response function.
6. Calculation of the deterministic clock errors according to (2).
7. Calculation of the final clock error signal by adding the results from point 5 and 6.

The next figures show the results of the simulation of four typical clock types, an active H-maser, a passive H-maser, a caesium time standard and a rubidium atomic frequency standard. Figure 2 shows over a short time and the fig. 3 over a long time the simulated clock time error. If we have a look on this pictures, we see the typical clock behaviours for the four clock types. As for an example we can see, that the rubidium atomic frequency standard has the worst long time behaviour, whereas the active H-maser has the best short time and the caesium standard has the best long time stability.

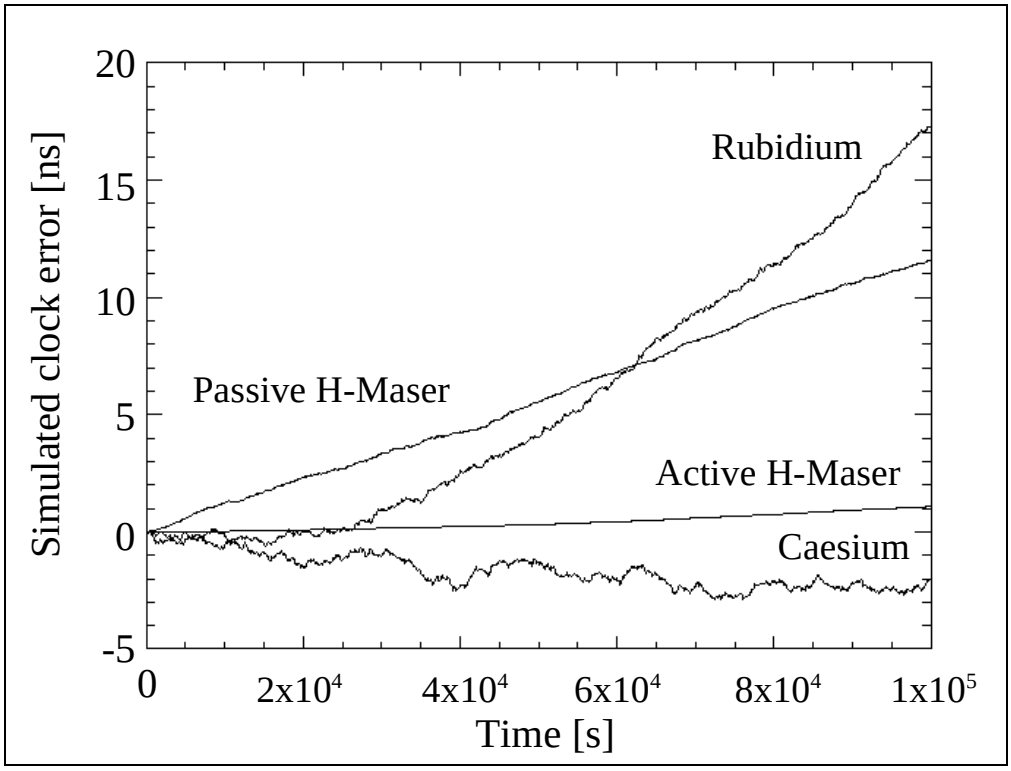

Fig. 2: Simulated short time clock errors for typical clock types

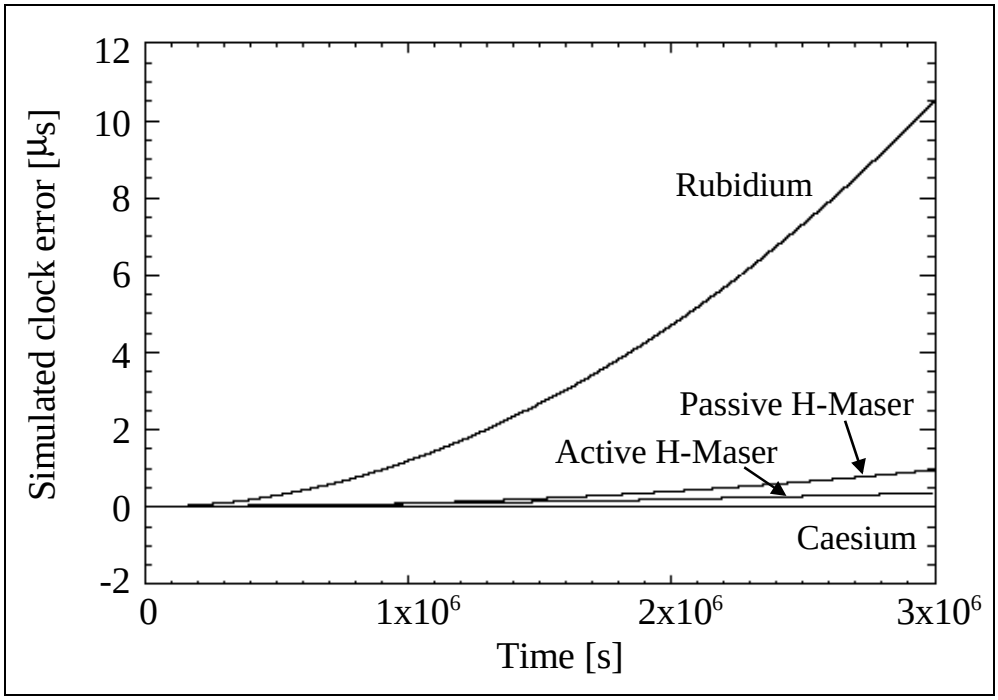

Fig. 3: Simulated long time clock errors for typical clock types

Finally the Allan deviations of the simulated clocks are depicted in the next figure.

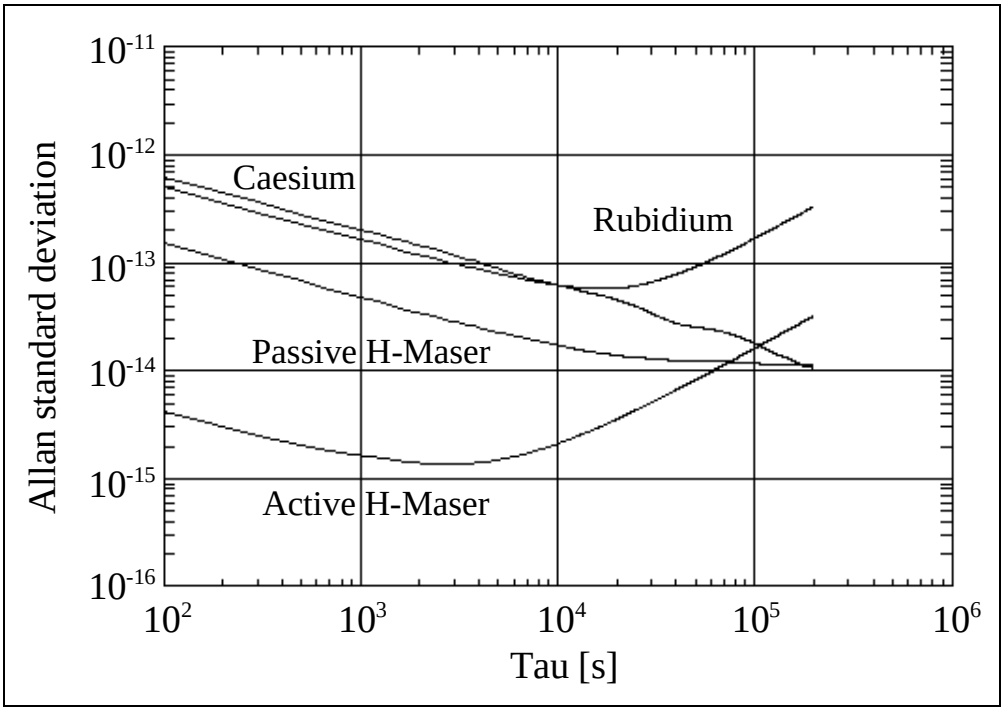

Fig. 4: Allan standard deviation of the simulated clocks

System Time Generation

After the error simulation of each individual physical clock in a chosen scenario of a navigation satellite system, the clock module "system time" calculates the error of the global navigation system time, which is an ensemble time of all or an user defined selection of the simulated clocks. Furthermore, the influence of used clocks on the

ensemble time can be adjusted by user defined weights. One realised method to calculate the error of the system time, resulting from a weighting least square formulation, is

$$x_{e,sys}(k) = \frac{\sum_{i=1}^{N} p_i \cdot x_{e,i}(k)}{\sum_{i=1}^{N} p_i} \quad , \tag{15}$$

where $x_{e,i}(k)$ is the clock error signal $x_e(k)$ of the ith clock and

$$p_i = b_i \cdot \frac{1}{A\sigma_i^2(\tau_{opt})} \tag{16}$$

is a weighting factor, which is the product of the user defined weighting factor b_i and the inverse Allan variance of the clock for a specific $\tau = \tau_{opt}$, for which the system time should be optimised.

As a simulation example, the fig. 5 shows the Allan deviation plots of two caesium time standards and two rubidium atomic frequency standards as well as the resulting system time optimised for $\tau_{opt} = 1000s$, calculated from this four clocks.

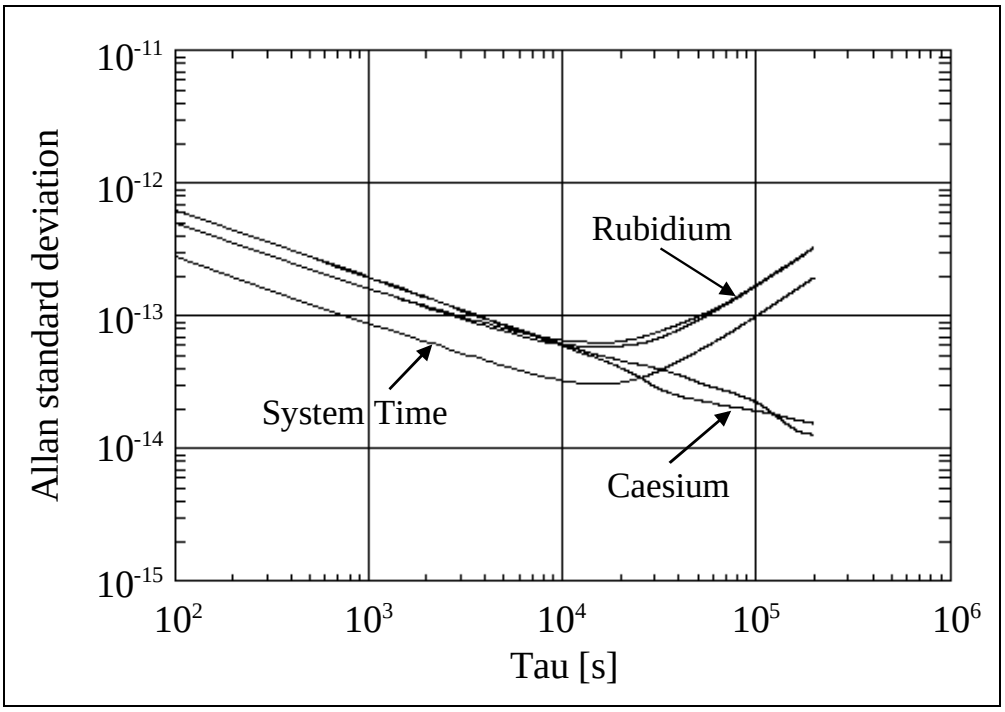

Fig. 5: Allan standard deviation of simulated clocks and system time

An additional implementation of other alternative algorithms for calculating the system time is planned for the future.

Predicted System Time Generation

The last time module "predicted system time" calculates the time correction coefficients A0, A1, A2 for each satellite clock. This parameters, which adapt the physical clock time to the system time, are included in the satellite navigation message.

For the difference between the i^{th} satellite clock and the calculated system time we get

$$x_{kor,i}(k) = x_{e,sys}(k) - x_{e,i}(k)\ , \tag{17}$$

which should be expressed by the following second order polynomial

$$x_{kor,i}(k) = A_0 + A_1 \cdot (k - k_0) + A_2 \cdot (k - k_0)^2 + \varepsilon(k) \tag{18}$$

for an interval of

$$k_0 < k < m + k\,, \tag{19}$$

where $\varepsilon(k)$ is the error between the polynomial and the actual value of $x_{kor,i}(k)$.

For the error signal we can suppose white Gaussian distributed noise with the properties:

$$E\{\varepsilon(k)\} = 0 \quad \text{and} \quad E\{\varepsilon(k)^2\} = q \tag{20}$$

If we now want to calculate the correction coefficients for the interval (19) we have m equations (measurements) like (18), which can be written in the following vector-matrix notation:

$$\underline{x}_{korr,i} = B \cdot \begin{bmatrix} A_0 \\ A_1 \\ A_2 \end{bmatrix} + \underline{\varepsilon} \quad \text{where} \quad B = \begin{bmatrix} 1 & 1 & 1 \\ 1 & 2 & 4 \\ 1 & 3 & 9 \\ \vdots & \vdots & \vdots \\ 1 & m & m^2 \end{bmatrix} \tag{20}$$

Finally, if we calculate the least square solution of (20), we get

$$\begin{bmatrix} A_0 \\ A_1 \\ A_2 \end{bmatrix} = \left(B^T \cdot B\right)^{-1} \cdot B^T \cdot \underline{x}_{korr,i}\ , \tag{21}$$

with which the correction coefficients for the i^{th} satellite can be estimated in an optimal manner.

Conclusion

The time specific modules, implemented in the end-to-end software simulator, calculate the physical clock errors of all used clocks in the simulated navigation system. Furthermore, the error of the system time and the time correction coefficients for each

satellite will be calculated too. With that the simulator is able to simulate all time depending aspects for a satellite navigation system under nearly realistic conditions.

References

[1]: A. Steingaß, P. Robertson, M. Angermann, J.Selva, J. Furthner, J. Hahn, A. Hornbostel, R. Krämer, H.P. Müller, E. Engler, T. Noack, S. Schlüter
"Modular end-to-end software simulator for navigation systems"
3rd European Symposium on Global Navigation Satellite Systems (GNSS'99), Genova, Italy, 5-8 October, 1999, pp. 385-391

[2]: J. Furthner, E. Engler, A. Steingass, M. Angermann, J. Hahn, A. Hornbostel, R. Krämer, H.P. Müller, T. Noack, P. Robertson, S. Schlüter, J. Selva
"Realisation of an End-to-End Software Simulator for Navigation Systems"
IJSC Special Edition on Satellite Navigation and Positioning, Wiley & Sons, 2000

[3]: P. Kartaschoff
"Frequency and Time"
Academic Press Inc. (London) Ltd, 1978, ISBN 0-12-400150-5

[4]: J.R.M. Hosking
"Fractional differencing"
Biometrika, Vol. 68, No. 1, 1981, pp. 165-176

[5]: N.J. Kasdin, T. Walter
"Discrete Simulation of Power Law Noise"
IEEE Frequency Control Symposium, 1992, pp. 274-283

[6]: J. Barnes, A. Chi, L. Cutler, D. Healey, D. Leeson, T. McGunigal, J. Mullen, W. Smith, R. Sydnor, R. Vessot, G. Winkler
"Characterization of Frequency Stability"
Transaction on Instrumentation and Measurement, Vol. IM-20, No.2,
May 1971, pp. 105-120

Simulation of Tropospheric Effects for Satellite Navigation

Achim Hornbostel
DLR Institute of Communication and Navigation
Oberpfaffenhofen, Germany

Abstract

The delay of satellite navigation signals due to the troposphere and its correction play an important role for the accuracy of the derived position solution. As part of an navigation end-to-end simulator a troposphere module was developed, which simulates group and phase delay, attenuation and noise due to dry gases, water vapor and rain. Simulation results are compared with different commonly used tropospheric correction models. Regional and temporal analyses of delay and signal-to-noise ratio and the effect of tropospheric delay on the position solution are shown for typical scenarii.

Introduction

The refractive index ($n > 1$) of the earth's neutral atmosphere reduces the propagation speed of radio frequency signals. The gradient of the refractive index with height causes additionally a curvature of the propagation path. Both effects lead in the sum to a delay of satellite navigation signals in comparison to free space propagation. This delay is commonly called tropospheric delay, although it includes contributions both by the troposphere and stratosphere.

The tropospheric delay can be separated in a wet component due to water vapor and a dry component due to the other atmospheric gases, which is dependent on atmospheric pressure and temperature. Typical values of the total vertical delay in zenith direction are about 2.5 m. Although the wet delay contributes normally only with 10%-20% to the total delay, the high temporal and spatial variability of the water vapor in the troposphere makes the wet delay to the most crucial component if accuracies in the decimetre or centimetre range are required.

An exact modelling of the tropospheric delay requires the knowledge of the actual vertical profiles of pressure, temperature and water vapor. This information is not available for most navigation users. Typical correction models [1-8] calculate the delay in vertical direction (zenith delay) from measured, predicted or long-time mean values of pressure, temperature and humidity on the earth surface and derive the delay at other elevation angels by multiplication with so-called mapping functions. Because these models have to make some assumptions for the shape of the vertical refractivity profile, which will never exactly represent the actual state of the atmosphere, a residual error will remain, even if the meteorological parameters at the surface can be measured without error.

As part of a modular software simulator for navigation systems (NAVSIM) a troposphere module, which simulates the group and phase delay, attenuation and noise due to dry gases, water vapor and rain was developed. In order to perform the simulation independently from correction models which may be used in the receiver, a ray-tracing algorithm is applied, which calculates the tropospheric delay by integration of the refractive index along the curved paths from the receiver location to each satellite in view. The refractivity profile in dependence of height is simulated with standard vertical profiles of temperature T, pressure P and partial pressure of water vapor P_w for different regions and seasons. Results of the ray-tracing algorithms are compared with an easy to use tropospheric correction model [3, 11] in order to show the usefulness and limitations of such models. More comprehensive comparisons of different correction models with ray-tracing results can be found in [9, 10].

The path attenuation due atmospheric gases is computed in a similar way as the delay by integration of the specific attenuation in dB/km, which is calculated as a function of height and frequency from the vertical atmospheric profiles. Optionally, in NAVSIM rain attenuation and rain delay can be simulated either for a reselected system availability utilising the ITU-R rain zone model [13] or, alternatively, with user defined rain rates and rain cell dimensions. Generally, the additional signal delay due to rain is two or three orders smaller than the delay by atmospheric gases. Finally, the thermal noise in path direction is directly derived from the total path attenuation (rain plus clear atmosphere) applying radiometric formulas. At L-band frequencies which are used by the current satellite navigation systems GPS and GLONASS attenuation and noise are generally low. However, at higher frequency bands, e.g. in C-band which is still in discussion for future systems, the rain attenuation and noise increase and can significantly reduce the signal-to-noise ratio during intense rainfall.

NAVSIM allows a global or regional and temporal analysis of the tropospheric delay, attenuation and noise seen by the user in dependence on the satellite configuration. Also the effect of propagation errors on the position solution can be simulated. Some examples will be shown.

Refractive Index and Delay

The tropospheric delay can be expressed as excess path in addition to the geometric path length by integration of the tropospheric refractivity $N=10^6\ (n-1)$ along the curved path through the neutral atmosphere, where n is the real part of the refractive index:

$$\Delta L = 10^{-6} \int_L N(s)\,ds \qquad (1)$$

The refractivity at a specific height depends on the vertical profiles of temperature T in Kelvin and the partial pressures of dry air P_d and water vapor P_w in mbar [14]

$$N = 77.6\frac{P_d}{T} + 64.8\frac{P_w}{T} + 3.776\cdot 10^5\,\frac{P_w}{T^2} = N_d + N_w \qquad (2)$$

The first term depending on P_d is called the dry component and the sum of the two other terms depending on P_w the wet component. Consequently, replacing N by N_d+N_w in (1), a dry and a wet delay can be defined. With substitution of P_d by P- P_w where P is the total air pressure, (2) can be rewritten as:

$$N = K_1 \frac{P}{T} + (K_2 - K_1)\frac{P_w}{T} + K_3 \frac{P_w}{T^2}, \qquad (3)$$

where K_1, K_2 and K_3 are the constants of (1).

Assuming that the air behaves as an ideal gas, an alternative form of equation (2) can be derived [11, 10]:

$$N = K_1 \cdot R_d \cdot \rho + (K_2 - K_1 \frac{R_d}{R_w})\frac{P_w}{T} + K_3 \frac{P_w}{T^2} = N_h + N_w', \qquad (4)$$

where ρ is the total air density in kg m^{-3}, and R_d =2.87 and R_w =4.61 are the specific gas constants for dry air and water vapor. The first term on the right hand side of (4) is called the hydrostatic component and the sum of the other two terms again the wet component. It is important to note that the hydrostatic component is not purely dry, but includes a small contribution by water vapor, and that the wet components in (2), (3) and (4) are slightly different.

Zenith Delay and Path Delay

The zenith delay can be calculated with (1) by integration of N in vertical direction from ground to the top of the neutral atmosphere. Common correction models do this separately for the dry or hydrostatic component and the wet component, where assumptions are made for the vertical profiles.

The *Hopfield* model [1] assumes a quartic profile for the dry component of the form:

$$N_d = N_{ds}\left(\frac{H_d - h}{H_d}\right)^4. \qquad (5)$$

H_d is the scale height (about 43 000m) for the dry atmosphere and depends on the surface temperature. For the wet component the same profile with a constant scale height H_w around 11 000 m is assumed. Performing the integration separately for the dry and wet component from the surface up to the scale heights H_d and H_w the zenith delay is simply:

$$\Delta L^Z = \Delta L_d^Z + \Delta L_w^Z = \frac{10^{-6}}{5}(N_{ds}H_d + N_{ws}H_w), \qquad (6)$$

where N_{ds} und N_{ws} are the dry and wet refractivity components according to (2) at the surface, i.e. at the height of the measurement station (not at sea level). The path delay into other directions with elevation angles E is derived by multiplying the wet

and dry zenith delay with so-called mapping functions:

$$\Delta L(E) = \Delta L_d^Z \cdot m_d(E) + \Delta L_w^Z \cdot m_w(E) \qquad (7)$$

Although mapping functions were suggested already by Hopfield, other mapping functions for application with the Hopfield zenith delay model were developed by *Black* [3], *Goad and Goodman* [4] and others. The Hopfield/Black model was employed with some small modifications in the coefficients for the GPS control segment [11,12, 20]. It is referenced here, because it is used later for comparison with the ray-tracing results:

$$\Delta L(E) = \frac{0.002312 P H_d \left[1+5(r_m - r_a)/H_d\right]}{148.98 T \sqrt{1-\left[\frac{r_a \cos(E)}{r_m + (1-C)H_d}\right]^2}} + \frac{0.0746 P_w H_w \left[1+5(r_m - r_a)/H_w\right]}{T^2 \sqrt{1-\left[\frac{r_a \cos(E)}{r_m + (1-C)H_w}\right]^2}}; \qquad (8)$$

r_a and r_m are the radial distances from the earth centre of the receiver antenna and of the monitor station, where the surface measurements of P, T and P_w are taken, and C is a constant equal to 0.85 for elevation angles E>5°. The wet scale height H_w is set here to a constant value of 13 000 m, and the dry scale height H_d is calculated from the surface temperature:

$$H_d = 148.98\,(T - 4.11) \qquad (9)$$

Applying (4), the hydrostatic component of the zenith delay can be written without any assumption for the vertical profile with the hydrostatic equation:

$$\Delta L_h^Z = 10^{-6} K_1 \cdot R_d \frac{P_s}{g_m}, \qquad (10)$$

where g_m is the acceleration due to gravity at the centre of mass of the vertical column of air, and P_S is the surface pressure. The hydrostatic zenith delay is applied e. g. in the models by *Saastamoinen* [2] and *Baby* [5], where g_m is modelled in dependence of height and latitude. Further models for the wet zenith delay are listed in [9, 10]. There are also a number of more or less sophisticated mapping functions, which map either the dry or hydrostatic and wet delay or the total delay. An overview is given in [9, 11]. In particular the mapping functions for hydrostatic and wet delay of the *Marini* [6] type with further improvements by *Herring* [7] and *Neill* [8] receive currently attention [20].

Ray-Tracing Algorithm

For solution of the integral (1) the atmosphere is thought to be composed of thin spherical layers of thickness Δh. Applying Snell's law for spherical shells the path length within each layer is:

$$\Delta s = \Delta a \frac{R_e(1 + a \cdot n(a))}{\sqrt{2a \cdot n(a) + a^2 n^2(a) + \sin^2(E)}} \,, \qquad (11)$$

where R_e is the Earth radius, $a=h/R_e$ is the normalised height, $n(a)=n(h)$ is the refractive index at height h, and E is the elevation angle in the initial layer at ground [3, 11]. For calculation of the refractive index for each layer with (2), the following standard atmospheres are implemented [15, 16, 17]:

- US-standard atmosphere (US)
- Summer mid-latitude atmosphere (SML) at 45°N
- Winter mid-latitude atmosphere (WML) at 45 °N
- Subartic summer atmosphere (SAS) at 60° N
- Subartic winter atmosphere (SAW) at 60° N
- Tropical annual average atmosphere (TAA) 15° N

It is assumed that the same atmospheres are valid for the southern hemisphere. The path attenuation by atmospheric gases is computed in a similar way as the delay by integration of the specific attenuation in dB/km, which is calculated as a function of height and frequency from the vertical profiles of T, P and P_w with equations given in [17], along the curved path.

Comparison of Ray-Tracing Results with the GPS Control Segment Model

Figure 1 and Figure 2 show a comparison of the ray-tracing results with the modified Hopfield/Black model used in the GPS control segment (8) for two different receiver heights r_a. Shown is the difference of model minus ray-tracing versus elevation angle for the different standard atmospheres listed above. In the ray-tracing the numerical integration was performed with an increment Δh =1 m up to a height of 100 km.

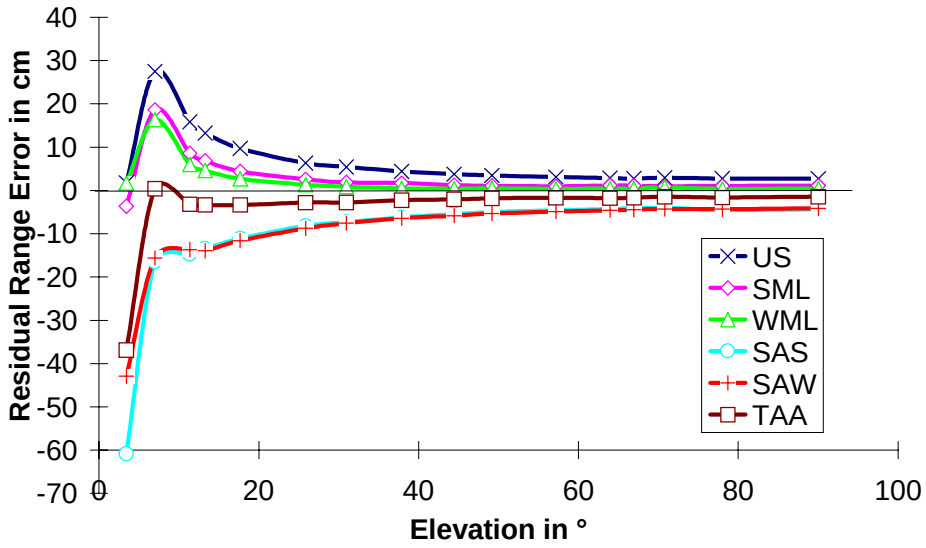

Figure 1 Comparison of ray-tracing results with GPS-model (r_m=0,r_a=10m).

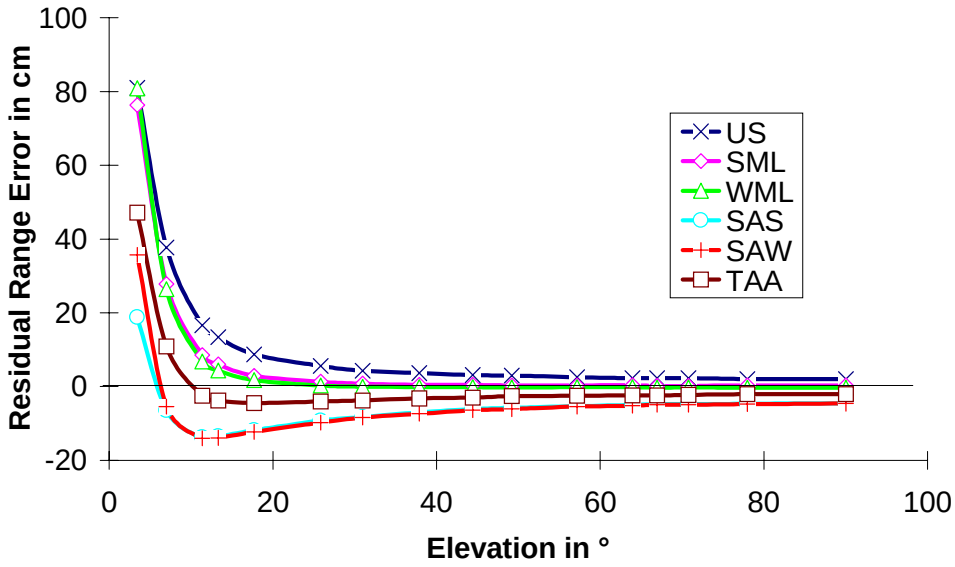

Figure 2 Comparison of ray-tracing results with GPS-model (r_m=0,r_a=500m).

The figures show that the model provides good results for elevation angles > 10°, where the modelling error can be kept below 20 cm. The maximum zenith error is 4 cm for the subartic atmospheres. For mid latitude and tropical atmospheres the error is less than 10 cm. The error (for E > 10°) can be even reduced to below 5 cm for the mid latitude atmospheres, if H_w is set to 12 km, and for the US-Standard atmosphere to less than 10 cm if H_w is set to 11 km. Also the error for the subartic summer atmosphere can be reduced if H_w is set to 15 km, but such height cannot be physically motivated.

For elevations E < 10° the mapping error by the Black mapping functions rapidly increases. For this elevations more sophisticated mapping functions should be applied. Table 1 shows a comparison of the mapping error in cm, if the zenith error is set to 0, for the mapping functions by Black, Goad & Goodman and Neill for the US-standard atmosphere and for the SAS atmosphere as worst case.

The table shows, that the mapping functions by Goad & Goodman [4, 18] yield excellent results for the US-standard atmosphere near sea level (r_a=10m), but that for elevations above10° also the error by the simple Black mapping function is tolerable. For the SAS atmosphere (and others not shown here) there is only a slight improvement by the Goad & Goodman functions. At a receiver height of 500 m there is no improvement at low elevation angles by the Goad & Goodman functions but some improvement for angles above 7°. The Neill mapping functions provide generally good results for elevation angles E > 2°- 3° in all cases, although there is no improvement for the US standard atmosphere at the receiver height 10m in comparison to the other mapping functions at these angles. It has to be noted, that the Neill mapping functions were designed for use with the hydrostatic and wet zenith delay rather than for the dry and wet component as they were applied here.

Elevation angle	0.5°	2.0°	3.4°	7.0°	11.4°	13.3°	17.8°	30.9
Black (US, r_a=10m)	-1707.1	-286.4	-37.9	5.9	2.2	1.6	0.8	0.1
G & G. (US, r_a=10m)	12.2	2.2	4.6	1.2	-0.04	-0.02	0.05	-0.002
Neill (US*, r_a=10m)	-61.5	-94.1	-39.8	-8.7	-3.0	-2.0	-0.9	-0.2
Black (SAS,r_a =10m)	-1649.4	-220.8	-0.17	17.4	6.8	5.0	3.0	1.1
G & G. (SAS,r_a=10m)	138.0	71.6	41.8	12.5	4.5	3.4	2.2	1.4
Neill (SAS, r_a=10m)	184	8.7	11.0	5.6	2.4	2.1	1.6	0.8
Black (US, r_a=500m)	-639	-37.0	49.2	20.8	6.0	4.2	1.9	0.2
G & G. (US, r_a=500m)	735	129.7	50.0	8.4	1.8	1.5	0.6	-0.02
Neill (US*, r_a=500m)	743	44.3	11.1	0.7	-0.4	0.04	-0.08	-0.14

*with mapping functions for 45° latitude summer.

Table 1 Mapping error in cm for US and SAS standard atmospheres with different mapping functions (r_m = 0 m).

Simulation of Rain Effects

Additionally to the clear atmosphere, rain effects can be simulated for a preselected system availability, either for a year or the so-called worst month, utilising the ITU-R rain model [13], where the rain zone and corresponding rain rate for a predefined user location and probability are automatically read from a file. Alternatively, a stratiform or cylindrical raincell model with user defined rain rate and cell dimensions can be applied. If rain rate and rain path geometry are determined by one of these models, the path attenuations and delays for each user-satellite path are calculated by multiplication of the specific rain attenuation and specific delay per km with the effective path lengths. The specific attenuation follows from regression coefficients delivered by the ITU-R rain model; for the computation of the specific delay the imaginary part of the refractive index of rain is calculated with the MPM89-model [19].

The thermal noise temperature seen in path direction is directly derived from the total path attenuation (rain plus clear atmosphere) applying the radiometric formula:

$$T_{noise} = T_m(1-10^{-0.1A}) + T_{cosmos} \cdot 10^{-0.1A}, \qquad (12)$$

where A is the path attenuation in dB, T_m is the effective medium temperature (ca. 270-280 K) and T_{cosmos} is the cosmic background temperature (2.7 K). Finally, the noise temperature is converted to the noise power density by multiplication with the Boltzmann constant.

Regional and Temporal Analysis

For demonstration, 1st January 2000 was chosen to compute the atmospheric scenario. Figure 3 presents the distribution of the vertical tropospheric delay including clear air effects and additional rain delay. The rain contribution was

calculated with the ITU-R rain zone model for a yearly probability of exceedence of 0.01% which corresponds to a system availability of 99.99%. The maximum rain delay is in the order of 2-3 cm and produces a visible enhancement of delay only in the tropical regions, where the highest rain rates occur. The delay is practically independent on frequency up to 30 GHz.

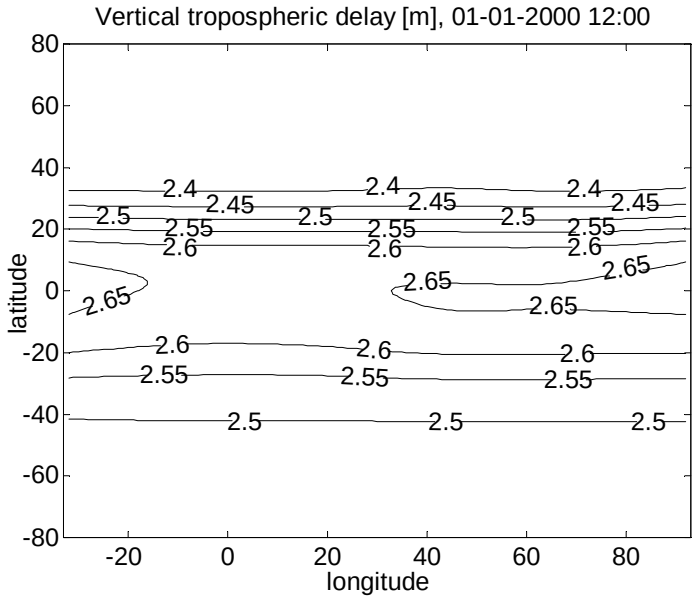

Figure 3 Distribution of vertical tropospheric delay including rain contribution in [m] for Europe and Africa.

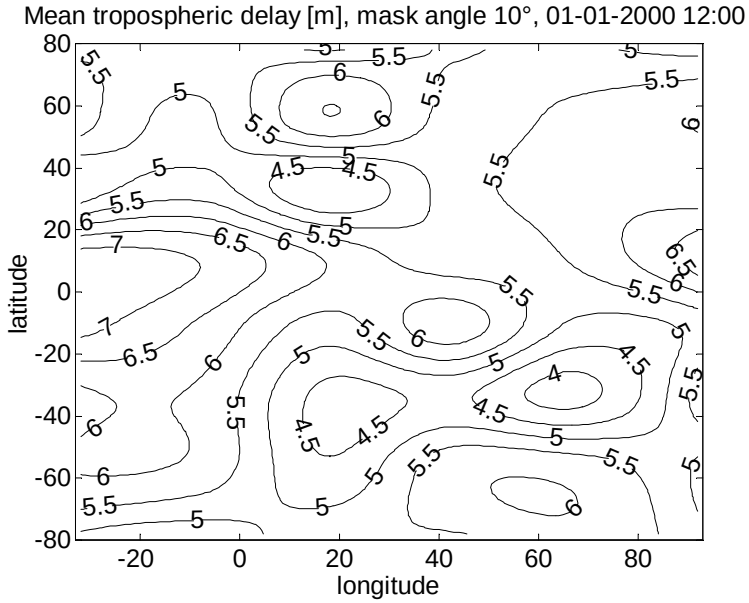

Figure 4 Distribution of mean tropospheric delay in [m] for Europe and Africa with mask angle 10°.

Figure 4 shows the mean tropospheric delay (clear atmosphere plus rain) received by virtual stations well-distributed in a region from –80° to 80° latitude and –30° to 80° longitude for a mask angle of 10° elevation. In this simulation the GPS

satellite constellation was chosen, but also other systems e.g. Galileo are possible. It has to be emphasised that the figures show the averaged values of all visible satellites appearing under elevation angles higher than the mask angle. The delay for a single satellite at the elevation angle 10° is about 15 m. Therefore, the distribution of delay in the figure is mainly due to the actual satellite constellation.

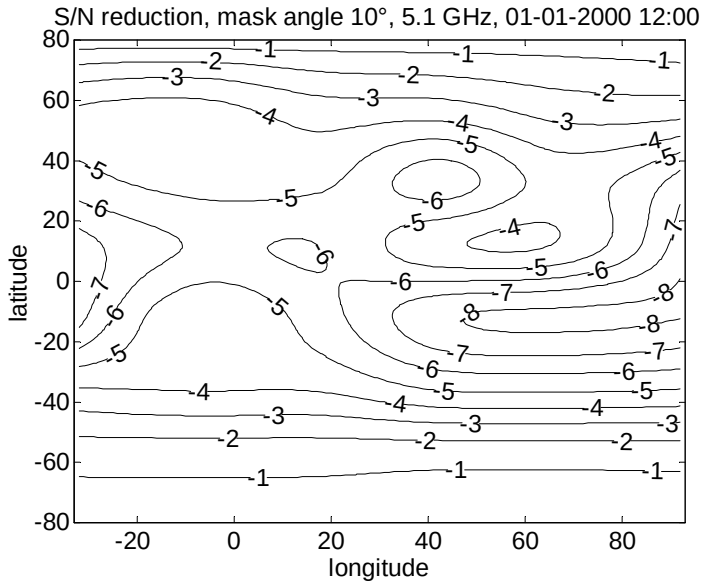

Figure 5 Reduction of signal-to-noise ratio in [dB] due to rain at C-band for a system availability of 99.99% (mean reduction for mask angle 10°).

In Figure 5 the reduction of the signal-to-noise ratio due to rain relative to the clear atmosphere level is shown. The simulation was performed with the GPS satellite constellation, but for C-band. At L-band the S/N reduction is less than 0.8 dB. Here the distribution is mainly by the ITU-R rain zones. In northern mid latitudes the S/N is reduced by 4-5 dB and in tropical regions by up to 8 dB as a mean value for all satellites in view at C-band.

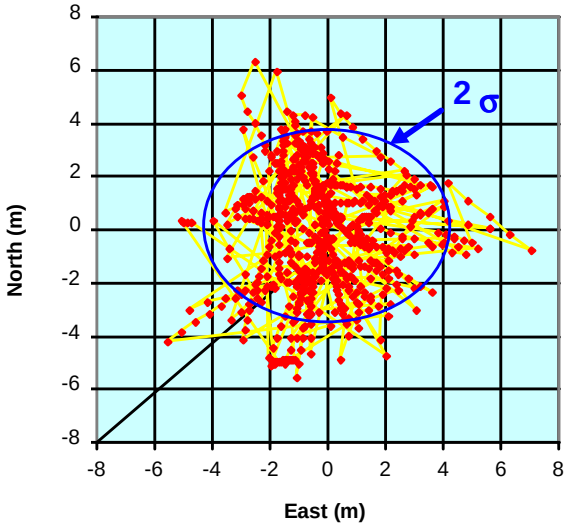

Figure 6 24 hours distribution of position solutions at 1st January 2000 for the receiver site Oberpfaffenhofen, mask angle 10°.

Figure 6 demonstrates how the tropospheric delay effects the position solution, if not corrected. The position solution was simulated for a complete day for a receiver location in Oberpfaffenhofen (latitude 48°N, longitude 11°E, height above sea level 595 m). The maximum error is about 6 m and the 2σ value is about 4 m. All other error sources except the clear atmosphere delay were excluded.

Conclusion

Within the end-to-end software simulator for satellite navigation NAVSIM tropospheric effects including delay, attenuation and noise are simulated. Ray-tracing results with standard atmospheres for different latitudes and seasons have been compared with the relatively simple modified Hopfield/Black model employed in the GPS control segment. The comparison shows that this model yields good results for elevation angles above 10° in particular for mid-latitude and tropical regions. However, for lower elevation angles more sophisticated mapping functions should be used. The mapping functions by Goad and Goodman produced excellent results for the US-standard atmosphere at a receiver height near sea level even for an elevation angle of 0.5°, but already at a receiver height of 500 m and for the other standard atmospheres the improvement was only small. Generally, the Neill mapping functions produced the best results for elevation angles above 3°. These results confirm the findings of other authors, e. g. it was recently suggested [20] to replace the Black mapping functions with the Neill mapping functions in the GPS control segment.

An analysis of the mean tropospheric delay at sea level for the GPS satellite constellation showed average values of 4.5 to 7 m for all satellites in view with a mask angle of 10°. The resulting 2σ error in the position solution due to the tropospheric delay is about 4 m for the same mask angle in mid latitudes. An analysis of vertical delay for the clear atmosphere showed values between 2.4 and 2.65 m. The additional vertical delay due to rain is in the order of 2-3 cm for high rain rates (>100 m/h) and practically negligible for low and moderate rain rates. Rain attenuation and noise are also negligible at L-Band, but increase rapidly with frequency and reduce the signal to noise ratio by up to 8 dB already in C-band in the average for a mask angle of 10°.

Finally, it should be emphasised, that the simulations shown here were made with mean standard tropospheric profiles. However, actual atmospheric profiles can significantly differ from this mean, e. g. in case of temperature inversion. Simulations of such situations are principally possible with the ray-tracing algorithm by implementation of measured radiosonde profiles.

References

[1] Hopfield, H. S.: "Two-Quartic Tropospheric Refractivity Profile for Correcting Satellite Data". Journal of Geophysical Research, Vol. 74, No. 18, August 20, 1969, pp. 4487-4499.

[2] Saastamoinen, J.: "Contributions to the Theory of Atmospheric Refraction". Bulletin Geodesique, 1973, Vol. 105, pp. 279-298, Vol. 106, pp. 383-397, Vol. 107, pp 13-34.

[3] Black, H. D.: "An Easily Implemented Algorithm for the Tropospheric Range Correction". Journal of Geophysical Research, Vol. 83, No. B4, April 10, 1978, pp. 1825-1828.
[4] Goad, C. C., Goodman, L.: "A modified Hopfield Tropospheric Refraction Correction Model". Presented Paper, AGU Annual Fall Meeting, San Francisco, 1974.
[5] Baby, H. P., Gole, P., and Laververgnat, J.,: ‘‘A Model for Tropospheric Excess Path Length of Radio Waves form Surface Meteorological Measurements’‘. Radio Science, Vol. 23, No. 6, 1988, pp. 803-807.
[6] Marini, J. W.: ‘‘Correction of Satellite Tracking for an Arbitrary Tropospheric Profile’‘. Radio Science, 7, pp. 223-231, 1972.
[7] Herring, T. A.: ‘‘Modelling Atmospheric Delay in Analysis of Space Geodetic Data’‘, in Munck J. C. de, Spoelstr T.A.T. (eds): Symposium on Refraction of Transatmospheric Signal in Geodesy, Netherlands Geod. Commis., New Ser. 36, pp. 157-164, 1992.
[8] Neill, A. E.: ‘‘Global Mapping Functions of the Atmosphere Delay at Radio Wavelengths’‘. Journal of Geophysical Research, Vol. 101, No. B2, 1996, pp. 3227-3246.
[9] Janes, H. W. , Langley, R. B., and Newby, S. P.: "Analysis of Tropospheric Delay Prediction Models ." Bulletin Geodesique, Vol. 65, 1991 , pp. 151-161.
[10] Mendes, V. B., Langley, R. B.: ‘‘Tropospheric Zenith Delay Prediction Accuracy for High-Precision GPS Positioning and Navigation’‘. Journal of the Institute of Navigation, Vol.46, No. 1, 1999, pp. 25-34.
[11] Spilker J.J. Jr.; Tropospheric Effects on GPS; in Parkinson B.W. et al.: Global Positioning System: Theory and Applications; Volume I; AIAA, Washington, 1996; pp. 517-546.
[12] Master Control Station Kalman-Filter Support Study Guide, 2nd ed. Oct.1993.
[13] ITU-R Recommendations PN 837-1 and 838, PN Series Volume ‘‘Propagation in Non-Ionized Media’‘ , ITU-R, Geneva, 1994.
[14] Thayer,G. D.: ‘‘An Improved Equation of Refractive Index of Air’‘. Radio Science, Vol. 9, 1994, pp. 803-807.
[15] Damosso, E., Stola, L. V., Brussard, G: ‘‘Characterisation oft the 50-70 GHz Band for Space Communications’‘. ESA Journal, Vol. 7, 1983, pp. 25-43.
[16] NOAA, U. S. Standard Atmosphere, 1976.
[17] Ulaby, F. T., Moore, R. K., Fung, A. K.: Microwave Remote Sensing, Vol. 1, Addison-Wesley, Publishing Company, London, 1981, pp. 261 ff.
[18] Hoffmann-Wellenhof, Lichtenberger H., and Collins, J.: GPS Theory and Practice, Springer Wien 1997, pp. 109-119.
[19] Liebe, H. J: ‘‘MPM-An Atmospheric Millimeter Wave Propagation Model’‘. Intern. Journal of Infrared and Millimeter Waves, Vol. 10., No. 6, 1989, pp. 631-650.
[20] Hay, C., Wong, J., "Enhancing GPS - Tropospheric Delay Prediction at the Master Control Station", GPS -World, Vol. 11, No. 1, Jan. 2000, pp. 56-62.

The ESA/ESOC 35-Meter Deep Space Antenna

Dennis Akins
SED Systems, a division of Calian Ltd.
Saskatoon, Saskatchewan, Canada

Rolf Martin
ESOC/ESA
Darmstadt, Germany

Dr. Konrad Pausch
Vertex Antennentechnik GmbH
Duisburg, Germany

Abstract

This paper describes the system design of the deep-space Telemetry, Tracking and Command (TT&C) antenna system that SED Systems has developed and is installing in New Norcia, Western Australia for the European Space Agency's (ESA) deep space ground station. The system incorporates a 35 meter parabolic reflector antenna on a full motion turning head pedestal with a beam waveguide feed system, cryogenically-cooled S-and X-band Low Noise Amplifiers (LNAs) and 20 kilowatt S- and X-band transmitters and all other front-end support equipment. The antenna is one of the largest in the world used for TT&C applications and represents the jewel in the crown of the European Space Operations Centre (ESOC) ground segment.

Introduction

In July of 1998, after a 10-month study phase, SED Systems of Saskatoon, Canada was awarded a contract by ESA's Space Operations Centre (ESOC) to supply this 35-meter Telemetry, Tracking and Command (TT&C) antenna system. Vertex Antennentechnik GmbH (VA) of Duisburg, Germany and Vertex Antenna Systems (VAS) of Santa Clara, California, USA are major subcontractors to SED with expertise in large antennas.

To be installed in late 2001, the antenna is required for deep space and highly elliptical-orbit missions. One of the most important of these missions is ESA's Rosetta program [1] in which a spacecraft, launched in 2003, will rendezvous some nine years later with the comet Wirtanen. On its way to the comet, the spacecraft will fly past and make measurements of two asteroids. Once in orbit around Wirtanen, the spacecraft will make scientific measurements and deploy a small landing package to explore the surface.

The ground station at New Norcia will send commands to the Rosetta spacecraft and will receive the data from it. Rosetta will be up to 900 million kilometers from the Earth, more than six times the distance from the Earth to the sun. The entire mission is scheduled for 10.5 years.

Requirements for the ESA Deep Space Antenna

The requirement for communications with a spacecraft over these long distances places very stringent Radio Frequency (RF) specifications on the ground station antenna system. Since weight and energy constraints limit the transmitter power and size of the antennas on board the

spacecraft, the earth station must provide sensitive receivers and powerful transmitters coupled to a high gain antenna to provide reliable communications. The key RF performance requirements for the ESA Deep Space Antenna (DSA) are given in Table 1.

Current ESA programs require various combinations of simultaneous receive and transmit operations in S-band and X-band. Some future ESA programs will use Ka-band downlinks, so the capability to upgrade the antenna in the future to accommodate these spacecraft is a requirement.

Frequency coordination issues imposed stringent sidelobe performance requirements that have to be satisfied in order to obtain the frequency operating license. These requirements, when taken with the high antenna gain required, were a significant design driver.

The high gain antenna required to satisfy the RF parameters implies a very narrow beamwidth. Consequently the ground segment antenna system pointing performance including accuracy stiffness and smooth motion, over a wide range of environmental conditions, are critical parameters. The antenna system is required to operate in program track mode with time-tagged azimuth and elevation coordinates being supplied from a precise computer generated orbital model. The travel limits, slew rates and accelerations are compatible with tracking an object effectively fixed in space, i.e. the earth's rotation provides the major component of motion. The performance requirements of the mechanical and servo subsystems are given in Table 2.

Systems Design Tradeoffs

The first step in the development of the system design was to determine the minimum antenna size required to satisfy the antenna gain to noise temperature ratio (G/T) and Effective Isotropic Radiated Power (EIRP) specifications together with the stringent sidelobe requirements. The initial analysis indicated that in order to obtain the required G/T for the downlinks, a parabolic reflector of at least 35 meters in diameter was required, combined with cryogenically-cooled LNAs. Further analysis based on the gain of a 35 meter antenna indicated that transmitter amplifiers capable of producing 20kW of output power were required to meet the EIRP requirements of the uplinks.

The next major system design steps were to perform two tradeoffs between candidate antenna design architectures. These tradeoffs considered the feasibility of each approach satisfying the technical performance requirements as well as associated cost and schedule parameters to determine an optimum solution.

The first tradeoff was between a standard Cassegrain antenna, and an axis centered beam waveguide (BWG) approach. A standard Cassegrain design consists of a complex multi-band feed at the focal point of a main reflector and subreflector. In this approach the feed moves with the reflector when tracking a spacecraft. The axis centered BWG approach uses a series of shaped metal reflectors to direct and focus the RF energy between a moveable reflector and subreflector in Cassegrain configuration and stationery RF feeds (one for each RF band) mounted in the antenna base. Dichroic mirrors in front of the feeds multiplex the different frequency bands by passing the higher frequency signals while reflecting the lower frequency signals. The centre line of the RF path is directed along the elevation and azimuth axes so that the RF energy makes the cross-axis transition without being affected by antenna motion

Requirement	S-Band	X-band	Ka-band (Future Consideration)
Receive Frequency Band (MHz)	2 200 - 2 300	8 400 - 8 500	31 800 – 32 300
G/T (dB/K) including Program Track Error	≥ 37.5	≥ 50.1	≥ 56
Receive Polarization	Left and Right Hand Circular Simultaneously		
Transmit Frequency Band (MHz)	2 025 - 2 120	7 145 – 7 235	Not Applicable
EIRP • **dBW - primary HPA** • **dBW - back-up HPA**	 ≥ 97 ≥ 87	 ≥ 107 ≥ 97	Not Applicable
Transmit Polarization	Left or Right Hand Circular - Selectable		Not Applicable
Sidelobe envelope (Transmit and Receive)	1st sidelobe: 13 dB below main beam. Further sidelobes: (29 - 25 log ϕ) dBi for ϕ ≤ 48 deg; -13 dBi for ϕ ≥ 48 deg.		

Table 1: RF Requirements

Requirement	Azimuth	Elevation
Travel Range (deg)	≥ 0 to 480	≥ 0 to 90
Slew Rate (deg/s)	≥ 0.4	≥ 0.4
Acceleration(deg/s^2)	≥ 0.4	≥ 0.4
Tracking Error (deg)	S-band: ≤ 0.026 deg X-band: ≤ 0.011 deg Ka-band: ≤ 0.006 deg (Optional)	
Operational Wind (km/h)	45 constant gusting to 60	
Temperature (deg C)	0 to 50	

Table 2: Mechanical and Servo Requirements

The tradeoff determined that the BWG configuration was technically superior as well as being cost and schedule effective. The major advantage of the BWG concept is that no rotary joints or long waveguide runs are needed at the antenna axes. This minimizes RF losses and the risk of Passive Intermodulation (PIM) generation. The BWG design allows for optimization of illumination, efficiency, gain and sidelobe performance for each band. It permits simultaneous operation in all specified bands. With this concept, High Power Amplifiers (HPAs) and cryogenically-cooled LNAs can be located in the equipment room at ground level, easing operation and maintenance activities.

The second tradeoff was between turning head and wheel and track pedestal designs. Both approaches use an elevation axis over azimuth axis configuration. The difference in the two approaches is in the implementation of the azimuth axis. The turning head uses a comparatively compact, precision circular bearing for azimuth rotation, while the wheel and track, as the name

implies, uses a large diameter circular track on which several wheel assemblies travel. These wheel assemblies are fixed to structural members that support rotating portions of the antenna.

The tradeoff determined that the TH approach was technically superior. The TH structure provides a better reflector surface and pointing accuracy in all operating conditions including wind disturbances and minimizes thermal effects compared to a WT approach. The wider stance of the WT design would seem to provide a more stable design, but the technical difficulties with the construction of the precision track and thermal effects on the support members negate this apparent advantage. Furthermore, the TH design provides indoor access to the azimuth housing that encloses the BWG, the servo encoders and the drive motors. The disadvantage of the TH concept when combined with an axis centered BWG is that the azimuth encoder cannot be mounted on axis. This problem is overcome by an off-axis geared encoder, calibrated before the BWG installation, when the axis is still free. Later re-calibration is possible by high precision reference marks.

The combined axis centered BWG and TH design configuration selected from the tradeoffs is shown as a conceptual layout in Figure 1. The elements of the BWG, i.e. feeds and mirrors are shown relative to the azimuth and elevation axes and the subreflector and main reflector. BWG mirror (M4a) is initially being implemented as a plane mirror that can be replaced by a dichroic mirror when Ka-band functionality is implemented. The location reserved for the future installation of Ka-band equipment is shown in the azimuth housing.

The system block diagram of the ESA DSA is given in Figure 2 showing the mechanical/structural elements, BWG, servo, uplink chains, and downlink chains, as well as other auxiliary subsystems. The major elements are briefly described in the following sections.

Antenna Mechanical Structure and Antenna Building

Physically the ESA DSA consists of a main- and subreflector assembly supported and pointed by a pedestal comprised of the elevation and azimuth portions. The pedestal is mounted on the antenna building. Figure 3 is a three-dimensional computer model showing the DSA after completion.

The main reflector is 35 meters in diameter. Its supporting structure is a truss constructed from steel pipes that also supports the quadropod and headpart for the subreflector. The reflector and supporting structure are counterbalanced about the elevation axis by ballast cantilevers.

The reflector surface has the shape of a corrected paraboloid. The individual high accuracy panels are made out of aluminum and are connected to the structure via adjustable studs.
The surface accuracy of the main reflector is specified with 0.3 mm-rms, which is sufficient for the Ka-band option without additional modification. The structural parts are painted white and the reflecting surfaces will receive a diffusely reflecting paint.

The subreflector, approximately 4.3 meters in diameter, is a shaped hyperboloid of aluminum cast design. The subreflector surface accuracy is specified with 0.2 mm-rms. The structure is designed to accommodate a motorized subreflector positioner required for Ka-band operation.

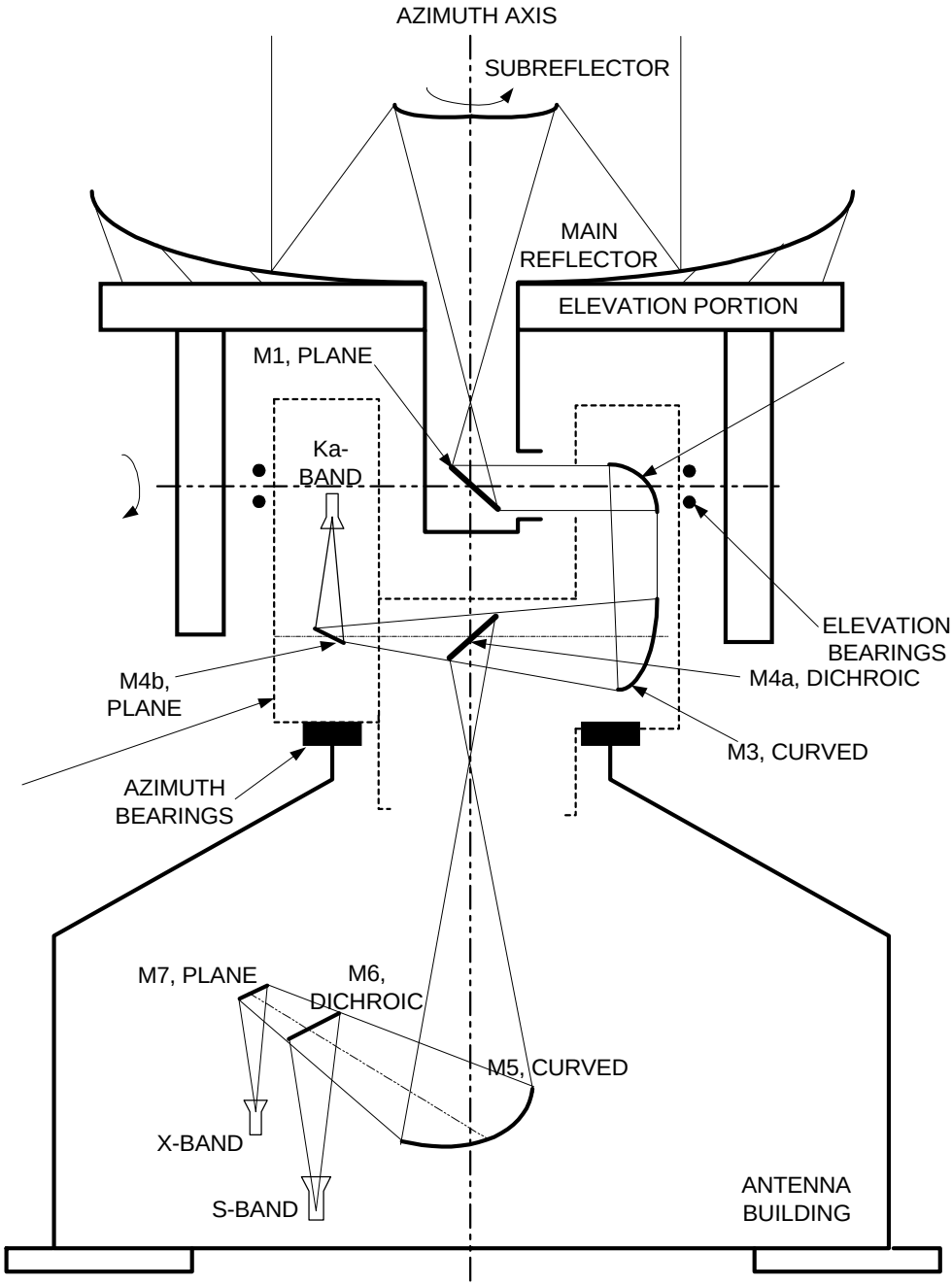

Figure 1: Layout of BWG Design in a Turning Head Pedestal

The rotating azimuth portion is a three story steel structure that supports the elevation portion on two fixed bearings that form the elevation axis. It houses the elevation and azimuth drives and encoders as well as the moveable elements of the BWG. Antenna azimuth motion is accomplished by two gearboxes each fitted with two servo motors. Elevation motion is realized by four gearboxes with one servo motor each, engaging toothed gear segments on the two ballast cantilevers. A room is reserved for the Ka-band equipment. The azimuth structure is clad with insulating panels on the front and back surfaces to minimize deformations due to differential thermal conditions.

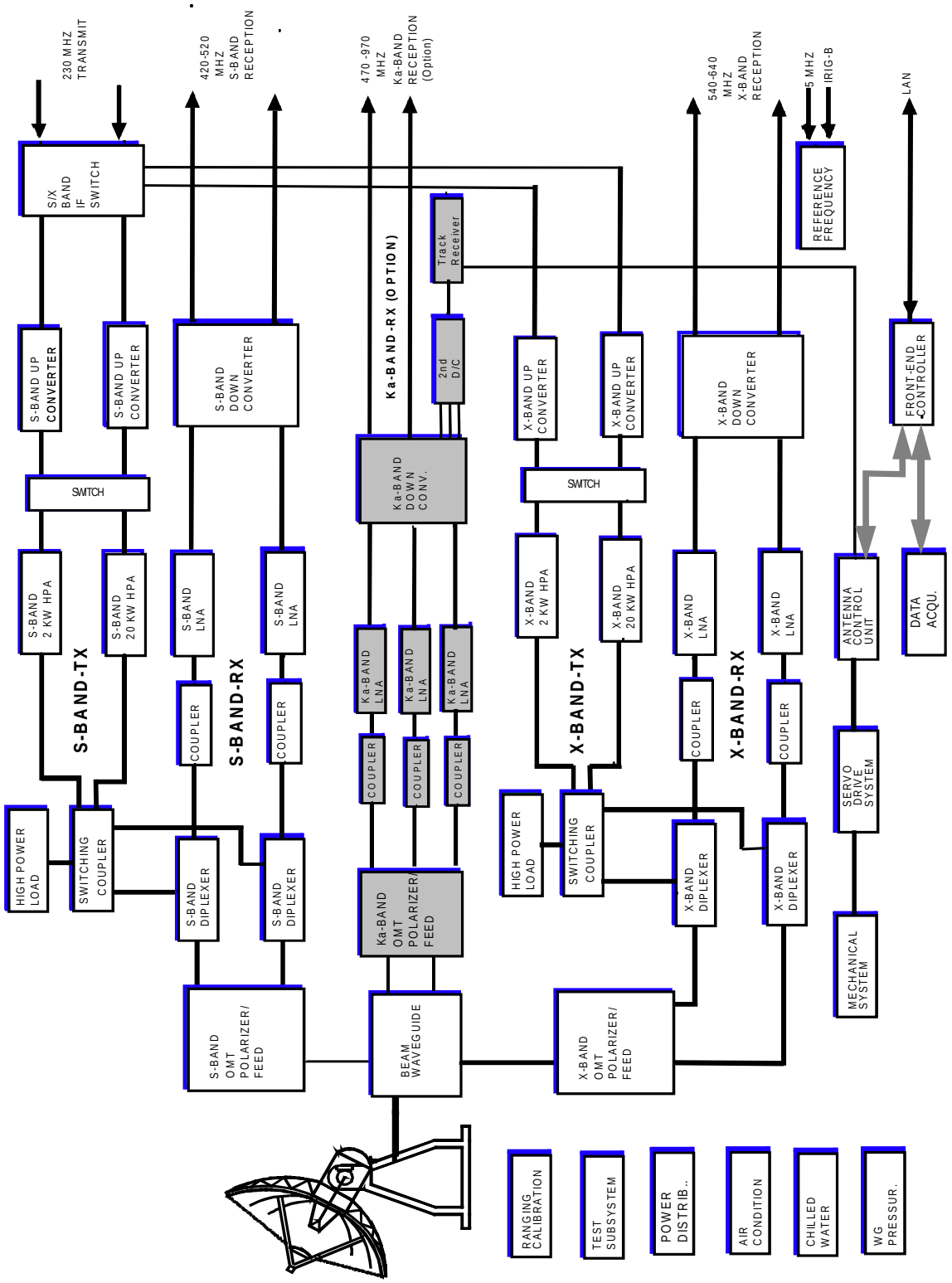

Figure 2: Deep Space Antenna Block Diagram

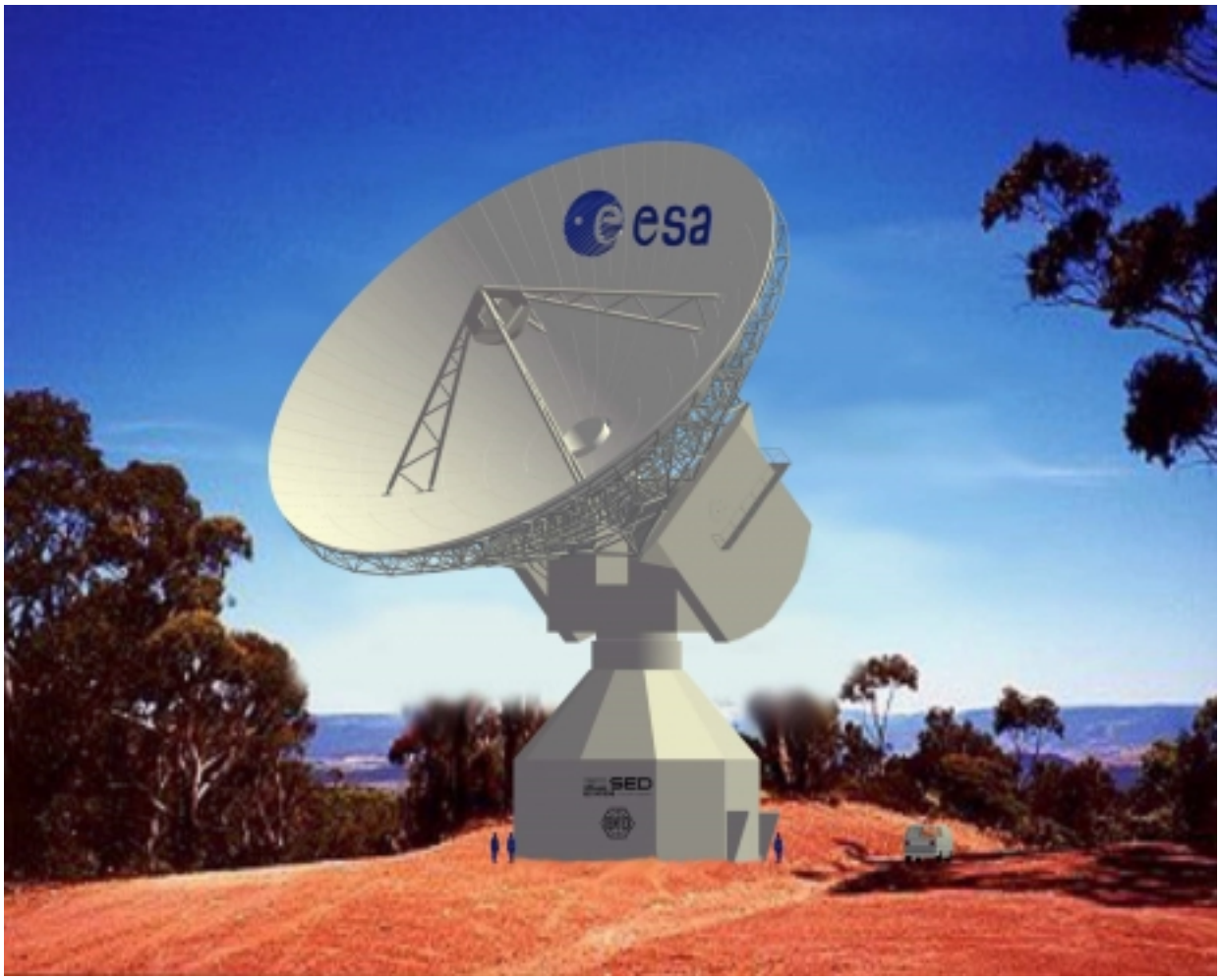

Figure 3: DSA 3-D Computer Model

The azimuth housing is mounted on the antenna building by means of an extremely stiff-three-row-roller bearing and a fixed steel base ring. Apart from horizontal and vertical loads, this bearing also transmits tilting moments, resulting from wind and seismic loads. The bearing is of sufficient size to allow the BWG and a spiral access staircase pass through the centre from the antenna building to the azimuth housing.

The antenna building is a ten-sided reinforced concrete structure with a conical roof that supports the antenna pedestal and provides an environmentally controlled enclosure for the stationery elements of the BWG system, RF feeds, and electronic equipment. The foundation is a reinforced concrete ring beam placed on an array of friction piles. The antenna building and foundation must withstand the loads presented by the antenna mechanical structure under operational wind conditions while deflecting less that 0.001 degrees. The outer walls are clad with insulating panels to minimize deflections of the antenna mounting interface due to differential thermal expansion.

The overall height of the antenna is around 40 meters and the total weight of the structure and equipment above the antenna building interface is approximately 620 tons. The weight of the main reflector is approximately 100 tons. The reflector and ballast cantilevers combined weigh

around 340 tons. The combined weight of the elevation portion and the rotating azimuth portion are approximately 540 tons.

BWG and RF Feeds

The ray optics with 6 mirrors for S-band and 7 mirrors for X-band are shown in Figure 1 labeled M1 through M7. The BWG creates an image of the S-band and X-band corrugated feed horns at the subreflector focus. The first mirror, M1, rotates in azimuth and elevation with the main and subreflector. A plane surface is used to ensure an imaged feed pattern that is independent of the elevation of the antenna. Mirrors M2 and M3 are parabola sectors. M4a is again a plane mirror in order to ensure an imaged feed pattern that is independent of the antenna azimuth position. M5 is an ellipsoid sector in order to allow smaller feedhorns in the pedestal room. M6 is a plane dichroic mirror that reflects in S-band and is transparent in X-band. M7 is a plane reflector used for X-band only.

The S-and X-band feeds are each comprised of a broadband corrugated horn, a mode launcher, a 90-degree circular motorized polarizer and an orthomode transducer. The orthomode transducer (OMT) provides two rectangular waveguide input/output ports, one for each sense of circular polarization. The polarizer can be rotated 90 degrees via circular waveguide rotary joints to change the polarization associated with each OMT port. A diplexer on each OMT port provides isolation between the transmit and receive signals for the corresponding frequency band to allow simultaneous transmit and receive operation in each band.

When the antenna is upgraded to Ka-band, M4a will be replaced by a dichroic mirror, transparent for Ka-band and reflecting for S- and X-band. A plane mirror, M4b, will be added to direct the RF energy to a Ka-band feed placed at the focus point. The Ka-band feed will contain elements similar to the other two feeds except diplexers are not included since transmission at Ka-band is not a requirement.

RF Downlinks

The S- and X-band downlinks have identical configurations. For each band, there are two LNAs, one connected directly to the receive arm of each diplexer followed by a dual channel downconverter.

Each LNA path consists of a vacuum dewar assembly, housing a cryogenically-cooled bandpass filter (BPF) and the first stage HEMT amplifier, and a second stage post amplifier at ambient temperature. The LNAs are cooled to 15 K to obtain the very low receive noise performance required to receive the weak signals from deep space. The overall noise contribution of the units amounts to approximately 11 K in S-band and approximately 18 K in X-band with a predicted gain of 56 dB in each band.

The rotatable polarizer in each feed allows rerouting the RHC or LHC polarized signals in the case of an LNA or downconverter failure. This configuration also minimizes the elements in front of the LNAs which contribute significant thermal noise, while providing the capability to simultaneously receive both RHC and LHC polarized signals.

The outputs of the downconverters shown in Figure 2 are further converted to 70 MHz by L-band downconverters and then digitally processed in the Intermediate Frequency Modem

System (IFMS), which is not shown in the antenna block diagram. The downconverters and IFMS are standard units, which have been developed for ESA for application throughout the ESOC ground segment network.

The planned Ka-band downlink configuration is similar to the other downlinks. The only difference is that a third channel providing a difference signal from the feed and a tracking receiver may be included to allow for an autotrack mode. The cryogenic LNA and downconverter elements required for the Ka-band downlink are not available off-the-shelf, but are under development at various equipment suppliers. When Ka-band functionality is added, the front-end components will be located in the azimuth housing next to the feed.

RF Uplink Subsystem

The S- and X-band uplinks are both arranged with a primary chain and a backup chain. The primary chain has a 20 kW HPA while the backup chain has a 2 kW HPA. Primary and backup upconverters are used for each band and IF/RF switching equipment provides for redundancy switching. This configuration allows transmission with either LHC or RHC polarization in a given band. The dichroic mirrors in the BWG permit the transmission of a 20 kW signal in S-band and in X-band simultaneously.

Two input signals, primary and backup, provided by the IFMSs (not shown in the block diagram), are routed by IF co-axial switches to the input of the S-band or X-band upconverter in the corresponding chain (i.e., primary or backup) for that band. RF co-axial switches at the outputs of the upconverters normally route the signals to the primary and backup HPAs respectively, but can cross connect these signals for redundancy purposes. The output of the primary HPA is selected and routed by waveguide switches to one of the two diplexer transmit ports for transmission as either an RHC or LHC polarized signal. The backup HPA is normally routed to a high power RF load, but can be selected for transmission by the waveguide switches. The high power load allows testing of the off-line HPA in parallel with on-line transmission with the other HPA.

The input to the upconverters is at a fixed frequency of 230 MHz that is translated in an agile manner (using a synthesized upconverter) to a selected output frequency in either X-band or S-band. The S-band upconverters are standard units using a single stage of upconversion, which have been developed for ESA for use throughout the ESOC ground segment network, while the X-band upconverters were developed using two-stage conversion for this project.

The primary HPAs are 20 kW water-cooled klystron amplifiers. The S-band amplifier has a 20 MHz instantaneous bandwidth, but is locally and remotely tunable across the transmit band. The X-band unit has a 90 MHz instantaneous bandwidth which covers the entire transmit band without tuning.

The backup HPAs are 2 kW air-cooled klystron amplifiers. The S-band and X-band units have 8 MHz and 30 MHz instantaneous bandwidths respectively. The instantaneous bandwidth of both klystrons is less than the full RF band, but both can be tuned locally or remotely across their respective transmit bands.

Servo Drive

The servo drive subsystem consists of the Antenna Control Unit (ACU), the interlock system, the servo amplifiers, motors and encoders.

The ACU is a PC-based system with VxWorks as operating system. It co-ordinates all actions within the servo system and interfaces to the Front End Controller (FEC) for receiving commands and program track data and for providing status information. The main operating modes of the servo subsystem are:

- RATE: The antenna moves with the selected speed.
- PRESET: The antenna moves to the selected position.
- PROGRAM TRACK: The antenna moves according track trajectories received from the FEC

Other modes include STOP, STOW and BORESIGHT POSITION.

The azimuth and elevation axes are equipped with anti-backlash drive units, using brushless motors. The actual positions and motions are measured by absolute, single turn, high resolution optical encoders (23 bit). The servo amplifiers and the entire control loop are fully digital and interconnected by a local bus system.

Unsafe and erroneous operating states are monitored and prevented by an interlock system, whose main component is an industrial Programmable Logic Controller (PLC).

Monitor and Control Subsystem

The Monitor and Control Subsystem provides remote monitoring and controlling for the whole antenna system. It consists of the following items.

- Front End Controller (FEC): A standard FEC 4, developed by ESA for the ESOC ground segment network that has been tailored to the specific requirements of this antenna. The FEC will interface via a Local Area Network (LAN) with the station computer located in the Main Equipment Room (MER) located in a building adjacent to the antenna building. An operator workstation located in the antenna building is connected to that LAN for local M&C purposes. The FEC has two IEEE busses. One will be used exclusively by the servo system, and the other will connect to all the other equipment in the antenna.
- Discrete input/output system: This equipment provides for collection of discrete alarms and status information, and for control of discrete switches, and the transfer of such information to/from the FEC. It is microprocessor-based.
- Adapters and Extenders: This equipment provides for conversion of non-IEEE-488 busses in equipment, to IEEE-488, to permit connection to the FEC.

Auxiliary Subsystems

In addition to the equipment and subsystems described in the preceding sections, the antenna contains several auxiliary subsystems with functions that are briefly described in the following paragraphs.

- Ranging calibration: This equipment provides RF loop-back paths by translating transmit signals into receive bands to facilitate the measurement of delays through the uplink and downlink chains. The measured results are used to correct spacecraft ranging measurements.

- Test subsystem: This subsystem is comprised of a power meter and a frequency counter and RF selection switches that sample and measure the RF signals at critical monitor points in the uplink and downlink chains.

- Frequency reference: This equipment distributes a 5 MHz signal and an IRIG-B signal derived from a MASER source. The 5 MHz signal is distributed to the IFMS, up and downconverters, and ranging calibration and test equipment to provide a common, phase stable reference frequency. The IRIG-B signal provides accurate time reference to the FEC for time tagging pointing coordinates and to the ACU to correlate antenna motion with these time tagged coordinates.

- Air conditioning: This equipment maintains the temperature of the AER (within 23 ±3 º C) and humidity below 70 %. Conditioned air is exhausted through the azimuth housing and BWG to minimize temperature differentials. Separate redundant air conditioning systems provide 18° ± 1°C air to critical equipment racks to minimize RF phase variations due to temperature changes.

- Chilled water: High pressure, deionized cooling water is provided to the 20 kW HPAs. Low pressure non-deionized cooling water is provided for the LNA cryogenic compressors, the RF loads, and the transmit waveguide and feed components.

- Waveguide pressurization: This unit provides pressurized dry air to the waveguide components and RF feeds to avoid the ingress of dust or moisture.

- Power Distribution: Short-break power from an adjacent power building is distributed from a centralized distribution and circuit breaker panel. Small Uninterruptible Power Supplies (UPSs) located in each equipment rack bay provide no-break power for outages less than several minutes.

Conclusion

The development of the ESA DSA is well advanced and on schedule for completion in late 2001. The system design and detailed design phases were completed in May 1999. The preparation of shop manufacturing drawings is nearing completion for the antenna pedestal mechanical structures and servo drives, and all the RF equipment. All major elements are on order or are in manufacture based on these drawings.

The civilworks detailed design of the antenna building including foundation, concrete structure, air conditioning, chilled water, and power distribution is nearly complete. The final design review is planned for late February 2000. Meanwhile, ESA has located a suitable site for the DSA approximately 140 km north of Perth, Western Australia on the Great Northern Highway. Site preparation activities and construction of the access road have commenced. These are planned to be completed in February 2000 so that construction of the antenna building can commence in March 2000.

The design of the DSA is tightly constrained by the performance specifications required for a deep space earth station. Tradeoffs have been made carefully to develop a compliant design making use of existing technologies whenever feasible. This approach has led to a cost effective design solution that can be implemented within the schedule constraints.

When the Deep Space Antenna is completed and commences operation, it will provide ESA with a state of the art TT&C facility capable of supporting a wide range of future space missions.

Definitions

ACU	Antenna Control Unit
AER	Antenna Equipment Room
BWG	Beam Waveguide
DSA	Deep Space Antenna
EIRP	Effective Isotropic Radiated Power
ESA	European Space Agency
ESOC	European Space Operations Centre
FEC	Front End Computer
G/T	gain to noise temperature ratio
HEMT	High Electron Mobility Transistor
IF	Intermediate Frequency
IFMS	Intermediate Frequency Modem System
IRIG-B	Standard B of the InterRange Instrumentation Group
LAN	Local Area Network
LNA	Low Noise Amplifier
MASER	Microwave Amplification by Stimulated Emission of Radiation
MER	Main Equipment Room
OMT	Orthomode Transducer
PIM	Passive Intermodulation
PLC	Programmable Logic Controller
RF	Radio Frequency
SED	SED Systems, a division of Calian
TH	Turning Head
TT&C	Telemetry, Tracking and Command
UPS	Uninterruptible Power Supplies
VA	Vertex Antennentechnik GmbH
VAS	Vertex Antenna Systems Limited
WT	Wheel and Track

References

[1] ESA Space Science Rosetta Website: http://sci.esa.int/rosetta/

The Software Scope between Operators and Complex Groundstation Equipment in a Multi Mission Scenario

Heiko Damerow (Heiko.Damerow@DLR.de)
Jens Richter (Jens.Richter@DLR.de)
DLR, German Remote Sensing Data Center
D-17235 Neustrelitz, Kalkhorstweg 53

Introduction

The ground station Neustrelitz is receiving data from several satellites in co-operation with national and international partners. Relevant working areas are reception planning, reception, archiving, cataloguing, processing and quality control. Starting from long-term experience in data reception a software system supporting operation manager and operators was developed. This system realizes a fast and reliable adoption on changing operation scenarios, a stable station monitoring and control and an objective collection of reception quality data (meta data).
This software system fulfills aspects of a monitoring and control system, but even the requirements of scheduled processes and configuration managment. It also offers an efficient and reliable operator interface. Further more it permits an efficient quality control.

The design considers the following aspects:

- Integration of devices and subsystems with very different functions, such as matrixes, direct archives, demodulators, receivers, antenna control units, bitsynchronizers and tape recoders (D1).
- minimal operator effort in a multi mission environment
- Creation of a operator interface, which provides efficient supervising, configuration and control capabilities for the whole ground station without information overload.
- Performing an operator independent and reliable collection of meta data.
- Realization of client/server relations.
- Structured and centralized storage of meta data.
- Flexible integration of devices.
- Definition and realization of interfaces between the system and data processors.
- Definition of abstractions and formalized procedures and generation of reusable and universal object-oriented software modules.
- Definition and realization of remote control interfaces.

The Ground Station Equipment

The ground station has been equipped with different devices and subsystems for the realization of current and future projects. The equipment has a very heterogen nature. The manufacturer delivers devices with variuos interfaces and levels of remote control properties.

With installation of a second X-band antenna and the modernisation of the LS-band antenna it was required and necessary to interconnect the antenna system with the other equipment by matrixes. The matrixes are the premise for dynamic reconfiguration of the needed data or signal pathes. Only by integration of matrixes it will be possible to use well checked redundant system components.

By receiving more and more missions it was also required to reconfigure the station in a very fast way or drive passages parallel.

All operations should be drive in maximum by one operator also in case of parallel receptions. The technical staff should have the possibility to drop down problems in short time, it requires they have to be well informed. For this reason a detailed and compete monitoring and logging is necessary.

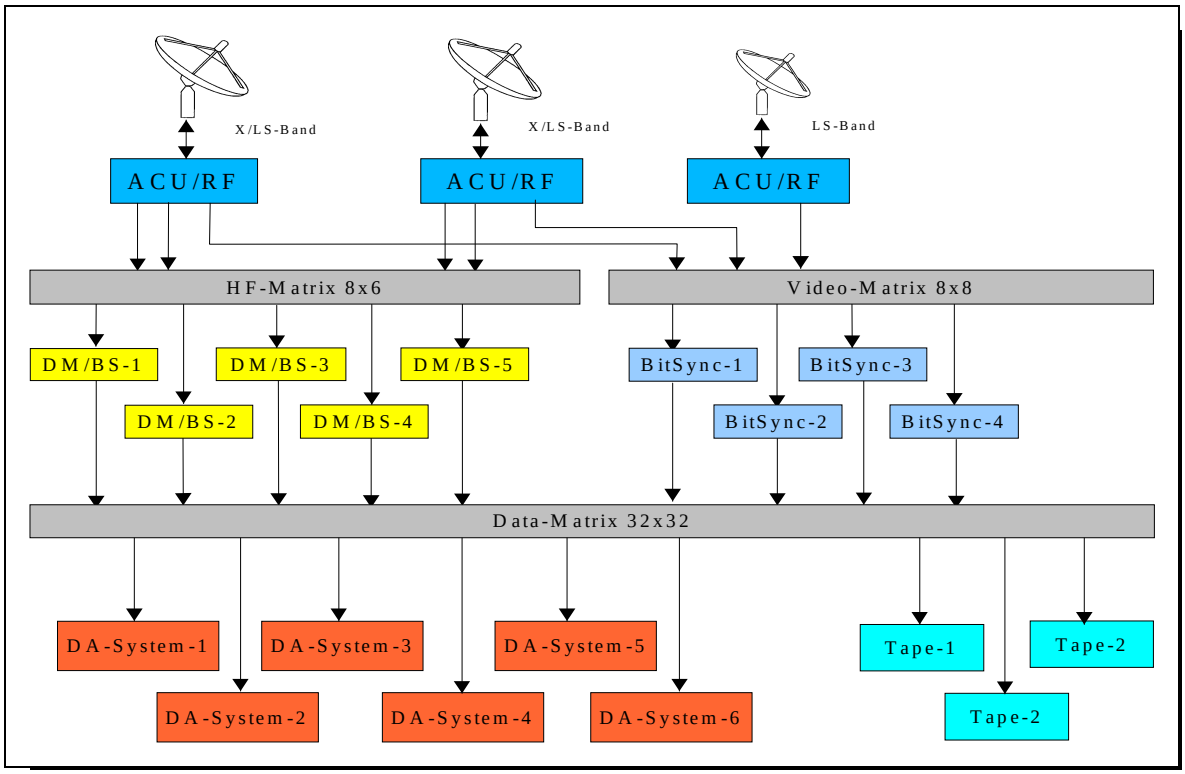

Figure 1 *Station Device and Subsystem Scheme*

Figure 1 shows approximately the current equipment of the Neustrelitz ground station. This scheme contents devices and subsystems. Devices are normaly components without any self steering capabilities, such as demodulators, matrixes or D1 tape machines. Subsystems are components which are able to drive complex procedure, e.g. direct archives as well as antenna control units. From view of the software also the subsystem is a kind of device.
The ground station has for the different missions redundant devices or subsystems. The **Table 1** gives an impression what that means.

For the realization of an efficient and reliable monitoring and control the devices and subsystems have to satisfy some requirements. These are an reliable remote control interface, detailed information about the common state (**Device State**) and the state concerning the data reception (**Lock State**). The **Lock State** means that the device is in a state to realize a save data reception in a good quality. The **Device State** provides information about the device condition itself and the control connection. Unfortunately each device realizes only a subset of this requirements and so it is necessary to integrate them in the station on a different level.

Manufacturer/Devices	*Supported Missions*
Antenna Systems	
Datron X/LS-band 1, 2	All missions in X- and LS-band
DLR L/S-Band	All mission in LS-band
DM/Bitsyncs	
L3 (BS 1-4)	All small satellite projects (up to 20 MBit NRZ-codes)
Datron (DM/BS 1,2,3)	IRS-1C, IRS-1D, ERS-2
Alcatel (DM/BS 4, 5)	Landsat-7, ERS-2, Radarsat, Envisat, MODIS
DA-Systems	
ACS (DAS 1,2)	Landsat-7
ISRO (DAS 3)	IRS-P3
DLR (DAS 4,5)	CHAMP, BIRD, GRACE, KORONAS-F, MODIS, all CCSDS-compliant missions up to 20 MBit $\cdot$ s^{-1}
McDonald-Dettweiler (DAS 6)	ERS-2 (up to 120 MBit $\cdot$ s^{-1})
SONY (Tape 1,2,3)	IRS-1C, IRS1C, Backup for all missions with data rates up to 128 MBit $\cdot$ s^{-1}

Table 1 *Redundant equipment of the ground station*

The Operator

The operator gets the station schedule from operation planning daily. This station schedule contents all passages with reflection of a needed antenna system and the needed transition time from one passage to the next one. This schedule considers all requests from the customers. Only if more passages than antennas are requested and the possibility of shortening is not enough it can happen that a passage has to be rejected. The transition time between two passages is about two minutes or shorter.

After loading the station schedule the operators job is to supervise the system. He has to act if he detects some failure by a device. If multible failueres are indicated the operator has to find out the technical reason.

The experience shows that in case of problems with the devices also any software has problems, e.g. temporary or complete fail of a device. The operator have the task to recognize the point of fail and overcome the problem in a short time. This often needs a reconfiguration of the station or a new initialisation of the failed device. If he does it manually he will need some time. Because it is not a standard situation the operator can make failures.

The manually change of interconnection beetween devices can cause problems concerning the data quality. Without software it is very effordable to report the reception process.

If more than one passage occures at the same time the operator have to supervise much more devices in parallel. In this cases he can miss an error or important events.

The Station Control Software

As described above the operator has some problems or tasks which he cannot solve without software in the required quality. The Station Control Software (**SCS**) supports the operators work and takes over all routine tasks. The software guaranties that once defined procedures can be fulfilled furthermore. The SCS offers also to get information in concentrated form with the opportunity to investigate the devices in more detail. A strictly separation of the configuration and

the operational view is realized.

To give the operator a tool which is easy to handle it is strictly necessary to introduce abstractions and rules:

all things are devices.
all devices have connectors for primary and secondary input signals
all devices have connectors for primary and secondary output signals
all devices provide meta data
all devices are providing a device status and a lock status
each mission uses a set of active and inactive devices
for each mission exist a number of parameter sets for each device and the mission itself

In conclusion the SCS has to be independend of missions. The operator will be liberated from parts of perception which are already registered by the software. The experience shows also that its necessary to supervice the device status and the lock status only. Therefore a special passage control window was defined. Below it will be explained in more detail.
Also for software updates (new missions or devices) the same procedures for configuration or operations will be used.

The Software Design

The design of SCS enables the integration of devices at different levels. Devices which not provide a remote control interface can also be integrated via the matrix.
All what the operator uses is transformed into objects. The object design is derived from terms like missions as well as device and other components including their relations to each other. This design contains common interfaces between device drivers and all components like scheduler, pass control or main logging control.
The scheduler is responsible for the resource sharing of devices. The operator will be informed if two passages want to use the same device. The scheduler is able to manage fast successsive sequences of device access. A further advantage of the scheduler is that it can take schedule requests from the orbit prediction, remote clients, operations planning or direct from operator.
The main logging control collects all messages from the devices. The logging control shows a subset of all messages on the screen and files the unfiltered messages on harddisk.
All configuration information like layouts, device parameters etc. are stored in a database.
The software distributes the tasks to several threads. Therefore it is possible to drive three and more missions at the same time with moderate response time. The software avoids problems with wrong hardware devices because each hardware device will be accessed by a own thread.
The following table demonstrates how many objects (like e.g. missions or configurations) can be handled by the SCS.

Feature	*Explanation*
Missions	> 15, includes the passage prediction from two lines
Devices for each mission	> 20
Number of configurations per mission	> 5
Integration of devices without direct support per mission	Yes (> 10), for matrix and resource management
Supported Hardware	Sony DIR-1000, Alcatel DMOD, Alcatel TMOD, Datron DMOD, Datron TMOD, DLR DAS, DLR GSC, L3 MBS-720, L3 DBS-530, L3 DBS-430, DLR DGEN, R&S SMIQ-03, Novotronik KSD-0241, Novotronik GTS-1115, Microdyne MRA-1400,
Used IF Typs	GPIB, Serial, Sockets, ftp, eMail, ISA,

Table 2 Technical parameter of SCS

Figure 2 shows the SCS with schedule control, logging control, control for steering of a Sony tape machine and two passage controls.

Figure 2 SCS Operator Interface

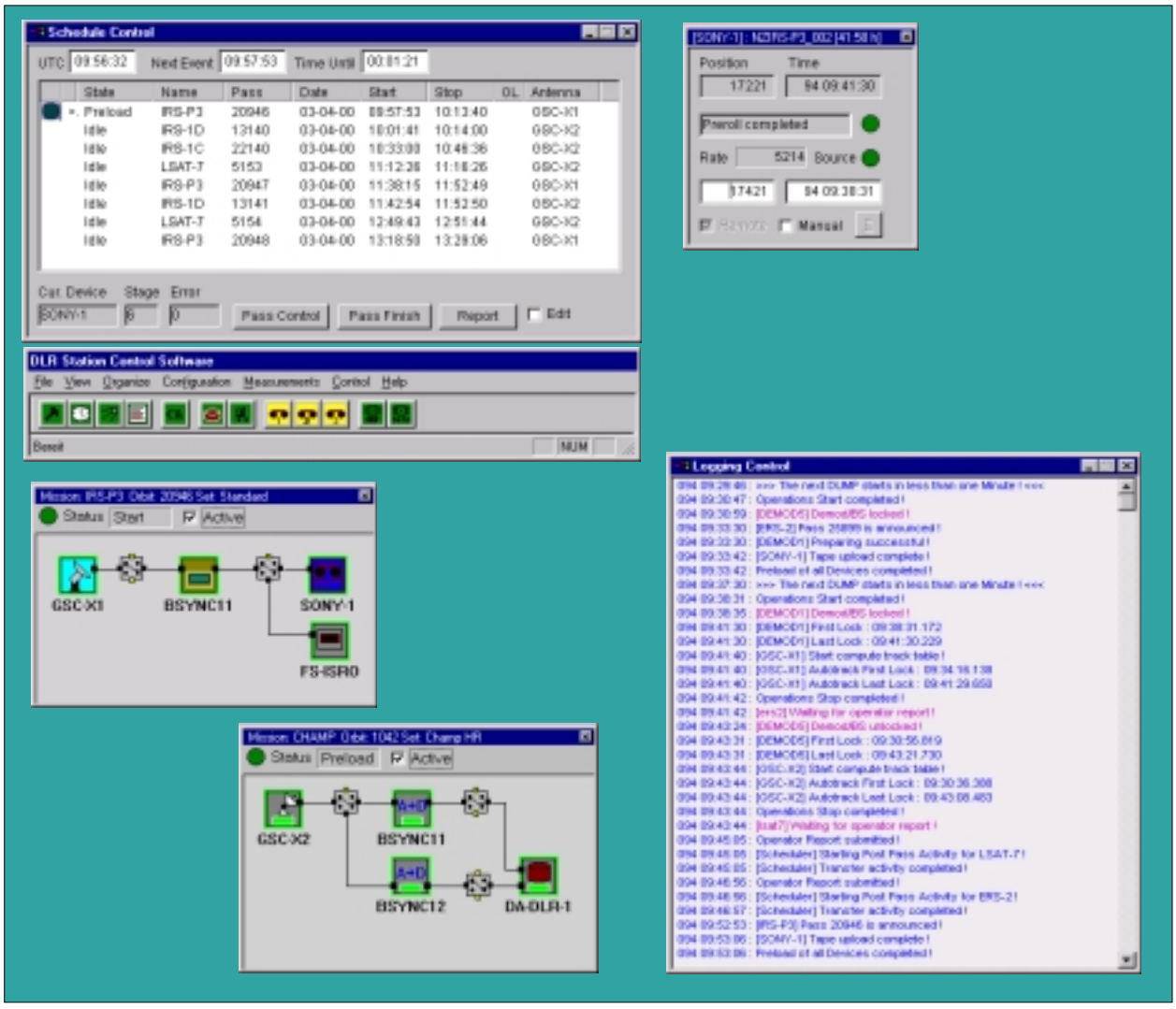

The Device Driver

There is one special device driver for each type of device. It consists of modules for configuration, for access to the hardware and for other purposes.
This driver don't influence the other software parts and offers the full freedom to adopting this special device. For example the device can be a subsystem, which can represent a direct archive system with remote control capability or a system which provides only meta data after a passage. If the device is a subsystem, it provides the meta data subset to the PostPass server directly (Figure 4).

The Passage Control

It was realized a special graphic window for the passage control. This window shows the current state of the passage at the actual time. The operator can start all interactions from the control if necessary. The passage control also expresses the current device layout and the selected set of configuration. Each passage has its own valid layout and set of parameters.

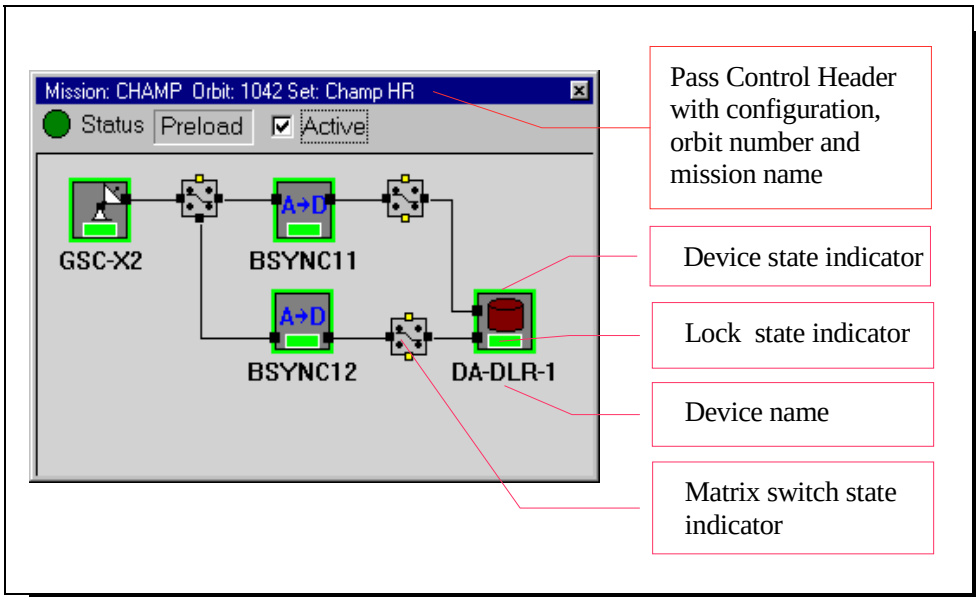

Figure 3 *The Passage Control Window*

Each reception procedure is devided into different phases which are scheduling, preparation, start, stop and transmission. **Table 3** shows the tasks which have to be realized during these phases.

Phase	***Tasks***
scheduling	- reselection of resources in accordance with the availability of the devices - schedule distribution to the subsystems
preparation	- loading of parameter set to the devices - reselection of resources if an error is not recoverable reloading of the configuration initiation of the preparation procedure of the devices
start	- initiation of the start procedure of the devices
stop	initiation of the stop procedure of the devices e.g. stopping of monitoring or data ingestion inquirement of the operator report
transmission	- distribution of all meta data to the PostPass Server

The pass control shows from the preparation until the end of the stop phase the states of the devices as well as the lock state. If some problems occure this will be shown by a red signal. Now the operator has the possibility to reconfigure the failed device or he can in the preparation phase select the redundant device. If there is need for more information he can open special windows from this control.

The CHAMP mission ground segment

CHAMP is a national geophysical mission which will be launched at the end of may 2000. The Raw Data Center (data reception, archiving and data distribution) for this mission is installed at the National Ground Segment in Neustrelitz.
Therefore a direct archive system was developed [1]. It has a remote control interface and provides metadata for system integration from the point of reception. Detailed and time resolved quality information are provided also in realtime. Mission independence is fulfilled by realizing of important parts of the CCSDS recommendations. Figure 4 shows the integration of this subsystems in the ground station.

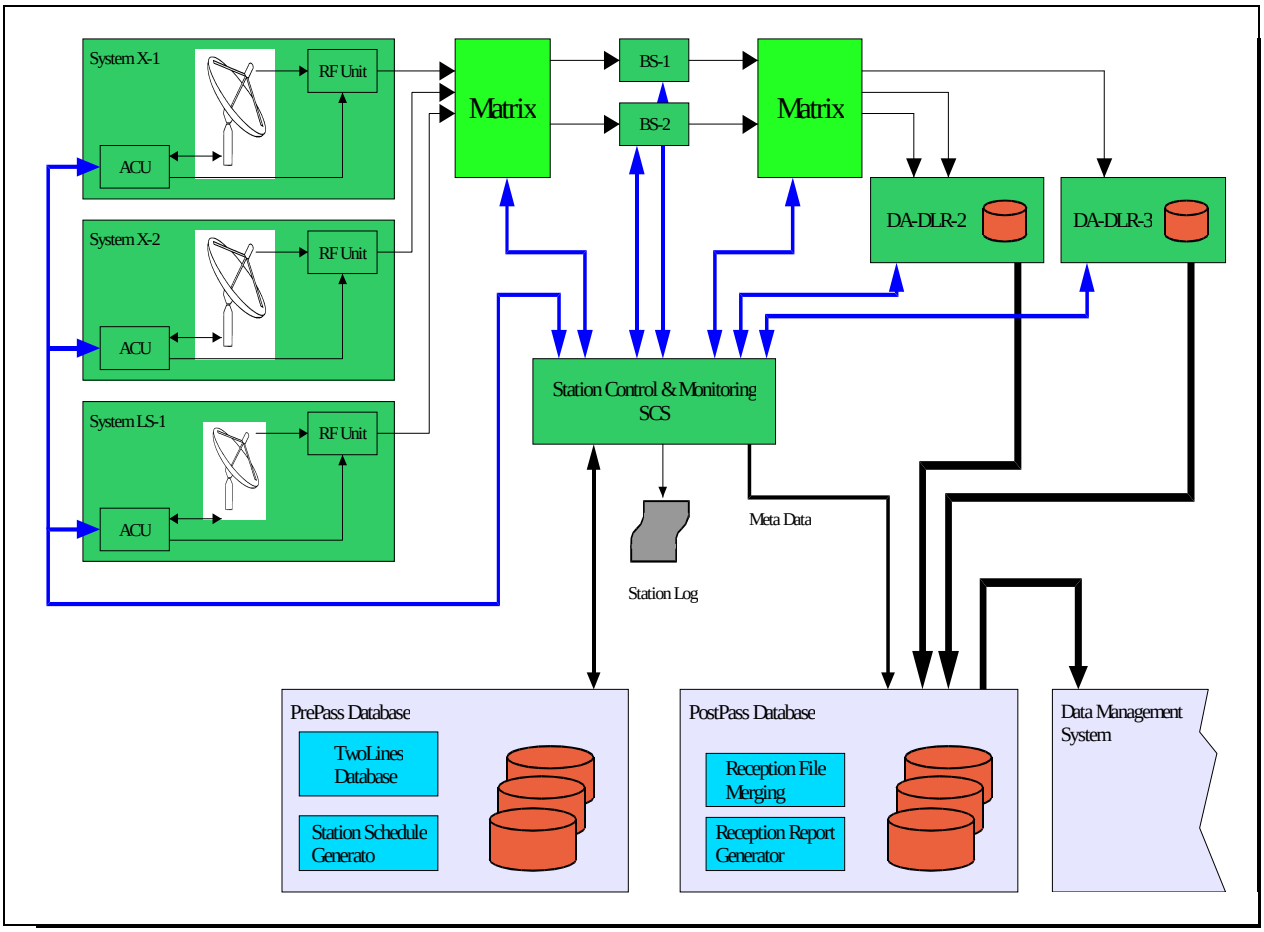

Figure 4 *The CHAMP reception subsystem*

Reporting and QS aspects

The meta information will be composed in dependence of the actual configuration of the passage. The composing will be executed at the PostPass Server. On this server the report generation subsystem ist established, which is responsible for the generation of all reports (technical or statistic reports). The generation of statistics and reports for the management is an important task of the operators. All monitor information and passage-related information will be collected and processed

during the reception process .
The collecting and concentration of the meta data is an direct condition for an efficient work of the technical staff and the operation manager, e.g. maintenance repair and quality control.
The meta data are filed in ASCII code. Three types of meta data are possible: **descriptions**, **tables** and **log's**. Descriptions are key-value pairs. There could be the same keys in different logical unit's of the meta data. While tables contain parameters which are filed in colums, log's are unstructured line oriented informations. In this way all forms of meta data can be represented. The meta data are hyper linked. The rules mentioned above make it easy to switch to the world of **XML**.

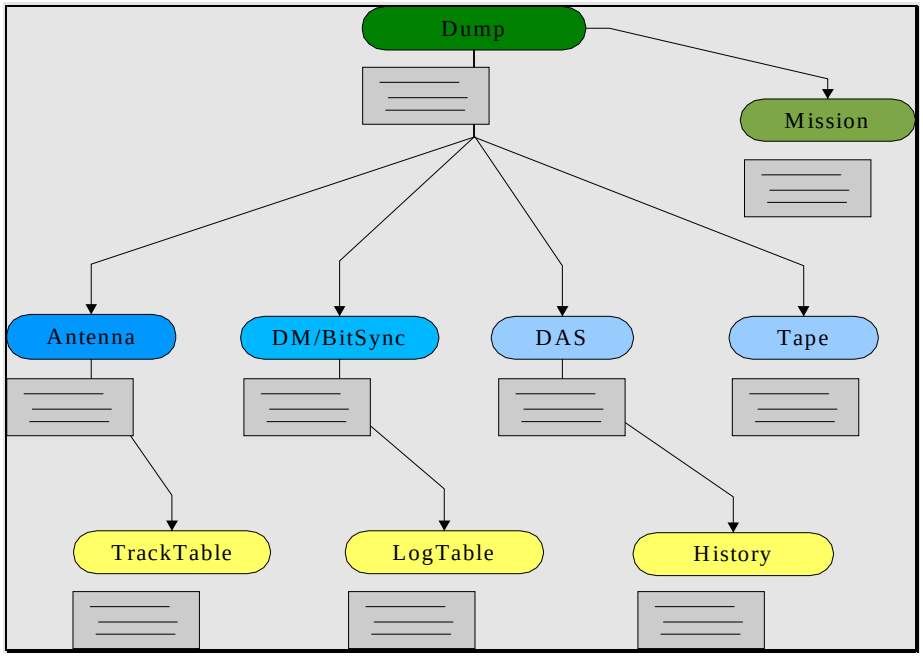

Figure 5 *Meta data structure*

For each mission a unified set of common description keys is defined. Each passage provides information according to this keys. So long term statistics are possible.
The meta data together with the received raw data are given as a pass oriented input directly into the data management system.

Conclusion

This contribution describes the realization of the software system for an efficient satellite data reception in multi mission scenario. Currently, the station control software performs the data reception for the missions ERS-2, LANDSAT-7, IRS-P3, IRS-1C, IRS-1D, CHAMP and BIRD. The used abstractions decrease the station complexibility from the operator view. The reporting system offers the advantage of automatic reporting and the possibility of an efficient quality control. The SCS realizes a homogeneous interface for the operator independed of various missions.

References

[1] J. Richter, H. Damerow; Universal PC-based Frame Synchronizing and Storage System for small satellites missions; Proceedings of the 2nd IAA Symposium on Small Satellites for Earth Observation, (1999) Berlin

Application areas: Man-Machine-Communication; Automation/Robotics

Keywords: M&C system; operator interface; automation; ground station; quality control

FORUM FQPSK

Feher Patented Quadrature Phase Shift Keying

Spectral Efficient Bit Rate Agile and IF Frequency Selectable FQPSK Commercial and Government Product Developments

Dr. Paul Eastman and R. B. Formeister
RF Networks
10201 N 21st Avenue, Unit 9
Phoenix, AZ 85021
United States of America
Voice: +1-602-861-3652
Facsimile: +1-602-861-0251

paul@rfnetworks.com
http://www.rfnetworks.com

Abstract

RF Networks developed one of the first flight tested practical modems to use the Feher-patented Quadrature Shift Keying (FQPSK) [1] modulation technique. The modem was developed, using as a base platform, a modem originally developed to transmit data over coaxial cable and microwave systems. Modifications were made to the modem to accommodate the patented modulation at baseband and to ruggedize the modem for prototype testing in flight telemetry applications.

Pioneering efforts resulted in the first transmitter/receiver pair to be flight proven utilizing the FQPSK modulation technique. Results of these tests confirmed an acceptable alternative to PCM-FM that provides a significantly improved spectral utilization. Current development of data rate agile transmitters and receivers for aircraft and missile telemetry for the US Air Force will be discussed in general terms.

Background

RF Networks was founded in 1993. The founders had been working for Fairchild Data Corporation, a prominent manufacturer of satellite and terrestrial communications products that had decided to drop the terrestrial product lines in favor of its core satellite business. Through the assistance of a European distributor based in Belgium, the founders, including the Fairchild Data Vice President of Engineering and the Terrestrial Line Marketing/Product Manager, we funded a buy out of one product line and began our initial efforts on the new modem that would eventually be used as a platform for the Feher-patented Quadrature Shift Keying (FQPSK) [1] modem.

In early 1995, RF Networks was approached by Dr. Kamilo Feher. Dr. Feher was aware that RF Networks produced a modem that used a phase shift keying modulation technique and wanted to adapt it to transmit and receive the patented Feher Quadrature Phase Shift Keying (FQPSK) modulation. It was determined that there were at least two separate modifications. The first was to modify the modulation circuitry to use the wavelet generation technique described in Dr. Feher's patents. The second involved modifying the demodulator to receive the transmitted OQPSK (Offset Quadrature Phase Shift Keyed) signal instead of the standard QPSK signal.

A Perspective of FQPSK Development at RF Networks

Dr. Feher originally supplied an external box to RF Networks. The box accepted a data stream and generated a baseband I and Q output. The output of the external box was injected into the RF Networks Model 5450 QPSK Modulator modulation input. The signal injection was in place of the I and Q generation from the normal QPSK baseband generator. This approach initially allowed RF Networks' engineering staff to experiment with the FQPSK signals at various data rates and power levels. This experimentation proved invaluable in the process of productizing Dr. Feher's concepts.

In the original implementation received from Dr. Feher, the internal clock was generated in a manner that that was uncoupled from the data. This caused a problem at various data rates as the rising edge of the clock signal varied its position relative to the center of the data signal. Normal circuit noise jitter would sometimes result in a noticeably increased bit error rate at certain power on cycles.

Initial testing of the modems proved very encouraging and led to additional interest to more closely examine the details of the FQPSK modulation technique. These details were quite apparent to us at RF Networks but were not obvious to the investigators - many of whom are presenting here at the FQPSK Forum at ETC-2000 in Garmisch-Partenkirchen, Germany. The modems were returned to RF Networks for the addition of special modifications. Special access was provided to make both I and Q channel baseband signals available. This was done for both the modulator and the demodulator. The modifications allowed the signals to be probed while protecting the modem from perturbations caused by voltage drops or transient inputs. To make the observed signaling more meaningful, the symbol clock was also brought out providing accurate timing.

An additional feature was also added to some demonstrator modem models to facilitate demonstration of the benefits of FQPSK over QPSK in a non-linear amplifier application. The modem was modified to allow a switch to control the modulation mode. (Figure 1) Using this switch, an operating modem could rapidly compare the two modulations under identical circumstances. By placing a non-linear amplifier following the output of the modem the spectral regeneration benefits became readily apparent. (See Figure 2) Similar modifications were added to the demodulator allowing investigators to compare the modulations over actual transmission services.

The feature was included on some demonstrator units whereby the output of the modulator could be fed into an amplifier circuit. A variable step attenuator was used to adjust the power applied to the amplifier input. With 20 dB of attenuation the amplifier acted in a linear manner. As the attenuation was decreased, the amplifier was driven approximately 8 dB into compression. A QPSK signal exhibited the expected spectral regrowth, spreading over several adjacent channels. The FQPSK spectrum showed no observable difference in shape as the attenuation was stepped over the same range.

From Commercial to Military Products

This particular modem set was demonstrated publicly at several venues including the ITC 1998 Exhibit Floor in San Diego, the AIAA Meeting in Washington DC in March 1998 and at the ITC 1999 Exhibit Floor in Las Vegas. It was also demonstrated to numerous private and governmental customers of FQPSK technology.

RF Networks began participation with the US Department of Defense FIRST (Family of Interoperable Range System Tranceivers) in February of 1996. The need for improved spectrum utilization was obvious. It became readily apparent that practical research into the real world transmission properties of FQPSK was needed before it could become the basis of a new telemetry standard. RF Networks was in a position to be able to economically adapt its products to the needs of those investigating potential modulations.

Our standard cable modem product was modified to meet the needs of FIRST researchers form the United States Army, Air Force and Navy. Since practical experimentation required transmission from an airborne platform, the modem needed to be stabilized for flight. Synthesizer robustness was increased to provide greater phase lock loop stability, internal support structures were added to decrease sensitivity to external vibration, and circular metal shell power connectors were added to the modem. Finally, the wavelet assembly software was redesigned to handle both the access and the timing stability needed to meet the requirements of data rates of 10 Mega-symbols per second or more.

Operational modems were delivered to three branches of the United States military for practical range testing. Flight testing of these modems proved the viability of FQPSK as a replacement for PCM/FM to provide for the expected higher spectral density requirements of the telemetry world. During this ETC-2000 conference Messrs. Law [2] and Jefferis [3] will be presenting results of their experimentation with operational FQPSK.

Additional fine tuning of the FQPSK spectral saving potential was investigated when a pair of Digcom's modems were brought back into RF Networks for modification through the additional spectral filtering. Both narrowband and wideband SAW filters were added to further constrain the occupied bandwidth. The results of these additions were discussed by Dr. Feher et al [4]. RF Networks also investigated higher cutoff rate demodulation filtering.

As the ARTM (Advanced Range Telemetry) Program [5] specification came together, RF Networks was once again called upon to assist in developing a specification that insured conformance and interoperability between all potential product developers. Specifically, Mr. Richard Formeister was asked to develop an unambiguous description of Dr. Feher's patent as well as the differential encoding methodology. Several other suggestions were also made to insure that any developed products would work in real world installations.

Confidence in our position as the industry leader in implementation and innovation led us to begin development of our new third generation products well in advance of the award of the U.S. Department of Defense (ARTM) contract. Heavy use of simulation has allowed us to investigate a number of details within the implementation of the FQPSK modulation. The responses, in the areas of phase transitions from one symbol to another, has proved to be extremely insightful and has led to what we consider will be a particularly strong performing product. Similar simulations using our existing products have confirmed the validity of this technique in comparison with known performance.

Using simulation to speed the process, RF Networks has already developed a complete baseband modulator using a number of innovative techniques. (Figure 3) These techniques can be made available to other parties as a part of an Intellectual Property transfer. The modulator has been used to drive and confirm the development of our Model 2120 Telemetry Demodulator, one of the ARTM deliverable items. We expect that this product will fully meet or exceed all program requirements and be available for commercial deliveries beginning in the fourth quarter of this year.

The current status and performance of the RF Networks Model 2120 Telemetry Demodulator will be discussed.

The following figures illustrate some of the typical results.

References

1. K. Feher et al.: U.S. Patents 4,339,724; 4,567,602; 4,644,565; 5,491,457; 5,784,402, post-patent improvements and other U.S. and international patents pending. For Feher patented FQPSK and Feher patented GMSK licensing and technology transfer information, on an equal-opportunity, non-discriminatory basis with uniform terms and at a fair market price contact: FQPSK Consortium- Digcom, Inc., c/o Dr. Kamilo Feher, 44685 Country Club Dr.; El Macero, CA 95618, USA . Tel. 530-753-0738; Fax 530-753-1788 E-mail: feherk@yahoo.com
2) E. Law: "IRIG FQPSK-B Standardization Progress Report," Member, RCC Telemetry Group, NAWCWD, US Navy, Pt. Mugu, California , USA, Proceedings of the European Telemetry Conference, ETC 2000, Garmisch-Partenkirchen, Germany, May 22-25, 2000
3. R. P. Jefferis: "FQPSK-B Performance in Air-to-Ground Telemetry," TYBRIN Corp., Edwards Air Force Base, California, USA, Proceedings of the European Telemetry Conference, ETC 2000, Garmisch-Partenkirchen, Germany, May 22-25, 2000
4. K. Feher: "Standardized Feher patented FQPSK Doubles and 2nd generation FQPSK Could Quadruple Spectral Efficiency of PCM/FM Telemetry, of Feher patented GMSK and of Alternatives", Proceedings of the European Telemetry Conference, ETC 2000, Garmisch-Partenkirchen, Germany, May 22-25, 2000
5. U.S. Department of Defense Solicitation F04611-99-R-0005; Advanced Range Telemetry Project; Edwards Air Force Base, California, USA.
6. IRIG STANDARD 106-00 "Telemetry Standards" [Note :For higher bit rates ,when better bandwidth efficiency is required, the IRIG 106-00 Telemetry Standard specifies the use of Feher' s patented Quadrature Phase Shift Keying (FQPSK-B) . This Standard has been approved for Public Release-Distribution is Unlimited. See

: http://technet0.jtce.jcs.mil/ RCC/manuals/106-00/ . Published by Secretariat of Range Commanders Council, U.S. Army, White Sands, New Mexico 88002-5110, USA , January 2000.
7. Digcom, Inc. : "FQPSK-B, Revision A1, Digcom –Feher Patented Technology Transfer Document, January 15,1999 " , El Macero ,CA, January 1999. [Note: This Digcom, Inc. proprietary document is available to Digcom's Licensees of the Feher patented FQPSK and GMSK Technologies , from Digcom, Inc]. The IRIG STANDARD 106-00 references (on page 2-5) this Digcom document for the use of the standard specified FQPSK-B. See : http://tecnet0.jcte.jcs.mil/RCC/manuals/106-00/ . For FQPSK –GMSK Technology Transfer and Licensing Contact: Digcom, Inc., c/o Dr. Kamilo Feher, 44685 Country Club Dr.; El Macero, CA 95618, USA Tel. 530-753-0738; Fax 530-753-1788 E-mail: feherk@yahoo.com
8. K. Feher : "*Wireless Digital Communications: Modulation & Spread Spectrum Applications"* - Book published by Prentice Hall, 1995. ISBN 0-13-098617-8

Figure 1 - Special FQPSK modifications to standard RF Networks modems.

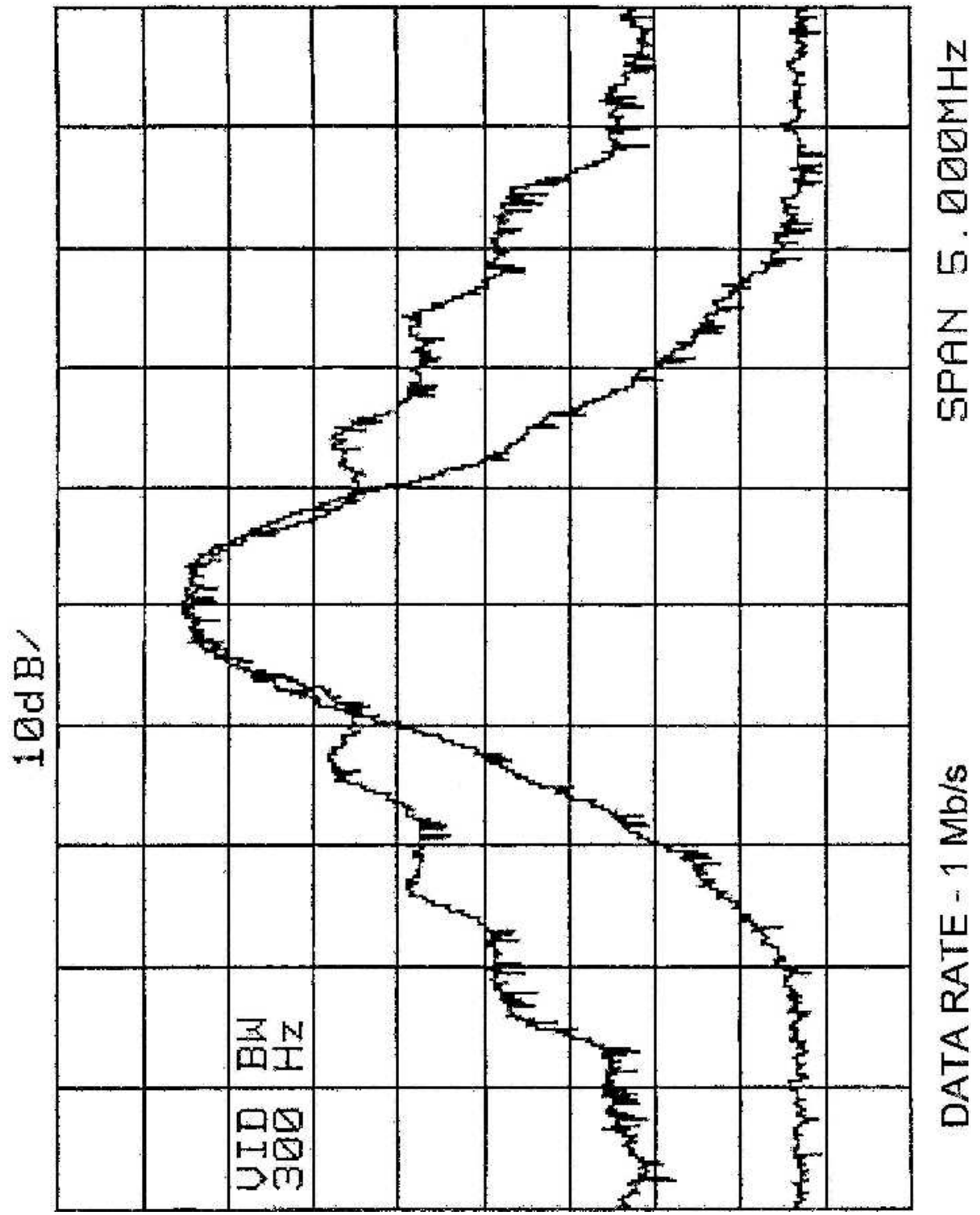

Figure 2 - RF Spectra for 1 Mb/s filtered FQPSK and QPSK (non-linear amplifier).

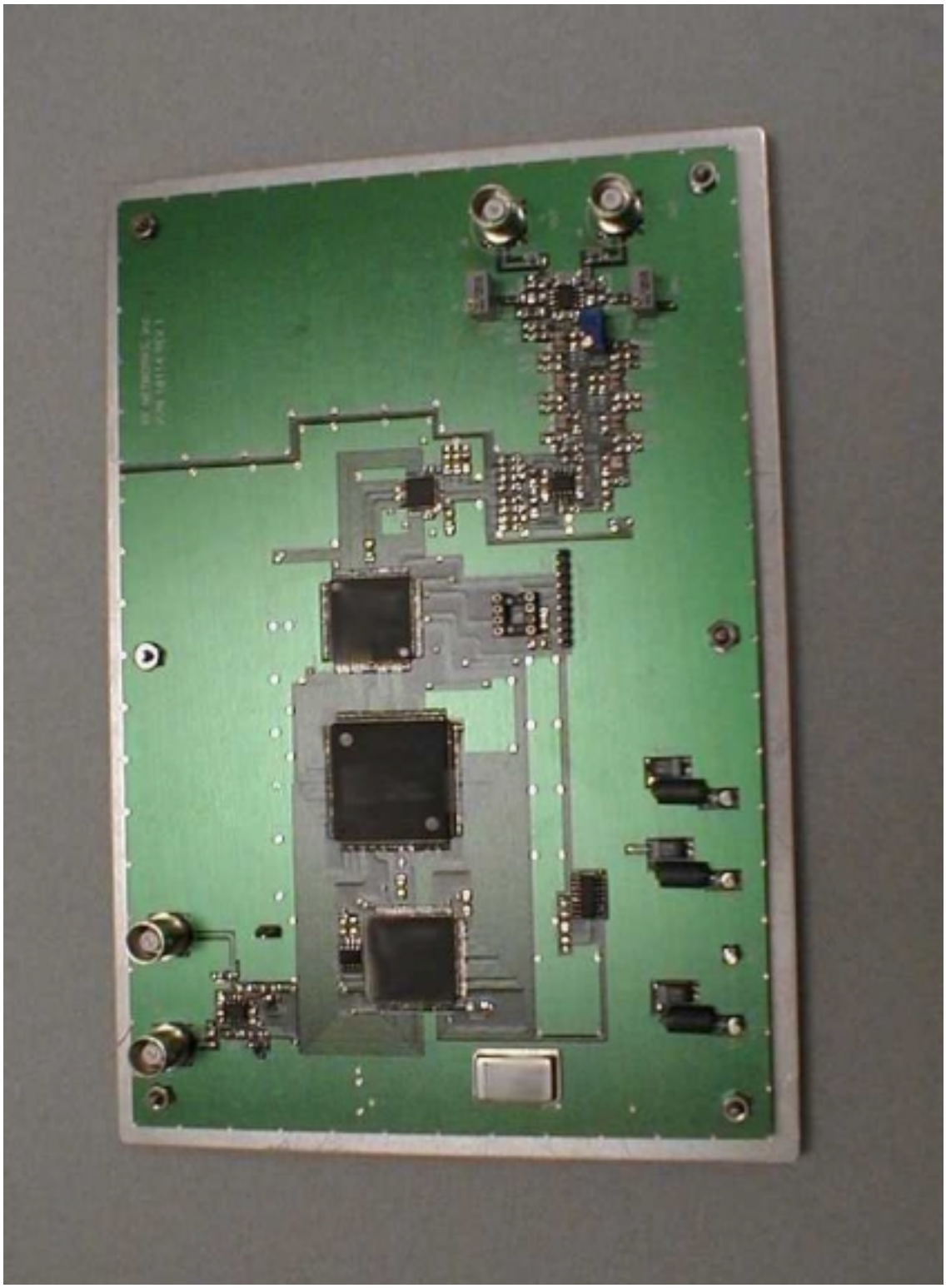

Figure 3 - RF Networks data rate agile FQPSK Baseband Modulator

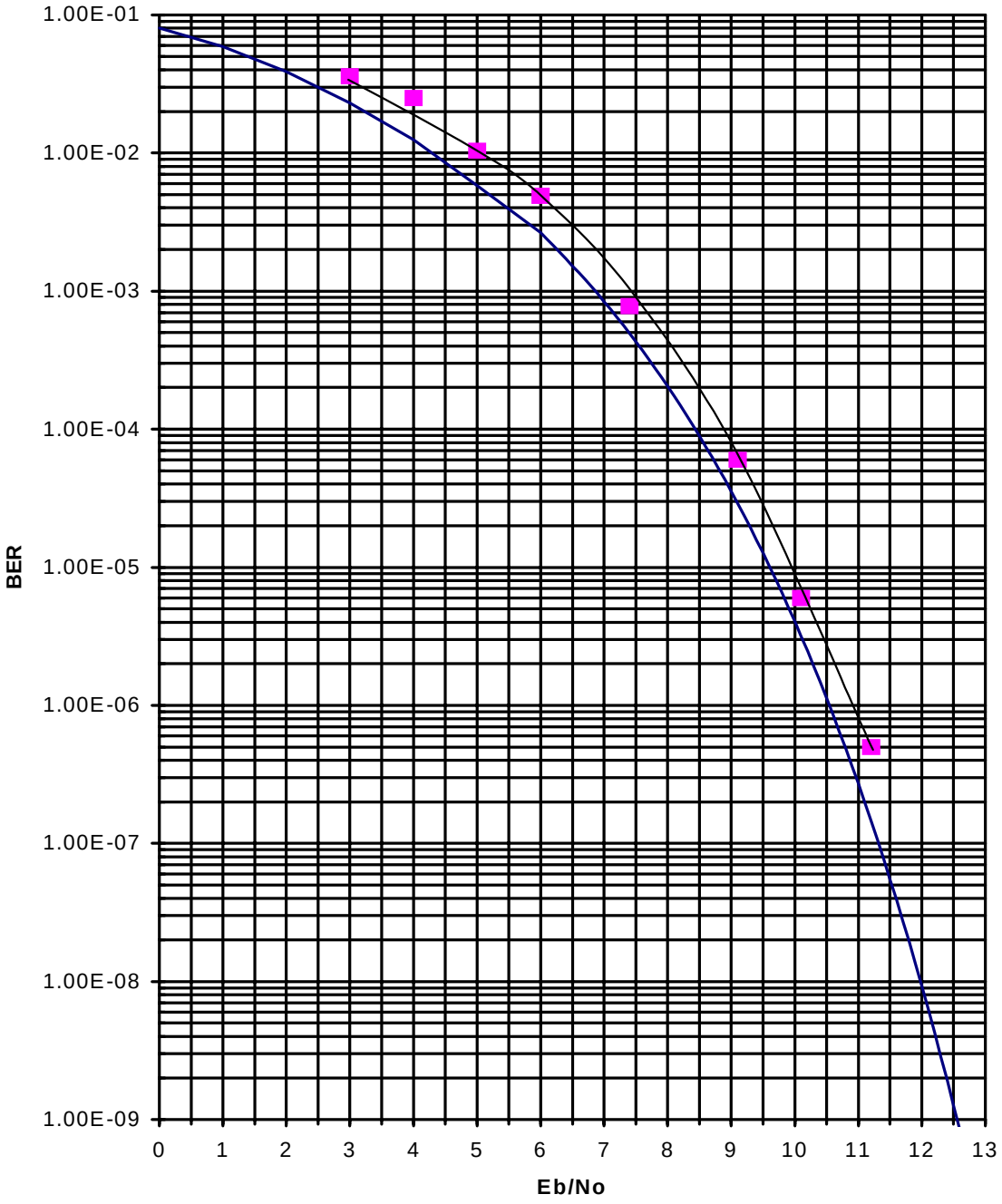

Figure 4 - BER for Standard QPSK at 1 Mbit/sec, 70 MHz center frequency

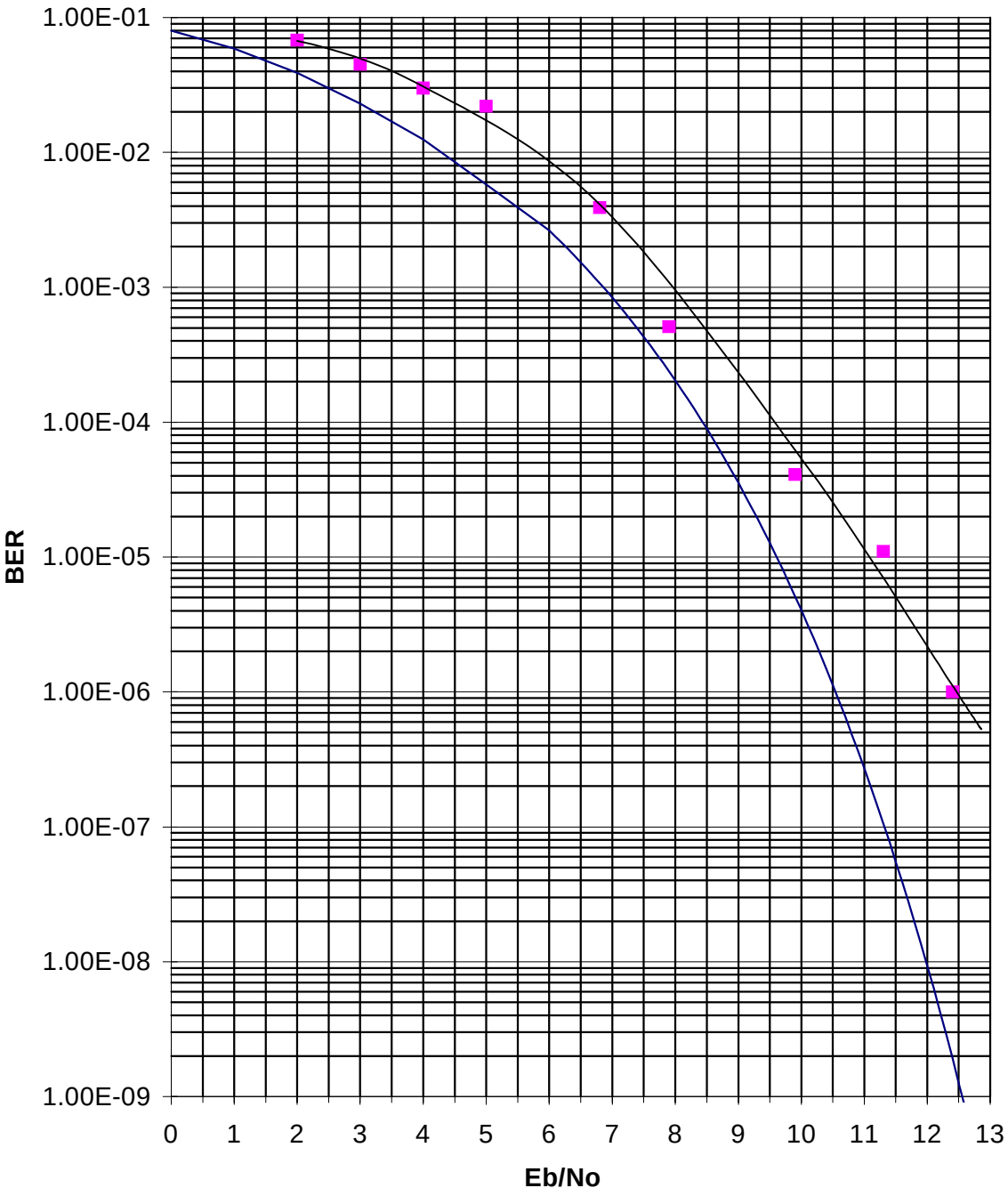

Figure 5 - BER for FQPSK at 1 Mbit/sec, 70 MHz center frequency

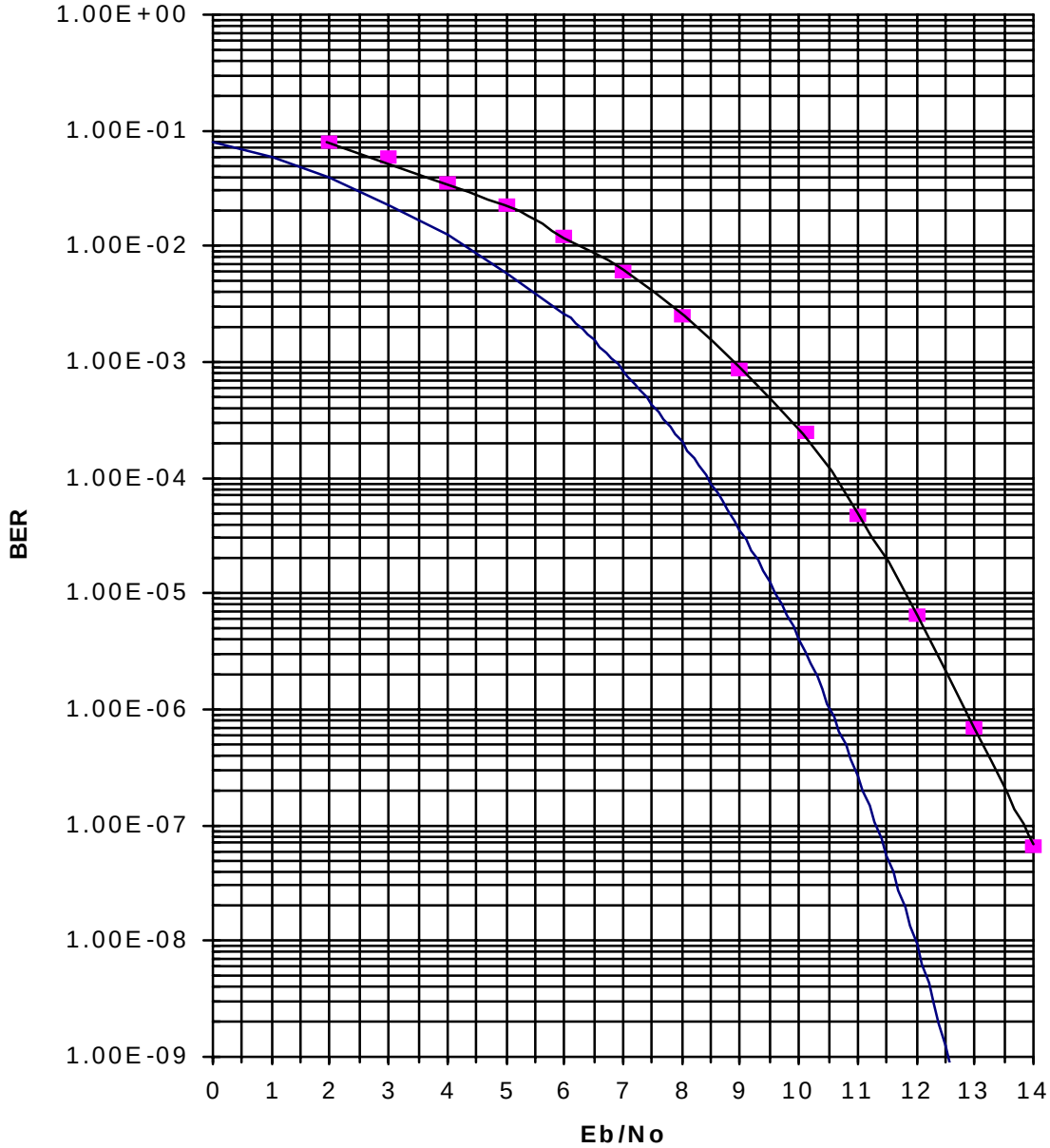

Figure 6 - BER for Standard QPSK at 5 Mbit/sec, 70 MHz center frequency, differential encoders ON, scramblers OFF, -45 dB Rx level, linear mode.

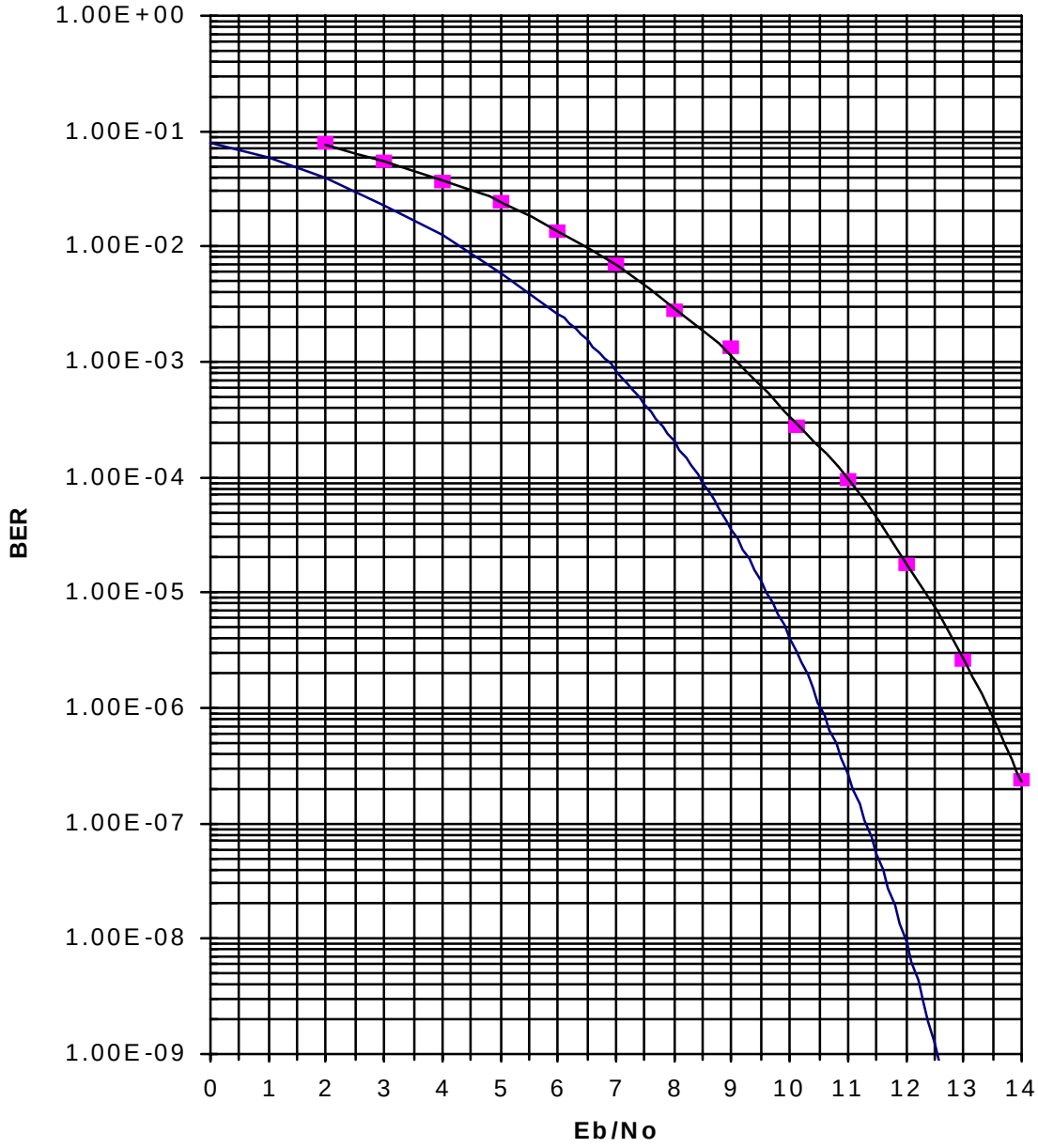

Figure 7 - BER for FQPSK at 5 Mbit/sec, 70 MHz center frequency, differential encoders ON, scramblers OFF, -45 dB Rx level, linear mode.

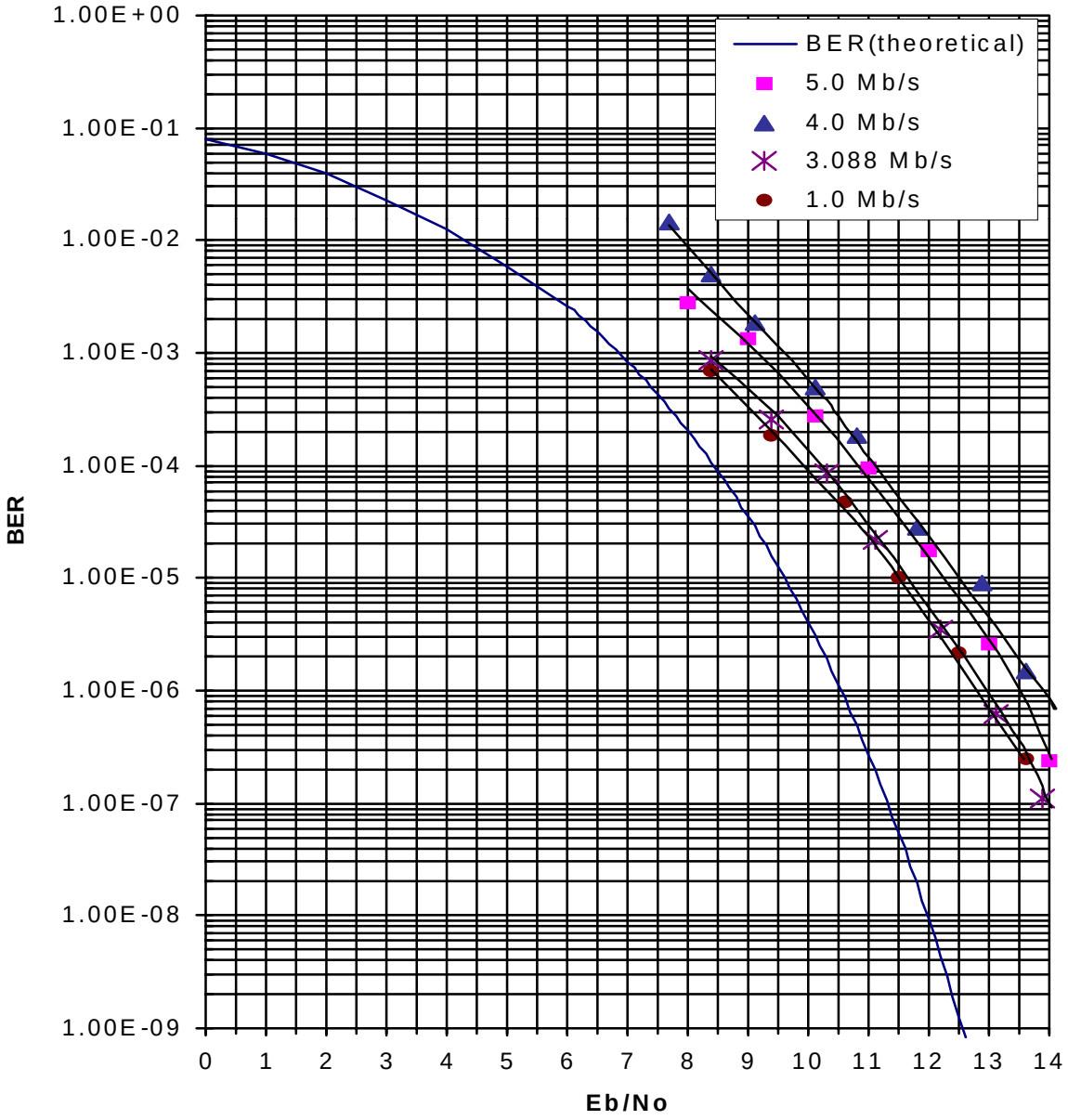

Figure 8 - Comparison of BER for FQPSK at 1.0 Mb/s, 3.088 Mb/s, 4.0 Mb/s, and 5.0 Mb/s

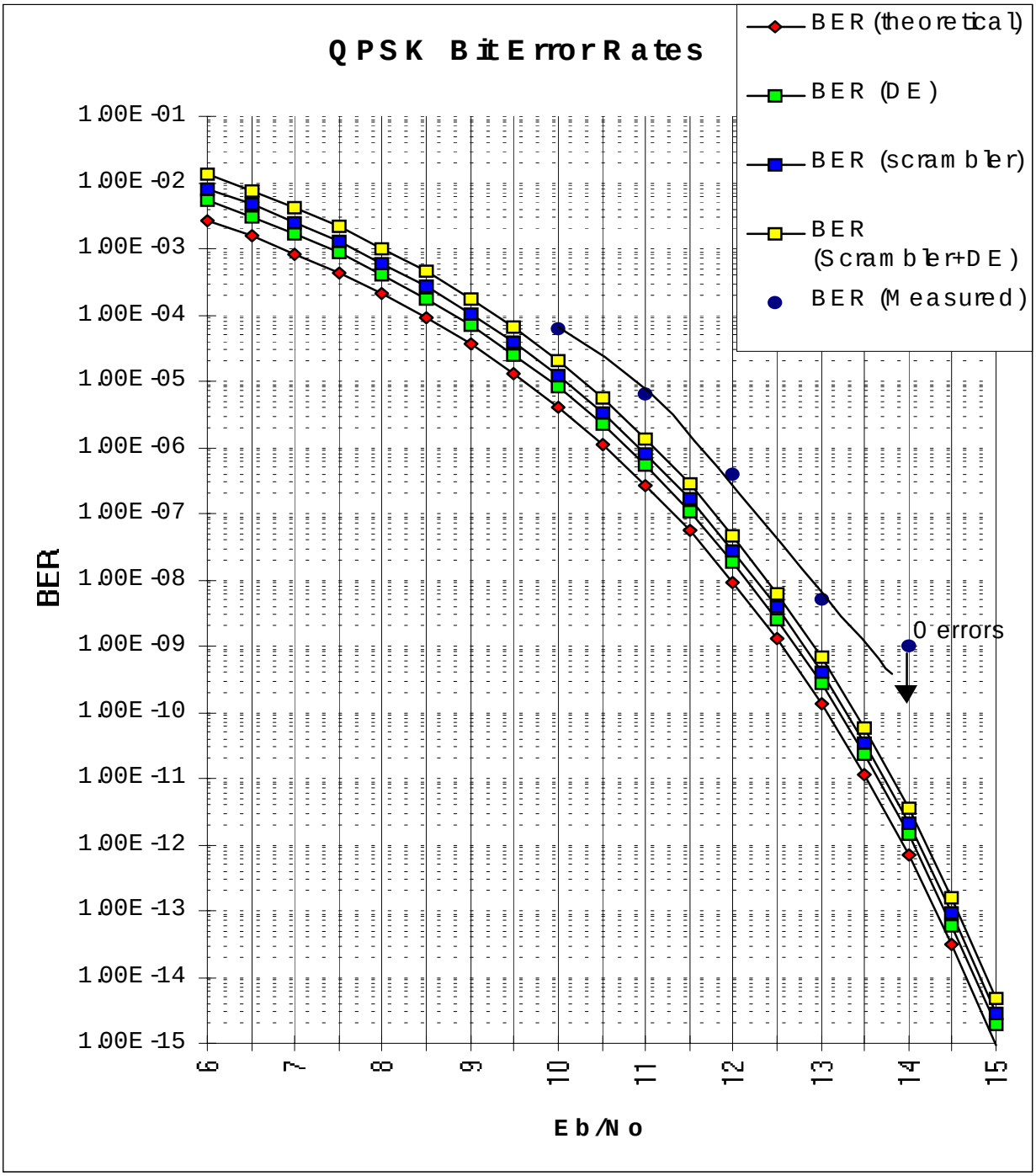

Figure 9 - Comparison of actual modem performance vs. Theory including the effects of differential encoding and scrambling.

PRODUCTION DESIGN OF GOVERNMENT STANDARDIZED SPECTRALLY EFFICIENT FQPSK[1,2] TRANSMITTERS©

Joe Bottenfield — Vice President, Engineering, bottenfield@herley.com

John Carle — Sr. RF Engineer, carle@herley.com

David Heft — Sr. Systems Engineer, heft@herley.com

Herley Industries, Inc.

10 Industry Drive

Lancaster, PA 17603

(717) 397-2777

http://www.herley.com

Abstract

Herley Industries has applied state of the art design for production techniques to develop of a line of dual use spectrally efficient digital data transmitters. Herley has been a global leader in the design and production of high tech RF and microwave products for more than 30 years. The resulting transmitters support variable data rates up to 20 Mbps and output power levels to 10 Watts in both the L and S frequency bands. The transmitter product line implements Feher's-patented Quadrature Phase Shift Keying (FQPSK) modulation technique, effectively doubling the spectral efficiency of conventional PCM-FM techniques. While the development of this transmitter product line represents the initial offering of Herley in the blossoming FQPSK industry, the design team has relied upon its extensive experience in producing RF and microwave products that represent the state of the art in design and manufacturing techniques. The end result has been the production of cost effective transmitters that meet the vibration, shock, EMI, altitude, and temperature requirements of missile and aircraft environments.

---

[1] Feher's-patented quadrature phase shift keying (FQPSK) is a variation of offset quadrature phase shift keying (OQPSK).

[2] K. Feher et al.: US Patents 4,567,602; 4,644,565; 5,491,457; and 5,784,402, post-patent improvements and other US and international patents pending.

Introduction

Increasing pressure on available bandwidth for range telemetry applications has led to the evaluation of various modulation techniques for the purpose of finding the appropriate balance between spectral efficiency, implementation cost, and impact to existing telemetry infrastructures. Feher's-patented Quadrature Phase Shift Keying (FQPSK) has emerged as the modulation method of choice for applications where available bandwidth is an issue and has been adopted as the standard for bandwidth efficient modulation in government standards such as IRIG 106-00.

The modulation characteristics of FQPSK allow the use of less expensive, more efficient, Non-Linear Amplification (NLA) techniques while providing a 2 to 1 improvement in spectral efficiency of GMSK, PCM-FM, and other modulation techniques.

Implementation of FQPSK for rugged use, including missile and aircraft applications, poses challenges in the areas of packaging (thermal transfer), phase noise performance, amplitude and phase balance, and frequency stability.

Herley Industries has designed a line of FQPSK transmitters for use in both commercial and military applications.

This paper provides an overview of Herley Industries and examines the challenges presented by an FQPSK transmitter implementation and the design techniques used to meet those challenges.

Overview of Herley Industries

From its incorporation in 1965, Herley Industries has designed and manufactured microwave devices for use in various tactical military programs.

Herley has grown to include both international and US domestic companies segregated into two divisions, Space and Communications, and Microwave Products.

The Space and Communications Group designs and produces an array of RF and microwave products from UHF to Ka-Band including; Telemetry (TM) Transmitters, Flight Termination Receivers, Command and Control Transponders, Radar Transponders, Identification Friend or Foe (IFF) Transponders, Frequency Multipliers, and highly integrated multi-function assemblies.

The Microwave Products Group designs and produces high power magnetrons, solid state receiver protectors, as well as complex microwave integrate circuits employed in military and commercial applications including Rear Warning Receivers, Electronics Countermeasure systems. The Microwave Products Group includes General Microwave Corporation which produces a variety of attenuation devices, IQ modulators, phase shifters, and microwave oscillators.

Herley joined the FQPSK Consortium in 1999 and has become the sole supplier of missile and aircraft TM Transmitters for the Advanced Range Telemetry (ARTM) program for the US Air Force.

FQPSK Transmitter Design

This section will include an examination of the requirements driving the design of an FQPSK Transmitter and the techniques used to meet those requirements.

Driving Requirements

- Fixed and Variable Rate FQPSK-B Revision A1 Modulation
  - Data rates from 1 to 20 Mbps
  - Differential Encoding of Data
  - Carrier Suppression: 25 dBc
  - I&Q Channel Defects: 30 dBc
- Carrier Frequency Range
  - L-Band: 1435.5 to 1534.5 MHz
  - S-Band: 2200.5 to 2389.5 MHz
- Carrier Frequency Stability: $\pm$ 20 ppm
- Single Side-Band (SSB) Phase Noise

Carrier Offset (kHz)	L(f) Upper Limit (dBc)
0.01	-30
0.1	-60
1	-82
10	-92
100	-102
1000	-102

- PSD Spectral Mask per IRIG 106-00
- Output Power: 2, 5 and 10 Watts
- Mechanical Outline
  - Fixed Rate: 180 cm^3 (11 in^3)
  - Variable Rate: 250 cm^3 (15.5 in^3)
- Operating Environment
  - Temperature: -40 ^oC to +85 ^oC

- Vibration: 15 grms, Random, 20 Hz to 2000 Hz
- Shock: 60 g, ½ sine impulse, 5 msec duration
- Acceleration: 40 g
- Altitude: sea level to 30,480 m (100,000 ft)
- Electromagnetic Interference: MIL-STD-461D for Aircraft

FQPSK Transmitter Functional Block Diagram

A functional block diagram of a FQPSK Transmitter is presented in Figure 1.

EMI Filter and DC/DC Converter

The EMI filter design has been incorporated in Herley transponders, receivers, and transmitters to reduce both conducted emissions from the transmitter as well as protecting the transmitter from conducted interference.

The EMI filter is connected to the DC/DC Converter. The input of the DC/DC Converter utilizes circuitry to prevent damage from Transient Surge Voltages, Spike Voltages and Reverse Voltage Protection. The DC/DC Converter and Linear Regulator convert the DC Input Voltage into the stable, regulated, DC levels required by the transmitter circuitry.

Frequency Synthesizer

The Frequency Synthesizer FQPSK Transmitter is locked to a surface mount Temperature Compensated Crystal Oscillator (TCXO) frequency stability over the specified temperature range.

The resulting synthesizer, and consequently the transmitter, output phase noise will be strongly influenced by the multiplied TCXO phase noise characteristic out to the edge of the loop bandwidth, after which the phase noise characteristic of the VCO will dominate.

Baseband Processor

The Baseband Processor includes input data and clock signal conditioning as well as performing the mechanics of FQPSK-B modulation. The following functions are performed by the Baseband Processor to generate the I and Q inputs for the Quadrature Modulator.

- Differential Encoding
- I&Q Symbol Splitting
- Symbol Cross-correlation
- Symbol to Wavelet Mapping
- Digital to Analog conversion
- Analog signal filtering and conditioning

For variable data rate implementations, the Baseband Processor performs additional digital filtering and interpolation functions to optimize the I and Q symbol streams.

Quadrature Modulator

The Quadrature Modulator accepts the I and Q analog data outputs from the Baseband Processor and the Local Oscillator output from the Frequency Synthesizer and use the I and Q data to Quadrature Phase Shift Key (QPSK) modulate the Local Oscillator carrier. The resulting RF output has the spectral characteristics of the FQPSK-B version A1 modulation by virtue of the filtering and data manipulation that takes place in the Baseband Processor.

Power Amplifier

The modulated signal is then amplified to its output power level using a Class C power amplifier.

FQPSK-B versus PCM-FM Transmitter Design

The design of an FQPSK-B Transmitter differs from that of a standard PCM-FM Transmitter in several areas, including:

- Carrier Frequency Stability required for FQPSK-B is more stringent than for PCM-FM
- SSB Phase Noise has more of an impact on Bit Error Rate (BER) performance for FQPSK-B
- FQPSK-B requires processing of data prior to modulation which is not required for PCM-FM

In return for the efforts required to implement FQPSK-B, the user is rewarded with greatly improved spectral efficiency as illustrated in Figures 2 and 3.

Designing for the Environment

Meeting the demands of missile and aircraft environments imposes additional considerations on the design of the Synthesizer (Exciter) to meet the Frequency Stability and SSB Phase Noise requirements.

The Reference Oscillator is the primary source of center frequency instabilities in the transmitter and temperature compensation is necessary to allow a crystal oscillator to meet the stability requirement over the military temperature range.

Transmitter SSB phase noise performance is determined by the Reference Oscillator within the Synthesizer Loop Bandwidth, and by the VCO outside the loop bandwidth. Therefore, the vibration performance of Reference Oscillator is critical for close-in phase noise performance. Both the Reference Oscillator and the VCO require attention to component staking and mounting to ensure adequate performance. Herley oscillator designs for coherent phase shift keyed applications have used a variety of materials and techniques for vibration damping including epoxies and preformed absorbers.

Designing to Eliminate Electro-Magnetic Interference (EMI)

The Herley FQPSK Transmitter is designed to meet the stringent Electro-Magnetic Interference requirements of US MIL-STD-461D/E for Aircraft applications. This operational environment necessitates the engineer pay particular attention to both the mechanical and electrical assembly of the transmitter. Figure 4 illustrates several areas of addressed by the EMI resistant design of the Herley FQPSK Transmitter.

Typical areas of concern for EMI designs include conductive gasketing, power-line filtering, signal line filtering, and suppression of spurious RF and harmonics.

As shown in Figure 4, all metal to metal interfaces and connector to chassis interfaces are subject to Radiated Emissions and Radiated Susceptibility testing. Electrically conductive and EMI resistant gasketing is be employed to prevent excessive radiation effects.

The other major area for EMI design techniques are the power, signal, and RF interfaces which are subject to Conducted Emissions and Conducted Susceptibility testing. To meet MIL-STD-461D/E in these areas, robust EMI filtering on the power lines and attention to RF spurious generation, including harmonics generated by oscillators and high speed digital components is required.

Packaging Considerations

Figure 5 presents an exploded view of the mechanical packaging design of the Herley FQPSK Transmitter. In the development of this package, design areas requiring special attention included:

- Isolation of the RF circuitry from spurs generated in the Baseband Processor and DC/DC Converter
- RF isolation within the RF chassis to prevent RF “sneak” paths.
- Signal transfer between chassis
- Effective heat transfer from the Power Amplifier to the chassis exterior

Conductive gasketing and the limitation of Baseband Processor chassis openings to those required for signal transfer, provide RF isolation.

Interior wall placement and continuity between the interior walls and the RF chassis cover provide effective RF isolation between functional sections of the RF chassis assembly. In this case the RF chassis cover includes the interfacing surface of the Baseband Processor chassis. Conductive gasketing is used to ensure continuity between the interior walls and the cover.

Power Amplifier heat removal is accomplished through the maintenance of thermally conductive material between the power transistor flanges and the chassis exterior.

FQPSK Transmitter Product Line

The Herley FQPSK Transmitter product line includes a wide range of frequency, data rate, output power, and input data/clock interfaces. The product line is segmented into two groups, Fixed Data Rate Transmitters and Variable Data Rate Transmitters. An overview of the available transmitters includes:

- Fixed Rate Transmitters,
  - Data Rates: 1 to 20 Mbps, factory set
  - Frequency: L-Band (1435.5 to 1534.5 MHz) and S-Band (2200.5 to 2389.5 MHz)
  - Output Power: 2 W and 5 W
  - Input Data/Clock Interface: TTL, ECL, and RS422
- Variable Rate
  - Data Rates: 1 to 20 Mbps, continuously variable
  - Frequency: L-Band (1435.5 to 1534.5 MHz) and S-Band (2200.5 to 2389.5 MHz)
  - Output Power: 10 W
  - Input Data/Clock Interface: TTL, ECL, and RS422

Conclusion

Feher's-patented Quadrature Phase Shift Keying (FQPSK) has emerged as the modulation method of choice for applications where available bandwidth is an issue and has been adopted as the standard for bandwidth efficient modulation in government standards such as IRIG 106-00.

Herley Industries has designed a line of state-of-the-art FQPSK transmitters for use in both commercial and military applications which meet the design challenges posed by missile and aircraft environments.

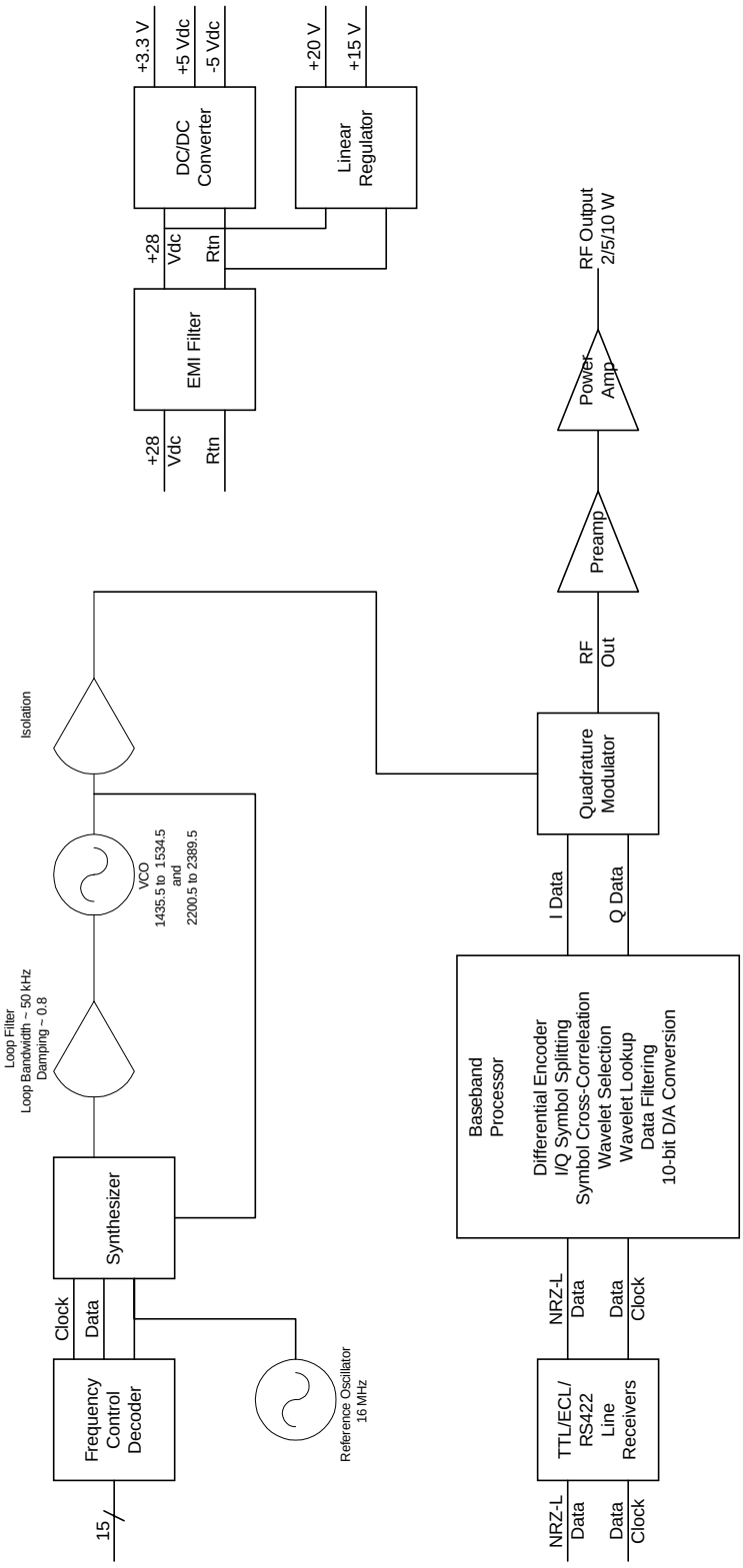

Figure 1. FQPSK Transmitter Functional Block Diagram

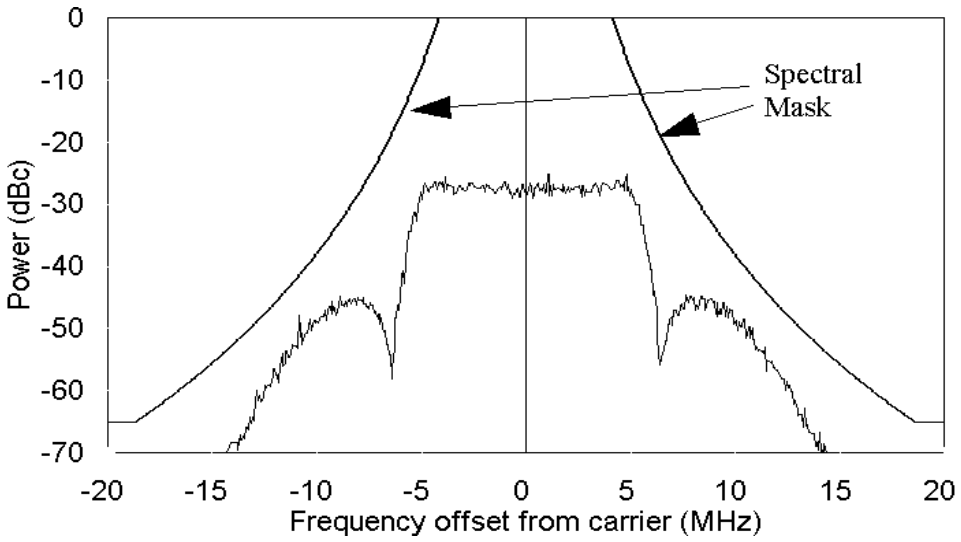

Figure 2. Typical PCM-FM Power Spectrum, 5Mbps

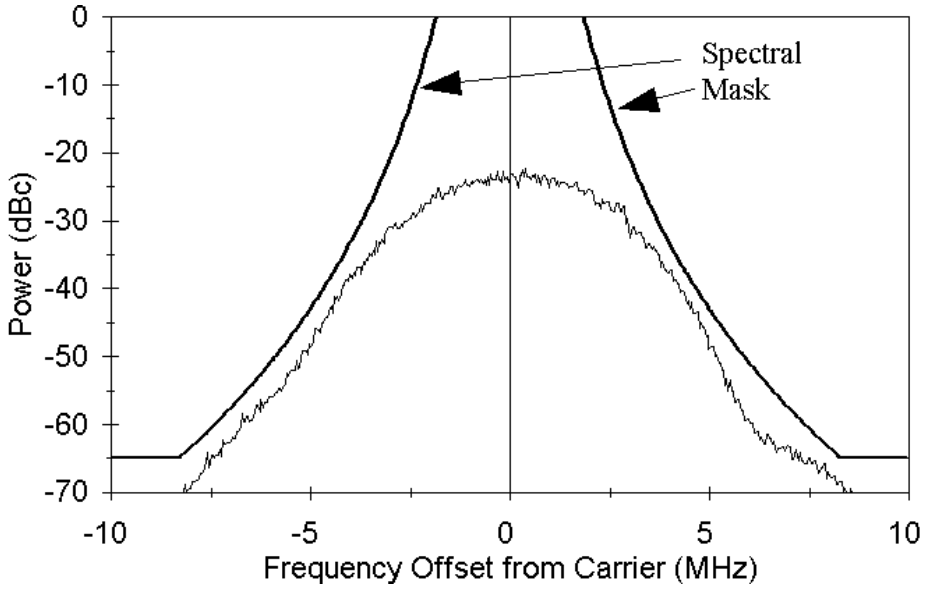

Figure 3. Typical FQPSK-B Power Spectrum, 5 Mbps

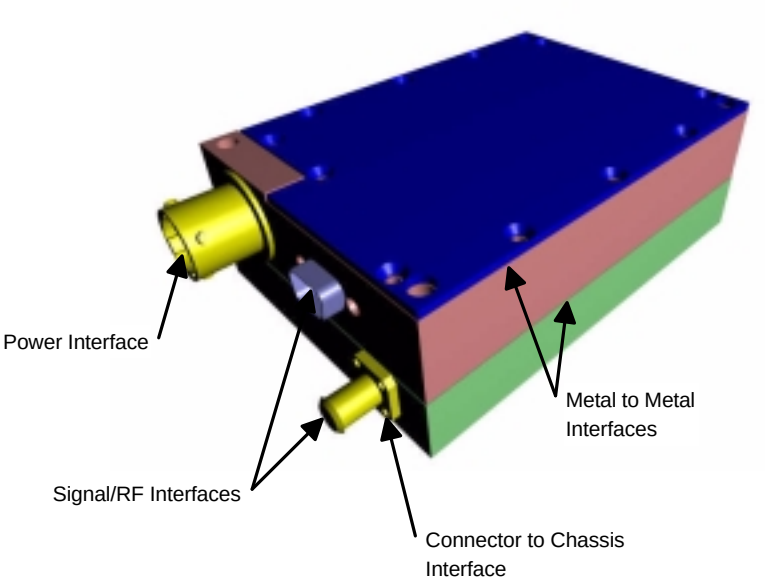

Figure 4. EMI Critical Areas

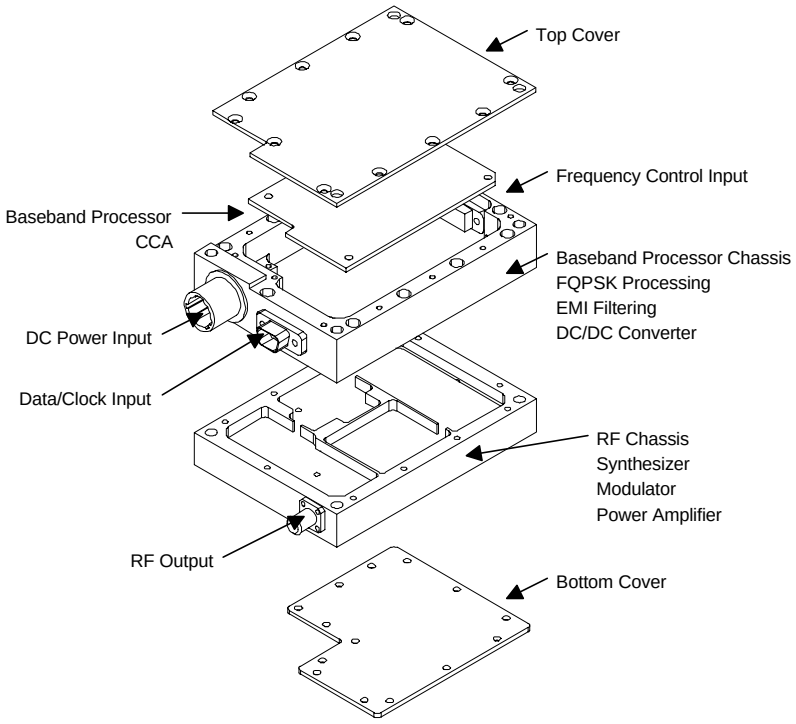

Figure 5. HV FQPSK Transmitter Packaging

An Off-line Coherent FQPSK-B Software Reference Receiver*

Haiping Tsou, Scott Darden, and Tsun-Yee Yan

Jet Propulsion Laboratory
California Institute of Technology
Pasadena, California, USA

ABSTRACT

Using Feher patented Quadrature Phase Shift Keying provides improved spectrum efficiency for high rate telemetry systems. This paper presents an off-line coherent FQPSK-B software reference receiver developed for hardware calibration under contract from the Advanced Range Telemetry (ARTM) program. This receiver is developed in Matlab/Simulink to be consistent with the software capacity available across a number of computing platforms at both ARTM and the Jet Propulsion Laboratory. It also offers a cost-effective approach to demonstrate the advance technologies. The functionality and key features of this receiver (including its internal software transmitter) will be addressed in this paper. Results from end-to-end system simulations are included as examples.

INTRODUCTION

Using Feher patented Quadrature Phase Shift Keying (Feher patented QPSK or FQPSK) improves spectrum efficiency for high rate telemetry systems. An off-line coherent software receiver has been developed for FQPSK-B modulation, a variant in the FQPSK family which includes proprietary designed filtering for additional spectrum containment [1]-[2]. It is intended to be used as (i) a stand-alone receiver offering a platform on which advanced technologies enabling further performance enhancement can be cost-effectively demonstrated, and (ii) a software tool that can be customized for testing and validating various hardware FQPSK-B transceivers under procurement consideration. Because of the testing requirements, the receiver has its own internal reference transmitter and a simple additive white Gaussian noise (AWGN) channel model and, therefore, is capable of performing end-to-end FQPSK-B system simulation and performance evaluation.

The software receiver consists of many functional modules developed in Matlab/Simulink, including differential encoding, FQPSK waveform generation, modulation, channel model, carrier and symbol synchronization, coherent demodulation and detection, differential decoding, and some real-time performance monitors and post-processing test result generators. These modules can be configured differently to carry out specific tasks in each of the receiver's four operating modes. For example, as a stand-alone receiver, it provides off-line demodulation, detection, and decoding of a sampled and digitized FQPSK-B signal from an external source, presumably a hardware

* The research described in this paper was carried out by the Jet Propulsion Laboratory, California Institute of Technology under contract with the National Aeronautic and Space Administration.

transmitter, to get the detected bit stream. Both demodulation and detection are performed coherently, which relies on the receiver's carrier and symbol synchronization loops to generate correct carrier phase reference and symbol timing. The bit error rate (BER) can be measured and compared to that of hardware receiver when the transmitted bit stream is available for BER calculation. The second mode is for hardware transmitter validation in which the software receiver is able to compare the demodulated hardware-generated signal with a reference signal realized by passing an internally generated baseband signal through the same receiver. The resulting error vector magnitude (EVM) measurement indicates hardware problems in the transmitter under test. The third and the fourth modes are for internal testing in which the software receiver functions as an end-to-end simulation system conducting BER and/or EVM tests under a set of user-specified conditions, including modulator imbalances and different filter designs. They can be used for trade-off studies on design parameters to realize a specification that meets certain design goals.

The FQPSK-B software receiver is developed on a Sun Workstation by using Matlab version 5.3 with Simulink toolboxes such as Communication Toolbox, DSP Toolbox, and Real Time Workshop. Because of the cross-platform compatibility of Matlab/Simulink, it can run on computers using operating systems such as UNIX, Window, and MacOS as long as a proper version of Matlab/Simulink is installed. It is also interesting to note that, because of the similarity between FQPSK and other conventional schemes in the QPSK family, the software receiver is flexible in handling many other types of QPSK signal or their derivatives with simple modifications.

The functionality and features of this Matlab/Simulink-based software receiver will be described in the next section, followed by a description of each of the four operation modes and their specific configurations for different applications. In addition, results from end-to-end system simulations using the internal reference transmitter are provided as examples, followed by a discussion of future works at the end of this paper.

FUNCTIONAL DESCRIPTION

The software receiver includes two major functional units: the internal transmitter and the coherent receiver. The functional block diagram of the internal transmitter is shown in Fig. 1, including a

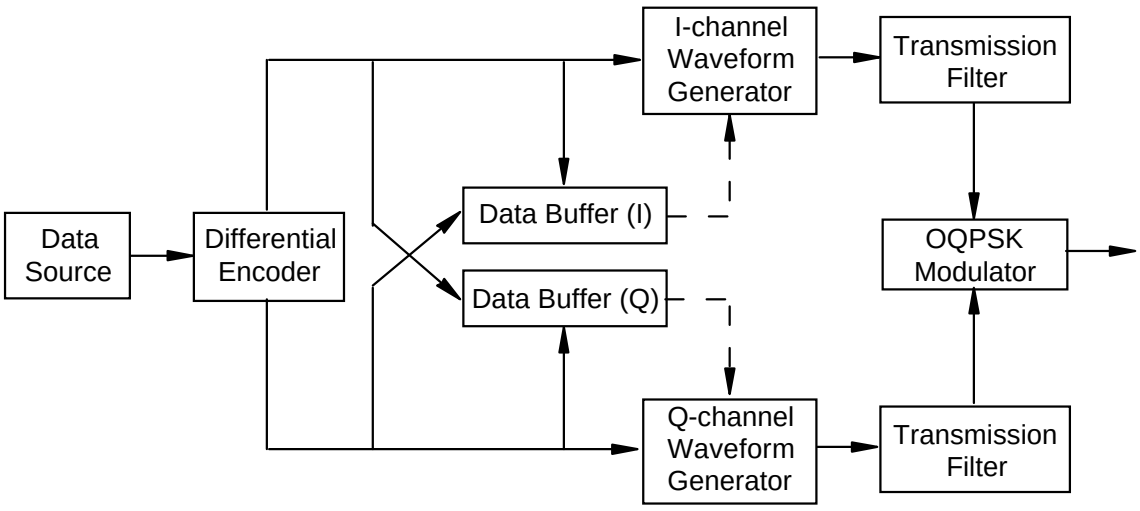

Figure 1 FQPSK-B Software Transmitter

data source (either a random or a fixed known sequence), a differential encoder, an FQPSK waveform generator (including data buffers facilitating cross-correlation between I-channel and Q-channel symbols), transmission filters and an offset QPSK (OQPSK) modulator. The functional block diagram of the coherent receiver is shown in Fig. 2, including an OQPSK carrier tracking loop, a symbol synchronizer providing correct timing for coherent detection, and a differential decoder.

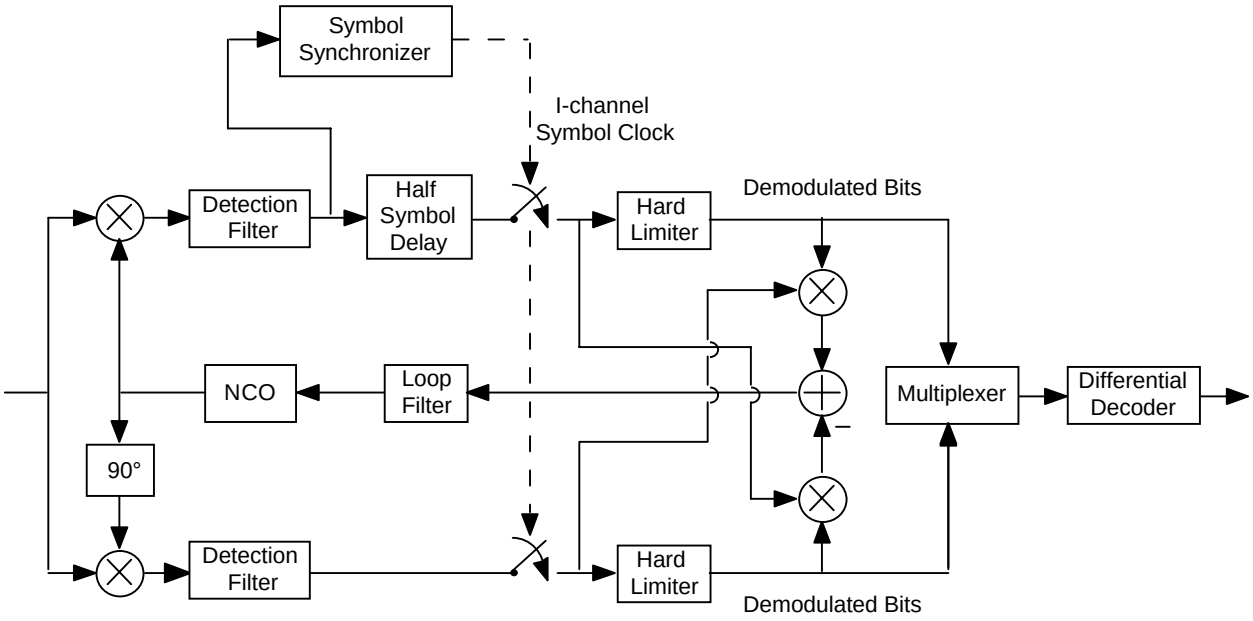

Figure 2 Coherent FQPSK-B Software Receiver

The receiver is developed based upon the assumption that the input signal is an FQPSK-B signal sampled at a fixed (known) rate that is high enough to avoid significant aliasing. The internal transmitter is able to generate such a sampled signal at either baseband or IF with floating-point values. On the other hand, the input from external hardware transmitters has to be a pre-recorded file consists of samples organized according to the Matlab standard I/O format. Typically, these samples are provided by the receiver's hardware front-end[1] that down-converts the received signal from RF to IF and then samples it to produce finite-bit quantized samples. These integer-valued samples will be internally converted to floating-point ones with average signal power normalized to one before being processed by the receiver.

Following are the description of the key functions of the transmitter and receiver.

Differential Encoding and Decoding

Differential coding is provided in the software transmitter according to the telemetry standards specified in [3]. Its use is to resolve phase ambiguity associated with QPSK-based modulations.

In the software transmitter, the binary source data stream, consisting of 0's and 1's with a bit duration of T_b seconds, is first differentially encoded. In particular, the k^{th} coded bit, denoted by B_k, is a function of the current source bit and the one before that, denoted by b_k and b_{k-1}, at the

[1] This is normally a hardware digital oscilloscope capable of down-conversion and sampling.

encoder input and the $(k-2)^{th}$ coded bit, B_{k-2}, at the encoder output. This function is written in the recursive formula as follows

$$B_k = \overline{b_k \oplus b_{k-1}} \oplus B_{k-2}, \qquad k \in N = \{0,1,2,\cdots\}$$

where the symbol $\oplus$ denotes the exclusive-or operator, the over-line represents the logical 'not' or inversion operator. The coded bit is then converted from binary format to a non-return-to-zero and leveled (NRZ-L) format by

$$\begin{aligned} 0 &\mapsto -1 \\ 1 &\mapsto +1 \end{aligned}$$

The coded NRZ-L bit stream is split into two, with even-numbered bits to be sent through the in-phase (I) channel and odd-numbered bits through the quadrature (Q) channel. On each channel, the coded bit has a duration that is twice of the source bit duration because of the split of coded bit stream. It is referred to as the symbol duration, $T_{sym} = 2T_b$, since a QPSK symbol represents two bits, one from each channel.

In the receiver, the decoding is performed after demodulation and data detection, rendering the following recursive relationship between coded and source bits.

$$b_k = \overline{B_k \oplus B_{k-2}} \oplus b_{k-1}, \qquad k \in N$$

Waveform Generation

The generation of baseband FQPSK signal in the internal software transmitter is based upon a method of performing a symbol-by-symbol cross-correlative mapping on selected I- and Q-channel symbols with a specific set of full-symbol waveforms (wavelets) [4]. To generate FQPSK-B signal requires additional filtering of the FQPSK signal. In the internal software transmitter, a low-pass filter is provided on each of the I- and Q-channel to serve as the transmission filter. The type of this filter and its order and cut-off frequency are user-specified parameters.

Modulation and Demodulation

The internal software transmitter can generate both baseband and modulated FQPSK-B signals. According to [3], the Q-channel signal is delayed with respect to the I-channel signal by one source bit, or equivalently a half symbol, resulting in a wavelet-coded baseband OQPSK signal which can be put onto a carrier to produce a modulated FQPSK-B signals at a user-specified frequency. The mapping between a transmitted symbol and the resultant phase is as follows:

I - channel Symbol	Q - channel Symbol	Corresponding Symbol Phase
+1	+1	45°
-1	+1	135°
-1	–1	225°
+1	–1	315°

In addition, the transmitter is capable of emulating an imperfect phase modulator with user-specified modulator imbalances defined in the following equation [5]

$$S(t) = [w_1(t) + a_1]\cos(2\pi f_c t + \theta_c) + G[w_2(t) + a_2]\sin(2\pi f_c t + \theta_c + \Delta\theta)$$

where G is the inter-channel amplitude imbalance, $\Delta\theta$ is the inter-channel phase imbalance, and a_1 and a_2 are I-channel and Q-channel dc biases, respectively. In this modulator imbalance model $w_1(t)$ and $w_2(t)$ represent I-channel and Q-channel signals, f_c is the carrier frequency, and θ_c is a random carrier phase.

On the receiver side, coherent demodulation requires a carrier reference established from the received signal. In particular, the carrier frequency f_c has to be estimated and the carrier phase θ_c has to be continuously tracked. The procedure to get an initial estimate of the carrier frequency and phase is referred to as carrier acquisition. It is done by first creating the carrier components from the received FQPSK-B signal with a full-wave, 4th-law detector [6], and then performing a discrete Fourier transform (DFT) on the detector output to have its frequency domain representation. A simple interpolation on the value of the peak bin around four times the fundamental (carrier) frequency and two values from adjacent bins on both sides of the peak bin produces the estimated frequency and phase.

The tracking of carrier phase is provided by a carrier tracking loop, as shown in Fig. 2, which results from a slight modification of a conventional QPSK cross-over Costas loop [7] by adding a half-symbol delay to its I-arm to compensate for the offset introduced between I- and Q-channel. Immediately after the carrier is acquired, carrier tracking commences with an initialization of the loop's numerically controlled oscillator (NCO) by using the estimated carrier frequency and phase. There are two user-specified low-pass arm filters serving as the detection filters for processing of the FQPSK-B signal. The loop filter implemented is a discrete-time low-pass filter with the following transfer function [8]

$$F(z) = G_1 + \frac{G_2}{1 - z^{-1}} + \frac{G_3}{\left(1 - z^{-1}\right)^2}$$

where

$$G_1 = rd/T_u$$

$$G_2 = rd^2/T_u$$

$$G_3 = k\,rd^3/T_u$$

and

$$d = \frac{4B_L T_u (r - k)}{r(r - k + 1)}$$

with T_u being the loop update interval in seconds, B_L being the loop bandwidth[2] in Hz, $r = 4\xi^2$ where ξ is the damping ratio, and k being the type III loop gain (e.g., $k = 0$ for a type II loop) with typical values ranging from 0.25 to 0.5. By specifying these parameters, a tracking loop with desired loop bandwidth can be exactly realized.

Coherent Detection

The software receiver performs coherent symbol-by-symbol hard decision separately on demodulated I-channel and Q-channel symbols. As shown in Fig. 2, this is done by sampling the detection filter output at proper times, presumably once at the mid-point of every symbol. Hence,

[2] This is the loop bandwidth by design. The actual loop bandwidth may be larger than this designed value depending on the product $B_L T_u$. Generally speaking, for $B_L T_u < 0.05$, the actual loop bandwidth is very close to the designed value.

the symbol clock epochs need to be established from the received signal, which is referred to as symbol synchronization. The software receiver uses a data transition tracking loop (DTTL) [9] to provide the estimated symbol timing. It takes the I-arm detection filter output as the input to its two-arm structure, with a full-symbol integration on a symbol and another full- or partial symbol integration centered at the symbol boundary. The latter provides an error signal to drive the estimated clock moving forwards or backwards when the integration window is not exactly centered at a symbol transition. The resulting I-channel symbol clock is at the mid-point of every Q-channel symbol because of the half-symbol inter-channel delay in the FQPSKB signal. It also enables mid-point sampling of I-channel symbols since they get an additional half-symbol delay in the receiver.

SYSTEM OPERATION

The software receiver is composed of four different set-ups, each being represented by an operating mode in which specific application of the software receiver is addressed with its own configuration. This section provides a description of these four operation modes, namely the receiver mode, the EVM mode, and internal end-to-end BER and EVM modes.

The Receiver Mode

This is the mode in which the software receiver functions as an offline coherent receiver that demodulates, detects, and decodes the received signal. In this mode the receiver accepts input from external source without using either of its internal software transmitters. Depending upon whether the recorded input is on a carrier, the operator can turn on or off the carrier acquisition and tracking subsystems. Other receiver parameters the operator can specify include

- data (bit) rate,
- window, DFT size, and zero-padding (if used) for DFT-based carrier acquisition,
- type, order, and BT_b-product of the detection filters,
- order, damping ratio, update interval, and loop bandwidth for carrier tracking loop,
- order, damping ratio, update interval, and loop bandwidth for symbol tracking loop.

During the real-time processing, the operator can monitor the progress by looking at a sample counter showing the number of samples being processed so far, and the tracking performance by bringing up the plots of residual phase and tracking variance versus time for carrier and/or symbol tracking. Besides these real-time indicators, the receiver will store the following data:

- detected soft I-channel and Q-channel samples (I/Q not aligned),
- detected soft I-channel and Q-channel samples (I/Q aligned),
- decoded bits,

into separate files for post processing. The detected I/Q-channel samples are the samples obtained by sampling the demodulated I/Q signal at the estimated symbol clock epochs provided by the symbol tracking. They are ‘soft’ since they are not passed through the hard decision yet. These sample files can be used to plot phasor diagrams for demodulated symbols before or after the one-bit I/Q-channel offset is removed. The decoded bit stream is the primary product of this mode. BER calculation can be performed on it if the transmitted bit stream is available for comparison, which requires a correlative matching process between the decoded and the source bit streams in the post processing to make them aligned.

The EVM Mode

This is the mode for hardware transmitter validation in which the signal from external hardware transmitter is demodulated, detected, and compared to the reference signal from the internal *continuous-time domain* software transmitter. The resulting error vectors provide indication of hardware problems in the transmitter under test. The set-up for EVM is divided into two sides. The reference side is a baseband end-to-end simulation system using the continuous-time domain transmitter to generate baseband FQPSK-B signal from a given periodic source bit stream used also on the test unit side. This baseband signal is then filtered by the detection filter of the software receiver, producing output samples to be saved into a reference sample file for later comparison[3]. On the test unit side, the same software receiver used on the reference side coherently demodulates the recorded IF signal from the hardware transmitter under test, rendering a test sample file at its detection filter output. This test samples are aligned with the reference samples by performing a correlative matching process between them. The EVM takes place at ideal symbol clock epochs that are readily available from the reference side by simply counting samples in the reference sample file.

The operator is able to specify receiver parameters other than those of detection filter, which remain fixed for both sides of EVM set-up, and get real-time performance monitoring as in the receiver mode. Two data files containing entire I-channel and Q-channel samples after the one-bit I/Q-channel offset is removed will be saved for post processing.

The EVM is done in the post processing, in which a correlative matching is performed to align the I/Q-channel sample files with the reference sample files using either I-channel or Q-channel samples and the aligned files are sampled at ideal detection times established by a sample count on the reference side to get the detected symbols. A resulting EVM file will be created, from which EVM statistics, including mean and standard deviation on magnitude and phase for all error vectors and for error vectors associated with individual symbols, are calculated and the following plots:

- Constellation plot -- a plot of error vectors on the signal constellation
- Normalized plot -- a scatter plot of error vectors in the vector space
- I/Q-channel magnitude errors vs. time

can be produced. In addition to EVM statistics and plots, phasor diagram (only with I/Q samples aligned) is also available in the post processing,

The Internal BER Mode

This is the mode for internal BER test in which the software transmitter-receiver pair functions as an end-to-end simulation system conducting BER test under a set of user-specified conditions. It differs from the receiver mode in the choice of signal source. In this mode, the internal discrete-time domain software transmitter is used to provide FQPSK-B signal either on a carrier or on baseband. A channel model is included in this end-to-end system. Currently, only an AWGN channel with a user-specified bit signal-to-noise ratio (SNR), denoted by E_b/N_o, is provided. More sophisticated channel models, including frequency selective multiple-way fading channel, can be easily added later.

---

[3] Getting a valid comparison requires the reference sample file to be generated by the internal software transmitter with parameters matching those used in the hardware transmitter under test. In addition, the detection filter has to be specified for this and will also be used on the reference side.

The operator can specify transmitter parameters such as

- data (bit) rate -- may include an offset,
- carrier frequency -- may include an offset,
- carrier phase,
- type, order, and BT_b-product of the transmission filters,
- source bit stream from a file or a noise seed if internal binary random number generator is used to generate source bit stream,

the channel parameter, E_b/N_o, and the receiver parameters such as

- data (bit) rate,
- window, DFT size, and zero-padding (if used) for DFT-based carrier acquisition,
- type, order, and BT_b-product of the detection filters,
- order, damping ratio, update interval, and loop bandwidth for carrier tracking loop,
- order, damping ratio, update interval, and loop bandwidth for symbol tracking loop.

Furthermore, the discrete-time domain transmitter is capable of accommodating modulator imbalances such as inter-channel amplitude and phase imbalances and I- and Q-channel dc biases, which allows the effect of modulator imbalances to be included with an end-to-end simulation.

The operation in this mode is all real-time. As in previous two modes, an operator can get real-time performance monitoring, including a BER counter showing coded and uncoded error performance.

The Internal EVM Mode

This is the mode for internal EVM test in which two software transmitter-receiver pairs form an end-to-end simulation system conducting EVM test under a set of user-specified conditions. Like the EVM test for external hardware transmitters, the two software transmitter-receiver pairs in the internal EVM test set-up constitute two sides: one for the reference and the other for the test unit. However, in this internal mode, the discrete-time domain software transmitter provides both the baseband signal for the reference side and the modulated signal for the test unit side. Both sides are synchronized so that EVM calculation can be performed in real-time without the need of a post-processing correlation to align signals from both sides. This set-up is intended for simulations to see the effect of (i) user-specified modulator imbalances added to the test unit, (ii) mismatched transmission filters, and (iii) receiver's demodulation and synchronization processing on the EVM results. An operator is able to monitor real-time performance, including selected EVM plots, with EVM statistics reported at the end of simulation.

EXAMPLE – THE BIT ERROR PERFORMANCE

This example shows the bit error performance for a baseband end-to-end system operated in the internal BER mode. Both coded and uncoded BER curves are shown here for bit SNR, E_b/N_o, from –3 to 10 dB. The uncoded BER curve agrees well with the one reported in [10]. As shown here, the degradation caused by differential encoding/decoding is

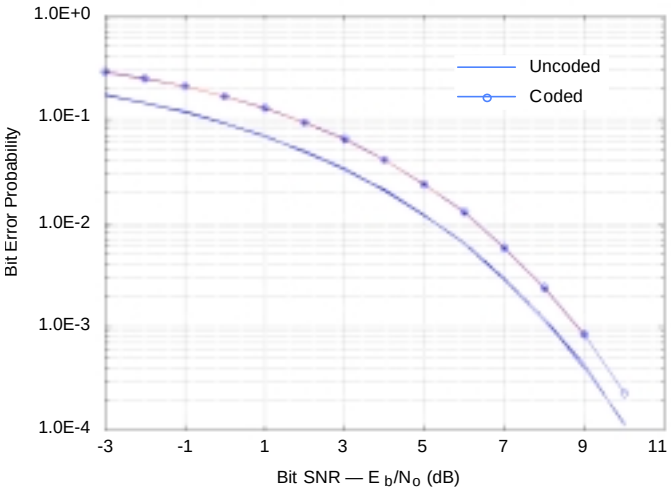

about 0.63 dB at BER=0.001. Simulation results obtained for systems including carrier and symbol tracking show no significant differences compared to these baseband curves, as long as sufficient loop SNRs are maintained.

EXAMPLE – The EVM Test

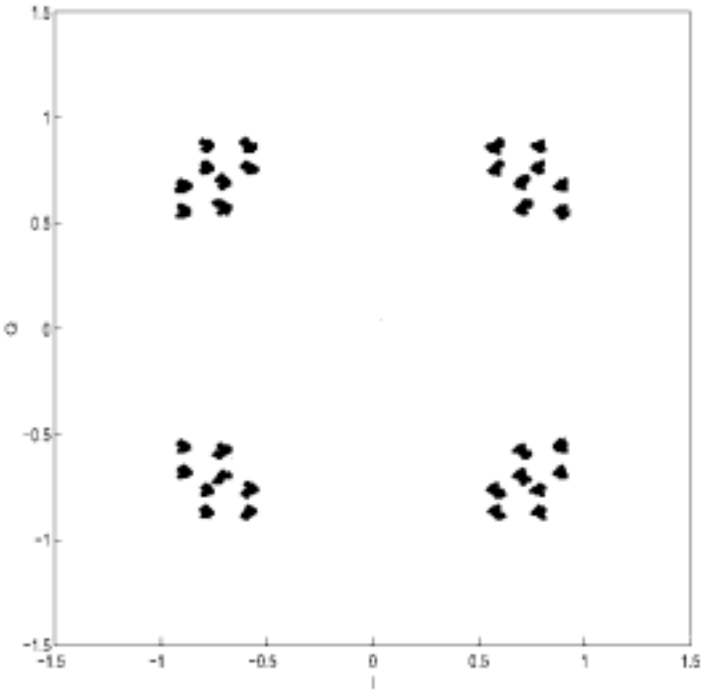

This example shows the results of an internal EVM test. The phasor diagram to the right is a constellation plot of the perfectly detected (reference) symbols from the receiver after the one-bit I/Q-channel offset is removed. In each quadrant, the corresponding FQPSK-B symbols form a distinct eight-cluster pattern. In the test unit, an amplitude imbalance is deliberately introduced to the Q-channel, making the amplitude of Q-channel symbols 5% smaller than that of I-channel symbols. After demodulation and detection, the error vectors are calculated by comparing both symbol streams symbol by symbol. In the following, two EVM plots are presented as an example. The constellation plot is the figure to the left in which each error vector is represented by an arrow pointing out from its corresponding reference symbol in the phasor diagram, while the normalized plot is the figure to the right that shows a scatter plot of end point of each error vector in a vector space. It is clearly indicated in these EVM plots that the amplitude imbalance exists in the transmitter under test by showing most arrows pointing roughly along the Q-channel direction in the constellation plot and a two-cluster distribution with an average separation approximately equal to 0.04 in the normalized plot.

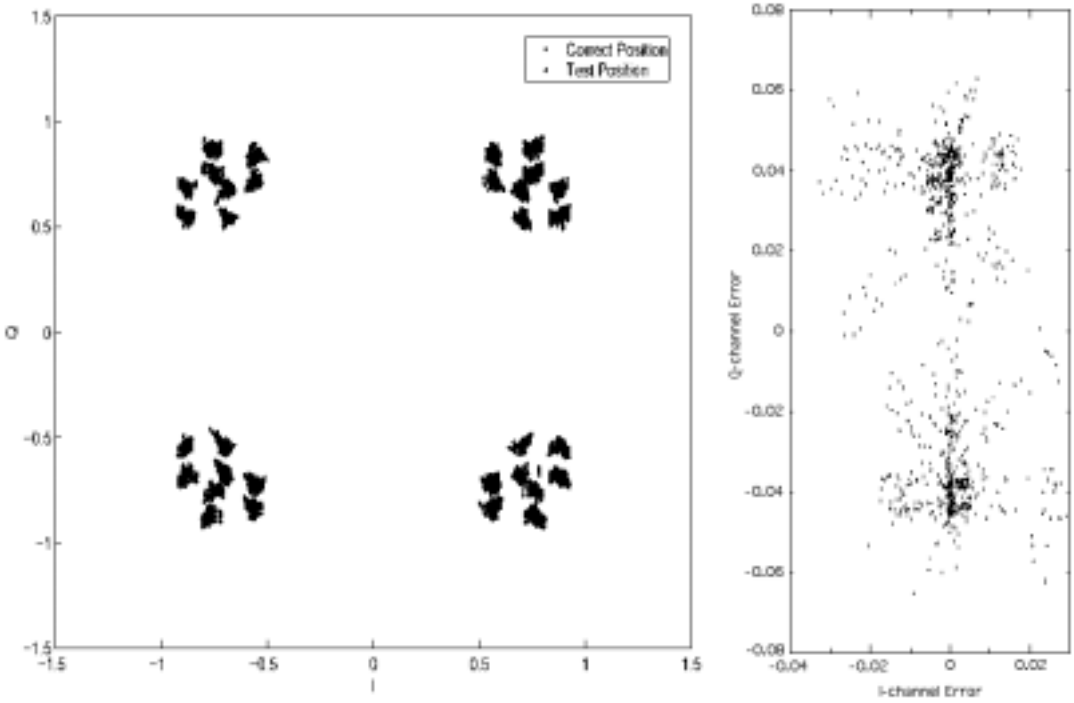

CONCLUSION

This paper presents the design and development of an off-line coherent FQPSK-B software reference receiver capable of being used for hardware validation and for advance technology development and demonstration. This Matlab/Simulink-based software receiver also includes end-to-end simulations that help a system design to meet certain performance goals. Because of its ease of use and versatility in flexible configurations for various tasks and even for other types of QPSK modulation, this software receiver provides a cost-effective approach with cross-platform compatibility for study, design and development of a quadrature-modulated communication system.

Currently, the software receiver is being modified to accommodate future studies include a frequency selective dynamic fading channel model and various equalizer techniques for mitigating the mobile fading effects.

REFERENCES

[1] K. Feher et al.: US Patents 4,567,602; 4,644,565; 5,491,457; and 5,784,402, post-patent improvements and other U.S. and international patents pending.

[2] "FQPSK-B, Revision A1," Digcom-Feher Patented Technology Transfer Document, Digcom Inc., January 15, 1999.

[3] "IRIG Standard 106-00: Telemetry Standards," Telemetry Group, Range Commanders Council, U.S. Army White Sands Missile Range, New Mexico, January 2000.

[4] M. K. Simon and T.-Y. Yan, "Cross-correlated Trellis Coded Quadrature Modulation," U.S. patents pending.

[5] H. Tsou, "The Combined Effect of Modulator Imbalances and Amplifier Nonlinearity on the Performance of Offset Quadrature-Phase-Shift-Keyed (OQPSK) Systems," *The TMO Progress Report 42-137*, Jet Propulsion Laboratory, Pasadena, California, May 15, 1999.

[6] W. B. Davenport, Jr. and W. L. Root, *An Introduction to the theory of Random Signals and Noise*, McGraw-Hill, New York, 1958.

[7] M. K. Simon, "On the Optimality of the MAP estimation Loop for Carrier Phase Tracking BPSK and QPSK Signals," *IEEE Trans. on Communications*, vol. COM-27, No. 1, January 1979.

[8] A. Blanchard, *Phase-Locked Loops: Application to Coherent Receiver Design*, John Wiley & Sons, Inc., New York, 1976.

[9] W. C. Lindsey and M. K. Simon, *Telecommunication Systems Engineering*, Prentice-Hall, Englewood Cliffs, New Jersey, 1973.

[10] T.-Y. Yan, *Advanced Range Telemetry Task Interim Report*, Jet Propulsion Laboratory, Pasadena, California, February 1999.

IRIG FQPSK-B STANDARDIZATION PROGRESS REPORT

Eugene L. Law
NAWCWD, Point Mugu, CA, USA

Abstract

This paper will provide an overview of the process used to develop the bandwidth efficient modulation sections of the Inter-Range Instrumentation Group (IRIG) standard[1]. The modulation method selected was Feher's patented quadrature phase shift keying (FQPSK-B)[2]. The important characteristics of a bandwidth efficient modulation method for aeronautical telemetry will be presented first followed by a summary of the results of the research, laboratory test, and flight test efforts. Future plans will then be summarized followed by the FQPSK-B sections of the current IRIG Telemetry Standard (the standard is available online at: http://tecnet0.jcte.jcs.mil/RCC/oldoc.htm).

Introduction

Telemetry data rates are increasing rapidly. At the same time, the total amount of available spectrum has decreased slowly. Therefore, the aeronautical telemetry community has been investigating modulation methods with more bandwidth efficiency than the commonly used non-return-to-zero level (NRZ-L) pulse code modulation/frequency modulation (PCM/FM)[1,3]. This paper will provide an overview of the efforts to develop a standard modulation method that will allow telemetry designers to pack more users/data into the available spectrum.

Important Characteristics

The important characteristics of a bandwidth efficient modulation method for aeronautical telemetry applications include:

- Bandwidth (99% and -25 dBm) and required pre-transmission filtering
- Bit error probability (BEP) vs. E_b/N_0 (signal energy per bit to noise power spectral density); 10^{-5} BEP or better is a common requirement
- Effect of non-linearities in transmitter and/or receiver (phase and amplitude)
- Adjacent channel interference, general interference performance
- Performance during multipath fading (frequency selective and flat)
- Recovery from multipath fading (frequency selective and flat)
- Data coding (level or differential)
- Effect of link dropouts (including reacquisition)
- Compatibility with existing equipment including tracking antennas, receivers, diversity combiners, etc.
- Power conversion efficiency (DC to RF)
- Cost, volume

Research

The initial phase included performing literature searches, funding investigative studies, and having discussions with various people working in the communications field. The Advanced Range

Telemetry (ARTM) program and the Telemetry Group of the Range Commanders Council sponsored the studies. Not surprisingly, several other projects were conducting similar studies at virtually the same time. One study that was ongoing at about the same time was by the space telemetry community[4]. The aeronautical telemetry and space telemetry studies both came to the conclusion that the two leading candidates were FQPSK-B and Gaussian minimum shift keying (GMSK). FQPSK-B hardware was available for both laboratory and flight testing but to date GMSK hardware (BT_b=0.2) with spectral efficiencies equal to FQPSK-B is not available for flight testing to the best of my knowledge. FQPSK-B is a variation of offset quadrature phase shift keying (OQPSK) with the in-phase (I) and quadrature (Q) waveforms selected such that $\sqrt{I^2+Q^2}$ is nearly constant[2].

Laboratory Testing

A variety of laboratory tests were performed at both the Naval Air Warfare Center Weapons Division and the Air Force Flight Test Center. The FQPSK-B hardware was at fixed bit rates of 1, 5, and 14.7 Mb/s. The FQPSK-B hardware performed well in the laboratory tests[5,6]. Summaries of the results of these tests for the characteristics of interest are:

Bandwidth: FQPSK-B 99% bandwidth is about 2/3 of that of optimum filtered NRZ PCM/FM; FQPSK-B –60 dBc and –25 dBm bandwidths are about ½ of that of optimum filtered NRZ PCM/FM

BEP vs E_b/N_0: FQPSK-B may require slightly higher E_b/N_0 than optimum PCM/FM for a 10^{-6} BEP but lower E_b/N_0 than non-optimum PCM/FM; FQPSK-B will require lower E_b/N_0 than optimum PCM/FM for a 10^{-3} BEP.

NLA effects: No significant differences observed.

ACI: FQPSK-B allows 2 transmitters of same bit rate to be packed about ½ as far apart as optimum NRZ PCM/FM, new FQPSK-B demodulators being developed under ARTM contract may allow even closer packing.

Multipath: FQPSK-B is slightly more sensitive to multipath fading than optimum NRZ PCM/FM but FQPSK-B is sensitive over a narrower frequency range so the net performance is similar. The FQPSK-B demodulator recovery time is acceptable as long as the demodulator loop bandwidth is a few kHz (this area needs more investigation).

Data coding: PCM/FM does not have a polarity ambiguity problem while FQPSK-B requires some method to solve the polarity ambiguity problems inherent in OQPSK. Differential encoding was selected as the method to solve polarity ambiguity. The purpose of the differential encoder/decoder is to resolve the phase ambiguities that are inherent in QPSK, OQPSK, and FQPSK-B modulation methods. The differential encoder/decoder used in this standard will cause one isolated symbol error to appear as two bits in error at the demodulator output. However, many aeronautical telemetry channels are dominated by fairly long burst error events and the effect of the differential encoder/decoder will often be masked by error bursts.

Link dropouts: The recovery time is acceptable as long as the demodulator loop bandwidth is a few kHz (this area needs more investigation).

Compatibility: FQPSK-B has been compatible with virtually all existing equipment with which it has been tried. The only exception is receivers with excessive phase noise.

The only problems encountered in laboratory testing with FQPSK-B were an increased susceptibility to phase noise and long acquisition and re-acquisition times with narrow demodulator loop bandwidths. One potential advantage of FQPSK-B is the ability to change bit rates without adjusting filter bandwidths or voltage levels as one has to with current PCM/FM transmitters.

Flight Testing

Flight tests were conducted at Edwards AFB, CA using a T-39 aircraft as the test platform. FQPSK-B and NRZ-L PCM/FM signals were radiated simultaneously as the aircraft flew around the test range. Tests were conducted with bit rates of 1, 5, and 14.7 Mb/s. At bit rates of 1 and 5 Mb/s the overall performance of both links was similar. Figure 1 shows the link availability[7] for portions of the 14.7 Mb/s flight. Link availability is basically the ratio of the number of seconds where the bit error probability is 10^{-5} or less to the total number of seconds. The points in the upper right hand corner show regions where multipath was the dominant source of errors and the points on the left hand side of the plot show regions where thermal noise was the dominant source of errors (low E_b/N_0 regions). FQPSK-B performed better than PCM/FM in both regions. The reasons are thought to be that the narrower bandwidth of FQPSK-B resulted in multipath affecting the data quality for a shorter time interval and that FQPSK-B has lower BEPs at low SNRs than PCM/FM. Overall, FQPSK-B performed as well as or better than NRZ PCM/FM during the flight tests. The flight tests were conducted with the equipment in fairly benign operating conditions. FQPSK-B tests in high shock and vibration environments will be conducted after production FQPSK-B hardware is available.

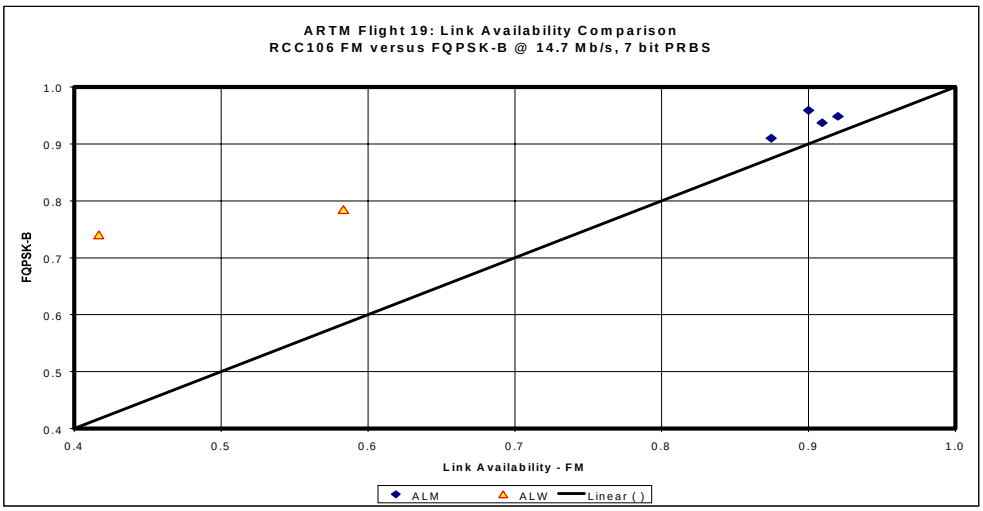

Notes:

1. Link operating condition designators:
   ALM – airborne, LOS, marginal SNR
   ALW – airborne, LOS, weak SNR
2. The two ALW points reflect conditions on the Edwards "racetrack" corridor @ 20k foot altitude. In each case the channel was dominated by thermal noise rather than multipath impairments. Under these conditions, the ARTM link availability definition breaks down and the FLA numbers will migrate towards zero as measurement period length increases. The points are posted here to illustrate the dramatic impact of low EIRP coupled with relatively large signal bandwidth.

Figure 1. FQPSK-B and NRZ-L PCM/FM link availability.

Future Plans

Production FQPSK-B transmitters and demodulators are being developed under ARTM contracts. Herley-Vega has the transmitter contract while RF Networks, L3-Microdyne, and L3-Aydin have demodulator contracts. Initial hardware deliveries are scheduled for mid-2000. A variety of laboratory and flight tests will be performed on this equipment. Edwards AFB is also in charge of a Small Business Innovative Research (SBIR) effort on bandwidth efficient modulation. The contract is in Phase II and initial hardware delivery is scheduled for early 2001. The contractor is Nova, Inc., Cincinnati, OH. Nova is developing a transmitter and receiver based on constant envelope, multi-h, continuous phase modulation. Computer simulations predict that the proposed modulation method will be 50% more bandwidth efficient than FQPSK-B with about the same BEP versus E_b/N_0 performance as FQPSK-B and NRZ PCM/FM.

Extracts from Telemetry Standards (IRIG 106-00) Chapter 2[1]

2.4.5 Modulation. The traditional modulation methods for aeronautical telemetry are frequency modulation and phase modulation. Frequency and phase modulation have a variety of desirable features but may not provide the required bandwidth efficiency especially for higher bit rates. When better bandwidth efficiency is required the standard method for digital signal transmission is FQPSK-B. FQPSK-B is nearly constant envelope and is compatible with non-linear amplifiers with minimal spectral regrowth and minimal degradation of detection efficiency. Additional FQPSK-B characteristics are discussed in section 7 of Appendix A.

2.4.5.1 Characteristics of FQPSK-B. FQPSK-B is described in the following Digcom Inc. document: "FQPSK-B, Revision A1 Digcom-Feher Patented Technology Transfer Document January 15, 1999". This document can be obtained under a license from:

Digcom Inc.
44685 Country Club Drive
El Macero, CA 95618
Telephone: 530-753-0738
FAX: 530-753-1788.

2.4.5.1.1 Differential encoding. Differential encoding shall be provided and shall be consistent with the following definitions. The NRZ-L data bit sequence $\{b_n\}$ is sampled periodically by the transmitter at time instants

$$t = nT_b \qquad n = 0,1,2,....$$

where T_b is the NRZ-L bit period. Using the bit index values n as references to the beginning of symbol periods, the differential encoder alternately assembles I channel and Q channel symbols to form the sequences

$$I_2, I_4, I_6, ...$$

and

$$Q_3, Q_5, Q_7, ...$$

according to the following rules:

$$I_{2n} = b_{2n} \oplus \overline{Q}_{(2n-1)} \qquad n > 0 \qquad (2\text{-}1)$$

$$Q_{(2n+1)} = b_{(2n+1)} \oplus I_{2n} \qquad n > 0 \qquad (2\text{-}2)$$

where $\oplus$ denotes the exclusive-or operator and the bar above a variable indicates the 'not' or inversion operator. Q channel symbols are offset (delayed) relative to I channel symbols by one bit period.

2.4.5.1.2 Data Randomization. The data input to the transmitter shall be randomized using either an encryptor which provides randomization or an IRIG 15-bit randomizer as described in Chapter 6 and Appendix D. The purpose of the randomizer is to prevent degenerative data patterns from degrading data quality.

2.4.5.1.3 Quadrature modulator phase map. Table 2-1 lists the mapping from the input to the modulator (after differential encoding and FQPSK-B wavelet assembly) to the carrier phase of the modulator output. The amplitudes in table 2-1 are ±a where "a" is a normalized amplitude.

TABLE 2-1. FQPSK-B PHASE MAP.

I Channel	Q Channel	Resultant Phase
a	**a**	**45 degrees**
-a	**a**	**135 degrees**
-a	**-a**	**225 degrees**
a	**-a**	**315 degrees**

2.4.5.1.4 Bit Rate. The bit rate range for FQPSK-B shall be between 1 Mb/s and 20 Mb/s.

2.4.5.1.5 Transmitter Phase Noise. The sum of all discrete spurious spectral components (single sideband) shall be less than -36 dBc. The continuous single sideband phase noise power spectral density (PSD) shall be below the curve shown in figure 2-1. The maximum frequency for the curve in figure 2-1 is one-fourth of the bit rate. For bit rates greater than 4 Mb/s, the phase noise PSD shall be less than –100 dBc/Hz between 1 MHz and one-fourth of the bit rate.

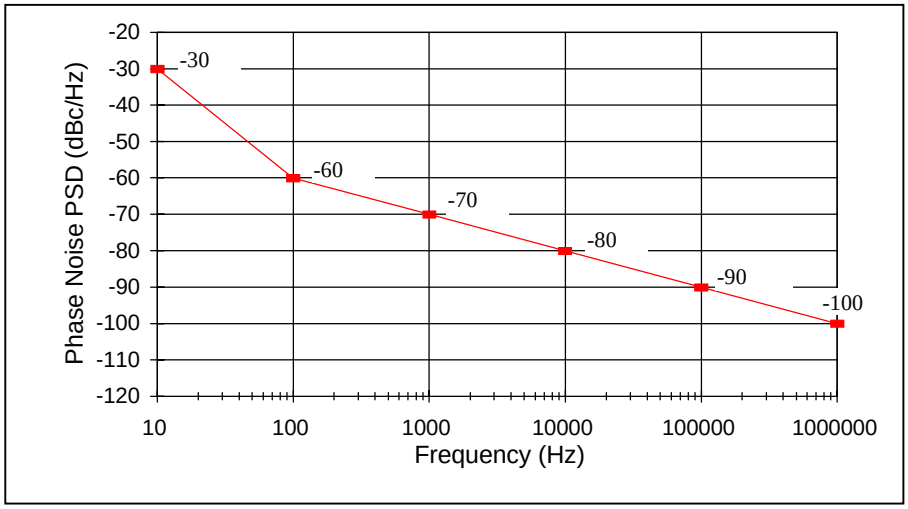

Figure 2-1. Continuous single sideband phase noise power spectral density.

2.4.5.1.6 Carrier Suppression. The remnant carrier level shall be no greater than -25 dBc. Paragraph 7.0 of Appendix A contains additional discussion of carrier suppression.

2.4.8 Modulated Transmitter Bandwidth[1] . Telemetry applications covered by this standard shall use 99 percent power bandwidth to define occupied bandwidth and -25 dBm bandwidth as the primary measure of spectral efficiency. The -25 dBm bandwidth is the minimum bandwidth which contains all spectral components which are -25 dBm or larger. A power level of -25 dBm is exactly equivalent to an attenuation of the transmitter power by $55 + 10\times\log(P)$ dB where P is the transmitter power expressed in watts. The spectra are assumed symmetrical about the transmitter's center frequency unless specified otherwise. All spectral components larger than $-(55 + 10\times\log(P))$ dBc at the transmitter output must be within the spectral mask calculated using the following equation:

$$M(f) = K + 90\log R - 100\log|f - f_c|; \qquad |f - f_c| \geq \frac{R}{m} \qquad (2\text{-}3)$$

where

$M(f)$ = power relative to P (i.e., units of dBc) at frequency f (MHz)
K = -20 for analog signals
K = -28 for binary signals;
K = -63 for quaternary signals (e.g., FQPSK-B)
f_c = transmitter center frequency (MHz)
R = bit rate (Mb/s) for digital signals or
$(\Delta f + f_{max})$ (MHz) for analog FM signals
m = number of states in modulating signal;
m = 2 for binary signals
m = 4 for quaternary signals and analog signals
Δ f = peak deviation
f_{max} = maximum modulation frequency

Note that the mask in this standard is different than and in general narrower than the mask contained in the 1996 and 1999 versions of the Telemetry Standards. Equation (2-3) does not apply to spectral components separated from the center frequency by less than *R/m*. The -25 dBm bandwidth is not required to be narrower than 1 MHz. Binary signals include all modulation signals with two states while quaternary signals include all modulation signals with four states (quadrature phase shift keying and FQPSK-B are two examples of four-state signals). Appendix A, paragraph 6.0 contains additional discussion and examples of this spectral mask.

2.5.3 Receiver Phase Noise. The sum of all discrete spurious spectral components (single sideband) shall be less than -39 dBc. The continuous single sideband phase noise power spectral density (PSD) shall be 3 dB below the curve shown in figure 2-1. The maximum frequency for the curve in figure 2-1 is one-fourth of the bit rate. For bit rates greater than 4 Mb/s, the phase noise PSD shall be less than –103 dBc/Hz between 1 MHz and one-fourth of the bit rate.

[1]These bandwidths are measured using a spectrum analyzer with the following settings: 10 kHz resolution bandwidth, 1 kHz video bandwidth, and max hold detector.

Selected Extracts from Telemetry Standards (IRIG 106-00) Appendix A[1]

From section 6.0 The first term in equation (A-9) *(equation A-9 is identical to equation 2-3)* accounts for bandwidth differences between modulation methods. Equation (A-9) can be rewritten as $M(f) = K - 10\log R - 100\log|(f-f_c)/R|$. When equation (A-9) is written this way, the $10\log R$ term accounts for the increased spectral spreading and decreased power per unit bandwidth as the modulation rate increases. The last term forces the spectral mask to roll off at 30 dB/octave (100 dB/decade). Any error detection or error correction bits, which are added to the data stream, are counted as bits for the purposes of this spectral mask. The quaternary signal spectral mask is based on the measured power spectrum of FQPSK-B. The binary signal spectral mask is primarily based on the power spectrum of a random binary NRZ PCM/FM signal with peak deviation equal to 0.35 times the bit rate and a multipole premodulation filter with a -3 dB frequency equal to 0.7 times the bit rate. The spectral mask includes the effects of reasonable component variations (unit-to-unit and temperature).

Figure A-9 shows the quaternary mask of equation (2-3) and the RF spectrum of a 1 Mb/s FQPSK-B signal. The transmitter power was assumed to be 10 watts in this example so the minimum value of the mask was –65 dBc. The peak value of the FQPSK-B signal was about −13 dBc.

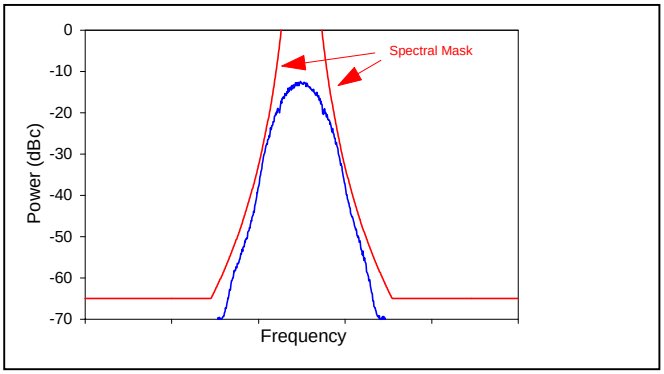

Figure A-9. Typical 1 Mb/s FQPSK-B signal and spectral mask.

Acknowledgment

The Advanced Range Telemetry (ARTM) Program and the member organizations of the Telemetry Group of the Range Commanders Council funded this effort.

Summary

Laboratory and flight tests of FQPSK-B have been conducted. The results of these tests indicate that FQPSK-B is a viable bandwidth efficient modulation method for aeronautical telemetry applications. The standard requires that data randomization and differential encoding be used when FQPSK-B is used in aeronautical telemetry applications. FQPSK-B is included in the 2000 edition of the IRIG Telemetry Standards (IRIG 106-00).

Keywords

FQPSK-B, PCM/FM, Telemetry Standards, spectral efficiency

References

1. Telemetry Group, Range Commanders Council: *Telemetry Standards.* IRIG Standard 106-00, Secretariat, Range Commanders Council, U.S. Army White Sands Missile Range, NM 88002-5110, January 2000, http://tecnet0.jcte.jcs.mil/RCC/manuals/106-00/ .

2. Feher et al. U.S. Patents: 4,567,602; 4,644,565; 5,491,457, 5,784,402; post-patent improvements and other U.S. and international patents pending; Digcom, Inc.; 44685 Country Club Drive; El Macero, CA 95618; USA; Tel. 530-753-0738; Fax 530-753-1788.

3. E. Law, D. Hust: *Telemetry Applications Handbook.* Technical publication #TP000044, Pacific Missile Test Center, Point Mugu, CA 93042, September 1987, also available as RCC document 119-88.

4. W. Martin, T. Yan, L. Lam: *CCSDS-SFCG Efficient Modulation Methods Study at NASA/JPL, Phase 3 End-to-End System Performance*, NASA/JPL SF17-28/D, September 1997.

5. E. Law, K. Feher: AFQPSK Versus PCM/FM for Aeronautical Telemetry Applications; Spectral Occupancy and Bit Error Probability Comparisons≅, Proceedings of the International Telemetering Conference, Las Vegas, October 27-30, 1997.

6. E.L. Law: "Robust, bandwidth efficient modulation methods for aeronautical telemetry applications; spectral occupancy, adjacent channel interference and bit error probability comparisons," Proceedings of the European Telemetry Conference, ETC'98, Garmisch-Partenkirchen, Germany, May 1998.

7. R. P. Jefferis: "Link availability and bit error clusters in aeronautical telemetry", Proceedings of the International Telemetering Conference, Las Vegas, October 26-28, 1999.

DESIGN AND PERFORMANCE OF A *FQPSK DEMODULATOR

Douglas C. O'Cull
L-3 Communications Microdyne
Ocala, Florida USA

ABSTRACT

This paper will discuss the design and performance of a Feher patented QPSK demodulator. This new demodulator also includes a built in bit sync with soft decision outputs. This paper will provide an overview on digital filtering used in the second IF filter which provides dynamic changing of the IF bandwidth.

INTRODUCTION

Many changes in today's telemetry environment have affected the use of standard range telemetry receivers. The most prevalent change is the increased data rate requirement for new telemetry missions. The increased data rate demand is requiring new modulation formats. However, legacy projects using low data rate methods will still have to be supported by range operation. Combine this with the decreasing spectrum issues and you have many issues to address. Most of these issues focus on the need to have a telemetry receiver that can be used for both high data rates (20 Mbps) and low data rates (10 kbps) applications. In addition the telemetry receiver will have to support multiple demodulation modes.

In the past designing a receiver that would support high and low data rates was difficult. Techniques used for high data rates required 70 MHz second IF Center Frequencies and Local Oscillators capable of tuning large ranges. These items made it difficult to build narrow filters and demodulators that would perform over many octaves of frequencies. Likewise, narrow band receivers used 20 MHz IF Center Frequencies which would not support wide IF filters. Today these challenges can be solved using digital sampling and filtering techniques.

The need for multi-mode demodulation can be solved using many of the digital techniques available through the advancement of function specific DSP technology. Demodulation mode can be controlled by on the fly programming of complex digital semiconductors. This enables demodulator design that can easily be re-configured and optimized for different modulation formats and rates.

DESIGN IMPLEMENTATION

The receiver design makes use of the latest digital signal processing IC's to facilitate a wide range of intended applications. This approach has merit in that it yields a "soft" radio that can be easily re-configured for changing applications. A block diagram of the receiver is shown below in Figure 1.

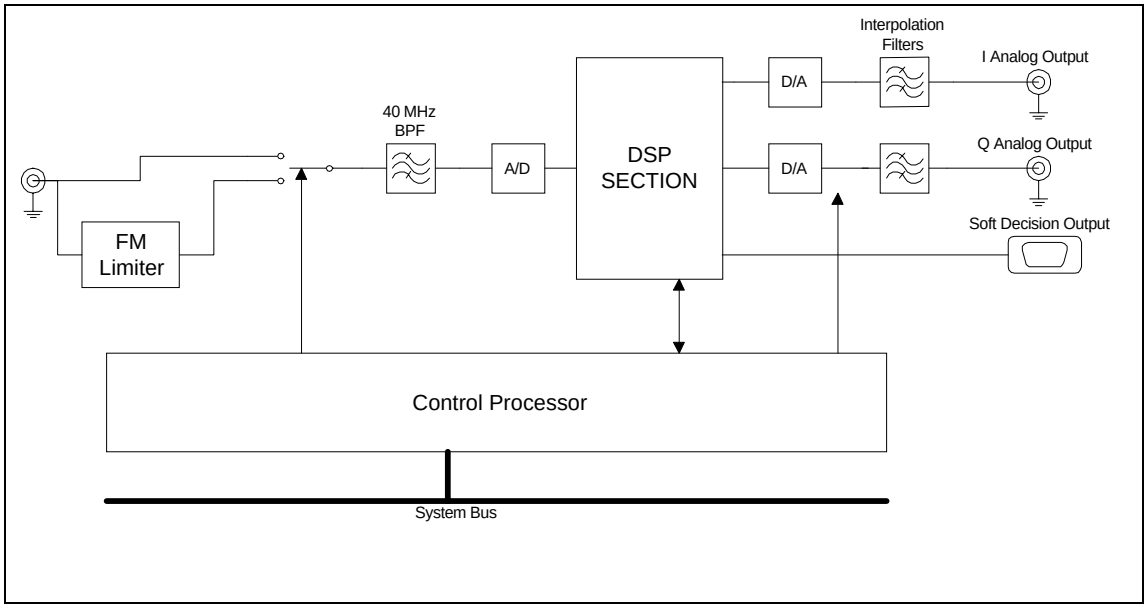

Figure 1 - Receiver Block Diagram

Input Sampling and Anti-Aliasing Filters

The input signal is centered at 70MHz and may be up to 20 MHz wide. The A/D converter has a 10-bit resolution. Wideband signals are sampled at 90 MHz while narrowband signals are sampled at 45 MHz. The distinction between wideband and narrowband is drawn from the partitioning of Digital Signal Processing (DSP) components and analog filters required for such a large range of signal bandwidths. There is some flexibility as to where the crossover occurs. As will be shown, the wideband-processing path is able to cover a range of bandwidths from 75 kHz to 20MHz. The narrowband-processing path is able to process signal bandwidths up to approximately 1 MHz and can easily handle the narrowest signal bandwidth of 10 kHz.

Alias Profile for 90 MHz Sampling

The sampling of the high bandwidth signals at 90 MHz creates replica's of the signal at multiples of the Nyquist (half the sampling) frequency as shown in Figure 2. The input signal is shown crosshatched. Any signals or noise below 45 MHz will alias back into the processing spectrum above 45 MHz. An analog anti-aliasing filter must be used to prevent these aliased components from interfering with the signal of interest.

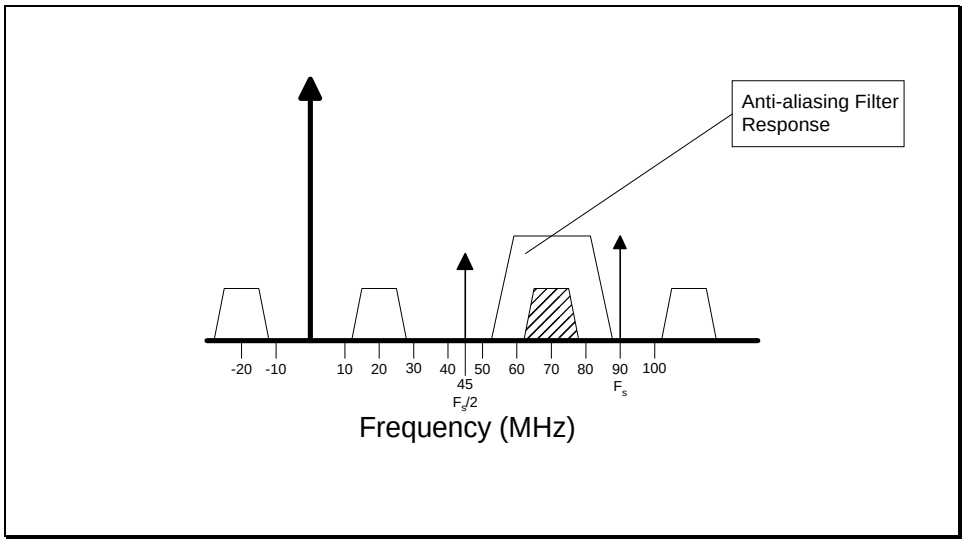

Figure 2 - Sampled Spectra and anti-aliasing filter for 90 MHz sampling

Design of the anti-aliasing filter is a compromise between minimizing group delay distortion (non-flat group delay) in the band of interest and controlling aliasing. Aliased components should be attenuated by 60 dB in the band of interest (50 to 90 MHz) in order to put them below the theoretical dynamic range of the 10-bit A/D (assuming equal spectral density). Signal components between 45 and 60 MHz will alias into the range between 30 and 45 MHz and therefore will not interfere with the band of interest. Signal components at 60 MHz and below will alias into the band of interest and therefore should be attenuated by at least 60 dB.

DSP Section

A block diagram of the DSP section is shown in Figure 3. The path through the Halfband Filter is for the wideband signals. The path through the Programmable Downconvertor is for the narrowband signals.

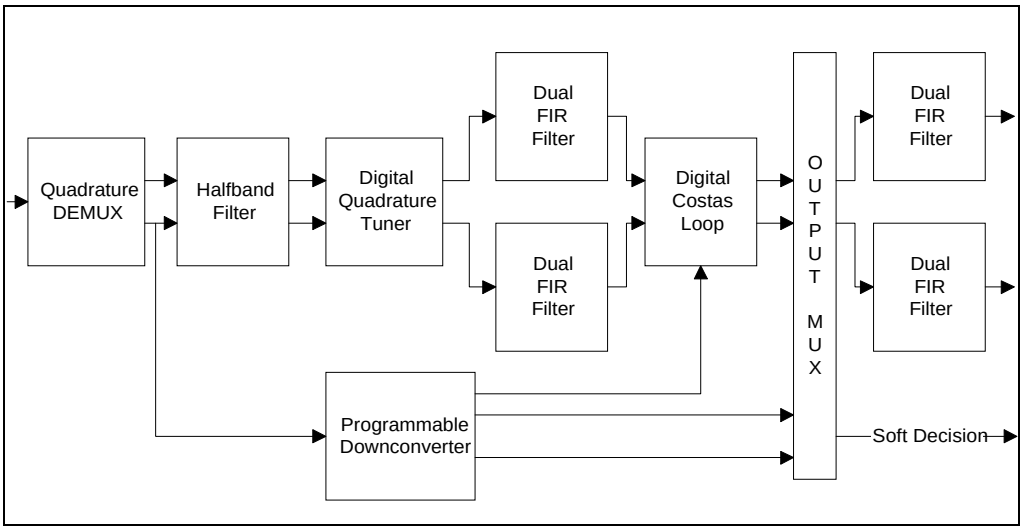

Figure 3 - DSP Section

WIDEBAND SIGNAL PROCESSING

The wideband path uses the Halfband Filter to perform the digital down conversion to a complex lowpass signal. The Halfband Filter also provides a filter which allows the sample rate to be decimated to half the input sample rate or 45 MHz. The quadrature demux logic externally de-multiplexes the two quadrature samples from the A/D and provides them to the Halfband Filter at the 45MHz rate.

The Halfband Filter shifts the spectrum by – Fs/4 (–22.5 MHz), which centers the signal just to the left of 0 Hz as shown in Figure 4. The Halfband Filter then provides real and imaginary components at the decimated sample rate of 45 MHz at the outputs. The Halfband filter removes the images created by decimation. Note that the bandwidth of the Halfband filter allows roughly 10 MHz of frequency uncertainty in either direction for the widest signal of interest.

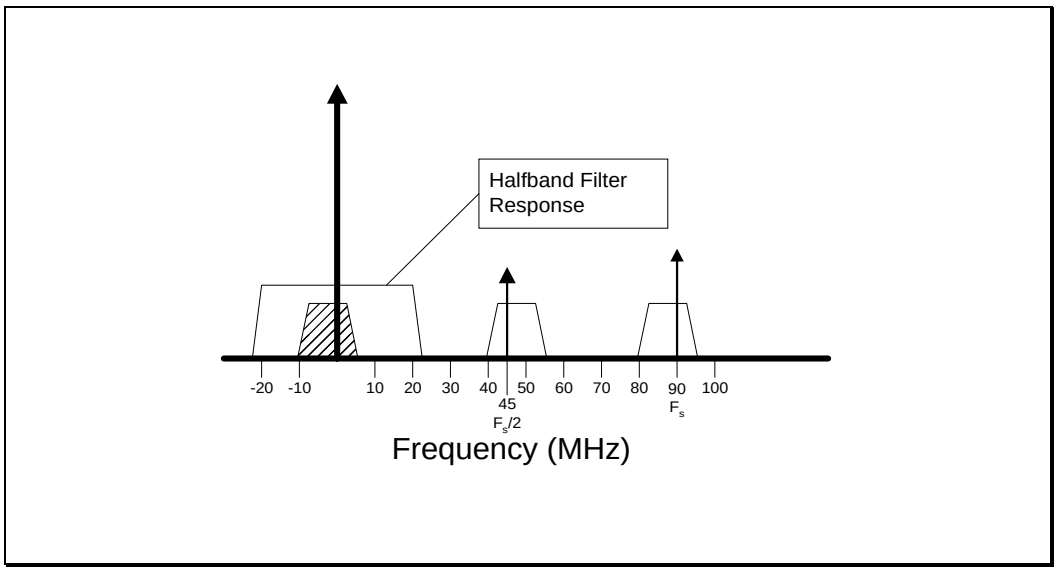

Figure 4 - Down Conversion by Halfband Filter

WIDEBAND CARRIER DEMODULATION

Wideband carrier demodulation is performed by the Digital Quadrature Tuner (DQT) and the Digital Costas Loop (DCL). These function specific DSPs form a digital version of the traditional second local oscillator/Costas loop phase coherent demodulator. The DQT is a digital equivalent of a tunable second local oscillator. The DCL receives a digital error word form the DCL and adjust the frequency of a numerical controller oscillator (NCO). This allows the demodulator to form a phase coherent carrier-tracking loop. This will be used for all phase coherent modulation formats such as PSK, BPSK and QPSK. For non-coherent application the DQT can be configured to a fixed frequency.

The Digital Costas Loop contains all the functional blocks of a traditional analog Costas loop. The quadrature signals are routed to quadrature mixers for carrier tracking. The output of the mix operation can be routed to programmable root raised cosine (RRC) filter for optimal

performance. Integrate and dump filters are also available. The outputs of the matched filters are routed to symbol tracking devices. This allows the demodulator to include a single channel variable bit synchronizer with soft decision outputs. The final output of the DCL provides both polar output and frequency discriminator outputs.

INTERPOLATION FILTERS

The dual FIR filter blocks shown after the output MUX in Figure 3 are used as interpolation (anti-imaging) filters for both the wideband and narrowband processing path. These interpolation filters allow a consistent output rate sample rate to be maintained at the output D/A Converters (DACs) over a wide range of decimation which, in turn, minimizes the number of analog interpolation filters required at the output of the DACs.

For the wideband processing path, the signals will be up-sampled to 45 MHz to allow a single analog interpolation filter to be used over the entire wideband range. The widest bandwidth signal required at the output is a 20 Mbps NRZ PCM signal where roughly 95% of the signal energy occurs below 20 MHz. Therefore, the analog interpolation filter should have its 3 dB cutoff at 20 MHz. The first sampling image will be centered at 45 MHz and have significant energy to 25 MHz (20 MHz below) for the 20 Mbps NRZ signal. The 20 MHz, 7 pole elliptical filter module has a stopband that is 50 dB down and a transition band of roughly 7 MHz. Most of the energy in the image would be attenuated by at least 60 dB.

PERFORMANCE

At the time of this writing, testing of this product is just beginning. Simulation and early performance estimates indicate that bit error rate (BER) performance will be within 1 dB of theoretical for both narrowband (10 kbps) and wideband (20 Mbps) applications. Full test data will be provided at the presentation of this paper or can be obtain by contacting the author.

CONCLUSION

The Microdyne FQD-7020 Demodulator and RCB-2000 Digital Receiver through the use of functional specific DSPs provides a robust solution for applications requiring both narrowband and wideband data applications. The use of digital techniques in filter and Costas loops allows the demodulator to be used for legacy product testing as well as testing of the latest state of the art products. These digital techniques allow the user to procure a single receiver for wideband and narrowband applications.

* Feher’s Patented QPSK licensed by Digcom, Inc.

FQPSK-B[1] PERFORMANCE IN AIR-TO-GROUND TELEMETRY

Robert P. Jefferis
TYBRIN Corporation
Edwards Air Force Base, California, USA

Abstract

Recent field tests validate the proposition that FQPSK-B modulation is a good candidate to replace two-level frequency modulation (FM) standards in many military air-to-ground test range applications. It provides improved spectral efficiency and power conversion efficiency comparable to FM transmitters. In addition, FQPSK-B links tested at 1, 5 and 15 megabits per second (Mb/s) have demonstrated link reliability comparable to FM systems. This paper presents FQPSK-B link reliability data acquired in flight tests conducted at Edwards Air Force Base, California, in 1998 and 1999. Multipath fading sensitivity data from laboratory tests are also presented.

Introduction

In 1996 a joint United States Army, Navy and Air Force project, the Advanced Range Telemetry project (ARTM)[2], began searching for practical modulation methods to improve spectral efficiency, reliability and utility of high bit rate, line-of-sight (LOS) air-to-ground telemetry links used in military aircraft and missile tests. The goal became a practical interim standard designed to stimulate orderly, reasonably priced migration of the DoD telemetry infrastructure to advanced telemetry techniques. By the end of 1997 a significant body of alternative studies, simulations and laboratory work identified FQPSK-B modulation [1] as a strong candidate [2,3]. This paper discusses recent field experience with FQPSK-B modulation, concentrating on link performance in real flight scenarios. Test methods are described and a specific definition of link reliability is presented. In the context of this definition, FQPSK-B performance is compared to that of benchmark PCM/FM[3] (FM) equipment [4]. Twenty hours of flight data from six T-39 jet aircraft sorties are represented.

Methodology

Considering the lack of reliable channel models for military test range channels and the difficulty of precise absolute link parameter measurements, the ARTM project concluded that meaningful evaluation of modulation techniques requires live side-by-side performance comparison against a standard, i.e., an A:B comparison method. This approach simplifies measurements and tends to minimize the number of uncontrolled test variables. Frequency modulation was the obvious choice for

[1] FQPSK-B is the acronym for “Feher’s Quadrature Phase Shift Keying”, type B [1]. Type B incorporates differential encoding.

[2] Sponsored by the United States Department of Defense (DoD) Central Test and Evaluation Investment Program.

[3] PCM/FM stands for pulse code modulation over frequency modulation as described in [4]. ARTM tests utilize fourth order Bessel baseband shaping filters with -3 dB cutoff frequency at 0.7 times bit rate. Modulation index is 0.7 in all cases.

comparison standard (system A) since it is the de facto standard in United States military flight tests. The method is illustrated in Figure 1. Two links are operated simultaneously, each transmitting the same maximal length pseudo-random binary sequence (PRBS) at the desired *bit* rate[4]. Standard, flight qualified FM transmitters are used with radio frequency (RF) power ratings ranging from 6 to 10 Watts. Flight qualified FQPSK-B transmitters are not available.

FIGURE 1 - BASIC MEASUREMENT SYSTEM

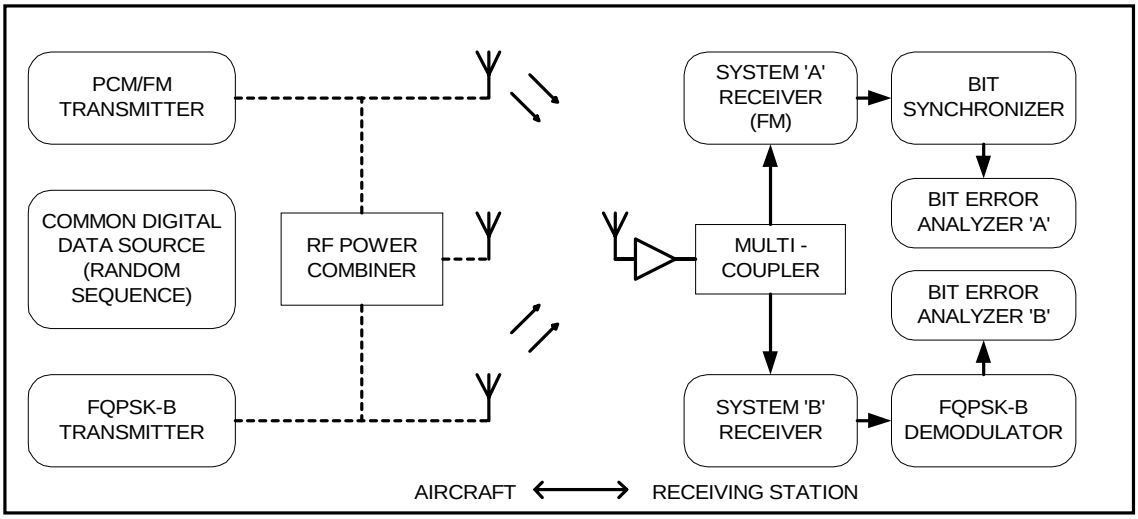

Commercial FQPSK-B modems[5] were modified to reduce vibration and temperature sensitivity and adjust detection loop bandwidth for this application. Modem output signals at an intermediate frequency (IF) of 70 megaHertz (MHz) are applied to an upconverter, a ten Watt linear amplifier (driven to full saturation for nonlinear operation) and a harmonic filter. A and B effective isotropic radiated power (EIRP) levels are equalized. A and B signals are transmitted at closely spaced carrier frequencies and are applied to similar antennas in close proximity to one another or to the same antenna via power combiner. System A and B signals are received with a single antenna[6] and a multicoupler routes RF signals to A and B receivers. FM receivers used are narrow band and wide bandwidth configurations of a receiver commonly used in DoD tests ranges[7]. The same receivers are used as downconverters for FQPSK-B signals. Auxiliary IF output signals are applied to the FQPSK-B demodulators which implement coherent, single symbol, hard-decision detection with differential decoding. Sophisticated bit error analyzers are connected to each system. These capture and *record* each and every bit error produced by both systems during a sortie. A and B bit error histories are correlated in time with Global Positioning System (GPS) timing markers imbedded in the bit error records. Postflight software analysis tools allow desired segments of flight data to be isolated and analyzed on a *bit-by-bit* basis. Ancillary measurements are recorded in the aircraft and in the receiving station to document aircraft position, aircraft orientation, time correlation

[4] All data presented here utilized a 2047 bit PRBS.
[5] Model 5450F, RF Networks Incorporated, Phoenix, Arizona.
[6] All tests utilized 2.4 and 4.6 meter parabolic reflector auto-tracking antennae.
[7] Model 700, Microdyne Corp., Ocala, Florida.

and channel conditions. Detailed discussion of these measurements and their implications is beyond the scope of this discussion.

A:B relative performance assessment relies primarily on bit error probability (BEP) and timing information. Bit error histories are used to calculate flight link availability (FLA) and error statistics. FLA is defined in [5]. It is an adaptation and extension of the concepts developed in [6]. Briefly, FLA is a normalized ratio:

$$FLA \equiv \frac{MP - \sum FS}{MP} \qquad (1)$$

MP is the measurement period or observation period in units of seconds. FS is a "failed second"[8]. FLA thus represents the amount of time in the MP that link BEP was better than 10^{-5} and is bound to the range [0,1]. FLA is cited in conjunction with an operating condition qualifier. Three course categories are used. Airborne, LOS, strong signal (ALS) denotes MP's associated with received carrier-to-noise ratio (CNR) high enough to consistently provide fade margins greater than 15 decibels (dB). Airborne, LOS, marginal signal (ALM) is assigned to records with fade margins in the range of 15 dB down to the CNR that would produce a thermal noise floor BEP of 10^{-8}. Airborne, LOS, weak signal (ALW) is assigned to data records where CNR is low enough to produce a BEP floor higher than 10^{-8}. Figure 2 introduces the graphic used to compare system performance. Ordered pairs [$FLA_{system\ A}$, $FLA_{system\ B}$] are cross-plotted. The diagonal line (unity slope and zero intercept) represents the line of equal performance. The collection of FLA data points superimposed on the point (1,1)

FIGURE 2 - LINK AVAILABILITY AT 1 Mb/s

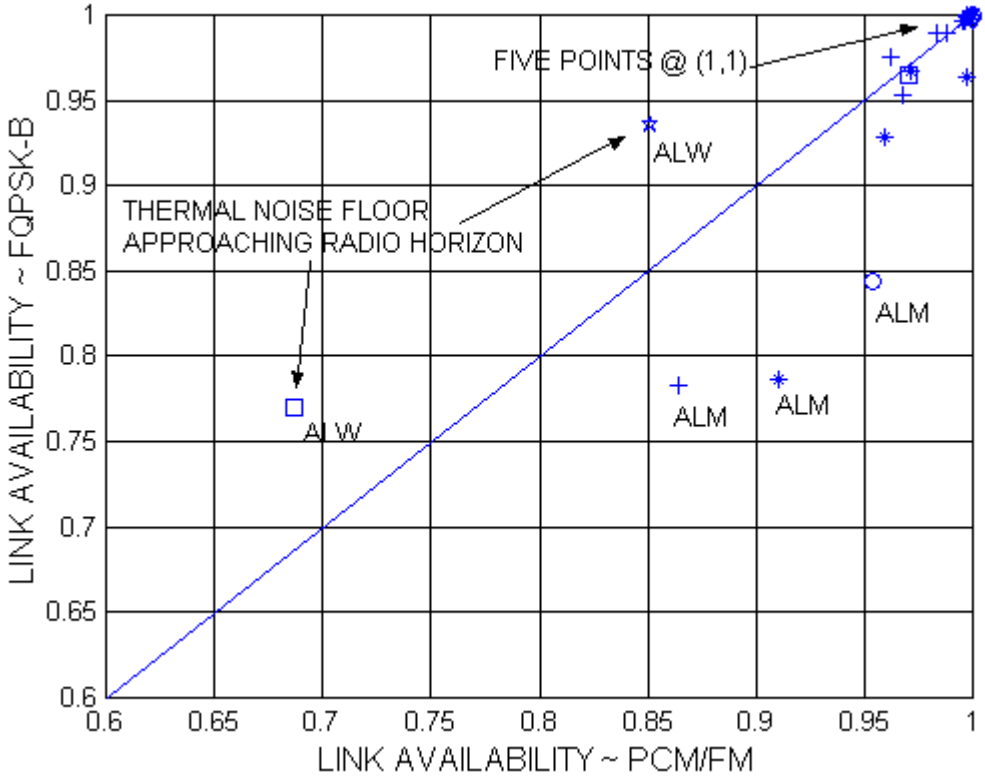

[8] A failed second is a one 1 second interval where measured BEP exceeds 10^{-5}.

represent 49 minutes of flight at altitudes[9] above three kilometers (km) and slant ranges[10] of 37 km to the radio horizon. These clearly show that under ALS and ALM conditions, in the absence of multipath fading or source antenna masking, both systems delivered error-free performance.

Flight Data

Figure 2 is the A:B FLA comparison from four sorties at 1 Mb/s. Approximately 8.3 hours of flight data are represented. Measurement periods range from 299 to 1440 seconds. Each different symbol represents a different flight corridor. All flight profiles are straight, level flight at constant pressure altitude and airspeed over a chosen terrain corridor. Airspeeds of 200 and 350 knots were used. Of particular interest are the points denoted with 'O' and '+' symbols. These flight profiles produce the largest number of multipath fade events because of low altitude, as low as 150 meters above ground level at a slant range of 93 km. Points associated with marginal signal strength are labeled ALM. Only three points indicate significant relative weakness in the FQPSK link. These are associated with marginal signal strength as well as severe multipath fading. Slow FQPSK-B system recovery from synchronization failures caused this degradation. Otherwise, these sorties show that the FQPSK-B link reliability is comparable to the FM system.

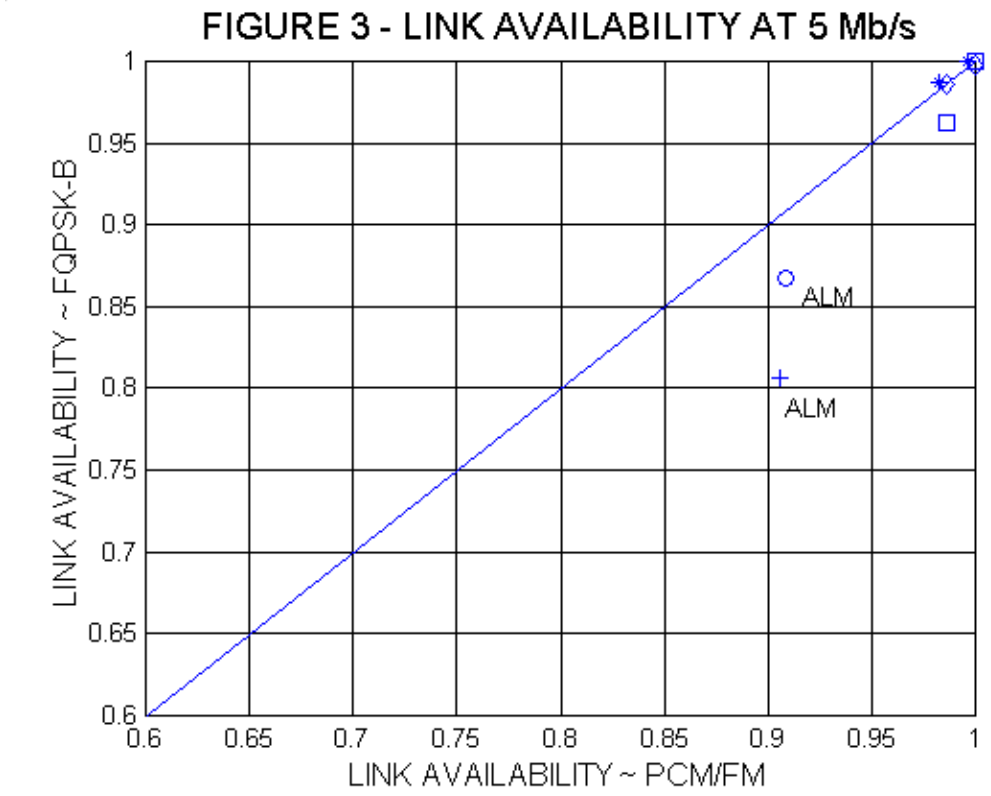

Figure 3 contains similar data from one sortie at 5 Mb/s. Again, the FQPSK-B link performance suffers under the same conditions as the 1 Mb/s data. In Figure 4, however, FQPSK demodulator loop bandwidth was increased and the 14.7 Mb/s

[9] Absolute or tapeline altitude above terrain level.
[10] Absolute straight line distance between transmit and receive antennae.

results are reversed. FQPSK performance is consistently better than the FM system. Another contributing factor to this FQPSK improvement is the fact that the FM

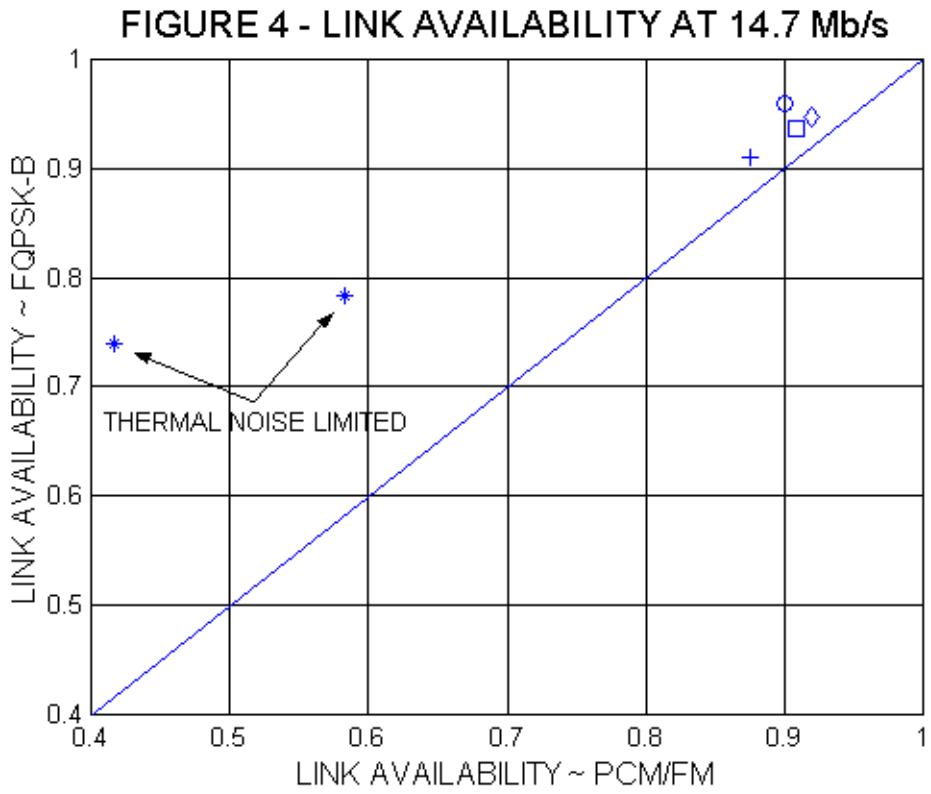

system bit synchronizer was operating near its rated bit rate limit and was less robust than at lower rates. At very low signal strength (ALW) thermal noise became a factor at slant ranges over 130 km. The two points noted as 'thermal noise limited' illustrate the coherent detection advantage in low CNR conditions. Ten to fifteen percent higher slant range capability has been noted in the FQPSK links under weak signal conditions.

Dispersive Fade Sensitivity

Most DoD telemetry links are designed to create and maintain ALS or ALM conditions. Recent channel sounding tests clearly indicate that dispersive fading (frequency selective) is the dominant channel impairment under these conditions [7]. From a practical standpoint, when high gain directional receiving antennae are used and the test vehicle is off the ground, then the following static channel impulse response model is useful [7]:

$$h(t) = \delta(t) + \sum_{k=1}^{K} \Gamma_k e^{j\gamma_k} \delta(t - \tau_k) \qquad (2)$$

δ is a unit impulse; the first term representing the LOS propagation path (ray). Γ is a real constant referred to as the reflection coefficient. γ is the phase difference between the LOS ray and ray k. τ (Tau) is the *difference* in transmit time between the LOS ray and ray k. In the frequency domain, the linear transfer function of equation (2) produces a series of nulls or notches in the channel spaced at 1/Tau Hertz intervals.

The absolute position of these notches is determined by γ. Notch depth is controlled by Γ.

A very high percentage of serious fade events can be modeled with K=1, i.e., a simple two-ray model. Sensitivity of data link performance to these events is strongly related to Γ and the *product* of bit rate R and Tau (RT). Figure 5 illustrates typical notch depth sensitivity of a wideband FM and FQPSK-B receiving system at two RT conditions. In this graph BEP is plotted against secondary ray path loss L in dB where:

$$L = 1/\Gamma \qquad (3)$$

At RT=0.1 the notch is wide relative to the main lobe of the modulated signals. Both systems exhibit a very steep depth sensitivity curve. At RT=1 the FM system is more sensitive to secondary ray power but still exhibits a steep, threshold-like characteristic.

FIGURE 5 ~ MULTIPATH DEPTH SENSITIVITY

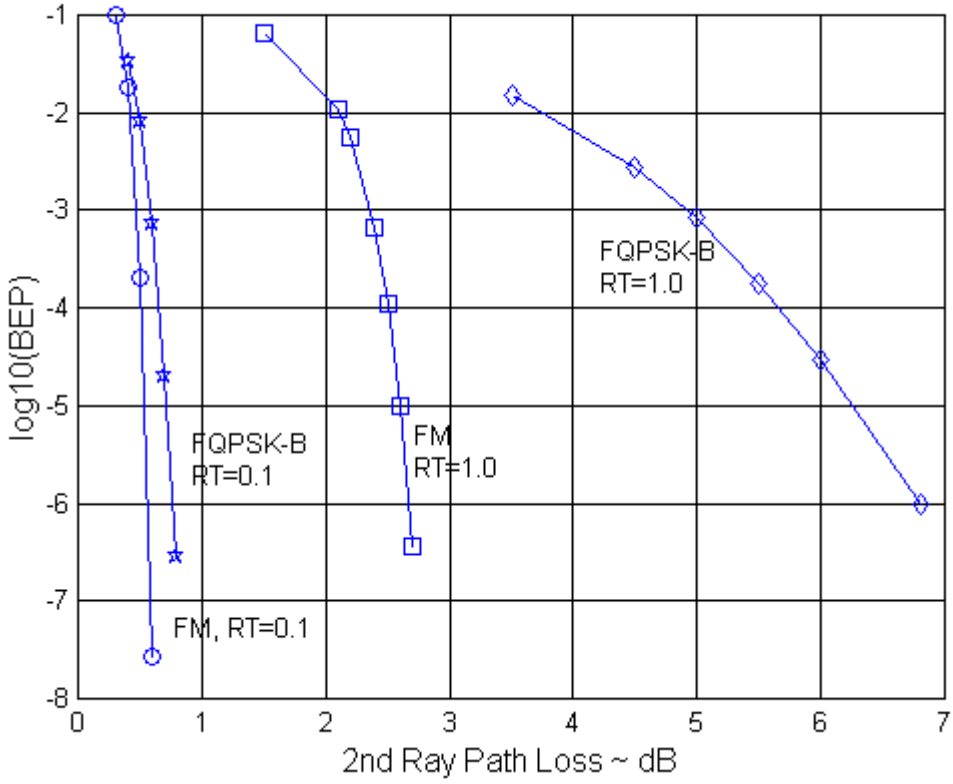

The FQPSK-B demodulator is even more sensitive (approximately 4 dB at BEP=10^{-6}) and there is no clear threshold. Flight test results over desert and mountainous terrain show that a very large number of short delay fade events (RT<0.05) are associated with low secondary ray path loss and both systems fail (loss of synchronization).

Figure 6 illustrates the *depth* of notch required to degrade BEP to 10^{-5} as RT varies (critical notch depth versus RT). Notch depth is expressed in dB relative to power in the LOS ray without channel impairment. At notch depths below or approaching critical, and RT values much smaller than about 0.1, fade induced passband gain slope, and group delay distortion become less significant factors in link degradation. As RT decreases to very small values, the fade becomes essentially 'flat' and absolute power loss becomes the dominant cause of bit errors and synchronization failures. In

this low RT range both systems perform approximately the same. As RT increases above 0.05, the notch depth sensitivity of both systems increases to some maximum value. In this example sensitivity levels off at approximately 12 and 10 dB for the FM and FQPSK-B system, respectively. It is important to note here that the results in Figures 5 and 6 include the effect of receiver and downconverter automatic gain control (AGC). Both systems are far more sensitive to these impairments if AGC is not used.

FIGURE 6 ~ MULTIPATH DELAY SENSITIVITY

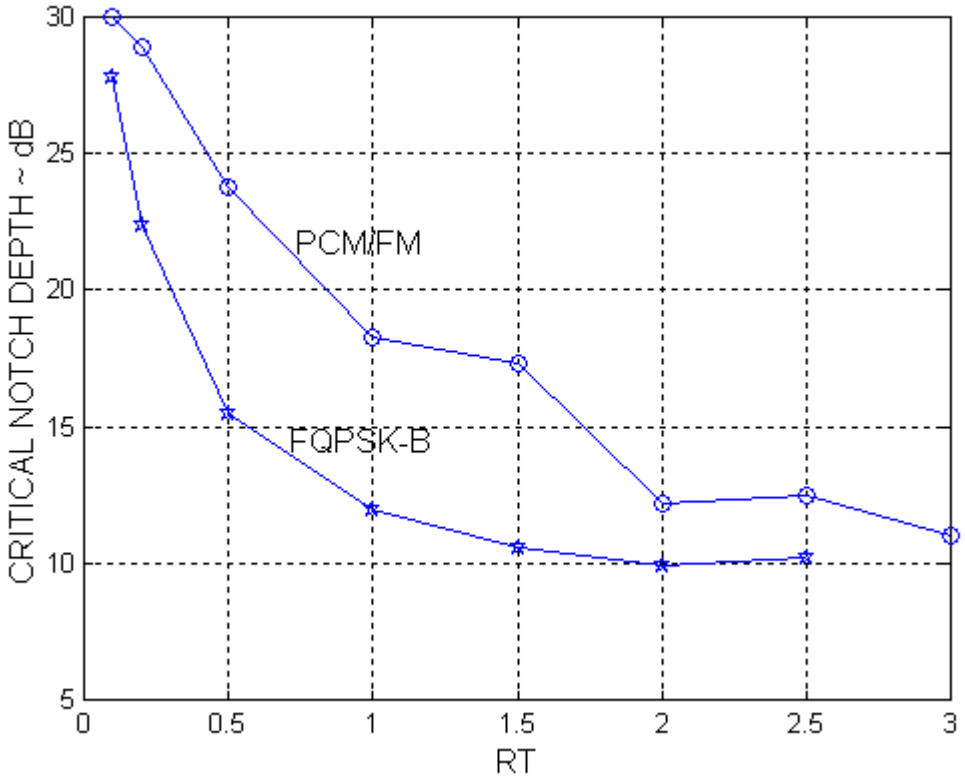

In general, slightly greater FQPSK-B receiver sensitivity to frequency selective fading is not regarded as a serious problem. The narrow FQPSK-B spectrum tends to be effected for shorter time intervals than the FM system as notches sweep across the receiving system passband. Thus, the higher sensitivity is partially self-compensating. Finally, a very high percentage of notches seen under ALM and ALS conditions are much deeper than critical notch depth. Both systems fail completely for the duration of the event. The overall difference in link availability depends on the short periods of time associated with fade onset and fade termination. These differences are generally considered negligible.

Known Weaknesses

Coherent detection is the source of two weaknesses in current FQPSK-B equipment. These are *not* peculiar to FQPSK. Rather, they are characteristic of coherent detection technology used in many QPSK and offset QPSK demodulators. FQPSK-B demodulators available today (analog and digital) rely on variations of the ubiquitous Costas loop for carrier phase and symbol timing recovery. Initial synchronization acquisition time and transient synchronization recovery time from events like severe

dispersive fades is longer than FM demodulator/bit synchronizer equipment. In addition, demodulator performance is strongly dependent on symbol zero-crossing transition density. In other words, good randomization is needed at the transmitter. Narrow loop bandwidth produces good synchronization thresholds at the expense of transient response capability. Further work is needed to identify 'optimum' loop bandwidth compromises in these applications. Three different loop bandwidths were used, ranging from 1 to 5 kHz. Acquisition and transient recovery periods were approximately one to two thousand times longer than the FM system. The impact of slow recovery depends on flight profile and vehicle speed. As long as severe frequency selective fade events are the dominant channel impairment and these events range in duration from hundreds of milliseconds to small numbers of seconds, the overall impact of slower synchronization on link reliability is considered negligible. However, if these events are very frequent and span much shorter periods of time, then FQPSK-B FLA may not be acceptable. High-speed synchronization methods would be required.

Conclusion

Performance data gathered in 1998 and 1999 demonstrated that FQPSK-B satisfies ARTM interim standard goals. Laboratory tests, flight tests and simulations have not identified any deficiencies significant enough to reject it. These results coupled with absence of serious alternatives prompted recommendation of FQPSK-B to the DoD Range Commander's Council telemetry standards committee.

Work In Progress

The ARTM project commissioned construction of first generation, flight worthy FQPSK-B transmitters and application specific demodulators in September 1999. Prototypes are scheduled for delivery in the summer of 2000. Meanwhile, the project is actively pursuing FQPSK-B receiver improvement initiatives. Significant investments are planned in 2000 and 2001 to identify optimum recovery loop parameters, implement prototype adaptive equalizers and test promising diversity techniques.

References

[1] K. Feher et al: U.S. patents 4,567,602; 4,339,724; 4,644,565; 5,491,457 and Canadian patents: 1,211,517; 1,130,871 and 1,265,851; Digcom, Inc., 44685 Country Club Drive; El Macero, California 95618; USA; Tel. 530-753-0738; Fax 530-753-1788.

[2] W. Martin, T. Yan, and L. Lam: *CCSDS-SFCG Efficient Modulation Methods Study at NASA/JPL, Phase 3 End-to-End System Performance*, NASA/JPL SF17-28/D, September 1997.

[3] E. Law, K. Feher, "FQPSK versus PCM/FM for Aeronautical Telemetry Applications: spectral Occupancy, Adjacent Channel Interference and Bit Error Probability Comparisons", *Proceedings of the International Telemetering Conference*, Las Vegas, Nevada, October 27-30, 1997, International Foundation for Telemetering, October 1997.

[4] *TELEMETRY STANDARDS, IRIG STANDARD 106-2000*, Range Commander's Council, Telemetry Group, Secretariat, White Sands Missile Range, White Sands, New Mexico, January, 2000.
[5] R. Jefferis, "Link Availability and Bit Error Clusters in Aeronautical Telemetry", *Proceedings of the International Telemetering Conference*, Las Vegas, Nevada, October 26-28, 1999, International Foundation for Telemetering, October 1999.
[6] International Telecommunication Union, "Error performance of an international digital connection operating at a bit rate below the primary rate and forming part of an integrated services digital network", ITU-T Recommendation G.821, August, 1996.
[7] Rice et al, "ARTM Channel Sounding Results - An Investigation of Frequency Selective Fading on Aeronautical Telemetry Channels", *Proceedings of the International Telemetering Conference*, Las Vegas, Nevada, October 25-28, 1999, International Foundation for Telemetering, October 1999.

Performance Enhancements of IRIG-106-00 Standardized FQPSK-B in a Complex Interference – RF Frequency Selective Faded Environment and Interoperability with Legacy Data Links

J. McCorduck*, M. Haghdad, J. S. Lin, K. Aflatouni, W. Gao, K. Feher,**
Email: engtec@aol.com, mhaghdad@ece.ucdavis.edu, linj@ece.ucdavis.edu, aflatoun@ece.ucdavis.edu, weito@ece.ucdavis.edu, feherk@yahoo.com
Department of Electrical and Computer Engineering
University of California
Davis, CA 95616

ABSTRACT:

Performance enhanced Feher's patented Quadrature Phase Shift Keying [1-4] systems are described.

One of the enhanced FQPSK increases the bandwidth efficiency of that of FQPSK-B by 50%. As the bandwidth efficiency of FQPSK-B doubles ($2\times$) that of PCM/FM, the enhanced FQPSK is triple ($3\times$) of that of PCM/FM. Another variation of the enhanced FQPSK has an end to end system loss of only 0.5 dB at BER=1×10^{-4} from ideal theory. With low redundancy FEC coding, e.g., RS(255,223), a BER=1×10^{-5} is achieved with an E_b/N_o of 6.5 dB.

Test and performance of experimental hardware and computer simulation results of FQPSK-B in a NLA complex interference environment are presented. Interference includes AWGN, CCI, and ACI, with single-tone and other FQPSK modulated interferers.

The results of the Tests & Evaluations (T&E) of ultra-fast adaptive Feher Equalizers (FE) are highlighted. It is demonstrated that for typical aeronautical telemetry RF frequency selective fading channels, having delay spreads in the 20 - 200 ns range, that the adaptive FE reduces the number of statistical outages by more than 60% without the need for training bits and without increasing the receiver synchronization time.

For complex frequency selective faded time dispersive dynamic RF environments, a smart multi-beam antenna selector combiner is described. Based on initial hardware experimental results, it is anticipated that outages will be reduced ten times over conventional combiners in selective faded environments.

Interoperability of IRIG-106-00 standardized FQPSK-B with legacy data links is discussed. In addition, the receive and transmit interoperability of FQPSK-B with future ultra-high spectrally efficient data-links is also discussed.

**Mr. McCorduck is with Entech Engineering and U.C. Davis*

***K. Feher is with U.C. Davis and the FQPSK Consortium, Digcom, Inc.; 44685 Country Club Drive, El Macero, CA 95618; Phone: (530)753-0738, FAX: (530)753-1788*

Section I: Spectrum and BER Performance Enhanced Alternatives of IRIG-106-00 Standardized FQPSK-B

Fig. 1 shows the computer simulated bit error rate (BER) for the proposed enhanced FQPSK, and the measured BER performance of FQPSK-B and PCM/FM for a 1Mb/s signal and 1 MHz IF filter bandwidths [5]. Compared with measured BER of FQPSK-B and PCM/FM, a BER of 1×10^{-5} can be achieved at an E_b/N_o of 1 to 1.5 dB lower with the proposed enhanced FQPSK using a simple threshold detector in the receiver.

The integrated adjacent channel interference (ACI) performance (with specific receiver filter) [6] of the enhanced FQPSK, FQPSK-B, and standardized GMSK (with transmitter low pass filter bandwidth BT_b = 0.3) NLA systems is shown in Fig. 2. The enhanced FQPSK shows about 50% better bandwidth efficiency than FQPSK-B, or triple ($3\times$) that of spectral efficiency of PCM/FM, while using the simplest transmitter filter among all. Detailed information about the proposed enhanced FQPSK is presented in [7].

To achieve better BER performance, low redundancy FEC can be applied to FQPSK systems. The computer simulated Reed-Solomon coded FQPSK-B with NASA standard RS(255,223) code and RS(255,239) code show significant improvement of BER performances. At BER=1×10^{-5}, The coding gain for FEC coded FQPSK-B is 4.7 dB and 3.4 dB, respectively. The results are shown in Fig. 3.

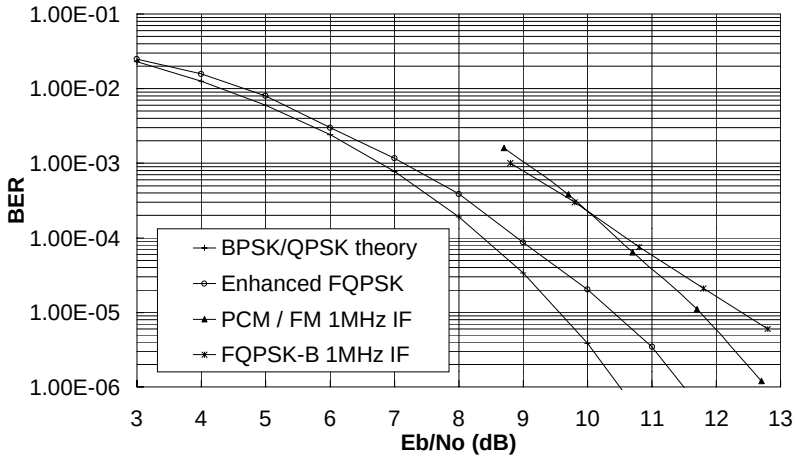

Figure 1: BER for enhanced FQPSK, and 1Mb/s FQPSK-B and PCM/FM. The BER performance of FQPSK-B and PCM/FM was measured for a 1Mb/s signal and 1 MHz IF filter bandwidth

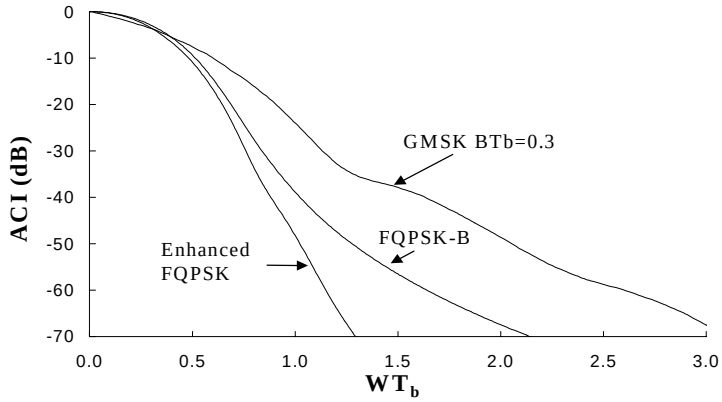

Figure 2: Adjacent channel interference performances of the enhanced FQPSK, FQPSK-B, and GMSK NLA systems. GMSK receiver used 4th order Gaussian bandpass filter with B_iT_b = 0.6 and transmitter filter bandwidths BT_b=0.3.

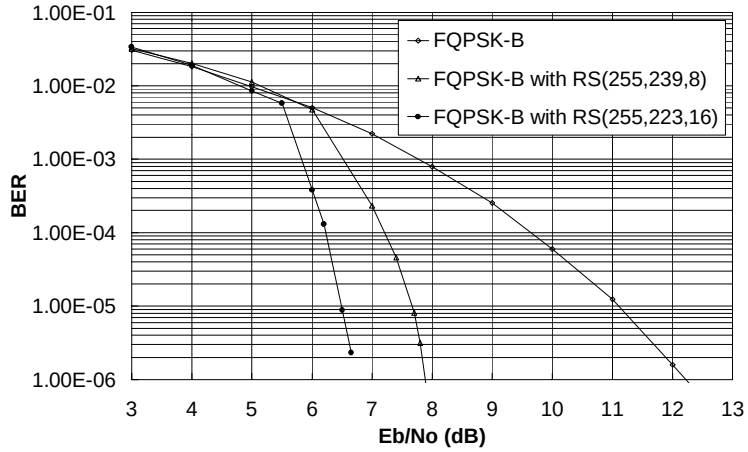

Figure 3: FEC coded FQPSK-B with Reed-Solomon codes.

Section II: FQPSK-B in a NLA Complex Interference Environment

Interference:

In a practical environment, the interference can be the ACI, CCI, AWGN or a combination of all of the above. Although in practical systems Noise, ACI and ACI are all present, in most cases, only one of these factors is dominant.

The spectrum of the CCI can have an arbitrary shape, a sinusoidal, FQPSK modulated or more complex combination of signals. Figures 4 and 5 show interference between a sinusoidal and a FQPSK modulated signal. Depends on the location of the CCI's center frequency relative to the FQPSK modulated signal's center frequency, the magnitude of the CCI varies. Consequently we get different BER result depends on the relative location of the CCI's center frequency. Both the simulation and measurements results are obtained for CCI with different relative center frequencies.

Simulations:
The simulation scheme is illustrated in Figure 6. The NRZ sequence goes through a FQPSK modulator and it is exposed to CCI, ACI and Additive Band-limited Noise. Then the signal passes trough a FQPSK demodulator and finally based on a comparison between the input and output sequence the BER is estimated.
Figure 7 shows the simulated BER results for a FQPSK modulated signal in the presence of an interfering sinusoidal signal (***A cos(2*π*fi*t)***) The results are obtained for different ***fi***.

Measurements:
The output from a signal generator is modulated and exposed to an interfering sinusoidal signal (***A cos(2*π*fi*t)***). In this measurement the CCI is the dominating factor and the ACI and AWGN are negligible. The resulting signal is demodulated and sent to a signal Comparator, which compares the original transmitted signal with the received signal. The number of error is counted and plotted as a BER curve. Figure 8 shows the BER after exposure to the CCI. The measurements was done at the bit rate of 1Mb/s at the center frequency of fc=10MHz.

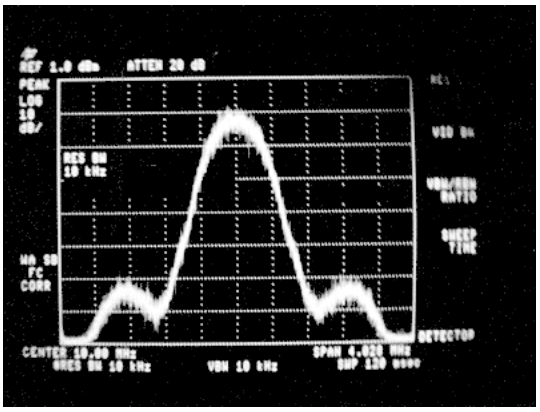

Figure 4: FQPSK spectrum

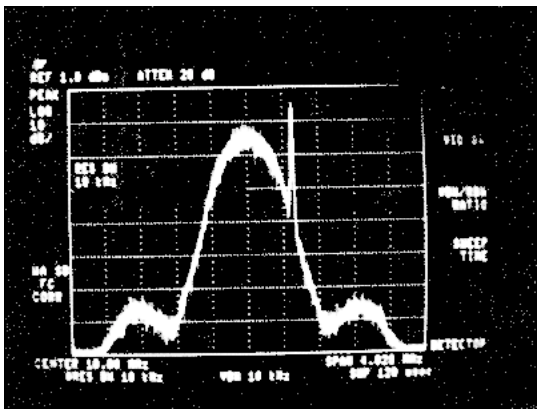

Figure 5: FQPSK spectrum with Interference

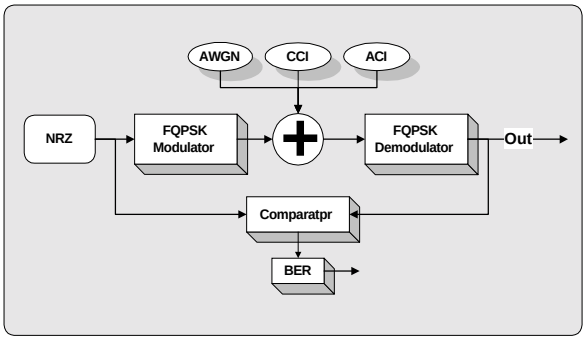

Figure 6: Conceptual system setup for simulation and measurement

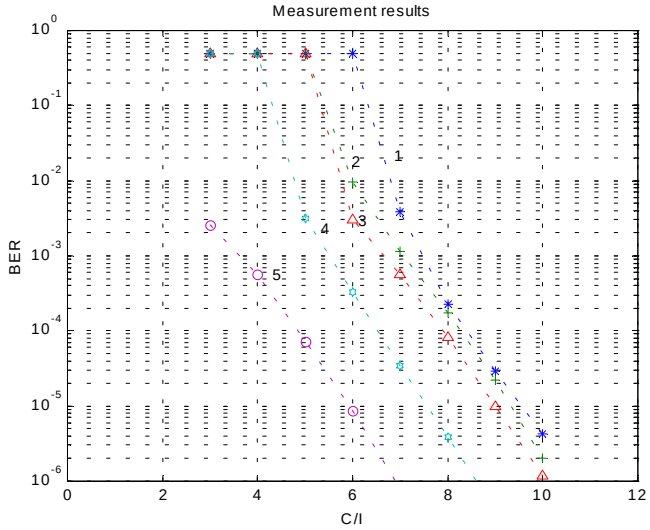

Figure 7: Measurement results at 1Mb/s for different CCI center frequencies

1) f=fc 2) f=fc-100KHz 3) f=fc-200KHz 4) f=fc-250KHz 5) f=fc-300KHz

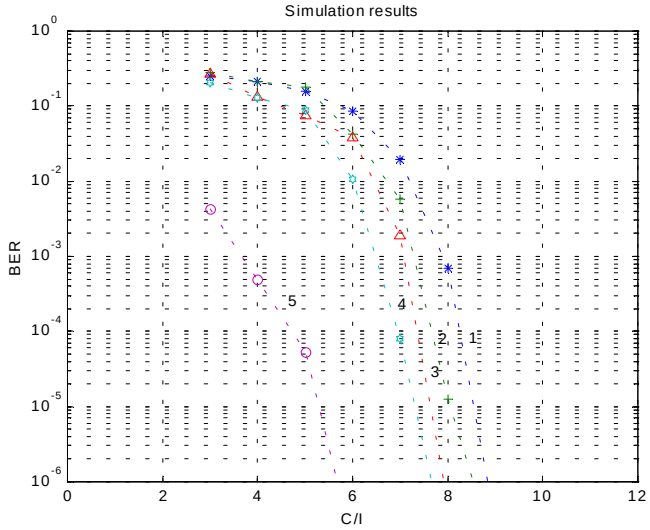

Figure 8: Simulation results at 1Mb/s for different CCI center frequencies

1) f=fc 2) f=fc-100KHz 3) f=fc-200KHz 4) f=fc-250KHz 5) f=fc-300KHz

Section III: Test and Evaluation of Adaptive Feher Equalization (FE)

In aeronautical telemetry communications, multipath interference occurs when reflected replicas with different delays of the transmitted signal arrive at the receive antenna. As a result, a multipath fade event happens and degrades the system performance. In general, the adaptive equalizer corrects the fading channel distortions by generating complimentary distortions of amplitude and associated group delay so that the frequency response of the overall system has a flat amplitude response and a constant group delay. To achieve that, however, many taps are needed. As a simple and robust approach, adaptive FE techniques show a significant performance improvement in

aeronautical frequency selective fading channel. A structure of this equalizer implemented in the intermediate frequency domain is shown in Figure 9. The equalizer is controlled by two parameters, c_1 and φ. Their values are adjusted by two different control signals respectively, which are generated based on a pseudo-error monitoring technique [8]. Unlike bit error rate (BER), pseudo-error (PSE) rate can be measured on-line and is directly proportional to BER.

A key point for the FE is to generate an extra notch to reduce the depth of a fade notch. It has been demonstrated that the spectrum of the equalized distortion signal is symmetrical when the PSE reaches its minimum. Figure 10 shows the concept of this equalizer. Experimental results of 1 Mb/s rate FQPSK-B system obtained in our laboratory frequency selective fading environment, which is closely related to the aeronautical telemetry-fading channel, have indicated that the FE based on PSE improves bit error rate (BER) by 6 dB at $P_e = 10^{-4}$ as shown in Figure 11.

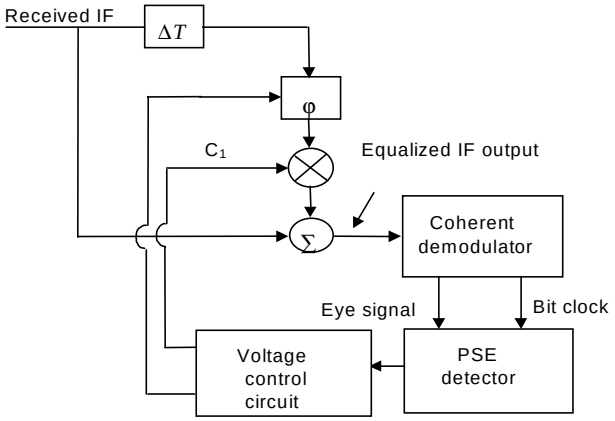

Figure 9: An adaptive FE based on a pseudo-error monitoring technique.

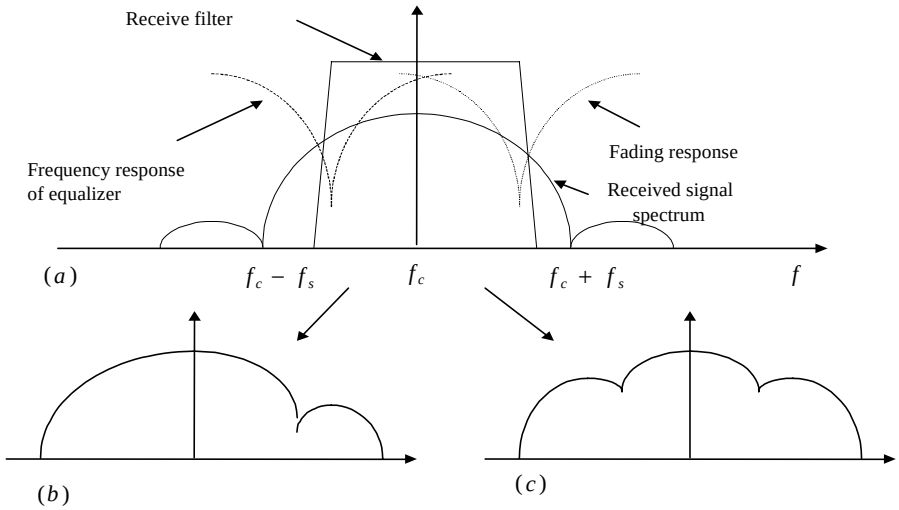

Figure 10: Concept of Feher's equalizer (FE). (a). Spectrum and frequency response. (b). Spectrum before FE. (c). Spectrum after FE.

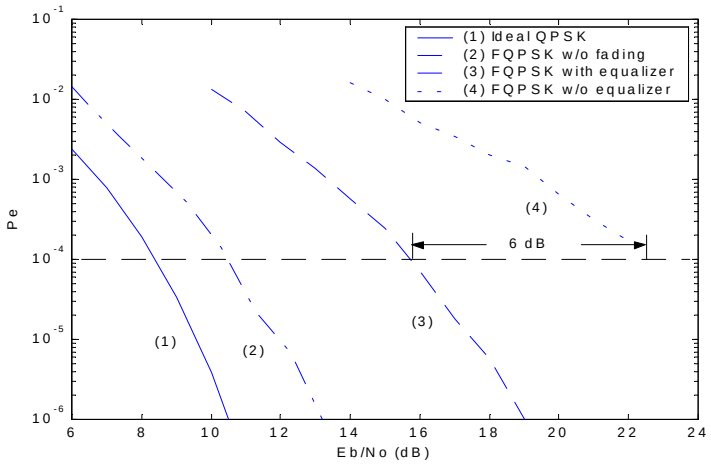

Figure 11: Measured BER for FQPSK with a bit rate of 1Mb/s in a two-path fading channel, where notch depth is 12 dB and notch is 200kHz above the carrier frequency

Section IV: The Smart Multi-Beam Antenna Selector – Feher Diversity (FD)

It has been shown that fast multipath fading severely degrades the average probability of error performance of radio transmission systems [9]. In order to achieve highly reliable digital data transmission without excessively increasing both transmitter power and co-channel reuse distance, it is indispensable to adopt an auxiliary technique that can cope with the fast multipath fading effect. It is well know that diversity reception is one of the most effective techniques for this purpose. The most suitable combining method of diversity branches for mobile radio applications is the selection method due to its simple implementation compare to other combining methods like maximal-ratio combining and equal-gain combining. The Feher Diversity (FD) technique includes a Non-Redundant Error Dection (NRED) based ultra fast control signal generated for selection of the true best signal with the lowest BER unlike other recently developed "optimal" combiners that choose the signal with the highest C/N that fail to perform in frequency selective faded environments. This method also has significant advantages over other BER measurement techniques that are based on counting the errors directly because it does not require redundancy in transmission in form of a test message or parity check digits in an error detection code or code violation detection.

Figure 12a. shows an undistorted signal with a lower C/N but better BER and Figure 12b shows a distorted signal with higher C/N but worse BER. Figure 13 shows the method of generating the ultra fast control signal for choosing the best diversity branch. Figure 14 shows the block diagram of the hitless switch that is used to select the best diversity branch without loosing any data while switching from one branch to the other is performed.

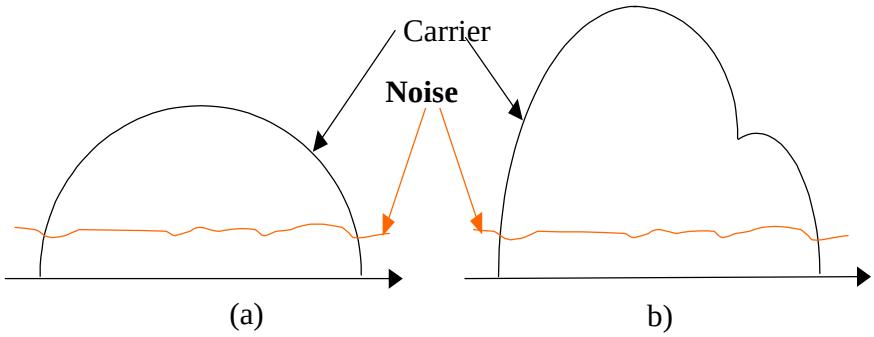

Figure 12: Distorted and undistorted signals

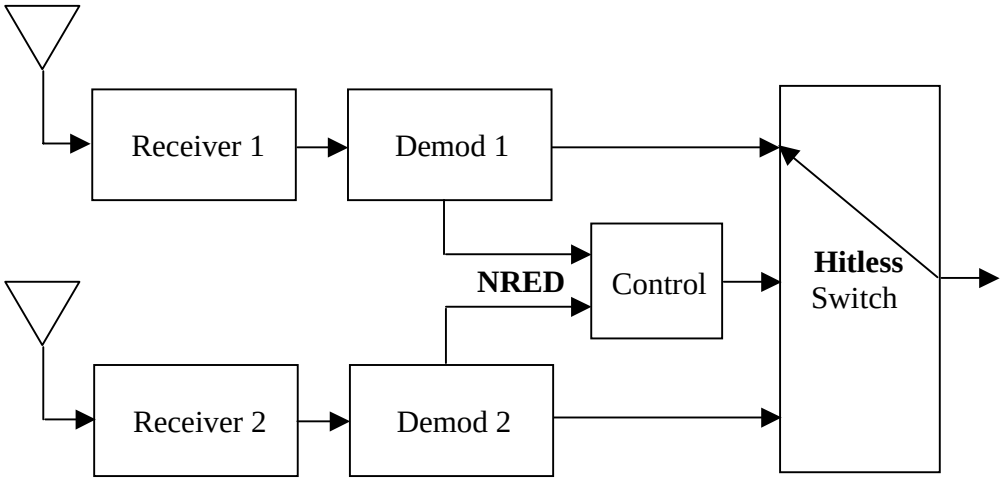

Figure 13: Switching method for choosing the best diversity branch

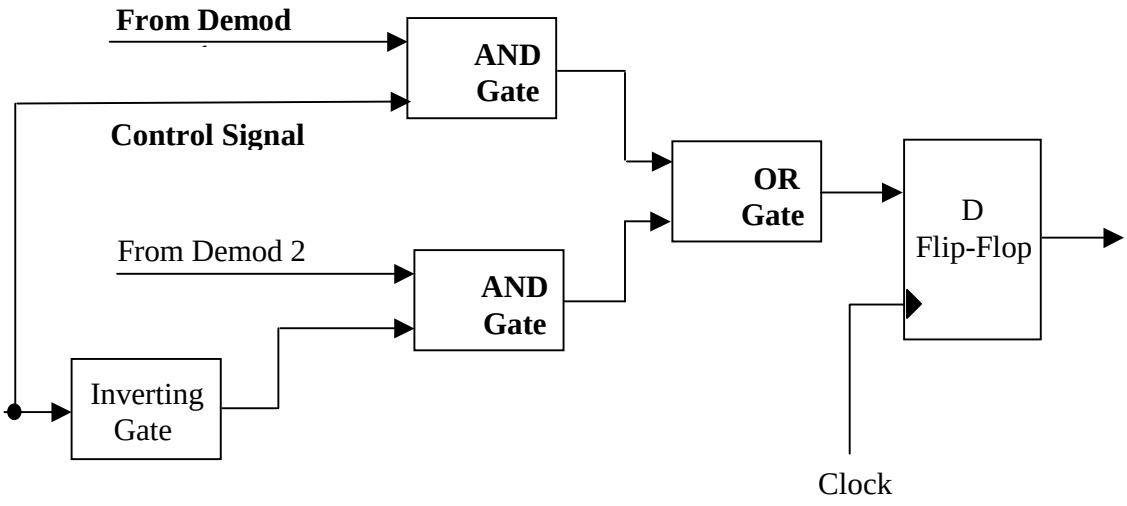

Figure 14: Block diagram of hitless switch

Section V: Interoperability of IRIG-106-00 Standard FQPSK-B with Legacy Data Links

The performance of interoperable FQPSK-B [1-3] transceivers with "legacy" data links – communications systems and benefits of such interoperable systems are described in this section. The term "legacy" is defined as the existing data links, which are currently deployed in many data link applications. Each combination of I and Q represents different resultant phase values. Also discussed in this section is forward compatibility of FQPSK-B with future data links. The interoperability and forward compatibility demonstrates the flexibility of this architecture for present and future data link applications.

With added pre-coding or differential encoding algorithms, FQPSK is interoperable with Minimum Shift Keying (MSK), Gaussian Minimum Shift Keying (GMSK), and Offset Quadrature Phase Shift Keying (OQPSK) transceiver data links. IRIG-106-00 defines the differential encoding algorithm below [3].

$$\mathbf{I}_{2n} = \mathbf{b}_{2n} \oplus \overline{\mathbf{Q}}_{(2n-1)}$$

$$\mathbf{Q}_{(2n+1)} = \mathbf{b}_{(2n+1)} \oplus \mathbf{I}_{2n} \qquad \text{for } n > 0$$

where $\mathbf{I}_2, \mathbf{I}_4, \mathbf{I}_6, \ldots$
and $\mathbf{Q}_3, \mathbf{Q}_5, \mathbf{Q}_7, \ldots$

$\mathbf{I}_n$ and $\mathbf{Q}_n$ represent the alternating quadrature data stream bits.

Interoperability explicitly states operation of FQPSK-B architecture as either a transmitter or receiver when installed with legacy GMSK, MSK, or OQPSK data links. The phase map of the FQPSK-B waveforms is illustrated in Figure 15[3]. Each combination of I and Q represents different resultant phase values. FQPSK can also be designed for forward compatibility with future data links such as the enhanced FQPSK defined in Section I, adaptive equalized FQPSK described in Section III, and FQAM (16 state FQPSK). Figure 16 represents the interoperability of FQPSK-B with the legacy data links. GMSK, MSK, and OQPSK are represented as the legacy systems.

I channel	Q Channel	Resultant Phase
A	A	45 Degrees
-A	A	135 Degrees
-A	-A	225 Degrees
A	-A	315 Degrees

Figure 15: FQPSK-B Quadrature Modulator Phase Map: (p. 2-6 IRIG STANDARD 106-00). Note that "A" is a normalized amplitude and the resultant phase is derived from the carrier of the modulated output.

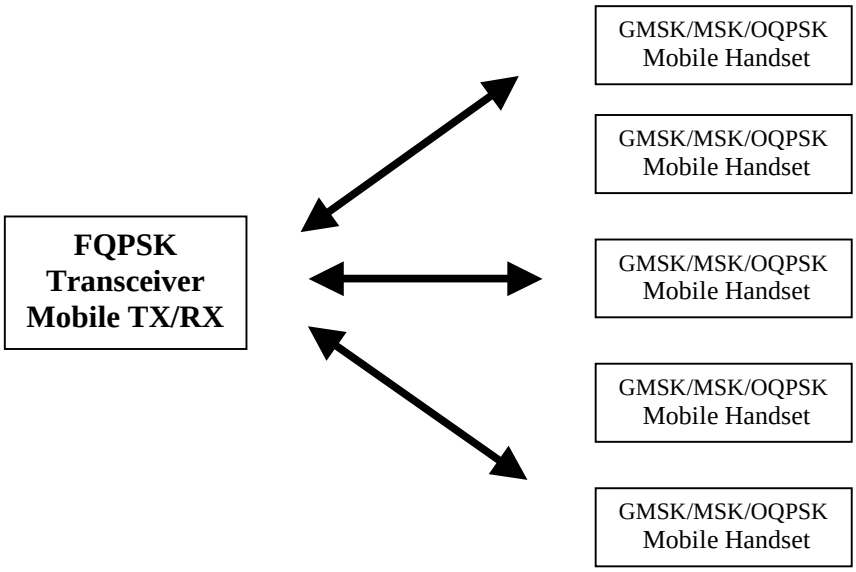

Figure 16: Proposed architecture for interoperability of FQPSK-B with legacy data links. Note that the FQPSK-B can be implemented for both transmitter and receiver applications as well as for future spectrally efficient data links.

References

1. K. Feher et al.: U.S. Patents 4,339,724; 4,567,602; 4,644,565; 5,491,457; 5,784,402, post-patent improvements and other U.S. and international patents pending. For Feher patented FQPSK and Feher patented GMSK licensing and technology transfer information, on an equal-opportunity, non-discriminatory basis with uniform terms and at a fair market price contact : FQPSK Consortium- Digcom, Inc., c/o Dr. Kamilo Feher, 44685 Country Club Dr.; El Macero, CA 95618, USA . Tel. 530-753-0738; Fax 530-753-1788 E-mail: feherk@yahoo.com
2. K. Feher .: "FQPSK Update: Commercial and Government Organizations Double Spectral Efficiency of "Dual-use" Systems," *Proc. of the International Telemetering Conference ITC/USA '99,* October 25-28, 1999, Las Vegas, NV, USA
3. IRIG STANDARD 106-00 "Telemetry Standards" [Note :For higher bit rates ,when better bandwidth efficiency is required, the IRIG 106-00 Telemetry Standard specifies the use of Feher' s patented Quadrature Phase Shift Keying (FQPSK-B) . This Standard has been approved for Public Release-Distribution is Unlimited. See : http://tecnet0.jcte.jcs.mil/RCC/manuals/106-00/ . Published by Secretariat of Range Commanders Council, U.S. Army, White Sands, New Mexico 88002-5110, USA , January 2000.
4. K. Feher : "*Wireless Digital Communications: Modulation & Spread Spectrum Applications"* - Book published by Prentice Hall, 1995. ISBN 0-13-098617-8
5. M.K. Simon and T.Y. Yan : " Unfiltered FQPSK: Another Interpretation and Further Enhancements ; Part-1 : Transmitter implementation and optimum reception," Applied Microwave & Wireless Journal, February 2000
6. E. Law and K. Feher, "FQPSK Versus PCM/FM for Aeronautical Telemetry Applications; Spectral Occupancy and Bit error rate Comparisons," Proceedings of the International Telemetry Conference, Las Vegas, NV, October 27-30, 1997
7. K. Feher, R. Jefferis, E. Law, "Spectral Efficiency and Adjacent Channel Interference Performance Definitions and Requirements for Telemetry Applications", Proceedings of the International Telemetry Conference, Las Vegas, NV, October 25-28, 1999
8. K. Feher and M. Keelty, "On-Line Pseudoerror Monitors for Digital Transmission Systems," *IEEE Trans. on Commu.*, vol. COM-26, No. 8, 1978
9. K. Feher, *"Advanced Digital Communications: Systems and Signal Processing Techniques"*, Crestone Engineering, Littleton, CO, 1996

Standardized Feher patented FQPSK Doubles and 2nd generation FQPSK could Quadruple Spectral Efficiency of PCM/FM Telemetry, of Feher patented GMSK and of Alternatives

Dr. Kamilo Feher
Professor, University of California Davis and
FQPSK Consortium -Digcom, Inc.,44685 Country Club Drive, El Macero, CA USA
Tel 530-753-0738; Fax 530-753-1788; [E-mail: feherk@yahoo.com]

Abstract

Spectrally efficient Feher's –patented Quadrature Phase Shift Keying (FQPSK) [1] developments, commercial and government "dual-use" FQPSK products ,Test and Evaluation(T&E) results, customer requirements, standards, USA and International Technology Transfer & Licensing programs of Feher patented GMSK and FQPSK are highlighted.

A List of FQPSK –GMSK Licensees, manufacturing companies & cooperating NASA, US Department of Defense (DoD), AIAA, International CCSDS programs/customers and member organizations of the FQPSK Consortium (1995-) is presented in Table 1.

Invitation is extended to the international community to join the FQPSK Consortium and benefit from the cost efficient , proven and leading spectral efficient/spectral saving FQPSK technology transfer and licensing program.

Multiyear studies of the US Department of Defense(DoD), NASA, AIAA and International Consultative Committee on Space Data Systems (CCSDS)- Space Frequency Coordination Group (SFCG) confirmed that FQPSK commercially available products offer the most spectrally efficient, robust performance flight tested data links and telemetry systems. During 1998 the AIAA recommended to the US Department of Defense (DoD), NASA and the CCSDS that FQPSK modulation be standardized. The recently issued Telemetry Standard IRIG 106-00 [Published January 2000- See: http://tecnet0.jcte.jcs.mil/RCC/manuals/106-00/] specified for higher bit rate better bandwidth efficiency telemetry systems the use of FQPSK-B. Numerous Government and Commercial systems/programs have immediate requirements for spectrally efficient telemetry systems , data links and other spectrally efficient wireless and broadcasting applications. For example, the US DoD' s Advanced Range Telemetry Program (ARTM) office has contracts with four(4) manufacturing organizations / vendors for procurement of spectrally efficient , bit rate agile 1Mb/s to 20Mb/s range S and L band FQPSK-B transmitters and receivers; NASA –GODDARD jointly with NASA/JPL are developing an ultra high bit rate (300Mb/s to 600Mb/s range) RF power and spectrally efficient FQPSK satellite system.

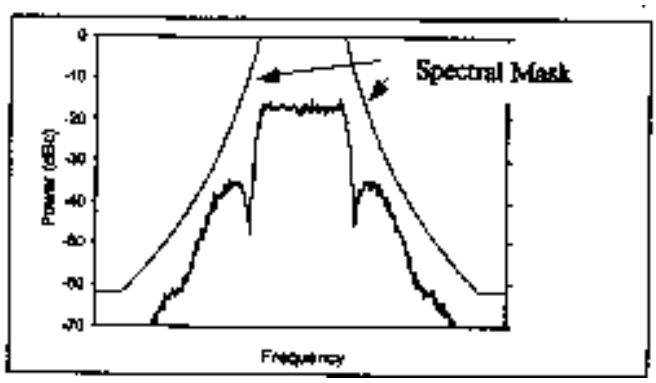

Figure A-7. Filtered 1 Mb/s RNRZ PCM/FM signal and spectral mask.

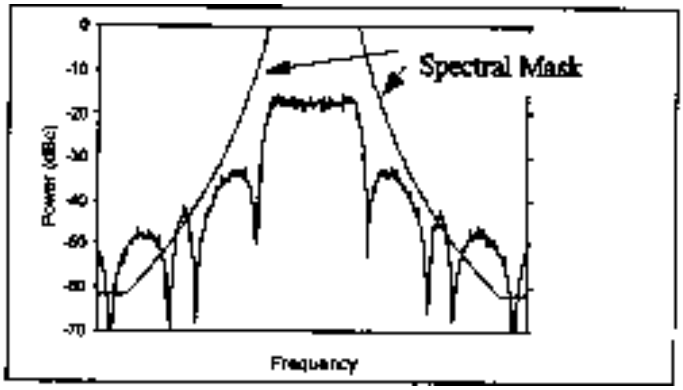

Figure A-8. Unfiltered 1 Mb/s RNRZ PCM/FM signal and spectral mask.

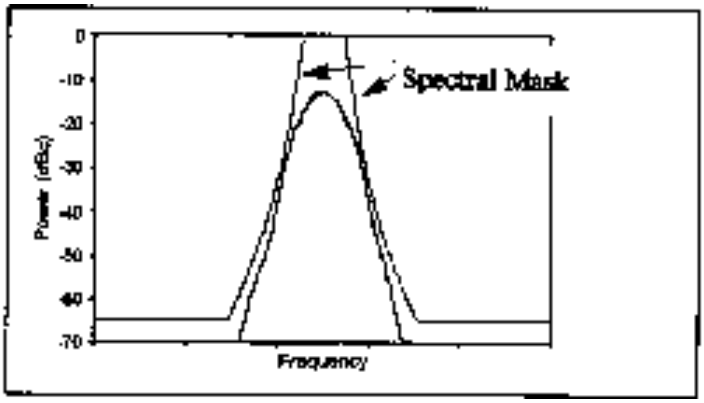

Figure A-9. Typical 1 Mb/s FQPSK-B signal and spectral mask.

Fig. 1 Spectrum and spectral mask of the telemetry IRIG STANDARD 106-00.
A comparison of the recently standardized Feher's- patented Quadrature Phase Shift Keying (FQPSK) spectrum with the PCM/FM spectrum illustrates the spectral efficiency advantage of the standardized FQPSK-B.
{From IRIG 106-00 Ref .[2] : http://tecnet0.jcte.jcs.mil/RCC/manuals/106-00/ }

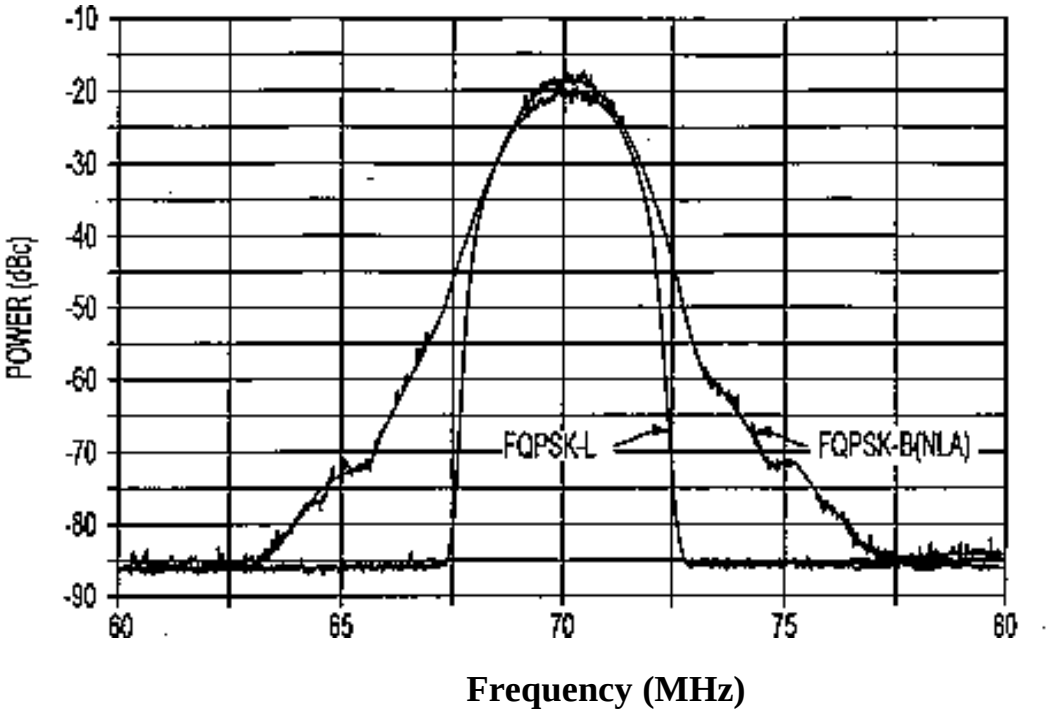

Fig. 2 Measured Spectrum of FQPSK–B Class C ,Non Linearly Amplified(NLA), fully saturated RF amplifier output, with 0dB Output Backo-Off (OBO) , at 5Mb/s rate 70MHz IF frequency and of one of the enhanced spectrum FQPSK-L systems with an approx. 2dB OBO.

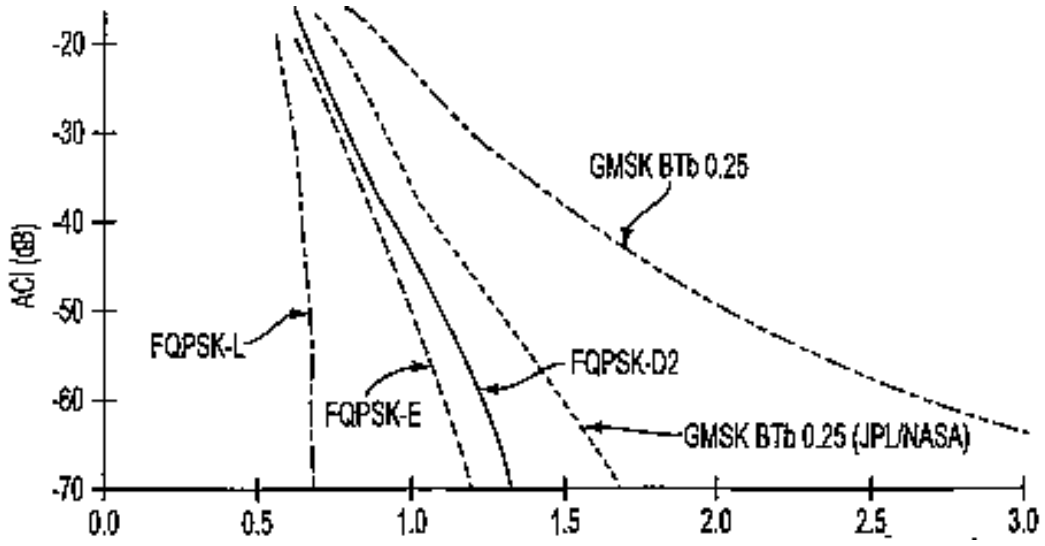

Fig. 3 Integrated out of band Adjacent Channel Interference (ACI) of Feher patented GMSK systems and of several Feher patented FQPSK systems.

IRIG STANDARD 106-00

TABLE A-1. 99% POWER BANDWIDTHS FOR VARIOUS DIGITAL MODULATION METHODS {From IRIG 106-00 Ref .[3]}

Description	99% Power Bandwidth
NRZ PCM/FM, premod filter BW=0.7R, Δf=0.35R	1.16 R
NRZ PCM/FM, no premod filter, Δf=0.25R	1.18 R
NRZ PCM/FM, no premod filter, Δf=0.35R	1.78 R
NRZ PCM/FM, no premod filter, Δf=0.40R	1.93 R
NRZ PCM/FM, premod filter BW=0.7R, Δf=0.40R	1.57 R
Minimum shift keying (MSK), no filter	1.18 R
FQPSK-B	0.78 R
PSK, no filter	19.30 R
Quadrature phase shift keying (QPSK), no filter	9.65 R
Offset QPSK (OQPSK), sinusoidal weighting	1.18 R

FQPSK-B

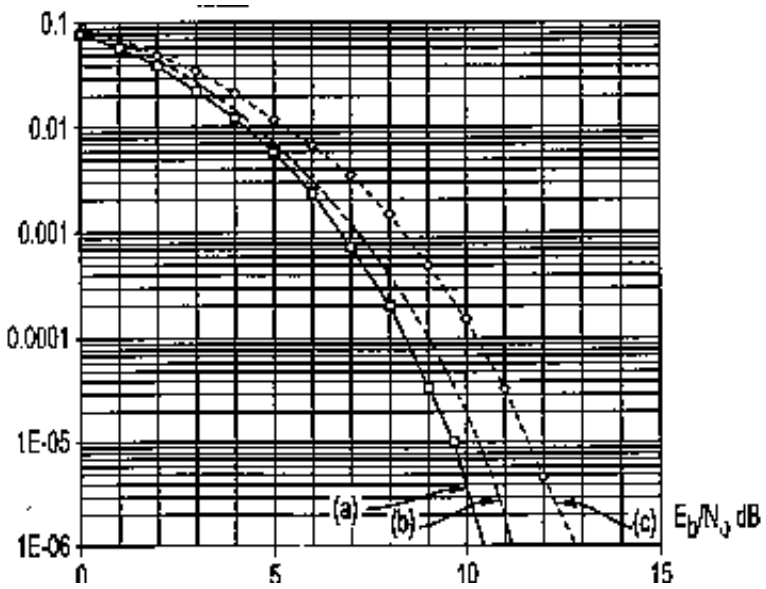

Fig. 4 Performance BER = f (Eb/No) of Non Linearly Amplified(NLA) or C-class amplified FQPSK and of Linearly Amplified Theoretical QPSK.
(a) is the ideal theoretical linearly amplified QPSK performance ;
(b) is the performance of a NLA enhanced FQPSK
(c) is the measured performance of a commercially available of the shelf FQPSK-B transceiver in a NLA mode operated in a bit rate agile mode in the 1Mb/s to 20Mb/s range (Note: this range and FQPSK-B have been specified in the ARTM- US DoD program)

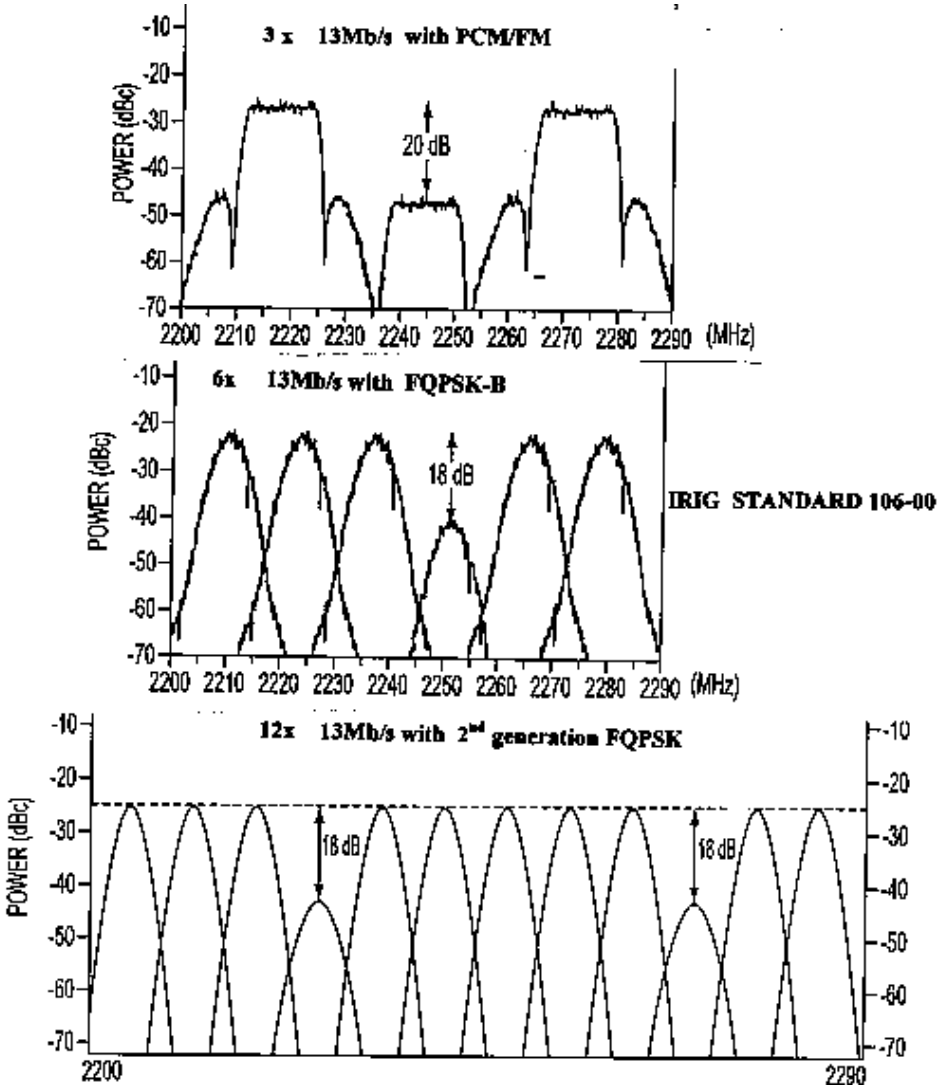

Fig. 5 The spectral efficiency advantages of FQPSK systems, over that of PCM/FM are illustrated in this illustrative example. With standardized PCM/FM in the RF authorized 90MHz " S" band (2200MHz to 2290MHz) 3 PCM/FM signals at 13Mb/s rate (having an aggregate rate of 39Mb/s) could be transmitted. The recently standardized IRIG 106-00 specified FQPSK-B doubles the number of PCM/FM telemetry signals to 6 FQPSK-B signals at 13Mb/s rate (having an aggregate rate of 78Mb/s) , while the 2nd generation of FQPSK signals will have the capability to quadruple the number of PCM/FM signals to 12 FQPSK-B signals at 13Mb/s rate (having an aggregate rate of 156Mb/s) .

****

TABLE 1. List of Feher patented FQPSK and Feher patented GMSK licensees, manufacturing companies & cooperating US Department of Defense (DoD), NASA, AIAA, International CCSDS and SFCG programs/customers and member organizations of the FQPSK Consortium (1995- 2000) :

L3 Communications, Inc:	Telemetry East-Aydin	Conic
	Interstate Electronics Co. (IEC)	Microdyne
Lockheed Martin	RF Networks, Inc.	Herley Industries-Vega
Tasc – Litton	Tybrin	EIP Microwave
Iota/NeoSoft	Emhiser Research Inc.	Applied Signal Tech.
	Broadcast Microwave Syst. Inc.	INTEL Corporation
US DoD:	SBIR(US Air Force)	ARTM-US Air Force -Edwards
CRADA-US Navy China Lake	CRADA-U.S. Navy -Pt. Mugu	1Mb/s to 20Mb/s FQPSK
FIRST;FIT ;Telemetry	TGRS	
NASA: TCA w/JPL-NASA	300Mb/s -600Mb/s FQPSK	NASA: Goddard, JPL
Standardization: AIAA	CCSDS; SFCG; ESA	FIT ; Telemetry IRIG 106-00
Universities:	NMSU	University of California ,Davis

****

Keywords:

Feher's patented Quadrature Phase Shift Keying (FQPSK) ; Feher's patented Gaussian Minimum Shift Keying(FGMSK) ; Gaussian Minimum Shift Keying; Spectral Efficient ; Bandwidth Efficient ; Quadrature Phase Shift Keying.

References

1. K. Feher et al.: U.S. Patents 4,339,724; 4,567,602; 4,644,565; 5,491,457; 5,784,402, post-patent improvements and other U.S. and international patents pending. For Feher patented FQPSK and Feher patented GMSK licensing and technology transfer information, on an equal-opportunity, non-discriminatory basis with uniform terms and at a fair market price contact : FQPSK Consortium-Digcom, Inc., c/o Dr. Kamilo Feher, 44685 Country Club Dr.; El Macero, CA 95618, USA . Tel. 530-753-0738; Fax 530-753-1788 E-mail: feherk@yahoo.com

2. IRIG STANDARD 106-00 "Telemetry Standards" [Note :For higher bit rates ,when better bandwidth efficiency is required, the IRIG 106-00 Telemetry Standard specifies the use of Feher' s patented Quadrature Phase Shift Keying (FQPSK-B) . This Standard has been approved for Public Release-Distribution is Unlimited. See : http://tecnet0.jcte.jcs.mil/RCC/manuals/106-00/ . Published by Secretariat of Range Commanders Council, U.S. Army, White Sands, New Mexico 88002-5110, USA , January 2000.

3 Digcom, Inc. : "FQPSK-B, Revision A1, Digcom –Feher Patented Technology Transfer Document, January 15,1999 " , El Macero ,CA, January 1999. [Note: This Digcom, Inc. proprietary document is available to Digcom's Licensees of the Feher patented FQPSK and GMSK Technologies , from Digcom, Inc]. The IRIG STANDARD 106-00 references (on page 2-5) this Digcom document for the use of the standard specified FQPSK-B. See : http://tecnet0.jcte.jcs.mil/RCC/manuals/106-00/ . For FQPSK –GMSK Technology Transfer and Licensing Contact: Digcom, Inc., c/o Dr. Kamilo Feher, 44685 Country Club Dr.; El Macero, CA 95618, USA Tel. 530-753-0738; Fax 530-753-1788 E-mail: feherk@yahoo.com

4 Feher : "*Wireless Digital Communications: Modulation & Spread Spectrum Applications"* - Book published by Prentice Hall, 1995. ISBN 0-13-098617-8

5 S. Kato and K. Feher: " XPSK: A new Cross-Correlated Phase Shift Keying Modulation Technique" IEEE Transactions on Communications ,vol.COM-31, May 1983

6 K. Feher ., R. Jefferis , E. Law : "Spectral Efficiency and Adjacent Channel Interference Performance Definitions and Requirements for Telemetry Applications," *Proc. of the International Telemetering Conference ITC/USA '99,* October 25-28, 1999, Las Vegas, NV, USA

7 G. Terziev , K. Feher .: "Adaptive Fast Blind Feher Equalizers (FE) for FQPSK," *Proc. of the International Telemetering Conference ITC/USA '99,* October 25-28, 1999, Las Vegas, NV, USA

8 W. Gao , S.H.Wang, K. Feher .: "Blind Equalization for FQPSK and FQAM Systems in Multipath Frequency Selective Fading Channels," *Proc. of the International Telemetering Conference ITC/USA '99,* October 25-28, 1999, Las Vegas, NV

9 G. Horcher .: "Design Considerations for Development of an Airborne FQPSK Transmitter," *Proc. of the International Telemetering Conference ITC/USA '99,* October 25-28, 1999, Las Vegas, NV

10 R.P. Jefferis.: "Link Availability and Bit Error Clusters in Aeronautical Telemetry," *Proc. of the International Telemetering Conference ITC/USA '99*, October 25-28, 1999, Las Vegas, NV

11 W.L.Martin, T.Y. Yan , L.V.Lam: CCSDS-SFCG Efficient Modulation Methods Study at NASA/JPL; Phase 3: End-to-End System Performance" , SFCG Meeting Report SF17-28/D. Published by JPL/NASA , Pasadena Ca, USA ,September 1997

12 E.L. Law .: "Estimating the Characteristics of the Aeronautical Telemetry Channel During Bit Error Events," *Proc. of the Internat. Telemet. Conf. ITC/USA '99,* October 25-28, 1999, Las Vegas, NV

13 M.K. Simon and T.Y. Yan : " Unfiltered FQPSK: Another Interpretation and Further Enhancements ; Part-1 : Transmitter implementation and optimum reception" [Dr. Marvin K Simon and Dr. Tsun-Yee Yan are with CalTech JPL-NASA] , Applied Microwave & Wireless Journal, www.amwireless.com February 2000

14 M.K. Simon and T.Y. Yan : " Performance Evaluation and Interpretation of Unfiltered Feher-patented Quadrature Phase Shift Keying(FQPSK) " JPL- TMO Progress Report 42-137 , May 15,1999 available from the JPL/NASA authors , California Institute of Technology(CalTech) -JPL/NASA ,Pasadena , CA, USA tel. 818-354-4321 or http://tmo.jpl.nasa.gov/progress_report/

15 E. Law and K. Feher : " FQPSK versus PCM/FM for Aeronautical Telemetry Applications; Spectral Occupancy and Bit Error Probability Comparisons " , *International Telemetering Conference ITC/USA '97,* October 27-30, 1997, Las Vegas, NV , USA

16 K. Feher : " FQPSK Transceivers Double the Spectral Efficiency of Wireless and Telemetry Systems " Applied Microwave & Wireless , June 1998 www.amwireless.com
17 D. Ernst ., A. Hooke , C. Irving , K. Leinhsart .: "International Standardization of Efficient Protocols for Aerospace Use," MITRE, NASA, U.S. Air Force and ESA-ESOC Chairman of CCSDS Panel-1, European Telemetry Conference ETC 2000, Garmisch-Partenkirchen, Germany, May 22-25, 2000
18 R. Jefferis ., E. Law : "Tutorial on Feher's Quadrature Phase Shift Keying (FQPSK) Technology and Applications," NAWCWD, U.S. Navy, Pt. Mugu, CA and Tybrin Corp., Edwards Air Force Base, CA, European Telemetry Conference ETC 2000, Garmisch-Partenkirchen, Germany, May 22-25, 2000
19 P. Eastman , R.B. Formeister : "Spectral Efficient Bit Rate Agile and IF Frequency Selectable FQPSK Commercial and Government Product Developments," RF Networks Inc., Phoenix, AZ, European Telemetry Conference ETC 2000, Garmisch-Partenkirchen, Germany, May 22-25, 2000
20 J. Bottenfield , J.Carle , D. Heft : "Production Design of Government Standardized Spectrally Efficient FQPSK Transmitters," Herley Industries, Inc. (Vega Div.), Lancaster, PA, European Telemetry Conference ETC 2000, Garmisch-Partenkirchen, Germany, May 22-25, 2000
21 H. Tsou , S. Darden , T.Y. Yan : "An Off-line Coherent FQPSK-B Software Reference Receiver," CalTech-JPL/NASA, Pasadena, CA, European Telemetry Conference ETC 2000, Garmisch-Partenkirchen, Germany, May 22-25, 2000
22 E. Law : "IRIG FQPSK-B Standardization Progress Report," Member, RCC Telemetry Group, NAWCWD, U.S. Navy, Pt. Mugu, CA, European Telemetry Conference ETC 2000, Garmisch-Partenkirchen, Germany, May 22-25, 2000
23 D. O'Cull : "FQPSK Demodulation and Performance," L-3 Communications, Inc., Microdyne Div., Ocala, FL, European Telemet. Conf. ETC 2000, Garmisch-Partenkirchen, Germany, May 22-25, 2000
24 R.P.Jefferis : "FQPSK-B Performance in Air-to-Ground Telemetry," Tybrin Corporation, Edwards Air Force Base, CA, European Telemetry Conference ETC 2000, Garmisch-Partenkirchen, Germany, May 22-25, 2000
25 J. McCorduck , M. Haghdad , J.S. Lin , K. Aflatouni , W. Gao , K. Feher.: "Performance Enhancements of IRIG-106-00 Standardized FQPSK-B in a Complex Interference - RF Frequency Selective Faded Environment and Interoperability with Legacy Data Links," European Telemet. Confer. ETC 2000, Garmisch-Partenkirchen, Germany, May 22-25, 2000
26 K. Feher: " Standardized Feher patented FQPSK Doubles and 2nd generation FQPSK Could Quadruple Spectral Efficiency of PCM/FM Telemetry, of Feher patented GMSK and of Alternatives", Proceedings of the European Telemetry Conference, ETC 2000, Garmisch-Partenkirchen, Germany, May 22-25, 2000

ICTS

International Consortium on Telemetry Spectrum (ICTS)

The **ICTS** is a recently proposed International Group of Telemetry Practioners whose main objective is to ensure the future availability of electromagnetic spectrum for telemetering. The participants of the meeting will discuss questions of Radio Frequency Spectrum Utilisation and other topics related. The following pages are showing the **ICTS Charter** and **By-Laws**.

ICTS CHARTER

INTERNATIONAL CONSORTIUM FOR TELEMETRY SPECTRUM

(APPROVAL DATE)

1. NAME

The name of the consortium shall be: International Consortium for Telemetry Spectrum (ICTS).

2. SPONSORSHIP

The ICTS is chartered under the sponsorship of the International Foundation for Telemetering (IFT).

3. OBJECTIVE

To establish a committee under the IFT that provides a loose coalition of telemetry practitioners who share a common goal of ensuring the availability of electromagnetic spectrum for telemetering.

4. SCOPE

The ICTS shall serve as a focal point to receive, review, coordinate, and disseminate information concerning telemetry spectrum for the well being of the individual ICTS members and their nations.

5. TASK

5.1. Determine the frequency allocations assigned to individual nations and regions for telemetering.

5.2 Alert telemetry practitioners on planned or proposed changes to spectrum allocations that affect telemetering.

5.3. Solicit comments from telemetry practitioners on the potential impact of planned or proposed changes to telemetry frequency band allocations.

5.4. Prepare and coordinate information papers for use by ICTS members in apprising their respective spectrum representatives.

6. ORGANIZATION

The leadership of the consortium shall be comprised of three officers and three regional coordinators.

The officers of the consortium shall consist of a Chair, Vice-Chair, and Secretary-Treasurer.

The regional coordinators shall consist of a coordinator for each of Regions 1,2 and 3, where these regions are as defined by the International Telecommunications Union (ITU).

7. ORGANIZATIONAL STRUCTURE

Through its Chair, the ICTS shall be responsible for adherence to its chartered objectives.

Regional coordinators shall coordinate the ICTS activities of ICTS members within their regions as defined by the ITU, and coordinate with the Officers in support of the goals of the consortium.

8. MEMBERSHIP

The consortium shall be open to membership for individuals or organizations who support the goals of the ICTS and have a business or professional stake in the use of the telemetry spectrum.

9. GENERAL

Revisions to the charter shall be formulated by the Officers and presented to the IFT for endorsement.

BY-LAWS

INTERNATIONAL CONSORTIUM FOR TELEMETRY SPECTUM

Approved (DATE)

1.0 Purpose

The purpose of the By-Laws will be to provide a working set of operational procedures for the successful implementation of the chartered International Consortium for Telemetry Spectrum (ICTS) objectives. The By-Laws shall at all times conform to the ICTS Charter.

1.1 Direction

Through its Chair, the ICTS shall be responsible for adherence to the ICTS Charter.

1.2 ICTS Year

The ICTS year shall begin immediately following the ICTS Annual Meeting, held in conjunction with the International Telemetering Conference.

2.0 Committees

The ICTS shall have standing committees consisting of a Nominating Committee and technical committees as defined herein.

2.1 Nominating Committee

The Nominating Committee shall propose ICTS Members and officers for approval by the membership. ICTS Members can also nominate prospective ICTS Members and officers via the Nominating Committee.

2.1.1 Membership

The Nominating Committee shall consist of the three ICTS Regional Coordinators. The Nominating Committee chairman will be elected by the standing ICTS membership.

2.1.2 Term of Membership

The Nominating Committee term of membership shall coincide with the term of office of the ICTS officers.

2.1.3 Duties

2.1.3.1 The Nominating Committee shall recommend persons to fill new, vacant or expiring membership positions at each ICTS Annual Meeting.

2.1.3.2 The Nominating Committee shall recommend the names of standing members to hold the positions of Secretary-Treasurer, Vice-Chair, and Regional Coordinators at the Annual Meeting in each even numbered year.

2.2 Technical Committees

The ICTS shall form committees as required to focus on specific areas of interest to the ICTS.

2.2.1 Formation

Committee chairs shall serve by appointment of the ICTS Chair. The ICTS Chair shall appoint ICTS Members and Alternates to serve on committees. The committee chair may appoint other Members as required. Committee members will be encouraged to attend committee meetings as called by the committee chair.

2.2.2 Task

Each committee shall perform the following functions:

(a) Research the specific area of interest.

(b) Comment on the potential impact to planned and existing telemetering applications.

(c) Communicate issues and impacts to ICTS Regional Coordinators for dissemination to ICTS members.

(d) Report on committee status at annual meetings.

(e) Perform other related tasks as assigned by the chair.

2.2.3 Function

Each of the committees shall function as a fact-finding group for the Consortium and shall obtain its information both by personal contact and by formal presentation of qualified individuals to the committee and/or Consortium. Presentations by non-ICTS members shall be on an invitation basis only and Members shall not release information as public information.

2.2.4 Recommendations

Upon completion of its investigations, each committee shall present its report to the full Consortium.

2.2.5 Release of Information

All external release of committee reports and correspondence shall be made in the name of the ICTS. Such release shall be made only with the approval of the ICTS Chair.

3.0 Membership

The ICTS shall have three categories of membership. The qualifications and other membership requirements are stated herein. The categories of ICTS membership shall be Regular, *ex-Officio*, and Emeritus.

3.1 Regular Members

The ICTS shall have a limited number of Regular members. No two Regular members shall be representatives of the same organization [as defined by the ICTS Nomination committee.]

3.1.1 Qualifications

In order to be qualified to serve as a member of ICTS a person must be actively engaged in telemetry-related activities, such as telemetering instrumentation, data systems, communications, and telemetry frequency management, or possess outstanding qualifications by virtue of long experience in these fields. The Nominating Committee shall recommend potential members based upon technical stature and capability to participate actively in ICTS activities.

3.1.2 Sphere of Interest

The Nominating Committee shall attempt to ensure that representatives of government and commercial entities shall each separately constitute a minimum of one-third of the regular ICTS membership. Any person meeting the requirements of Section 3.1.1, including but not limited to those in commercial, governmental, and academic entities, may constitute the remaining one-third.

3.1.2.1 Government Entity Definition

Government entities are defined to include agencies of federal, state, or local governments, and not-for-profit organizations under contract to them.

3.1.2.2 Commercial Entity Definition

Commercial entities are defined as manufacturers, vendors of equipment, software, or systems, companies that use telemetry equipment, and suppliers of telemetry-related services, such as consulting.

3.1.2.3 Government Entity Definition

Academic entities are defined as colleges and universities who provide educational and research services in the field of telemetry.

3.1.3 Regular Member Selection

Prospective Regular Members who have been nominated by the Nominating Committee shall be confirmed at either the annual meeting or at second meeting scheduled each year to coincide with the European Telemetering Conference (odd-numbered years) or European Test and Telemetry Conference (even-numbered years). Confirmation will require a majority vote among ICTS members present.

3.1.4 Resignation of Membership

If a member resigns or is otherwise unable to serve a complete term, the Nominating Committee shall recommend a qualified replacement.

3.1.5 Alternates

Each Regular Member can nominate a permanent Alternate who is in the member's own sphere of interest and meets the same qualifications as a Regular Member. The Alternate shall be kept informed of the Consortium activities and will be expected to actively serve on a committee, as required. The Alternate will be encouraged to attend all meetings. The Alternate shall vote in the absence of the Regular Member.

3.1.6 Sponsorship

Each Regular Member shall assure the ICTS of his/her ability to meet the obligations of membership upon becoming a member. The obligations include the time and costs associated with attending at least one ICTS meeting per year. This assurance may come from the Member or the Member's employing organization.

3.2 Ex-Officio Member

The chair of the IFT may appoint a representative to serve as liaison between the IFT and the ICTS. This representative shall be an *Ex-Officio* Member of the ICTS.

There shall be one Ex-Officio member of the ICTS as defined herein. The Ex-Officio member of the ICTS shall have voting rights on all issues, but may not hold the office of Chair, Vice-Chair, Secretary-Treasurer, or Regional Coordinator.

3.3 Members Emeriti

The ICTS may elect Members Emeriti from time to time as appropriate. A Member Emeritus shall have the right to attend all ICTS meetings, be a committee chair, and have voting rights on all issues before the ICTS. A Member Emeritus is obliged to participate actively in ICTS affairs within the constraints of their situation.

The qualifications for Member Emeritus shall be:

- The Member shall have been a Regular Member of the ICTS for at five years and shall have been active in ICTS matters during his/her tenure.
- The Member shall no longer be an employee of an organization defined in Section 3.1.2.1 of the By-Laws.
- The Member shall be desirous of maintaining an active interest and participation in ICTS matters.
- Nomination for Membership Emeritus shall be by unanimous vote of the ICTS Officers. Any Member or past Member may recommend a person for Membership Emeritus.
- If recommendation is not by request of the prospective Member Emeritus, the member shall indicate their desire to serve actively as a Member Emeritus prior to the vote of the full Consortium on their election.

4.0 Organization

The Consortium shall have the following Officers: Chair, Vice-Chair, and Secretary-Treasurer.

There shall also be three Regional Coordinators. The Regional Coordinators shall consist of an International Telecommunications Union (ITU) Region 1 Coordinator, an ITU Region 2 Coordinator, and an ITU Region 3 Coordinator.

4.1 ICTS Officers

The Vice-Chair and Secretary-Treasurer shall be elected from the Membership. The Vice-Chair shall succeed the outgoing Chair.

4.1.1 Term of Office

Officers shall serve for a two-year term of office beginning at the start of the ICTS Year in even-numbered calendar years.

4.1.2 Officer Succession

The Secretary-Treasurer may be re-elected. If the Chair is unable to serve out their term of office, the Vice-Chair shall serve the Chair's remaining term of office. Upon completion of the remaining term of office, the Vice-Chair will continue to fulfill a two-year term as Chair.

4.1.3 Officer Elections

Nominations for Vice-Chair and Secretary-Treasurer shall be submitted to the Nominating Committee. Elections will be held in even-numbered calendar years at the ICTS Annual Meeting. Members who are unable to attend may vote by proxy via their Alternate or via their Regional Coordinators.

4.2 ICTS Regional Coordinators

There shall be an ICTS Regional Coordinator for each ITU Region. Regional Coordinators shall be elected by the ICTS Members within each specific Region.

4.2.1 Term of Office

Regional Coordinators shall serve for a two-year term coinciding with the ICTS Officers term of office. Regional Coordinators may be re-elected.

4.2.2 Regional Coordinator Elections

Each current Regional Coordinator will be responsible for soliciting nominations and holding elections for their replacement. Only Members in their Region shall be eligible to nominate, vote, and serve. Each Regional Coordinator shall hold elections prior to the ICTS Annual Meeting. Regional Coordinators shall announce their replacement at the ICTS annual meeting.

5.0 Meetings

There shall be a minimum of two (2) scheduled ICTS meetings per year.

5.1 Meeting Schedule

The ICTS Annual meeting shall be held in conjunction with the International Telemetering Conference each year. A second meeting shall be scheduled each year to coincide with the European Telemetering Conference (odd years) or European Test and Telemetry Conference (even years).

5.2 Notice

At least four weeks written notice shall be required to call an official meeting. In exceptional cases the Chair may schedule or reschedule a meeting on shorter notice, but not less than two weeks.

5.3 Attendance

Members are expected to attend at least one regularly scheduled meeting per year. The Alternate shall attend meetings when the Member is unable to attend. Failure to regularly attend scheduled meetings can be considered grounds for termination of Membership.

6.0 Requirements for Transaction of Business

The official actions of the ICTS shall be classified as Policy Matters, Routine Matters, or ICTS Positions as defined herein. For the purposes of this section, the word Member refers to Regular Members or their Alternate in case of absence, Members Emeritus, and *ex-Officio* Members.

6.1 Policy Matters

Policy Approval shall require the concurrence of two-thirds (2/3) of all voting Members, which will also constitute a quorum, at the Annual Meeting. All policy matters will be presented to ICTS members at least thirty (30) calendar days before the Annual Meeting to allow input and voting by Members unable to attend.

A policy matter is defined as any of the following:

- Election of Officers
- Selection of Members or Alternates
- Amendment, Suspension or Adoption of By-Laws
- Any recommendation that goes outside the ICTS

6.2 Routine Matters

Official action of the Consortium on routine business matters shall be determined by the concurring vote of a majority of the Members present.

6.3 ICTS Positions

In special cases, the ICTS may propose to publish an "ICTS Position" on an issue. ICTS Positions require 100% agreement by voting members and an endorsement by the IFT.

6.4 Ability to Transact Business Outside of Scheduled Meetings

Not withstanding anything else in this section, all matters may be submitted for a vote of the membership outside of a meeting when appropriate ("mail vote"). The matter shall be submitted and votes received in a format that may be retained for permanent records, e.g. letter mail, facsimile, or email hardcopy. The Chair shall provide notice and pertinent information and at least 30 calendar days prior to the set date for return votes. The number of affirmative votes required shall be as defined under "Policy Matters" and "Routine Matters" above.

7.0 Business

The ICTS shall confine its activities to the Scope of work outlined under Section 3 of its Charter.

7.1 Program

At the beginning of each ICTS year the Officers shall prepare a program for the year's activity and submit it for approval of the membership. Implementation of the outlined tasks shall be via duly constituted committees.

7.2 Reporting

The ICTS Chair shall submit an annual written report and a separate financial statement to the IFT. The annual written report shall be submitted for timely inclusion in *The Proceedings of the International Telemetering Conference.* The financial statement shall be prepared by the Secretary/Treasurer prior to the Annual Meeting and shall include a budget and request for sponsorship support for the coming year.

8.0 By-Laws

8.1 Adoption or Amendment

By-laws may be adopted or amended by an affirmative vote of committee members as defined in 6.0, Requirements for Transaction of Business. Changes to the By-Laws shall be approved by the Sponsoring Organization before taking effect.

8.2 Suspension

These By-laws may be suspended by an affirmative vote of committee members as defined in 6.0, Requirements for Transaction of Business.